AD722250

AD

USAAVLABS TECHNICAL REPORT 70-67

STABILITY AND CONTROL HANDBOOK FOR COMPOUND HELICOPTERS

By

E. K. Garay

E. Kisielowski

February 1971

EUSTIS DIRECTORATE
U. S. ARMY AIR MOBILITY RESEARCH AND DEVELOPMENT LABORATORY
FORT EUSTIS, VIRGINIA

CONTRACT DAAJ02-69-C-0023

DYNASCIENCES CORPORATION

BLUE BELL, PENNSYLVANIA

625

Disclaimers

The findings in this report are not to be construed as an official Department of the Army position unless so designated by other authorized documents.

When Government drawings, specifications, or other data are used for any purpose other than in connection with a definitely related Government procurement operation, the United States Government thereby incurs no responsibility nor any obligation whatsoever; and the fact that the Government may have formulated, furnished, or in any way supplied the said drawings, specifications, or other data is not to be regarded by implication or otherwise as in any manner licensing the holder or any other person or corporation, or conveying any rights or permission, to manufacture, use, or sell any patented invention that may in any way be related thereto.

Disposition Instructions

Destroy this report when no longer needed. Do not return it to the originator.

DEPARTMENT OF THE ARMY
EUSTIS DIRECTORATE
U.S. ARMY AIR MOBILITY RESEARCH AND DEVELOPMENT LABORATORY
FORT EUSTIS, VIRGINIA 23604

This report has been reviewed by the Eustis Directorate, U. S. Army Air Mobility Research and Development Laboratory and is considered to be technically sound. The report is published for the exchange of information and appropriate application.

Task 1F162204A14233
Contract DAAJ02-69-C-0023
USAAVLABS Technical Report 70-67

February 1971

STABILITY AND CONTROL HANDBOOK FOR COMPOUND HELICOPTERS

Dynasciences Report No. DCR-314

by

E. K. Garay
E. Kisielowski

Prepared by

Dynasciences Corporation
Blue Bell, Pennsylvania

for

Eustis Directorate
U.S. Army Air Mobility Research and Development Laboratory
Fort Eustis, Virginia

ABSTRACT

This handbook contains analytical methods and stability data for determining the dynamic stability and control characteristics of generalized single-rotor compound helicopter configurations. The methods use calculation procedures which are considerably simplified through the extensive use of information presented in graphs and charts. These charts are applicable to articulated, teetering, and hingeless rotor systems and cover a range of flight conditions from hover to high forward speeds.

The charts for low forward speeds (advance ratios, $\mu \leq 0.2$) were obtained from the rotor performance data based on classical rotor theory. However, the high-speed charts ($\mu \geq 0.3$) exclude the major assumptions of classical theory and include blade compressibility, stall, reverse flow, large inflow ratios, etc.

The information presented herein is suitable for extensive digital and analog computer studies as well as for rapid manual computations such as required for preliminary design applications.

FOREWORD

This handbook was prepared by the Dynasciences Corporation, Blue Bell, Pennsylvania, for the Eustis Directorate, U. S. Army Air Mobility Research and Development Laboratory, Fort Eustis, Virginia, under Contract DAAJ02-69-C-0023, Task 1F162204A14233, during the period from April 1969 through June 1970.

The work contained in this report incorporates recently available compound helicopter performance and stability information and represents a modification and extension of the U. S. Army Stability and Control Handbook for Helicopters published as USAAVLABS Technical Report 67-63 in August 1967.

The Army technical representatives were Mr. R. P. Smith and Mr. G. W. Fosdick, who were assisted by Mr. W. D. Vann and Major A. Gilewicz. The contributions of the Army personnel to this work are gratefully acknowledged. The following Dynasciences Corporation personnel contributed to this work:

Mr. E. Kisielowski	Director of Aeronautical Research
Mr. E. K. Garay	Sr. Aeronautical Engineer
Miss L. G. Haskins	Jr. Engineer

CONTENTS

Page

Page

Page

Page

LIST OF ILLUSTRATIONS

Figure		Page
10	Calculated Characteristics of a Rotor With 0° Twist for $\mu = 0.3$ and $M_T = 0.7$ . . .	5.2-27
11	Calculated Characteristics of a Rotor With 0° Twist for $\mu = 0.3$ and $M_T = 0.9$ . . .	5.2-29
12	Calculated Characteristics of a Rotor With -4° Twist for $\mu = 0.3$ and $M_T = 0.8$ . . .	5.2-31
13	Calculated Characteristics of a Rotor With -8° Twist for $\mu = 0.3$ and $M_T = 0.8$ . . .	5.2-33
Section 5.3		
1	Geometric Characteristics of Four Single-Rotor Helicopter Fuselage Models. (Reference 1)	5.3-3
2	Geometric Characteristics of Two Full-Scale Single-Rotor Helicopter Fuselages. (Reference 1)	5.3-6
3	Drag Coefficients for Several Single-Rotor Helicopter Fuselages for $\beta_S = 0$	5.3-8
4	Lift Coefficients for Several Single-Rotor Helicopter Fuselages Versus Fuselage Angle of Attack for $\beta_S = 0$	5.3-10
5	Side Force Coefficient for Several Single-Rotor Helicopter Fuselages Versus Fuselage Angle of Attack for $\beta_S = 0$ . . .	5.3-11
6	Side Force Coefficient Versus Sideslip Angle, β_S, for Constant Values of α_{FUS} - Model A . .	5.3-12
7	Side Force Coefficient Versus Sideslip Angle, β_S, for Constant Values of α_{FUS} - Model B . .	5.3-13

Figure		Page

LIST OF TABLES

LIST OF SYMBOLS

A, a_m	constants as defined in the text
AR	aspect ratio
$A_{X_{FUS}}$	fuselage frontal area, ft^2
$A_{Y_{FUS}}$	fuselage side area, ft^2
$A_{Z_{FUS}}$	fuselage planform area, ft^2
A_1	lateral cyclic tilt of the control axis relative to the shaft, positive to the right, rad
a	rotor blade lift curve slope, or lift curve slope of an aerodynamic aurface
a_{mn}	element of a determinant, m^{th} row and n^{th} column
a_0	blade coning angle, rad; also airfoil section lift curve slope,/rad
a_1	longitudinal flapping angle, positive when flapping up at front, rad
B, b_m	constants as defined in the text
B_T	tip loss factor (0.97)
B_1	longitudinal cyclic tilt of control axis relative to shaft, positive when forward, rad
b	number of blades; also span of aerodynamic surface, ft
b_1	lateral flapping angle, positive when flapping down to the right, rad
C	constant as defined in the text
C_D	drag coefficient of an aerodynamic surface
C_D'	drag coefficient of a rotor = D/T.F.
$C_{D_{FUS}}$	fuselage drag coefficient $= D_{FUS}/\frac{1}{2}\rho V_0^2 A_{X_{FUS}}$
C_{D_0}	profile drag coefficient of an aerodynamic surface

ΔC_{d_f}	increment in airfoil section drag coefficient with deflected flap
C_f	turbulent flat plate skin-friction coefficient
C.G.	aircraft C.G. position
C_H	rotor H-force coefficient $= H/T.F.$
C_L	lift coefficient of an aerodynamic surface $= L/\frac{1}{2}\rho V_0^2 S$
C_L'	lift coefficient of a rotor $= L/T.F.$
C_l	two-dimensional airfoil section lift coefficient
$C_{L_{FUS}}$	fuselage lift coefficient $= L_{FUS}/\frac{1}{2}\rho V_0^2 A_{Z_{FUS}}$
$C_{\mathcal{L}_{FUS}}$	fuselage rolling moment coefficient $= \mathcal{L}_{FUS}/\frac{1}{2}\rho V_0^2 A_{X_{FUS}} \ell_{FUS}$
$C_{M_{FUS}}$	fuselage pitching moment coefficients $= M_{FUS}/\frac{1}{2}\rho V_0^2 A_{X_{FUS}} \ell_{FUS}$
$C_{N_{FUS}}$	fuselage yawing moment coefficient $= N_{FUS}/\frac{1}{2}\rho V_0^2 A_{X_{FUS}} \ell_{FUS}$
C_P	propeller power coefficient $= 2\pi C_Q$
C_Q	rotor torque coefficient $= Q/(T.F.)R$
C_S	propeller side-force coefficient $= S/\rho n^2 D^4$
C_T	propeller thrust coefficient $= T/\rho n^2 D^4$
C_Y'	rotor side force coefficient $= Y/T.F.$
$C_{Y_{FUS}}$	fuselage side force coefficient $= Y_{FUS}/\frac{1}{2}\rho V_0^2 A_{Y_{FUS}}$
c	blade chord, or airfoil section chord, ft
$\bar{c}$	mean aerodynamic chord of lifting surface, ft
c_f	flap or control chord measured parallel to plane of symmetry

c_{ROOT} — chord of a lifting surface at the root, ft

c_{TIP} — chord of a lifting surface at the tip, ft

D — aerodynamic drag force of an aircraft component, positive in the direction of wind, lb

D_j — diameter of jet exit nozzle, ft

D_n, d_n — constants as defined in the text

d — fuselage diameter, ft; also distance of the vortex sheet median plane below the wing trailing edge measured normal to the direction of airflow, ft.

E, e_n — constants as defined in the text

e — blade hinge offset, ft; also span efficiency factor $1.1(a/A\!\!\!R)/[R(a/A\!\!\!R)+(1-R)\pi]$

e_v — virtual blade hinge offset, ft

F, f_n — constants as defined in the text

$\vec{F}$ — force vector $= X\vec{i} + Y\vec{j} + Z\vec{k}$, lb

$F(\Lambda)$ — stability characteristic equation

$f_n(\Lambda)$ — operator function for aircraft response

G_n, g_n — constants as defined in the text

g — acceleration due to gravity, ft/sec^2

H — rotor H-force, component of the resultant rotor force perpendicular to the control axis, lb

H_n, h_n — constants as defined in the text

h, h_1 — vertical tail heights as defined in the text

I — rotor moment of inertia about axis of rotation, slug-ft^2

I_b — blade moment of inertia about flapping hinge, slug-ft^2

I_{XX} — aircraft moment of inertia about the body X-axis, slug-ft^2

I_{YY}	aircraft moment of inertia about the body Y-axis, slug-ft^2
I_{ZZ}	aircraft moment of inertia about the body Z-axis, slug-ft^2
I_{XY}, I_{YZ}, I_{XZ}	aircraft products of inertia pertaining to body X, Y, Z system of axis, slug-ft^2
i	geometric incidence of an aircraft component relative to the body X-axis, rad
i, j, k	unit vectors along body X, Y, and Z axis respectively
i_n	constants as defined in the text
J	advance ratio of a propeller $= \pi V_0/(\Omega R)_p$
$J_1, J_2, \ldots$	pilot authority ratios pertaining to stability augmentation system
K_b	factor used in estimating the lift effectiveness of flaps and control surfaces at subsonic speeds
K_n, k_n	constants as defined in the text
$K_{FR}, K_{FFUS}, \ldots$	downwash interference factors pertaining to various aerodynamic components as defined by the subscripts
K_V	fuselage download factor
K'	flap span factor
k	aerodynamic surface roughness height, in.
L	aerodynamic lift force of an aircraft component, perpendicular to local wind vector, lb; also airfoil thickness location parameter
$\mathcal{L}$	rolling moment of an aircraft component, positive down to the right, ft-lb
$\mathcal{L}_W, \mathcal{L}_\phi, \ldots$	rolling moment total derivatives
$\vec{\ell}$	position vector of an aircraft component, relative to aircraft C. C. position, ft
ℓ_x	longitudinal moment arm, positive when the point of application of the force vector is forward from the C. G. position, ft

ℓ_Y lateral moment arm, positive when the point of application of the force vector is to the right from the C. G. position, ft

ℓ_Z normal (vertical) moment arm, positive when the point of application of the force vector is below C. G. position, ft

M pitching moment of an aircraft component, positive nose-up, ft-lb; also Mach number

$\vec{M}$ moment vector $= \mathcal{L}\vec{i} + M\vec{j} + N\vec{k}$, ft-lb

$M_u, M_\theta, \ldots$ pitching moment total derivatives

M_S first moment of blade mass about the flapping hinge, slug-ft

M_T Mach number of advancing blade tip

N yawing moment of an aircraft component, positive to the right, ft-lb

N_P normal force of auxiliary propulsion unit, positive up, lb

$N_v, N_\psi, \ldots$ yawing moment total stability derivatives

n number of propellers

P period of oscillation, sec

p angular rolling velocity ($\dot{\phi}$), positive down to the right, rad/sec

Q rotor/propeller torque, ft-lb

q angular pitching velocity ($\dot{\theta}$), positive nose-up, rad/sec

q_o dynamic pressure $= \frac{1}{2}\rho V_o^2$, lb/ft^2

R rotor radius, ft; also leading-edge suction parameter, ratio of actual to maximum theoretical value of the lifting surface leading-edge suction

R^* Routh discriminant

R_ℓ Reynolds number based on length, ℓ

r	angular yawing velocity ($\dot{\psi}$), positive nose to the right, rad/sec; also leading-edge radius of aerodynamic surface; also radial distance corrected for jet deflection due to slipstream from the jet axis to the elevator hinge line
r_1	radial distance from jet thrust axis to the elevator hinge line
S	area of an aerodynamic surface, ft^2; also propeller side force
S^*	constant as defined in the text
s	semi span of wing, $b_W/2$
T	rotor/propeller thrust, force acting along the shaft or control axis, lb
T.F.	thrust factor = $\rho\pi R^2(\Omega R)^2$, lb
$T_{1/2}$	time required for a disturbance to damp to one-half of its initial amplitude
T_2	time required for a disturbance to double its initial amplitude
t	time, sec; also airfoil thickness, ft
u	longitudinal velocity component, along body X-axis, $=u_0+\bar{u}$ positive forward, ft/sec
$\vec{V}$	instantaneous velocity vector $= u\vec{i}+v\vec{j}+w\vec{k}$, ft/sec
V_0	steady state, or trim value of the resultant velocity vector $=\sqrt{u_0+v_0+w_0}$, ft/sec
V_S	velocity of sound in standard atmospheric condition, ft/sec
v	lateral velocity component along body Y-axis $=v_0+\bar{v}$, positive to the right, ft/sec
v_i	rotor induced velocity, ft/sec
W	aircraft gross weight, lb
w	normal velocity component along body Z-axis, $=w_0+\bar{w}$, positive down, ft/sec

X	longitudinal force along body X-axis, positive forward, lb
$X_u, X_\theta, \ldots$	total stability derivatives of the longitudinal X-force
x	distance, parallel to the direction of airflow, between the wing quarter chord point at the root and the horizontal tail quarter chord point
x_j	axial distance upstream from a jet exit nozzle at which a jet, in accordance with the law of jet spreading that holds at large distances from the exit, would have zero cross section
x_t	is the chordwise position of maximum thickness
x_1	the axial distance along the jet thrust axis from the theoretical origin of the jet (x_j) to a perpendicular to the elevator hinge line
Y	lateral force along the body Y-axis, positive to the right, lb
$Y_v, Y_\phi, \ldots$	total stability derivatives of the lateral Y-force
y	aerodynamic control span ordinate from plane of symmetry, ft
Z	normal force along the body Z-axis, positive down, lb
$Z_u, Z_\theta, \ldots$	total stability derivatives of the normal Z-force
A	amplitude of an oscillation
α	remote wind angle of attack relative to body X-axis, $\tan^{-1}(w/u)$ positive nose-up, rad
α_c	rotor angle of attack; angle between axis of no feathering and a plane perpendicular to flight path, positive when axis is inclined rearward, rad
β	blade flapping angle $= a_0 - a_1 \cos\Psi - b_1 \sin\Psi$, rad; also Prandtl-Glauert compressibility correction factor $\sqrt{1-M^2}$

β_s	aircraft sideslip angle $= \tan^{-1}(v/u)$, positive when wind vector is to the right of body X-axis, rad
Γ	rotor dihedral angle $= i_F - i_R$, rad
γ	Lock inertia number $= \rho acR^4/I_b$
γ_c	aircraft climb angle, rad
Δ	discriminant, increment, or perturbation from trim
δ_a	aileron deflection angle, right aileron up is positive, rad
δ_e	elevator deflection angle, positive down, rad
δ_r	rudder deflection angle, trailing edge left is positive, rad
$\delta_0, \delta_1, \delta_2$	blade drag constants defining drag polar
ϵ	downwash interference angle, rad
ζ, η	constants as defined in the text
η	dimensionless distance from plane of symmetry to edge of flap or control surface, $y/(b/2)$
Θ	blade collective pitch $= J\theta_C + \theta_S$, rad
θ	pitch attitude, positive nose-up, rad
θ_C	blade collective pitch due to pilot control input, rad
θ_S	blade collective pitch due to stability augmentation system input, rad
$\theta_{.75}$	blade section pitch angle at 0.75 rotor radius, rad
θ_0	collective pitch at blade root, rad
θ_1	blade twist angle per unit spanwise distance, rad
K_n	constants for solidity correction of local stability derivatives

κ	ratio of actual to theoretical two-dimensional lift curve slope, $a_0/2\pi$
Λ	operator = d( )/dt ; also aerodynamic surface sweepback angle, positive rearward, deg
λ	rotor inflow ratio = $(V_0 \sin \alpha_c - v_i)/\Omega R$, also lifting surface taper ratio c_{TIP}/c_{ROOT}
μ	rotor tip speed ratio = $V_0 \cos \alpha_c/\Omega R$
ν	constant as defined in the text
Π_n	constants as defined in the text
π	constant = 3.14
ρ	air density, slug/ft^3
Σ	summation
σ	rotor solidity = $bc/\pi R$
ς	constant as defined in the text
τ	time constant; also airfoil section trailing-edge angle, deg
Υ	taper ratio correction factor
Φ	phase angle, rad
ϕ	aircraft roll attitude, positive to the right, rad
X	rotor wake angle = $a_1 + \tan^{-1}(-\mu/\lambda)$, rad
χ	generalized body space angle, rad
$\vec{X}$	vectorial, angular displacement relative to body X, Y, Z axes = $\phi\vec{i} + \theta\vec{j} + \psi\vec{k}$, rad
Ψ	blade azimuth position, rad
ψ	aircraft yaw attitude, positive nose to the right, rad
Ω	rotor rotational speed, rad/sec
$\bar{\Omega}$	nondimensional rotor frequency parameter, ω_1/Ω

ω_1	first natural flapping frequency of rotor, rad/sec
$\vec{\omega}$	instantaneous angular velocity vector $= p\vec{i} + q\vec{j} + r\vec{k}$, rad/sec
$\perp$	perpendicular to

SUBSCRIPTS

A	aerodynamic
C	control
CUT	pertaining to Reynolds number cutoff limit
exp	exposed planform area of an aerodynamic surface
F	pertaining to front rotor
FR,FFUS	effects of front rotor on rear rotor, front rotor on fuselage, etc
f	flap
G	pertaining to gravity
HUB	pertaining to rotor hub
I	pertaining to inertia
i	an integer 1, 2, 3 ..., or i^{th} aircraft component; also pertaining to inboard edge of aerodynamic control surface
j	pertaining to jet exit nozzle or orifice
L	pertaining to lift
LER	pertaining to leading-edge radius of a lifting surface
L.S.	pertaining to lifting surface
$\mathcal{L}$	pertaining to rolling moment
M	pertaining to pitching moment
m,n	integers as defined in the text
N	pertaining to yawing moment

O	pertaining to initial condition or steady state; also to outboard edge of aerodynamic control surface
P	propeller or auxiliary propulsive device
R	rear rotor; also right
S	stability augmentation system
T	horizontal tailplane
TOT	total
TR	tail rotor
VT	vertical tailplane
W	wing
wet	pertaining to total wetted area of aerodynamic surface
X	longitudinal direction
Y	lateral direction
Z	normal (vertical) direction

Dots denote time rate of change of variables

Bars denote perturbation values

SECTION I. INTRODUCTION

In recent years a considerable portion of the U. S. Army research activity in the rotary-wing field has been directed toward improving the high-speed performance of the helicopter. The design approach which emerged for alleviating the high-speed rotor blade stall and compressibility problems has been to unload the rotor by adding wings to generate lift and auxiliary thrust devices for additional propulsion. Since the means for producing lift and propulsive thrust on the helicopter have now been compounded, this configuration is commonly referred to as a compound helicopter. The compound helicopter is flown as a conventional helicopter in the low-speed range. However, as forward speed is increased, the lift requirement of the rotor is reduced as the load is transferred more to the wing, and also the forward propulsion requirement is shifted more from the rotor to the auxiliary propulsion system. Rotor stall problems are thus alleviated by the unloading of the rotor, and since the rotor can now be slowed down, the compressibility problems are avoided.

Although the performance objectives of many of the compound helicopters now flying were attained, many new stability and control problems appeared that still require extensive investigation in order to achieve satisfactory flying qualities. Some of the problems arose because the level of control moment available from the unloaded rotor was reduced, while the increased inertia and air load damping of the wings increased the control moment requirements. A solution to this problem was found by integrating conventional aircraft control surfaces into the control system to augment the control available from the rotor at high speeds. However, many other stability and control problems associated with compound helicopters are still being investigated and have yet to be resolved.

One of the most important considerations in the design of a compound helicopter is to provide the aircraft with adequate dynamic stability and control characteristics consistent with its performance and mission requirements. Therefore, stability and control analyses have become an important part of the preliminary design of compound helicopters.

The prime objective of this program is to summarize the existing state of the art of compound helicopter dynamic stability and control and to provide, under one volume, systematic engineering methods for predicting the dynamic stability and control characteristics of generalized compound helicopter configurations.

The stability methods, procedures, and data contained herein represent a revision and expansion of the work performed under USAAVLABS Contract DA44-177-AMC-197(T), and published as USAAVLABS Technical Report 67-63, August 1967.

The present handbook incorporates recently published rotor performance data and stability charts covering the forward speed range from hovering to advance ratio of $\mu = 1.0$. The stability data for advance ratios to $\mu \leq 0.3$ was derived from classical rotor theory, whereas the data from $\mu = 0.3$ to $\mu = 1.0$ include the effects of rotor blade compressibility, reverse flow, and blade stall. The stability methods presented herein apply to fully articulated, teetering, and hingeless configurations and are suitable for preliminary design purposes as well as for extensive digital and analog computer studies.

The compound helicopter equations of motion presented in this handbook are derived without resorting to simplifying small angle assumptions or any decoupling of the longitudinal from the lateral-directional degrees of freedom. They include six degrees of freedom of aircraft motion, and three degrees of freedom of stability augmentation system. The analyses apply to absolutely arbitrary (non-zero) aircraft attitudes and angular rates and as such they can be used for maneuvering flight conditions as well as for steady level flight. Although this handbook deals specifically with single rotor compound helicopters, provisions are made for analyses of tandem rotors or any other types of compound helicopter configurations.

The analytical methods presented herein have been verified against the recently available flight test data of typical compound helicopters. Good correlations thus obtained indicate that the analytical stability methods presented in this handbook are well within the required degree of accuracy, and as such they can be confidently used for predicting the dynamic stability and control characteristics of generalized compound helicopter configurations.

Comments concerning this work are invited and should be directed to the Eustis Directorate, U. S. Army Air Mobility Research and Development Laboratory, Fort Eustis, Virginia 23604.

SECTION 2. GUIDE TO THE HANDBOOK

The main objective of this handbook is to provide, under one cover, a comprehensive summary of analytical methods for predicting stability and control characteristics of generalized compound helicopter configurations.

The handbook is organized in such a way that it is self-sufficient. For a given flight condition and configuration, the complete set of stability derivatives can be calculated and the required compound helicopter stability and response characteristics can be determined. The use of reliable test data, especially for the fuselage characteristics, is strongly recommended.

The various sections of the handbook have been numbered with a decimal system which provides maximum flexibility for revising, deleting, or supplementing any of the material, with a minimum disturbance to the remainder of the volume. The following pattern was developed for the numbering system:

Section:	An orderly numbering system is used, with numbers having not more than two parts separated by a decimal point, e.g., 3.2 or 10.1.
Subsection:	Subsections have numbers with more than two parts, e.g., 3.1.2 or 10.2.1.
Page:	The page number consists of the section number followed by a dash. Example: Page 3.1-20.
Figures:	Figure numbers follow a numerical sequence starting from 1 for each section.
Tables:	Table numbers follow a numerical sequence starting from I for each section.
Equations:	Equation numbers (where required) follow a numerical sequence starting from 1 for each section.
References:	References are located at the end of each section. References are numbered in sequence starting from 1.

The overall organization of the handbook proceeds in a computational sequence from the general to the particular. Hence, the equations of motion are presented before the total derivatives, which in turn precede the local and isolated derivatives.

For digital computer work, the general equations of motion, Section 4, can be used directly. For analog computer work or hand calculations, the stability characteristics of a helicopter are obtained by proceeding as follows:

Determine trim conditions	Section 5
Determine the isolated derivatives	Section 7.5
Correct the isolated derivatives for rotor solidity	Section 7.4
Determine local derivatives	Section 7.3
Determine total derivatives	Section 7.1
Determine characteristic equation	Section 8.1
Determine roots of the characteristic equation	Section 8.5
Determine control derivatives	Section 7.2
Determine response to control input	Section 10

The effects of variations of the main design parameters on the dynamic stability and control characteristics of compound helicopters can be used directly for preliminary design applications.

SECTION 3. DEFINITIONS

3.1 DEFINITION OF AXIS SYSTEM

Sketch 1 below shows a right-angled coordinate axis system commonly used in stability work.

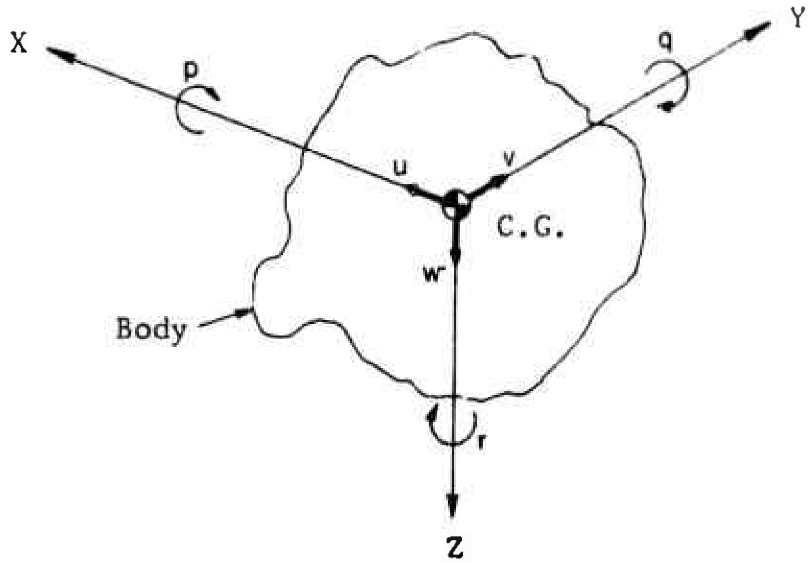

Sketch 1. Definition of Axis System.

In analyzing aircraft stability, a variety of reference axes can be used. Descriptions of various axes systems are presented in References 1 and 2.

In general, the choice of the appropriate reference axis depends on the nature of the stability problem and the aircraft configuration to be analyzed.

The most common systems of reference axes presently in use are:

(a) Gravity Axes
(b) Stability Axes
(c) Wind Axes
(d) Body Axes

The following subsections contain brief descriptions of these axes systems.

3.1.1 Gravity Axes

Gravity axes refer to a right-handed system of Cartesian coordinates with the origin either fixed at a point on the surface of the earth or fixed at the aircraft mass center (moving with the aircraft).

In each case, the Z-axis is pointing to the center of the earth (positive downward), the X-axis is directed along the horizon (positive forward), and the Y-axis is oriented to form a right-handed orthogonal axes system (positive towards right).

The gravity or earth fixed axes are primarily useful as a reference system for the gravity vector, aircraft altitude, horizontal distance, and orientation. The use of these axes introduces certain simplifications in the stability analyses, in that the linear velocity components (u, v. w) along X, Y, Z axes are independent of aircraft rotation about the C.G. and are only functions of aircraft translation and the climb angle (γ_c). It follows that in the derivation of the equations of motion, the aerodynamic force contribution is accounted for through the sine or cosine of climb angle (γ_c). Further simplifications occur for level flight ($\gamma_c = 0$). However, the use of gravity axes introduces rather cumbersome corrections to aircraft inertia terms and products of inertia in accounting for aircraft rotation.

3.1.2 Stability Axes

The stability axes represent a right-handed system of Cartesian coordinates, with the origin located at the aircraft C.G. and with the axes chosen so that the positive X-axis points in the direction of motion of the airplane (into the relative wind) in a reference condition of steady trimmed flight. The Z-axis is perpendicular to the relative wind in the reference condition and is positive downward; the Y-axis is oriented to form a right-handed orthogonal axis system (positive to the right). The stability axes remain fixed to the aircraft during the transient conditions or perturbed motion.

The use of stability axes eliminates the terms w_0 and v_0 which are zero in steady symmetric flight and thus introduces substantial simplifications into the aerodynamic terms. In addition, the use of stability axes enables the aerodynamic forces and moments at the trimmed condition to the estimated directly from wind-tunnel results which are automatically resolved parallel and perpendicular to the wind when using a tunnel-fixed balance.

In this system, the only linear velocity component that remains is u, which is independent of aircraft rotation (as in the case of gravity axes) and represents perturbation of the forward velocity vector. However, the moment and product of inertia terms will generally vary for each initial flight condition since the axes will be differently oriented in the aircraft for each trim condition. In general, these terms are assumed to be constant in the equations of motion. This limits the use of the stability axes system to small disturbance motions.

3.1.3 Wind Axes

The wind axis system is a right-handed, orthogonal system of axes, with the origin located at the aircraft C.G. and with the axes chosen so that the positive X-axis always points into the relative wind. The Z-axis is perpendicular to the relative wind and is positive downward, and the Y-axis is oriented to form a right-handed orthogonal axis system (positive to the right).

The wind axes are primarily useful as a reference system for wind-tunnel measurements taken with a tunnel-fixed balance. In flight where the aircraft moves about the wind axes, the moments of inertia and products of inertia are constantly varying. Thus the wind axis system can only be used to analyze aircraft motions when the changes in moments of inertia and products of inertia can be assumed to be negligible.

3.1.4 Body Axes

The body axis system refers to a right-handed, orthogonal system of axes fixed at aircraft C.G., rotating and translating with the aircraft. The X-axis is aligned along a reference line (datum line) fixed to the vehicle (positive pointing forward). The Z-axis is perpendicular to X-axis, positive toward the bottom of the vehicle. The Y-axis is mutually perpendicular to X and Z, positive when pointing to the right.

The use of the axes fixed to the vehicle insures that the inertia terms in the equations of motion are constant (independent of flight conditions); furthermore, by coinciding one of the body axes with a principal axis of inertia, certain products of inertia terms can be eliminated. In this axis system, the aerodynamic forces and moments depend on relative velocity orientation with respect to the body as defined by the angles α and β_s .

Body axes are particularly useful in the study of aircraft dynamics, since velocities and accelerations with respect to these axes are the same as those that would be experienced by a pilot or would be measured by the instruments mounted in the aircraft.

3.1.5 Choice of Axes

Since it is more convenient to express the aerodynamic and gravitational forces and moments with respect to body axes than to express inertia forces and moments with respect to wind stability or gravity axes, a body axis coordinate system has been selected for the work in this handbook.

For this axis system, the following definitions are made:

(a) Linear Velocities

$$\vec{V} = u\vec{i} + v\vec{j} + w\vec{k}$$

In the above definition, the velocity components u, v, and w consist of the sum of initial (trim) values u , v , and w and of their perturbation values, respectively.

(b) Angular Displacements

$$\vec{\chi} = \phi\vec{i} + \theta\vec{j} + \psi\vec{k}$$

(c) Angular Velocities About C.G.

$$\vec{\omega} = p\vec{i} + q\vec{j} + r\vec{k}$$

(d) Forces

$$\vec{F} = X\vec{i} + Y\vec{j} + Z\vec{k}$$

(e) Moments

$$\vec{M} = \mathcal{L}\vec{i} + M\vec{j} + N\vec{k}$$

(f) Moment Arms

$$\vec{\ell} = \ell_x \vec{i} + \ell_y \vec{j} + \ell_z \vec{k}$$

LITERATURE CITED

1. Thelander, J. A., AIRCRAFT MOTION ANALYSIS, Technical Documentary Report FDL-TDR-64-70, Air Force Flight Dynamics Laboratory, Air Force Systems Command, Wright-Patterson Air Force Base, Ohio, March 1965.

2. DYNAMICS OF THE AIRFRAME, Bu Aer Report AE-61-4 II, Bureau of Aeronautics, Navy Department (presently Bureau of Naval Weapons, Naval Air Systems Command Headquarters), Washington, D. C., September 1952.

3.2 STABILITY VARIABLES

3.2.1 Independent Variables

Following are the selected independent stability variables:

(a) Linear Velocity Components (ft/sec) u, v and w - defined in Subsection 3.1.4(a)

(b) The Angular Displacements (radians) ϕ , θ, and ψ - defined in Subsection 3.1.4(b)

3.2.2 Dependent Variables

(a) **Free-Stream Angle of Attack (radians)**

$$\alpha = \tan^{-1}\left(\frac{w}{u}\right)$$

The perturbation angle of attack is given by:

$$\bar{\alpha} \simeq \frac{\bar{w}}{u_0}$$

(b) Sideslip Angle (radians)

$$\beta_s = \tan^{-1}\left(\frac{v}{u}\right)$$

The perturbation sideslip angle is given by:

$$\bar{\beta}_s \simeq \frac{\bar{v}}{u_0}$$

(c) Interference Angles (radians)

Changes of local velocity due to aerodynamic interactions are accounted for by the interference angles

$\epsilon_F, \epsilon_R, \epsilon_{FUS}, \epsilon_W, \epsilon_T, \epsilon_{TR}, \epsilon_{VT}$ etc.

3.3 ILLUSTRATION OF PARAMETERS AND SIGN CONVENTION

A typical single-rotor compound helicopter configuration, along with the definition of the parameters and sign conventions used herein, is presented in Figure 1.

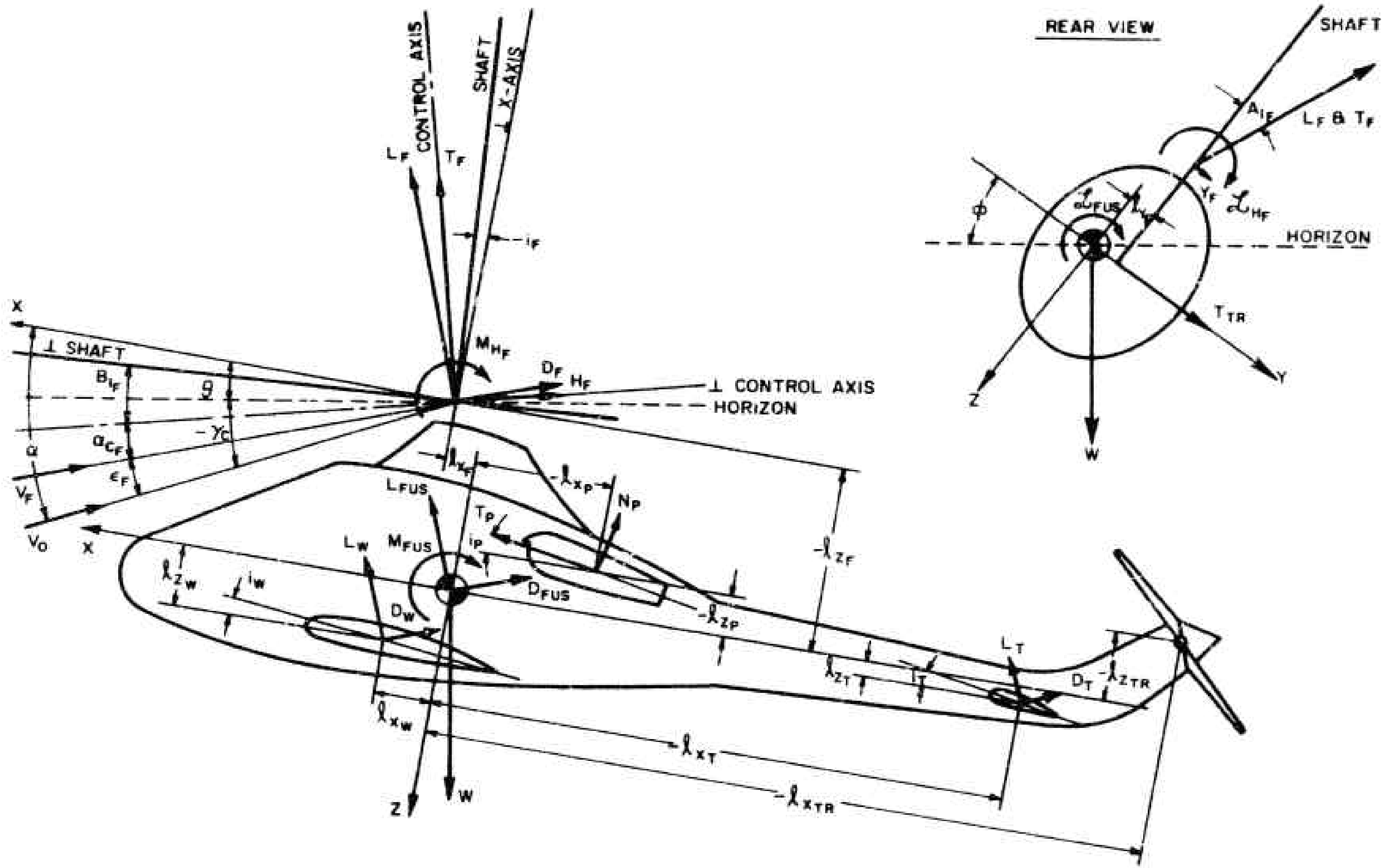

Figure 1. Definition of Parameters and Sign Convention for a Single-Rotor Compound Helicopter.

SECTION 4. EQUATIONS OF MOTION

The generalized equations presented herein pertain to 6 degrees of freedom of coupled longitudinal and lateral aircraft motions about the body system of axes described in Subsection 3.1.4. A detailed derivation of the equations of motion is presented in Reference 1.

The analysis is performed for a generalized aircraft configuration, which may consist of the following components:

(a) Single Rotor
(b) Two rotors in tandem rotor configuration
(c) Fuselage
(d) Horizontal tailplane
(e) Vertical tail
(f) Tail rotor
(g) Propellers or jet engines
(h) Wings
(i) Various stabilization devices

The equations of motion presented in this section can be adapted to various types of compound helicopters, single rotor helicopters, and tandem rotor helicopters by selecting those aerodynamic and design components which pertain to the helicopter under consideration and by eliminating the components which do not apply. To insure the generality of the equations, all products of inertia are retained.

From the theoretical derivations presented in Reference 1, the equations of motion for a generalized aircraft configuration are:

(a) The X-Force Equation

$$X=(X)_F+(X)_R+(X)_{FUS}+(X)_W+(X)_T+(X)_{VT}+(X)_{TR}+\sum_{i=1}^{n}(X)_{P_i}+W\sin\phi\sin\psi$$

$$-W\cos\phi\sin\theta\cos\psi-\frac{W}{g}(\dot{u}+qw-rv)=0$$

where

$$(X)_F=\left[(L_F\cos A_{I_F}-Y_F\sin A_{I_F})\sin(\alpha-\epsilon_F)-D_F\cos(\alpha-\epsilon_F)\right]\cos\beta_S$$

$$-(L_F\sin A_{I_F}+Y_F\cos A_{I_F})\sin\beta_S$$

$$(X)_R=\left[(L_R\cos A_{I_R}+Y_R\sin A_{I_R})\sin(\alpha-\epsilon_R)-D_R\cos(\alpha-\epsilon_R)\right]\cos\beta_S$$

$$-(L_R\sin A_{I_R}-Y_R\cos A_{I_R})\sin\beta_S$$

$$(X)_{FUS}=\left[L_{FUS}\sin(\alpha-\epsilon_{FUS})-D_{FUS}\cos(\alpha-\epsilon_{FUS})\right]\cos\beta_S-Y_{FUS}\sin\beta_S$$

$$(X)_W=\left[L_W\sin(\alpha-\epsilon_W)-D_W\cos(\alpha-\epsilon_W)\right]\cos\beta_S$$

$$(X)_T=\left[L_T\sin(\alpha-\epsilon_T)-D_T\cos(\alpha-\epsilon_T)\right]\cos\beta_S$$

$$(X)_{VT}=-D_{VT}\cos(\alpha-\epsilon_{VT})\cos\beta_S+L_{VT}\sin\beta_S$$

$$(X)_{TR}=\left[Y_{TR}\sin(\alpha-\epsilon_{TR})-D_{TR}\cos(\alpha-\epsilon_{TR})\right]\cos\beta_S-T_{TR}\sin\beta_S$$

$$(X)_{P_i}=T_{P_i}\cos i_{P_i}-N_{P_i}\sin i_{P_i}$$

(b) The Y-Force Equation

$$Y = (Y)_F + (Y)_R + (Y)_{FUS} + (Y)_W + (Y)_T + (Y)_{VT} + (Y)_{TR} + \sum_{i=1}^{n} (Y)_{P_i} + W \sin\phi \cos\psi$$

$$+ W \cos\phi \sin\theta \sin\psi - \frac{W}{g}(\dot{v} + ru - pw) = 0$$

where

$$(Y)_F = \left[(L_F \cos A_{I_F} - Y_F \sin A_{I_F}) \sin(\alpha - \epsilon_F) - D_F \cos(\alpha - \epsilon_F)\right] \sin\beta_S$$

$$+ (L_F \sin A_{I_F} + Y_F \cos A_{I_F}) \cos\beta_S$$

$$(Y)_R = \left[(L_R \cos A_{I_R} + Y_R \sin A_{I_R}) \sin(\alpha - \epsilon_R) - D_R \cos(\alpha - \epsilon_R)\right] \sin\beta_S$$

$$+ (L_R \sin A_{I_R} - Y_R \cos A_{I_R}) \cos\beta_S$$

$$(Y)_{FUS} = \left[L_{FUS} \sin(\alpha - \epsilon_{FUS}) - D_{FUS} \cos(\alpha - \epsilon_{FUS})\right] \sin\beta_S + Y_{FUS} \cos\beta_S$$

$$(Y)_W = \left[L_W \sin(\alpha - \epsilon_W) - D_W \cos(\alpha - \epsilon_W)\right] \sin\beta_S$$

$$(Y)_T = \left[L_T \sin(\alpha - \epsilon_T) - D_T \cos(\alpha - \epsilon_T)\right] \sin\beta_S$$

$$(Y)_{VT} = -D_{VT} \cos(\alpha - \epsilon_{VT}) \sin\beta_S - L_{VT} \cos\beta_S$$

$$(Y)_{TR} = \left[Y_{TR} \sin(\alpha - \epsilon_{TR}) - D_{TR} \cos(\alpha - \epsilon_{TR})\right] \sin\beta_S + T_{TR} \cos\beta_S$$

$$(Y)_{P_i} = Y_{P_i}$$

(c) The Z-Force Equation

$$Z = (Z)_F + (Z)_R + (Z)_{FUS} + (Z)_W + (Z)_T + (Z)_{VT} + (Z)_{TR} + \sum_{i=1}^{n} (Z)_{P_i} + W \cos\phi \cos\theta$$

$$- \frac{W}{g} (\dot{w} + pv - qu) = 0$$

where

$$(Z)_F = -\left[D_F \sin(\alpha - \epsilon_F) + (L_F \cos A_{1_F} - Y_F \sin A_{1_F}) \cos(\alpha - \epsilon_F)\right]$$

$$(Z)_R = -\left[D_R \sin(\alpha - \epsilon_R) + (L_R \cos A_{1_R} + Y_R \sin A_{1_R}) \cos(\alpha - \epsilon_R)\right]$$

$$(Z)_{FUS} = -\left[D_{FUS} \sin(\alpha - \epsilon_{FUS}) + L_{FUS} \cos(\alpha - \epsilon_{FUS})\right]$$

$$(Z)_W = -\left[D_W \sin(\alpha - \epsilon_W) + L_W \cos(\alpha - \epsilon_W)\right]$$

$$(Z)_T = -\left[D_T \sin(\alpha - \epsilon_T) + L_T \cos(\alpha - \epsilon_T)\right]$$

$$(Z)_{VT} = -D_{VT} \sin(\alpha - \epsilon_{VT})$$

$$(Z)_{TR} = -\left[D_{TR} \sin(\alpha - \epsilon_{TR}) + Y_{TR} \cos(\alpha - \epsilon_{TR})\right]$$

$$(Z)_{P_i} = -\left[T_{P_i} \sin i_{P_i} + N_{P_i} \cos i_{P_i}\right]$$

(d) The Rolling Moment Equation ($\mathcal{L}$)

$$\mathcal{L} = \sum_{i=1}^{n} (\mathcal{L})_i = \sum_{i=1}^{n} \left[(Z)_i \ell_{Y_i} - (Y)_i \ell_{Z_i} + (\mathcal{L}_0)_i \right] + \mathcal{L}_I$$

$$\mathcal{L} = (Z)_F \ell_{Y_F} - (Y)_F \ell_{Z_F} + (Z)_R \ell_{Y_R} - (Y)_R \ell_{Z_R}$$

$$+ (Z)_W \ell_{Y_W} - (Y)_W \ell_{Z_W} + (Z)_T \ell_{Y_T} - (Y)_T \ell_{Z_T}$$

$$+ (Z)_{VT} \ell_{Y_{VT}} - (Y)_{VT} \ell_{Z_{VT}} + (Z)_{TR} \ell_{Y_{TR}} - (Y)_{TR} \ell_{Z_{TR}}$$

$$+ \sum_{i=1}^{n} \left[(Z)_{P_i} \ell_{Y_{P_i}} - (Y)_{P_i} \ell_{Z_{P_i}} + Q_{P_i} \right] + \mathcal{L}_{FUS} + \mathcal{L}_{HUB_F} - \mathcal{L}_{HUB_R}$$

$$- \dot{p} I_{XX} + I_{XZ} (\dot{r} + pq) + rq (I_{YY} - I_{ZZ}) + I_{XY} (\dot{q} - rp)$$

$$+ I_{YZ} (q^2 - r^2) = 0$$

where i refers to the i^{th} aircraft component and is evaluated by letting i = 1, 2, 3, etc., or the appropriate component designation.

Also sub I refers to inertia terms. Similar notation is used in the pitching and yawing moment equations given below.

(e) The Pitching Moment Equation (M)

$$M = \sum_{i=1}^{n} (M)_i = \sum_{i=1}^{n} \left[(X)_i \ell_{Z_i} - (Z)_i \ell_{X_i} + (M_0)_i \right] + M_I$$

$$M = (X)_F \ell_{Z_F} - (Z)_F \ell_{X_F} + (X)_R \ell_{Z_R} - (Z)_R \ell_{X_R}$$

$$+(X)_W \ell_{Z_W} - (Z)_W \ell_{X_W} + (X)_T \ell_{Z_T} - (Z)_T \ell_{X_T}$$

$$+(X)_{VT} \ell_{Z_{VT}} - (Z)_{VT} \ell_{X_{VT}} + (X)_{TR} \ell_{Z_{TR}} - (Z)_{TR} \ell_{X_{TR}}$$

$$+\sum_{i=1}^{n} \left[(X)_{P_i} \ell_{Z_{P_i}} - (Z)_{P_i} \ell_{X_{P_i}} + M_{P_i} \right] + M_{FUS} + M_{HUB_F} + M_{HUB_R} + Q_{TR}$$

$$-\dot{q} I_{YY} + I_{XZ}(r^2 - p^2) - rp(I_{XX} - I_{ZZ})$$

$$+ I_{XY}(\dot{p} + rq) + I_{YZ}(\dot{r} - pq) = 0$$

(f) <u>The Yawing Moment Equation (N)</u>

$$N = \sum_{i=1}^{n} (N)_i = \sum_{i=1}^{n} \left[(Y)_i \ell_{X_i} - (X)_i \ell_{Y_i} + (N_0)_i \right] + N_I$$

$$N = (Y)_F \ell_{X_F} - (X)_F \ell_{Y_F} + (Y)_R \ell_{X_R} - (X)_R \ell_{Y_R}$$

$$+ (Y)_W \ell_{X_W} - (X)_W \ell_{Y_W} + (Y)_T \ell_{X_T} - (X)_T \ell_{Y_T}$$

$$+ (Y)_{VT} \ell_{X_{VT}} - (X)_{VT} \ell_{Y_{VT}} + (Y)_{TR} \ell_{X_{TR}} - (X)_{TR} \ell_{Y_{TR}}$$

$$+\sum_{i=1}^{n} \left[(Y)_{P_i} \ell_{X_{P_i}} - (X)_{P_i} \ell_{Y_{P_i}} \right] + N_{FUS} + Q_F - Q_R$$

$$-\dot{r} I_{ZZ} + I_{XZ}(\dot{p} - qr) - pq(I_{YY} - I_{XX})$$

$$+ I_{XY}(p^2 - q^2) + I_{YZ}(\dot{q} + pr) = 0$$

LITERATURE CITED

1. Kisielowski, E., Perlmutter, A. A., and Tang, J., STABILITY AND CONTROL HANDBOOK FOR HELICOPTERS, Dynasciences Corporation; USAAVLABS Technical Report 67-63, U. S. Army Aviation Materiel Laboratories, Fort Eustis, Virginia, August 1967, AD 662 259.

SECTION 5. EVALUATION OF TRIM CONDITIONS

The trim, or steady state, equilibrium conditions for a compound helicopter can be obtained by simultaneously solving the equations of motion given in Section 4 with all the acceleration and inertia terms set equal to zero. The procedure used in this section is to obtain the longitudinal trim conditions first, and then use these conditions in the three lateral equations of motion to obtain the complete equilibrium conditions for the aircraft.

In order to evaluate the trim conditions for a generalized compound helicopter configuration, the following design parameters must be determined:

(a) The aircraft gross weight W, lb
(b) The fuselage projected areas; frontal $A_{X_{FUS}}$, side $A_{Y_{FUS}}$, and planform $A_{Z_{FUS}}$, ft^2
(c) The fuselage overall length ℓ_{FUS}, ft
(d) The locations of the rotor hub (or hubs) and tail rotor hub relative to the aircraft C.G. position, ft $\ell_{X_F}, \ell_{Y_F}, \ell_{Z_F}$; $\ell_{X_R}, \ell_{Y_R}, \ell_{Z_R}$; $\ell_{X_{TR}}, \ell_{Y_{TR}}, \ell_{Z_{TR}}$
(e) The rotor radii R_F, R_R, and R_{TR}, ft
(f) The rotor solidities σ_F, σ_R, σ_{TR}
(g) The rotor rotational speeds $(\Omega R)_F$, $(\Omega R)_R$, and $(\Omega R)_{TR}$, rad/sec
(h) The blade Lock inertia numbers γ_F, γ_R, and γ_{TR}.
(i) The blade twists θ_{1_F}, θ_{1_R}, and $\theta_{1_{TR}}$.
(j) The blade mass moments of inertia M_{S_F}, and M_{S_R}, slugs-ft
(k) The flapping hinge offsets e_F and e_R
(l) The number of blades b per rotor
(m) The tip loss factor, $B_T = 0.97$
(n) The geometric, fixed incidences relative to the fuselage of the wing i_W, horizontal tail i_T, vertical tail i_{VT}, auxiliary propulsion thrust vectors i_{P_1}, and the rotor shaft inclinations i_F, i_R, and i_{TR}.
(o) The lift curve slopes of the rotor blades, wing, horizontal tail, vertical tail, etc.
(p) The area of the wing S_W, horizontal tailplane S_T, and vertical tail S_{VT}, ft^2
(q) The moment arms ℓ_X, ℓ_Y, and ℓ_Z of the wing, horizontal tail, vertical tail, etc.
(r) The geometry such as the chord, span, etc., of each conventional aircraft control surface.
(s) The geometry of the auxiliary propulsion unit(s)
(t) The geometry of external appendages such as fuel tanks, cargo pods, etc.
(u) The first natural flapping frequency ω_1, rad/sec, if hingeless elastic rotors are used.

5.1 TRIM CONDITIONS FOR SINGLE ROTOR COMPOUND HELICOPTERS

5.1.1 Hovering

The procedure given below for calculating the rotor trim conditions while hovering uses the expressions for rotor thrust, constant inflow, and coning angle presented in Reference 1. Also, the effect of thrust of the auxiliary propulsion units is included in the computations.

The simplifying assumptions made in Reference 1, such as constant induced velocity, no radial flow, and tip loss factor $B_T = 0.97$ are incorporated in this procedure.

The vertical trim condition for hovering can be calculated as follows:

$$T_F = \frac{K_V W}{1 - \frac{S_{Wexp}}{\pi R_F^2}} - \sum_{i=1}^{n} T_{P_i} \sin(\theta + i_{P_i})$$

where

K_V = fuselage download factor (approximately 1.05)

$$C_{T_F} = \left(\frac{T}{T.F.}\right)_F$$

where

$$(T.F.)_F = \rho \pi \left[R^2 (\Omega R)^2\right]_F$$

$$\lambda_F = -\sqrt{\frac{C_{T_F}}{2}}$$

$$\theta_{.75} = \frac{\left(\frac{2C_T}{a\sigma} - 0.4704\lambda\right)_F}{0.3042}$$

$$a_{0_F} = \left[\frac{\gamma}{2}(0.2213\,\theta_{.75} + 0.3042\lambda)\right]_F$$

5.1.2 Forward Speed

For calculating the forward speed trim conditions for compound helicopters, rotor performance charts are used. Such charts for rotors operating at high forward speeds, corresponding to advance ratios from μ = 0.25 to μ = 1.4, are presented in Reference 2. The charts presented in Reference 2 incorporate the effects of blade stall, compressible flow, and large inflow angles. For extreme operating conditions, the tabulated data in Reference 3 can be used to extend the charts presented in Reference 2. For low forward speeds the performance charts presented in Section 5.2 of this report can be used for speeds corresponding to advance ratios of $\mu \leq 0.2$. These charts were obtained from the results of Reference 4.

The trim procedur for forward flight is performed as follows:

(a) Determine the required design parameters for a single rotor compound helicopter as specified on page 5-1. Include the design parameters for any additional lifting surfaces such as large support pylons for the auxiliary engines and also external appendages such as fuel tanks.

(b) Establish the compound helicopter operating conditions such as V_0, ρ, V_S, $(\Omega R)_F$, $(\Omega R)_{TR}$, $(\Omega R)_P$, T_{P_i}.

Then compute

$$\mu_F = \frac{V_0}{(\Omega R)_F} \qquad \mu_{TR} = \frac{V_0}{(\Omega R)_{TR}}$$

$$(M_T)_F = \frac{V_0 + (\Omega R)_F}{V_S} \qquad (M_T)_{TR} = \frac{V_0 + (\Omega R)_{TR}}{V_S}$$

$$(T.F.)_F = \left[\rho \pi R^2 (\Omega R)^2\right]_F \qquad (T.F.)_{TR} = \left[\rho \pi R^2 (\Omega R)^2\right]_{TR}$$

$$q_0 = \frac{1}{2} \rho V_0^2$$

Also for auxiliary propulsion units using propellers, calculate the advance ratio $J_i = \pi V_0/(\Omega R)$ and propeller activity factor $(A.F.)_i$ as defined in the particular propeller test data to be used.

(c) Choose a fuselage angle of attack α_{FUS} for which the first estimates of trim will be obtained. If no knowledge of the flight conditions is available, the first iteration can be performed at $\alpha_{FUS} = 0^{\circ}$. If some knowledge of the flight conditions is available, use the best estimate of the trimmed fuselage flight attitude that can be obtained in order to reduce the number of iterations required for convergence to trim.

For the selected value of α_{FUS}, obtain fuselage lift and drag coefficients $C_{L_{FUS}}$ and $C_{D_{FUS}}$, then calculate

$$D_{FUS} = C_{D_{FUS}} q_o A_{X_{FUS}} \qquad L_{FUS} = C_{L_{FUS}} q_o A_{Z_{FUS}}$$

Include the effect of all nonlifting surface components or appendages in the above computations.

(d) From Section 5.4, obtain the wing and horizontal tail lift curve slopes, a_W and a_T. Then calculate first approximations of the wing and tail lift and drag forces at the selected value of α_{FUS}, thus:

$$\alpha_W = (\alpha_{FUS} + \epsilon_{FUS}) + (i_W - \epsilon_W) \qquad \alpha_T = (\alpha_{FUS} + \epsilon_{FUS}) + (i_T - \epsilon_T)$$

$$C_{L_W} = a_W(\alpha_W - \alpha_{o_W}) \qquad C_{L_T} = a_T(\alpha_T - \alpha_{o_T})$$

$$C_{D_W} = \left(C_{D_o} + \frac{C_L^2}{\pi AR}\right)_W \qquad C_{D_T} = \left(C_{D_o} + \frac{C_L^2}{\pi AR}\right)_T$$

where the section profile drag coefficients $(C_{D_o})_W$ and $(C_{D_o})_T$ can be estimated from Section 5.4 or assumed as

$$(C_{D_o})_W = (C_{D_o})_T \approx 0.01$$

Compute wing and tail lift and drag forces, thus:

$$L_W = C_{L_W} q_o S_W \qquad L_T = C_{L_T} q_o S_T$$

$D_W = C_{D_W} q_o S_W$ $\qquad$ $D_T = C_{D_T} q_o S_T$

Note that for the first iteration, the interference angles ϵ_{FUS}, ϵ_W, and ϵ_T above are set equal to zero.

(e) Calculate the first approximation for the main rotor lift and drag forces, thus:

$$L_F = W - L_{FUS} - L_W - L_T - \sum_{i=1}^{n} T_{P_i} \sin(i_{P_i} + \alpha)$$

$$D_F = -D_{FUS} - D_W - D_T + \sum_{i=1}^{n} T_{P_i} \cos(i_{P_i} + \alpha)$$

Also compute the corresponding rotor lift and drag coefficients

$$\left(\frac{C_L'}{\sigma}\right)_F = \frac{L_F}{[(T.F.)\sigma]_F}$$

$$\left(\frac{C_D'}{\sigma}\right)_F = \frac{D_F}{[(T.F.)\sigma]_F}$$

(f) Using (C_L'/σ) from step (e), obtain the values for the required interference angles. For the first approximation use $\lambda_F = 0$, thus:

$$\epsilon_{FUS} = K_{FFUS}\left[\frac{\sigma}{2\mu\sqrt{\mu^2+\lambda^2}}\left(\frac{C_L'}{\sigma}\right)57.3\right]_F \quad \text{deg}$$

$$\epsilon_W = K_{FW}\left[\frac{\sigma}{2\mu\sqrt{\mu^2+\lambda^2}}\left(\frac{C_L'}{\sigma}\right)57.3\right]_F \quad \text{deg}$$

$$\epsilon_T = (K_{FT} + K_{WT})\left[\frac{\sigma}{2\mu\sqrt{\mu^2+\lambda^2}}\left(\frac{C_L'}{\sigma}\right)57.3\right]_F \quad \text{deg}$$

$$\epsilon_{TR} = K_{FTR}\left[\frac{\sigma}{2\mu\sqrt{\mu^2+\lambda^2}}\left(\frac{C_L'}{\sigma}\right)57.3\right]_F \quad \text{deg}$$

(g) Repeat steps (d) through (f), incorporating the interference angles from step (f) until the values converge.

(h) Calculate the chart values of rotor lift and drag coefficients corresponding to rotor solidity of $\sigma_F = 0.1$, using the methods in Reference 2, thus:

$$\left[\left(\frac{C_L'}{\sigma}\right)_{0.1}\right]_F = \left(\frac{C_L'}{\sigma}\right)_F$$

$$\left[\left(\frac{C_D'}{\sigma}\right)_{0.1}\right]_F = \left[\frac{C_D'}{\sigma} - \frac{\Delta\sigma}{2\mu^2}\left(\frac{C_L'}{\sigma}\right)^2\right]_F$$

where

$$(\Delta\sigma)_F = \sigma_F - 0.1$$

(i) Using the values of $[(C_L'/\sigma)_{0.1}]_F$ and $[(C_D'/\sigma)_{0.1}]_F$ from step (h) and θ_{1_F}, M_{T_F}, and μ_F from steps (a) and (b), enter the appropriate trim charts, presented in Section 5.2.1 or References 2 and 3, and obtain the first approximations for the following rotor trim parameters corresponding to $\sigma = 0.1$:

$$\left[(\alpha_c)_{0.1}\right]_F,\ a_{1_F},\ b_{1_F},\ a_{0_F},\ \theta_{.75_F},\ \lambda_F,\ (C_Q/\sigma)_F$$

Note that b_{1_F}, a_{0_F}, and θ_{75_F} have to be obtained only after final trim has been established.

(j) Calculate main rotor angle of attack α_{c_F} and rotor torque Q_F as follows:

$$\alpha_{c_F} = \left[(\alpha_c)_{0.1} \div \frac{\Delta\sigma}{2\mu^2}\left(\frac{C_L'}{\sigma}\right)\right]_F$$

$$Q_F = \left[(T.F.)R\sigma\left(\frac{C_Q}{\sigma}\right)\right]_F$$

(k) Using the trim parameters obtained in the steps above, assume two values of $C_{M_{FUS}}$ and calculate α_{FUS} from the following equation:

$$\alpha_{FUS} = \frac{NUM}{DEN} - \epsilon_{FUS}$$

where

$$NUM = (\ell_{x_F} L_F - \ell_{z_F} D_F) + (\ell_{x_W} L_W - \ell_{z_W} D_W) + (\ell_{x_T} L_T - \ell_{z_T} D\ )$$

$$+ \sum_{i=1}^{n} \left[(T_{P_i} - N_{P_i} i_{P_i}) \ell_{z_{P_i}} + (T_{P_i} i_{P_i} + N_{P_i}) \ell_{x_{P_i}} + M_{P_i} \right]$$

$$+ \left[\frac{e b \Omega^2 M_S}{2} (a_1 - B_1) \right]_F + M_{FUS} + Q_{TR}$$

$$DEN = -(\ell_{z_F} L_F + \ell_{x_F} D_F) - (\ell_{z_W} L_W + \ell_{x_W} D_W) - (\ell_{z_T} L_T + \ell_{x_T} D_T)$$

$$M_{FUS} = C_{M_{FUS}} q_o A_{x_{FUS}} \ell_{FUS}$$

$$B_{1_F} \ -(\alpha_{FUS} + \epsilon_{FUS}) - \alpha_{C_F} + i_F$$

$Q_{TR} = 0$ for the first iteration

and N_{P_i} and M_{P_i} are obtained from Section 5.7.

The straight line obtained by connecting the two points thus calculated is superimposed on the experimental fuselage pitching moment curve of ($C_{M_{FUS}}$ versus α_{FUS}). The point of intersection will yield the new fuselage trim angle of attack, α_{FUS}, to be used in the next iteration.

If no point of intersection is obtained because the calculated fuselage pitching moment curve lies above or below the experimental curve, then the new estimate of α_{FUS} to be used in the next iteration is estimated as follows:

(a) If the calculated fuselage pitching moment curve lies below the experimental curve at the assumed value of α_{FUS} then this indicates that the estimated value of α_{FUS} is too low since not enough fuselage pitching moment was calculated to agree with the experimentally determined fuselage pitching moment. A larger value of α_{FUS} should thus be

assumed for the next iteration.

(b) If the calculated fuselage pitching moment lies above the experimental curve at the assumed value of α_{FUS}, then a similar argument to that above will indicate that the magnitude of α_{FUS} should be reduced for the next iteration.

If multiple points of intersection are obtained, then the magnitude of α_{FUS} for the next iteration should be increased or reduced as explained above until the experimental and calculated fuselage pitching moment curves intersect at the same α_{FUS} for which the calculations were performed.

(l) Using α_{FUS} from step (k), enter fuselage charts and obtain

$C_{L_{FUS}}$, $C_{D_{FUS}}$, $C_{Y_{FUS}}$, $C_{\mathcal{L}_{FUS}}$, $C_{M_{FUS}}$, and $C_{N_{FUS}}$.

Then calculate the following fuselage trim values:

$$L_{FUS} = C_{L_{FUS}} q_0 A_{Z_{FUS}} \qquad D_{FUS} = C_{D_{FUS}} q_0 A_{X_{FUS}}$$

$$Y_{FUS} = C_{Y_{FUS}} q_0 A_{Y_{FUS}} \qquad \mathcal{L}_{FUS} = C_{\mathcal{L}_{FUS}} q_0 A_{X_{FUS}} \ell_{FUS}$$

$$M_{FUS} = C_{M_{FUS}} q_0 A_{X_{FUS}} \ell_{FUS} \qquad N_{FUS} = C_{N_{FUS}} q_0 A_{X_{FUS}} \ell_{FUS}$$

(m) Using the values of N_{FUS} from step (l) and Q_F from step (j), determine the following tail-rotor parameters:

$$T_{TR} = \frac{N_{FUS} + Q_F}{-\ell_{X_{TR}}}$$

$$\left(\frac{C_L'}{\sigma}\right)_{TR} = \left[\frac{T}{(T.F.)\sigma}\right]_{TR}$$

(n) Knowing the tail-rotor parameters μ_{TR}, $(M_T)_{TR}$, and $\theta_{I_{TR}}$ from step (b), and using the value of $(C_L'/\sigma)_{TR}$ from step (m) and $\alpha_{C_{TR}} = 0$, enter the appropriate performance charts and obtain the following tail-rotor trim values:

$$\left[\left(\frac{C_D'}{\sigma}\right)_{0.1}\right]_{TR},\ \left(\frac{C_Q}{\sigma}\right)_{TR},\ \lambda_{TR},\ \theta_{75_{TR}},\ a_{o_{TR}},\ a_{1_{TR}},\ b_{1_{TR}}$$

then compute

$$\left(\frac{C_Q'}{\sigma}\right)_{TR} = \left[\left(\frac{C_D'}{\sigma}\right)_{0.1} + \frac{\Delta\sigma}{2\mu^2}\left(\frac{C_L'}{\sigma}\right)^2\right]_{TR}$$

$$D_{TR} = \left[(T.F.)\sigma\,\frac{C_Q'}{\sigma}\right]_{TR}$$

and

$$Q_{TR} = \left[(T.F.)\,\sigma\,R\left(\frac{C_Q}{\sigma}\right)\right]_{TR}$$

(o) Using values of ϵ_{FUS} from step (f) and α_{FUS} from step (k), calculate

$$\alpha = \alpha_{FUS} + \epsilon_{FUS}$$

and then using the values of a_W and a_T obtained in step (c), obtain

$$\alpha_W = \alpha + i_W - \epsilon_W$$

$$C_{L_W} = a_W(\alpha_W - \alpha_{o_W})$$

$$L_W = C_{L_W} q_o S_W$$

$$C_{D_W} = \left[C_{D_o} + \frac{C_L^2}{\pi \mathcal{R} e}\right]_W$$

$$D_W = C_{D_W} q_o S_W$$

If no elevator control or incidence control is used on the horizontal tail, then the tail lift and drag are calculated using the same equations as above but reading subscript T for subscript W in each equation.

If an elevator control is used, the control derivative $C_{L_{\delta_e}}$ must be obtained from Section 5.6. Using the value of B_{I_F} from step (k), the corresponding elevator angle δ_e is then read from the aircraft control rigging curve (B_{I_F} and δ_e versus control position)

Then calculate:

$$\alpha_T = \alpha + i_T - \epsilon_T$$

$$C_{L_T} = a_T (\alpha_T - \alpha_{o_T}) + C_{L_{\delta_e}} \delta_e$$

$$L_T = C_{L_T} q_0 S_T$$

$$C_{D_T} = \left[C_{D_o} + \frac{C_L^2}{\pi A\!\!\!R e} \right]_T$$

$$D_T = C_{D_T} q_0 S_T$$

Deflected flaps on the wing can be accounted for in a similar manner.

(p) Using the trim parameters obtained above and assuming $A_{I_F} = \phi = Y_{TR} = \gamma_c = \beta_S = 0$, the X and Z equations from Section 4 are solved simultaneously, making the usual small-angle assumptions, to obtain a better approximation for the main rotor drag and lift, thus:

$$L_F = \frac{K_1 \alpha - K_2}{1 + \alpha^2}$$

$$D_F = L_F \alpha - K_1$$

where

$$K_1 = W\alpha - L_{FUS}(\alpha - \epsilon_{FUS}) - L_W(\alpha + i_W - \epsilon_W) - L_T(\alpha + i_T - \epsilon_T)$$

$$+ D_{FUS} + D_W + D_T + D_{TR} - \sum_{i=1}^{n}(T_{P_i} - N_{P_i}\, i_{P_i})$$

and

$$K_2 = D_{FUS}(\alpha - \epsilon_{FUS}) + D_W(\alpha + i_W - \epsilon_W) + D_T(\alpha + i_T - \epsilon_T)$$

$$+ D_{TR}(\alpha - \epsilon_{TR}) + L_{FUS} + L_W + L_T + \sum_{i=1}^{n}(T_{P_i}\, i_{P_i} + N_{P_i}) - W$$

Then obtain

$$\left(\frac{C_L'}{\sigma}\right)_F = \left[\left(\frac{C_L'}{\sigma}\right)_{0.1}\right]_F = \left[\frac{L}{(T.F.)\sigma}\right]_F$$

$$\left(\frac{C_D'}{\sigma}\right)_F = \left[\frac{D}{(T.F.)\sigma}\right]_F$$

and compute

$$\left[\left(\frac{C_D'}{\sigma}\right)_{0.1}\right]_F = \left[\frac{C_D'}{\sigma} - \frac{\Delta\sigma}{2\mu^2}\left(\frac{C_L'}{\sigma}\right)^2\right]_F$$

(q) Repeat steps (f) through (p) with new values of $[(C_L'/\sigma)_{0.1}]_F$ and $[(C_D'/\sigma)_{0.1}]_F$ until convergence is achieved, yielding the final trim values.

In general, for $\alpha \leq 5^\circ$, the above iteration procedure is very rapidly convergent, and therefore one or two iterations are sufficient to obtain the final trim conditions.

(r) Calculate main rotor side force, thus:

$$Y_F = \Big[(T.F.)\sigma \frac{a}{2}\Big(-\frac{3}{4}\mu\theta_{.75}a_0 + \frac{1}{3}\theta_{.75}b_1 + \frac{3}{8}\mu^2\theta_{.75}b_1 + \frac{3}{4}\lambda b_1$$

$$+ \frac{1}{6}a_0 a_1 - \frac{3}{2}\mu\lambda a_0 - \mu^2 a_0 a_1 + \frac{1}{4}\mu a_1 b_1 + \frac{1}{8}\mu^2\lambda b_1\Big]_F$$

(s) Equations must now be obtained for the forces and moments due to lateral and directional aerodynamic (conventional aircraft) controls, if they are employed, or due to flow asymmetries, if such effects are evident in the test data. It is usually possible to relate the movement of the conventional aircraft type controls to the helicopter control movements by means of the experimental control rigging curves for the compound helicopter being investigated. Those relationships are usually linear or of some simple nonlinear form such that the following function can be obtained:

$$\delta_a = \text{function}\ \left[A_{1_F}\right]$$

$$\delta_r = \text{function}\ \left[(\theta_{.75})_{TR}\right]$$

Using the control design parameters from page 5-1 and the methods in Section 5.6, obtain the control derivatives

$$C_{\mathcal{L}_{\delta_a}} = \frac{\partial(\mathcal{L}_W/q_0 S_W b_W}{\partial\delta_a} \quad \text{per aileron}$$

$$C_{L_{\delta_r}} = \frac{\partial(L_{VT}/q_0 S_{VT}}{\partial\delta_r}$$

Then calculate

$$\mathcal{L}_W = -L_W \ell_{Y_W} = q_0 S_W b_W (C_{\mathcal{L}_{\delta_a}})_W (\delta_{a_R} - \delta_{r_L})$$

$$= \text{function}\ (A_{1_F})$$

$$L_{VT} = (a_{VT}\beta_S + C_{L_{\delta_r}}\delta_r)q_0 S_{VT}$$

$$= \text{function}\ (\beta_S)$$

Test data for the aircraft being analyzed might indicate additional moments that could be included in the analysis, such as a rolling moment due to asymmetric horizontal tail lift.

(t) From the curves of the experimental lateral fuselage characteristics, obtain slopes $\partial C_{Y_{FUS}}/\partial \beta_S$, $\partial C_{\mathcal{L}_{FUS}}/\partial \beta_S$, and $\partial C_{N_{FUS}}/\partial \beta_S$. Using the coefficients $C_{Y_{FUS}}$, $C_{\mathcal{L}_{FUS}}$, and $C_{N_{FUS}}$ obtained in step (1) at $\beta_S = 0$, obtain expressions for the fuselage lateral characteristics, thus:

$$C_{Y_{FUS}} = C_{Y_{FUS}\,\beta_S=0} + \frac{\partial C_{Y_{FUS}}}{\partial \beta_S}\beta_S$$

$$C_{\mathcal{L}_{FUS}} = C_{\mathcal{L}_{FUS}\,\beta_S=0} + \frac{\partial C_{\mathcal{L}_{FUS}}}{\partial \beta_S}\beta_S$$

$$C_{N_{FUS}} = C_{N_{FUS}\,\beta_S=0} + \frac{\partial C_{N_{FUS}}}{\partial \beta_S}\beta_S$$

(u) Using the trim conditions calculated above, obtain the main rotor lateral cyclic (A_{1_F}) and sideslip angle (β_S) from a simultaneous solution of the rolling and yawing moment equations, thus:

$$\beta_S = \frac{K_5 K_7 - K_4 K_8}{K_4 K_6 - K_3 K_7} \quad \text{rad}$$

$$A_{1_F} = -\frac{K_3 \beta_S + K_5}{K_4} \quad \text{rad}$$

where

$$K_3 = (L_F \alpha_F - D_F)\lambda_{X_F} + Y_F \lambda_{Y_F} + (L_W \alpha_W - D_W)\lambda_{X_W} + (L_T \alpha_T - D_T)\lambda_{X_T}$$
$$- a_{VT} q_0 S_{VT} \lambda_{X_{VT}} - D_{TR}\lambda_{X_{TR}} + T_{TR}\lambda_{Y_{TR}} + \frac{\partial C_{N_{FUS}}}{\partial \beta_S} q_0 A_{X_{FUS}} \lambda_{FUS}$$

$$K_4 = L_F \lambda_{X_F} + Y_F \alpha_F \lambda_{Y_F} + 2 q_0 S_W b_W C_{\mathcal{L}_{\delta_a}} \frac{\partial \delta_a}{\partial A_{1_F}} \alpha_W$$

$$K_5 = Y_F \ell_{X_F} - (L_F \alpha_F - D_F)\ell_{Y_F} + 2q_o S_W b_W C_{\ell_{\delta_a}} \delta_a \Big|_{A_{1_F}=0} \alpha_W - L_T \ell_{Y_T} \alpha_T$$

$$- C_{L_{\delta_r}} \delta_r q_o S_{VT} \ell_{X_{VT}} + T_{TR} \ell_{X_{TR}} + D_{TR} \ell_{Y_{TR}} + C_{N_{FUS}}\Big|_{\beta=0} q_o A_{X_{FUS}} \ell_{FUS}$$

$$+ Q_F + \sum_{i=1}^{n} \left[Y_{P_i} \ell_{X_{P_i}} - (T_{P_i} - N_{P_i} i_{P_i}) \ell_{Y_{P_i}} \right]$$

$$K_6 = -(L_F \alpha_F - D_F)\ell_{Z_F} - (L_W \alpha_W - D_W)\ell_{Z_W} - (L_T \alpha_T - D_T)\ell_{Z_T}$$

$$+ a_{VT} q_o S_{VT} \ell_{Z_{VT}} + D_{TR} \ell_{Z_{TR}} + \frac{\partial C_{\ell_{FUS}}}{\partial \beta_S} q_o A_{X_{FUS}} \ell_{FUS}$$

$$K_7 = -Y_F \ell_{Y_F} - L_F \ell_{Z_F} + 2q_o S_W b_W C_{\ell_{\delta_a}} \frac{\partial \delta_a}{\partial A_{1_F}} + \left[\frac{eb\Omega^2 M_S}{2}\right]_F$$

$$K_8 = -(D_F \alpha_F - L_F)\ell_{Y_F} - Y_F \ell_{Z_F} + 2q_o S_W b_W C_{\ell_{\delta_a}} \delta_a \Big|_{A_{1_F}=0} - L_T \ell_{Y_T}$$

$$+ C_{L_{\delta_r}} \delta_r q_o S_{VT} \ell_{Z_{VT}} - D_{TR} \ell_{Y_{TR}} \alpha_{TR} - T_{TR} \ell_{Z_{TR}} + C_{\ell_{FUS}}\Big|_{\beta=0} q_o A_{X_{FUS}} \ell_{FUS}$$

$$- \sum_{i=1}^{n} \left[(T_{P_i} i_{P_i} + N_{P_i}) \ell_{Y_{P_i}} + Q_{P_i} \right] + \left[\frac{eb\Omega^2 M_S b_1}{2}\right]_F$$

and the slope $\partial\delta_a/\partial A_{1_F}$ is obtained from the appropriate aileron control rigging curves for the aircraft being examined.

(v) Substitute the values of A_{1_F} and β_S from step (u) and solve for the aircraft roll attitude, ϕ, using the side force equation, thus

$$\phi = -\frac{K_9 \beta_S + L_F A_{1_F} + K_{10}}{W}$$

where

$$K_9 = L_F \alpha_F - D_F + L_{FUS} \alpha_{FUS} - D_{FUS} + \frac{\partial C_{Y_{FUS}}}{\partial \beta_S} q_o A_{Y_{FUS}} + L_W \alpha_W$$

$$- D_W + L_T \alpha_T - D_T - a_{VT} q_c S_{VT} - D_{TR}$$

$$K_{10} = Y_F + C_{Y_{FUS}\,\beta_s=0} q_o A_{Y_{FUS}} - C_{L_{\delta_r}} \delta_r q_o S_{VT} + T_{TR}$$

(w) Knowing the value of β_S from step (u), obtain better approximations for Y_{FUS}, $\mathcal{L}_{FUS}$, and N_{FUS} from step (1) using values of $C_{Y_{FUS}}$, $C_{\mathcal{L}_{FUS}}$, and $C_{N_{FUS}}$ from step (t) and compute new values for L_{VT} and D_{VT} from step (s).

<u>LITERATURE CITED</u>

1. Gessow, A., and Meyers, G. C., Jr., AERODYNAMICS OF THE HELICOPTER, The MacMillan Company, New York, 1952.

2. Tanner, W. H., CHARTS FOR ESTIMATING ROTARY WING PERFORMANCE IN HOVER AND AT HIGH FORWARD SPEEDS, United Aircraft Corporation, NASA Contractor Report CR-114, National Aeronautics and Space Administration, Washington D. C., November 1964.

3. Tanner, W. H., TABLES FOR ESTIMATING ROTARY WING PERFORMANCE AT HIGH FORWARD SPEEDS, United Aircraft Corporation, NASA Contractor Report, CR-115, National Aeronautics and Space Administration, Washington, D. C., November 1964.

4. STABILITY AND CONTROL HANDBOOK FOR HELICOPTERS, TRECOM Report 60-43, U. S. Army Transportation Research Command (presently, U. S. Army Aviation Materiel Laboratories), Fort Eustis, Virginia, August 1960.

5.2 ROTOR CHARACTERISTICS

This section contains rotor performance data presented in the form of charts which can be used to evaluate the trim condition of compound helicopter configurations. Although these charts have been specifically developed for fully articulated rotor systems having rotor solidity of $\sigma = 0.1$, they are equally applicable for analyses of teetering and hingeless rotor systems.

The correlation of the analytical results for fully articulated rotors having zero hinge offsets with the teetering rotor wind-tunnel test data of Reference 1 has shown that the performance charts presented herein apply to a variety of teetering rotor configurations with **small** to moderate teetering angles.

The performance data for a hingeless system can be obtained from the results of a fully articulated rotor system through the use of a virtual hinge-offset concept. This concept is based on the fact that hingeless rotor systems, because of their elasticity, are subjected to a "flapping motion" similar to that associated with articulated rotors. The fundamental parameter governing this motion is the frequency of the first harmonic flapwise bending mode. Therefore, the basic problem is to represent a hingeless rotor system with a virtual hinge offset, by an equivalent articulated rotor. A comprehensive discussion of the subject matter is presented in References 2 and 3, from which the following relationship is obtained for the **virtual hinge-offset for hingeless rotors:**

$$\frac{e_V}{R} = \frac{\overline{\Omega}^2 - 1}{\overline{\Omega}^2 + \frac{1}{2}}$$

where

$\overline{\Omega}$ is the nondimensional rotor frequency parameter (ω_1 / Ω)

ω_1 is the natural frequency of the rotor first flapping mode when the blade is rotating, rad/sec

Ω is the rotor rotational speed, rad/sec

The natural frequency ω_1 is a function of the rotor blade's mass and stiffness distribution and the rotor speed.

This parameter can be obtained using the methods of Reference 4. Thus, by using the concept of an equivalent articulated rotor applied to the hingeless rotor, the rotor trim and stability derivatives can now be evaluated by the conventional helicopter methods presented in the following sections.

5.2.1 Trim Charts for Rotor Solidity, $\sigma = 0.1$

Classical rotor aerodynamic theories, such as those presented in References 5 and 6, use several simplifying assumptions which limit the applicability of the resulting equations to low forward speeds. To increase the range of applicability, some of these assumptions have been eliminated in Reference 7, which presents charts of pertinent aerodynamic rotor parameters for the tip speed ratios ranging from $\mu = 0.3$ to $\mu = 1.4$. These charts include the effects of blade compressibility and retreating blade stall and do not rely upon small-angle assumptions of the classical theory. However, the charts are prepared for only one value of rotor solidity, $\sigma = 0.1$, and do not include the rotor Y-force data.

In applying the above performance charts for rotor solidity different from $\sigma = 0.1$, appropriate solidity correction factors were used as presented in Reference 7. The required Y-force data were generated by using the equation of Reference 6. together with the pertinent performance results obtainable from Reference 8. The charts for rotor inflow ratio λ and the blade flapping parameters a_0 and b_1, which were not included in Reference 7, were derived from the results of Reference 8 and are presented in this section.

All low-speed performance charts for $\mu = 0.1$ and 0.2 were derived from the classical rotor performance results of Reference 9 and are presented in Figures 1 and 2. The high-speed charts which are not included in Reference 7 are presented in Figures 3 through 13.

The performance charts of Reference 7 and those presented here are derived for constant values of μ, M_T, and θ_1. The relationships between the basic rotor performance parameters, such as C_L'/σ, C_D'/σ, C_Q/σ, a_1, α_c, and $\theta_{.75}$, are presented in the form of carpet plots. The parameters such as λ, a_0, and b_1 for all values of μ are presented as a function of rotor angle of attack, α_c, for constant values of C_L'/σ. Using the above parameters, the rotor side force coefficient can be computed from the following equation:

$$\frac{C_Y'}{\sigma} = \frac{a}{2}\left(-\frac{3}{4}\mu\,\theta_{.75}a_0 + \frac{1}{3}\theta_{.75}b_1 + \frac{3}{8}\mu^2\theta_{.75}b_1 + \frac{3}{4}\lambda b_1\right.$$

$$\left. + \frac{1}{6}a_0a_1 - \frac{3}{2}\mu\lambda a_0 - \mu^2 a_0a_1 + \frac{1}{4}\mu a_1b_1 + \frac{1}{8}\mu^2\lambda b_1\right)$$

The use of the above-mentioned performance charts with the analytical expressions wherever necessary constitutes an integral part of the stability method presented in this Handbook.

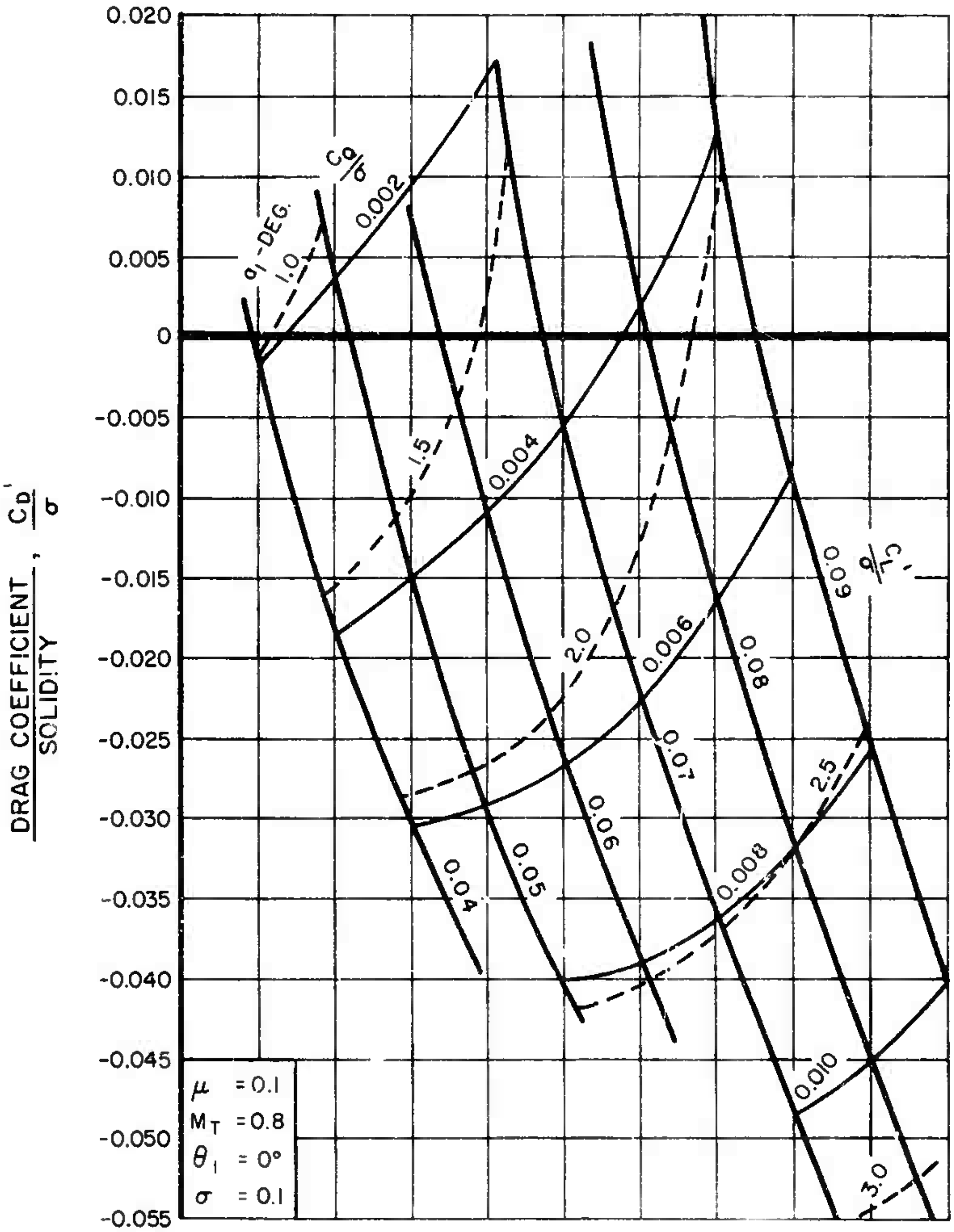

(a) $\frac{C_Q}{\sigma}$ and a_1

Figure 1. Calculated Characteristics of a Rotor With 0° Twist for μ = 0.1 and M_T = 0.8.

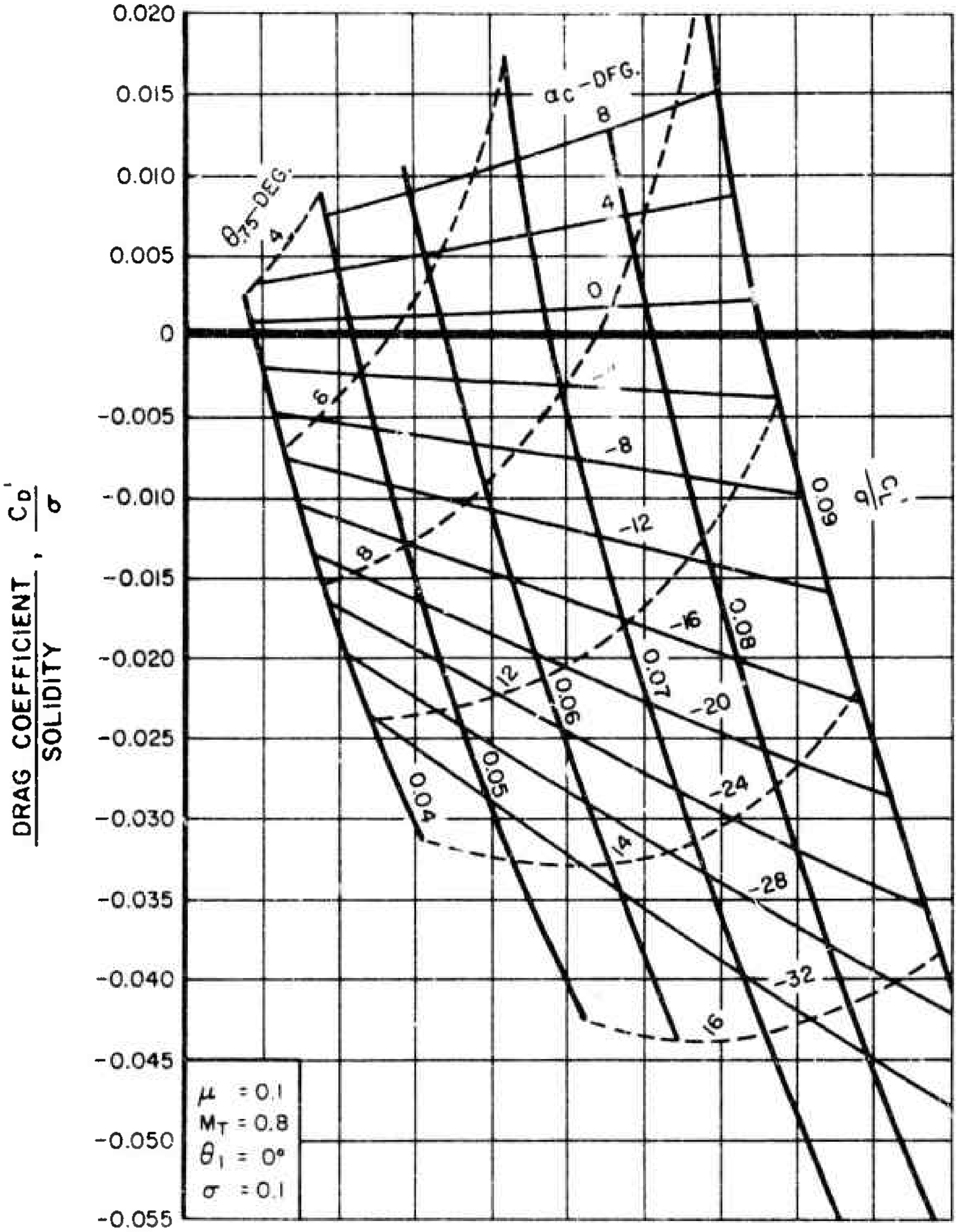

(b) α_c and $\theta_{.75}$

Figure 1. Continued.

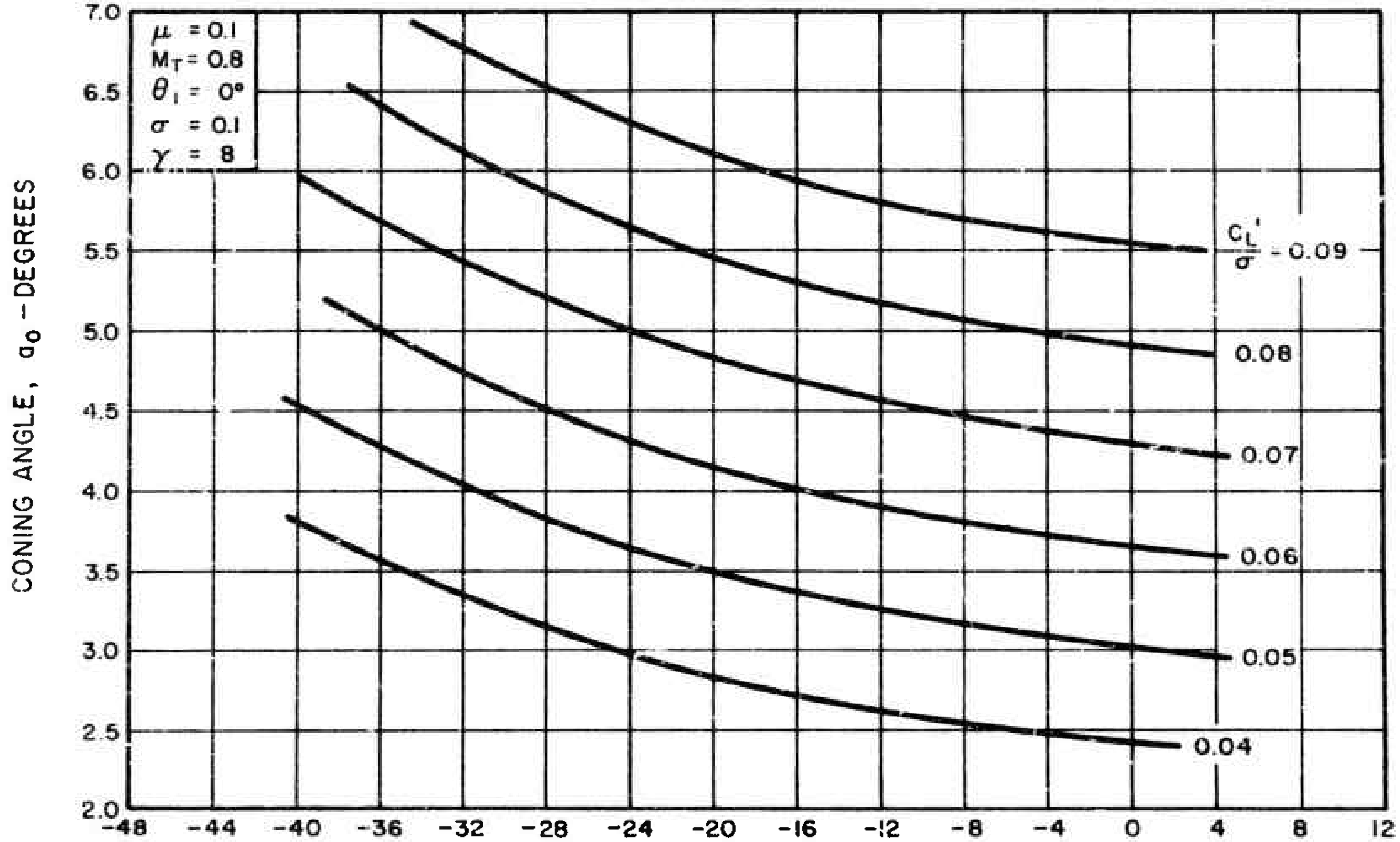

(c) a_0

Figure 1. Continued.

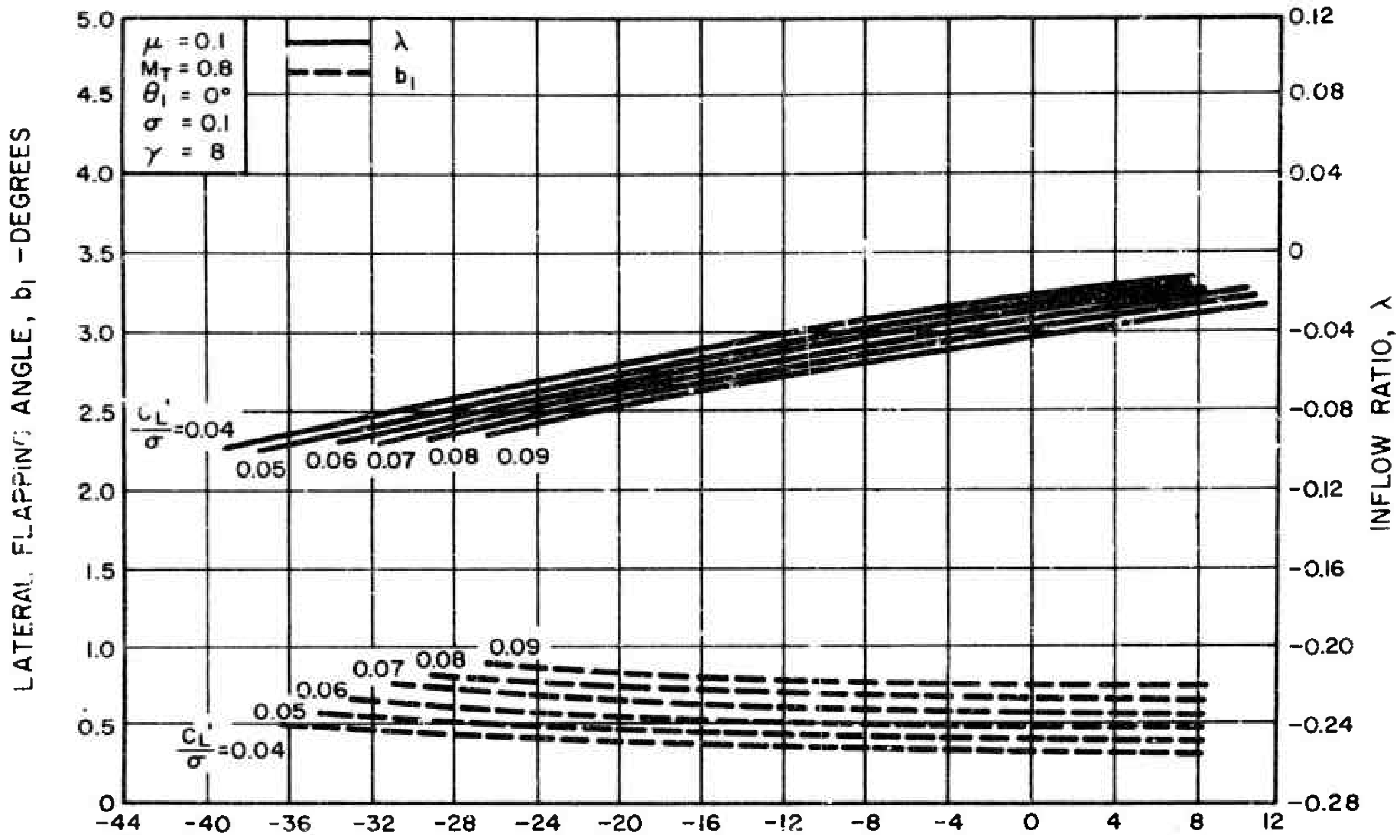

(d) b_1 and λ

Figure 1. Concluded.

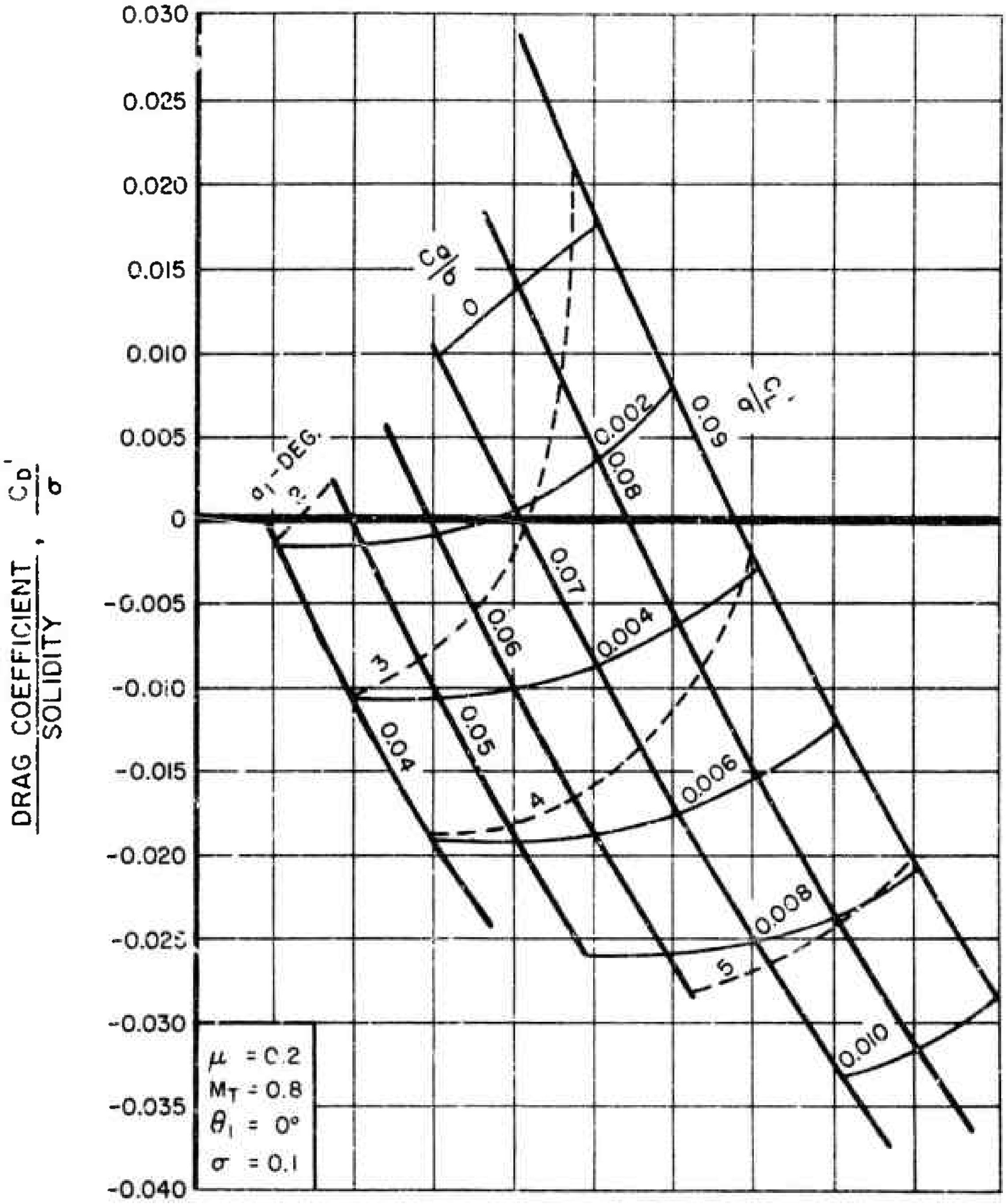

(a) $\frac{C_Q}{\sigma}$ and a_1

Figure 2. Calculated Characteristics of a Rotor With 0° Twist for μ = 0.2 and M_T = 0.8.

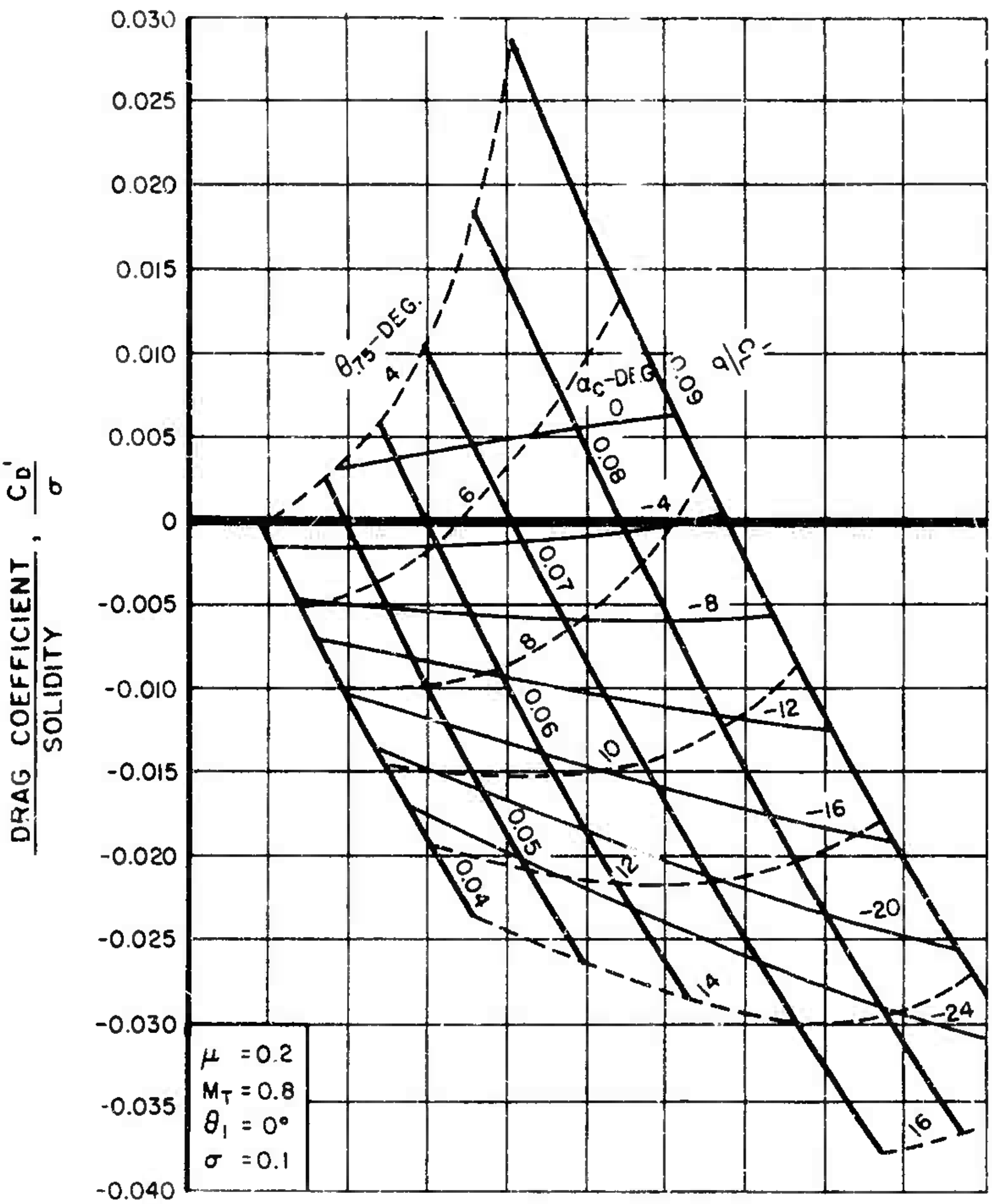

(b) α_c and $\theta_{.75}$

Figure 2. Continued.

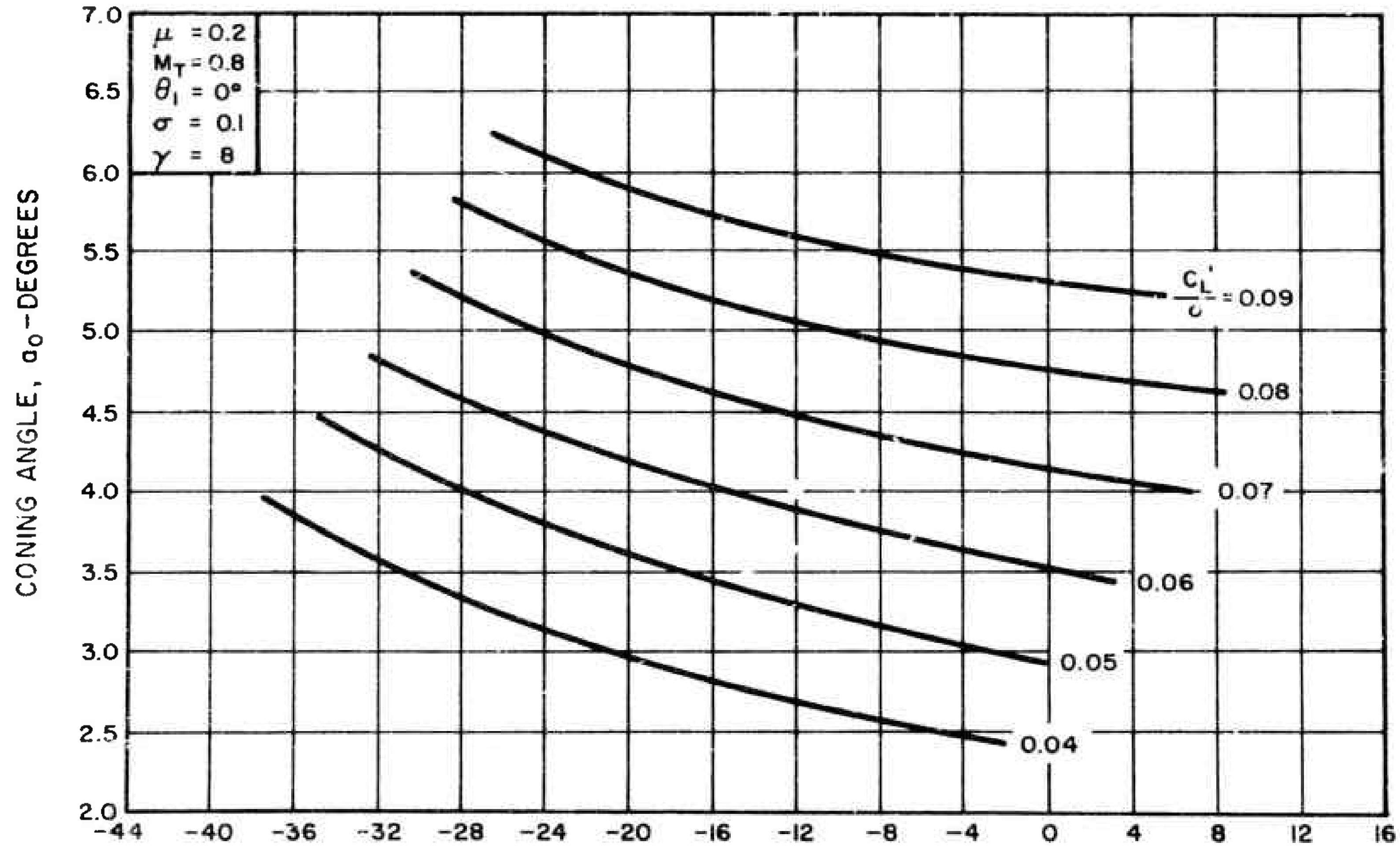

ROTOR ANGLE OF ATTACK, α_C—DEGREES

(c) a_0

Figure 2. Continued.

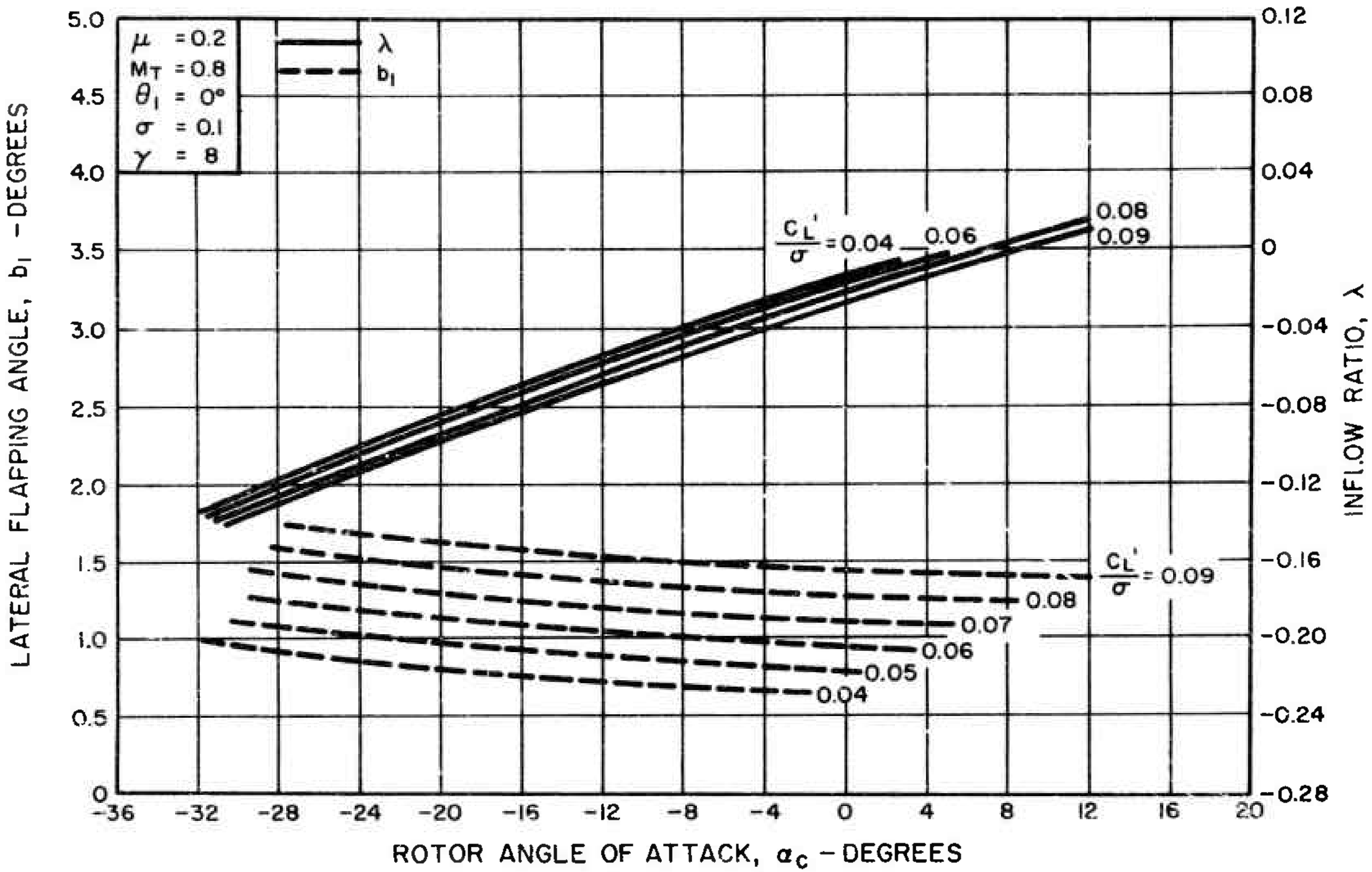

(d) b_1 and λ

Figure 2. Concluded.

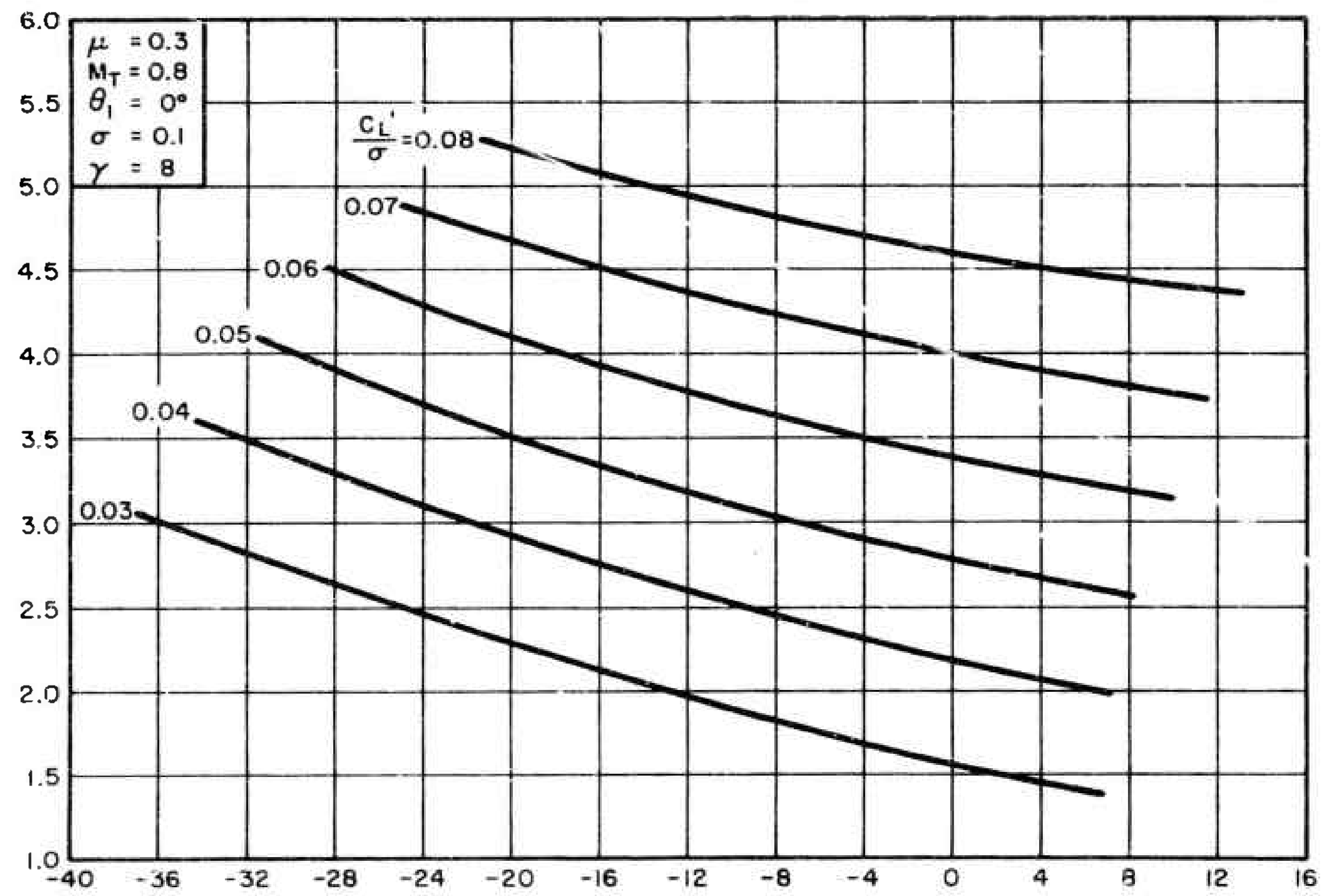

(a) a_0

Figure 3. Calculated Characteristics of a Rotor With 0° Twist for $\mu = 0.3$ and $M_T = 0.8$.

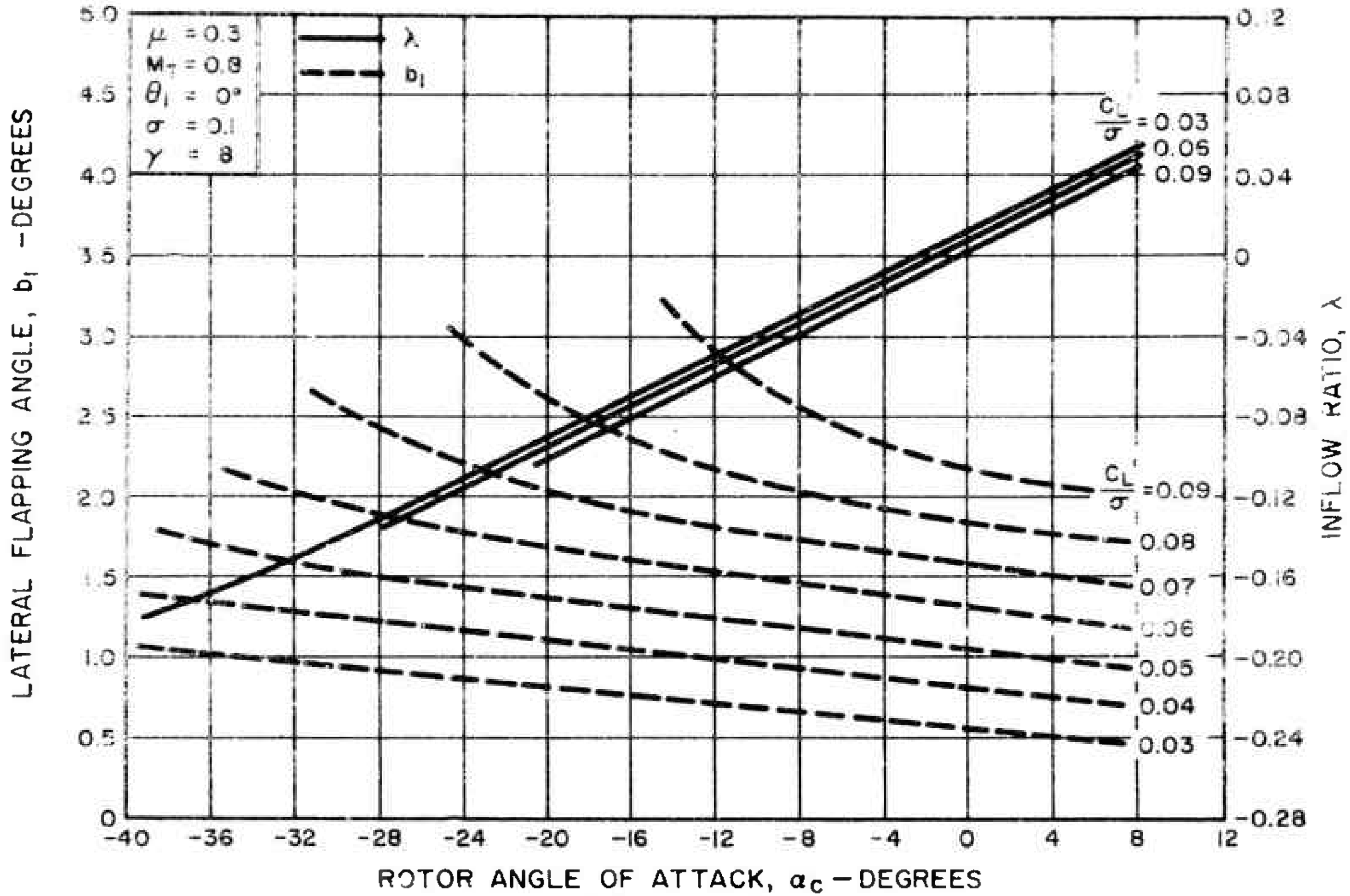

(b) b_1 and λ

Figure 3. Concluded.

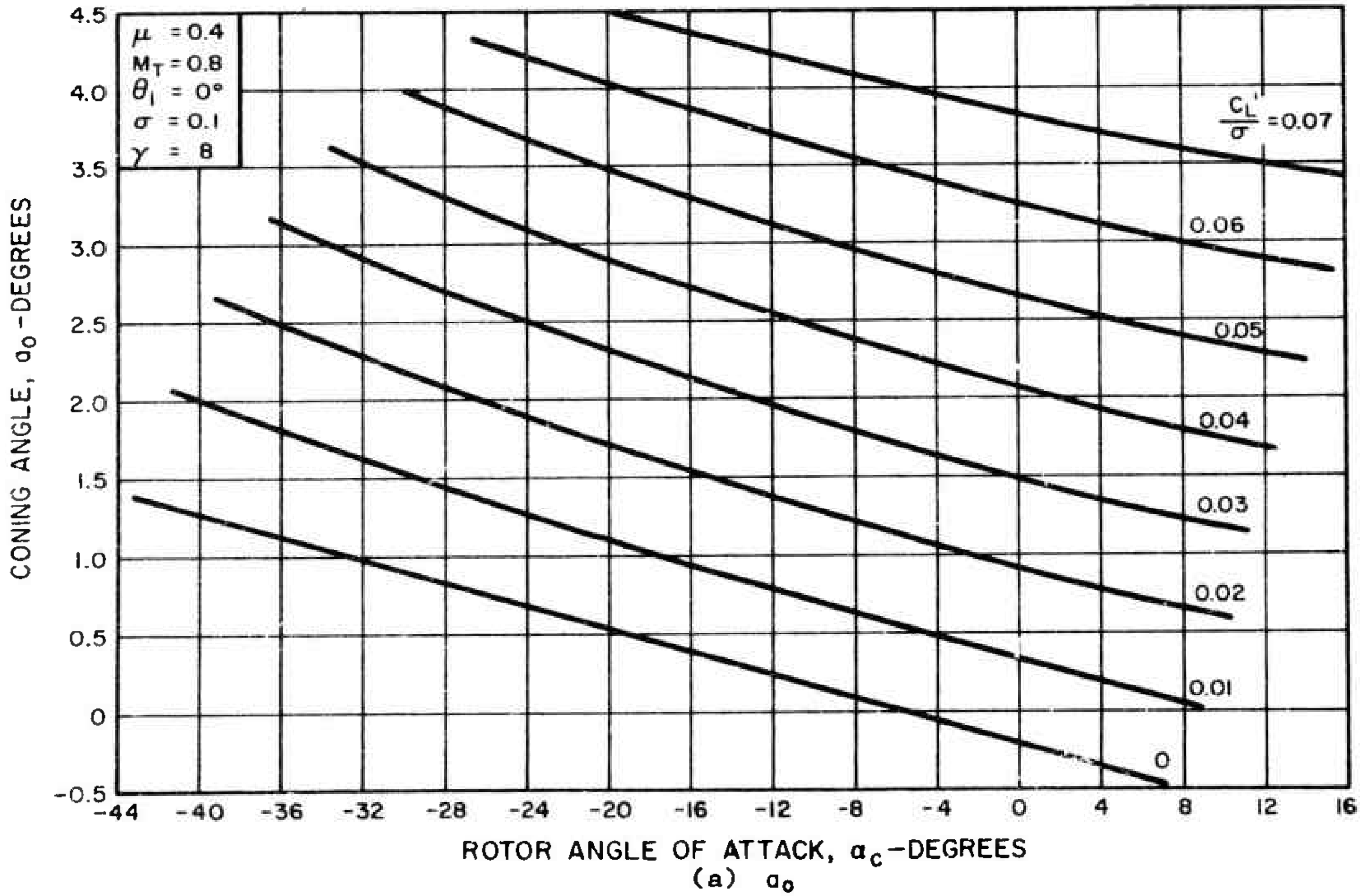

(a) a_0

Figure 4. Calculated Characteristics of a Rotor With $0°$ Twist for $\mu = 0.4$ and $M_T = 0.8$.

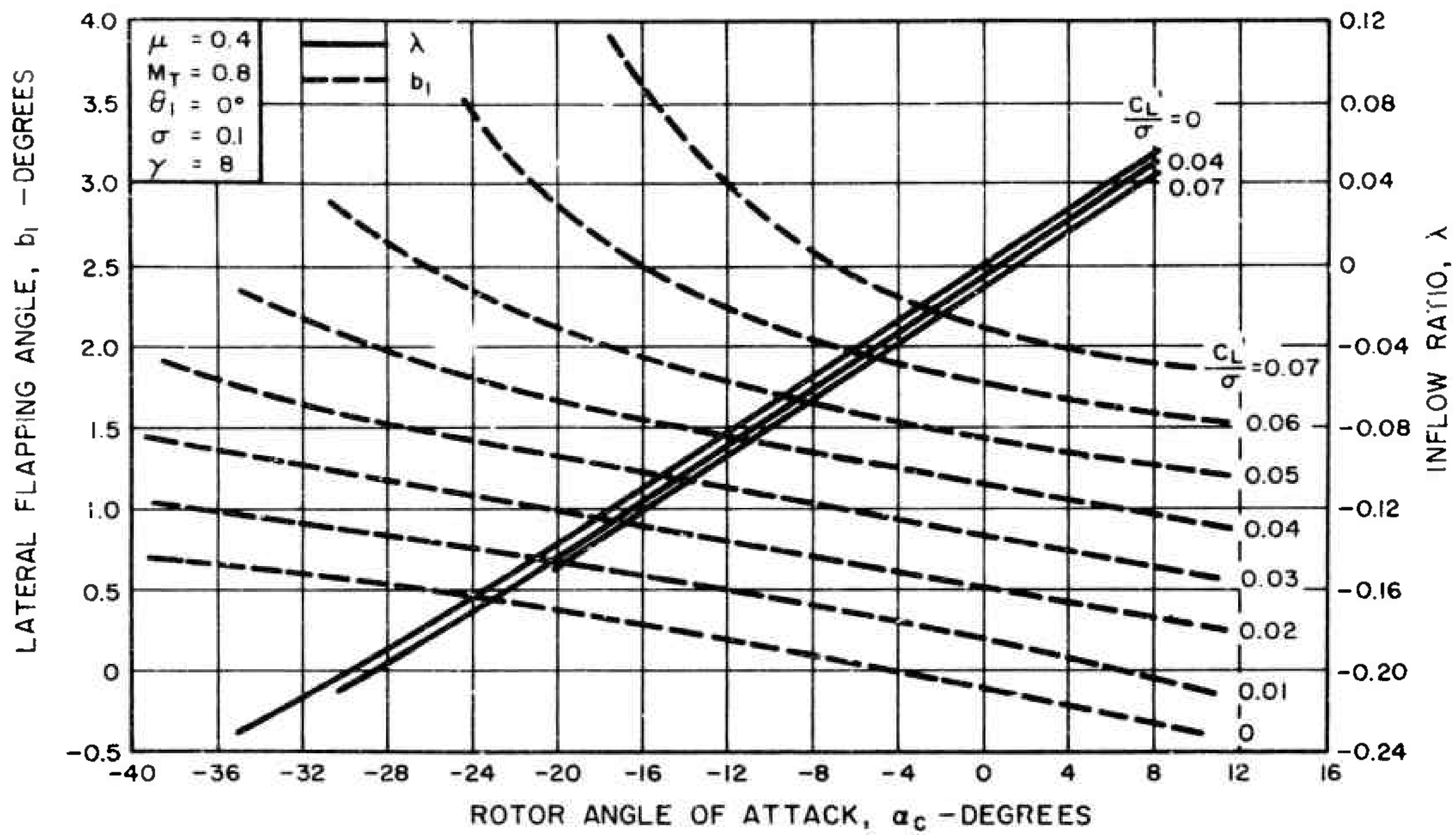

(b) b_1 and λ

Figure 4. Concluded.

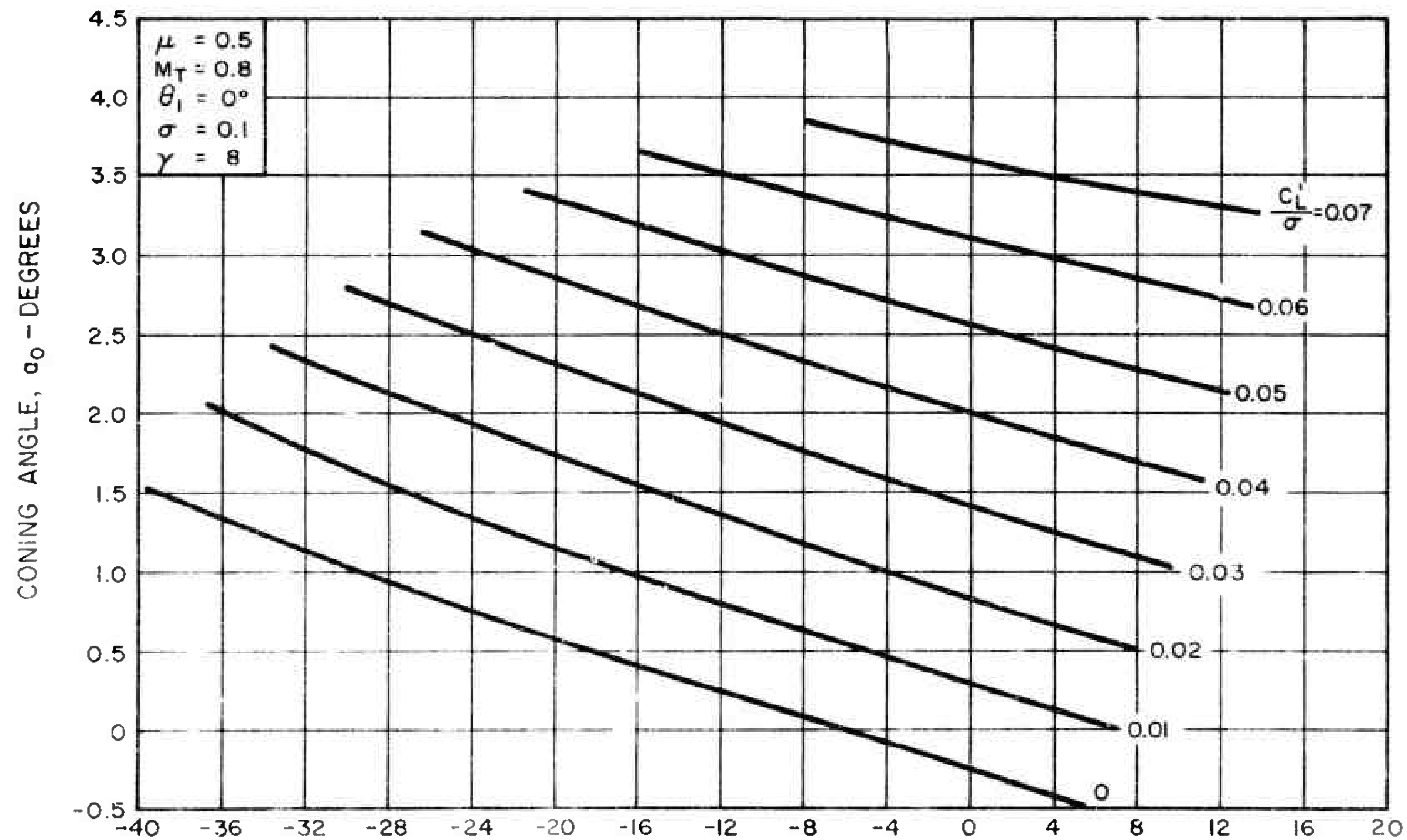

(a) a_0

Figure 5. Calculated Characteristics of a Rotor With 0° Twist for μ = 0.5 and M_T = 0.8.

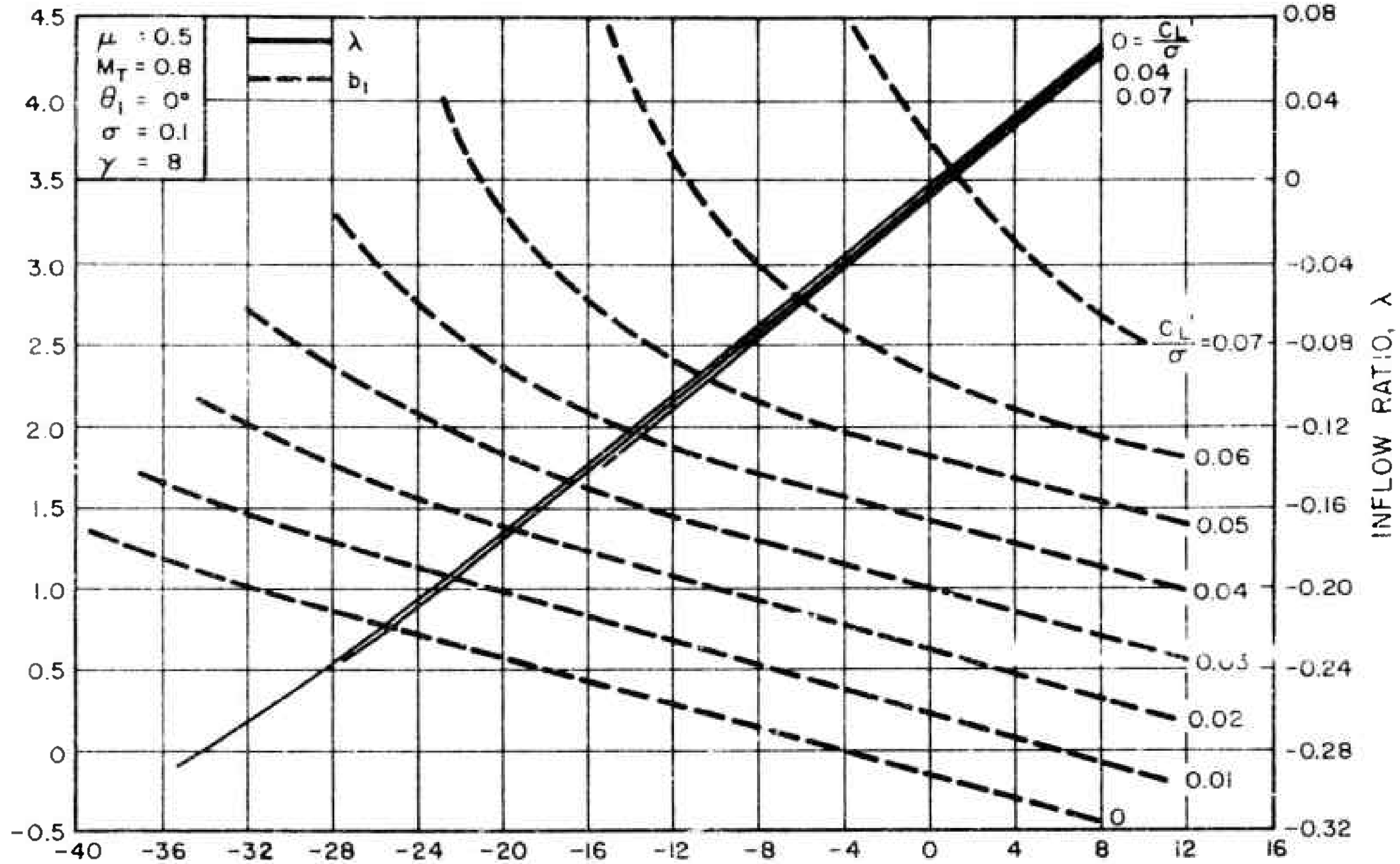

(b) b_1 and λ

Figure 5. Concluded.

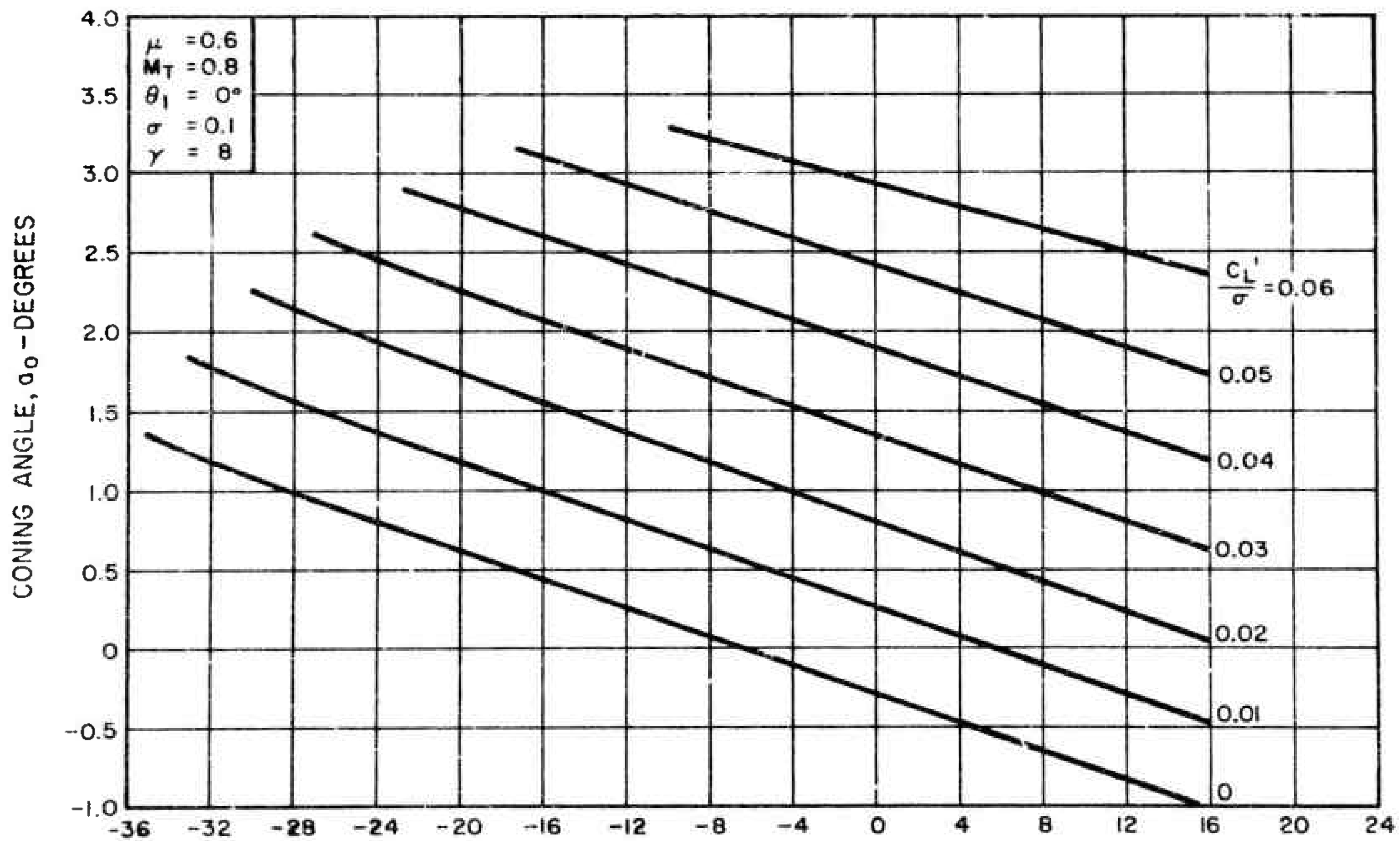

(a) a_0

Figure 6. Calculated Characteristics of a Rotor With 0^{o} Twist for $\mu = 0.6$ and $M_T = 0.8$.

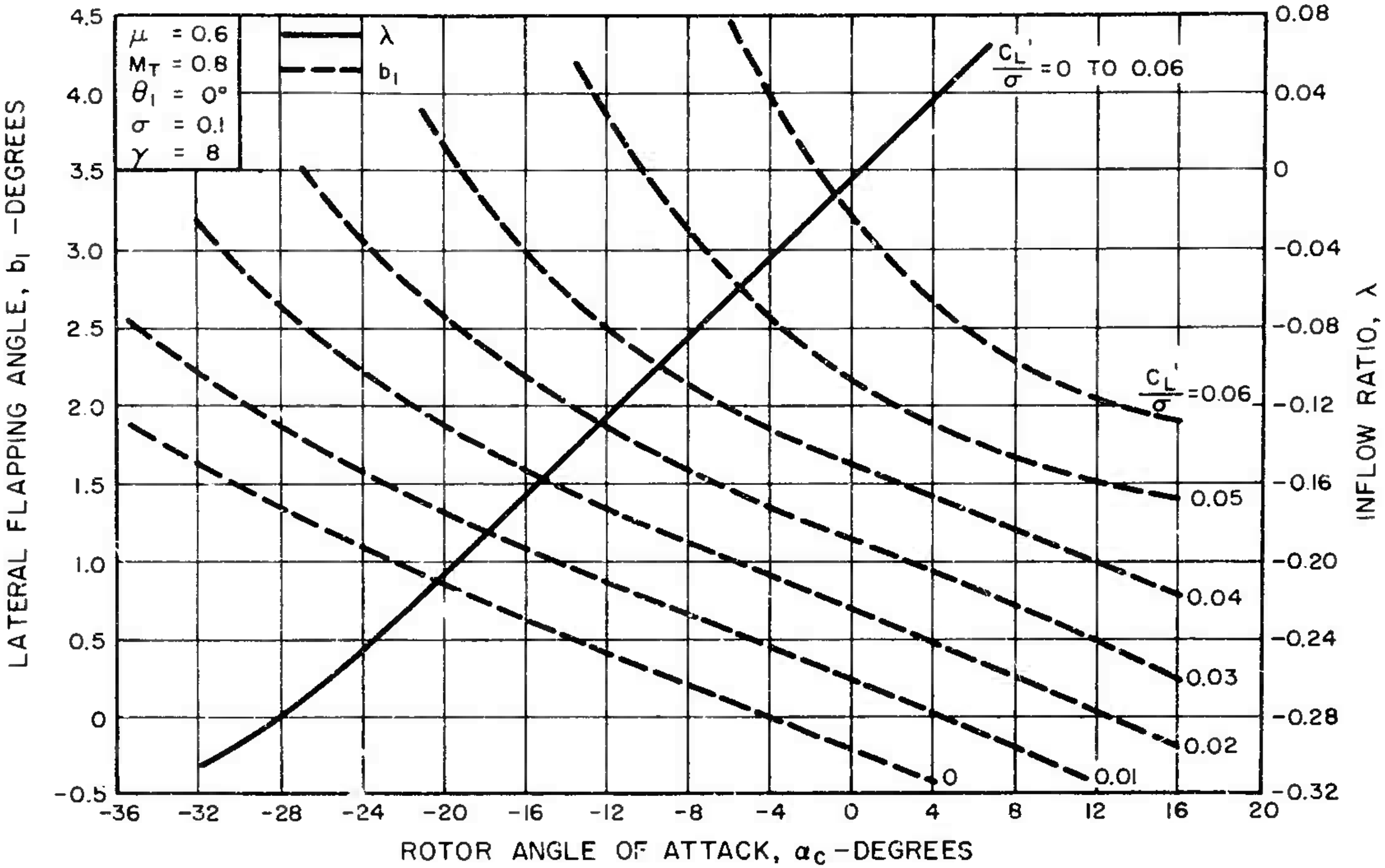

(b) b_1 and λ

Figure 6. Concluded.

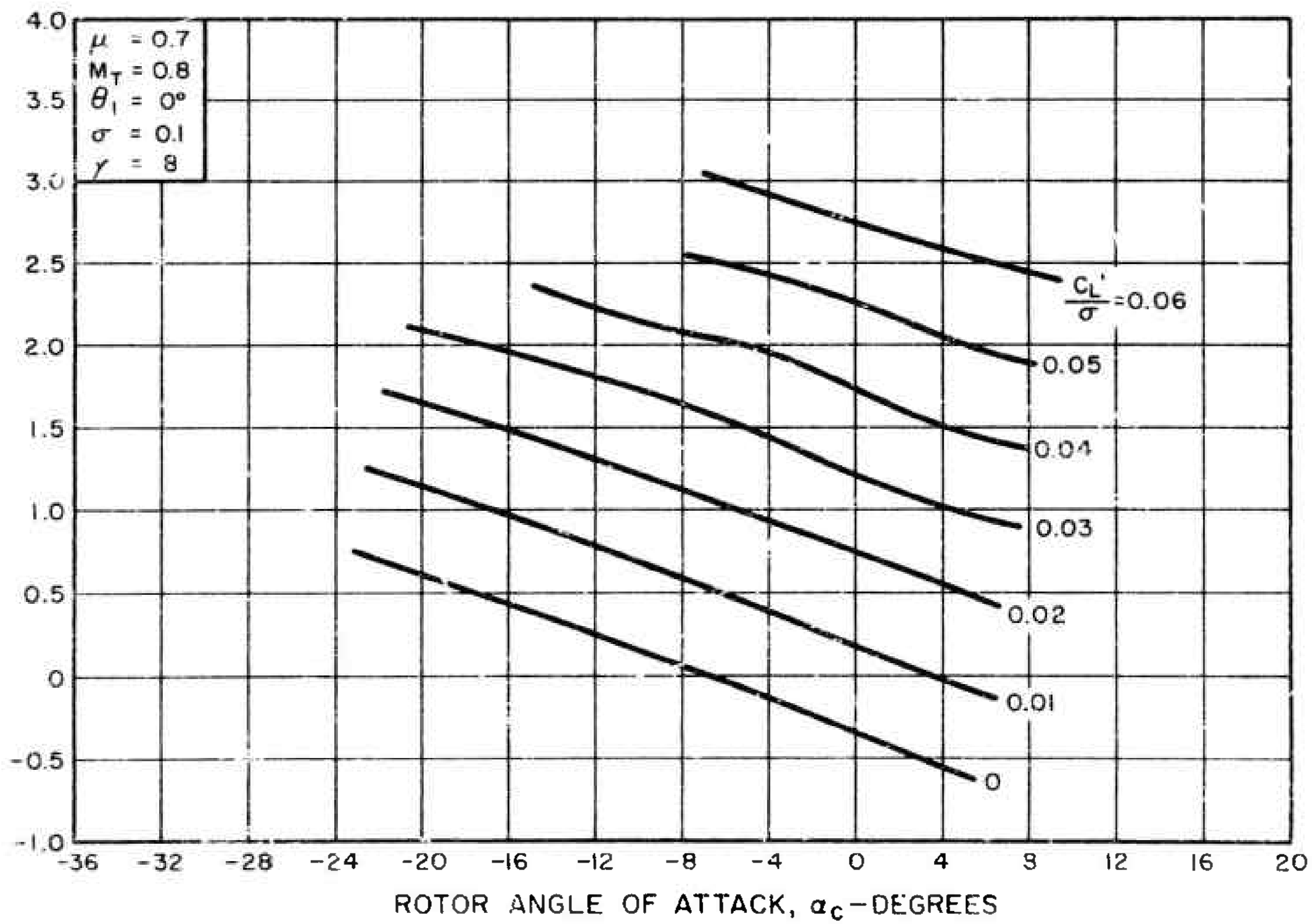

(a) a_0

Figure 7. Calculated Characteristics of a Rotor With 0° Twist for $\mu = 0.7$ and $M_T = 0.8$.

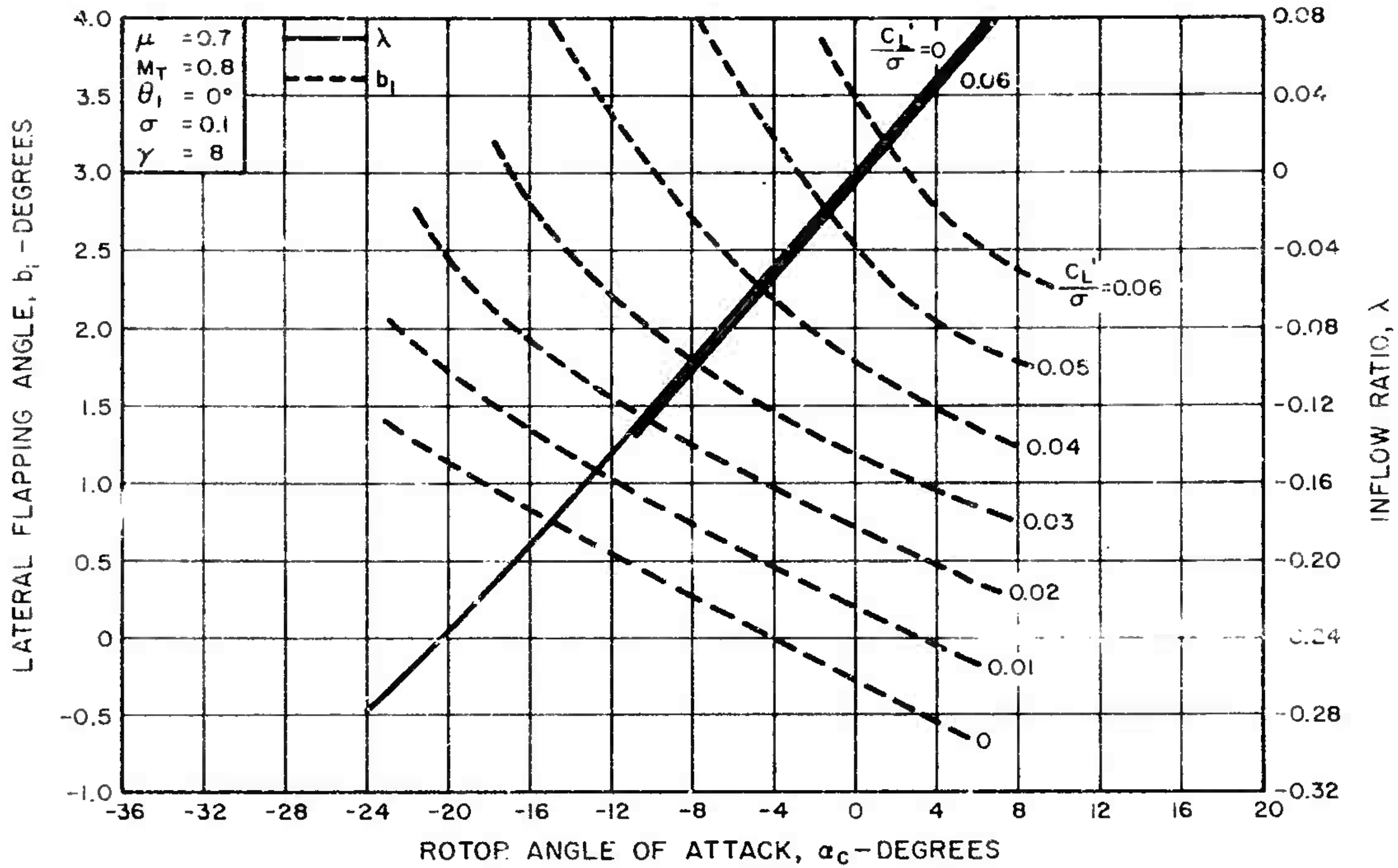

(b) b_1 and λ

Figure 7. Concluded.

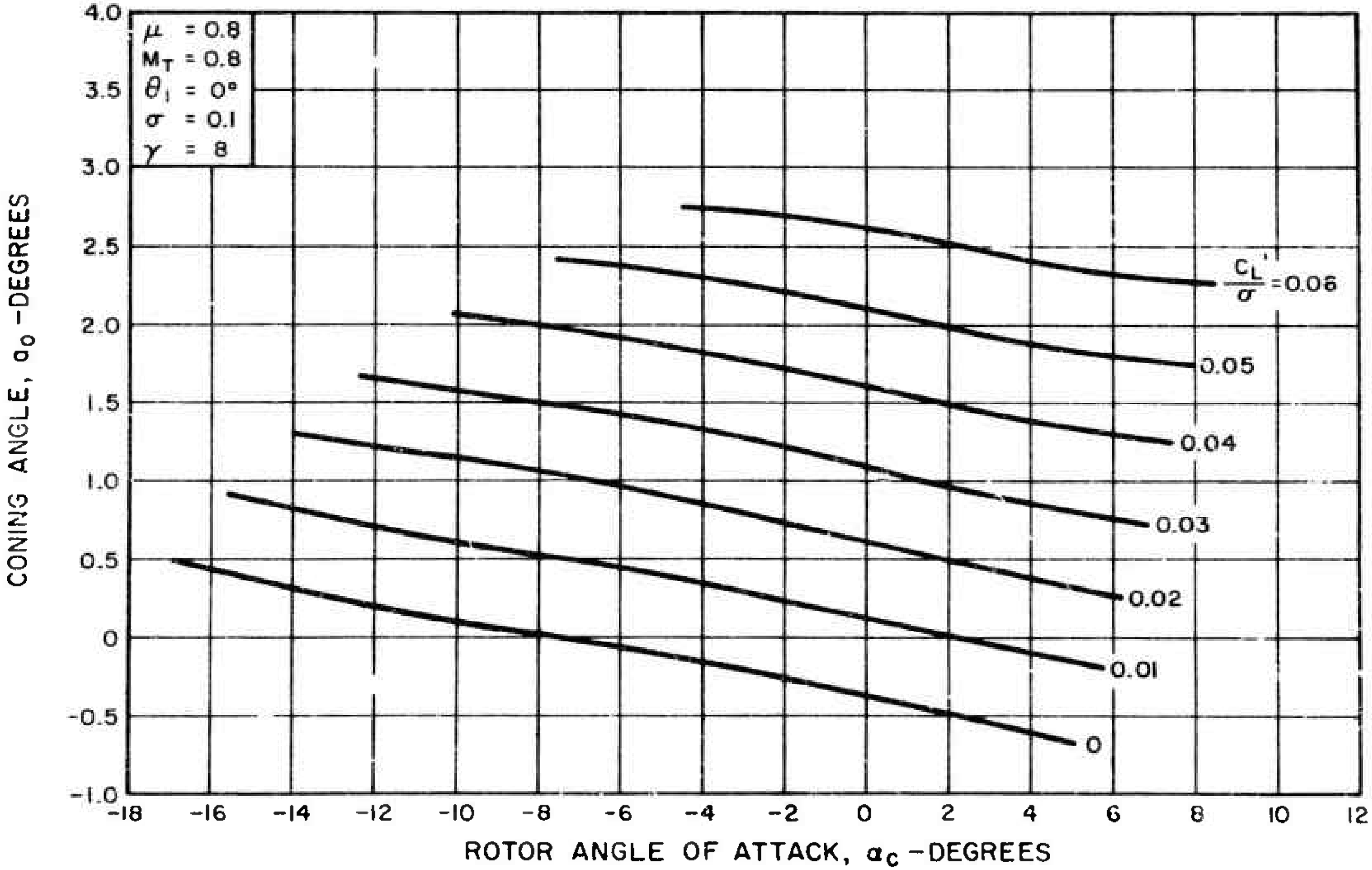

(a) a_0

Figure 8. Calculated Characteristics of a Rotor With 0° Twist for μ = 0.8 and M_T = 0.8.

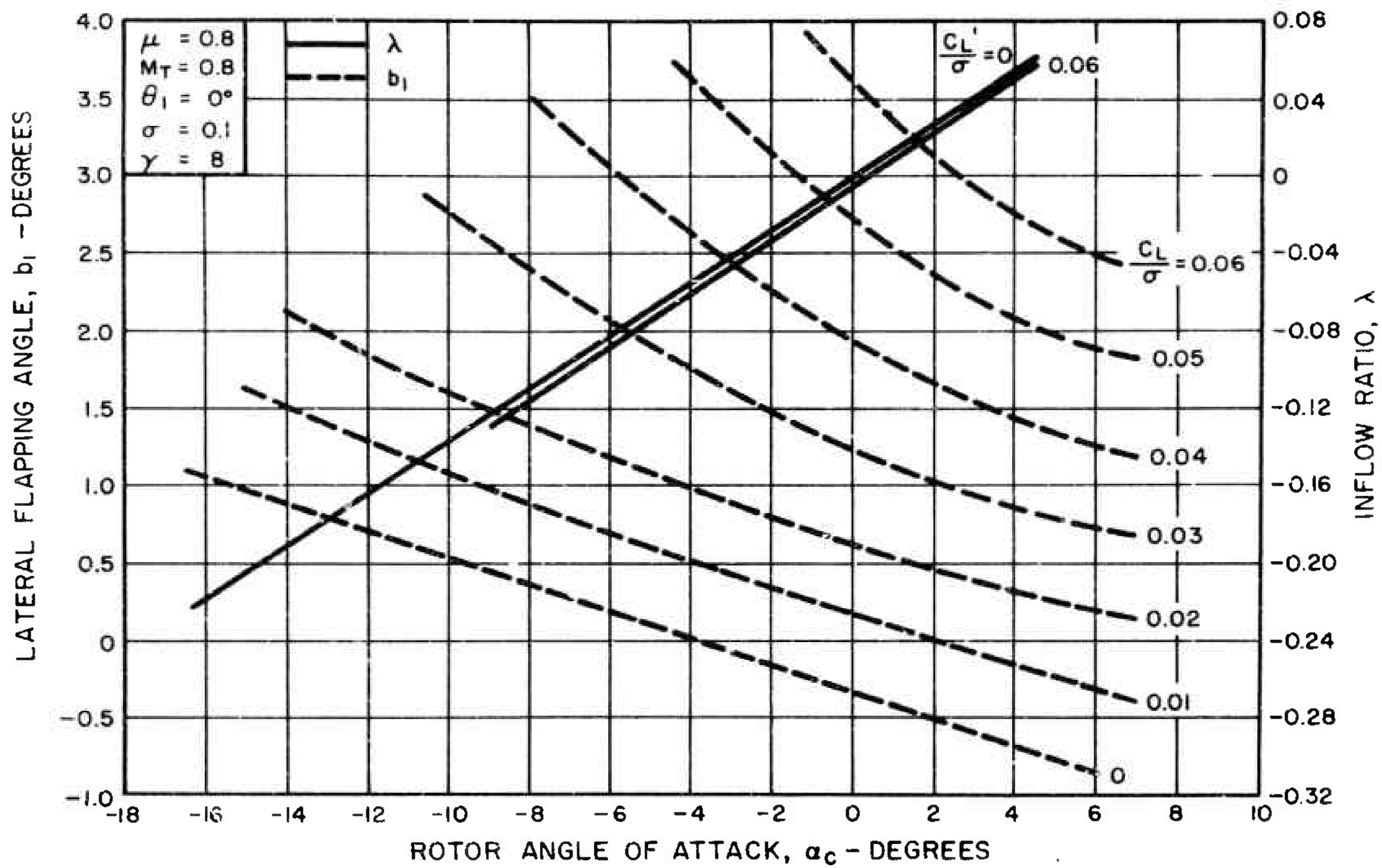

(b) b_1 and λ

Figure 8. Concluded.

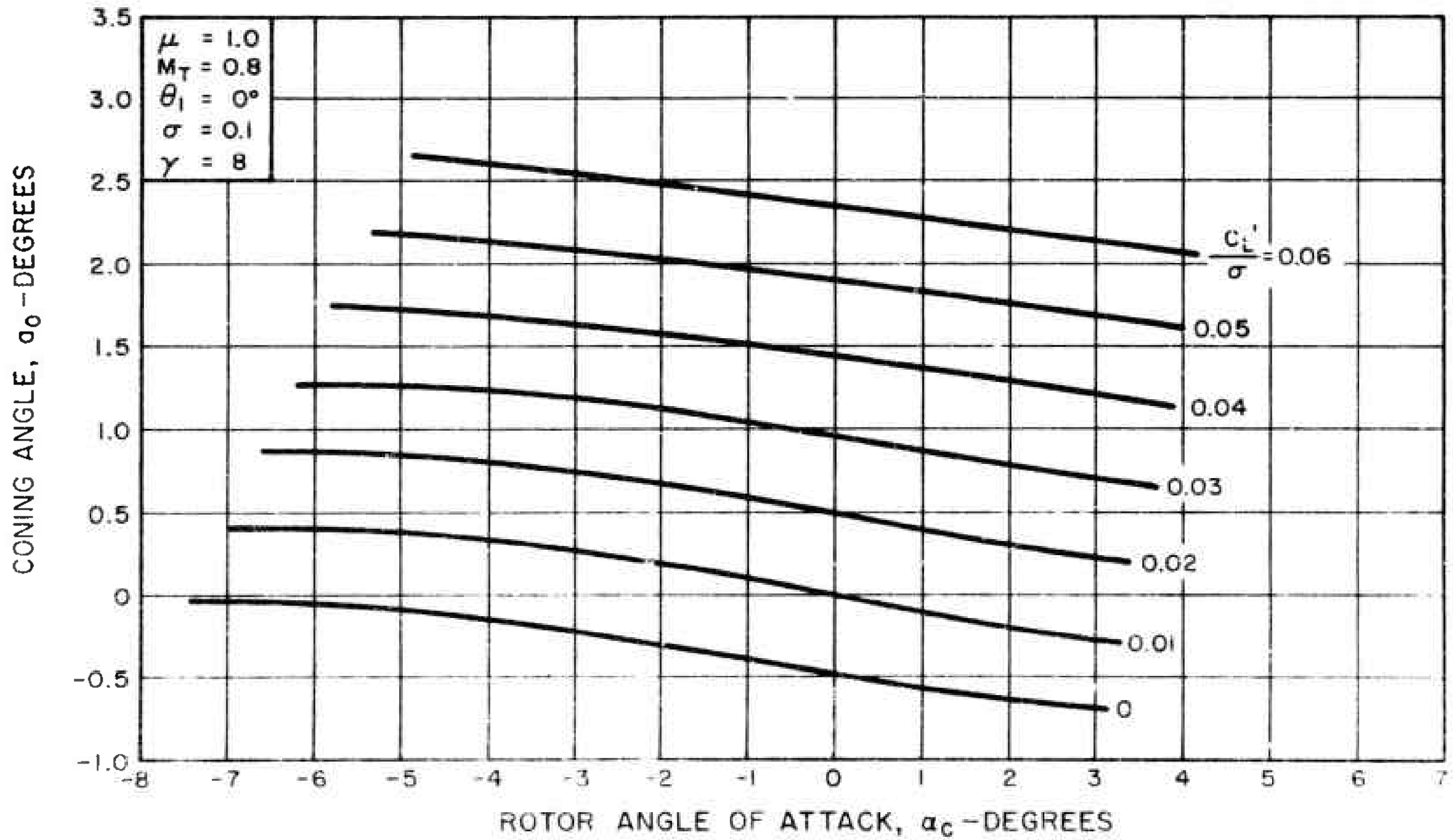

(a) a_0

Figure 9. Calculated Characteristics of a Rotor With 0° Twist For μ = 1.0 and M_T = 0.8.

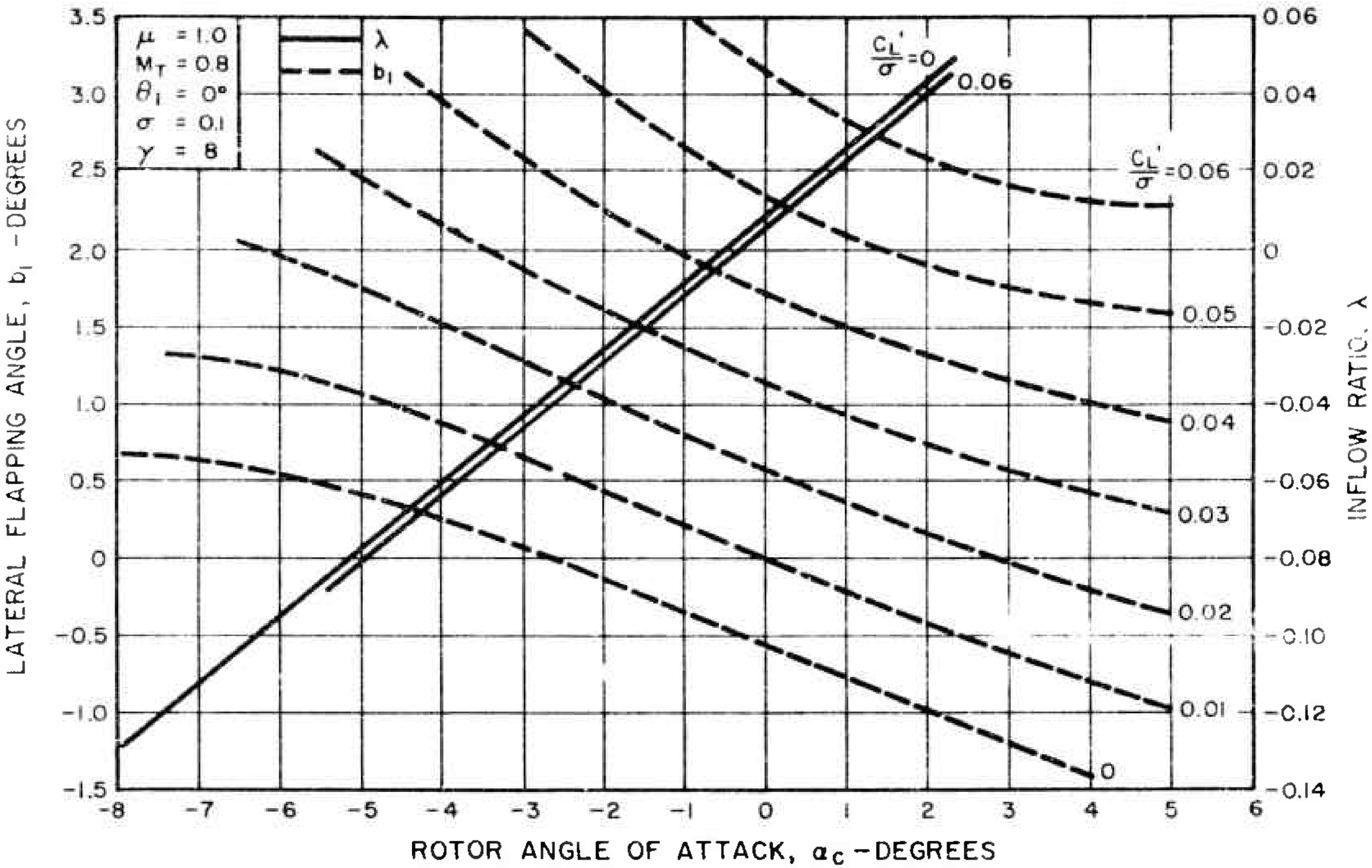

(b) b_1 and λ

Figure 9. Concluded.

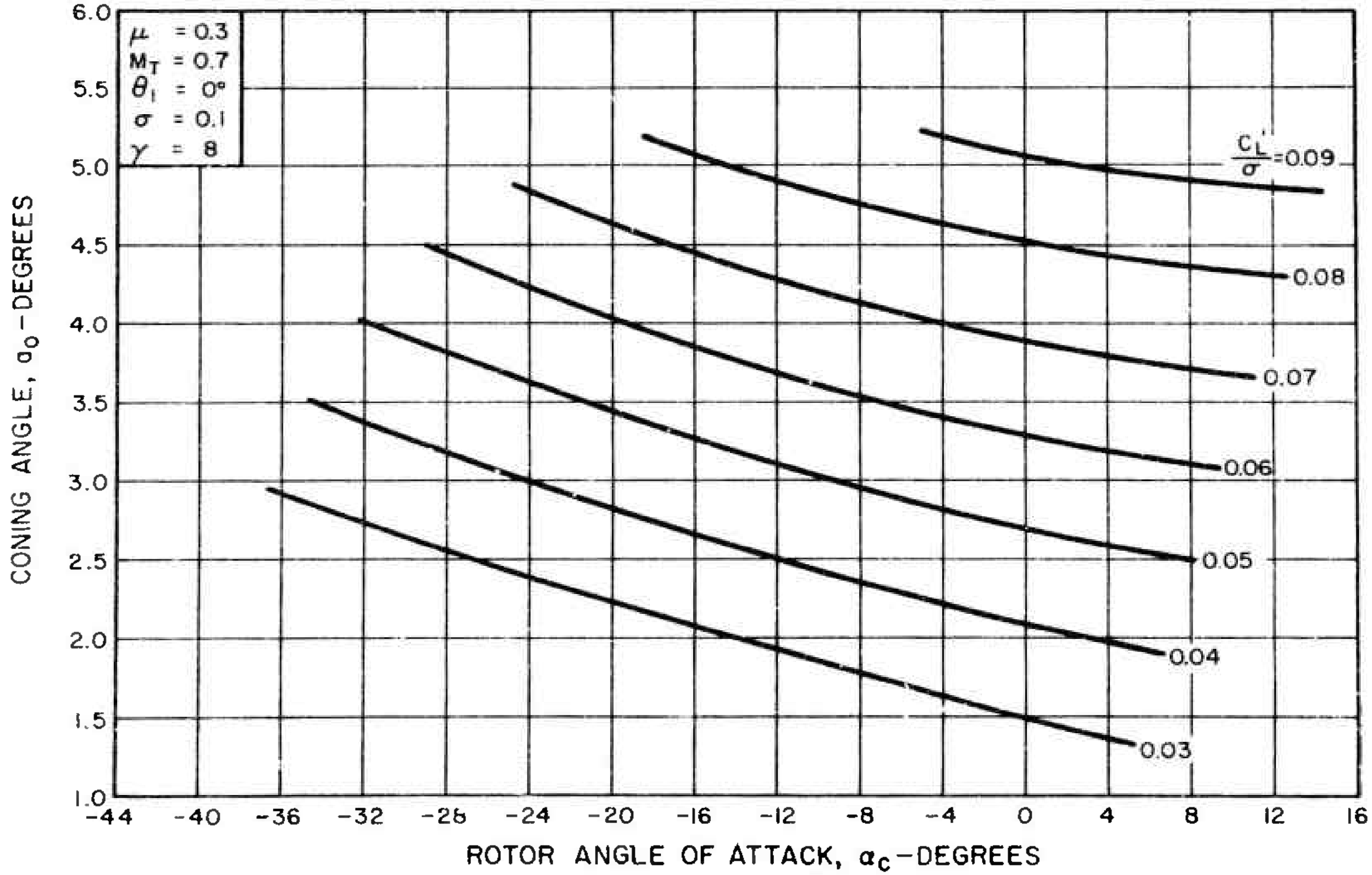

(a) a_o

Figure 10. Calculated Characteristics of a Rotor With 0^o Twist for μ = 0.3 and M_T = 0.7.

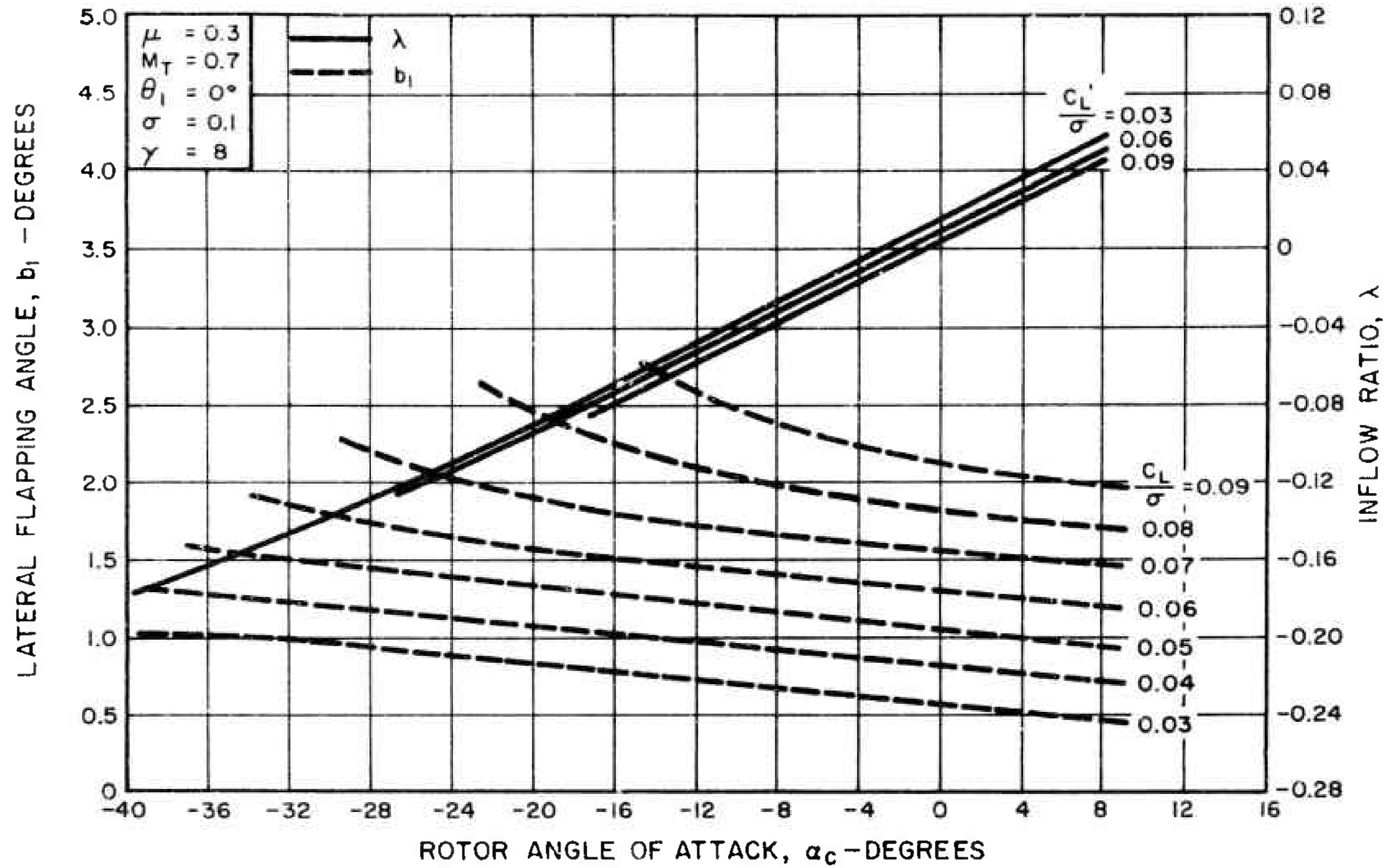

(b) b_1 and λ

Figure 10. Concluded.

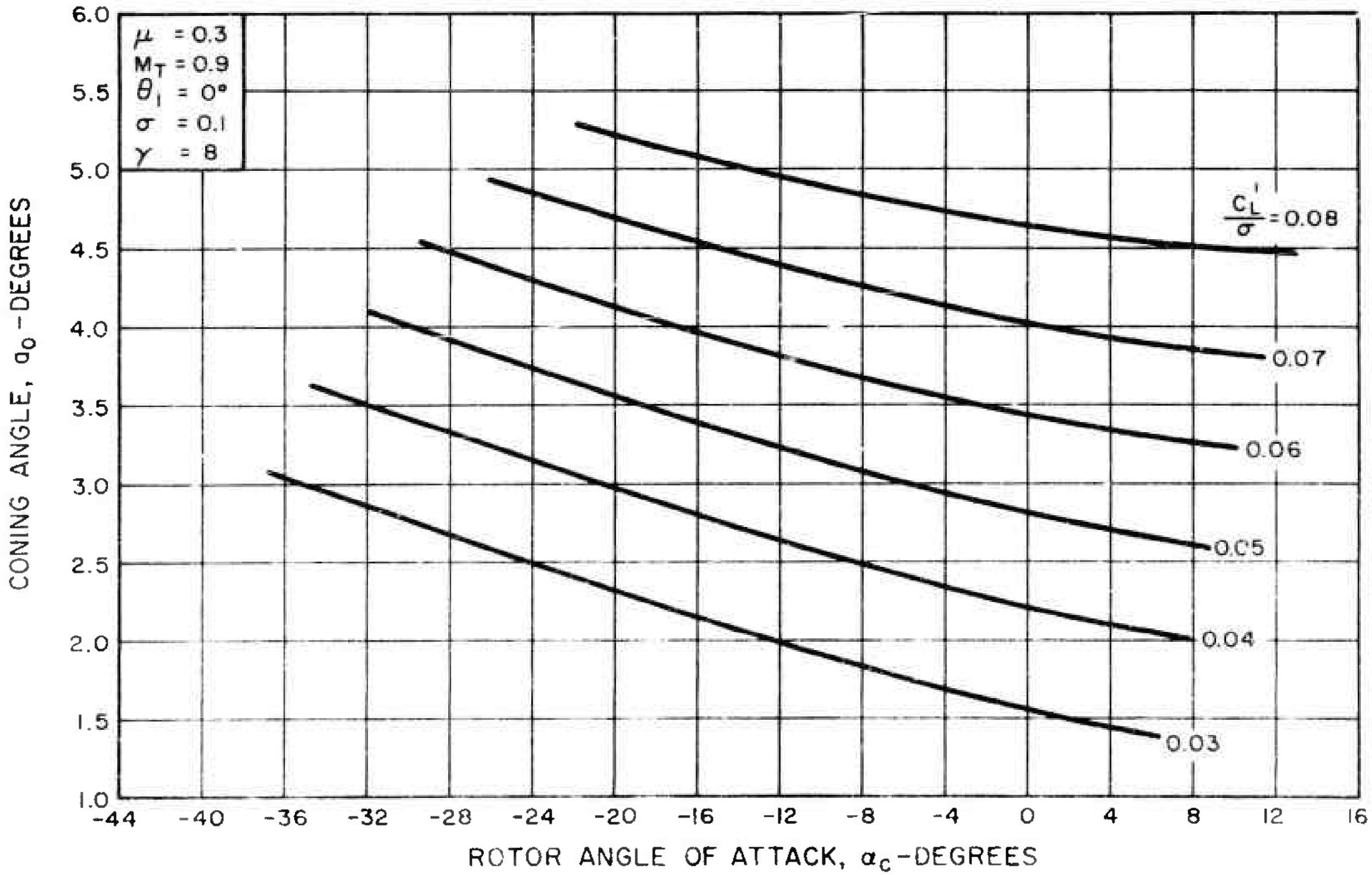

(a) a_0

Figure 11. Calculated Characteristics of a Rotor With 0° Twist for $\mu = 0.3$ and $M_T = 0.9$

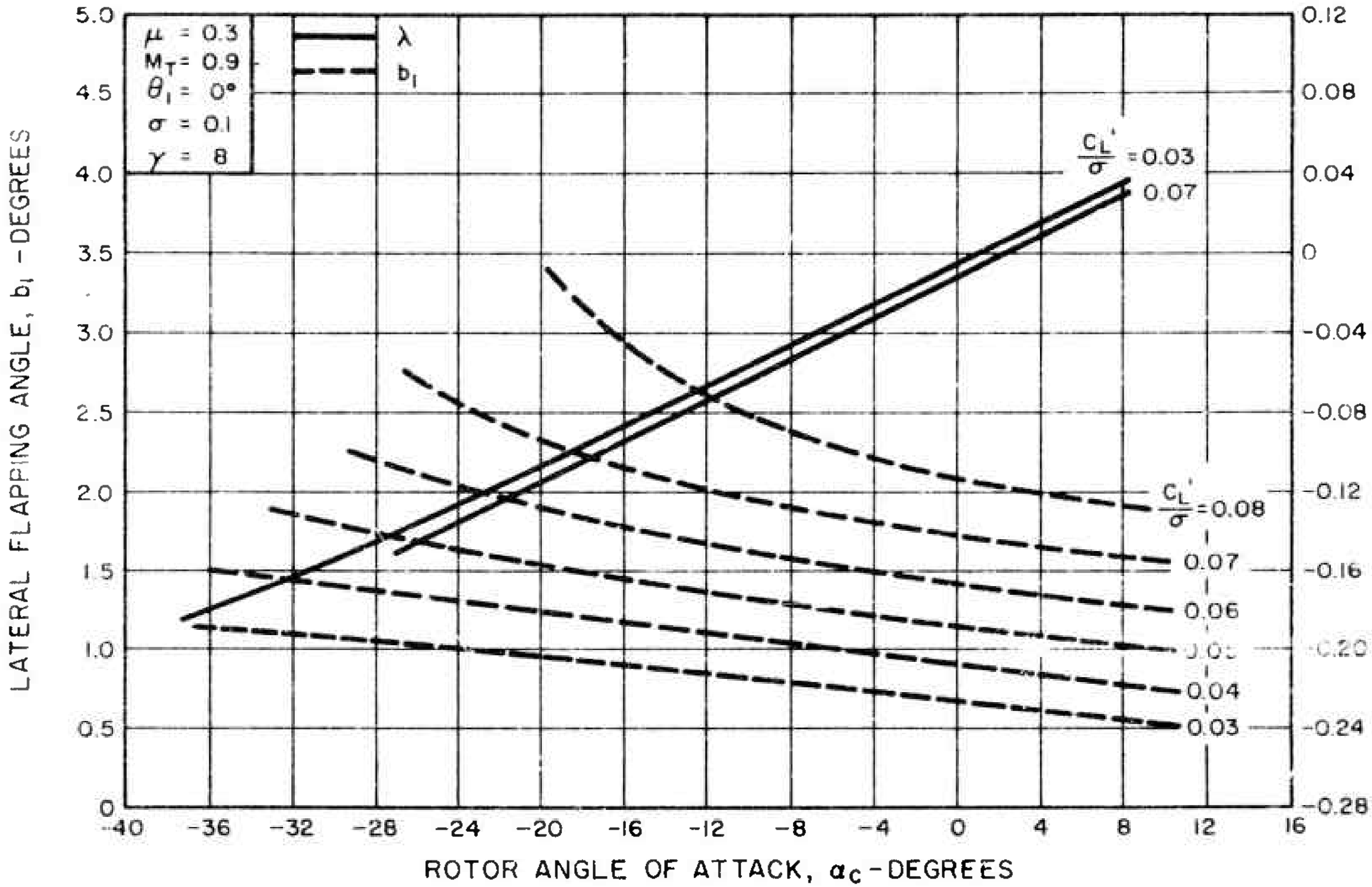

(b) b_1 and λ

Figure 11. Concluded.

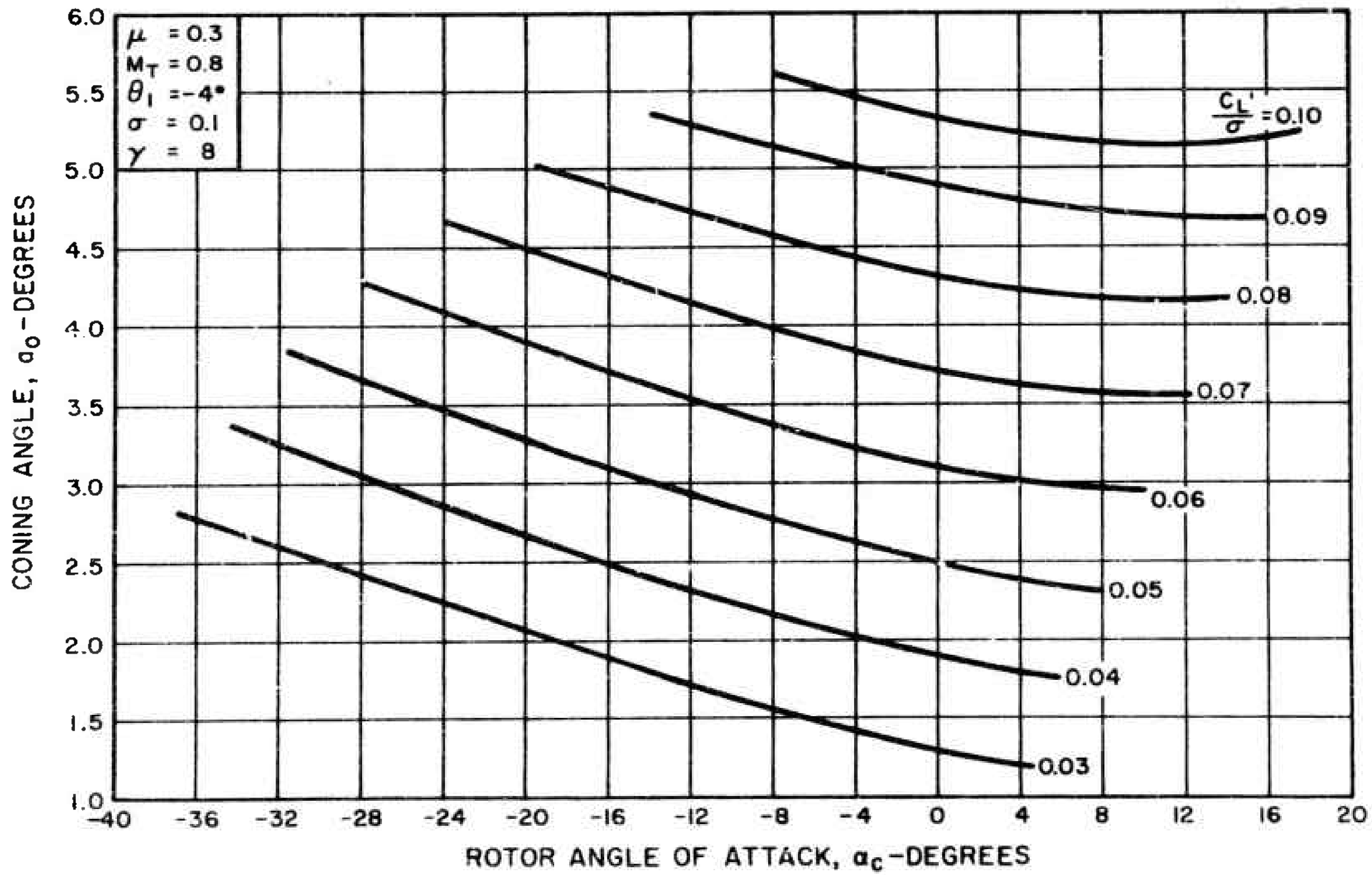

(a) a_0

Figure 12. Calculated Characteristics of a Rotor With -4° Twist for μ = 0.3 and M_T = 0.8.

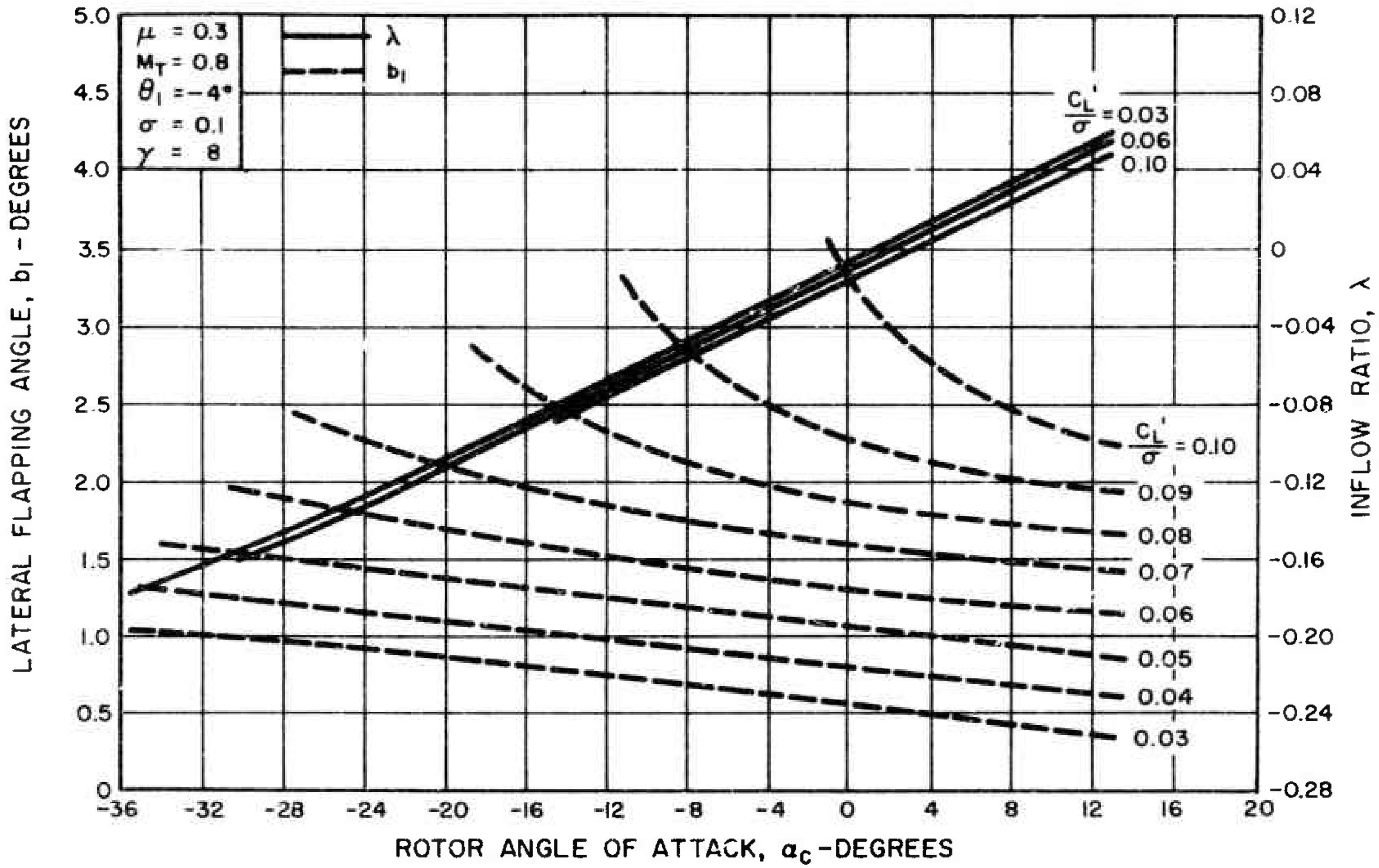

(b) b_1 and λ

Figure 12. Concluded.

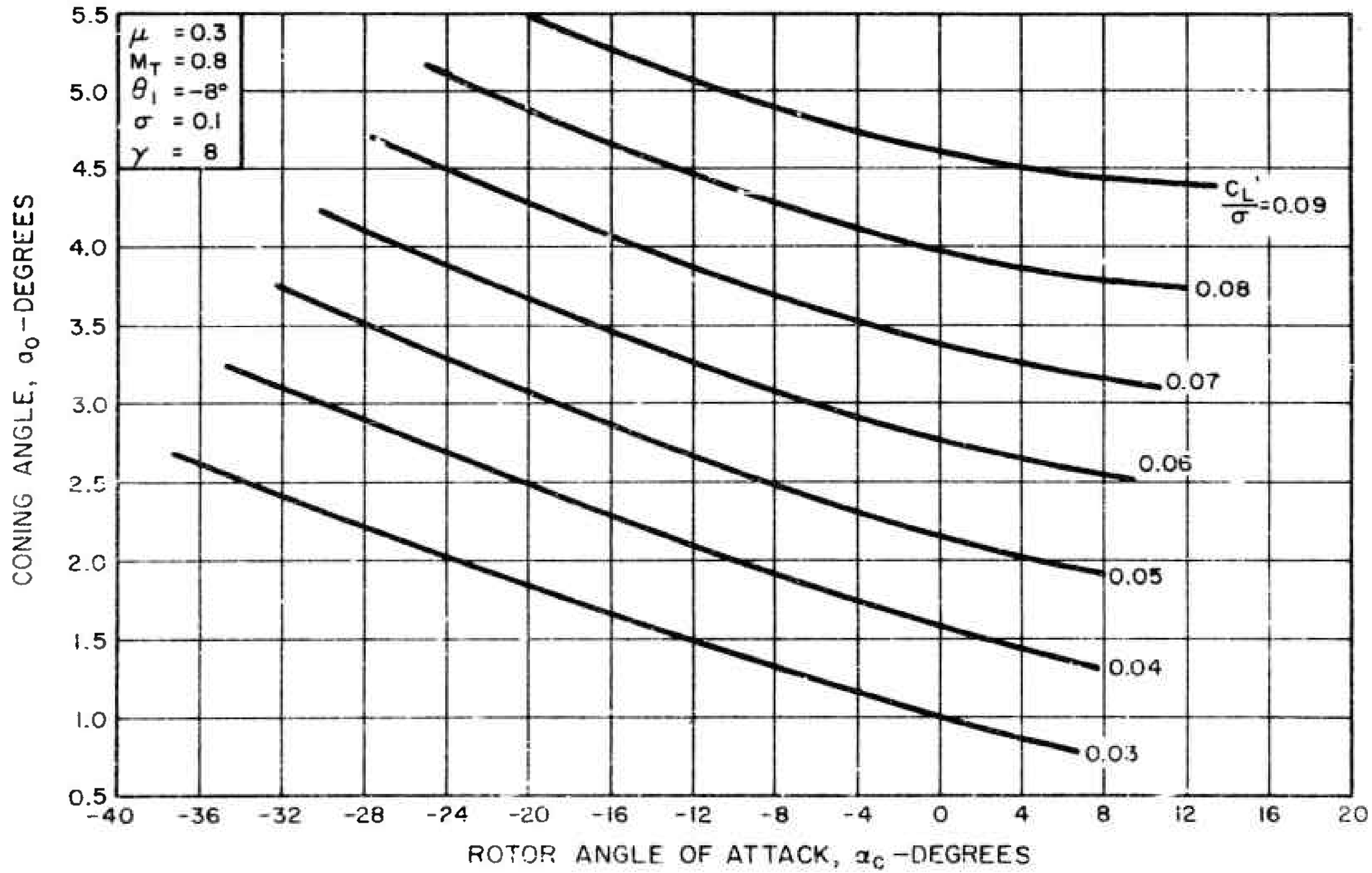

(a) a_0

Figure 13. Calculated Characteristics of a Rotor With -8° Twist for μ = 0.3 and M = 0.8.

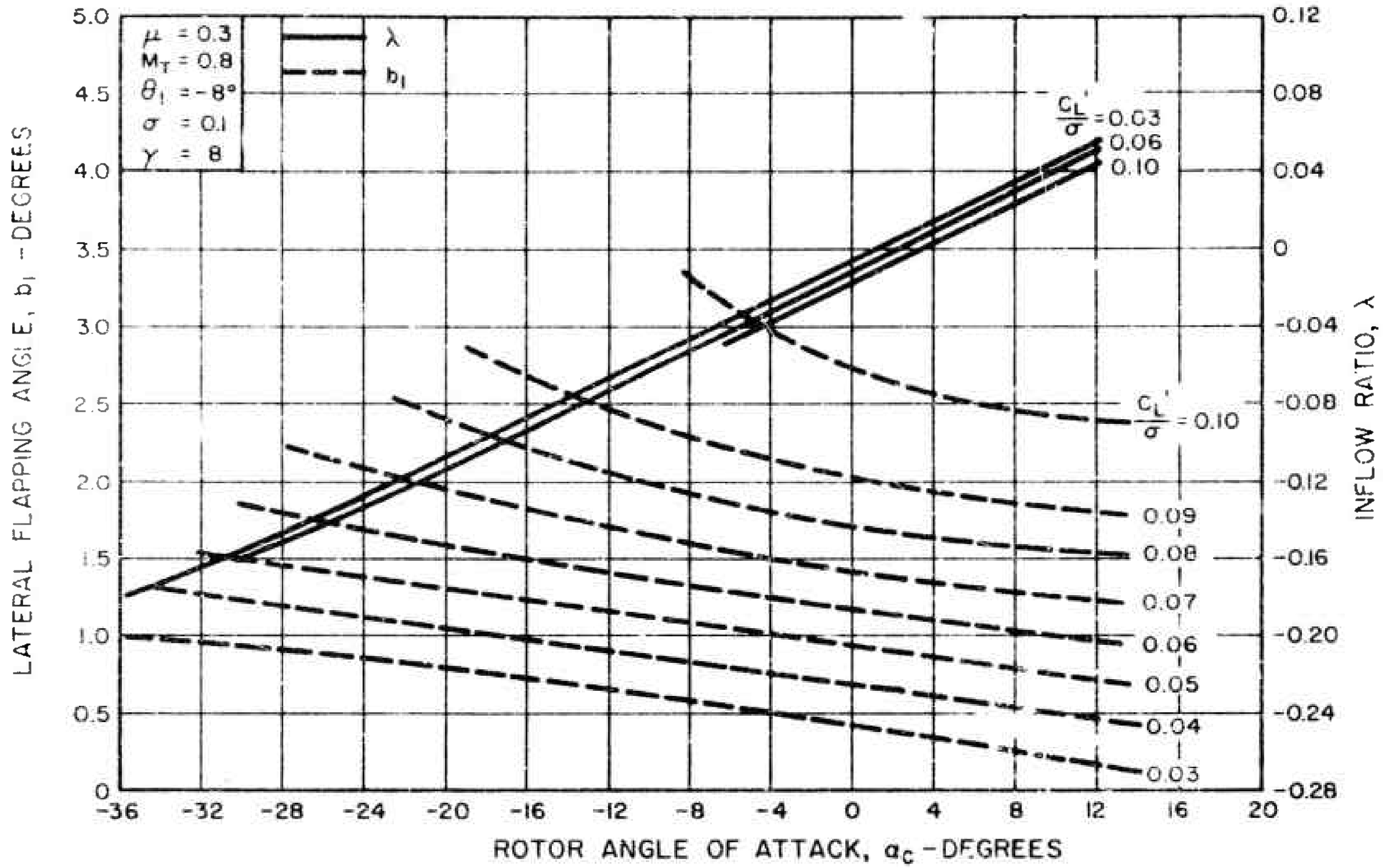

(b) b_1 and λ

Figure 13. Concluded.

LITERATURE CITED

1. Charles, Bruce D., and Tanner, Watson H., WIND TUNNEL INVESTIGATION OF SEMIRIGID FULL-SCALE ROTORS OPERATING AT HIGH ADVANCE RATIOS, Bell Helicopter Company; USAAVLABS Technical Report 69-2, U. S. Army Aviation Materiel Laboratories, Ft. Eustis, Virginia, January 1969, AD684396.

2. Reichert, G., and Oelker, P., HANDLING QUALITIES WITH THE BOLKOW RIGID ROTOR SYSTEM, Bolkow GmbH, Germany; paper presented at the 24th Annual National Forum of the American Helicopter Society, May 1968.

3. Reichert, G., FLUGMECHANISCHE BESONDERHEITEN DES GELENKLOSEN HUBSCHRAVBERROTORS, Wissenschaftl. Gesellschaft fur Luftund Raumfahrt (WGLR), Jahrbuch 1965 (translated by NASA - Langley Research Center).

4. Yntema, Robert T., SIMPLIFIED PROCEDURES AND CHARTS FOR THE RAPID ESTIMATION OF BENDING FREQUENCIES OF ROTATING BEAMS, Langley Aeronautical Laboratory; NACA Technical Note 3459, National Advisory Committee for Aeronautics, Langley Field, Virginia, June 1955.

5. Bailey, F. E., Jr., A SIMPLIFIED THEORETICAL METHOD OF DETERMINING CHARACTERISTICS OF A LIFTING ROTOR IN FORWARD FLIGHT, NACA Report No. 716, National Advisory Committee for Aeronautics (presently, National Aeronautics and Space Administration), Washington, D. C., 1941.

6. Gessow, A., and Crim, A. D., AN EXTENSION OF LIFTING ROTOR THEORY TO COVER OPERATIONS AT LARGE ANGLES OF ATTACK AND HIGH INFLOW CONDITIONS, NACA Technical Note TN-2665, National Advisory Committee for Aeronautics (presently, National Aeronautics and Space Administration), Washington, D. C., 1952.

7. Tanner, W. H., CHARTS FOR ESTIMATING ROTARY WING PERFORMANCE IN HOVER AND AT HIGH FORWARD SPEEDS, NASA Contractor Report CR-114, National Aeronautics and Space Administration, Washington, D. C., November 1964.

8. Tanner, W. H., TABLES FOR ESTIMATING ROTARY WING PERFORMANCE AT HIGH FORWARD SPEEDS, NASA Contractor Report CR-115, National Aeronautics and Space Administration, Washington, D. C., November 1964.

9. STABILITY AND CONTROL HANDBOOK FOR HELICOPTERS, TRECOM Report 60-43, U. S. Army Transportation Research Command (presently, U. S. Army Aviation Materiel Laboratories), Fort Eustis, Virginia, August 1960.

5.3 FUSELAGE CHARACTERISTICS

Typical compound helicopter fuselages are of shapes which do not lend themselves easily to theoretical aerodynamic analysis. It is necessary, therefore, to rely on experimental data for accurate determination of fuselage characteristics. As an aid for preliminary stability calculations, some of the published helicopter fuselage experimental data are summarized in this section. The data have been rearranged to be consistent with the nomenclature of this handbook.

The following characteristics must be determined:

Fuselage Drag Coefficient

$$C_{D_{FUS}} = \frac{D_{FUS}}{q_0 A_{X_{FUS}}}$$

Fuselage Lift Coefficient

$$C_{L_{FUS}} = \frac{L_{FUS}}{q_0 A_{Z_{FUS}}}$$

Fuselage Side Force Coefficient

$$C_{Y_{FUS}} = \frac{Y_{FUS}}{q_0 A_{Y_{FUS}}}$$

Fuselage Pitching Moment Coefficient

$$C_{M_{FUS}} = \frac{M_{FUS}}{q_0 A_{X_{FUS}} \ell_{FUS}}$$

Fuselage Yawing Moment Coefficient

$$C_{N_{FUS}} = \frac{N_{FUS}}{q_0 A_{X_{FUS}} \ell_{FUS}}$$

Fuselage Rolling Moment Coefficient

$$C_{\mathcal{L}_{FUS}} = \frac{\mathcal{L}_{FUS}}{q_0 \, A_{X_{FUS}} \, \ell_{FUS}}$$

Test data for several fuselages of small helicopters are presented in References 1 and 2. Reference 1 presents model data for all three force and three moment coefficients for a range of angles of attack and sideslip. Reference 2 presents the lift, drag, and pitching moment coefficients for two full-scale helicopters. The geometric characteristics of these fuselages are shown in Figures 1 and 2.

For fuselage shapes differing greatly from those described in this section, the methods in either Reference 3 or Reference 4 can be used to obtain the required characteristics.

5.3.1 Drag Coefficient

The variation of the drag coefficient with angle of attack at $\beta_S = 0$ is shown in Figure 3. It is noted from Figure 3 that $C_{D_{FUS}}$ is relatively constant with α_{FUS} for the model fuselages, Models A through D. It is also seen that the small-scale fuselages are aerodynamically substantially cleaner than the full-scale fuselages, Model E and F.

The relationship between drag coefficient and equivalent flat plate drag area is as follows:

$$S_{FUS} = C_{D_{FUS}} A_{X_{FUS}} \quad ft^2$$

5.3.2 Lift Coefficient

The variation of lift coefficient with angle of attack at $\beta_S = 0$ is shown in Figure 4. The fuselage download factor, K_V, is related to the lift coefficient as follows:

$$K_V = \frac{q_0 \, C_{L_{FUS}} \, A_{Z_{FUS}}}{W}$$

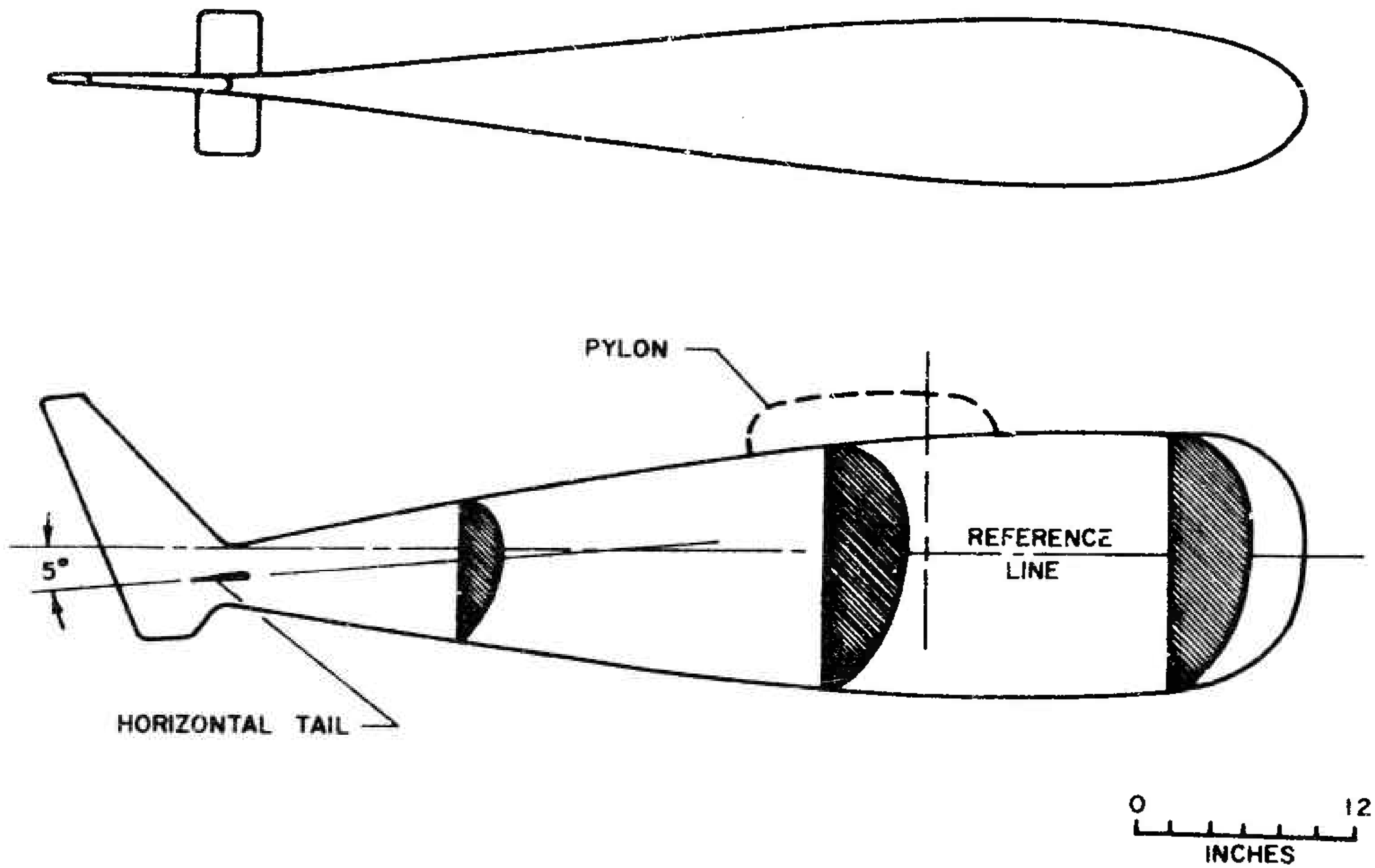

(a) MODEL A

Figure 1. Geometric Characteristics of Four Single-Rotor Helicopter Fuselage Models. (Reference 1)

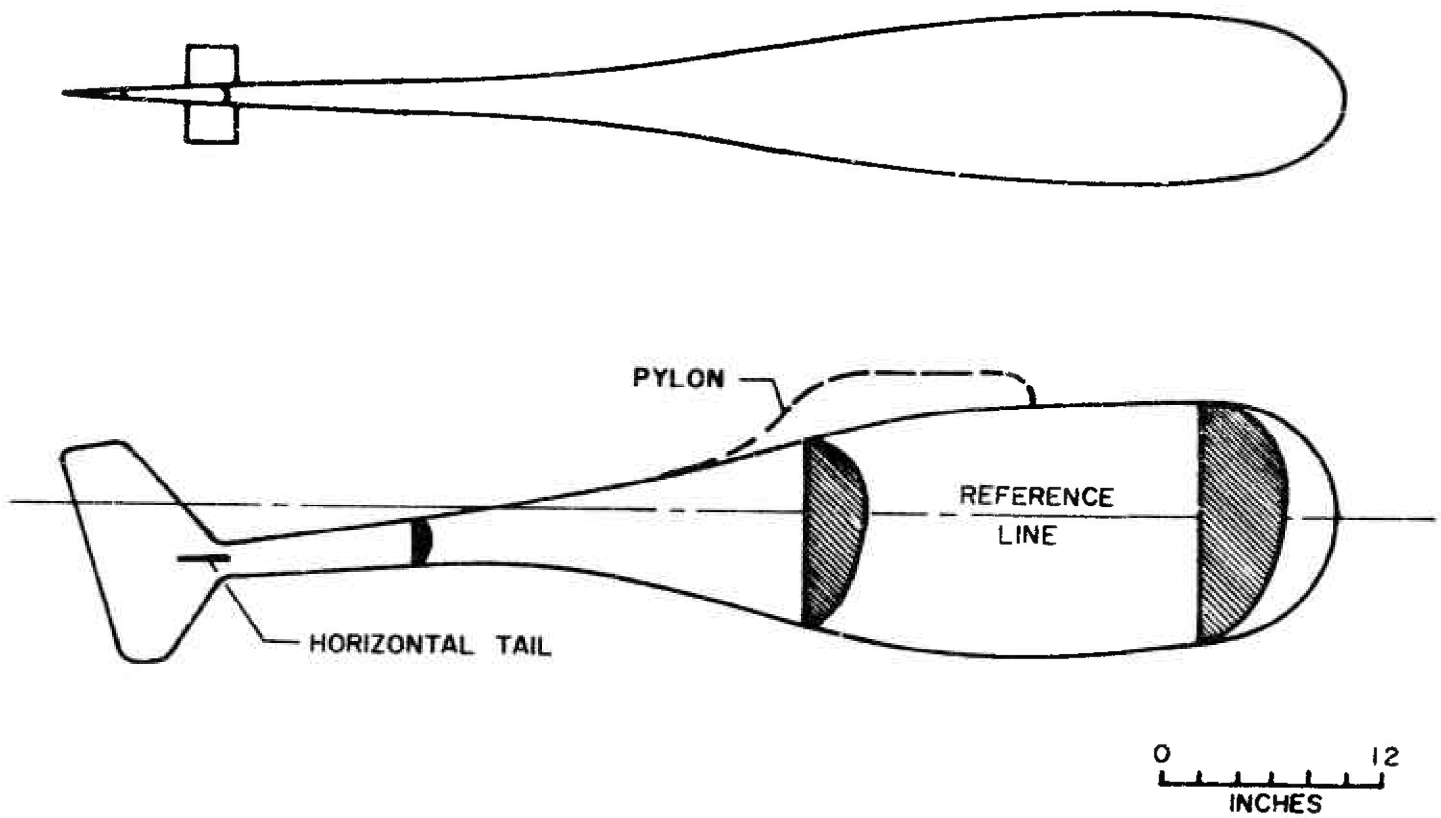

(b) MODEL B

Figure 1. Continued

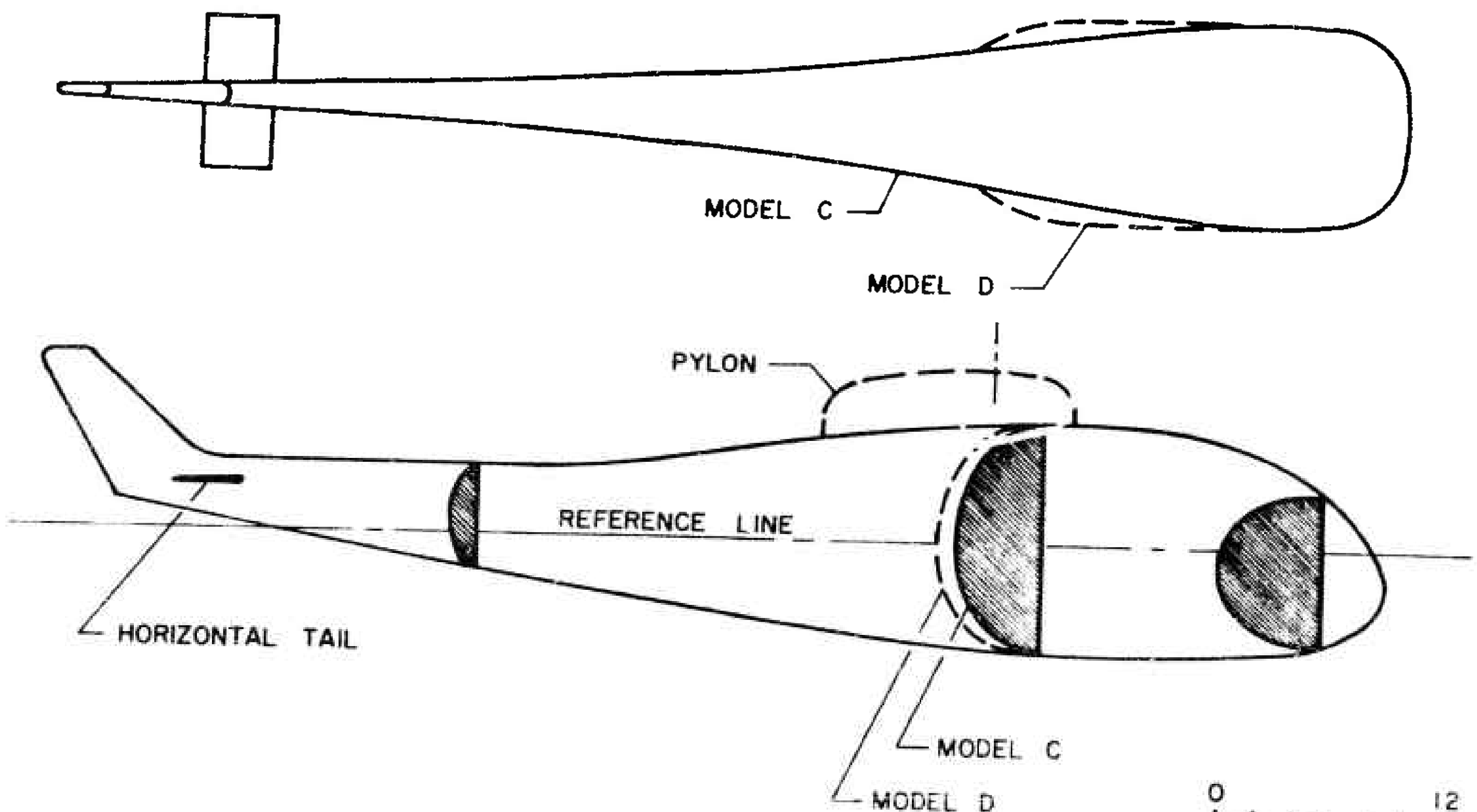

(c) MODELS C AND D

Figure 1. Concluded.

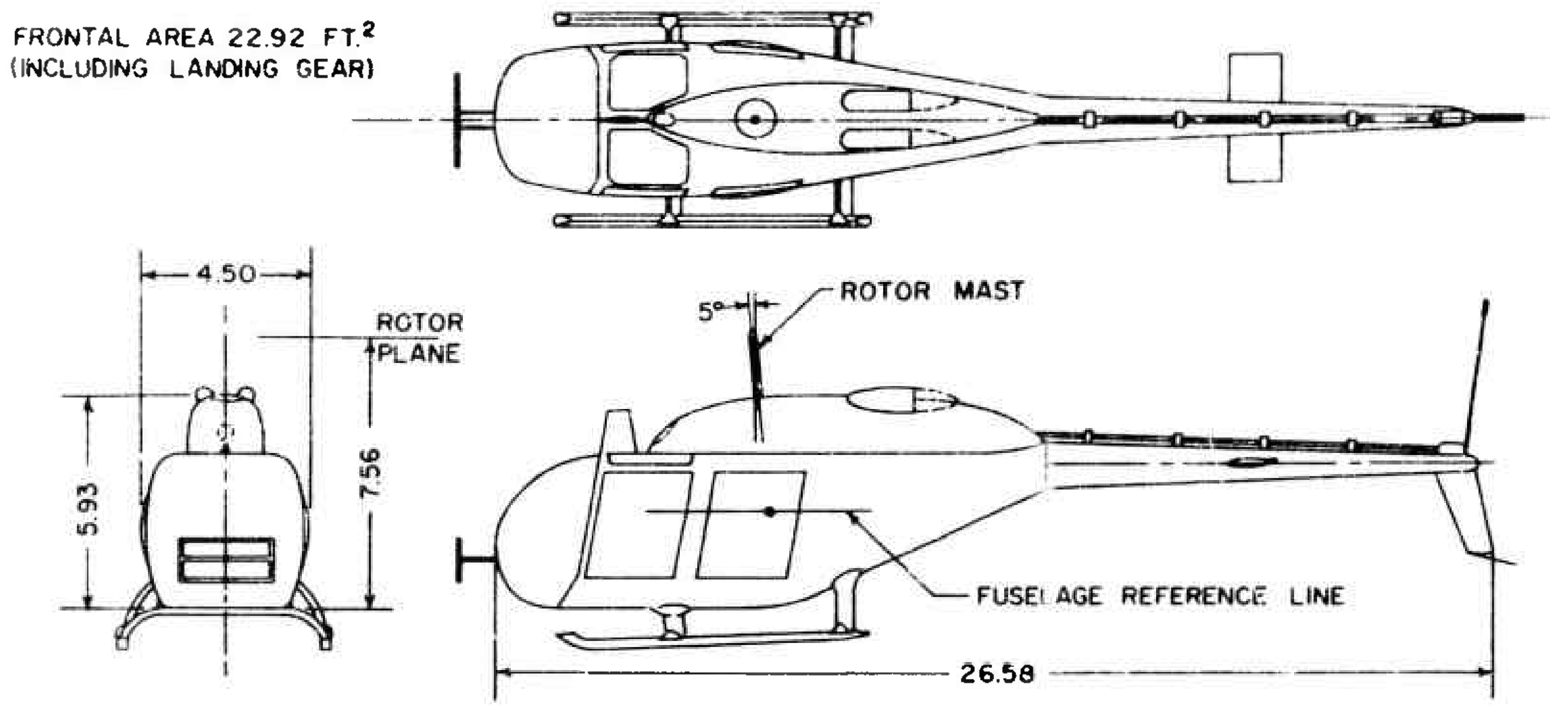

(ALL DIMENSIONS IN FEET)

Figure 2. Geometric Characteristics of Two Full-Scale Single-Rotor Helicopter Fuselages. (Reference 2)

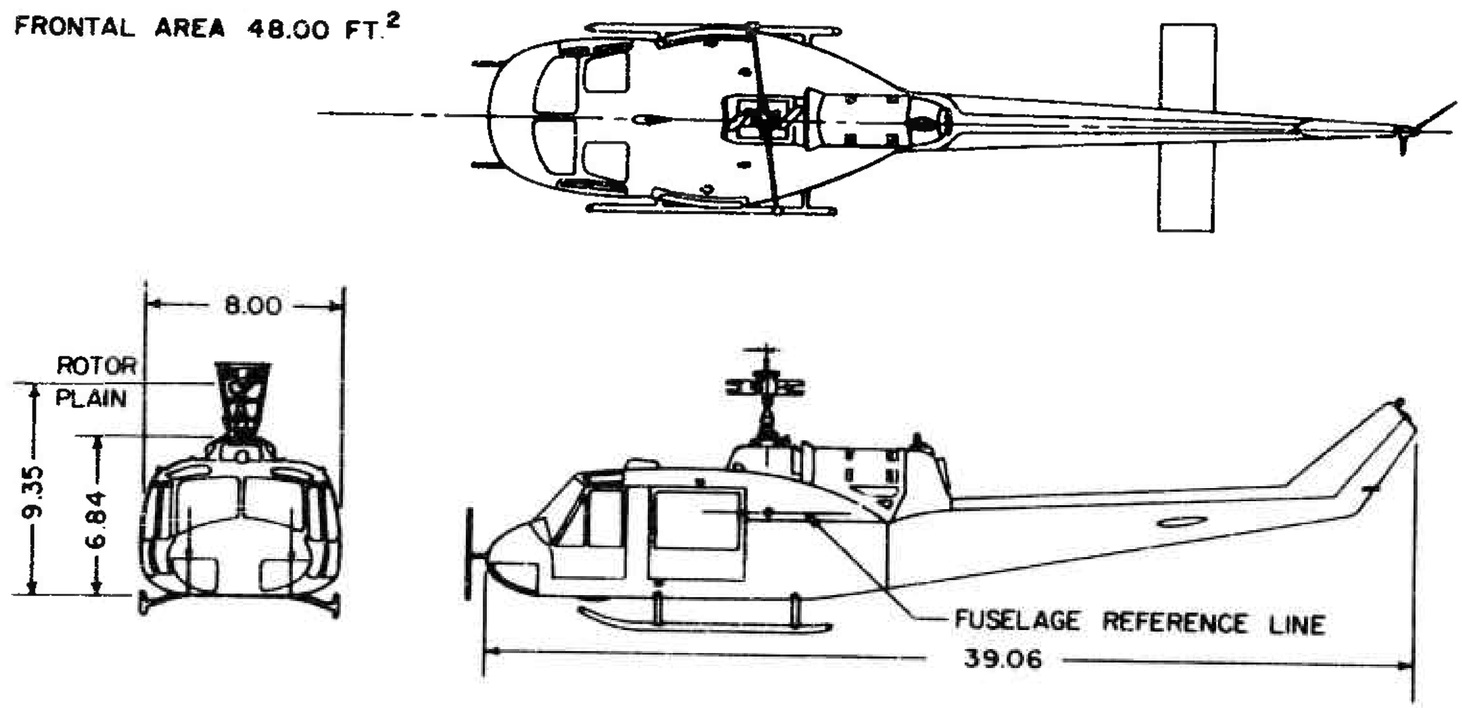

(ALL DIMENSIONS IN FEET)

Figure 2. Concluded.

5.3.3 Y-Force Coefficient

The variation of Y-Force Coefficient with angle of attack at $\beta_S = 0$ is shown in Figure 5. No $C_{Y_{FUS}}$ data were available for the full-scale helicopter fuselages of Reference 2. Figure 6 though 9 present $C_{Y_{FUS}}$ data for Models A through D, respectively, as a function of β_S for several values of α_{FUS}.

5.3.4 Pitching Moment Coefficient

The variation of pitching moment coefficient with angle of attack at $\beta_S = 0$ is shown in Figure 10 for all six models.

5.3.5 Rolling Moment Coefficient

The variation of rolling moment coefficient with angle of attack at $\beta_S = 0$ for the four fuselage models is shown in Figure 11. The variation of rolling moment coefficient $C_{\ell_{FUS}}$ with sideslip is shown in Figures 12 through 15.

5.3.6 Yawing Moment Coefficient

The variation of yawing moment coefficient, with angle of attack at $\beta_S = 0$ for the four fuselage models is shown in Figure 16. The variation of yawing moment coefficient $C_{N_{FUS}}$ with sideslip is shown in Figures 17 through 20.

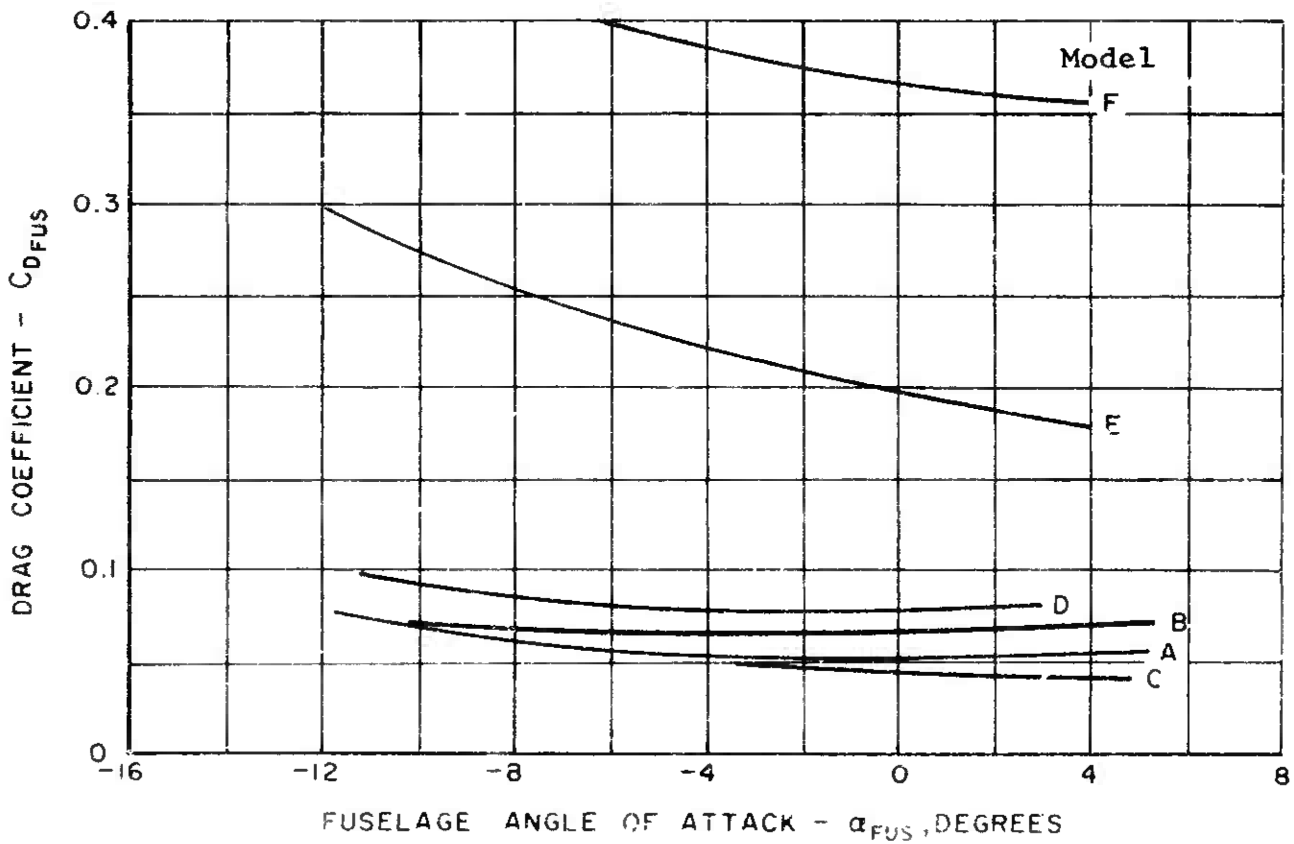

Figure 3. Drag Coefficients for Several Single-Rotor Helicopter Fuselages Versus Fuselage Angle of Attack for $\beta_S = 0$.

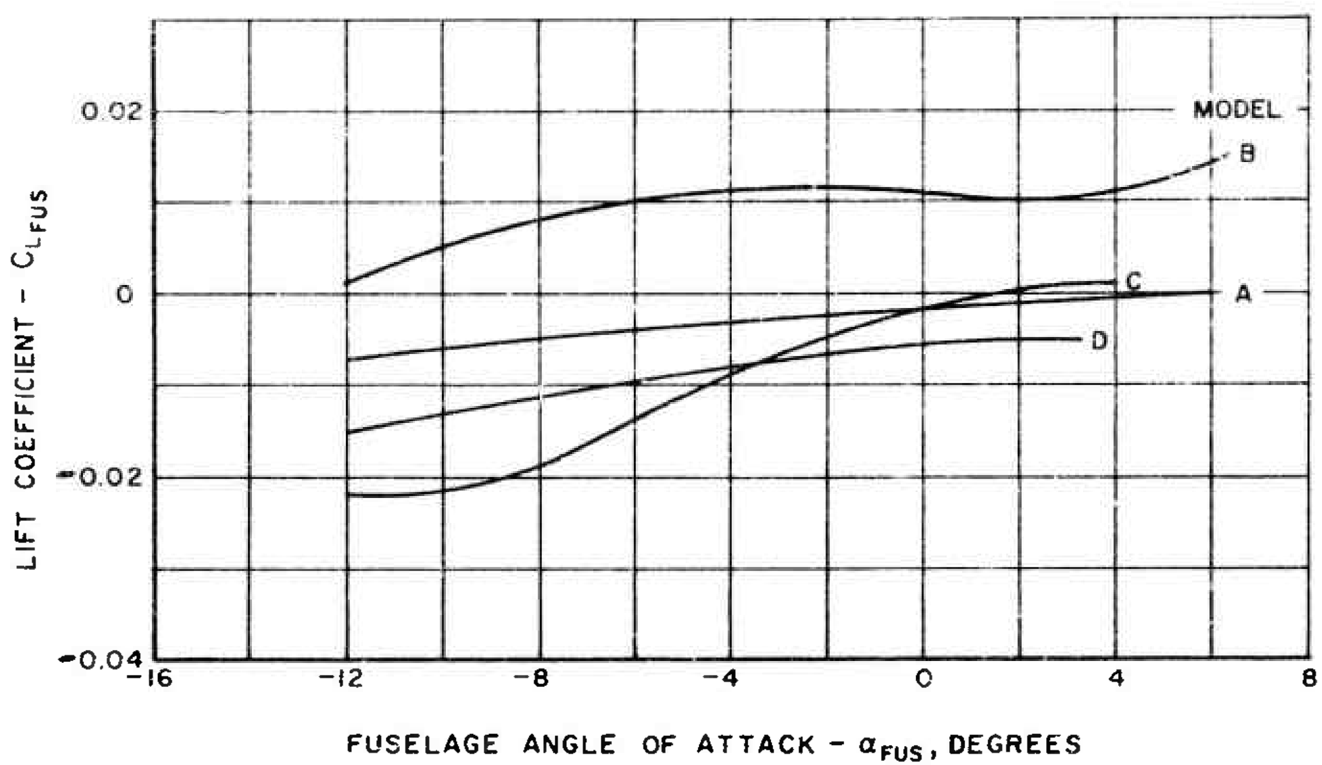

Figure 4. Lift Coefficients for Several Single-Rotor Helicopter Fuselages Versus Fuselage Angle of Attack for $\beta_S = 0$.

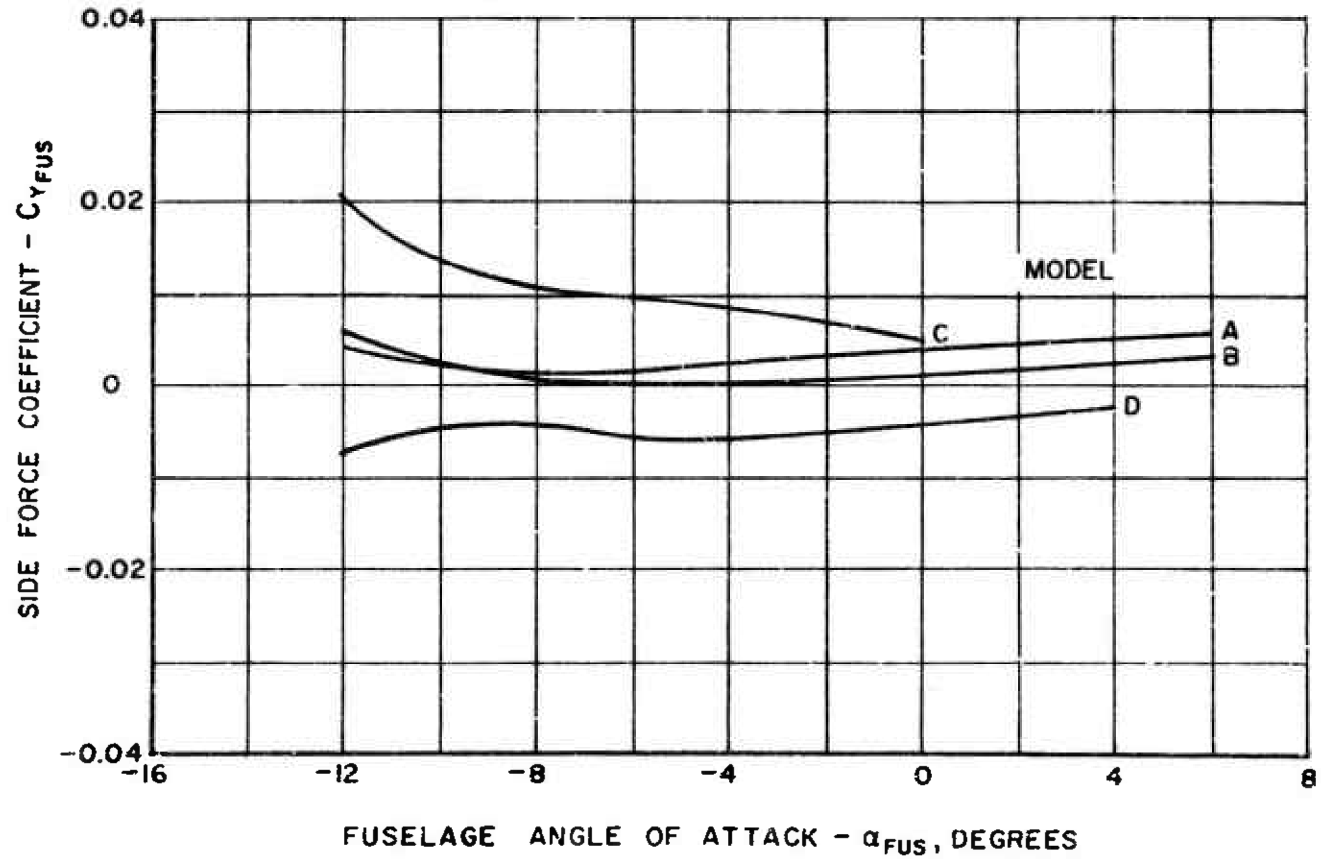

Figure 5. Side Force Coefficient for Several Single-Rotor Helicopter Fuselages Versus Fuselage Angle of Attack for $\beta_s = 0$.

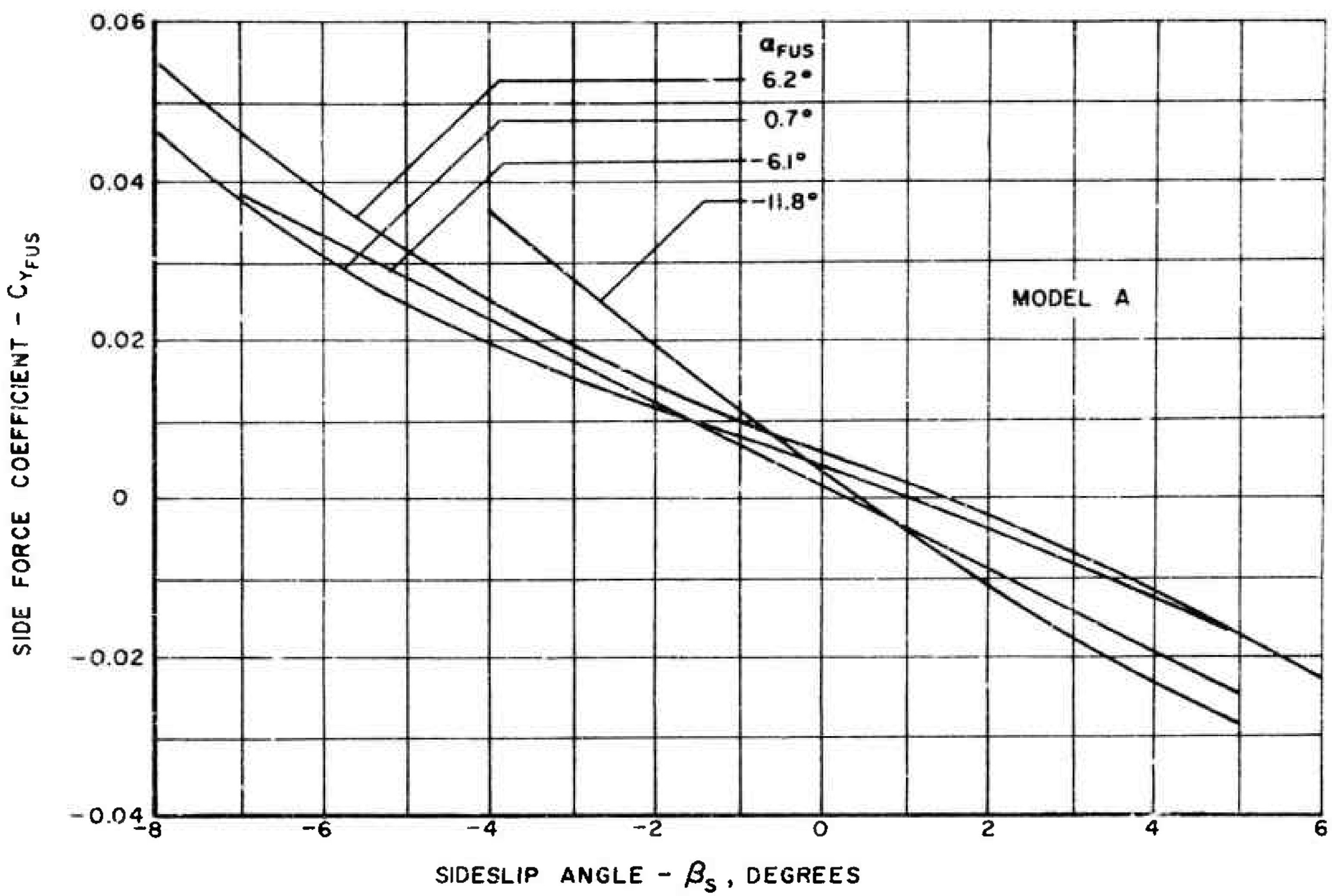

Figure 6. Side Force Coefficient Versus Sideslip Angle, β_S, for Constant Values of α_{FUS} - Model A.

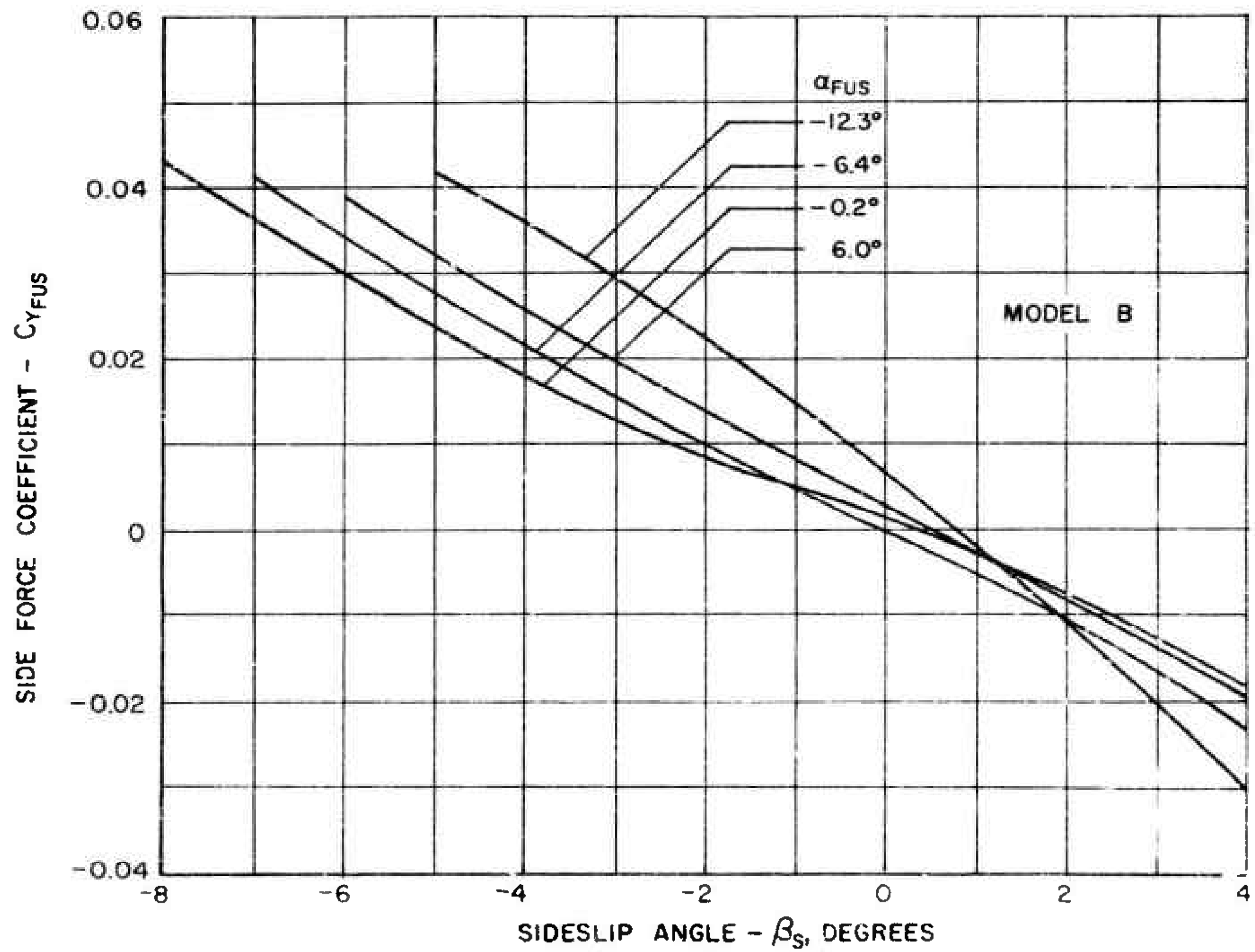

Figure 7. Side Force Coefficient Versus Sideslip Angle, β_S, for Constant Values of α_{FUS} - Model B.

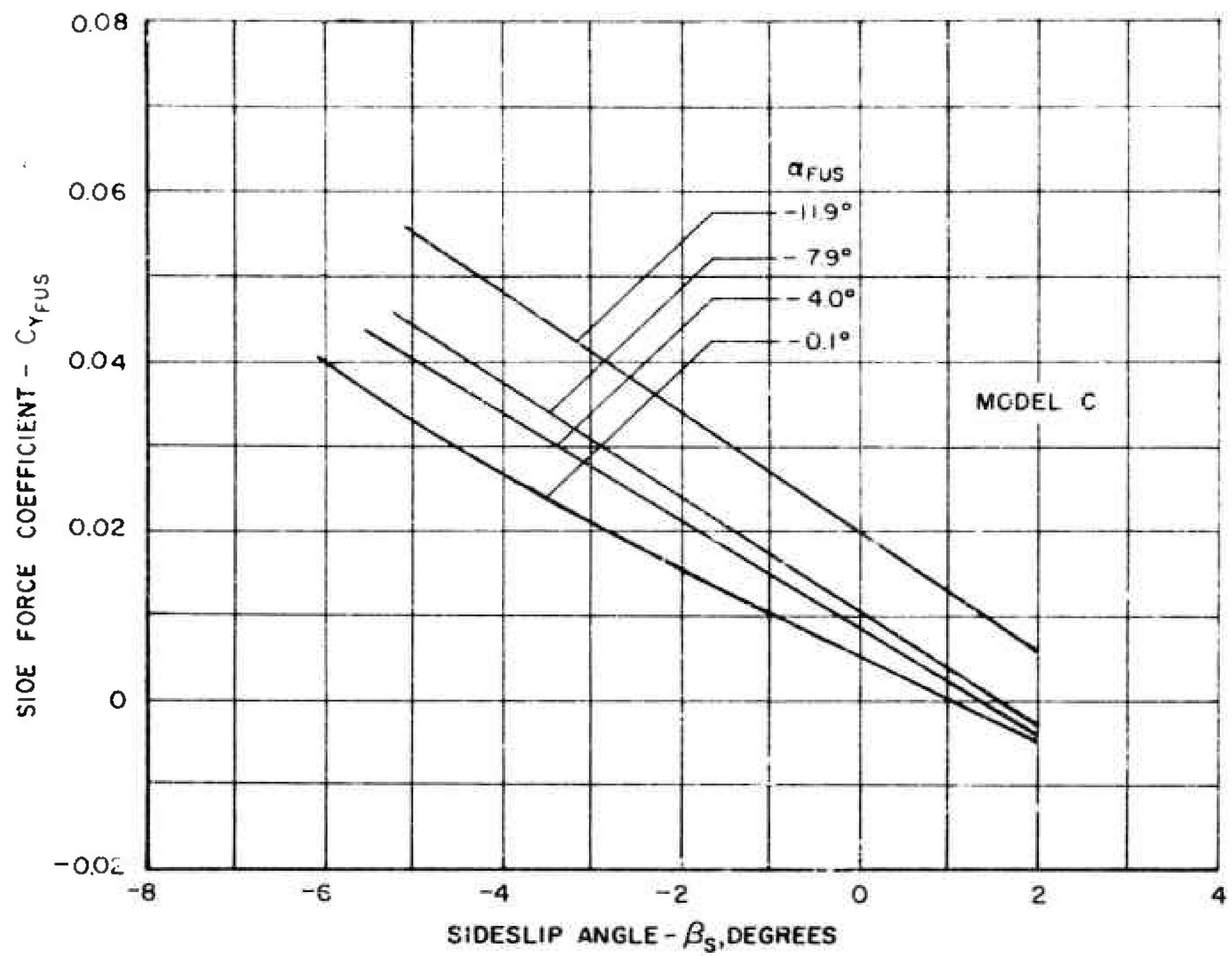

Figure 8. Side Force Coefficient Versus Sideslip Angle, β_S, for Constant Values of α_{FUS} - Model C.

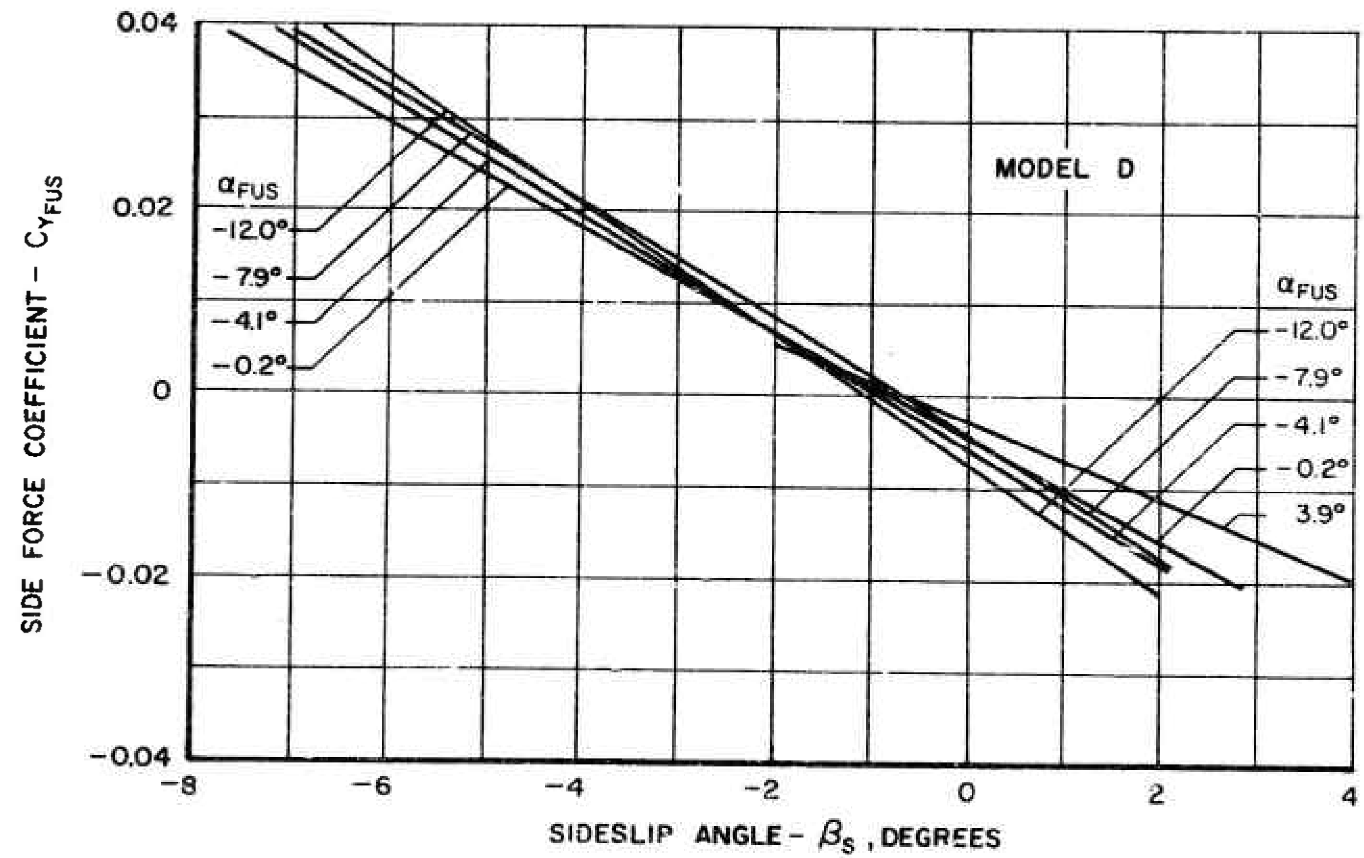

Figure 9. Side Force Coefficient Versus Sideslip Angle, β_S, for Constant Values of α_{FUS} - Model D.

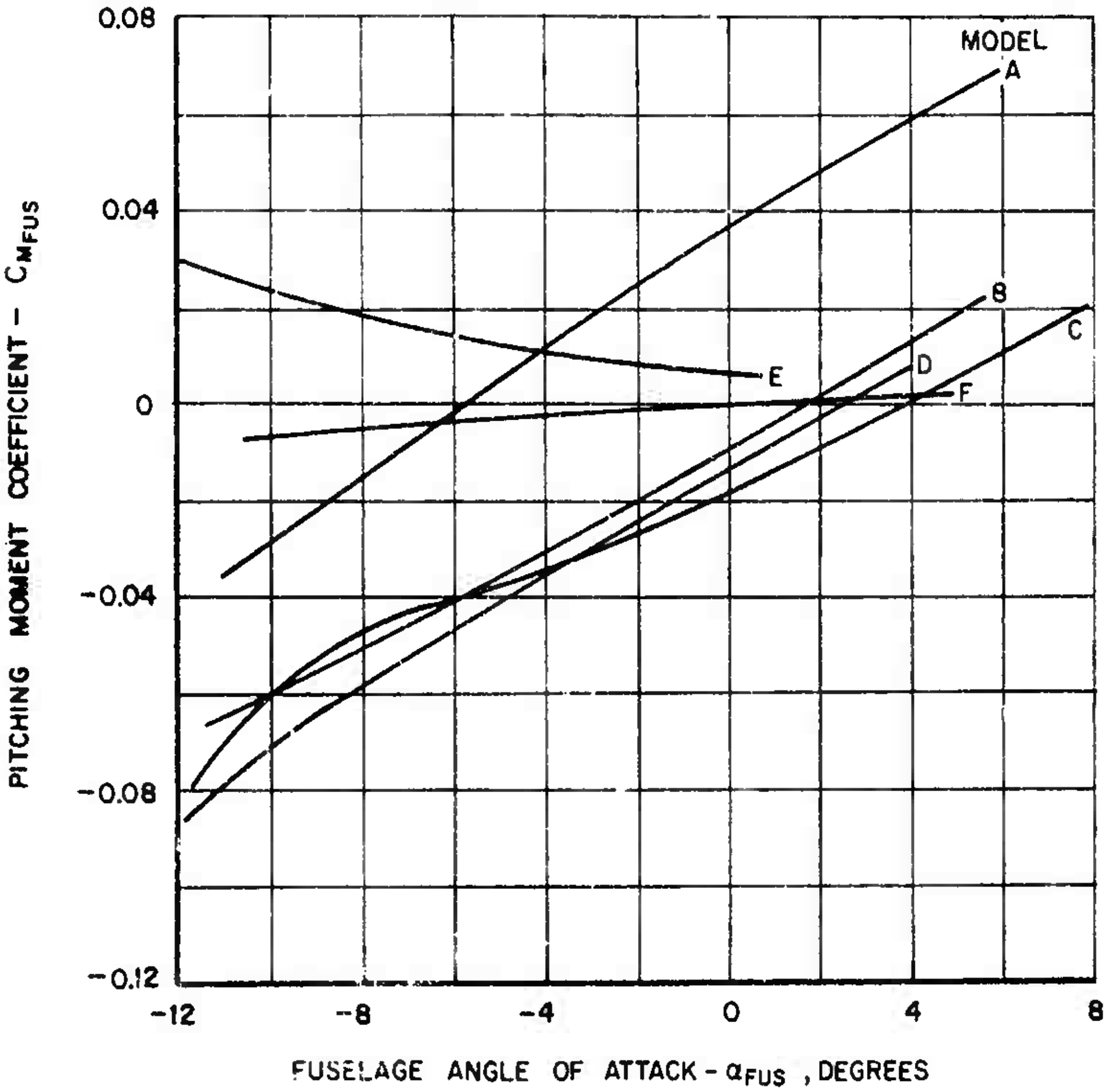

Figure 10. Pitching Moment Coefficient for Several Single-Rotor Helicopter Fuselages Versus Fuselage Angle of Attack For $\beta_S = 0$.

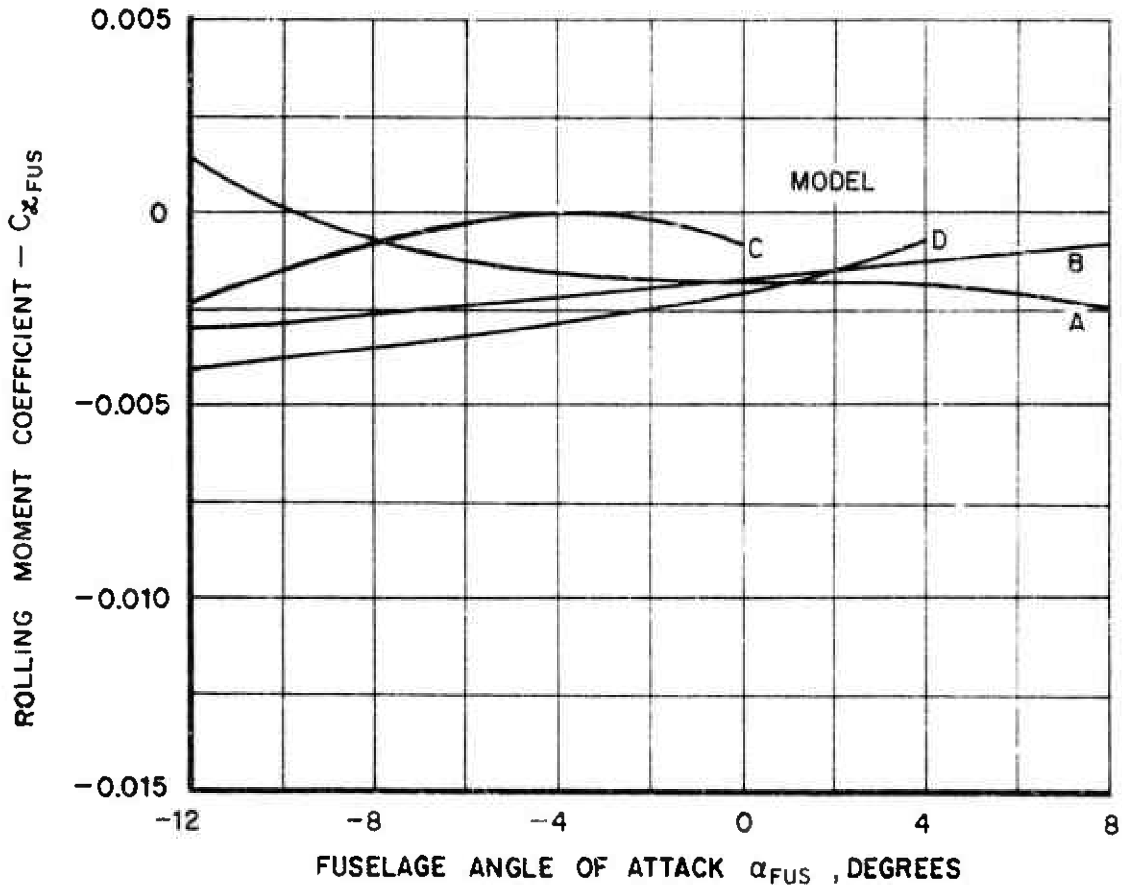

Figure 11. Rolling Moment Coefficient for Several Single-Rotor Helicopter Fuselages Versus Fuselage Angle of Attack for $\beta_S = 0$.

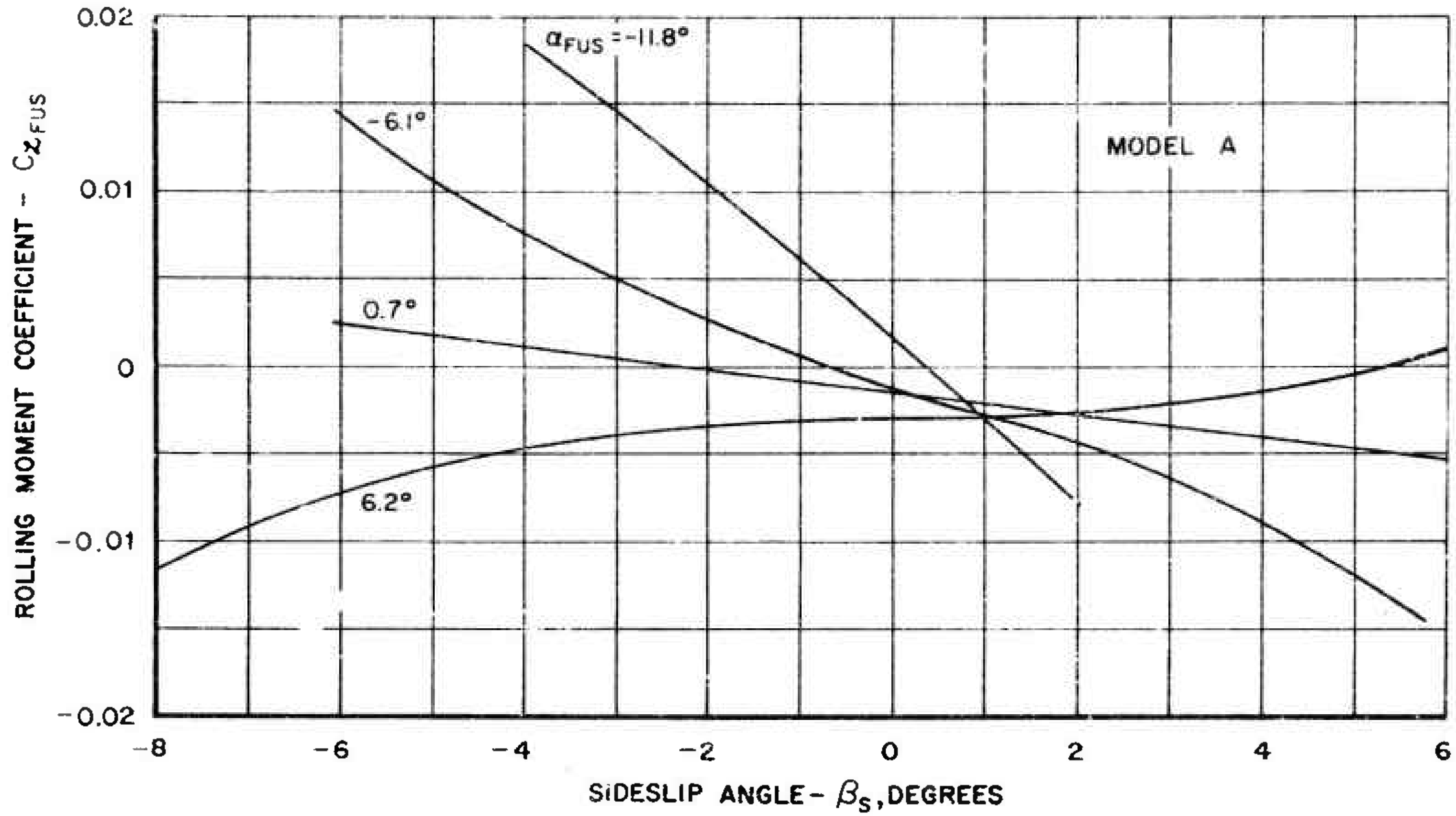

Figure 12. Rolling Moment Coefficient Versus Sideslip Angle, β_S, for Constant Values of α_{FUS} - Model A.

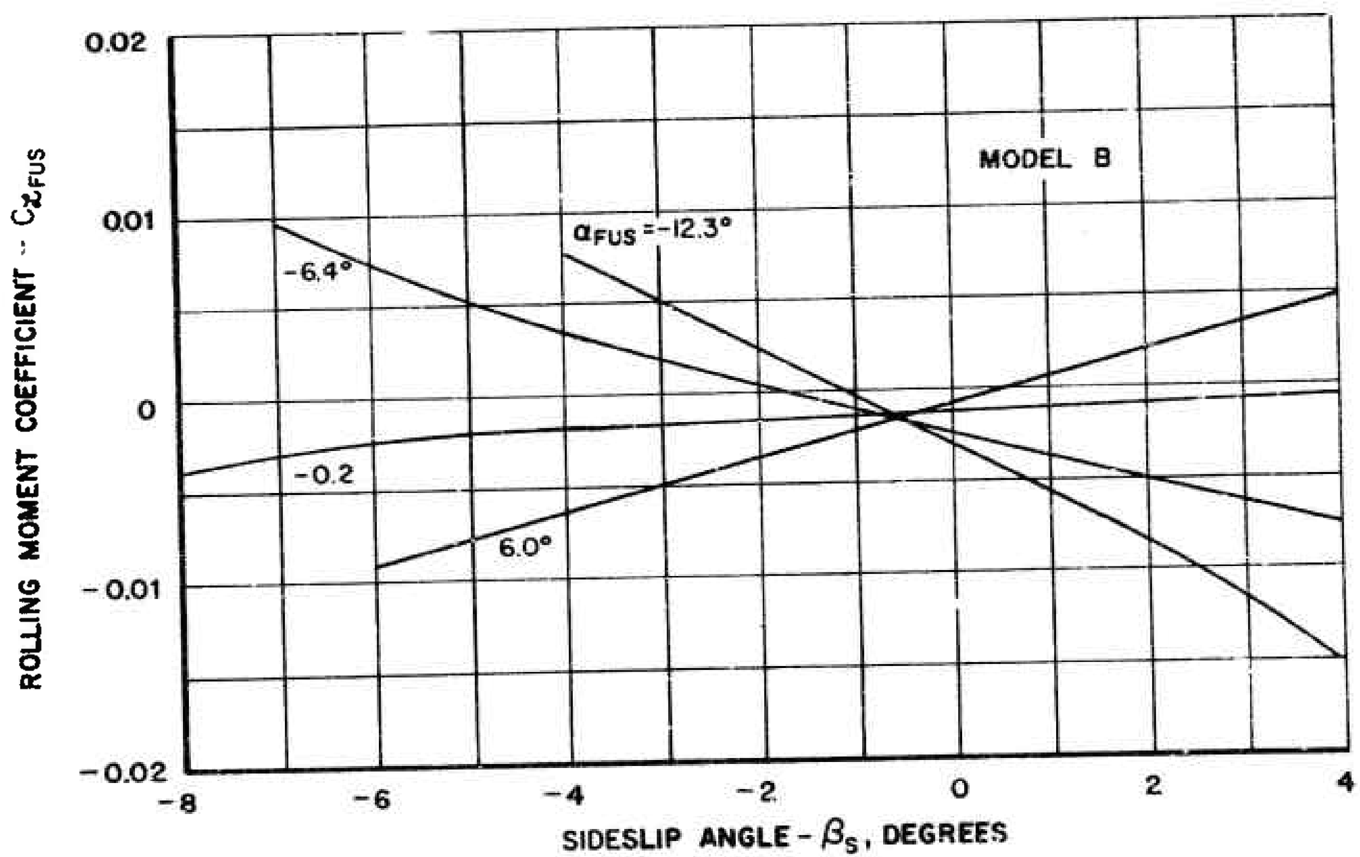

Figure 13. Rolling Moment Coefficient Versus Sideslip Angle, β_S, for Constant Values of α_{FUS} - Model B.

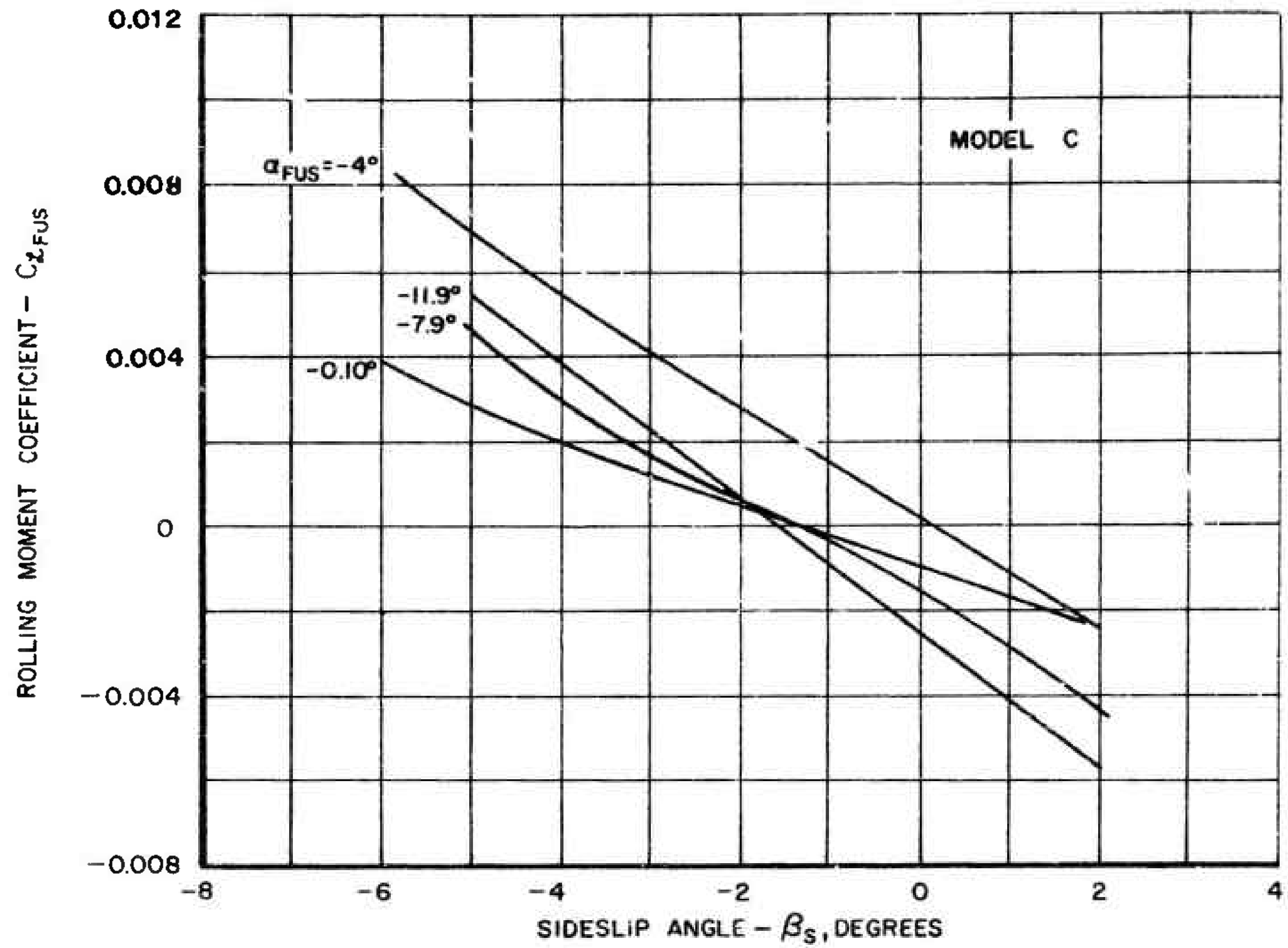

Figure 14. Rolling Moment Coefficient Versus Sideslip Angle, β_S, for Constant Values of α_{FUS} - Model C.

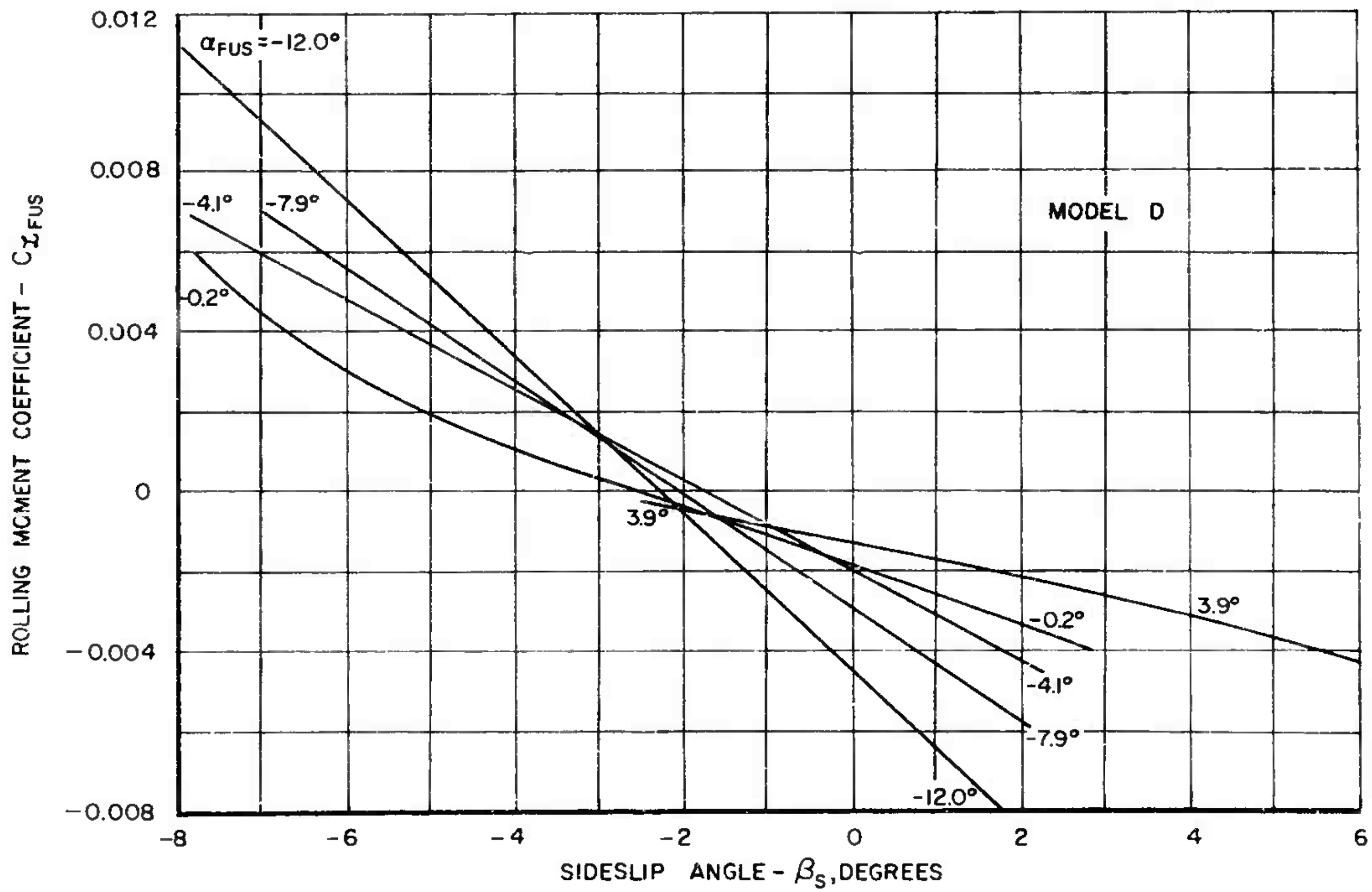

Figure 15. Rolling Moment Coefficient Versus Sideslip Angle, β_S, for Constant Values of α_{FUS} - Model D.

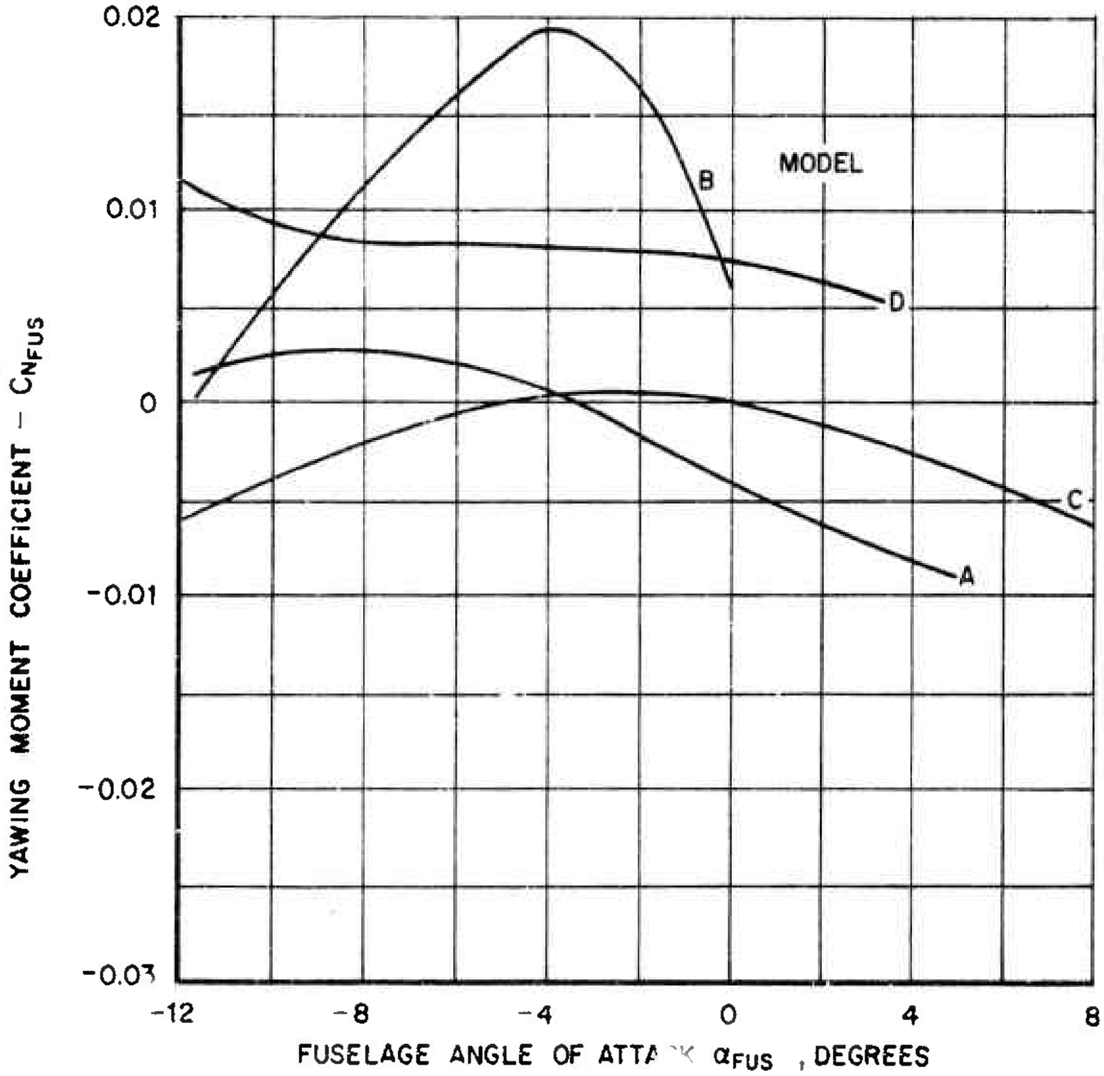

Figure 16. Yawing Moment Coefficient for Several Single-Rotor Helicopter Fuselages Versus Fuselage Angle of Attack for $\beta_S = 0$.

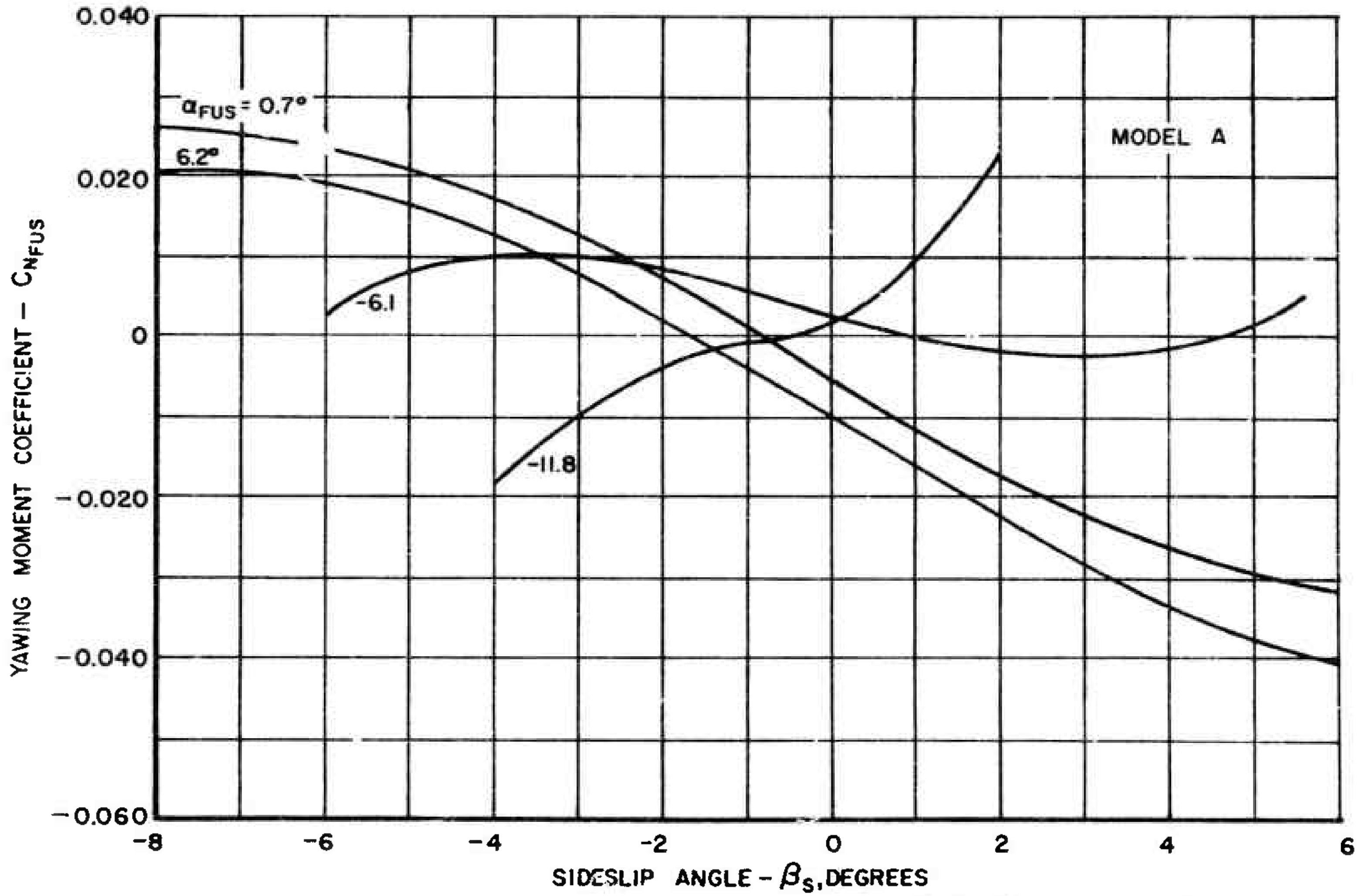

Figure 17. Yawing Moment Coefficient Versus Sideslip Angle, β_S, for Constant Values of α_{FUS} - Model A.

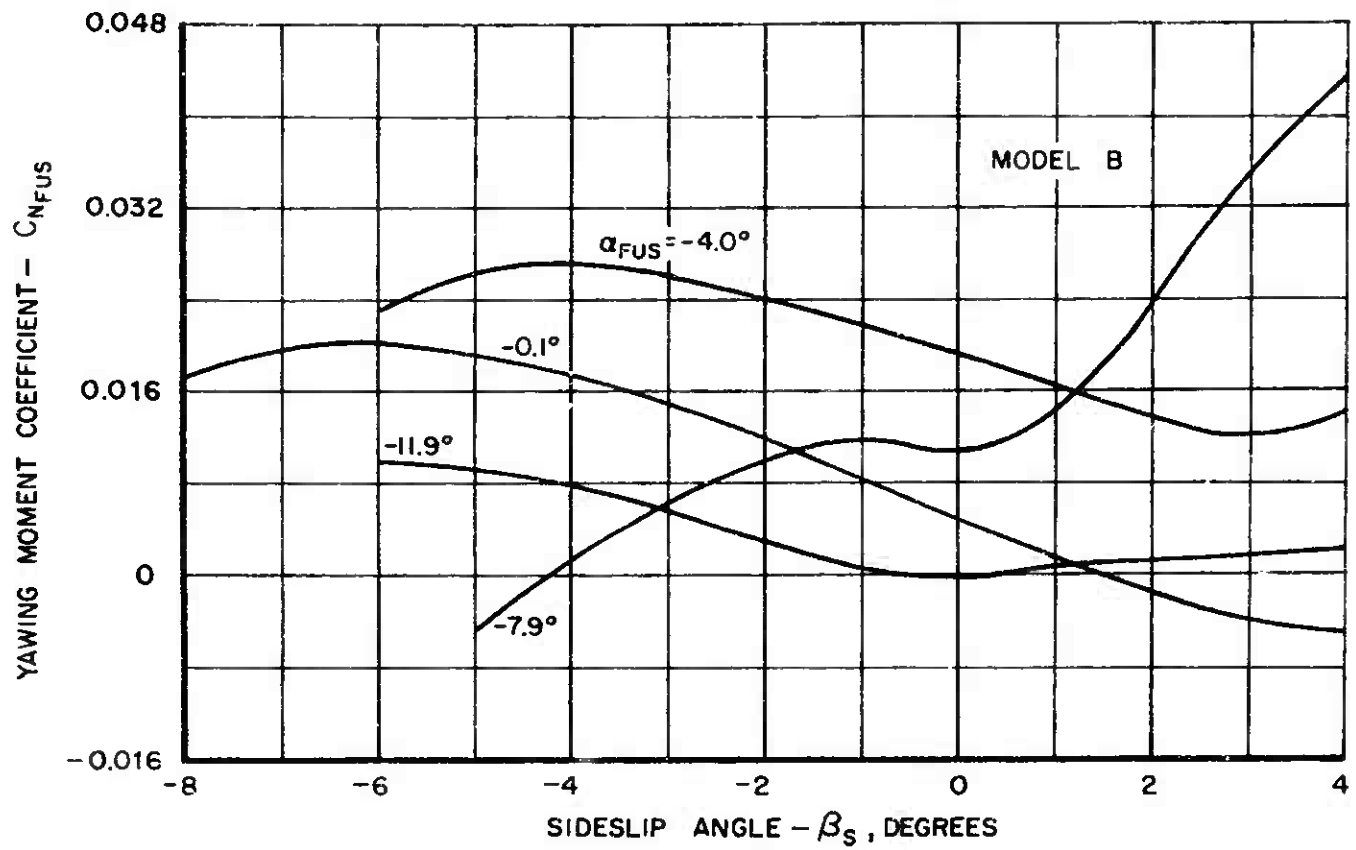

Figure 18. Yawing Moment Coefficient Versus Sideslip Angle, β_S, for Constant Values of α_{FUS} - Model B.

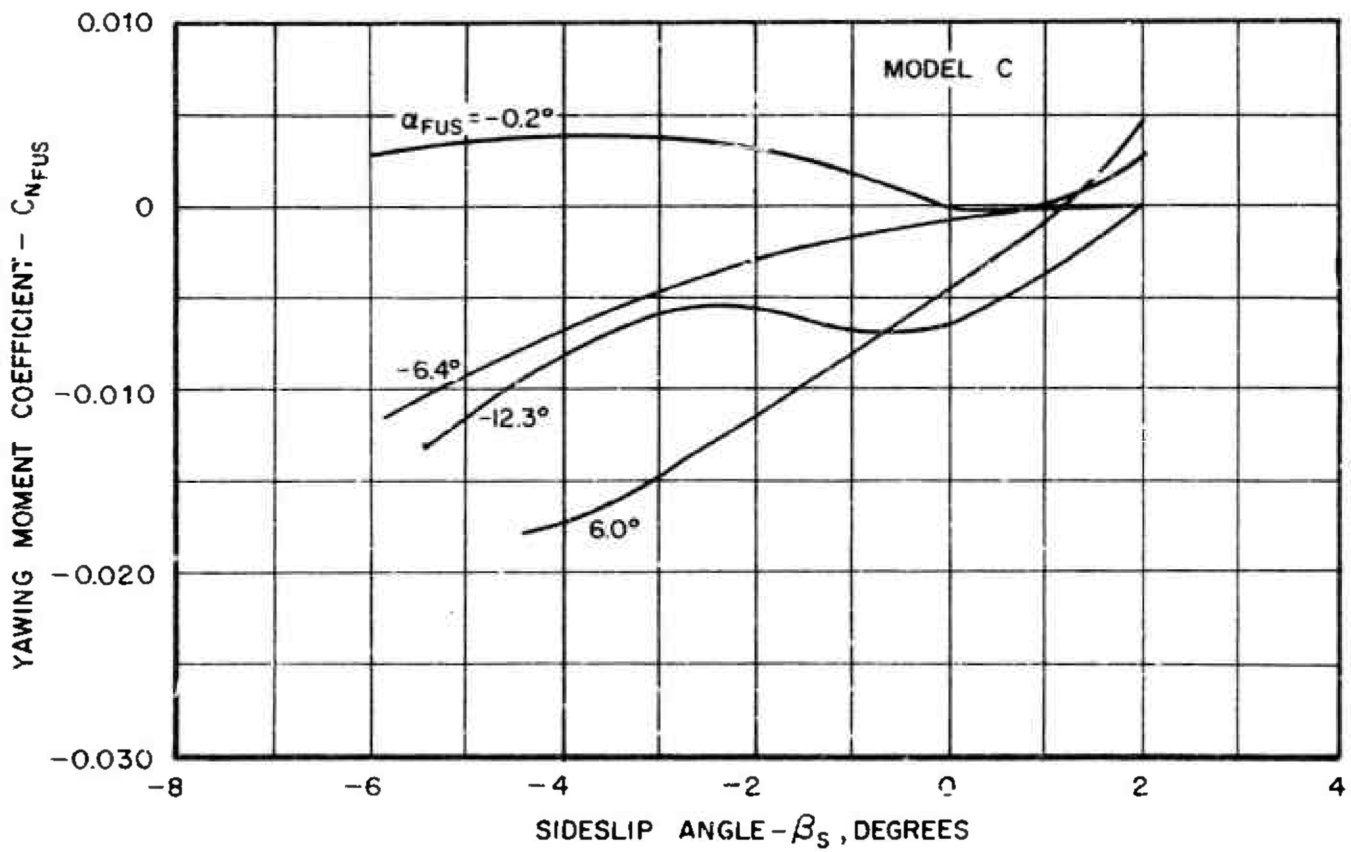

Figure 19. Yawing Moment Coefficient Versus Sideslip Angle, β_S, for Constant Values of α_{FUS} - Model C.

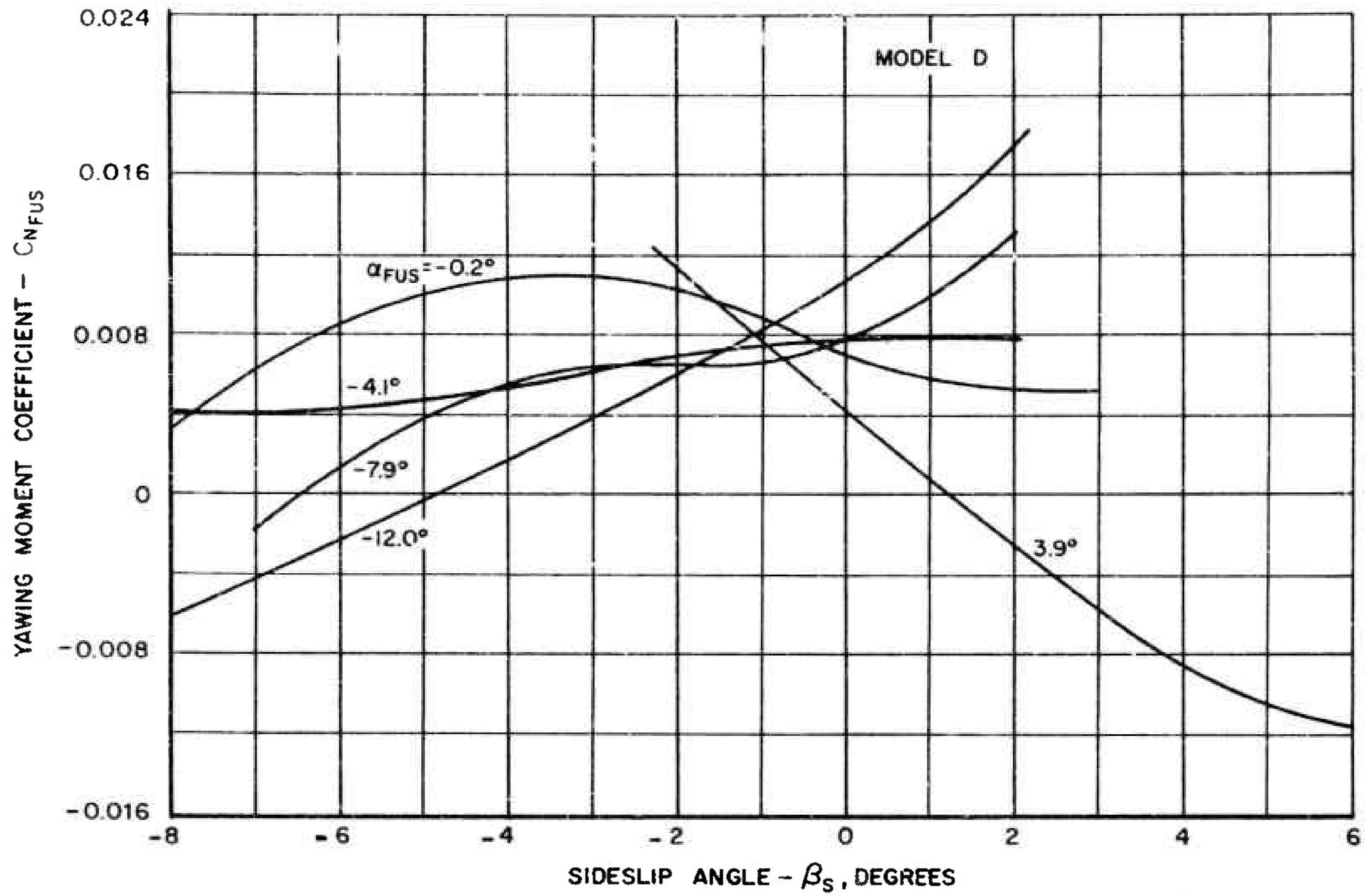

Figure 20. Yawing Moment Coefficient Versus Sideslip Angle, β_S, for Constant Values of α_{FUS} - Model D.

LITERATURE CITED

1. Sweet, G. E., and Jenkins, J. L., WIND TUNNEL INVESTIGATION OF THE DRAG AND STATIC STABILITY CHARACTERISTICS OF FOUR HELICOPTER FUSELAGE MODELS, NASA TND-1363, National Aeronautics and Space Administration, Washington, D. C., July 1962.

2. Biggers, J. C., McCloud, J. L., and Patterakis, P., WIND TUNNEL TESTS OF TWO FULL-SCALE HELICOPTER FUSELAGES, NASA TND-1548, National Aeronautics and Space Administration, Washington, D. C., October 1962.

3. USAF STABILITY AND CONTROL HANDBOOK (DATCOM), Flight Control Division, Air Force Flight Dynamics Laboratory, Wright-Patterson Air Force Base, Ohio, October 1960, Revised July 1963.

4. ROYAL AERONAUTICAL SOCIETY DATA SHEETS (VOLUMES III and IV), Royal Aeronautical Society of Great Britain, 1955.

5.4 LIFTING SURFACE CHARACTERISTICS

The aerodynamic characteristics of lifting surfaces are documented in numerous NACA and NASA publications. As described in References 1 and 2, the aerodynamic coefficients and their derivatives with respect to pertinent stability parameters depend on the specific geometric configuration of the lifting surface. The following methods extracted from Reference 1 give reliable estimates for a straight tapered lifting surface such as a wing or tail operating in the typical compound helicopter Mach number range, $M \leq 0.6$.

The wing lift coefficient is given by:

$$C_{L_W} = \frac{L_W}{\frac{1}{2}\rho V_0^2 S_W} = a_W(\alpha_W - \alpha_{o_W})$$

where

$$\alpha_W = \alpha + i_W - \epsilon_W$$

and

$$\frac{a_W}{A\!\!R} = \frac{2\pi}{2+\sqrt{\frac{A\!\!R^2\beta^2}{\kappa^2}\left(1+\frac{\tan^2\Lambda_{c/2}}{\beta^2}\right)+4}}$$

$A\!\!R$ = Wing aspect ratio.

β = Prandtl-Gleuert compressibility correction factor, $\sqrt{1-M^2}$

M = Free-stream Mach number.

$\Lambda_{c/2}$ = Wing midchord sweep angle.

κ = $\frac{a_{o_W}}{2\pi}$

a_{o_W} = Wing section (defined parallel to free stream) lift curve slope (per radian).

α_{o_W} = Wing zero lift angle

The three-dimensional lift curve slope of the wing is obtained using Figure 1.

Also, the wing drag coefficient is given by:

$$C_{D_W} = \frac{D_W}{\frac{1}{2}\rho V_o^2 S_W} = C_{D_{o_W}} + \frac{C_{L_W}^2}{\pi A\!\!R\, e}$$

The wing section profile drag coefficient is given by:

$$C_{D_{o_W}} = C_f \left[1 + L\left(\frac{t}{c}\right) + 100\left(\frac{t}{c}\right)^4 \right] R_{L.S.} \left[\frac{S_{wet}}{S_{exp}}\right]\left[\frac{S_{exp}}{S_W}\right]$$

The turbulent flat plate skin-friction coefficient C_f is obtained as a function of Mach number M and the Reynolds number $R_{\bar{c}}$ based on the mean aerodynamic chord $\bar{c}$. This is accomplished as follows:

First, the wing surface roughness height k is obtained from Table I, and the admissible roughness parameter $\bar{c}/k$ is computed. This roughness parameter, together with the computed Mach number, is used in Figure 2 to obtain the cutoff, Reynolds number, R_{cut} . Figure 3 is then entered and the value of C_f is obtained corresponding to either the computed or the cutoff Reynolds number, whichever is lower.

The airfoil thickness location parameter L is taken as $L = 1.2$ for $(t/c)_{max}$ located at $x_t \geq 0.30c$ and $L = 2.0$ for $(t/c)_{max}$ located at $x_t < 0.30c$. Using the appropriate value of L , the bracketed term $[1 + L(t/c) + 100(t/c)^4]$ in the equation for $C_{D_{o_W}}$ can be obtained directly from Figure 4.

The lifting surface correlation factor $R_{L.S.}$ can be obtained from Figure 5.

Finally, the ratio of S_{wet}/S_{exp} can be determined from Figure 6 in terms of airfoil average section thickness ratio. The ratio of S_{exp}/S_W is a function of a given wing geometry.

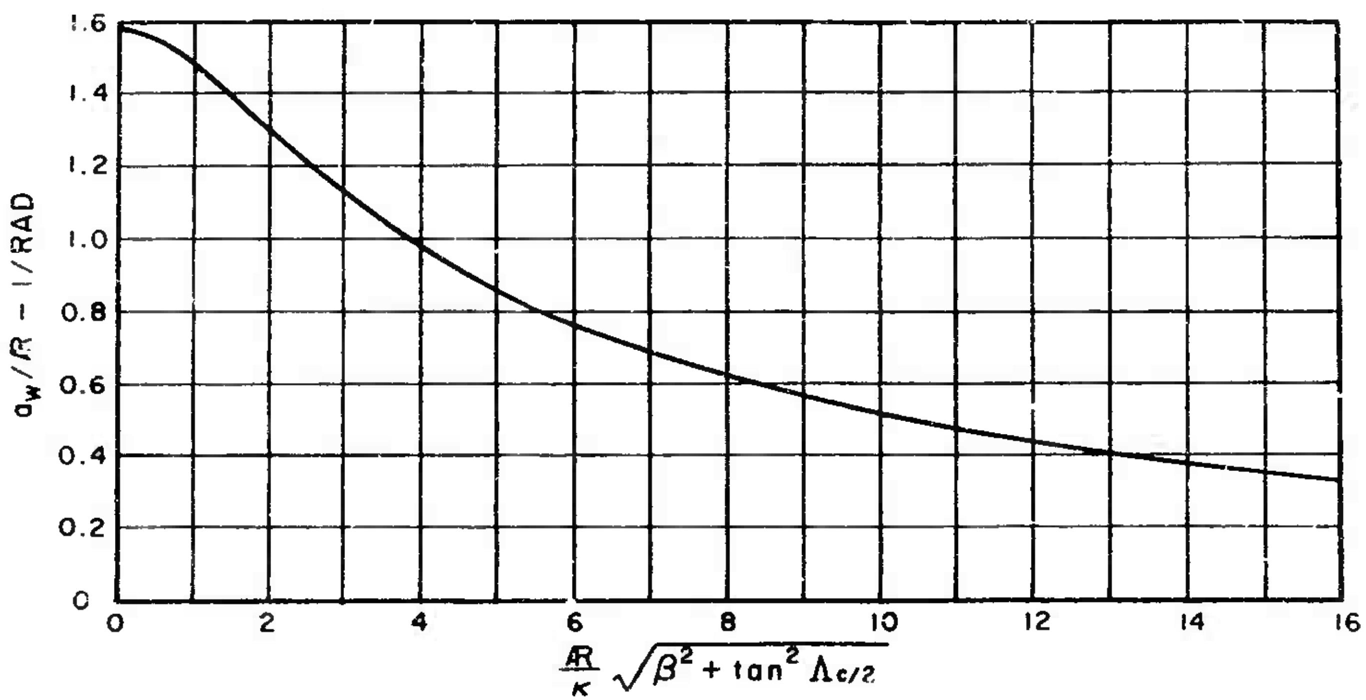

Figure 1. Subsonic Wing Lift-Curve Slope.

TABLE I

REPRESENTATIVE VALUES OF SURFACE-ROUGHNESS HEIGHT

Type of Surface	Equivalent Sand Roughness k (inches)
Aerodynamically smooth	0
Polished metal or wood	$0.02\text{-}0.08 \times 10^{-3}$
Natural sheet metal	0.16×10^{-3}
Smooth matte paint, carefully applied	0.25×10^{-3}
Standard camouflage paint, average application	0.40×10^{-3}
Camouflage paint, mass-production spray	1.20×10^{-3}
Dip-galvanized metal surface	6.00×10^{-3}
Natural surface of cast iron	10.00×10^{-3}

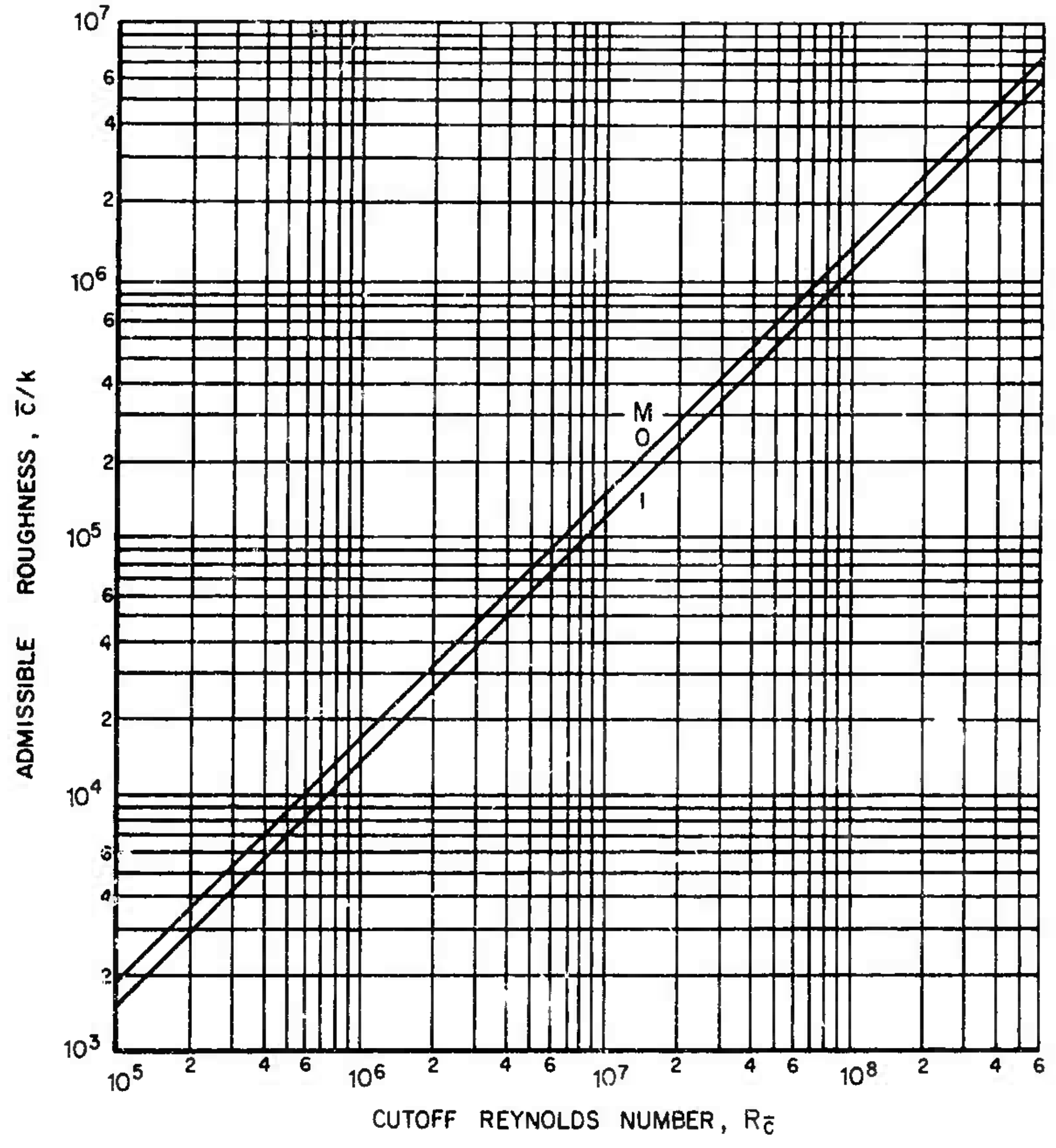

Figure 2. Cutoff Reynolds Number Versus Admissible Roughness.

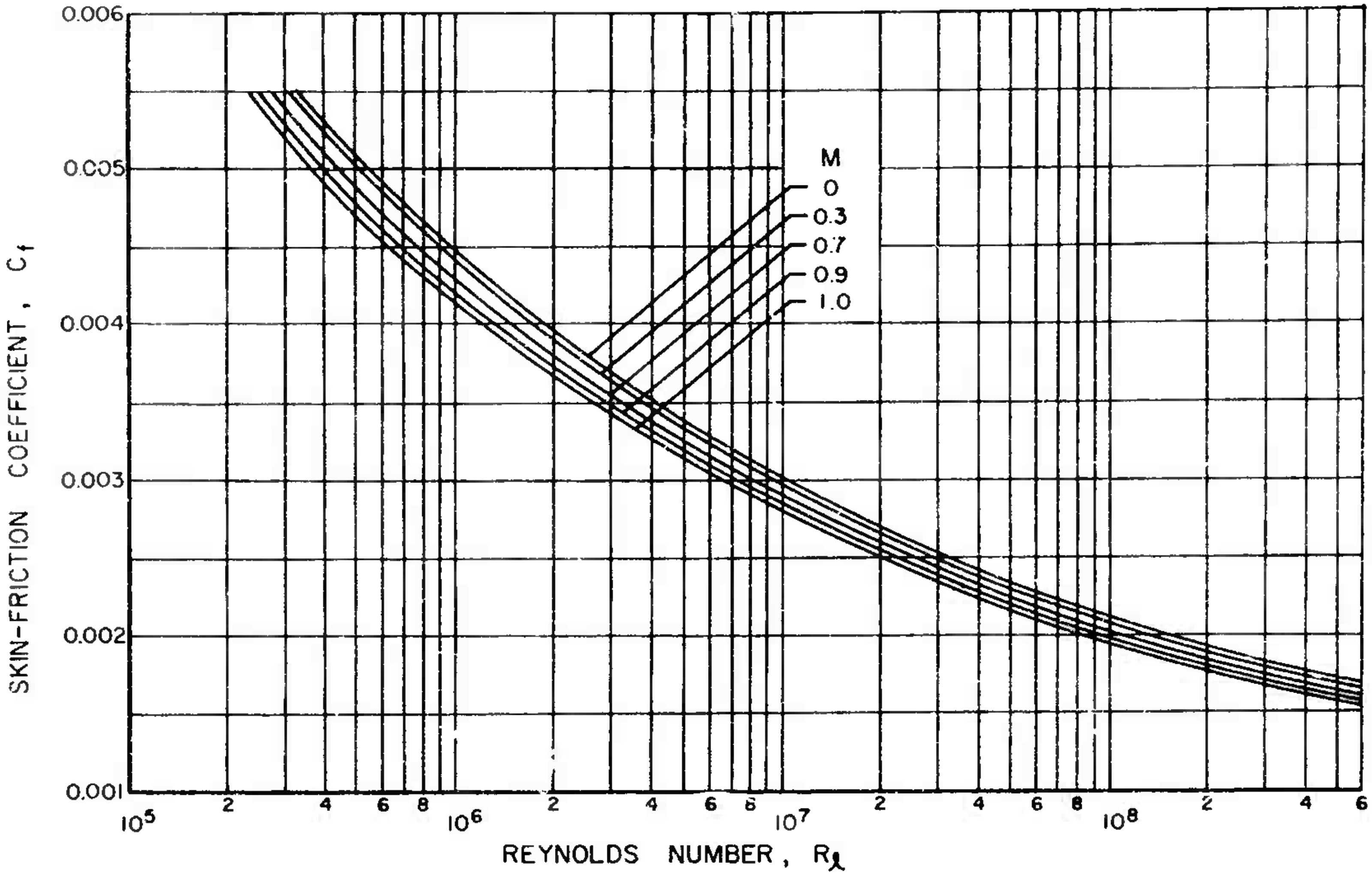

Figure 3. Turbulent Mean Skin-Friction Coefficient on an Insulated Flat Plate Versus Reynolds Number.

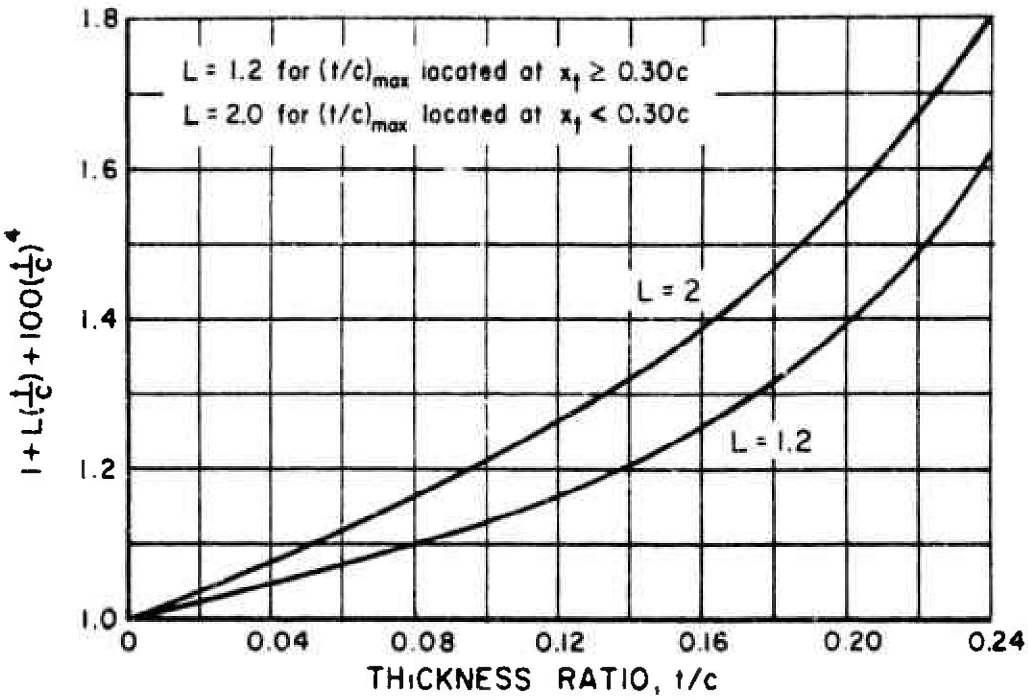

Figure 4. Subsonic Wing Minimum-Drag Factor Versus Wing Thickness Ratio.

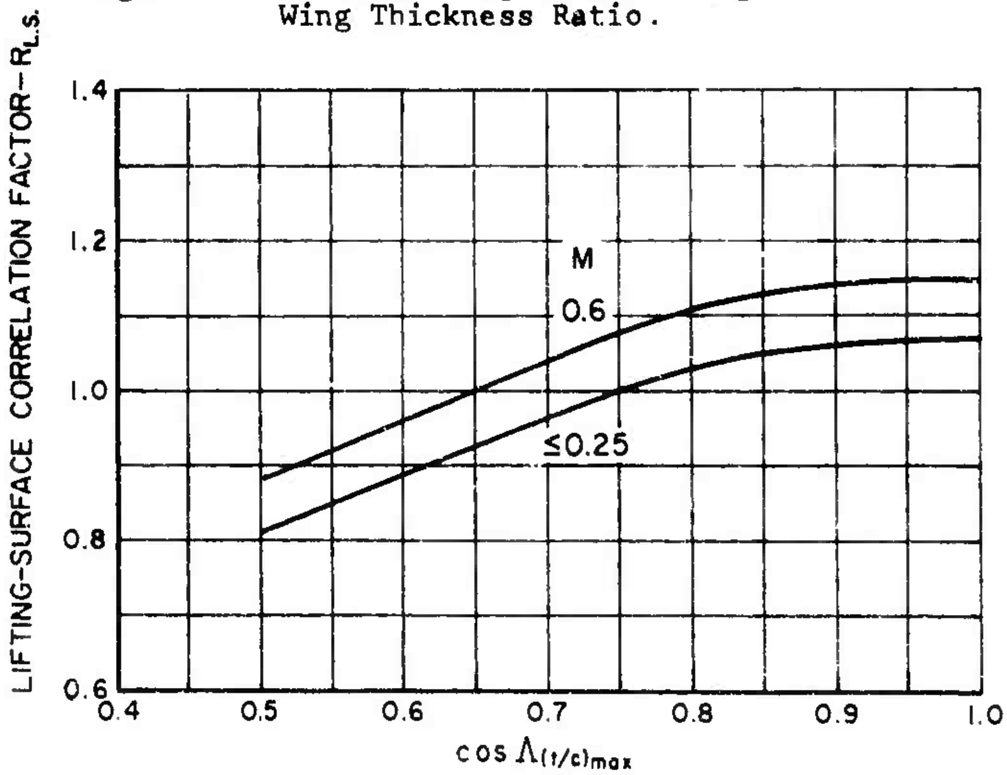

Figure 5. Lifting-Surface Correlation Factor for Subsonic Drag Versus Sweep Factor of Wing Maximum Thickness Line.

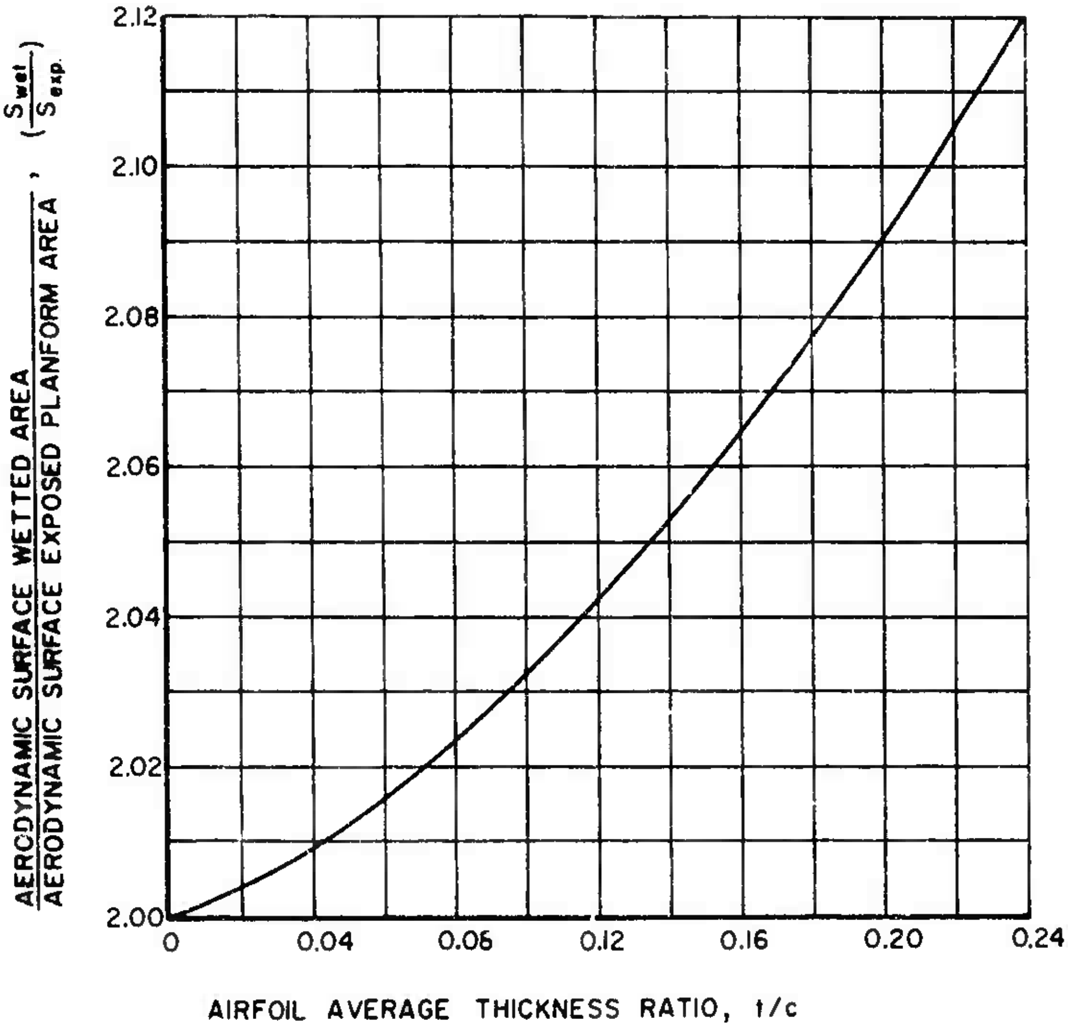

Figure 6. Thickness Correction to Wetted Area.

The span efficiency factor (e) appearing in the induced drag portion of the total wing drag is given by

$$e = \frac{1.1(a_w/AR)}{R(a_w/AR)+(1-R)\pi}$$

where R is the leading edge suction parameter defined as the ratio of the actual to the maximum theoretical value of the leading edge suction. This parameter is presented in Figure 7 as a function of leading-edge radius Reynolds number $R_{\ell_{LER}}$, aspect ratio AR , wing sweepback Λ_{LE} , and Mach number M for the values of $R_{\ell_{LER}} \cot \Lambda_{LE}\sqrt{1-M^2\cos^2\Lambda_{LE}}$ smaller than 1.3×10^5, the parameter R can be obtained from Figure 7(a) ; for the values larger than 1.3×10^5, Figure 7(b) is used.

The leading-edge radius Reynolds number $R_{\ell_{LER}}$ is based on the leading-edge radius r /c of the airfoil at the mean aerodynamic chord. The value of r / c for a variety of airfoil families can be determined using Figure 8. For the family of airfoils not shown in Figure 8, the leading-edge radius should be obtained from existing airfoil data.

To account for wing twist or complicated wing planforms, the methods of Reference 1 should be used.

The methods outlined above, although specifically developed for wings, can be directly applied to horizontal tailplanes.

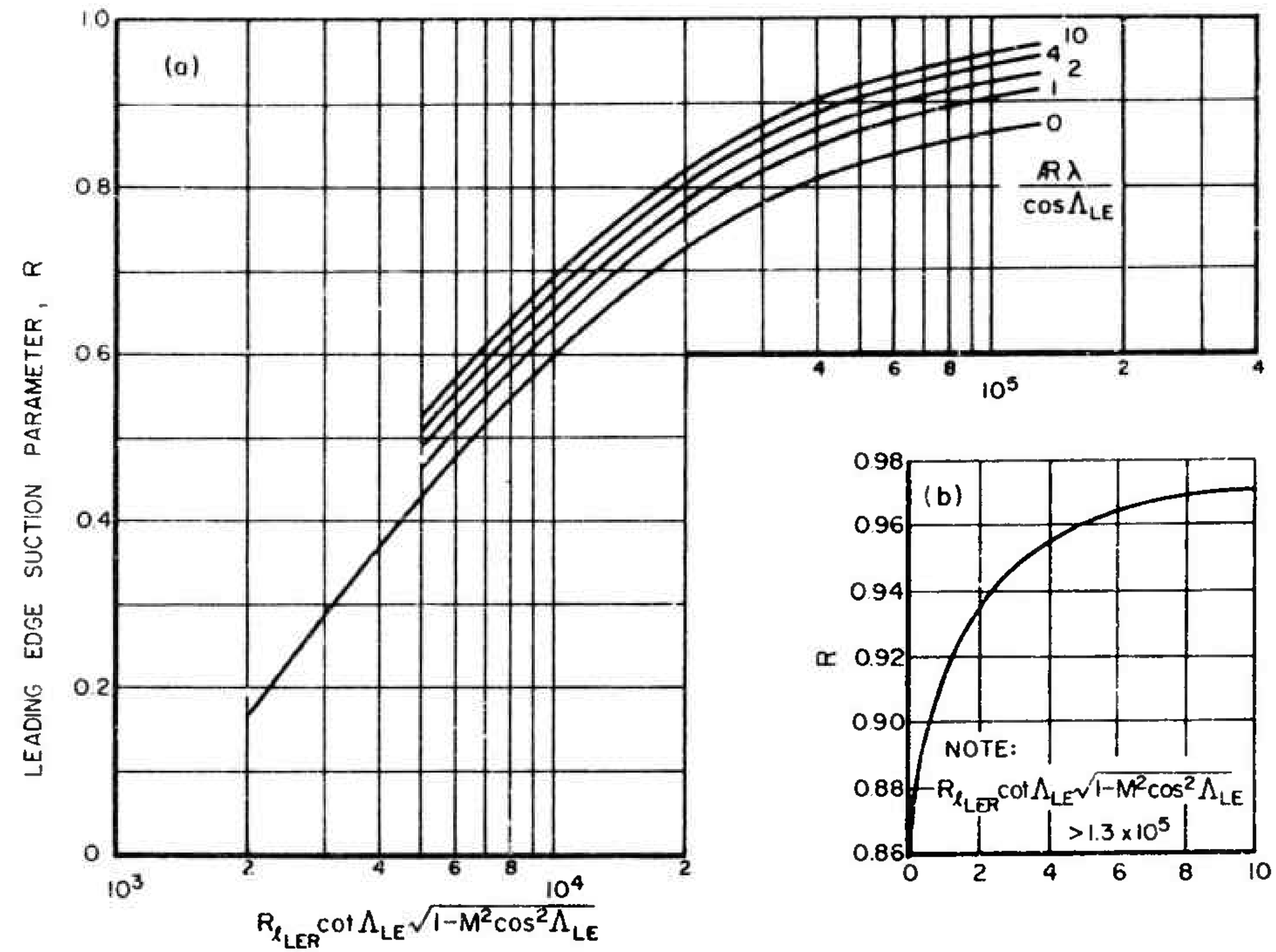

Figure 7. Leading-Edge Suction Parameter as a Function of Leading-Edge Radius Reynolds Number at Subsonic Speeds, $M \leq 0.8$.

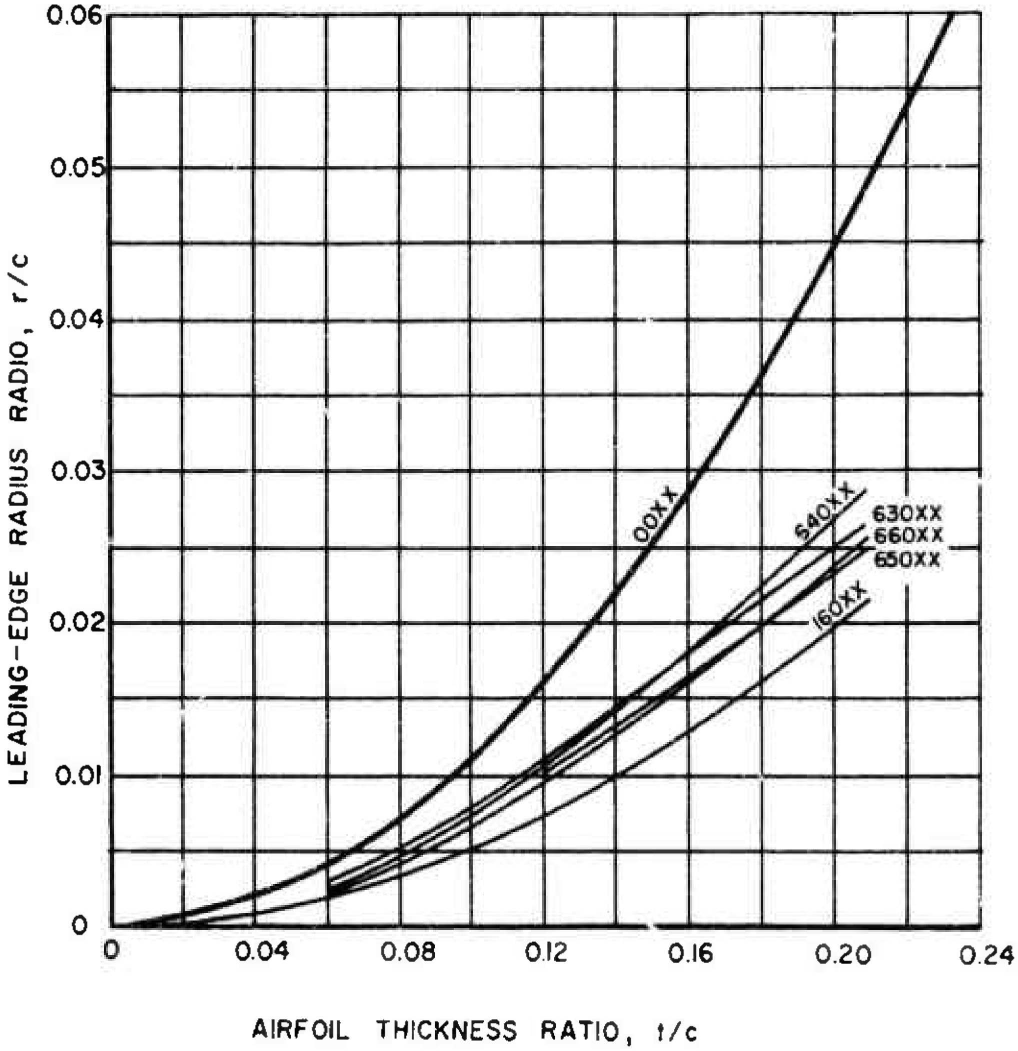

Figure 8. Leading-Edge Radius Ratio versus Thickness Ratio of Airfoils.

LITERATURE CITED

1. USAF STABILITY AND CONTROL HANDBOOK (DATCOM), Flight Control Division, Air Force Flight Dynamics Laboratory Wright-Patterson Air Force Base, Ohio, October 1960, Revised July 1963.

2. ROYAL AERONAUTICAL SOCIETY DATA SHEETS (VOLUMES II and III), Royal Aeronautical Society of Great Britain, 1955.

5.5 VERTICAL TAIL CHARACTERISTICS

The aerodynamic characteristics of vertical tail surfaces are influenced by the geometry of the body, wing, horizontal tail, main rotor, and tail rotor, and by the location of the vertical tail relative to these components. The effects of main and tail rotors on the vertical tail are generally small and can be neglected. The effects of the body, wing, and horizontal tail on lift and drag characteristics of vertical fins can be obtained from the comprehensive compilation of test data of Reference 1. This document provides data for estimating the lift curve slope a_{VT} for various vertical tail configurations such as:

(a) body merging into the vertical tail
(b) twin vertical tails
(c) vertical tail mounted on a body of circular cross section

The vertical tail lift and drag characteristics can be calculated in terms of the appropriate lift curve slope and the tail geometry as follows:

$$C_{L_{VT}} = a_{VT}\,\beta_S$$

$$L_{VT} = C_{L_{VT}}\,q_o\,S_{VT}$$

$$C_{D_{VT}} = \left[C_{d_o} + \frac{C_L^2}{\pi AR}\right]_{VT}$$

$$D_{VT} = C_{D_{VT}}\,q_o\,S_{VT}$$

where the vertical tail profile drag coefficient, $C_{d_{o_{VT}}}$, can be obtained using methods presented for wings in Section 5.4.

The procedures for determining a_{VT} for various vertical tail configurations are presented in the following subsections.

5.5.1 Body Merging into Single Vertical Tail

The calculation procedure for this configuration is as follows:

(a) Obtain the required geometric parameters S_{VT}, h, h_l, d, and c as defined in Figure 1(a), and find the trailing-edge angle of the vertical tail airfoil section, τ.

(b) Compute the ratio of h_l/h and calculate the aspect ratio $A\!R_{VT}$ based on S_{VT}, thus:

$$A\!R_{VT} = \frac{h^2}{S_{VT}}$$

(c) Using the value of h_l/h, obtain $(A\!R_e/A\!R)_{VT}$ from Figure 1(b), where $A\!R_{e_{VT}}$ is the aspect ratio allowing for the end plate effect of the horizontal tailplane. Then, compute the effective aspect ratio from

$$A\!R_{e_{VT}} = \left(\frac{A\!R_e}{A\!R}\right)_{VT} A\!R_{VT}$$

(d) Knowing the values of $A\!R_{e_{VT}}$ and τ, obtain a'_{VT}, the lift curve slope of the vertical tail considered as an airfoil of rectangular planform, from Figure 1(c).

(e) Using the ratio of d/h, determine a_{VT}/a'_{VT} from Figure 1(d), where a_{VT} is the required lift curve slope of the vertical tail allowing for wing, body, and horizontal tail effects.
Compute a_{VT} thus:

$$a_{VT} = \left(\frac{a_{VT}}{a'_{VT}}\right) a'_{VT}$$

5.5.2 Twin Vertical Tails

The calculation procedure for this configuration is as follows:

(a) Obtain the required geometric parameters h, h_l, b_T, d, and the area of each vertical tail S_{VT}, as defined in Figure 2(a). Also obtain the fuselage length ℓ_{FUS}, and the trailing-edge angle of the vertical tail airfoil section τ, in degrees.

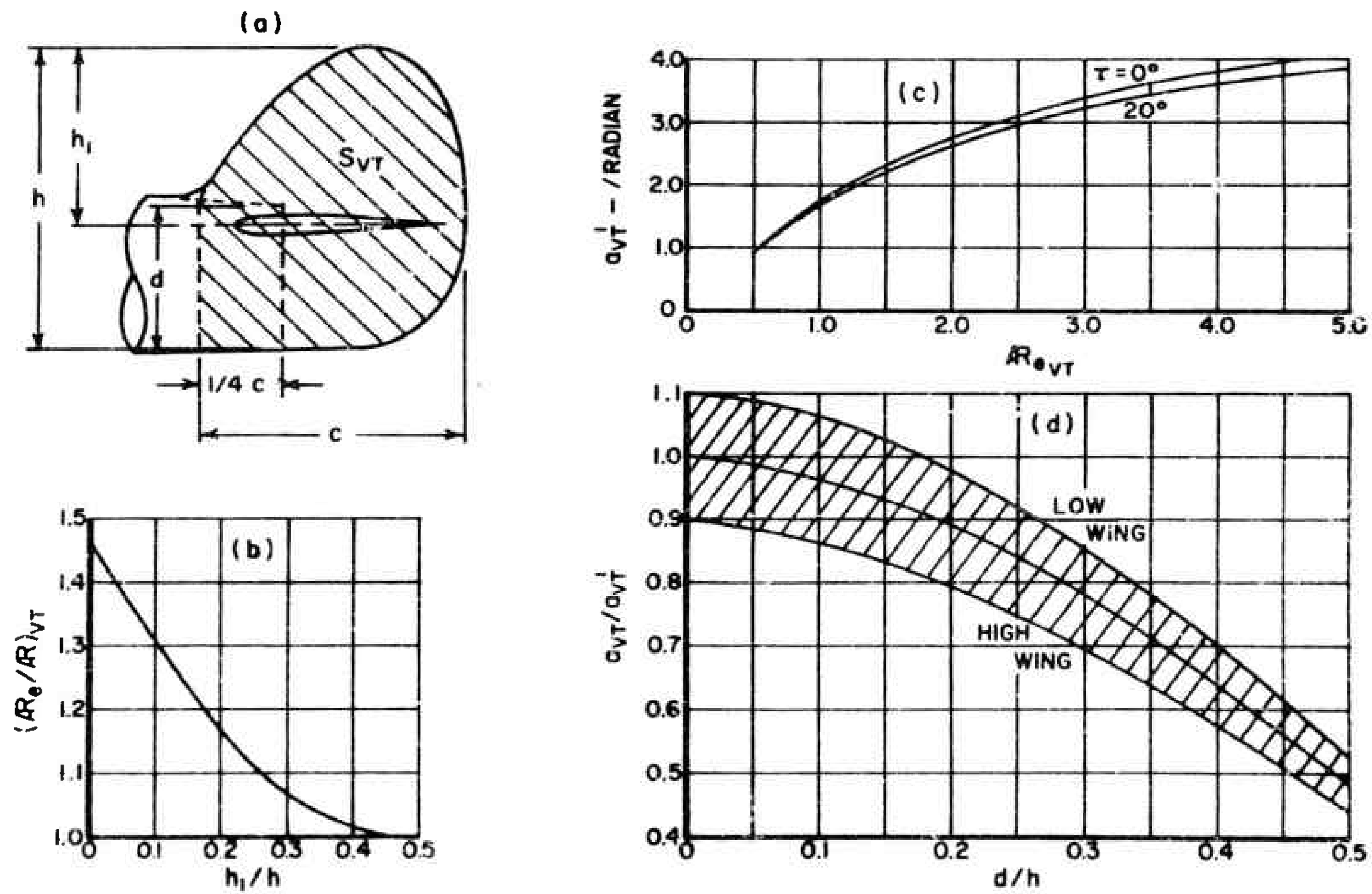

Figure 1. Lift-Curve Slope for a Vertical Tailplane With the Body Shape Merging Into the Tailplane (Reproduced from Royal Aeronautical Society Data Sheet Controls 01.01.01).

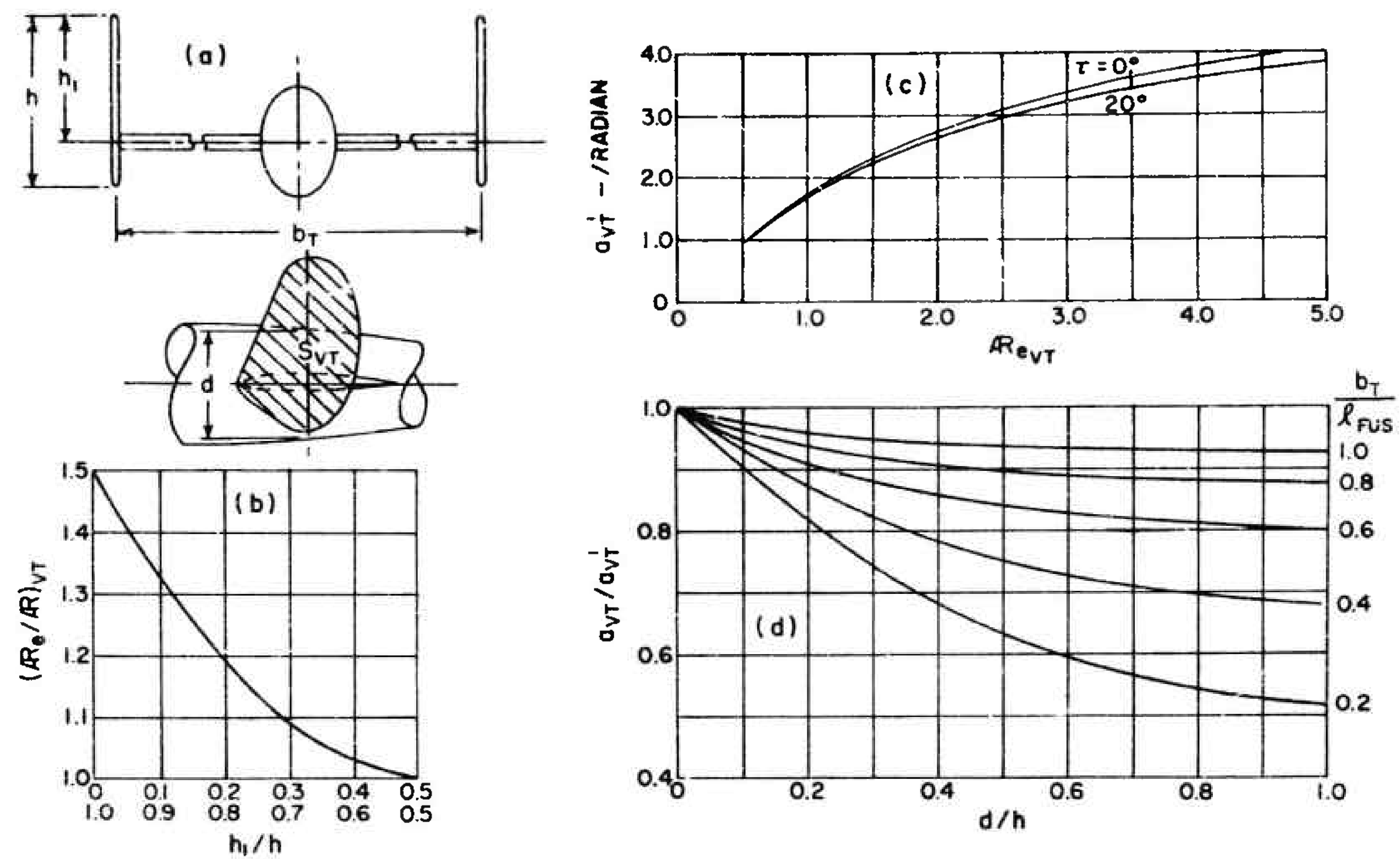

Figure 2. Lift-Curve Slope for Twin Vertical Tailplanes (Reproduced From Royal Aeronautical Society Data Sheet Controls 01.01.02).

(b) Compute aspect ratio of each vertical tail using

$$A_{VT} = \frac{h^2}{S_{VT}}$$

(c) Compute the ratio h_l/h and obtain $(A_e/A)_{VT}$ from Figure 2(b), where $A_{e_{VT}}$ is the equivalent aspect ratio of each vertical tail, allowing for the end-plate effect of the horizontal tail. Then calculate

$$A_{e_{VT}} = \left(\frac{A_e}{A}\right)_{VT} A_{VT}$$

(d) Knowing the values of $A_{e_{VT}}$ and τ, obtain a'_{VT}, the lift curve slope of the vertical tail considered as an airfoil of rectangular planform, from Figure 2(c).

(e) Using the ratios d/h and t_r/ℓ_{US}, determine a_{VT}/a'_{VT} from Figure 2(d). Then calculate a_{VT} thus:

$$a_{VT} = \left(\frac{a_{VT}}{a'_{VT}}\right) a'_{VT}$$

where

a_{VT} is the required mean lift-curve slope of the twin vertical tails allowing for body and additional horizontal tail-plane effects.

5.5.3 Single Vertical Tail on Body of Circular Cross Section

The calculation procedure for this configuration is as follows:

(a) Obtain the required geometric parameters h, h_l, D, $\Lambda_{c/4_{VT}}$ and S_{VT} as defined in Figure 3(a), and find the taper ratio of the vertical tail, λ_{VT}.

(b) Compute the aspect ratio of the vertical tail using

$$A_{VT} = \frac{h^2}{S_{VT}}$$

(c) Obtain the aspect ratio correction factor, k, from Figure 4(a) or by using the formula

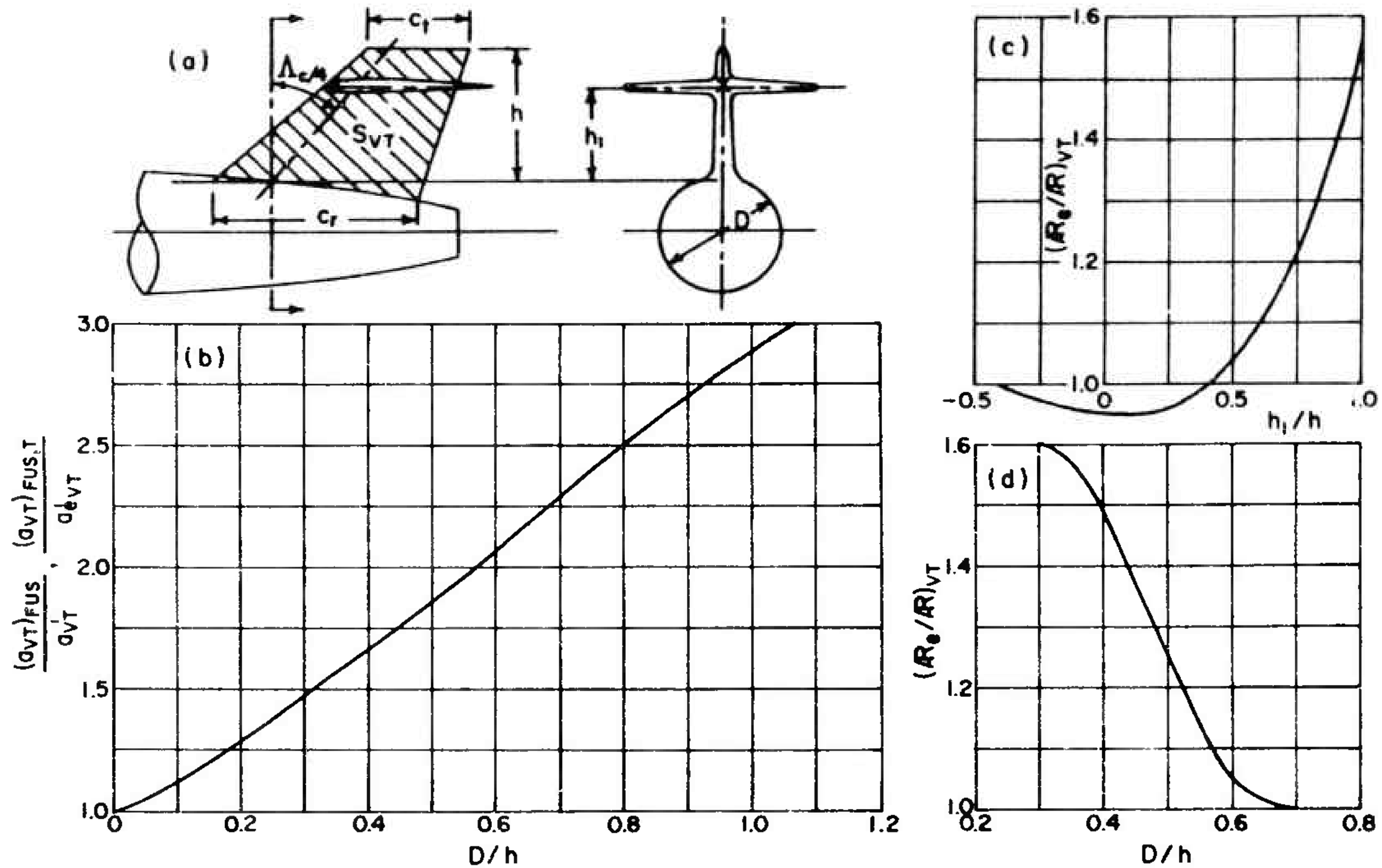

Figure 3. Lift-Curve Slope for Single Vertical Tailplane on a Body of Circular Cross Section. (Reproduced From Royal Aeronautical Society Data Sheet Controls 01.01.05).

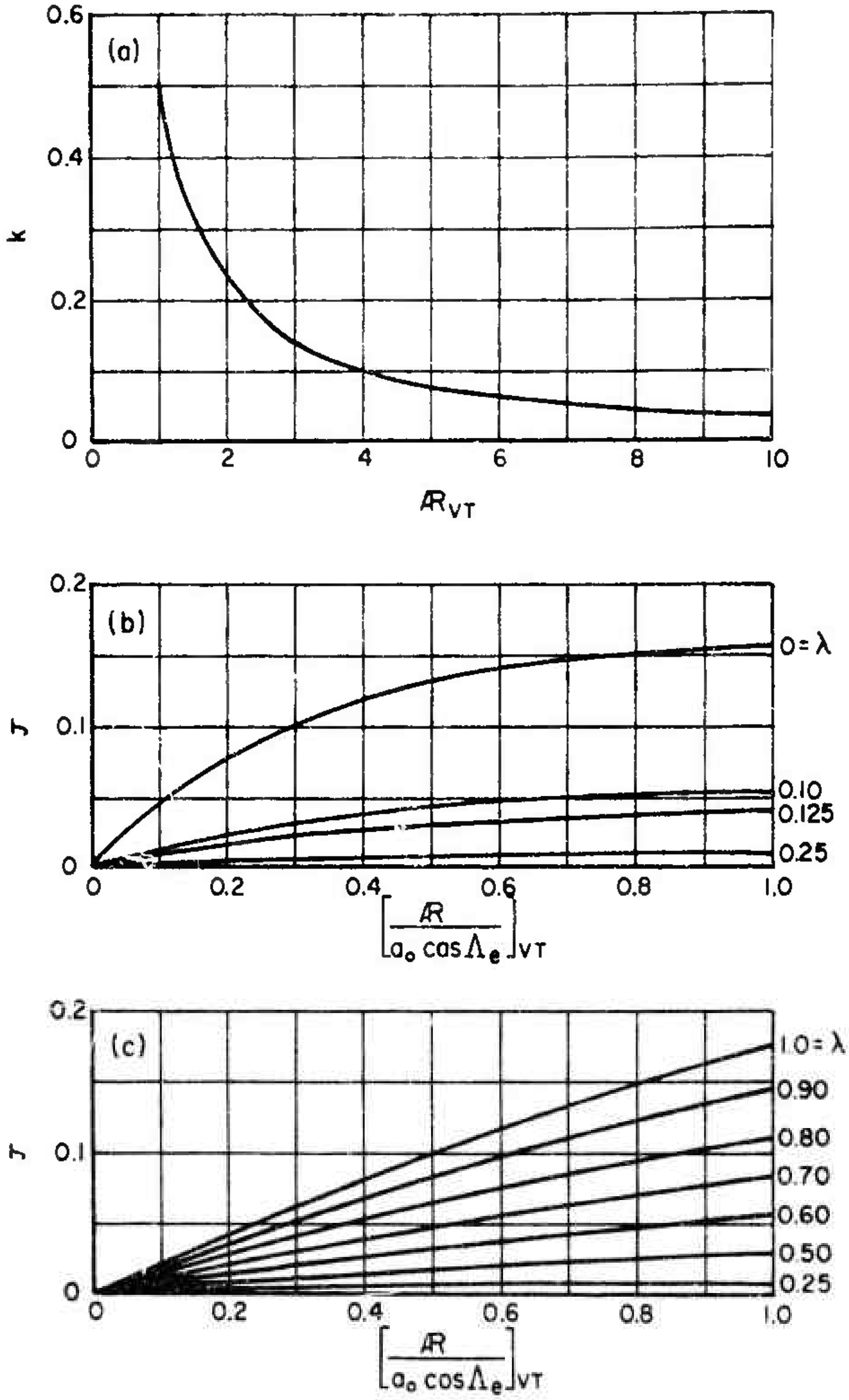

Figure 4. Lift-Curve Slope for Swept and Tapered Vertical Tailplanes. (Reproduced From Royal Aeronautical Society Data Sheet Wings 01.01.01).

$$k = \frac{1}{\pi A\!\!R_{VT}} \left[1 + \frac{A\!\!R_{VT}}{2} \left\{ \sqrt{(1 + \frac{4}{A\!\!R_{VT}^2})} - 1 \right\} \right]$$

(d) Calculate the effective sweep angle of the vertical tail, $\Lambda_{e_{VT}}$, from

$$\tan \Lambda_{e_{VT}} = \left[\tan \Lambda_{c/4} - \frac{\Lambda_{c/4}}{45 A\!\!R (1+\lambda)} \right]_{VT}$$

(e) From either Reference 1 or Reference 2, obtain the two-dimensional or section lift-curve slope, $a_{0_{VT}}$.

(f) From Figure 4(b) or 4(c) obtain the taper ratio correction factor τ, as a function of λ_{VT} and $A\!\!R_{VT} / a_{0_{VT}} \cos \Lambda_{e_{VT}}$.

(g) Then calculate the isolated vertical tail lift-curve slope a'_{VT} from

$$\frac{1}{a'_{VT}} = \frac{1}{a_{0_{VT}} \cos \Lambda_{e_{VT}}} + (1 + \tau) k$$

(h) The lift-curve slope of the vertical tail in the presence of the body $(a_{VT})_{FUS}$ is then obtained from Figure 3(b), which gives $(a_{VT})_{FUS} / a'_{VT}$ in terms of D/h.

The effect of the addition of a horizontal tail is expressed as a change in vertical tail aspect ratio; that is, $A\!\!R_{e_{VT}}$ is so chosen that $(a_{VT})_{FUS,T} / a'_{e_{VT}}$ is the same function of D/h as $(a_{VT})_{FUS} / a'_{VT}$. The aspect ratio $A\!\!R_{e_{VT}}$ is found from either Figure 3(c) or 3(d).

(i) Recalculate k from step (c), $\Lambda_{e_{VT}}$ from step (d), and τ from step (f), using the appropriate value of $A\!\!R_{e_{VT}}$ in every case. Then obtain $(a_{VT})_{FUS,T}$, the vertical tail lift-curve slope, allowing for the body and horizontal tail effects from Figure 3(b), thus:

$$(a_{VT})_{FUS,T} = \left(\frac{(a_{VT})_{FUS,T}}{a'_{e_{VT}}}\right) a'_{e_{VT}}$$

(j) A factor based on good engineering judgement must be applied to account for the effect of wing position on the lift-curve slope of the vertical tail. For a wing

mounted low on the fuselage, the vertical tail lift-curve slope may be increased by a factor of as much as 1.4, whereas the decreased sidewash with the wing at the top of the body may reduce the vertical tail lift-curve slope by a factor of as much as 0.7.

LITERATURE CITED

1. ROYAL AERONAUTICAL SOCIETY DATA SHEETS (VOLUME IV), Royal Aeronautical Society of Great Britain, 1955.

2. USAF STABILITY AND CONTROL HANDBOOK (DATCOM), Flight Control Division, Air Force Flight Dynamics Laboratory Wright-Patterson Air Force Base, Ohio, October 1960, Revised July 1963.

5.6 CONVENTIONAL AIRCRAFT CONTROL CHARACTERISTICS

Presented in this section are practical engineering methods for estimating the primary effects of fully or partially deflected conventional aircraft control surfaces. More rigorous treatment of the subject is presented in References 1 and 2.

5.6.1 Longitudinal Control

Longitudinal control is achieved by means of an elevator on the horizontal tail or by means of a movable horizontal tailplane. The effect of the elevator on tailplane lift can be determined simply by calculating the control effectiveness derivative $C_{L_{\delta_e}}$ using the nomogram in Figure 1. The increment of tailplane lift due to elevator deflection can then be obtained as $\Delta C_{L_T} = C_{L_{\delta_e}} \delta_e$. The calculation procedures for determining $C_{L_{\delta_e}}$ as shown in Figure 1 are self-explanatory and do not require any further discussion.

5.6.2 Lateral Control

Lateral control is achieved using ailerons, flaperons, or differential spoilers. There are many varieties of spoilers that can be used for lateral control, therefore the reader is referred to Reference 1 for methods of estimating their effect. The primary effect of ailerons and flaperons is to induce a rolling moment about the X-axis of the wing. The magnitude of the rolling moment can be determined by obtaining the control effectiveness derivative $C_{\ell_{\delta_a}}$ per aileron from the nomogram in Figure 2 and by summing the effects of both port and starboard wings. A secondary effect of aileron deflection is to produce a yawing moment due to asymmetric wing drag. This effect, if required, can be calculated using Reference 1.

5.6.3 Directional Control

Directional control is achieved by means of a rudder located on the vertical tail. The primary effect on the lift of the vertical tail can be estimated by determining the rudder control effectiveness derivative, $C_{L_{\delta_r}}$. This derivative can be obtained from Figure 1 in the same manner as $C_{L_{\delta_e}}$ by replacing δ_e with δ_r. Then the increment of lift on the vertical tail due to rudder deflection can be obtained from

$$\Delta C_{L_{VT}} = C_{L_{\delta_r}} \delta_r$$

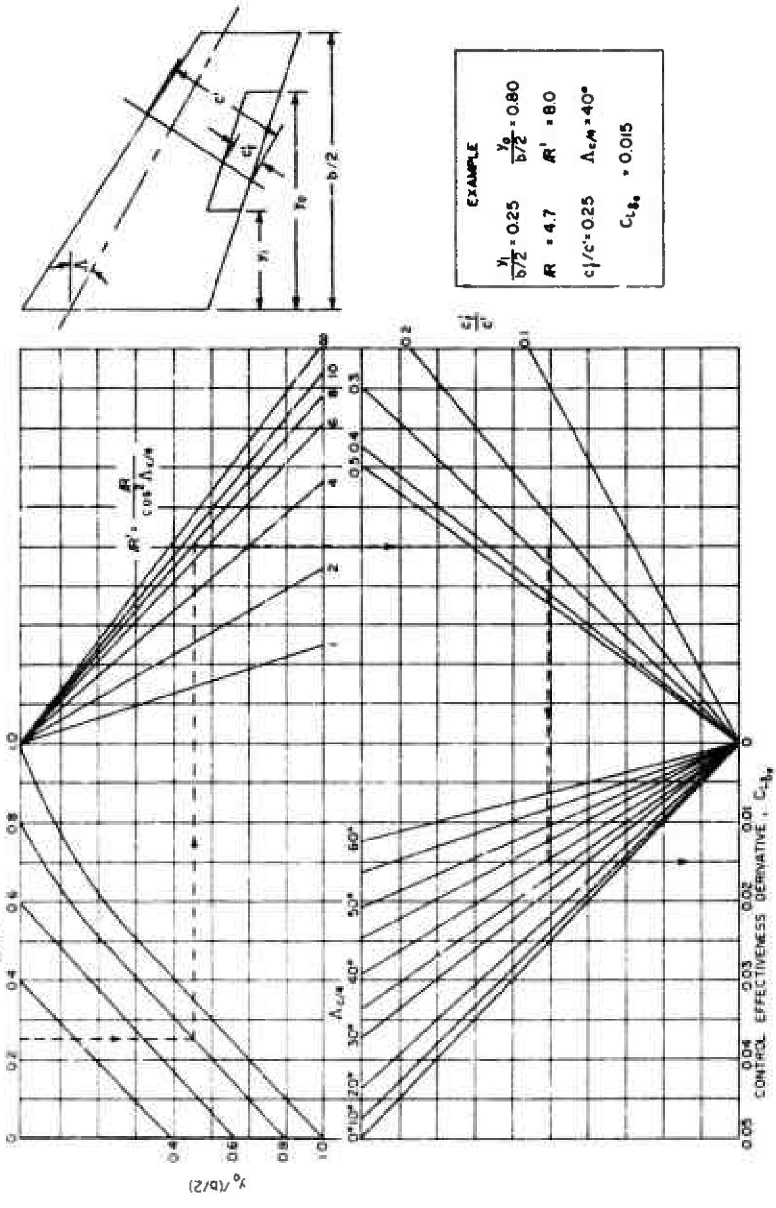

Figure 1. Subsonic Elevator Lift Effectiveness (Gap not Sealed).

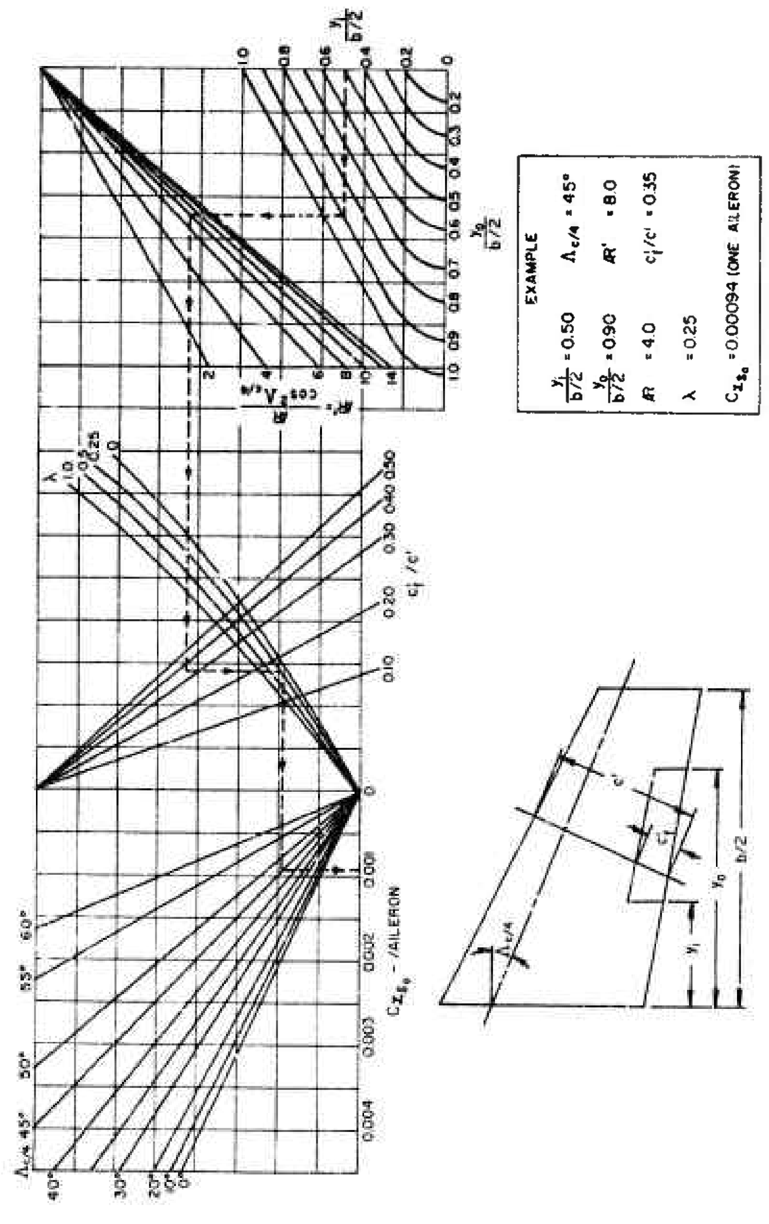

Figure 2. Subsonic Aileron Effectiveness.

5.6.4 Wing Lift Controls

Wing lift can be controlled through the use of trailing-edge flaps, leading-edge flaps, spoilers, slots, slats, etc. Since the most common form of wing lift control device used on compound helicopters is the plain trailing-edge flap, the following methods for estimating the effect of flap deflection on wing lift, drag, and pitching moment are confined to plain trailing-edge flaps. For information on the effects of spoilers, slats, etc., the reader is referred to Reference 1.

5.6.4.1 Lift Due to Flap Deflection

The change in wing lift caused by deflecting a plain trailing-edge flap by an amount δ_f is given by $\Delta C_L = C_{L_{\delta_f}} \delta_f$. The derivative $C_{L_{\delta_f}}$ can be obtained from Figure 1 in the same manner as $C_{L_{\delta_e}}$ by replacing δ_e by δ_f and using the appropriate wing geometric parameters.

5.6.4.2 Drag Due to Flap Deflection

Deflection of a plain trailing-edge flap causes an increase in both wing profile drag and wing induced drag. The change in overall wing drag is given by

$$\Delta C_D = (K_{b_o} - K_{b_i})\Delta C_{d_f} + K' \frac{(C_{L_{\delta_f}} \delta_f)}{\pi R_W}$$

where K_{b_o} or K_{b_i}, ΔC_{d_f}, and K' are obtained using Figures 3, 4, and 5 respectively, and $C_{L_{\delta_f}}$ is obtained under 5.6.4.1 above.

5.6.4.3 Pitching Moment Due to Flap Deflection

Large changes in pitching moment can result from deflection of a trailing-edge flap. The magnitude of the pitching moment change is given by

$$\Delta C_M = C_{M_{\delta_f}} \delta_f$$

where the derivative $C_{M_{\delta_f}}$ is obtained from the nomogram presented in Figure 6. A value of $C_{\ell_{\delta_f}}$, the rolling moment derivative due to one flap being deflected, is required to use this nomogram. This is easily obtained from Figure 2 in the same manner as required to obtain the derivative $C_{\ell_{\delta_a}}$ described under 5.6.2 above.

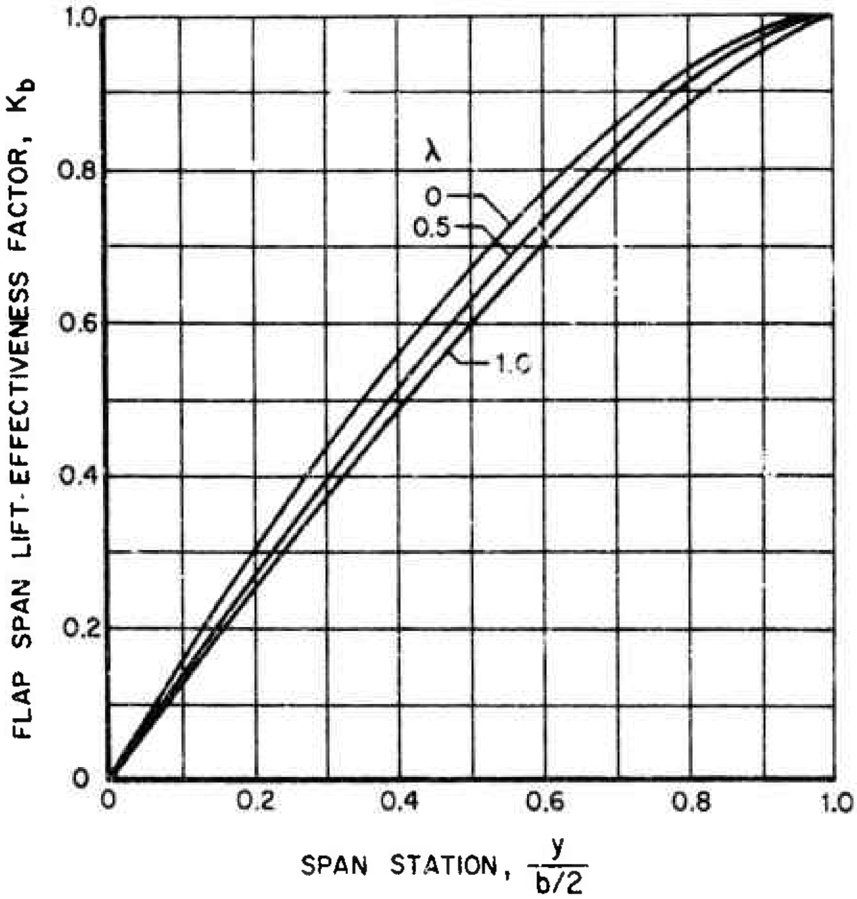

Figure 3. Span Factor for Inboard Flaps.

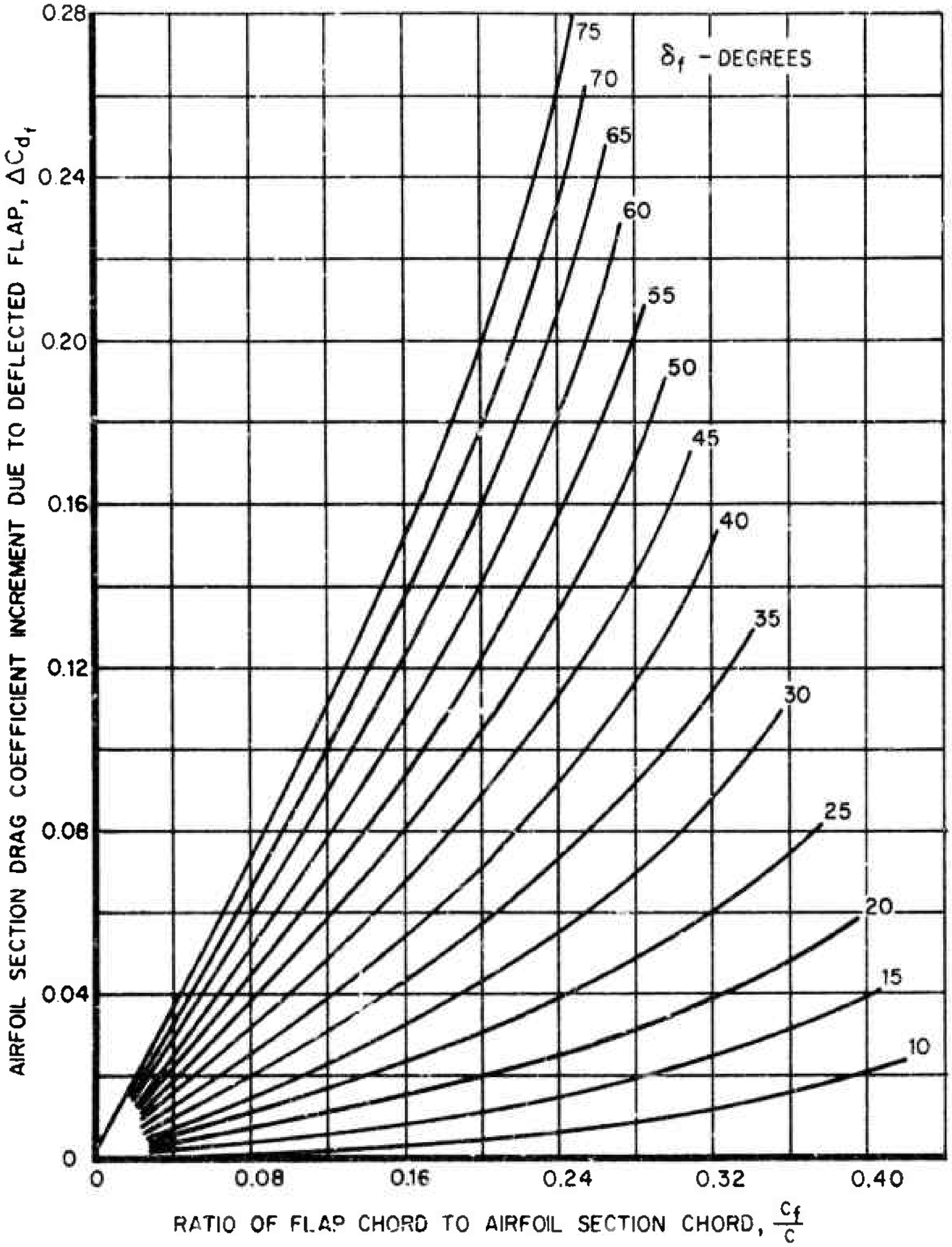

Figure 4. Two-Dimensional Drag Increment Due to Plain Flaps.

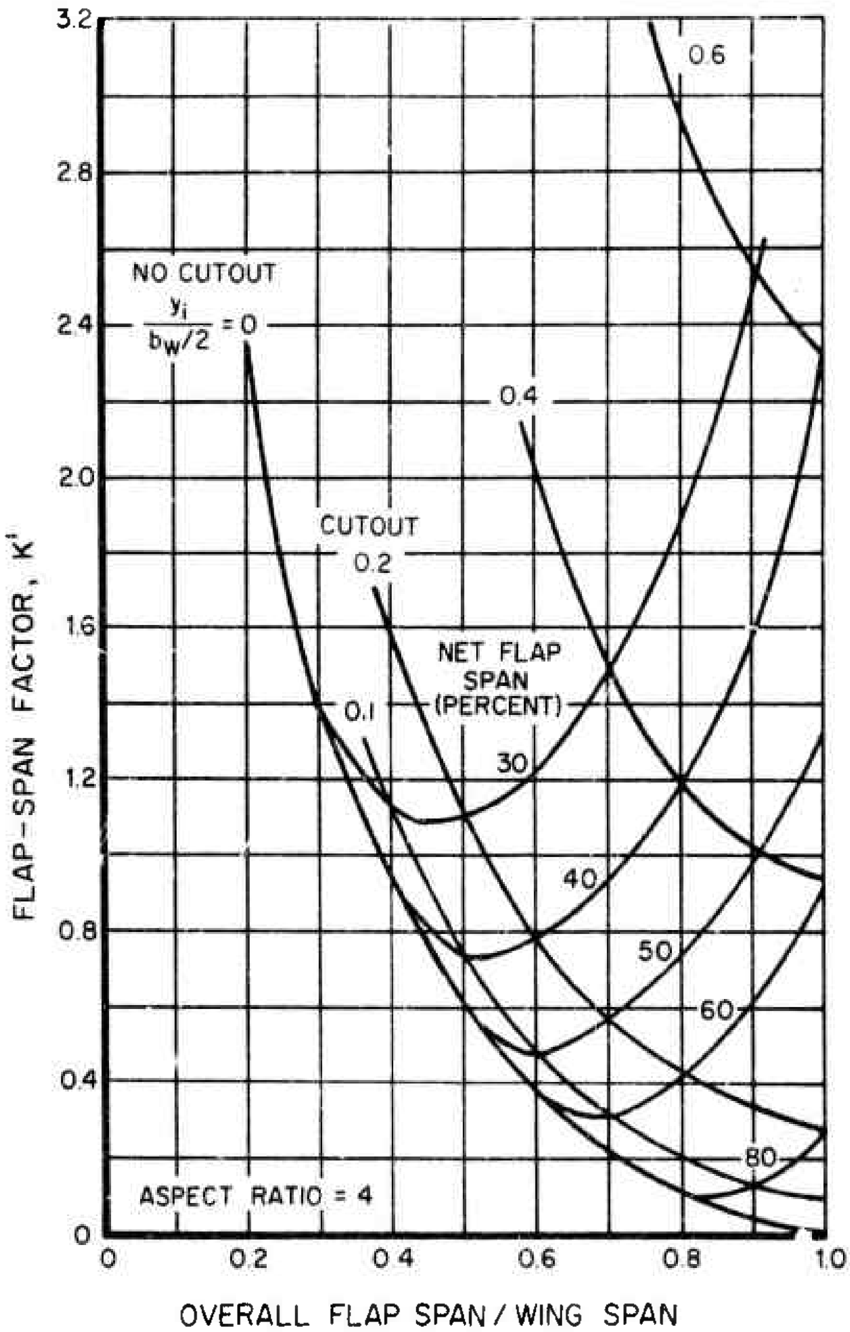

Figure 5. Factor K' for Calculating Induced Drag of an Elliptic Wing With Part-Span Flaps and Cutout.

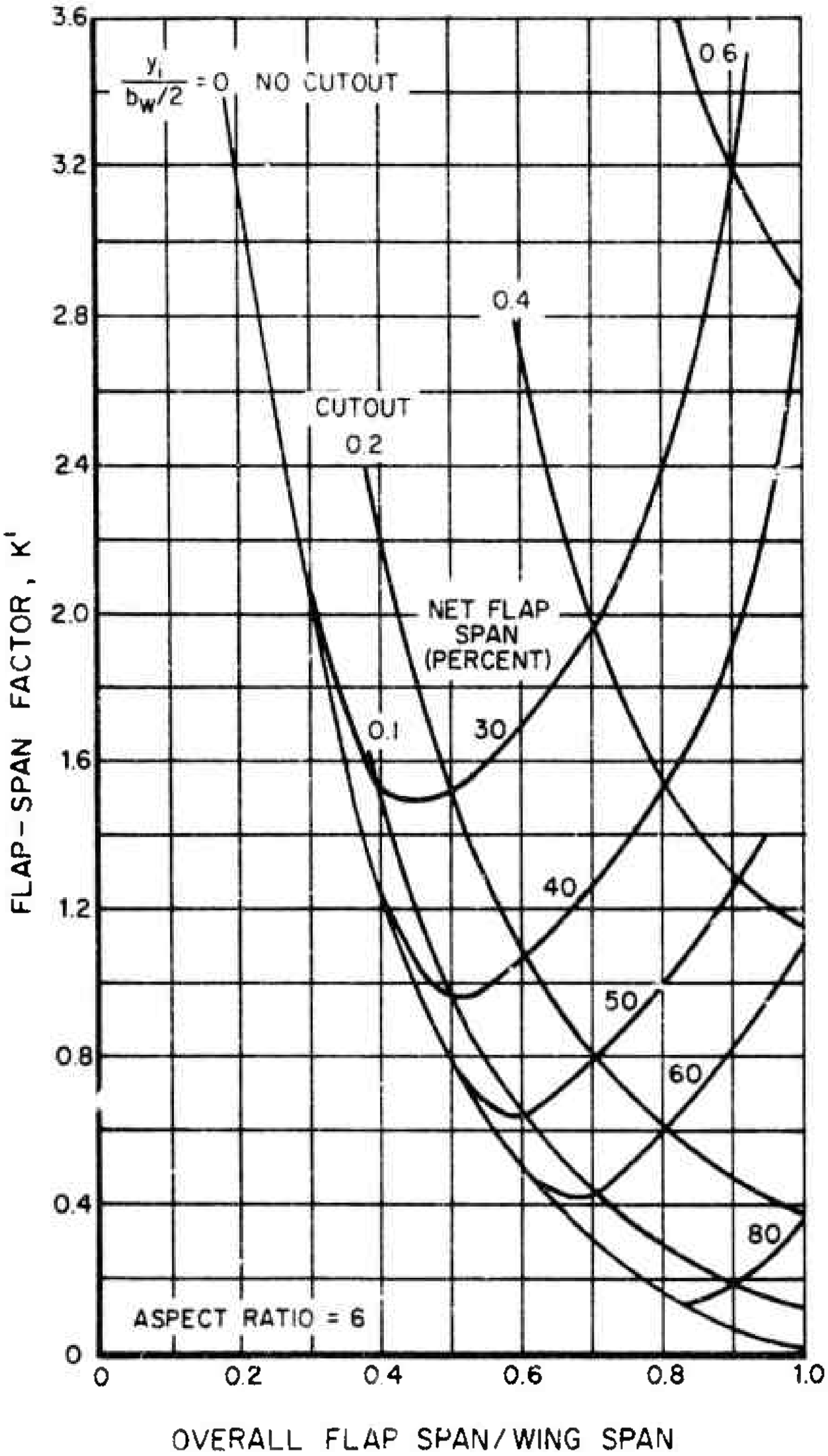

Figure 5. Continued.

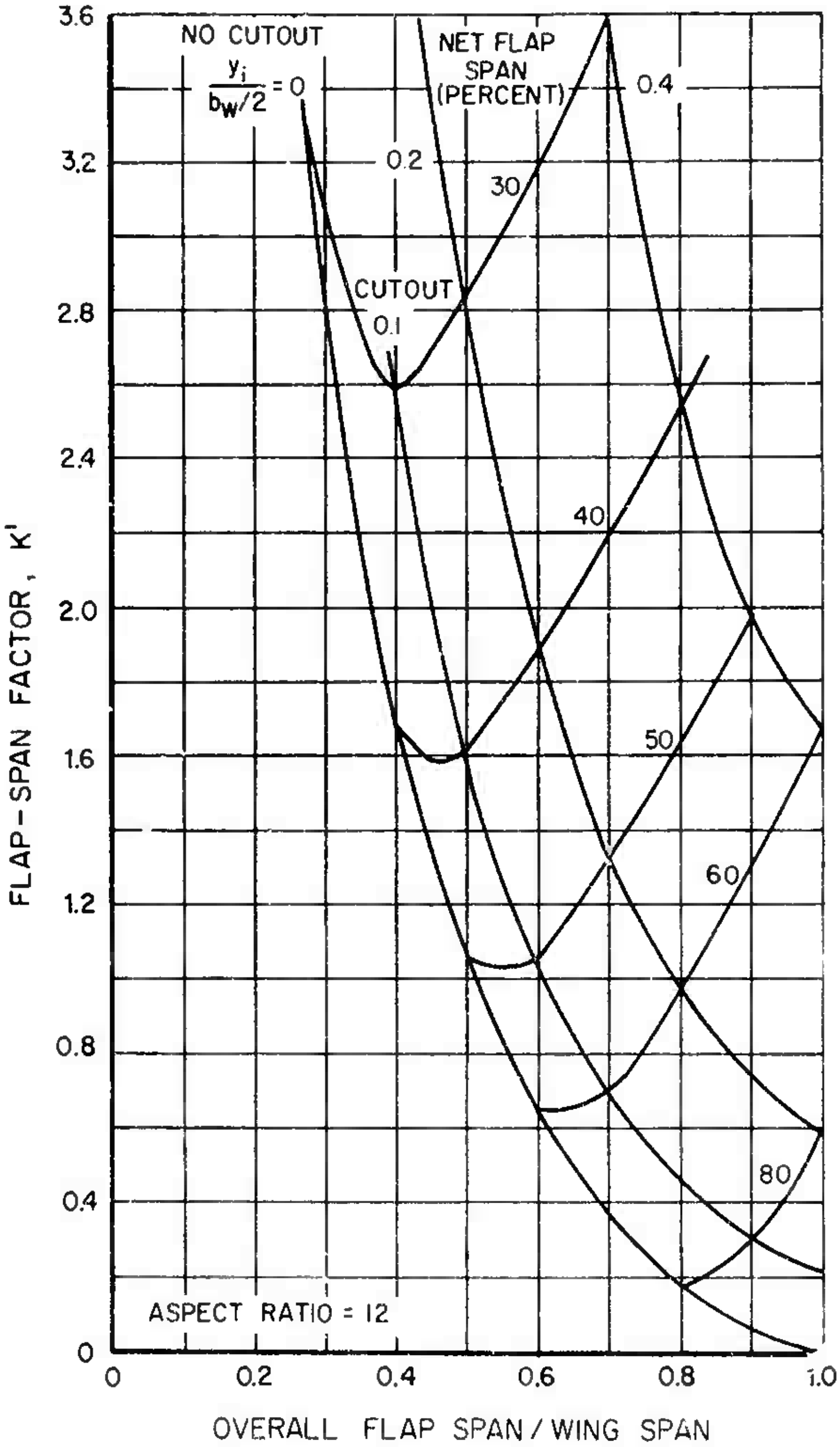

Figure 5. Concluded.

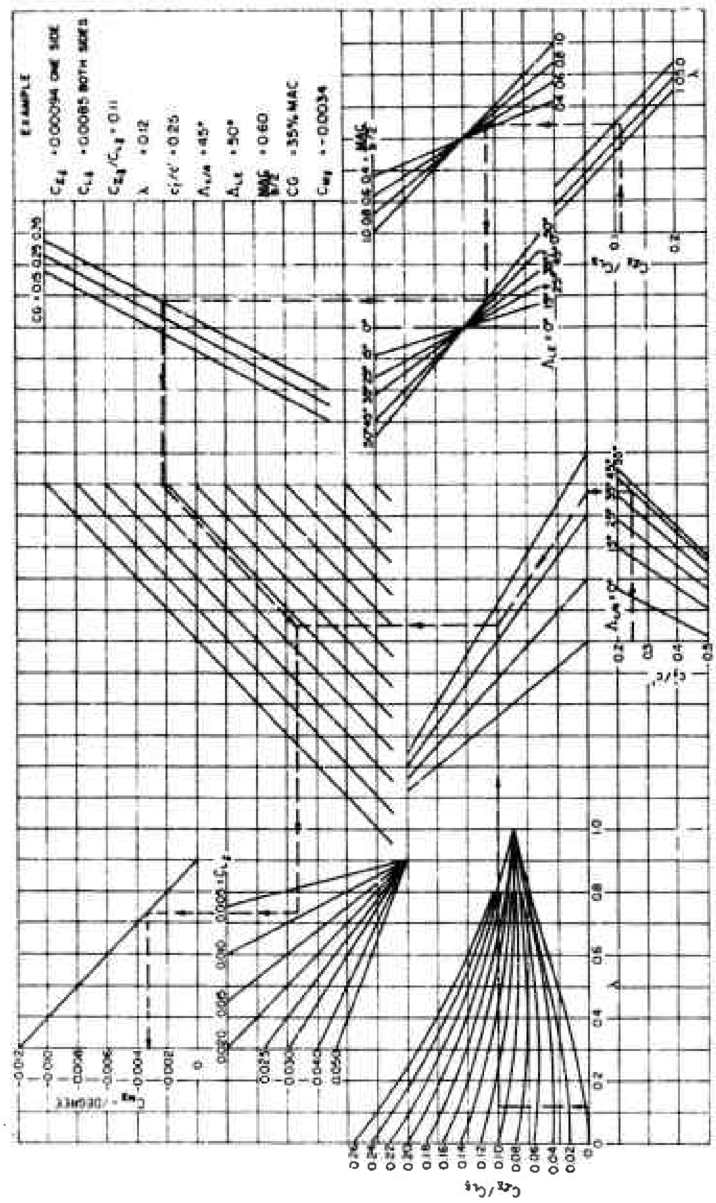

Figure 6. Pitching Moment Effectiveness, Subsonic C_{M_δ}.

The procedures presented in Subsections 5.6.4.2 and 5.6.4.3 for estimating the increments of drag and pitching moment, respectively, due to deflected wing flap, can be used if required to estimate these increments for deflected ailerons and elevators.

LITERATURE CITED

1. Ellison, D. E., and Malthan, L. V., USAF STABILITY AND CONTROL DATCOM, McDonnell Douglas Corporation, Douglas Aircraft Division, Flight Control Division, Air Force Flight Dynamics Laboratory, Wright-Patterson Air Force Base, Ohio, October 1960 (Revised to June 1969).

2. ROYAL AERONAUTICAL SOCIETY DATA SHEETS (VOLUME IV), Royal Aeronautical Society of Great Britain, 1955.

5.7 AUXILIARY PROPULSION CHARACTERISTICS

Compound helicopters can employ propellers, ducted propellers, turbojets, and fanjets to unload their rotors propulsively and thus increase their speed capability. Most research compound helicopters to date have employed jet engines for this purpose even though these engines are relatively inefficient in the compound helicopter speed range.

This section presents some basic performance data for the three propulsive systems which may he used in the design of compound helicopters. These systems include open propellers, ducted propellers, and jet engines. Because of the large variations of performance parameters and the specific geometry of each propulsive system, it is not expedient to present the required performance information for each propulsive system in the handbook format. For this reason it is recommended that the appropriate test data be used wherever possible. However, if such data are not available, the reference material cited in this section should be adequate for determining the required performance parameters for the specific propulsive systems under consideration.

5.7.1 Propellers

The characteristics of a propeller operating in a flow field parallel to the shaft axis are completely defined once thrust T and shaft torque Q are known at the trim condition. However, when a propeller operates in an unsymmetrical flow field ($\alpha_p \neq 0^\circ$ and/or $\beta_s \neq 0^\circ$), then oscillating airloads are generated on the propeller blades which result in propeller shaft in-plane forces and out-of-plane moments. The positive directions of these propeller forces and moments are shown in the sketch below.

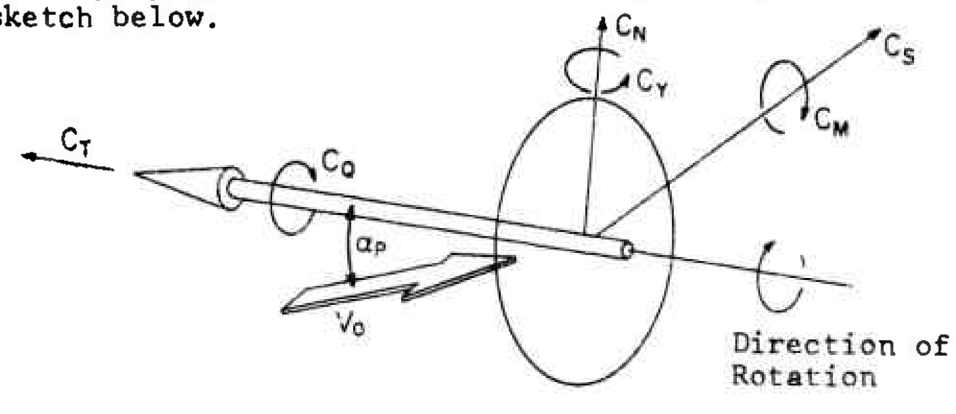

Directions of Propeller Forces and Moments.

The standard NASA propeller coefficients shown in the sketch are defined as:

$C_T = \frac{T}{\rho n^2 D^4}$, thrust coefficient

$C_N = \frac{N}{\rho n^2 D^4}$, normal-force coefficient

$C_S = \frac{S}{\rho n^2 D^4}$, side-force coefficient

$C_Q = \frac{Q}{\rho n^2 D^5}$, torque coefficient

$C_M = \frac{M}{\rho n^2 D^5}$, pitching moment coefficient

$C_Y = \frac{Y}{\rho n^2 D^5}$, yawing moment coefficient

$C_P = 2\pi C_Q$, power coefficient

where n = propeller rotational speed, rps

D = propeller diameter, ft

In addition, the following parameters are required to define the propeller and its operating condition:

B = number of blades

β = propeller blade angle measured at 0.75R, deg

$J = \frac{V_0}{nD}$, advance ratio

$J' = \frac{V_0 \cos \alpha_P}{nD}$, advance ratio based on velocity component normal to propeller disc

$$AF = \frac{10,000}{16} \int_{0.2}^{1.0} \left(\frac{b}{D}\right)\left(\frac{r}{R}\right)^3 d\left(\frac{r}{R}\right)$$, activity factor per blade

where b = blade chord at radius r, ft

R = propeller radius, ft

The activity factor, AF, is a measure of the blade's ability to absorb power; as such, it would be a better parameter for comparing different propellers than the solidity factor σ, which does not account for variations in blade width along the blade span. Any two propellers may have the same solidity, but if one has most of its blade area at the root while the other has most of its area at the tip, their capacities for absorbing power will be widely different.

It should be noted that the nomenclature and definition of propeller parameters vary greatly in the literature, and caution should be exercised when comparing the results of one report against another.

Many theoretical and semiempirical methods for estimating propeller forces and moments are available in the literature, such as those given in References 1 through 9. Although these methods are useful for calculating trim conditions, most of them do not provide any direct methods for calculating all the required propeller stability derivatives. If theoretical methods must be used to determine the propeller characteristics, References 1 and 2 are recommended because they do provide means for estimating most of the stability derivatives. However, even these methods require some empirical data in order to obtain accurate estimates.

If the propeller shaft horsepower is known, the charts in Reference 10 provide a simple means for accurately determining the thrust and torque for 2-, 3-, and 4-bladed propellers.

This report recommends the use of propeller test data to obtain the propeller characteristics and stability derivatives. A good compilation of such propeller test data is contained in References 11 through 14. By using test data for a propeller similar to the one under investigation, the required parameters can be quickly obtained for design purposes.

The propeller coefficients C_T, C_P, C_N, C_M, and C_Y are normally presented in any of the following formats:

Coefficients versus $J(J')$ for various β at constant values of α_P

Coefficients versus $J(J')$ for various α_P at constant values of β

Coefficients versus α_P for various $J(J')$ at constant values of β

Any of the above presentations can be cross plotted to obtain the required data. The coefficient C_S is normally assumed to be negligible for angle-of-attack variations. The propeller characteristics are obtained by reading C_T, $C_P = 2\pi C_Q$, C_N, C_M, and C_Y at the trim conditions. The stability derivatives of the coefficients versus J or J' and α_P are also obtained by graphically taking slopes at the trim conditions.

In sideslip (β_S), the symmetry in the propeller disc plane allows the propeller parameters to be determined by assuming α_P to be similar to β_S so that:

$$C_T = C_T$$

$$C_Q = C_Q$$

$$C_S \approx C_N$$

$$C_M \approx -C_Y$$

$$C_N = 0$$

$$C_Y \approx C_M$$

5.7.2 Ducted Propellers

Ducted propellers are attractive for use on compound helicopters mainly because they reduce the size of the propeller required to produce a given thrust. This increase in propulsive thrust is generated by the negative pressure distributions over the leading edge of the duct shroud and by the increase in flow rate through the propeller, which increases its efficiency. Also, at an angle of attack the shroud acts as an aerodynamic lifting surface, thus generating lift which may be used for control purposes.

Because of the many design and operating parameters that can vary for a ducted propeller, it is recommended that test data be used to accurately determine the characteristics of a given system. The test data presented in Reference 15 are particularly useful for this purpose.

References 16 through 18 can be used to estimate the characteristics of a ducted propeller if test data are not available. References 18 through 21 can be used to estimate the stability derivatives for these systems.

5.7.3 Jet Engines

Turbojet and fanjet characteristics are best obtained from test data or engine manufacturers' curves for the specific engines being used. Generally, only the thrust (T_{P_i}), the engine torque (Q_{P_i}), and the normal force at the inlet (N_{P_i}) are required to define trim. Of these parameters, the thrust is usually known either by measurement or by assuming a value. However, unless engine test data are available, the effect of engine torque (Q_{P_i}) is usually neglected since it is generally small. Reference 22 may be employed if more detailed estimates of jet engine characteristics are required.

If the static thrust is known, the decrease in thrust with forward speed can be estimated using Figure 1, which was obtained from Reference 23. This graph can be used to obtain typical values of the forward speed derivative $\partial T_{P_i}/\partial u$ by graphically taking slopes at the trimmed airspeed.

For preliminary design purposes, the normal force acting at the intake of a jet engine can be found from

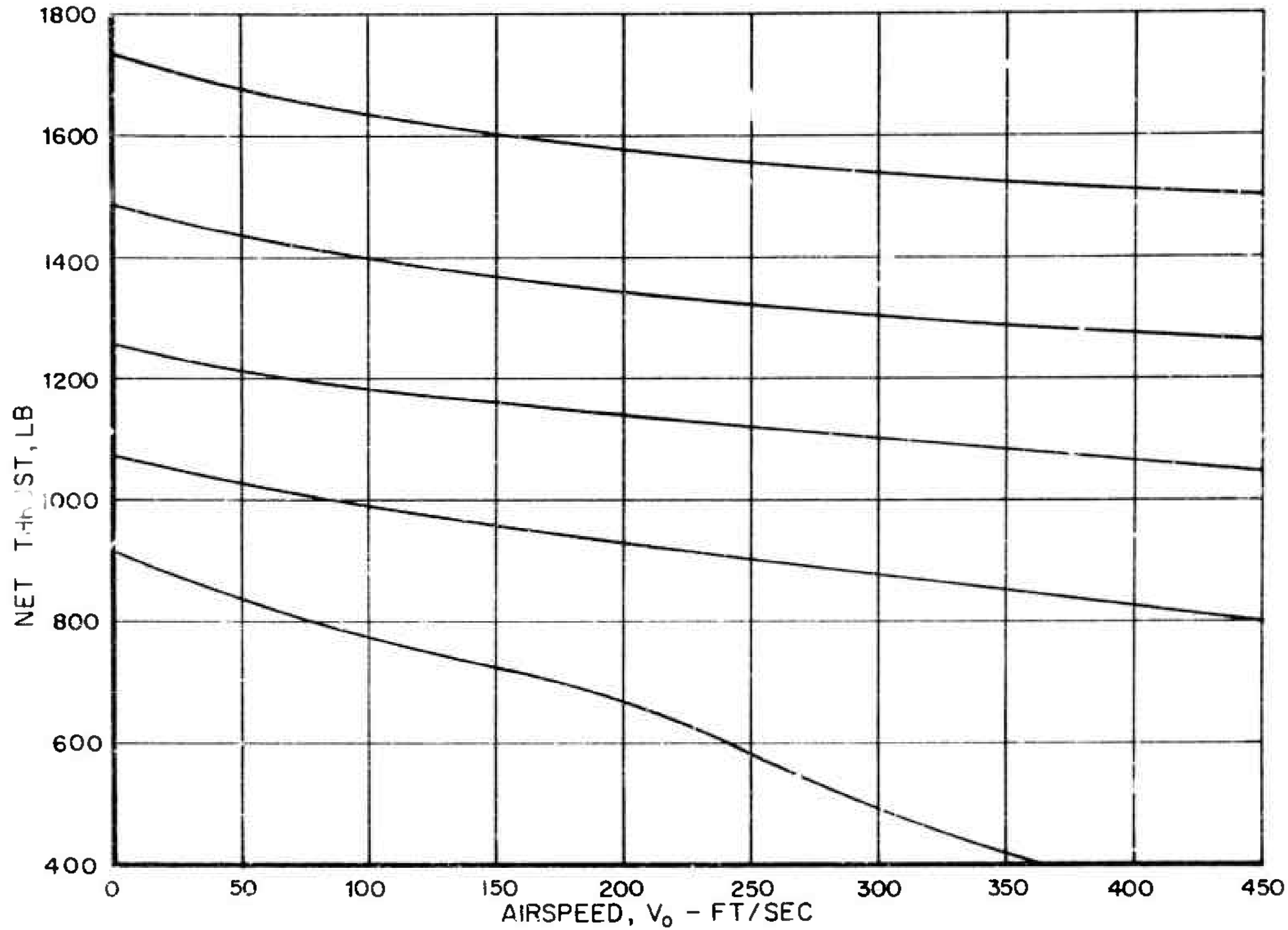

Figure 1. Typical Jet Engine Thrust Variation With Forward Speed (Reference 23).

momentum considerations. The air passing through a propulsive duct experiences, in general, a change in magnitude and direction. The change in magnitude is the principal source of thrust, and the change in direction produces the normal force which acts normal to the thrust vector at the inlet. The magnitude of the normal force can be estimated with the aid of the sketch below.

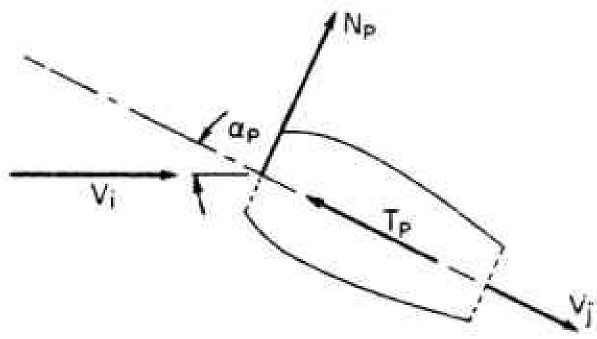

Jet Engine Force and Velocity Vectors.

Let the mass flow through the duct be m' slugs per second and the velocity vectors at the inlet and exhaust be V_i and V_j respectively. The magnitude of V_i can be expressed in terms of the mass flow m' and inlet area A_i ; thus

$$V_i = m'/A_i \rho_i$$

Application of the momentum principle then shows that the normal force or component of the momentum change can be expressed as

$$N_P = m' V_i \sin \alpha_P$$

$$= \rho_i V_i^2 A_i \sin \alpha_P$$

If we now assume free-stream conditions at the inlet such that $V_i \approx V_0$ and $\rho_i \approx \rho_0$, then

$$N_p = \rho_0 V_0^2 A_i \sin \alpha_p$$

$$= 2 q_0 A_i \sin(\alpha - \epsilon_p + i_p)$$

This expression is plotted in Figure 2 in a form suitable for graphical evaluation of the derivative $\partial N_p / \partial \alpha_p$.

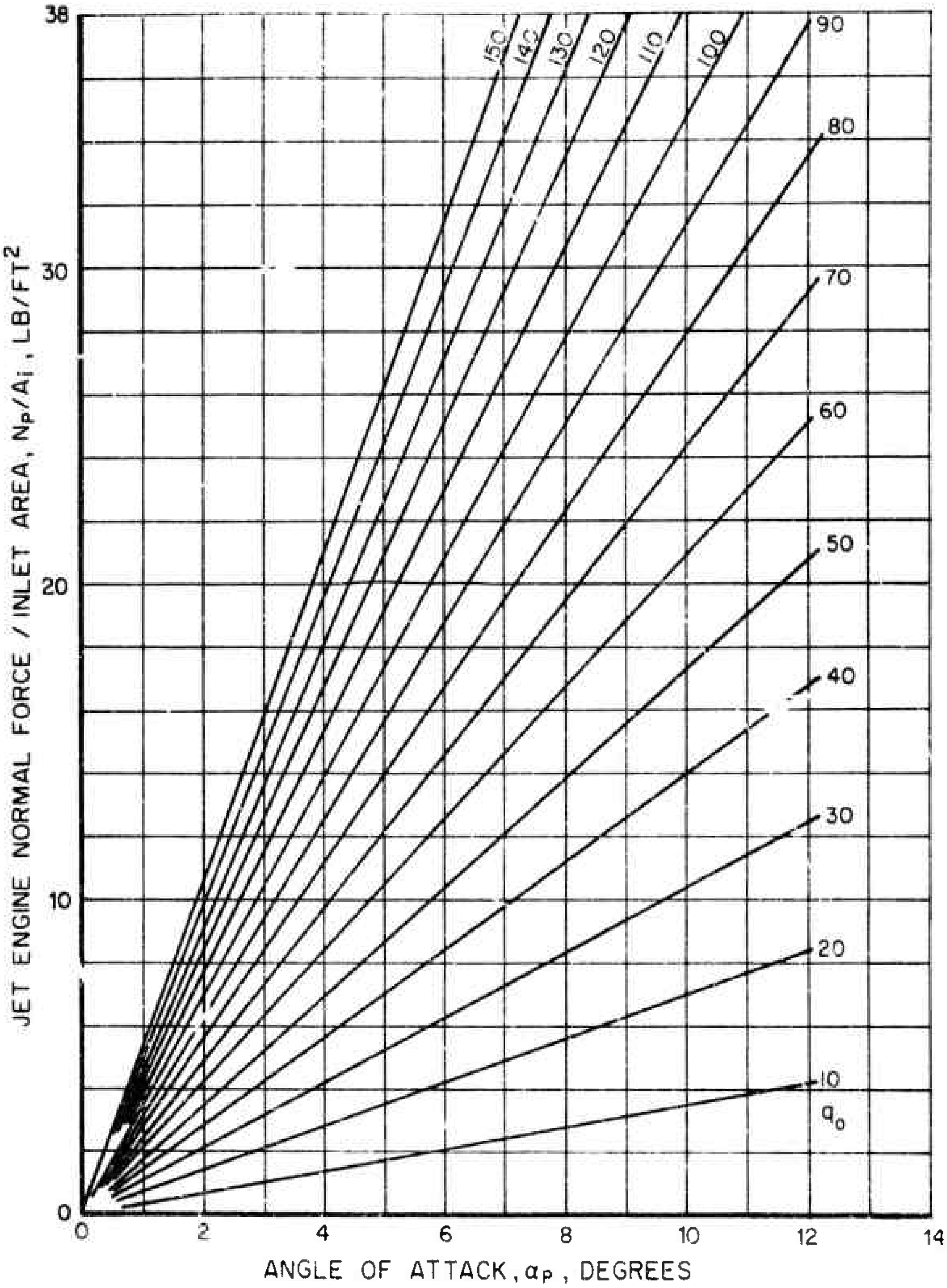

Figure 2. Jet Engine Normal Force From Momentum Considerations Versus Angle of Attack, α_p.

LITERATURE CITED

1. De Young, John, PROPELLER AT HIGH INCIDENCE, Journal of Aircraft, Vol. 2, No. 3, May-June 1965, pp 241-250.

2. Ellison, D. E., and Malthan, L. V., USAF STABILITY AND CONTROL DATCOM, McDonnell Douglas Corporation, Douglas Aircraft Division; Flight Control Division, Air Force Flight Dynamics Laboratory, Wright-Patterson Air Force Base, Ohio, October 1960 (Revised to June 1969).

3. Hall, Gerald, F., A METHOD OF ANALYSIS FOR PROPELLERS AT EXTREME ANGLES OF ATTACK, Journal of Aircraft, Vol. 6, No. 1, January-February 1969, pp 52-58.

4. Shenkman, Albert M., GENERALIZED PERFORMANCE OF CONVENTIONAL PROPELLERS FOR VTOL-STOL AIRCRAFT, Hamilton Standard, Report No. HS-1829, United Aircraft Corporation, Windsor Locks, Connecticut, March 1958.

5. Lock, C. N. H., A GRAPHICAL METHOD OF CALCULATING THE PERFORMANCE OF AN AIRSCREW, R. & M. No. 1849, Aeronautical Research Committee, London, England, August 1938.

6. Crigler, John L., and Gilman, Jean, Jr., CALCULATION OF AERODYNAMIC FORCES ON A PROPELLER IN PITCH OR YAW, NACA TN 2585, 1952. (Supersedes NACA RM L8K26).

7. Crigler, John L., COMPARISON OF CALCULATED AND EXPERIMENTAL PROPELLER CHARACTERISTICS FOR FOUR-, SIX-, AND EIGHT-BLADE SINGLE-ROTATING PROPELLERS, NACA WR L-362, 1944. (Formerly NACA ACR 4B04).

8. Ribner, Herbert S., FORMULAS FOR PROPELLERS IN YAW AND CHARTS OF THE SIDE-FORCE DERIVATIVE, NACA Rep. 819, 1945. (Supersedes NACA ARR 3E19).

9. Ribner, Herbert S., PROPELLERS IN YAW, NACA Rep. 820, 1945. (Supersedes NACA ARR 3L09).

10. Borst, H. V., A SHORT METHOD TO PROPELLER PERFORMANCE, Curtiss-Wright Corporation, Caldwell, N. J., July 1959.

11. McLemore, H. Clyde, and Cannon, Michael D., AERODYNAMIC INVESTIGATION OF A FOUR-BLADE PROPELLER OPERATING THROUGH AN ANGLE-OF-ATTACH RANGE FROM 0° to 180°, Langley Aeronautical Laboratory, NACA TN 3228, National Advisory Committee for Aeronautics, Washington, D. C., June 1954.

12. Yaggy, Paul F., and Rogallo, Vernon L., A WIND-TUNNEL INVESTIGATION OF THREE PROPELLERS THROUGH AN ANGLE-OF-ATTACK RANGE FROM 0° to 85°, Ames Research Center, NASA TN D-318, National Aeronautics and Space Administration, Washington, D. C., May 1960.

13. Wickens, R. H., AERODYNAMIC FORCE AND MOMENT CHARACTERISTICS OF A FOUR-BLADED PROPELLER YAWED THROUGH 120 DEGREES, National Aeronautical Establishment, Aeronautical Report LR-454, National Research Council of Canada, Ottawa, Canada, May 1966.

14. Olcott, John W., TESTS OF A HAMILTON STANDARD FOUR-WAY 21-INCH-DIAMETER MODEL PROPELLER EMPLOYING THE U. S. NAVY AIRBORNE MODEL TEST FACILITY, Princeton University, Report No. 675, Princeton University, Princeton, N. J., April 1964.

15. Black, Donald M., Wainauski, Harry S., and Rohrback, Carl, SHROUDED PROPELLERS - A COMPREHENSIVE PERFORMANCE STUDY, United Aircraft Corporation, No. 68-994, AIAA Fifth Annual Meeting and Technical Display, Philadelphia, Pa. October 1968.

16. Meyerhoff, L., and Zvengrowski, P., DUCTED PROPELLER STUDY, Eastern Research Group (ERG Doc. 947), U. S. Army Transportation Research Command, Fort Eustis, Virginia, January 1962.

17. Theodorsen, Theodore, THEORETICAL INVESTIGATION OF DUCTED PROPELLER AERODYNAMICS, VOL. 1, Republic Aviation Corporation; TRECOM Technical Report CRD 3860, U. S. Army Transportation Research Command, Fort Eustis, Virginia, August 1960.

18. Kriebel, A. R., THEORETICAL INVESTIGATION OF STATIC COEFFICIENTS STABILITY DERIVATIVES, AND INTERFERENCE FOR DUCTED PROPELLERS, Vidya, Report No. 112 Itek Corporation, Palo Alto, California, March 1964.

19. Kriebel, A. R., Sacks, A. H., and Nielsen, J. N., THEORETICAL INVESTIGATION OF DYNAMIC STABILITY DERIVATIVES OF DUCTED PROPELLERS, Vidya, Technical Report No. 63-95, Itek Corporation, Palo Alto, California, January 1963.

20. Kriebel, A. R., THEORETICAL STABILITY DERIVATIVES FOR A DUCTED PROPELLER, Vidya, Itek Corporation, Palo Alto, California, October 1963.

21. Kriebel, A. R., THEORETICAL STABILITY DERIVATIVES FOR A DUCTED PROPELLER, Journal of Aircraft, Vol. 1, No. 4, July-August 1964, pp 203-210.

22. Ribner, Herbert S., FIELD OF FLOW ABOUT A JET AND EFFECT OF JETS ON STABILITY OF JET-PROPELLER AIRPLANES, NACA WR L-213 (ARC No. L6C13), National Advisory Committee for Aeronautics, Langley Field, Virginia, March 1946.

23. Van Wyckhouse, J. F., HIGH-PERFORMANCE UH-1 COMPOUND HELICOPTER MANEUVER FLIGHT TEST PROGRAM, Bell Helicopter Company; USAAVLABS Technical Report 66-17, U. S. Army Aviation Materiel Laboratories, Fort Eustis, Virginia, February 1966, AD630927.

5.8 DOWNWASH INTERFERENCE EFFECTS

Interference effects between aerodynamic components can be expressed in terms of changes of local velocity and local angle of attack. Changes in the effective velocity due to aerodynamic interference are generally small and are herein neglected. Changes in local angle of attack, however, can be appreciable. In general, the local angle of attack of an aerodynamic component can be expressed in terms of the remote stream angle of attack and interference angles as follows:

$$\alpha_{LOCAL} = \alpha + i - \epsilon$$

where

α = remote wind angle of attack relative to the X-axis

i = the geometric inclination of the specific aerodynamic component considered with respect to the X-axis

ϵ = aerodynamic interference angle

For the compound helicopter configurations considered here, the aerodynamic interference is generated mainly by the downwash velocities of the rotors, the downwash velocity behind the wing, and the jet-induced downwash behind the auxiliary jet engines.

5.8.1 Rotor Interference Effects

The rotor downwash can affect any other rotor, the fuselage, and any lifting surface attached to the fuselage. The downwash velocity of a rotor varies with time as well as with location. The determination of the effect of such varying velocity distribution on the lift and drag of a rotor, fuselage, or lifting surface is an exceedingly complicated task; in fact, to be consistent with other assumptions made, it is not required in the stability and control analysis. It is adequate to assume that the effective change of angle of attack of an aerodynamic component due to rotor downwash is equal to the average downwash velocity of the rotor, divided by the free-stream velocity, and multiplied by an appropriate downwash interference factor. Hence, the angle due to downwash interference of the front rotor on the rear rotor of a tandem helicopter is given by

$$\epsilon_R = K_{FR}\left(\frac{V_{i_F}}{V_o}\right)$$

where K_{FR} is the interference factor of the front rotor on the rear rotor, as identified by the subscripts FR; V_{i_F} is the average induced velocity at the front rotor plane. The term V_{i_F} is obtained by use of the momentum equation as follows:

$$\frac{V_{i_F}}{V_o} = \tan \alpha_{c_F} - \left(\frac{\lambda}{\mu}\right)_F = \left[\frac{\sigma}{2\mu\sqrt{\mu^2+\lambda^2}}\left(\frac{C_L'}{\sigma}\right)\right]_F$$

The downwash interference angles of the front rotor on the rear of a tandem-rotor helicopter or front and rear rotors on other aerodynamic components can therefore be written as follows:

(a) Front Rotor on Rear Rotor

$$\epsilon_R = K_{FR}\left[\tan \alpha_c - \left(\frac{\lambda}{\mu}\right)\right]_F$$

(b) Fuselage

$$\epsilon_{FUS} = K_{FFUS}\left[\tan \alpha_c - \left(\frac{\lambda}{\mu}\right)\right]_F + K_{RFUS}\left[\tan \alpha_c - \left(\frac{\lambda}{\mu}\right)\right]_R$$

(c) Wing

$$\epsilon_W = K_{FW}\left[\tan \alpha_c - \left(\frac{\lambda}{\mu}\right)\right]_F + K_{RW}\left[\tan \alpha_c - \left(\frac{\lambda}{\mu}\right)\right]_R$$

(d) Horizontal Tail Surface

$$\epsilon_T = K_{FT}\left[\tan \alpha_c - \left(\frac{\lambda}{\mu}\right)\right]_F + K_{RT}\left[\tan \alpha_c - \left(\frac{\lambda}{\mu}\right)\right]_R$$

(e) Vertical Tail Surface

$$\epsilon_{VT} = K_{FVT}\left[\tan \alpha_c - \left(\frac{\lambda}{\mu}\right)\right]_F + K_{RVT}\left[\tan \alpha_c - \left(\frac{\lambda}{\mu}\right)\right]_R$$

(f) Rear Rotor on Front Rotor

$$\epsilon_F = K_{RF}\left[\tan\ \alpha_C - \left(\frac{\lambda}{\mu}\right)\right]_R$$

(g) Tail Rotor

$$\epsilon_{TR} = K_{FTR}\left[\tan\ \alpha_C - \left(\frac{\lambda}{\mu}\right)\right]_F + K_{RTR}\left[\tan\ \alpha_C - \left(\frac{\lambda}{\mu}\right)\right]_R$$

On the basis of data on the downwash behind a single rotor, such as Reference 1, it has been concluded by other investigators that a presentation of the downwash factor as a function of wake angle will yield more accurate results. The wake angle is defined by

$$X = a_{\parallel} + \tan^{-1}\left[\frac{1}{\left(-\frac{\lambda}{\mu}\right)}\right]$$

The variation of the interference factor K_{FR} as a function of X, (presented in Figure 1) neglecting rotor overlap and differential rotor height, may be taken as that suggested in Reference 2.

This factor is obtained from the theory of Reference 3 and represents the value of the ratio of the downwash at the location of the center of the rear rotor to the downwash at the center of the front rotor. The theory is based on the downwash due to one isolated rotor and, hence, neglects the effect of the presence of the rear rotor on the resultant flow of the front rotor. Correlation with test data, similar to those obtained in Reference 4, is required to check the validity of neglecting the effect of the rear rotor on the forward rotor. It is recommended that until better information becomes available, the value of K_{FR}, as presented in Figure 1, should be used. It is also recommended that K_{FT} be taken equal to K_{FR}. Very little information is available on the effects of the rear rotor on the front rotor, therefore some investigators recommend the use of $K_{RF} = -0.08$ to indicate the existence of a slight upwash. Until more reliable data becomes available, it is recommended that $K_{RF} = 0$ be used.

Measurements of fuselage lift and drag reported in Reference 5 indicate that for a single rotor helicopter, K_{FFUS} is approximately 1.0. Also, test data presented in

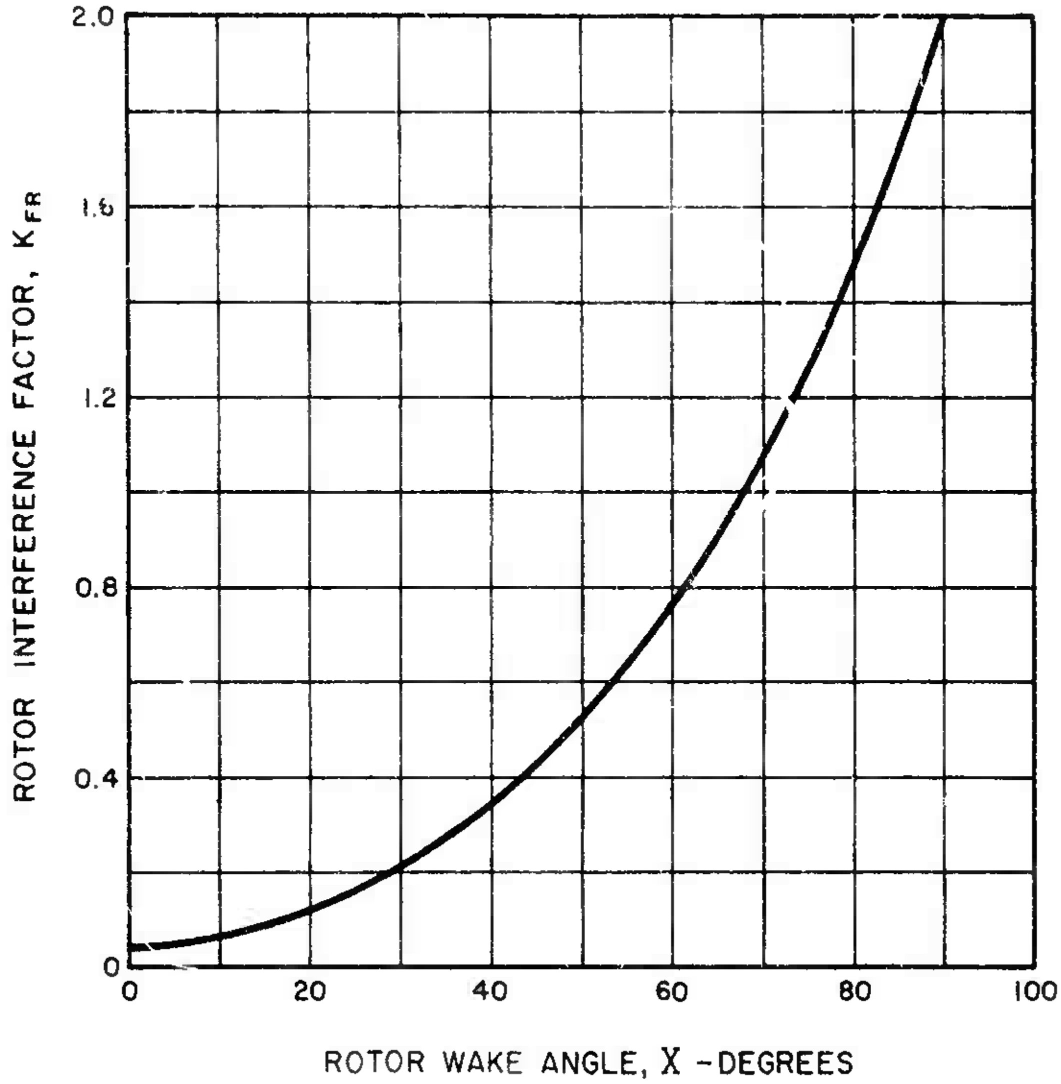

Figure 1. Rotor Interference Factor, K_{FR}, Versus Rotor Wake Angle, X.

Reference 5 on the horizontal tail interference factor are reproduced here as Figure 2. These data were obtained for the horizontal tail, located approximately one rotor radius behind the rotor center. Based on these data, it is recommended that K_{FT} = 1.0 be used.

In summary, the following values for the downwash interference factors are recommended:

K_{FR} — see Figure 1

$K_{FT} = K_{FVT} = K_{FTR} = K_{FR} = K_{FFUS} = 1.0$

$K_{RT} = K_{RVT} = K_{RTR} = K_{RFUS} = 1.0$

$K_{RF} = 0$

The interference factor of the front rotor or the rear rotor, if any, on the wing can be obtained from the experimental results of Reference 6 reproduced herein in Figure 3. This figure shows the variation of the rotor-wing interference factor K_{FW} as a function of wing vertical location relative to the rotor $(\ell_{Z_W}-\ell_{Z_F})/2R_F$ and the wing size.

5.8.2 Wing Interference Effects

The primary interference effect of a wing is to induce a downwash angle (ϵ_T) at the tail. This effect can be estimated from Figures 4 and 5, which have been reproduced from Reference 7. The results shown in these figures are presented as a function of location of the tailplane relative to the wing for a series of values of aspect ratio (AR_W = 6, 9, and 12) and taper ratios (λ_W = 1, 2, 3 and 5). For interpolation, values of ϵ_T/C_{L_W} should be cross plotted against $1/AR_W$. The charts apply to subsonic flow only, and to wings with sweep less than 15 degrees.

The calculation procedure for obtaining ϵ_T is as follows:

(a) From the aircraft geometry, obtain b_W, AR_W, λ_W, and x, which is the distance measured parallel to the direction of airflow between the quarter chord point of the wing root chord and the quarter chord point of the horizontal tail. Also obtain C_{L_W} from Section 5.4.

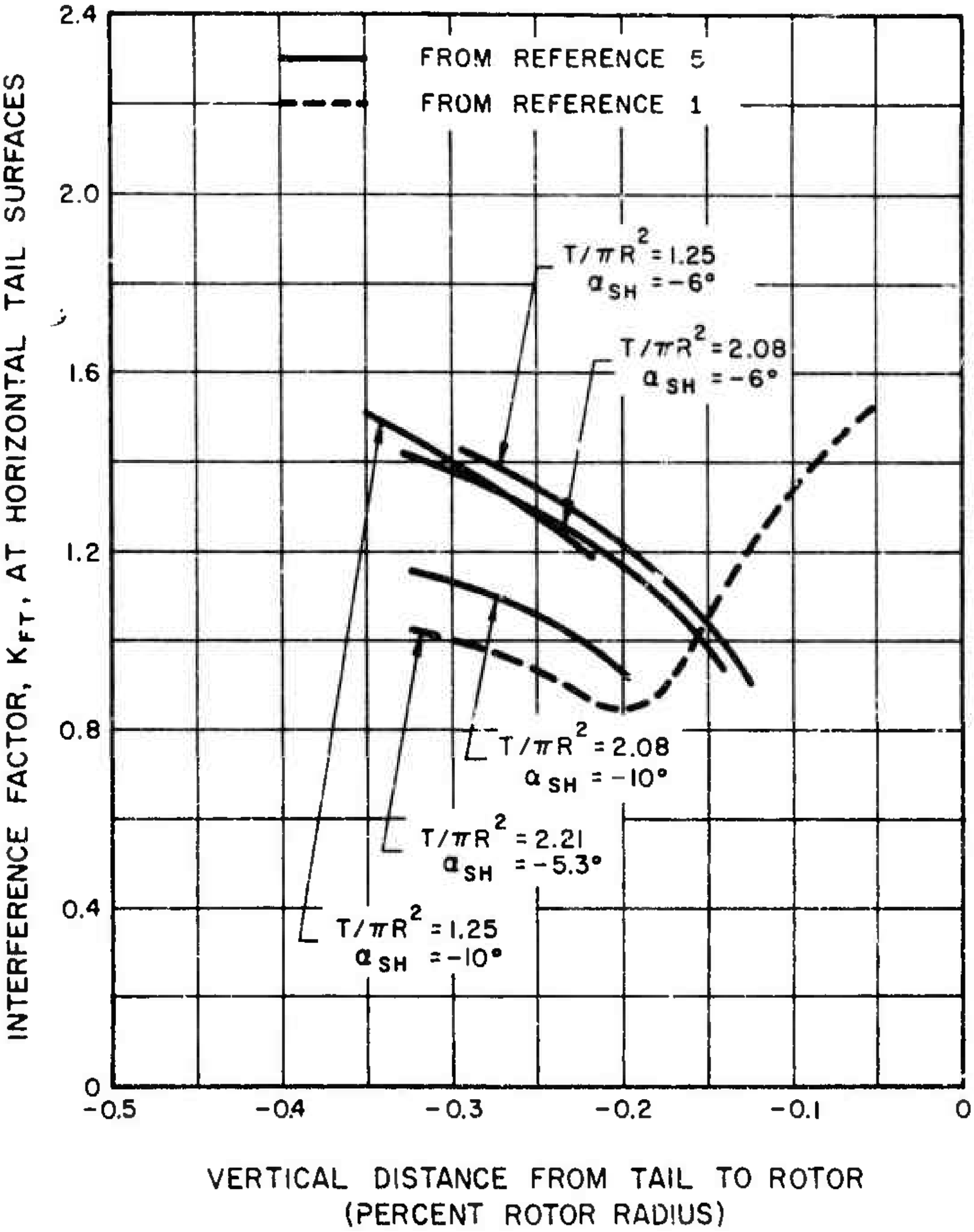

Figure 2. Interference Factor, K_{FT} at a "Half-Tee" Tail Versus Vertical Distance From Tail to Rotor.

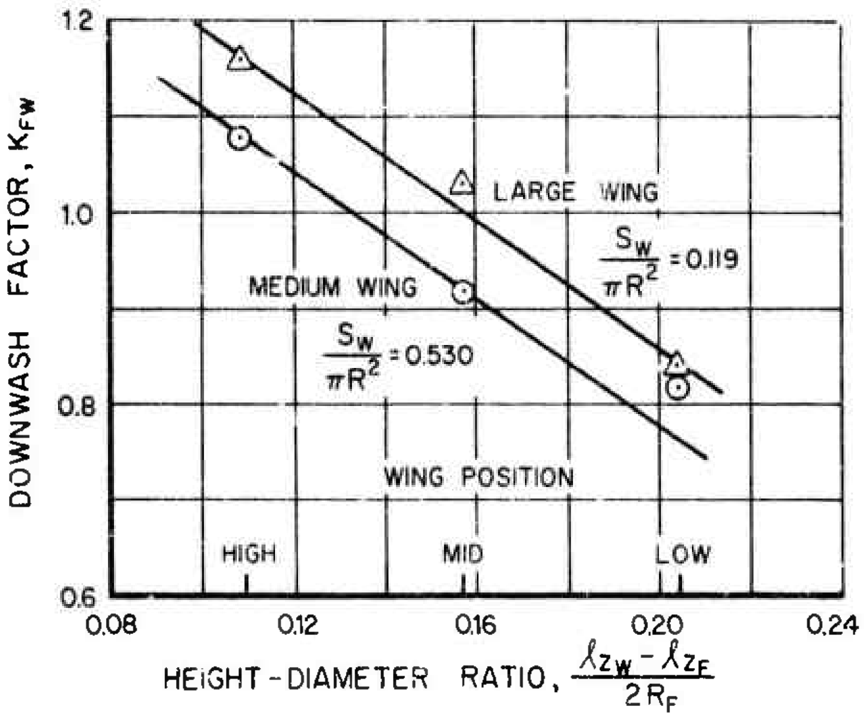

Figure 3. Wing Position Versus Downwash Factor for the Large and Medium Wings.

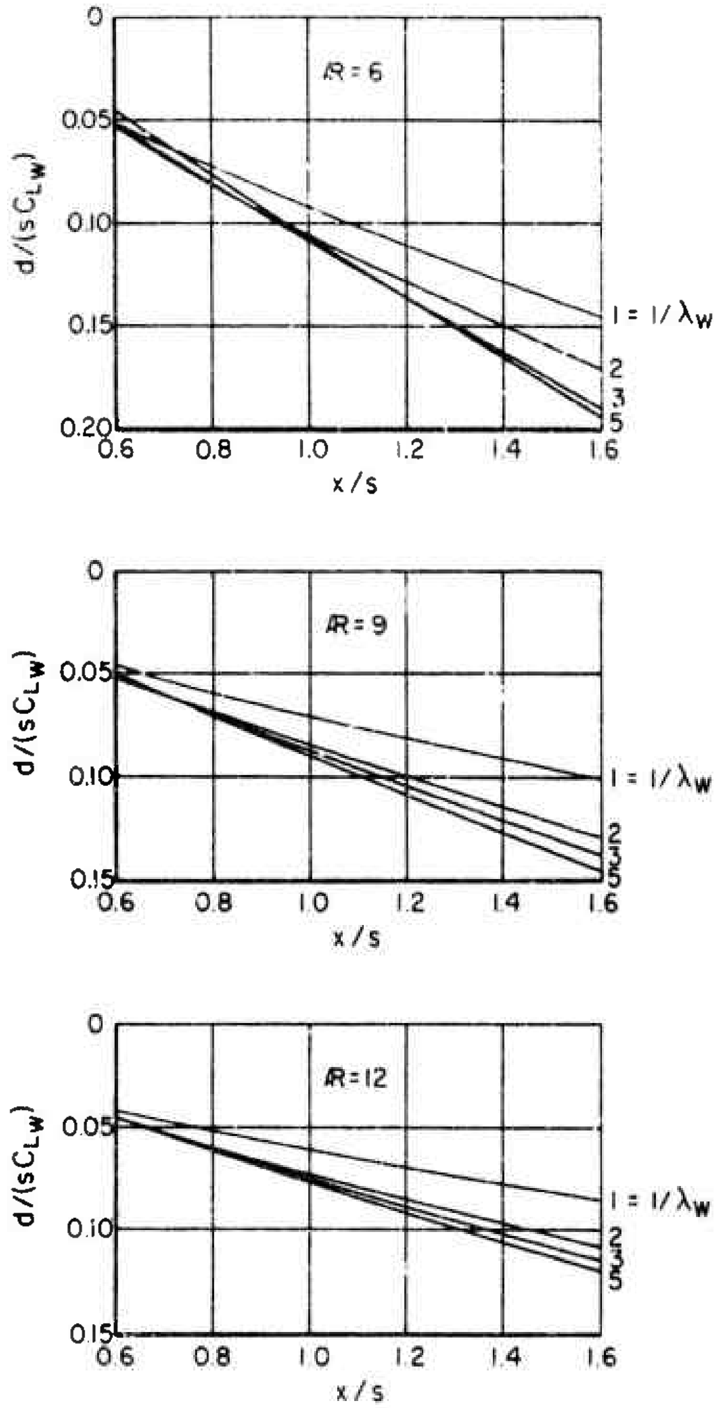

Figure 4. Displacement of Vortex Median Plane.

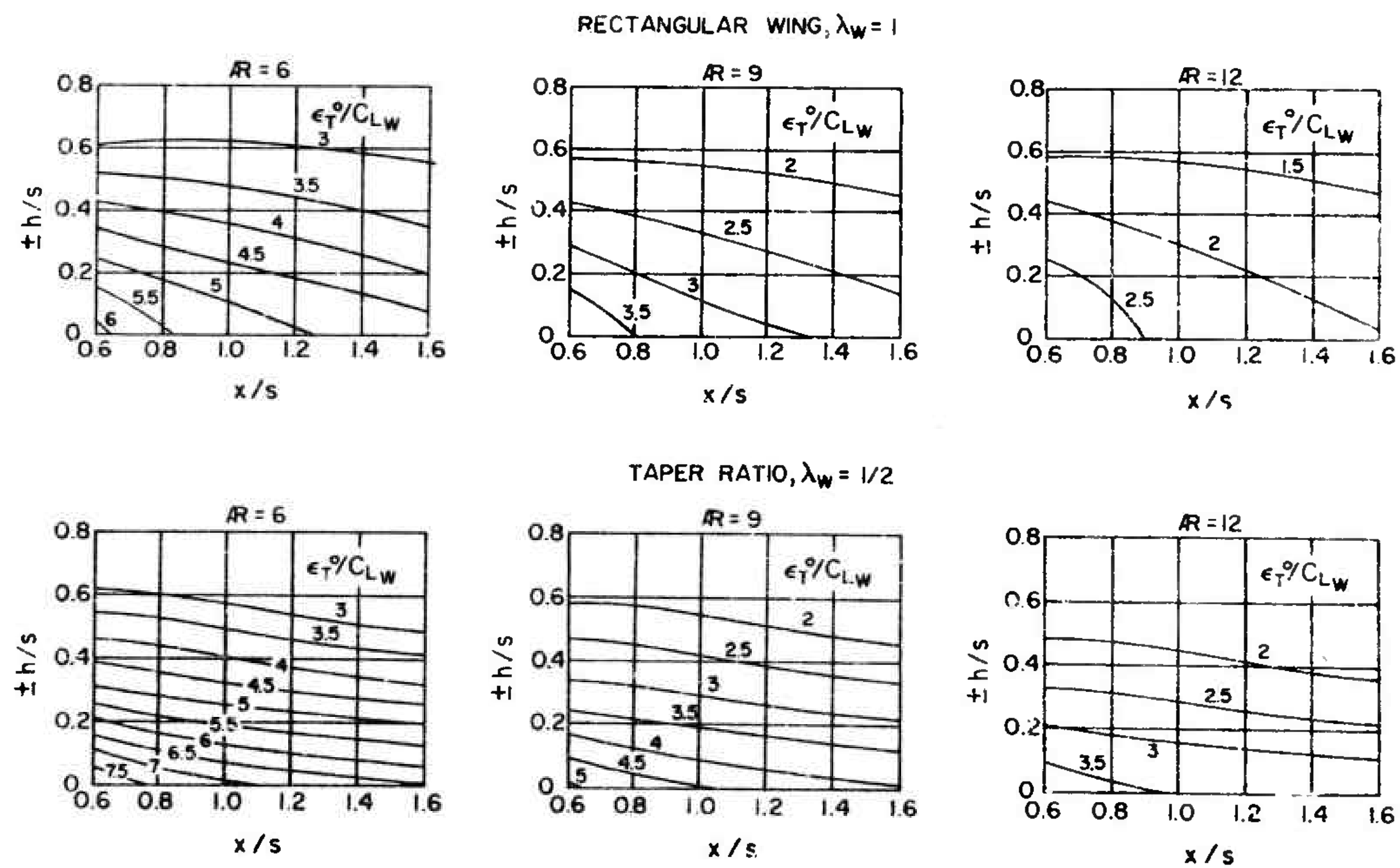

Figure 5. Downwash Behind Wings of Taper Ratios, λ_W = 1, 1/2, 1/3, 1/5.

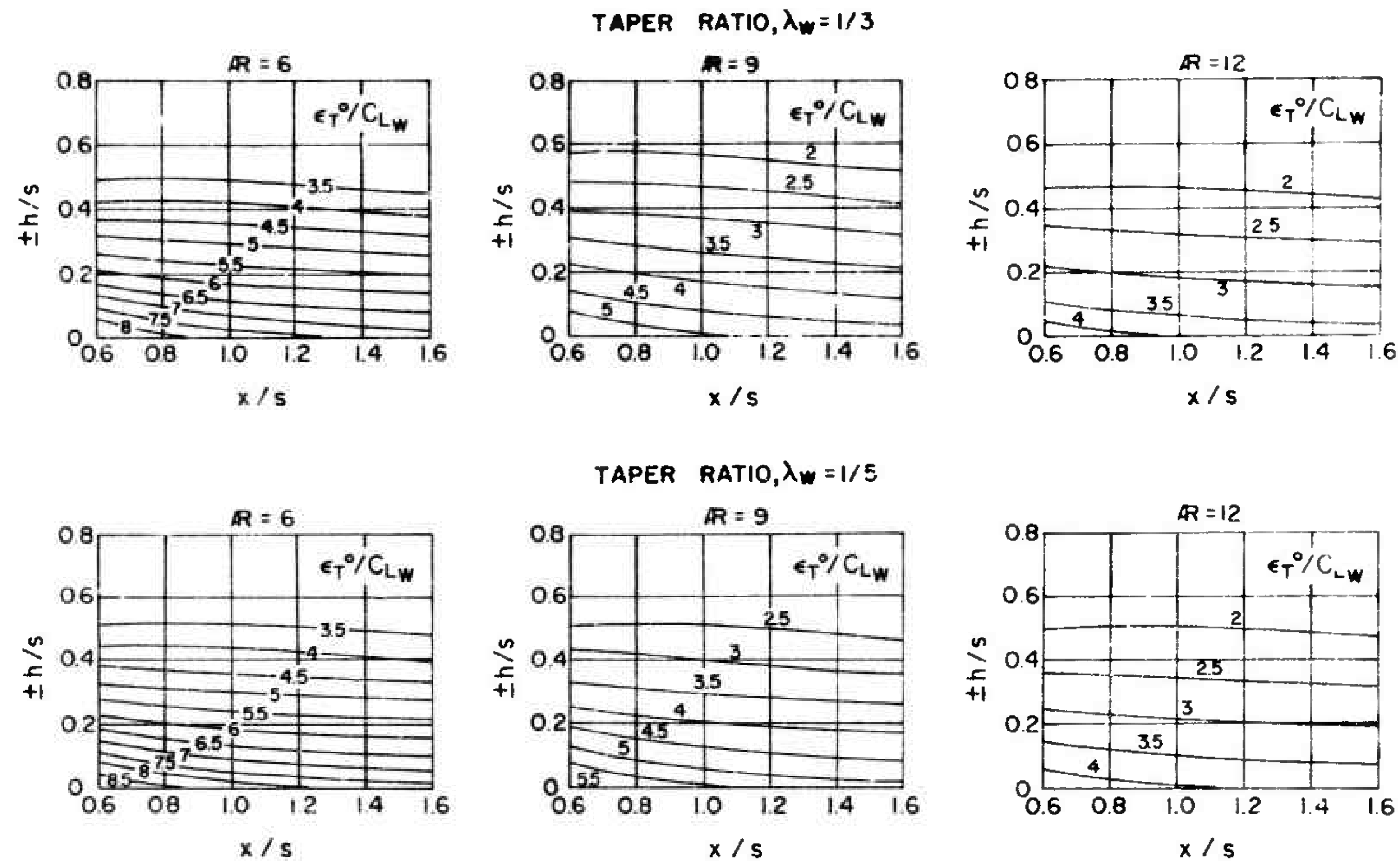

Figure 5. Concluded.

(b) Calculate

$$s = \frac{b_W}{2}$$

(c) Using the values of λ_W and AR_W from step (a) and the ratio x/s, obtain $d/(sC_{L_W})$ from Figure 4. The parameter d is the distance of the vortex sheet median plane below the wing trailing edge, measured normal to the direction of airflow.

(d) From aircraft geometry, obtain h the distance to the quarter chord point of the horizontal tail (up or down), from the vortex sheet median plane, measured normal to the airflow (i.e., from the position defined by x and d).

(e) For the wing parameters AR_W, λ_W obtained in step (a) and the ratios x/s and $\pm h/s$, determine ϵ_T/C_{L_W} from Figure 5. Finally, obtain the downwash angle at the tail due to the wing, thus:

$$\epsilon = \left(\frac{\epsilon_T}{C_{L_W}}\right) C_{L_W}$$

For more detailed estimates of wing downwash angles or for configurations not covered by the above method, the wing downwash charts in Reference 8 can be used.

5.8.3 Jet Induced Downwash

The downwash angle induced on the horizontal tail by one or more jets may be estimated by using the results presented in Figures 6, and 7, reproduced from Reference 9. The calculation procedure is as follows:

(a) Calculate the theoretical origin of the jet x_j to be 2.3 jet exit diameters (D_j) upstream of the jet exit, thus

$$x_j = 2.3 D_j$$

(b) From the aircraft geometry obtain:

(i) the axial distance (x_1) along the jet thrust axis from the theoretical origin of the jet to a

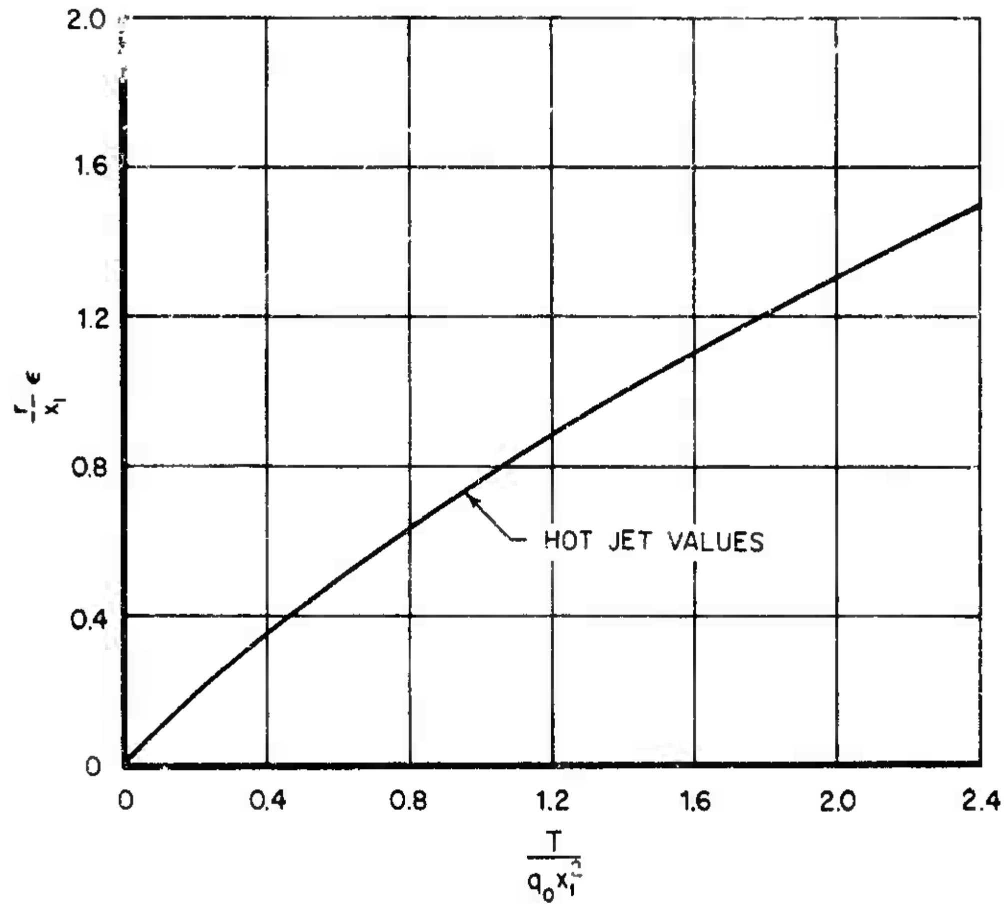

Figure 6. Flow Inclination Outside a Jet.

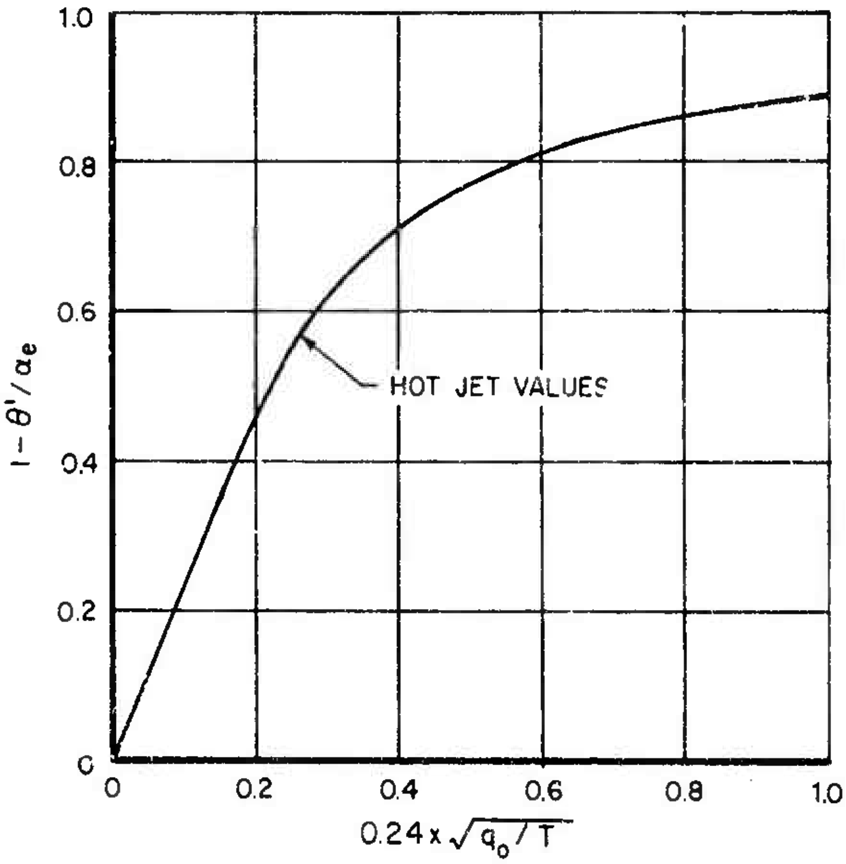

Figure 7. Angular Deviation of Jet Due to Angle of Attack.

perpendicular to the elevator hinge line

(ii) the radial distance r_l from the jet thrust axis to the elevator hinge line

(c) Using the value of x_l from step (b), compute $T_P/q_0 x_l^2$ and obtain the value of $r\epsilon/x_l$ from Figure 6.

(d) From Figure 7 obtain values of $(1-\theta'/\alpha_e)$ for appropriate values of $0.24 x_l\sqrt{q_0/T_P}$ and at $0.24 x_j\sqrt{q_0/T_P}$ where

θ' is the local inclination of the jet axis to the general flow

α_e is the angle of attack of the thrust axis relative to the average flow between the jet and tail

(e) Sum the two values of $(1-\theta'/\alpha_e)$ obtained in step (d) and divide the result by 2 to obtain $(1-\theta'/\alpha_e)_{avg.}$

(f) Obtain the downwash angle at the horizontal tail due to the wing, ϵ_T, from Section 5.8.2 and use this to obtain

$$\alpha_e = \alpha_p - \epsilon_T \quad \text{degrees}$$

(g) Find the actual location of the jet center line relative to the tail (r), thus:

$$r = r_l + \Delta r$$

where the change due to jet deflection in the radial distance r_l is given by

$$\Delta r = -\frac{\alpha_e}{57.3}(x_l - x_j)(1-\theta'/\alpha_e)_{avg.}$$

(h) Using the value of r from step (g) and x_l from step (b), obtain the jet-induced flow inclination (ϵ) from the value of $r\epsilon/x_l$ obtained in step (c), thus

$$\epsilon = \left(\frac{r\epsilon}{x_l}\right)\frac{x_l}{r}$$

(i) From Figure 8 obtain the ratio (ϵ_T/ϵ) as a function of $2d/b_T$ and r/b_T. Using the value of ϵ from step (h), obtain the estimate of the mean induced downwash angle over the horizontal tail, thus:

$$\epsilon_T = \left(\frac{\epsilon_T}{\epsilon}\right)\epsilon$$

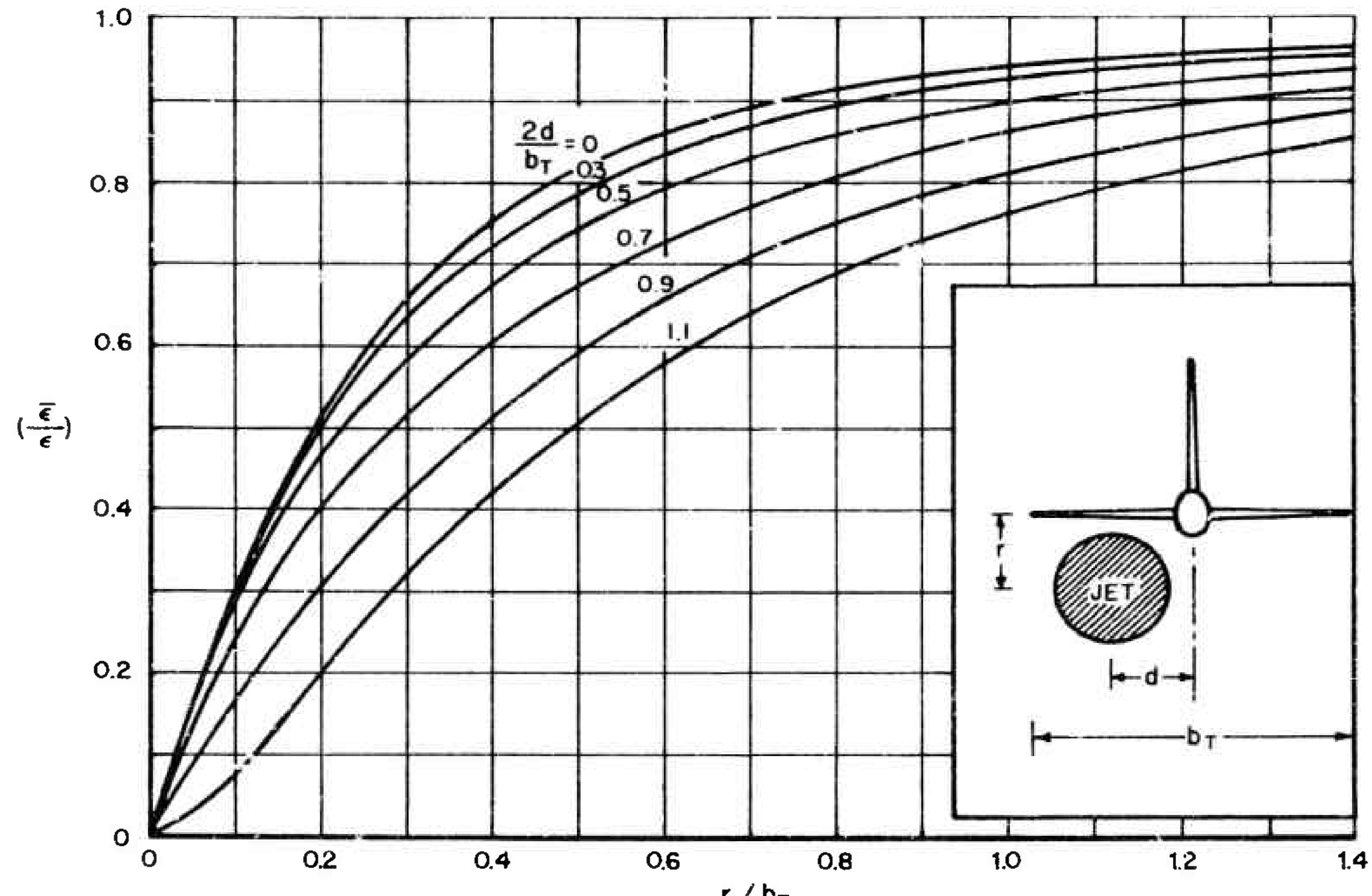

Figure 8. Ratio of the Effective Mean Downwash $\bar{\epsilon}$ Induced by the Jet Over the Tailplane to the Flow Inclination ϵ Induced at a Radius r .

LITERATURE CITED

1. Heyson, H. H., and Katzoff, S., INDUCED VELOCITY NEAR A LIFTING ROTOR WITH NONUNIFORM DISK LOADING, NACA Report 1319, National Advisory Committee for Aeronautics (presently, National Aeronautics and Space Administration), Washington, D. C., 1957.

2. Prouty, W., AN ANALYTICAL STUDY OF THE LONGITUDINAL STABILITY OF TANDEM ROTOR HELICOPTERS, Bell Helicopter Corporation Report No. 299-099-113, Fort Worth, Texas, 1959.

3. Castles, W., Jr., and DeLeeux, J. H., THE NORMAL COMPONENT OF THE INDUCED VELOCITY IN THE VICINITY OF A LIFTING ROTOR AND SOME EXAMPLES OF ITS APPLICATION, NACA Technical Note TN-2912, National Advisory Committee for Aeronautics (presently, National Aeronautics and Space Administration), Washington, D. C., March 1953.

4. Halliday, A. S., and Cox, D. K., WIND TUNNEL EXPERIMENTS ON A MODEL OF A TANDEM ROTOR HELICOPTER, British Aeronautical Research Council Report No. 19829, London, England, January 1958.

5. Pruyn, R. R., STUDIES OF ROTORCRAFT AERODYNAMIC PROBLEMS AIMED AT REDUCING PARASITE DRAG, ROTOR-AIRFRAME INTERFERENCE EFFECTS AND IMPROVING AIRFRAME STATIC STABILITY, WADC Technical Report No. 61-124, Wright Air Development Division, Air Research and Development Command, Wright-Patterson Air Force Base, Ohio, November 1961.

6. Bain, Lawrence J., and Landgrebe, Anton J., INVESTIGATION OF COMPOUND HELICOPTER AERODYNAMIC INTERFERENCE EFFECTS, Sikorsky Aircraft Division, United Aircraft Corporation, USAAVLABS Technical Report 67-44, U. S. Army Aviation Materiel Laboratories, Fort Eustis, Virginia, November 1967, AD665427.

7. ROYAL AERONAUTICAL SOCIETY DATA SHEETS (VOLUME III), Royal Aeronautical Society of Great Britain, 1955.

8. Katzoff, S., and Silverstein, A., DESIGN CHARTS FOR PREDICTING DOWNWASH ANGLES AND WAKE CHARACTERISTICS BEHIND PLAIN AND FLAPPED WINGS, Langley Memorial Aeronautical Laboratory, NACA Report 648, National Advisory Committee for Aeronautics, Langley Field, Virginia, 1938.

9. Ribner, Herbert S., FIELD OF FLOW ABOUT A JET AND EFFECT OF JETS ON STABILITY OF JET-PROPELLED AIRPLANES, NACA WR L-213 (ARC No. L6C13) National Advisory Committee for Aeronautics, Langley Field, Virginia, March 1946.

SECTION 6. PERTURBATION EQUATIONS OF MOTION

In accordance with the commonly used stability analysis procedure, only small perturbations about the trim conditions are considered. This is accomplished by linearizing the equations of motion presented in Section 4. The variables θ, $\dot{\theta}$, etc., denote changes from trim conditions of aircraft pitch attitude, pitch rate, etc. The parameters A_{1_C} , B_{1_C} , θ_C , and θ_{TR} denote pilot control inputs in lateral and longitudinal cyclic pitch, main rotor collective pitch, and tail rotor collective pitch, respectively. J_1 and J_2 are the pilot's authority ratios in the longitudinal and lateral control, respectively. The terms X_θ, $X_{\dot{\theta}}$, etc., are the total or composite aircraft stability derivatives and denote the rate of change of forces or moments with respect to the subscript variable evaluated at the trim conditions. The composite or total stability derivatives are presented in Section 7.

The perturbation equations of motion can be expressed as follows:

(a) The X-Force Equation

$$X_u \bar{u} + X_{\dot{u}} \dot{\bar{u}} + X_v \bar{v} + X_w \bar{w} + X_{\dot{w}} \dot{\bar{w}} + X_\theta \bar{\theta} + X_{\dot{\theta}} \dot{\bar{\theta}} + X_{\dot{\phi}} \dot{\bar{\phi}} + X_{\dot{\psi}} \bar{\psi}$$

$$+ J_1 (X_{B_{1_C}} \bar{B}_{1_C} + X_{\dot{B}_{1_C}} \dot{\bar{B}}_{1_C}) + X_{B_{1_S}} \bar{B}_{1_S} + X_{\dot{B}_{1_S}} \dot{\bar{B}}_{1_S}$$

$$+ J_2 (X_{A_{1_C}} \bar{A}_{1_C} + X_{\dot{A}_{1_C}} \dot{\bar{A}}_{1_C}) + X_{A_{1_S}} \bar{A}_{1_S} + X_{\dot{A}_{1_S}} \dot{\bar{A}}_{1_S}$$

$$+ J_3 (X_{\delta_{r_C}} \bar{\delta}_{r_C} + X_{\dot{\delta}_{r_C}} \dot{\bar{\delta}}_{r_C}) + X_{\delta_{r_S}} \bar{\delta}_{r_S} + X_{\dot{\delta}_{r_S}} \dot{\bar{\delta}}_{r_S}$$

$$+ J_4 (X_{\theta_C} \bar{\theta}_C + X_{\dot{\theta}_C} \dot{\bar{\theta}}_C) + X_{\theta_S} \bar{\theta}_S + X_{\dot{\theta}_S} \dot{\bar{\theta}}_S = 0$$

(b) The Y-Force Equation

$$Y_u\bar{u}+Y_v\bar{v}+Y_{\dot{v}}\dot{\bar{v}}+Y_w\bar{w}+Y_{\dot{\theta}}\dot{\bar{\theta}}+Y_\phi\bar{\phi}+Y_{\dot{\phi}}\dot{\bar{\phi}}+Y_\psi\bar{\psi}+Y_{\dot{\psi}}\dot{\bar{\psi}}$$

$$+J_1(Y_{B_{1_C}}\bar{B}_{1_C}+Y_{\dot{B}_{1_C}}\dot{\bar{B}}_{1_C})+Y_{B_{1_S}}\bar{B}_{1_S}+Y_{\dot{B}_{1_S}}\dot{\bar{B}}_{1_S}$$

$$+J_2(Y_{A_{1_C}}\bar{A}_{1_C}+Y_{\dot{A}_{1_C}}\dot{\bar{A}}_{1_C})+Y_{A_{1_S}}\bar{A}_{1_S}+Y_{\dot{A}_{1_S}}\dot{\bar{A}}_{1_S}$$

$$+J_3(Y_{\delta_{r_C}}\bar{\delta}_{r_C}+Y_{\dot{\delta}_{r_C}}\dot{\bar{\delta}}_{r_C})+Y_{\delta_{r_S}}\bar{\delta}_{r_S}+Y_{\dot{\delta}_{r_S}}\dot{\bar{\delta}}_{r_S}$$

$$+J_4(Y_{\theta_C}\bar{\theta}_C+Y_{\dot{\theta}_C}\dot{\bar{\theta}}_C)+Y_{\theta_S}\bar{\theta}_S+Y_{\dot{\theta}_S}\dot{\bar{\theta}}_S=0$$

(c) The Z-Force Equation

$$Z_u\bar{u}+Z_v\bar{v}+Z_w\bar{w}+Z_{\dot{w}}\dot{\bar{w}}+Z_\theta\bar{\theta}+Z_{\dot{\theta}}\dot{\bar{\theta}}+Z_{\dot{\phi}}\dot{\bar{\phi}}+Z_{\dot{\psi}}\dot{\bar{\psi}}$$

$$+J_1(Z_{B_{1_C}}\bar{B}_{1_C}+Z_{\dot{B}_{1_C}}\dot{\bar{B}}_{1_C})+Z_{B_{1_S}}\bar{B}_{1_S}+Z_{\dot{B}_{1_S}}\dot{\bar{B}}_{1_S}$$

$$+J_2(Z_{A_{1_C}}\bar{A}_{1_C}+Z_{\dot{A}_{1_C}}\dot{\bar{A}}_{1_C})+Z_{A_{1_S}}\bar{A}_{1_S}+Z_{\dot{A}_{1_S}}\dot{\bar{A}}_{1_S}$$

$$+J_3(Z_{\delta_{r_C}}\bar{\delta}_{r_C}+Z_{\dot{\delta}_{r_C}}\dot{\bar{\delta}}_{r_C})+Z_{\delta_{r_S}}\bar{\delta}_{r_S}+Z_{\dot{\delta}_{r_S}}\dot{\bar{\delta}}_{r_S}$$

$$+J_4(Z_{\theta_C}\bar{\theta}_C+Z_{\dot{\theta}_C}\dot{\bar{\theta}}_C)+Z_{\theta_S}\bar{\theta}_S+Z_{\dot{\theta}_S}\dot{\bar{\theta}}_S=0$$

(d) The Rolling Moment Equation ($\mathcal{L}$)

$$\mathcal{L}_u \bar{u} + \mathcal{L}_v \bar{v} + \mathcal{L}_w \bar{w} + \mathcal{L}_{\dot{w}} \dot{\bar{w}} + \mathcal{L}_{\dot{\theta}} \dot{\bar{\theta}} + \mathcal{L}_{\ddot{\theta}} \ddot{\bar{\theta}}$$

$$+ \mathcal{L}_{\dot{\phi}} \dot{\bar{\phi}} + \mathcal{L}_{\ddot{\phi}} \ddot{\bar{\phi}} + \mathcal{L}_{\dot{\psi}} \dot{\bar{\psi}} + \mathcal{L}_{\ddot{\psi}} \ddot{\bar{\psi}}$$

$$+ J_1 (\mathcal{L}_{B_{1_c}} \bar{B}_{1_c} + \mathcal{L}_{\dot{B}_{1_c}} \dot{\bar{B}}_{1_c}) + \mathcal{L}_{B_{1_s}} \bar{B}_{1_s} + \mathcal{L}_{\dot{B}_{1_s}} \dot{\bar{B}}_{1_s}$$

$$+ J_2 (\mathcal{L}_{A_{1_c}} \bar{A}_{1_c} + \mathcal{L}_{\dot{A}_{1_c}} \dot{\bar{A}}_{1_c}) + \mathcal{L}_{A_{1_s}} \bar{A}_{1_s} + \mathcal{L}_{\dot{A}_{1_s}} \dot{\bar{A}}_{1_s}$$

$$+ J_3 (\mathcal{L}_{\delta_{r_c}} \bar{\delta}_{r_c} + \mathcal{L}_{\dot{\delta}_{r_c}} \dot{\bar{\delta}}_{r_c}) + \mathcal{L}_{\delta_{r_s}} \bar{\delta}_{r_s} + \mathcal{L}_{\dot{\delta}_{r_s}} \dot{\bar{\delta}}_{r_s}$$

$$+ J_4 (\mathcal{L}_{\theta_c} \bar{\theta}_c + \mathcal{L}_{\dot{\theta}_c} \dot{\bar{\theta}}_c) + \mathcal{L}_{\theta_s} \bar{\theta}_s + \mathcal{L}_{\dot{\theta}_s} \dot{\bar{\theta}}_s = 0$$

(e) The Pitching Moment Equation (M)

$$M_u \bar{u} + M_v \bar{v} + M_w \bar{w} + M_{\dot{w}} \dot{\bar{w}} + M_{\dot{\theta}} \dot{\bar{\theta}} + M_{\ddot{\theta}} \ddot{\bar{\theta}}$$

$$+ M_{\dot{\phi}} \dot{\bar{\phi}} + M_{\ddot{\phi}} \ddot{\bar{\phi}} + M_{\dot{\psi}} \dot{\bar{\psi}} + M_{\ddot{\psi}} \ddot{\bar{\psi}}$$

$$+ J_1 (M_{B_{1_c}} \bar{B}_{1_c} + M_{\dot{B}_{1_c}} \dot{\bar{B}}_{1_c}) + M_{B_{1_s}} \bar{B}_{1_s} + M_{\dot{B}_{1_s}} \dot{\bar{B}}_{1_s}$$

$$+ J_2 (M_{A_{1_c}} \bar{A}_{1_c} + M_{\dot{A}_{1_c}} \dot{\bar{A}}_{1_c}) + M_{A_{1_s}} \bar{A}_{1_s} + M_{\dot{A}_{1_s}} \dot{\bar{A}}_{1_s}$$

$$+ J_3 (M_{\delta_{r_c}} \bar{\delta}_{r_c} + M_{\dot{\delta}_{r_c}} \dot{\bar{\delta}}_{r_c}) + M_{\delta_{r_s}} \bar{\delta}_{r_s} + M_{\dot{\delta}_{r_s}} \dot{\bar{\delta}}_{r_s}$$

$$+J_4(M_{\theta_c}\bar{\theta}_c+M_{\dot{\theta}_c}\dot{\bar{\theta}}_c)+M_{\theta_s}\bar{\theta}_s+M_{\dot{\theta}_s}\dot{\bar{\theta}}_s=0$$

(f) The Yawing Moment Equation (N)

$$N_u\bar{u}+N_v\bar{v}+N_w\bar{w}+N_{\dot{w}}\dot{\bar{w}}+N_{\dot{\theta}}\dot{\bar{\theta}}+N_{\ddot{\theta}}\ddot{\bar{\theta}}$$

$$+N_{\dot{\phi}}\dot{\bar{\Phi}}+N_{\ddot{\phi}}\ddot{\bar{\Phi}}+N_{\dot{\psi}}\dot{\bar{\Psi}}+N_{\ddot{\psi}}\ddot{\bar{\Psi}}$$

$$+J_1(N_{B_{1_c}}\bar{B}_{1_c}+N_{\dot{B}_{1_c}}\dot{\bar{B}}_{1_c})+N_{B_{1_s}}\bar{B}_{1_s}+N_{\dot{B}_{1_s}}\dot{\bar{B}}_{1_s}$$

$$+J_2(N_{A_{1_c}}\bar{A}_{1_c}+N_{\dot{A}_{1_c}}\dot{\bar{A}}_{1_c})+N_{A_{1_s}}\bar{A}_{1_s}+N_{\dot{A}_{1_s}}\dot{\bar{A}}_{1_s}$$

$$+J_3(N_{\delta_{r_c}}\bar{\delta}_{r_c}+N_{\dot{\delta}_{r_c}}\dot{\bar{\delta}}_{r_c})+N_{\delta_{r_s}}\bar{\delta}_{r_s}+N_{\dot{\delta}_{r_s}}\dot{\bar{\delta}}_{r_s}$$

$$+J_4(N_{\theta_c}\bar{\theta}_c+N_{\dot{\theta}_c}\dot{\bar{\theta}}_c)+N_{\theta_s}\bar{\theta}_s+N_{\dot{\theta}_s}\dot{\bar{\theta}}_s=0$$

(g) The Stabilization Equations

Generalized stability augmentation system equations are as follows:

$$\dot{\bar{B}}_{1_s}=-\bar{B}_{1_s}(D_1+D_2\bar{B}_{1_s})+k_1\bar{\theta}+k_2\dot{\bar{\theta}}+k_3\bar{u}+k_4\bar{w}$$

$$\dot{\bar{A}}_{1_s}=-\bar{A}_{1_s}(D_1+D_2\bar{A}_{1_s})+k_5\bar{\Phi}-k_6\dot{\bar{\Phi}}-k_7\bar{v}$$

$$\dot{\bar{\delta}}_{r_s}=-k_8\bar{\delta}_{r_s}-k_9\bar{v}-k_{10}\dot{\bar{\psi}}$$

The simplified "lagged rate" stabilization system can be represented by

$$\dot{\overline{B_{1_s}}} = -D_1 \overline{B_{1_s}} + k_2 \dot{\overline{\theta}}$$

$$\dot{\overline{A_{1_s}}} = -D_1 \overline{A_{1_s}} - k_6 \dot{\overline{\phi}}$$

$$\dot{\overline{\delta_{r_s}}} = -k_8 \overline{\delta_{r_s}} - k_{10} \dot{\overline{\psi}}$$

where

D_1 and D_2 are damping constants

k_1, k_2 ....etc. are the linkage ratios.

SECTION 7. STABILITY DERIVATIVES

7.1 TOTAL STABILITY DERIVATIVES

The total aircraft stability derivatives are obtained by differentiating the equations of motion (presented in Section 4) with respect to the appropriate stability variables. The derivatives presented herein are not limited to small-angle assumptions for initial trim conditions as used in Reference 1. These derivatives apply to completely arbitrary (non-zero) angular attitudes and angular rates. As such they can be used for stability analyses of compound helicopters in maneuvering flight conditions as well as in steady, level flight.

7.1.1 The X-Force Derivatives

7.1.1.1 X_u

$$X_u = (X_u)_F + (X_u)_R + (X_u)_{FUS} + (X_u)_W + (X_u)_T + (X_u)_{VT} + (X_u)_{TR} + \sum_{i=1}^{n} (X_u)_{P_i}$$

where

$$(X_u)_F = \frac{\partial (X)_F}{\partial u} = X_{u_F} + X_{\alpha_F} \frac{\partial \alpha_F}{\partial u}$$

$$X_{u_F} = \left[\frac{\partial (X)_F}{\partial u_F} = \left(\frac{\partial L_F}{\partial u_F} \cos A_{I_F} - \frac{\partial Y_F}{\partial u_F} \sin A_{I_F}\right) \sin(\alpha - \epsilon_F) - \frac{\partial D_F}{\partial u_F} \cos(\alpha - \epsilon_F)\right] \cos\beta_S$$

$$-\left(\frac{\partial L_F}{\partial u_F} \sin A_{I_F} + \frac{\partial Y_F}{\partial u_F} \cos A_{I_F}\right) \sin \beta_S$$

$$X_{\alpha_F} = \frac{\partial (X)_F}{\partial \alpha_F} = \left[\left(\frac{\partial L_F}{\partial \alpha_F} \cos A_{I_F} - \frac{\partial Y_F}{\partial \alpha_F} \sin A_{I_F}\right) \sin(\alpha - \epsilon_F) - \frac{\partial D_F}{\partial \alpha_F} \cos(\alpha - \epsilon_F)\right.$$

$$\left. + (L_F \cos A_{I_F} - Y_F \sin A_{I_F}) \cos(\alpha - \epsilon_F) + D_F \sin(\alpha - \epsilon_F)\right] \cos \beta_S$$

$$-\left(\frac{\partial L_F}{\partial \alpha_F} \sin A_{I_F} + \frac{\partial Y_F}{\partial \alpha_F} \cos A_{I_F}\right) \sin \beta_S$$

$$\frac{\partial \alpha_F}{\partial u} = -\frac{\partial \epsilon_F}{\partial u} = -\frac{K_{RF}}{V_O}\left(\frac{\lambda}{\mu} - \frac{\partial \lambda}{\partial \mu}\right)_R$$

$$(X_u)_R = \frac{\partial (X)_R}{\partial u} = X_{u_R} + X_{\alpha_R}\frac{\partial \alpha_R}{\partial u}$$

$$X_{u_R} = \frac{\partial (X)_R}{\partial u_R} = \left[\left(\frac{\partial L_R}{\partial u_R}\cos A_{1_R} + \frac{\partial Y_R}{\partial u_R}\sin A_{1_R}\right)\sin(\alpha - \epsilon_R) - \frac{\partial D_R}{\partial u_R}\cos(\alpha - \epsilon_R)\right]\cos\beta_S$$

$$-\left(\frac{\partial L_R}{\partial u_R}\sin A_{1_R} - \frac{\partial Y_R}{\partial \alpha_R}\cos A_{1_F}\right)\sin\beta_S$$

$$X_{\alpha_R} = \frac{\partial (X)_R}{\partial \alpha_R} = \left(\frac{\partial L_R}{\partial \alpha_R}\cos A_{1_R} + \frac{\partial Y_R}{\partial \alpha_R}\sin A_{1_R}\right)\sin(\alpha - \epsilon_R) - \frac{\partial D_R}{\partial \alpha_R}\cos(\alpha - \epsilon_R)$$

$$+ (L_R\cos A_{1_R} + Y_R\sin A_{1_R})\cos(\alpha - \epsilon_R) + D_R\sin(\alpha - \epsilon_R)\Big]\cos\beta_S$$

$$-\left(\frac{\partial L_R}{\partial \alpha_R}\sin A_{1_R} - \frac{\partial Y_R}{\partial \alpha_R}\cos A_{1_R}\right)\sin\beta_S$$

$$\frac{\partial \alpha_R}{\partial u} = -\frac{\partial \epsilon_R}{\partial u} = -\frac{K_{FR}}{V_O}\left(\frac{\lambda}{\mu} - \frac{\partial \lambda}{\partial \mu}\right)_F$$

$$(X_u)_{FUS} = \frac{\partial (X)_{FUS}}{\partial u} = X_{u_{FUS}} + X_{\alpha_{FUS}}\frac{\partial \alpha_{FUS}}{\partial u}$$

$$X_{u_{FUS}} = \frac{\partial (X)_{FUS}}{\partial u_{FUS}} = \left[\frac{\partial L_{FUS}}{\partial u_{FUS}}\sin(\alpha - \epsilon_{FUS}) - \frac{\partial D_{FUS}}{\partial u_{FUS}}\cos(\alpha - \epsilon_{FUS})\right]\cos\beta_S$$

$$-\frac{\partial Y_{FUS}}{\partial u_{FUS}}\sin\beta_S$$

$$X_{\alpha_{FUS}} = \frac{\partial (X)_{FUS}}{\partial \alpha_{FUS}} = \frac{\partial L_{FUS}}{\partial \alpha_{FUS}}\sin(\alpha - \epsilon_{FUS}) - \frac{\partial D_{FUS}}{\partial \alpha_{FUS}}\cos(\alpha - \epsilon_{FUS})$$

$$+ L_{FUS}\cos(\alpha - \epsilon_{FUS}) + D_{FUS}\sin(\alpha - \epsilon_{FUS})\Big]\cos\beta_S$$

$$- \frac{\partial Y_{FUS}}{\partial \alpha_{FUS}} \sin \beta_S$$

$$\frac{\partial \alpha_{FUS}}{\partial u} = - \frac{\partial \epsilon_{FUS}}{\partial u} = - \frac{K_{F\,FUS}}{V_0} \left(\frac{\lambda}{\mu} - \frac{\partial \lambda}{\partial \mu}\right)_F - \frac{K_{R\,FUS}}{V_0} \left(\frac{\lambda}{\mu} - \frac{\partial \lambda}{\partial \mu}\right)_R$$

$$(X_u)_W = \frac{\partial (X)_W}{\partial u} = X_{u_W} + X_{\alpha_W} \frac{\partial \alpha_W}{\partial u}$$

$$X_{u_W} = \frac{\partial (X)_W}{\partial u_W} = \left[\frac{\partial L_W}{\partial u_W} \sin (\alpha - \epsilon_W) - \frac{\partial D_W}{\partial u_W} \cos (\alpha - \epsilon_W) \right] \cos \beta_S$$

$$X_{\alpha_W} = \frac{\partial (X)_W}{\partial \alpha_W} = \left[\frac{\partial L_W}{\partial \alpha_W} \sin (\alpha - \epsilon_W) - \frac{\partial D_W}{\partial \alpha_W} \cos (\alpha - \epsilon_W) \right.$$

$$\left. + L_W \cos (\alpha - \epsilon_W) + D_W \sin (\alpha - \epsilon_W) \right] \cos \beta_S$$

$$\frac{\partial \alpha_W}{\partial u} = - \frac{\partial \epsilon_W}{\partial u} = - \frac{K_{FW}}{V_0} \left(\frac{\lambda}{\mu} - \frac{\partial \lambda}{\partial \mu}\right)_F - \frac{K_{RW}}{V_0} \left(\frac{\lambda}{\mu} - \frac{\partial \lambda}{\partial \mu}\right)_R$$

$$(X_u)_T = \frac{\partial (X)_T}{\partial u} = X_{u_T} + X_{\alpha_T} \frac{\partial \alpha_T}{\partial u}$$

$$X_{u_T} = \frac{\partial (X)_T}{\partial u_T} = \left[\frac{\partial L_T}{\partial u_T} \sin (\alpha - \epsilon_T) - \frac{\partial D_T}{\partial u_T} \cos (\alpha - \epsilon_T) \right] \cos \beta_S$$

$$X_{\alpha_T} = \frac{\partial (X)_T}{\partial \alpha_T} = \left[\frac{\partial L_T}{\partial \alpha_T} \sin (\alpha - \epsilon_T) - \frac{\partial D_T}{\partial \alpha_T} \cos (\alpha - \epsilon_T) \right.$$

$$\left. + L_T \cos (\alpha - \epsilon_T) + D_T \sin (\alpha - \epsilon_T) \right] \cos \beta_S$$

$$\frac{\partial \alpha_T}{\partial u} = - \frac{\partial \epsilon_T}{\partial u} = - \frac{K_{FT}}{V_0} \left(\frac{\lambda}{\mu} - \frac{\partial \lambda}{\partial \mu}\right)_F - \frac{K_{RT}}{V_0} \left(\frac{\lambda}{\mu} - \frac{\partial \lambda}{\partial \mu}\right)_R$$

$$(X_u)_{VT} = \frac{\partial (X)_{VT}}{\partial u} = X_{u_{VT}} + X_{\alpha_{VT}} \frac{\partial \alpha_{VT}}{\partial u}$$

$$X_{u_{VT}} = \frac{\partial(X)_{VT}}{\partial u_{VT}} = -\frac{\partial D_{VT}}{\partial u_{VT}} \cos(\alpha - \epsilon_{VT}) \cos\beta_s + \frac{\partial L_{VT}}{\partial u_{VT}} \sin\beta_s$$

$$X_{\alpha_{VT}} = \frac{\partial(X)_{VT}}{\partial \alpha_{VT}} = \left[-\frac{\partial D_{VT}}{\partial \alpha_{VT}} \cos(\alpha - \epsilon_{VT}) + D_{VT} \sin(\alpha - \epsilon_{VT})\right] \cos\beta_s$$

$$+ \frac{\partial L_{VT}}{\partial \alpha_{VT}} \sin\beta_s$$

$$\frac{\partial \alpha_{VT}}{\partial u} = -\frac{\partial \epsilon_{VT}}{\partial u} = -\frac{K_{F\,VT}}{V_0}\left(\frac{\lambda}{\mu} - \frac{\partial\lambda}{\partial\mu}\right)_F - \frac{K_{R\,VT}}{V_0}\left(\frac{\lambda}{\mu} - \frac{\partial\lambda}{\partial\mu}\right)_R$$

$$(X_u)_{TR} = \frac{\partial(X)_{TR}}{\partial u_{TR}} = X_{u_{TR}} + X_{\alpha_{TR}} \frac{\partial \alpha_{TR}}{\partial u}$$

$$X_{u_{TR}} = \frac{\partial(X)_{TR}}{\partial u_{TR}} = \left[\frac{\partial Y_{TR}}{\partial u_{TR}} \sin(\alpha - \epsilon_{TR}) - \frac{\partial D_{TR}}{\partial u_{TR}} \cos(\alpha - \epsilon_{TR})\right] \cos\beta_s$$

$$- \frac{\partial T_{TR}}{\partial u_{TR}} \sin\beta_s$$

$$X_{\alpha_{TR}} = \frac{\partial(X)_{TR}}{\partial \alpha_{TR}} = \left[\frac{\partial Y_{TR}}{\partial \alpha_{TR}} \sin(\alpha - \epsilon_{TR}) - \frac{\partial D_{TR}}{\partial \alpha_{TR}} \cos(\alpha - \epsilon_{TR})\right.$$

$$\left. + Y_{TR} \cos(\alpha - \epsilon_{TR}) + D_{TR} \sin(\alpha - \epsilon_{TR})\right] \cos\beta_s$$

$$- \frac{\partial T_{TR}}{\partial \alpha_{TR}} \sin\beta_s$$

$$\frac{\partial \alpha_{TR}}{\partial u} = -\frac{\partial \epsilon_{TR}}{\partial u} = -\frac{K_{F\,TR}}{V_0}\left(\frac{\lambda}{\mu} - \frac{\partial\lambda}{\partial\mu}\right)_F - \frac{K_{R\,TR}}{V_0}\left(\frac{\lambda}{\mu} - \frac{\partial\lambda}{\partial\mu}\right)_R$$

$$(X_u)_{P_i} = \frac{\partial(X)_{P_i}}{\partial u} = X_{u_{P_i}} + X_{\alpha_{P_i}} \frac{\partial \alpha_{P_i}}{\partial u}$$

$$X_{u_{P_i}} = \frac{\partial(X)_{P_i}}{\partial u_{P_i}} = \frac{\partial T_{P_i}}{\partial u_{P_i}} \cos i_{P_i} - \frac{\partial N_{P_i}}{\partial u_{P_i}} \sin i_{P_i}$$

$$X_{\alpha_{P_i}} = \frac{\partial(X)_{P_i}}{\partial \alpha_{P_i}} = \frac{\partial T_{P_i}}{\partial \alpha_{P_i}} \cos i_{P_i} - \frac{\partial N_{P_i}}{\partial \alpha_{P_i}} \sin i_{P_i}$$

$$\frac{\partial \alpha_{P_i}}{\partial u} = - \frac{\partial \epsilon_{P_i}}{\partial u} = - \frac{K_{FP_i}}{V_0}\left(\frac{\lambda}{\mu} - \frac{\partial \lambda}{\partial \mu}\right)_F - \frac{K_{RP_i}}{V_0}\left(\frac{\lambda}{\mu} - \frac{\partial \lambda}{\partial \mu}\right)_R$$

7.1.1.2 $X_{\dot{u}}$

$$X_{\dot{u}} = -\frac{W}{g}$$

7.1.1.3 X_v

$$X_v = (X_v)_F + (X_v)_R + (X_v)_{FUS} + (X_v)_W + (X_v)_T + (X_v)_{VT} + (X_v)_{TR} + \sum_{i=1}^{n} (X_v)_{P_i}$$

where

$$(X_v)_F = \frac{\partial(X)_F}{\partial v} = \frac{1}{V_0} \frac{\partial(X)_F}{\partial \beta_S} = \frac{-1}{V_0}(L_F \sin A_{1_F} + Y_F \cos A_{1_F}) \cos \beta_S - \frac{1}{V_0}\Big[(L_F \cos A_{1_F} - Y_F \sin A_{1_F}) \sin(\alpha - \epsilon_F) - D_F \cos(\alpha - \epsilon_F)\Big] \sin \beta_S$$

$$(X_v)_R = \frac{\partial(X)_R}{\partial v} = \frac{1}{V_0} \frac{\partial(X)_R}{\partial \beta_S} = \frac{-1}{V_0}(L_R \sin A_{1_R} - Y_R \cos A_{1_R}) \cos \beta_S - \frac{1}{V_0}\Big[(L_R \cos A_{1_R} + Y_R \sin A_{1_R}) \sin(\alpha - \epsilon_R) - D_R \cos(\alpha - \epsilon_R)\Big] \sin \beta_S$$

$$(X_v)_{FUS} = \frac{\partial(X)_{FUS}}{\partial v} = \frac{1}{V_0} \frac{\partial(X)_{FUS}}{\partial \beta_S} = \frac{1}{V_0}\left[\frac{\partial L_{FUS}}{\partial \beta_S} \sin(\alpha - \epsilon_{FUS}) - \frac{\partial D_{FUS}}{\partial \beta_S} \cos(\alpha - \epsilon_{FUS}) - Y_{FUS}\right] \cos \beta_S - \frac{1}{V_0}\left[L_{FUS} \sin(\alpha - \epsilon_{FUS}) - D_{FUS} \cos(\alpha - \epsilon_{FUS}) + \frac{\partial Y_{FUS}}{\partial \beta_S}\right] \sin \beta_S$$

$$(X_v)_W = \frac{\partial(X)_W}{\partial v} = \frac{1}{V_0}\frac{\partial(X)_W}{\partial\beta_s} = \frac{-1}{V_0}\left[L_W \sin(\alpha-\epsilon_W) - D_W\cos(\alpha-\epsilon_W)\right]\sin\beta_s$$

$$(X_v)_T = \frac{\partial(X)_T}{\partial v} = \frac{1}{V_0}\frac{\partial(X)_T}{\partial\beta_s} = \frac{-1}{V_0}\left[L_T \sin(\alpha-\epsilon_T) - D_T\cos(\alpha-\epsilon_T)\right]\sin\beta_s$$

$$(X_v)_{VT} = \frac{\partial(X)_{VT}}{\partial v} = \frac{1}{V_0}\frac{\partial(X)_{VT}}{\partial\beta_s} = \frac{1}{V_0}\left[L_{VT} - \frac{\partial D_{VT}}{\partial\beta_s}\cos(\alpha-\epsilon_{VT})\right]\cos\beta_s$$

$$+\frac{1}{V_0}\left[D_{VT}\cos(\alpha-\epsilon_{VT}) + \frac{\partial D_{VT}}{\partial\beta_s}\right]\sin\beta_s$$

$$(X_v)_{TR} = \frac{\partial(X)_{TR}}{\partial v} = \frac{1}{V_0}\frac{\partial(X)_{TR}}{\partial\beta_s} = \frac{1}{V_0}\left[-\frac{\partial Y_{TR}}{\partial\beta_s}\sin(\alpha-\epsilon_{TR}) - \frac{\partial D_{TR}}{\partial\beta_s}\cos(\alpha-\epsilon_{TR}) - T_{TR}\right]\cos\beta_s$$

$$-\frac{1}{V_0}\left[Y_{TR}\sin(\alpha-\epsilon_{TR}) - D_{TR}\cos(\alpha-\epsilon_{TR}) + \frac{\partial T_{TR}}{\partial\beta_s}\right]\sin\beta_s$$

$$(X_v)_{P_i} = \frac{\partial(X)_{P_i}}{\partial v} = \frac{1}{V_0}\frac{\partial(X)_{P_i}}{\partial\beta_s} = \frac{1}{V_0}\left(\frac{\partial T_{P_i}}{\partial\beta_s}\cos i_{P_i} - \frac{\partial N_{P_i}}{\partial\beta_s}\sin i_{P_i}\right)$$

7.1.1.4 X_w

$$X_w = (X_w)_F + (X_w)_R + (X_w)_{FUS} + (X_w)_W + (X_w)_T + (X_w)_{VT} + (X_w)_{TR} + \sum_{i=1}^{n}(X_w)_{P_i} - \frac{W}{g}q$$

where

$$(X_w)_F = \frac{\partial(X)_F}{\partial w} = X_{w_F}\frac{\partial\alpha_F}{\partial\alpha}$$

$$X_{w_F} = \frac{\partial(X)_F}{\partial w_F} = \frac{1}{V_0}\frac{\partial(X)_F}{\partial\alpha_F} = \frac{1}{V_0}X_{\alpha_F}$$

$$\frac{\partial\alpha_F}{\partial\alpha} = 1 - \frac{\partial\epsilon_F}{\partial\alpha} = 1 - K_{RF}\left[1 - \frac{1}{\mu}\left(\frac{\partial\lambda}{\partial\alpha_C}\right)\right]_R$$

$$(X_w)_R = \frac{\partial (X)_R}{\partial w} = X_{w_R} \frac{\partial \alpha_R}{\partial \alpha}$$

$$X_{w_R} = \frac{\partial (X)_R}{\partial w_R} = \frac{1}{V_0} \frac{\partial (X)_R}{\partial \alpha_R} = \frac{1}{V_0} X_{\alpha_R}$$

$$\frac{\partial \alpha_R}{\partial \alpha} = 1 - \frac{\partial \epsilon_R}{\partial \alpha} = 1 - K_{FR}\left[1 - \frac{1}{\mu}\left(\frac{\partial \lambda}{\partial \alpha_C}\right)\right]_F$$

$$(X_w)_{FUS} = \frac{\partial (X)_{FUS}}{\partial w} = X_{w_{FUS}} \frac{\partial \alpha_{FUS}}{\partial \alpha}$$

$$X_{w_{FUS}} = \frac{\partial (X)_{FUS}}{\partial w_{FUS}} = \frac{1}{V_0} \frac{\partial (X)_{FUS}}{\partial \alpha_{FUS}} = \frac{1}{V_0} X_{\alpha_{FUS}}$$

$$\frac{\partial \alpha_{FUS}}{\partial \alpha} = 1 - \frac{\partial \epsilon_{FUS}}{\partial \alpha} = 1 - K_{F\,FUS}\left(1 - \frac{1}{\mu}\frac{\partial \lambda}{\partial \alpha_C}\right)_F - K_{R\,FUS}\left(1 - \frac{1}{\mu}\frac{\partial \lambda}{\partial \alpha_C}\right)_R$$

$$(X_w)_W = \frac{\partial (X)_W}{\partial w} = X_{w_W} \frac{\partial \alpha_W}{\partial \alpha}$$

$$X_{w_W} = \frac{\partial (X)_W}{\partial w_W} = \frac{1}{V_0} \frac{\partial (X)_W}{\partial \alpha_W} = \frac{1}{V_0} X_{\alpha_W}$$

$$\frac{\partial \alpha_W}{\partial \alpha} = 1 - \frac{\partial \epsilon_W}{\partial \alpha} = 1 - K_{FW}\left(1 - \frac{1}{\mu}\frac{\partial \lambda}{\partial \alpha_C}\right)_F - K_{RW}\left(1 - \frac{1}{\mu}\frac{\partial \lambda}{\partial \alpha_C}\right)_R$$

$$(X_w)_T = \frac{\partial (X)_T}{\partial w} = X_{w_T} \frac{\partial \alpha_T}{\partial \alpha}$$

$$X_{w_T} = \frac{\partial (X)_T}{\partial w_T} = \frac{1}{V_0} \frac{\partial (X)_T}{\partial \alpha_T} = \frac{1}{V_0} X_{\alpha_T}$$

$$\frac{\partial \alpha_T}{\partial \alpha} = 1 - \frac{\partial \epsilon_T}{\partial \alpha} = 1 - K_{FT}\left(1 - \frac{1}{\mu}\frac{\partial \lambda}{\partial \alpha_C}\right)_F - K_{RT}\left(1 - \frac{1}{\mu}\frac{\partial \lambda}{\partial \alpha_C}\right)_R$$

$$(X_w)_{VT} = \frac{\partial (X)_{VT}}{\partial w} = \frac{1}{V_0} X_{w_{VT}} \frac{\partial \alpha_{VT}}{\partial \alpha}$$

$$X_{w_{VT}} = \frac{\partial (X)_{VT}}{\partial w_{VT}} = \frac{1}{V_0} \frac{\partial (X)_{VT}}{\partial \alpha_{VT}} = \frac{1}{V_0} X_{\alpha_{VT}}$$

$$\frac{\partial \alpha_{VT}}{\partial \alpha} = 1 - \frac{\partial \epsilon_{VT}}{\partial \alpha} = 1 - K_{FVT}\left(1 - \frac{1}{\mu}\frac{\partial \lambda}{\partial \alpha_{C}}\right)_F - K_{RVT}\left(1 - \frac{1}{\mu}\frac{\partial \lambda}{\partial \alpha_{C}}\right)_R$$

$$(X_w)_{TR} = \frac{\partial (X)_{TR}}{\partial w} = \frac{1}{V_0} X_{w_{TR}} \frac{\partial \alpha_{TR}}{\partial \alpha}$$

$$X_{w_{TR}} = \frac{\partial (X)_{TR}}{\partial w_{TR}} = \frac{1}{V_0} \frac{\partial (X)_{TR}}{\partial \alpha_{TR}} = \frac{1}{V_0} X_{\alpha_{TR}}$$

$$\frac{\partial \alpha_{TR}}{\partial \alpha} = 1 - \frac{\partial \epsilon_{TR}}{\partial \alpha} = 1 - K_{FTR}\left(1 - \frac{1}{\mu}\frac{\partial \lambda}{\partial \alpha_{C}}\right)_F - K_{RTR}\left(1 - \frac{1}{\mu}\frac{\partial \lambda}{\partial \alpha_{C}}\right)_R$$

$$(X_w)_{P_i} = \frac{\partial (X)_{P_i}}{\partial w} = \frac{1}{V_0} X_{w_{P_i}} \frac{\partial \alpha_{P_i}}{\partial \alpha}$$

$$X_{w_{P_i}} = \frac{\partial (X)_{P_i}}{\partial w_{P_i}} = \frac{1}{V_0} \frac{\partial (X)_{P_i}}{\partial \alpha_{P_i}} = \frac{1}{V_0} X_{\alpha_{P_i}}$$

$$\frac{\partial \alpha_{P_i}}{\partial \alpha} = 1 - \frac{\partial \epsilon_{P_i}}{\partial \alpha} = 1 - K_{FP_i}\left(1 - \frac{1}{\mu}\frac{\partial \lambda}{\partial \alpha_{C}}\right)_F - K_{RP_i}\left(1 - \frac{1}{\mu}\frac{\partial \lambda}{\partial \alpha_{C}}\right)_R$$

<u>7.1.1.5 $X_{\dot{w}}$</u>

$$X_{\dot{w}} = (X_{\dot{w}})_R + (X_{\dot{w}})_T + (X_{\dot{w}})_{VT} + (X_{\dot{w}})_{TR}$$

where

$$(X_{\dot{w}})_R = \frac{\partial (X)_R}{\partial \dot{w}} = \frac{1}{V_0} \frac{\partial (X)_R}{\partial \dot{\alpha}} = \frac{1}{V_0} X_{\alpha_R} \frac{\partial \alpha_R}{\partial \dot{\alpha}}$$

$$\frac{\partial \alpha_R}{\partial \dot{\alpha}} = - \frac{\partial \epsilon_R}{\partial \dot{\alpha}} = - \frac{\partial \epsilon_R}{\partial \alpha}\left(\frac{\ell x_F - \ell x_R}{V_0}\right) = -K_{FR}\left(1 - \frac{1}{\mu}\frac{\partial \lambda}{\partial \alpha_{C_F}}\right)\left(\frac{\ell x_F - \ell x_R}{V_0}\right)$$

$$(X_{\dot w})_T = \frac{\partial (X)_T}{\partial \dot w} = \frac{1}{V_0}\frac{\partial (X)_T}{\partial \dot\alpha} = \frac{1}{V_0} X_{\alpha_T}\frac{\partial \alpha_T}{\partial \dot\alpha}$$

$$\frac{\partial \alpha_T}{\partial \dot\alpha} = -\frac{\partial \epsilon_T}{\partial \dot\alpha} = -\frac{\partial \epsilon_T}{\partial \alpha}\left(\frac{\ell x_F - \ell x_T}{V_0}\right) = -\left[K_{FT}\left(1-\frac{1}{\mu}\frac{\partial \lambda}{\partial \alpha_C}\right)_F + K_{RT}\left(1-\frac{1}{\mu}\frac{\partial \lambda}{\partial \alpha_C}\right)_R\right]\left(\frac{\ell x_F - \ell x_T}{V_0}\right)$$

$$(X_{\dot w})_{VT} = \frac{\partial (X)_{VT}}{\partial \dot w} = \frac{1}{V_0}\frac{\partial (X)_{VT}}{\partial \dot\alpha} = \frac{1}{V_0} X_{\alpha_{VT}}\frac{\partial \alpha_{VT}}{\partial \dot\alpha}$$

$$\frac{\partial \alpha_{VT}}{\partial \dot\alpha} = -\frac{\partial \epsilon_{VT}}{\partial \dot\alpha} = -\left[K_{FVT}\left(1-\frac{1}{\mu}\frac{\partial \lambda}{\partial \alpha_C}\right)_F + K_{RVT}\left(1-\frac{1}{\mu}\frac{\partial \lambda}{\partial \alpha_C}\right)_R\right]\left(\frac{\ell x_F - \ell x_{VT}}{V_0}\right)$$

$$(X_{\dot w})_{TR} = \frac{\partial (X)_{TR}}{\partial \dot w} = \frac{1}{V_0}\frac{\partial (X)_{TR}}{\partial \dot\alpha} = \frac{1}{V_0} X_{\alpha_{TR}}\frac{\partial \alpha_{TR}}{\partial \dot\alpha}$$

$$\frac{\partial \alpha_{TR}}{\partial \dot\alpha} = -\frac{\partial \epsilon_{TR}}{\partial \dot\alpha} = -\left[K_{FTR}\left(1-\frac{1}{\mu}\frac{\partial \lambda}{\partial \alpha_C}\right)_F + K_{RTR}\left(1-\frac{1}{\mu}\frac{\partial \lambda}{\partial \alpha_C}\right)_R\right]\left(\frac{\ell x_F - \ell x_{TR}}{V_0}\right)$$

7.1.1.6 X_θ

$$X_\theta = -W \cos\theta \cos\phi \cos\psi$$

7.1.1.7 $X_{\dot\theta}$

$$X_{\dot\theta} = (X_{\dot\theta})_F + (X_{\dot\theta})_R + (X_{\dot\theta})_W + (X_{\dot\theta})_T + (X_{\dot\theta})_{VT} + (X_{\dot\theta})_{TR} + \sum_{i=1}^{n}(X_{\dot\theta})_{P_i} - \frac{W}{g} V_0 \sin\alpha$$

where

$$(X_{\dot\theta})_F = \frac{\partial (X)_F}{\partial \dot\theta} = X_{u_F}\ell_{z_F} - X_{w_F}\ell_{x_F} + \left(\frac{\partial X}{\partial a_1}\right)_F \frac{\partial a_{1_F}}{\partial q} + \left(\frac{\partial X}{\partial b_1}\right)_F \frac{\partial b_{1_F}}{\partial q}$$

$$\left(\frac{\partial X}{\partial a_1}\right)_F = \left(\frac{\partial L_F}{\partial a_{1_F}} \cos A_{1_F} - \frac{\partial Y_F}{\partial a_{1_F}} \sin A_{1_F}\right) \sin(\alpha - \epsilon_F) - \frac{\partial D_F}{\partial a_{1_F}} \cos(\alpha - \epsilon_F)$$

$$\left(\frac{\partial X}{\partial b_1}\right)_F = \left(\frac{\partial L_F}{\partial b_{1_F}} \cos A_{1_F} - \frac{\partial Y_F}{\partial b_{1_F}} \sin A_{1_F}\right) \sin(\alpha - \epsilon_F) - \frac{\partial D_F}{\partial b_{1_F}} \cos(\alpha - \epsilon_F)$$

$$(X_{\dot\theta})_R = X_{u_R} \ell_{z_R} - X_{w_R} \ell_{x_R} + \left(\frac{\partial X}{\partial a_1}\right)_R \frac{\partial a_{1_R}}{\partial q} + \left(\frac{\partial X}{\partial b_1}\right)_R \frac{\partial b_{1_R}}{\partial q}$$

$$\left(\frac{\partial X}{\partial a_1}\right)_R = \left(\frac{\partial L_R}{\partial a_{1_R}} \cos A_{1_R} + \frac{\partial Y_R}{\partial a_{1_R}} \sin A_{1_R}\right) \sin(\alpha - \epsilon_R) - \frac{\partial D_R}{\partial a_{1_R}} \cos(\alpha - \epsilon_R)$$

$$\left(\frac{\partial X}{\partial b_1}\right)_R = \left(\frac{\partial L_R}{\partial b_{1_R}} \cos A_{1_R} + \frac{\partial Y_R}{\partial b_{1_R}} \sin A_{1_R}\right) \sin(\alpha - \epsilon_R) - \frac{\partial D_R}{\partial b_{1_R}} \cos(\alpha - \epsilon_R)$$

$$(X_{\dot\theta})_W = \frac{\partial (X)_W}{\partial \dot\theta} = X_{u_W} \ell_{z_W} - X_{w_W} \ell_{x_W}$$

$$(X_{\dot\theta})_T = \frac{\partial (X)_T}{\partial \dot\theta} = X_{u_T} \ell_{z_T} - X_{w_T} \ell_{x_T}$$

$$(X_{\dot\theta})_{VT} = \frac{\partial (X)_{VT}}{\partial \dot\theta} = X_{u_{VT}} \ell_{z_{VT}} - X_{w_{VT}} \ell_{x_{VT}}$$

$$(X_{\dot\theta})_{TR} = \frac{\partial (X)_{TR}}{\partial \dot\theta} = X_{u_{TR}} \ell_{z_{TR}} - X_{w_{TR}} \ell_{x_{TR}}$$

$$(X_{\dot\theta})_{P_i} = \frac{\partial (X)_{P_i}}{\partial \dot\theta} = X_{u_{P_i}} \ell_{z_{P_i}} - X_{w_{P_i}} \ell_{x_{P_i}}$$

7.1.1.8 X_ϕ

$$X_\phi = W \sin\psi \cos\phi + W \sin\phi \sin\theta \cos\psi$$

7.1.1.9 $X_{\dot\phi}$

$$X_{\dot\phi} = (X_{\dot\phi})_F + (X_{\dot\phi})_R + (X_{\dot\phi})_W + (X_{\dot\phi})_T + (X_{\dot\phi})_{VT} + (X_{\dot\phi})_{TR} + \sum_{i=1}^{n} (X_{\dot\phi})_{P_i}$$

where

$$(X_{\dot\phi})_F = \frac{\partial(X)_F}{\partial\dot\phi} = X_{W_F}\, \ell_{Y_F} - X_{V_F}\, \ell_{Z_F} + (\frac{\partial X}{\partial a_1})_F \frac{\partial a_{1F}}{\partial p} + (\frac{\partial X}{\partial b_1})_F \frac{\partial b_{1F}}{\partial p}$$

$$(X_{\dot\phi})_R = \frac{\partial(X)_R}{\partial\dot\phi} = X_{W_R}\, \ell_{Y_R} - X_{V_R}\, \ell_{Z_R} + (\frac{\partial X}{\partial a_1})_R \frac{\partial a_{1R}}{\partial p} + (\frac{\partial X}{\partial b_1})_R \frac{\partial b_{1R}}{\partial p}$$

$$(X_{\dot\phi})_W = \frac{\partial(X)_W}{\partial\dot\phi} = X_{W_W}\, \ell_{Y_W} - X_{V_W}\, \ell_{Z_W}$$

$$(X_{\dot\phi})_T = \frac{\partial(X)_T}{\partial\dot\phi} = X_{W_T}\, \ell_{Y_T} - X_{V_T}\, \ell_{Z_T}$$

$$(X_{\dot\phi})_{VT} = \frac{\partial(X)_{VT}}{\partial\dot\phi} = X_{W_{VT}}\, \ell_{Y_{VT}} - X_{V_{VT}}\, \ell_{Z_{VT}}$$

$$(X_{\dot\phi})_{TR} = \frac{\partial(X)_{TR}}{\partial\dot\phi} = X_{W_{TR}}\, \ell_{Y_{TR}} - X_{V_{TR}}\, \ell_{Z_{TR}}$$

$$(X_{\dot\phi})_{P_i} = \frac{\partial(X)_{P_i}}{\partial\dot\phi} = X_{W_{P_i}}\, \ell_{Y_{P_i}} - X_{V_{P_i}}\, \ell_{Z_{P_i}}$$

7.1.1.10 $X_{\dot\psi}$

$$X_{\dot\psi} = (X_{\dot\psi})_F + (X_{\dot\psi})_R + (X_{\dot\psi})_W + (X_{\dot\psi})_T + (X_{\dot\psi})_{VT} + (X_{\dot\psi})_{TR} + \sum_{i=1}^{n} (X_{\dot\psi})_{P_i} + \frac{W}{g} V_a \sin \beta_s$$

where

$$(X_{\dot\psi})_F = \frac{\partial(X)_F}{\partial\dot\psi} = X_{V_F}\, \ell_{X_F} - X_{U_F}\, \ell_{Y_F} + (\frac{\partial X}{\partial a_1})_F \frac{\partial a_{1F}}{\partial r} + (\frac{\partial X}{\partial b_1})_F \frac{\partial b_{1F}}{\partial r}$$

$$(X_{\dot\psi})_R = \frac{\partial(X)_R}{\partial\dot\psi} = X_{V_R}\, \ell_{X_R} - X_{U_R}\, \ell_{Y_R} + (\frac{\partial X}{\partial a_1})_R \frac{\partial a_{1R}}{\partial r} + (\frac{\partial X}{\partial b_1})_R \frac{\partial b_{1R}}{\partial r}$$

$$(X_{\dot\psi})_W = \frac{\partial (X)_W}{\partial \dot\psi} = X_{v_W} \ \ell_{X_W} - X_{u_W} \ell_{Y_W}$$

$$(X_{\dot\psi})_T = \frac{\partial (X)_T}{\partial \dot\psi} = X_{v_T} \ \ell_{X_T} - X_{u_T} \ell_{Y_T}$$

$$(X_{\dot\psi})_{VT} = \frac{\partial (X)_{VT}}{\partial \dot\psi} = X_{v_{VT}} \ \ell_{X_{VT}} - X_{u_{VT}} \ell_{Y_{VT}}$$

$$(X_{\dot\psi})_{TR} = \frac{\partial (X)_{TR}}{\partial \dot\psi} = X_{v_{TR}} \ell_{X_{TR}} - X_{u_{TR}} \ell_{Y_{TR}}$$

$$(X_{\dot\psi})_{P_i} = \frac{\partial (X)_{P_i}}{\partial \dot\psi} = X_{v_{P_i}} \ell_{X_{P_i}} - X_{u_{P_i}} \ell_{Y_{P_i}}$$

7.1.2 The Y-Force Derivatives

7.1.2.1 Y_u

$$Y_u = (Y_u)_F + (Y_u)_R + (Y_u)_{FUS} + (Y_u)_W + (Y_u)_T + (Y_u)_{VT} + (Y_u)_{TR} + \sum_{i=1}^{n} (Y_u)_{P_i} - \frac{W}{g} r$$

where

$$(Y_u)_F = \frac{\partial (X)_F}{\partial u} = Y_{u_F} + Y_{\alpha_F} \frac{\partial \alpha_F}{\partial u}$$

$$Y_{u_F} = \frac{\partial (Y)_F}{\partial u_F} = \left[\frac{\partial L_F}{\partial u_F} \sin A_{l_F} + \frac{\partial Y_F}{\partial u_F} \cos A_{l_F}\right] \cos \beta_S + \left[\left(\frac{\partial L_F}{\partial u_F} \cos A_{l_F}\right.\right.$$

$$\left.\left. - \frac{\partial Y_F}{\partial u_F} \sin A_{l_F}\right) \sin(\alpha - \epsilon_F) - \frac{\partial D_F}{\partial u_F} \cos(\alpha - \epsilon_F)\right] \sin \beta_S$$

$$Y_{\alpha_F} = \frac{\partial (Y)_F}{\partial \alpha_F} = \left[\frac{\partial L_F}{\partial \alpha_F} \sin A_{I_F} + \frac{\partial Y_F}{\partial \alpha_F} \cos A_{I_F}\right] \cos \beta_S$$

$$+ \left[\left(\frac{\partial L_F}{\partial \alpha_F} \cos A_{I_F} - \frac{\partial Y_F}{\partial \alpha_F} \sin A_{I_F} + D_F\right) \sin(\alpha - \epsilon_F)\right.$$

$$\left.\left(L_F \cos A_{I_F} - Y_F \sin A_{I_F} + \frac{\partial D_F}{\partial \alpha_F}\right) \cos(\alpha - \epsilon_F)\right] \sin \beta_S$$

$$(Y_u)_R = \frac{\partial (Y)_R}{\partial u} = Y_{u_R} + Y_{\alpha_R} \frac{\partial \alpha_R}{\partial u}$$

$$Y_{u_R} = \frac{\partial (Y)_R}{\partial u_R} = \left[\frac{\partial L_R}{\partial u_R} \sin A_{I_R} - \frac{\partial Y_R}{\partial u_R} \cos A_{I_R}\right] \cos \beta_S + \left[\frac{\partial L_R}{\partial u_R} \cos A_{I_R}\right.$$

$$\left.+ \frac{\partial Y_R}{\partial u_R} \sin A_{I_R}\right) \sin(\alpha - \epsilon_R) - \frac{\partial D_R}{\partial u_R} \cos(\alpha - \epsilon_R)\Big] \sin \beta_S$$

$$Y_{\alpha_R} = \frac{\partial (Y)_R}{\partial \alpha_R} = \left[\frac{\partial L_R}{\partial \alpha_R} \sin A_{I_R} - \frac{\partial Y_R}{\partial \alpha_R} \cos A_{I_R}\right] \cos \beta_S$$

$$+ \left[\left(\frac{\partial L_R}{\partial \alpha_R} \cos A_{I_R} + \frac{\partial Y_R}{\partial \alpha_R} \sin A_{I_R} + D_R\right) \sin(\alpha - \epsilon_R)\right.$$

$$\left.+ \left(L_R \cos A_{I_R} + Y_R \sin A_{I_R} - \frac{\partial D_R}{\partial \alpha_R} \cos(\alpha - \epsilon_R)\right] \sin \beta_S$$

$$(Y_u)_{FUS} = \frac{\partial (Y)_{FUS}}{\partial u} = Y_{u_{FUS}} + Y_{\alpha_{FUS}} \frac{\partial \alpha_{FUS}}{\partial u}$$

$$Y_{u_{FUS}} = \frac{\partial (Y)_{FUS}}{\partial u_{FUS}} = \frac{\partial Y_{FUS}}{\partial u_{FUS}} \cos \beta_S + \left[\frac{\partial L_{FUS}}{\partial u_{FUS}} \sin(\alpha - \epsilon_{FUS})\right.$$

$$\left.- \frac{\partial D_{FUS}}{\partial u_{FUS}} \cos(\alpha - \epsilon_{FUS})\right] \sin \beta_S$$

$$Y_{\alpha_{FUS}} = \frac{\partial (Y)_{FUS}}{\partial \alpha_{FUS}} = \frac{\partial Y_{FUS}}{\partial \alpha_{FUS}} \cos \beta_s + \left[\left(\frac{\partial L_{FUS}}{\partial \alpha_{FUS}} + D_{FUS} \right) \sin(\alpha - \epsilon_{FUS}) \right.$$

$$\left. + \left(L_{FUS} - \frac{\partial D_{FUS}}{\partial \alpha_{FUS}} \right) \cos(\alpha - \epsilon_{FUS}) \right] \sin \beta_s$$

$$(Y_u)_W = \frac{\partial (Y)_W}{\partial u_W} = Y_{u_W} + Y_{\alpha_W} \frac{\partial \alpha_W}{\partial u}$$

$$Y_{u_W} = \frac{\partial (Y)_W}{\partial u_W} = \left[\frac{\partial L_W}{\partial u_W} \sin(\alpha - \epsilon_W) - \frac{\partial D_W}{\partial u_W} \cos(\alpha - \epsilon_W) \right] \sin \beta_s$$

$$Y_{\alpha_W} = \frac{\partial (Y)_W}{\partial \alpha_W} = \left[\left(\frac{\partial L_W}{\partial \alpha_W} + D_W \right) \sin(\alpha - \epsilon_W) + \left(L_W - \frac{\partial D_W}{\partial \alpha_W} \right) \cos(\alpha - \epsilon_W) \right] \sin \beta_s$$

$$(Yu)_T = \frac{\partial (Y)_T}{\partial u_T} = Y_{u_T} + Y_{\alpha_T} \frac{\partial \alpha_T}{\partial u}$$

$$Y_{u_T} = \frac{\partial (Y)_T}{\partial u_T} = \left[\frac{\partial L_T}{\partial u_T} \sin(\alpha - \epsilon_T) - \frac{\partial D_T}{\partial u_T} \cos(\alpha - \epsilon_T) \right] \sin \beta_s$$

$$Y_{\alpha_T} = \frac{\partial (Y)_T}{\partial u_T} = \left[\left(\frac{\partial L_T}{\partial \alpha_T} + D_T \right) \sin(\alpha - \epsilon_T) + \left(L_T - \frac{\partial D_T}{\partial \alpha_T} \right) \cos(\alpha - \epsilon_T) \right] \sin \beta_s$$

$$(Y_u)_{VT} = \frac{\partial (Y)_{VT}}{\partial u} = Y_{u_{VT}} + Y_{\alpha_{VT}} \frac{\partial \alpha_{VT}}{\partial u}$$

$$Y_{u_{VT}} = \frac{\partial (Y)_{VT}}{\partial u_{VT}} = - \frac{\partial L_{VT}}{\partial u_{VT}} \cos \beta_s - \frac{\partial D_{VT}}{\partial u_{VT}} \cos(\alpha - \epsilon_{VT}) \sin \beta_s$$

$$Y_{\alpha_{VT}} = \frac{\partial (Y)_{VT}}{\partial \alpha_{VT}} = - \frac{\partial L_{VT}}{\partial \alpha_{VT}} \cos \beta_s - \left[\frac{\partial D_{VT}}{\partial \alpha_{VT}} \cos(\alpha - \epsilon_{VT}) \right.$$

$$\left. - D_{VT} \sin(\alpha - \epsilon_{VT}) \right] \sin \beta_s$$

$$(Y_u)_{TR} = \frac{\partial (Y)_{TR}}{\partial u} = Y_{u_{TR}} + Y_{\alpha_{TR}} \frac{\partial \alpha_{TR}}{\partial u}$$

$$Y_{u_{TR}} = \frac{\partial (Y)_{TR}}{\partial u_{TR}} = \frac{\partial T_{TR}}{\partial u_{TR}} \cos\beta_S + \left[\frac{\partial Y_{TR}}{\partial u_{TR}} \sin(\alpha - \epsilon_{TR}) - \frac{\partial D_{TR}}{\partial u_{TR}} \cos(\alpha - \epsilon_{TR})\right] \sin\beta_S$$

$$Y_{\alpha_{TR}} = \frac{\partial (Y)_{TR}}{\partial \alpha_{TR}} = \frac{\partial T_{TR}}{\partial \alpha_{TR}} \cos\beta_S + \left[\left(\frac{\partial Y_{TR}}{\partial \alpha_{TR}} + D_{TR}\right) \sin(\alpha - \epsilon_{TR}) - \left(\frac{\partial D_{TR}}{\partial \alpha_{TR}} - Y_{TR}\right) \cos(\alpha - \epsilon_{TR})\right] \sin\beta_S$$

$$(Y_u)_{P_i} = \frac{\partial (Y)_{P_i}}{\partial u} = Y_{u_{P_i}} + Y_{\alpha_{P_i}} \frac{\partial \alpha_{P_i}}{\partial u}$$

$$Y_{u_{P_i}} = \frac{\partial (Y)_{P_i}}{\partial u_{P_i}} = \frac{\partial Y_{P_i}}{\partial u_{P_i}}$$

$$Y_{\alpha_{P_i}} = \frac{\partial (Y)_{P_i}}{\partial \alpha_{P_i}} = \frac{\partial Y_{P_i}}{\partial \alpha_{P_i}}$$

7.1.2.2 Y_V

$$Y_V = (Y_V)_F + (Y_V)_R + (Y_V)_{FUS} + (Y_V)_W + (Y_V)_T + (Y_V)_{VT} + (Y_V)_{TR} + \sum_{i=1}^{n} (Y_V)_{P_i}$$

where

$$(Y_V)_F = \frac{\partial (Y)_F}{\partial v} = \frac{1}{V_0} \frac{\partial (Y)_F}{\partial \beta_S} = \frac{1}{V_0}\left[(L_F \cos A_{I_F} - Y_F \sin A_{I_F}) \sin(\alpha - \epsilon_F) - D_F \cos(\alpha - \epsilon_F)\right] \cos\beta_S - \frac{1}{V_0}\left[L_F \sin A_{I_F} + Y_F \cos A_{I_F}\right] \sin\beta_S$$

$$(Y_V)_R = \frac{\partial (Y)_R}{\partial v} = \frac{1}{V_0} \frac{\partial (Y)_R}{\partial \beta_S} = \frac{1}{V_0}\left[(L_R \cos A_{I_R} + Y_R \sin A_{I_R}) \sin(\alpha - \epsilon_R) - D_R \cos(\alpha - \epsilon_R)\right] \cos\beta_S$$

$$-\frac{1}{V_0}\left[L_R \sin A_{I_R} - Y_R \cos A_{I_R}\right]\sin\beta_s$$

$$(Y_v)_{FUS} = \frac{\partial(Y)_{FUS}}{\partial v} = \frac{1}{V_0}\frac{\partial(Y)_{FUS}}{\partial\beta_s} = \frac{1}{V_0}\left[L_{FUS}\sin(\alpha-\epsilon_{FUS}) - D_{FUS}\cos(\alpha-\epsilon_{FUS}) + \frac{\partial Y_{FUS}}{\partial\beta_s}\right]\cos\beta_s$$

$$+\frac{1}{V_0}\left[\frac{\partial L_{FUS}}{\partial\beta_s}\sin(\alpha-\epsilon_{FUS}) - \frac{\partial D_{FUS}}{\partial\beta_s}\cos(\alpha-\epsilon_{FUS}) - Y_{FUS}\right]\sin\beta_s$$

$$(Y_v)_W = \frac{\partial(Y)_W}{\partial v} = \frac{1}{V_0}\frac{\partial(Y)_W}{\partial\beta_s} = \frac{1}{V_0}\left[L_W\sin(\alpha-\epsilon_W) - D_W\cos(\alpha-\epsilon_W)\right]\cos\beta_s$$

$$(Y_v)_T = \frac{\partial(Y)_T}{\partial v} = \frac{1}{V_0}\frac{\partial(Y)_T}{\partial\beta_s} = \frac{1}{V_0}\left[L_T\sin(\alpha-\epsilon_T) - D_T\cos(\alpha-\epsilon_T)\right]\cos\beta_s$$

$$(Y_v)_{VT} = \frac{\partial(Y)_{VT}}{\partial v} = \frac{1}{V_0}\frac{\partial(Y)_{VT}}{\partial\beta_s} = \frac{1}{V_0}\left[-D_{VT}\cos(\alpha-\epsilon_{VT}) - \frac{\partial L_{VT}}{\partial\beta_s}\right]\cos\beta_s$$

$$-\frac{1}{V_0}\left[\frac{\partial D_{VT}}{\partial\beta_s}\cos(\alpha-\epsilon_{VT}) + L_{VT}\right]\sin\beta_s$$

$$(Y_v)_{TR} = \frac{\partial(Y)_{TR}}{\partial v} = \frac{1}{V_0}\frac{\partial(Y)_{TR}}{\partial\beta_s} = \frac{1}{V_0}\left[Y_{TR}\sin(\alpha-\epsilon_{TR}) - D_{TR}\cos(\alpha-\epsilon_{TR}) + \frac{\partial T_{TR}}{\partial\beta_s}\right]\cos\beta_s$$

$$+\frac{1}{V_0}\left[\frac{\partial Y_{TR}}{\partial\beta_s}\sin(\alpha-\epsilon_{TR}) - \frac{\partial D_{TR}}{\partial\beta_s}\cos(\alpha-\epsilon_{TR}) - T_{TR}\right]\sin\beta_s$$

$$(Y_v)_{P_i} = \frac{\partial(Y)_{P_i}}{\partial v} = \frac{1}{V_0}\frac{\partial(Y)_{P_i}}{\partial\beta_s} = \frac{1}{V_0}\frac{\partial Y_{P_i}}{\partial\beta_s}$$

7.1.2.3 $Y_{\dot{v}}$

$$Y_{\dot{v}} = -\frac{W}{g}$$

7.1.2.4 Y_w

$$Y_w = (Y_w)_F + (Y_w)_R + (Y_w)_{FUS} + (Y_w)_W + (Y_w)_T + (Y_w)_{VT} + (Y_w)_{TR} + \sum_{i=1}^{n}(Y_w)_{P_i} - \frac{W}{g}p$$

where

$$(Y_w)_F = \frac{\partial (Y)_F}{\partial w} = Y_{w_F} \frac{\partial \alpha_F}{\partial \alpha}$$

$$Y_{w_F} = \frac{\partial (Y)_F}{\partial w_F} = \frac{1}{V_0} \frac{\partial (Y)_F}{\partial \alpha_F} = \frac{1}{V_0} Y_{\alpha_F}$$

$$(Y_w)_R = \frac{\partial (Y)_R}{\partial w} = Y_{w_R} \frac{\partial \alpha_R}{\partial \alpha}$$

$$Y_{w_R} = \frac{\partial (Y)_R}{\partial w_R} = \frac{1}{V_0} \frac{\partial (Y)_R}{\partial \alpha_R} = \frac{1}{V_0} Y_{\alpha_R}$$

$$(Y_w)_{FUS} = \frac{\partial (Y)_{FUS}}{\partial w} = Y_{w_{FUS}} \frac{\partial \alpha_{FUS}}{\partial \alpha}$$

$$Y_{w_{FUS}} = \frac{\partial (Y)_{FUS}}{\partial w_{FUS}} = \frac{1}{V_0} \frac{\partial (Y)_{FUS}}{\partial \alpha_{FUS}} = \frac{1}{V_0} Y_{\alpha_{FUS}}$$

$$(Y_w)_W = \frac{\partial (Y)_W}{\partial w} = Y_{w_W} \frac{\partial \alpha_W}{\partial \alpha}$$

$$Y_{w_W} = \frac{\partial (Y)_W}{\partial w_W} = \frac{1}{V_0} \frac{\partial (Y)_W}{\partial \alpha_W} = \frac{1}{V_0} Y_{\alpha_W}$$

$$(Y_w)_T = \frac{\partial (Y)_T}{\partial w} = Y_{w_T} \frac{\partial \alpha_T}{\partial \alpha}$$

$$Y_{w_T} = \frac{\partial (Y)_T}{\partial w_T} = \frac{1}{V_0} \frac{\partial (Y)_T}{\partial \alpha_T} = \frac{1}{V_0} Y_{\alpha_T}$$

$$(Y_w)_{VT} = \frac{\partial (Y)_{VT}}{\partial w} \quad Y_{w_{VT}} \frac{\partial \alpha_{VT}}{\partial \alpha}$$

$$Y_{w_{VT}} = \frac{\partial (Y)_{VT}}{\partial w_{VT}} = \frac{1}{V_0} \frac{\partial (Y)_{VT}}{\partial \alpha_{VT}} = \frac{1}{V_0} Y_{\alpha_{VT}}$$

$$(Y_w)_{TR} = \frac{\partial (Y)_{TR}}{\partial w} = Y_{w_{TR}} \frac{\partial \alpha_{TR}}{\partial \alpha}$$

$$Y_{w_{TR}} = \frac{\partial (Y)_{TR}}{\partial w_{TR}} = \frac{1}{V_0} \frac{\partial (Y)_{TR}}{\partial \alpha_{TR}} = \frac{1}{V_0} Y_{\alpha_{TR}}$$

$$(Y_w)_{P_i} = \frac{\partial (Y)_{P_i}}{\partial w} = Y_{w_{P_i}} \frac{\partial \alpha_{P_i}}{\partial \alpha}$$

$$Y_{w_{P_i}} = \frac{\partial (Y)_{P_i}}{\partial w_{P_i}} = \frac{1}{V_0} \frac{\partial (Y)_{P_i}}{\partial \alpha_{P_i}} = \frac{1}{V_0} Y_{\alpha_{P_i}}$$

7.1.2.5 Y_θ

$$Y_\theta = W \cos\phi \cos\theta \sin\psi$$

7.1.2.6 $Y_{\dot\theta}$

$$Y_{\dot\theta} = (Y_{\dot\theta})_F + (Y_{\dot\theta})_R + (Y_{\dot\theta})_W + (Y_{\dot\theta})_T + (Y_{\dot\theta})_{VT} + (Y_{\dot\theta})_{TR} + \sum_{i=1}^{n} (Y_{\dot\theta})_{P_i}$$

where

$$(Y_{\dot\theta})_F = \frac{\partial (Y)_F}{\partial \dot\theta} = Y_{u_F} \ell_{z_F} - Y_{w_F} \ell_{x_F} + \left(\frac{\partial Y}{\partial a_1}\right)_F \frac{\partial a_{1_F}}{\partial q} + \left(\frac{\partial Y}{\partial b_1}\right)_F \frac{\partial b_{1_F}}{\partial q}$$

$$\left(\frac{\partial Y}{\partial a_1}\right)_F = \frac{\partial L_F}{\partial a_{1_F}} \sin A_{1_F} + \frac{\partial Y_F}{\partial a_{1_F}} \cos A_{1_F}$$

$$\left(\frac{\partial Y}{\partial b_1}\right)_F = \frac{\partial L_F}{\partial b_{1_F}} \sin A_{1_F} + \frac{\partial Y_F}{\partial b_{1_F}} \cos A_{1_F}$$

$$(Y_{\dot\theta})_R = \frac{\partial (Y)_R}{\partial \dot\theta} = Y_{u_R} \ell_{z_R} - Y_{w_R} \ell_{x_R} + \left(\frac{\partial Y}{\partial a_1}\right)_R \frac{\partial a_{1_R}}{\partial q} + \left(\frac{\partial Y}{\partial b_1}\right)_R \frac{\partial b_{1_R}}{\partial q}$$

$$\left(\frac{\partial Y}{\partial a_1}\right)_R = \frac{\partial L_R}{\partial a_{1_R}} \sin A_{1_R} - \frac{\partial Y_R}{\partial a_{1_R}} \cos A_{1_R}$$

$$\left(\frac{\partial Y}{\partial b_1}\right)_R = \frac{\partial L_R}{\partial b_{1_R}} \sin A_{1_R} - \frac{\partial Y_R}{\partial b_{1_R}} \cos A_{1_R}$$

$$(Y_{\dot\theta})_W = \frac{\partial(Y)_W}{\partial\dot\theta} = Y_{u_W}\ell_{z_W} - Y_{w_W}\ell_{x_W}$$

$$(Y_{\dot\theta})_T = \frac{\partial(Y)_T}{\partial\dot\theta} = Y_{u_T}\ell_{z_T} - Y_{w_T}\ell_{x_T}$$

$$(Y_{\dot\theta})_{VT} = \frac{\partial(Y)_{VT}}{\partial\dot\theta} = Y_{u_{VT}}\ell_{z_{VT}} - Y_{w_{VT}}\ell_{x_{VT}}$$

$$(Y_{\dot\theta})_{TR} = \frac{\partial(Y)_{TR}}{\partial\dot\theta} = Y_{u_{TR}}\ell_{z_{TR}} - Y_{w_{TR}}\ell_{x_{TR}}$$

$$(Y_{\dot\theta})_{P_i} = \frac{\partial(Y)_{P_i}}{\partial\dot\theta} = Y_{u_{P_i}}\ell_{z_{P_i}} - Y_{w_{P_i}}\ell_{x_{P_i}}$$

7.1.2.7 Y_ϕ

$$Y_\phi = W\cos\phi\cos\psi - W\sin\phi\sin\theta\sin\psi$$

7.1.2.8 $Y_{\dot\phi}$

$$Y_{\dot\phi} = (Y_{\dot\phi})_F + (Y_{\dot\phi})_R + (Y_{\dot\phi})_W + (Y_{\dot\phi})_T + (Y_{\dot\phi})_{VT} + (Y_{\dot\phi})_{TR} + \sum_{i=1}^{n}(Y_{\dot\phi})_{P_i} + \frac{W}{g}V_0\sin\alpha$$

where

$$(Y_{\dot\phi})_F = \frac{\partial(Y)_F}{\partial\dot\phi} = Y_{w_F}\ell_{Y_F} - Y_{v_F}\ell_{z_F} + \left(\frac{\partial Y}{\partial a_1}\right)_F\frac{\partial a_{1_F}}{\partial p} + \left(\frac{\partial Y}{\partial b_1}\right)_F\frac{\partial b_{1_F}}{\partial p}$$

$$(Y_{\dot\phi})_R = \frac{\partial(Y)_R}{\partial\dot\phi} = Y_{w_R}\ell_{Y_R} - Y_{v_R}\ell_{z_R} + \left(\frac{\partial Y}{\partial a_1}\right)_R\frac{\partial a_{1_R}}{\partial p} + \left(\frac{\partial Y}{\partial b_1}\right)_R\frac{\partial b_{1_R}}{\partial p}$$

$$(Y_{\dot\phi})_W = \frac{\partial(Y)_W}{\partial\dot\phi} = Y_{w_W}\ell_{Y_W} - Y_{v_W}\ell_{z_W}$$

$$(Y_{\dot\phi})_T = \frac{\partial(Y)_T}{\partial\dot\phi} = Y_{w_T}\ell_{Y_T} - Y_{v_T}\ell_{z_T}$$

$$(Y\dot{\phi})_{VT} = \frac{\partial(Y)_{VT}}{\partial\dot{\phi}} = Y_{W_{VT}}\ \ell_{Y_{VT}} - Y_{V_{VT}}\ell_{Z_{VT}}$$

$$(Y\dot{\phi})_{TR} = \frac{\partial(Y)_{TR}}{\partial\dot{\phi}} = Y_{W_{TR}}\ \ell_{Y_{TR}} - Y_{V_{TR}}\ell_{Z_{TR}}$$

$$(Y\dot{\phi})_{P_i} = \frac{\partial(Y)_{P_i}}{\partial\dot{\phi}} = Y_{W_{P_i}}\ \ell_{Y_{P_i}} - Y_{V_{P_i}}\ell_{Z_{P_i}}$$

<u>7.1.2.9 Y_ψ</u>

$$Y_\psi = W\ \sin\theta\ \cos\phi\ \cos\psi\ - W\sin\phi\ \sin\psi$$

<u>7.1.2.10 $Y_{\dot{\psi}}$</u>

$$Y_{\dot{\psi}} = (Y_{\dot{\psi}})_F + (Y_{\dot{\psi}})_R + (Y_{\dot{\psi}})_W + (Y_{\dot{\psi}})_T + (Y_{\dot{\psi}})_{VT} + (Y_{\dot{\psi}})_{TR} + \sum_{i=1}^{n} (Y_{\dot{\psi}})_{P_i} - \frac{W}{g} V_0$$

where

$$(Y_{\dot{\psi}})_F = \frac{\partial(Y)_F}{\partial\dot{\psi}} = Y_{V_F}\ \ell_{X_F} - Y_{U_F}\ \ell_{Y_F}\ + \left(\frac{\partial Y}{\partial a_1}\right)_F \frac{\partial a_{1_F}}{\partial r} + \left(\frac{\partial Y}{\partial b_1}\right)_F \frac{\partial b_{1_F}}{\partial r}$$

$$(Y_{\dot{\psi}})_R = \frac{\partial(Y)_R}{\partial\dot{\psi}} = Y_{V_R}\ \ell_{X_R} - Y_{U_R}\ \ell_{Y_R}\ + \left(\frac{\partial Y}{\partial a_1}\right)_R \frac{\partial a_{1_R}}{\partial r} + \left(\frac{\partial Y}{\partial b_1}\right)_R \frac{\partial b_{1_R}}{\partial r}$$

$$(Y_{\dot{\psi}})_W = \frac{\partial(Y)_W}{\partial\dot{\psi}} = Y_{V_W}\ \ell_{X_W} - Y_{U_W}\ \ell_{Y_W}$$

$$(Y_{\dot{\psi}})_T = \frac{\partial(Y)_T}{\partial\dot{\psi}} = Y_{V_T}\ \ell_{X_T} - Y_{U_T}\ \ell_{Y_T}$$

$$(Y_{\dot{\psi}})_{VT} = \frac{\partial(Y)_{VT}}{\partial\dot{\psi}} = Y_{V_{VT}}\ \ell_{X_{VT}} - Y_{U_{VT}}\ell_{Y_{VT}}$$

$$(Y_{\dot{\psi}})_{TR} = \frac{\partial(Y)_{TR}}{\partial\dot{\psi}} = Y_{V_{TR}}\ \ell_{X_{TR}} - Y_{U_{TR}}\ell_{Y_{TR}}$$

$$(Y_{\dot\psi})_{P_i} = \frac{\partial (Y)_{P_i}}{\partial \dot\psi} = Y_{V_{P_i}} \ell_{X_{P_i}} - Y_{U_{P_i}} \ell_{Y_{P_i}}$$

7.1.3 The Z-Force Derivatives

7.1.3.1 Z_u

$$Z_u = (Z_u)_F + (Z_u)_R + (Z_u)_{FUS} + (Z_u)_W + (Z_u)_T + (Z_u)_{VT} + (Z_u)_{TR} + \sum_{i=1}^{n} (Z_u)_{P_i}$$

where

$$(Z_u)_F = \frac{\partial (Z)_F}{\partial u} = Z_{u_F} + Z_{\alpha_F} \frac{\partial \alpha_F}{\partial u}$$

$$Z_{u_F} = \frac{\partial (Z)_F}{\partial u_F} = -\left[\frac{\partial D_F}{\partial u_F} \sin(\alpha - \epsilon_F) + \left(\frac{\partial L_F}{\partial u_F} \cos A_{I_F} - \frac{\partial Y_F}{\partial u_F} \sin A_{I_F}\right) \cos(\alpha - \epsilon_F)\right]$$

$$Z_{\alpha_F} = \frac{\partial (Z)_F}{\partial \alpha_F} = -\left[\frac{\partial D_F}{\partial \alpha_F} \sin(\alpha - \epsilon_F) + \left(\frac{\partial L_F}{\partial \alpha_F} \cos A_{I_F} - \frac{\partial Y_F}{\partial \alpha_F} \sin A_{I_F}\right) \cos(\alpha - \epsilon_F)\right]$$

$$-\left[D_F \cos(\alpha - \epsilon_F) - (L_F \cos A_{I_F} - Y_F \sin A_{I_F}) \sin(\alpha - \epsilon_F)\right]$$

$$(Z_u)_R = \frac{\partial (Z)_R}{\partial u} = Z_{u_R} + Z_{\alpha_R} \frac{\partial \alpha_R}{\partial u}$$

$$Z_{u_R} = \frac{\partial (Z)_R}{\partial u_R} = -\left[\frac{\partial D_R}{\partial u_R} \sin(\alpha - \epsilon_R) + \left(\frac{\partial L_R}{\partial u_R} \cos A_{I_R} + \frac{\partial Y_R}{\partial u_R} \sin A_{I_R}\right) \cos(\alpha - \epsilon_R)\right]$$

$$Z_{\alpha_R} = \frac{\partial (Z)_R}{\partial \alpha_R} = -\left[\frac{\partial D_R}{\partial \alpha_R} \sin(\alpha - \epsilon_R) + \left(\frac{\partial L_R}{\partial \alpha_R} \cos A_{I_R} + \frac{\partial Y_R}{\partial \alpha_R} \sin A_{I_R}\right) \cos(\alpha - \epsilon_R)\right]$$

$$-\left[D_R \cos(\alpha - \epsilon_R) - (L_R \cos A_{I_R} + Y_R \sin A_{I_R}) \sin(\alpha - \epsilon_R)\right]$$

$$(Z_u)_{FUS} = \frac{\partial (Z)_{FUS}}{\partial u} = Z_{u_{FUS}} + Z_{\alpha_{FUS}} \frac{\partial \alpha_{FUS}}{\partial u}$$

$$Z_{u_{FUS}} = \frac{\partial (Z)_{FUS}}{\partial u_{FUS}} = -\left[\frac{\partial D_{FUS}}{\partial u_{FUS}} \sin(\alpha - \epsilon_{FUS}) + \frac{\partial L_{FUS}}{\partial u_{FUS}} \cos(\alpha - \epsilon_{FUS})\right]$$

$$Z_{\alpha_{FUS}} = \frac{\partial (Z)_{FUS}}{\partial \alpha_{FUS}} = -\left[\frac{\partial D_{FUS}}{\partial \alpha_{FUS}} \sin(\alpha - \epsilon_{FUS}) + \frac{\partial L_{FUS}}{\partial \alpha_{FUS}} \cos(\alpha - \epsilon_{FUS})\right]$$

$$-\left[D_{FUS} \cos(\alpha - \epsilon_{FUS}) - L_{FUS} \sin(\alpha - \epsilon_{FUS})\right]$$

$$(Z_u)_W = \frac{\partial (Z)_W}{\partial u} = Z_{u_W} + Z_{\alpha_W} \frac{\partial \alpha_W}{\partial u}$$

$$Z_{u_W} = \frac{\partial (Z)_W}{\partial u_W} = -\left[\frac{\partial D_W}{\partial u_W} \sin(\alpha - \epsilon_W) + \frac{\partial L_W}{\partial u_W} \cos(\alpha - \epsilon_W)\right]$$

$$Z_{\alpha_W} = \frac{\partial (Z)_W}{\partial \alpha_W} = -\left[\frac{\partial D_W}{\partial \alpha_W} \sin(\alpha - \epsilon_W) + \frac{\partial L_W}{\partial \alpha_W} \cos(\alpha - \epsilon_W)\right]$$

$$-\left[D_W \cos(\alpha - \epsilon_W) - L_W \sin(\alpha - \epsilon_W)\right]$$

$$(Z_u)_T = \frac{\partial (Z)_T}{\partial u} = Z_{u_T} + Z_{\alpha_T} \frac{\partial \alpha_T}{\partial u}$$

$$Z_{u_T} = \frac{\partial (Z)_T}{\partial u_T} = -\left[\frac{\partial D_T}{\partial u_T} \sin(\alpha - \epsilon_T) + \frac{\partial L_T}{\partial u_T} \cos(\alpha - \epsilon_T)\right]$$

$$Z_{\alpha_T} = \frac{\partial (Z)_T}{\partial \alpha_T} = -\left[\frac{\partial D_T}{\partial \alpha_T} \sin(\alpha - \epsilon_T) + \frac{\partial L_T}{\partial \alpha_T} \cos(\alpha - \epsilon_T)\right]$$

$$-\left[D_T \cos(\alpha - \epsilon_T) - L_T \sin(\alpha - \epsilon_T)\right]$$

$$(Z_u)_{VT} = \frac{\partial (Z)_{VT}}{\partial u} = Z_{u_{VT}} + Z_{\alpha_{VT}} \frac{\partial \alpha_{VT}}{\partial u}$$

$$Z_{u_{VT}} = \frac{\partial (Z)_{VT}}{\partial u_{VT}} = - \frac{\partial D_{VT}}{\partial u_{VT}} \sin(\alpha - \epsilon_{VT})$$

$$Z_{\alpha_{VT}} = \frac{\partial (Z)_{VT}}{\partial \alpha_{VT}} = - \frac{\partial D_{VT}}{\partial \alpha_{VT}} \sin(\alpha - \epsilon_{VT}) - D_{VT} \cos(\alpha - \epsilon_{VT})$$

$$(Z_u)_{TR} = \frac{\partial (Z)_{TR}}{\partial u} = Z_{u_{TR}} + Z_{\alpha_{TR}} \frac{\partial \alpha_{TR}}{\partial u}$$

$$Z_{u_{TR}} = \frac{\partial (Z)_{TR}}{\partial u_{TR}} = -\left[\frac{\partial D_{TR}}{\partial u_{TR}} \sin(\alpha - \epsilon_{TR}) + \frac{\partial Y_{TR}}{\partial u_{TR}} \cos(\alpha - \epsilon_{TR}) \right]$$

$$Z_{\alpha_{TR}} = \frac{\partial (Z)_{TR}}{\partial \alpha_{TR}} = -\left[\frac{\partial D_{TR}}{\partial \alpha_{TR}} \sin(\alpha - \epsilon_{TR}) + \frac{\partial Y_{TR}}{\partial \alpha_{TR}} \cos(\alpha - \epsilon_{TR}) \right]$$

$$- \left[D_{TR} \cos(\alpha - \epsilon_{TR}) - Y_{TR} \sin(\alpha - \epsilon_{TR}) \right]$$

$$(Z_u)_{P_i} = \frac{\partial (Z)_{P_i}}{\partial u} = Z_{u_{P_i}} + Z_{\alpha_{P_i}} \frac{\partial \alpha_{P_i}}{\partial u}$$

$$Z_{u_{P_i}} = \frac{\partial (Z)_{P_i}}{\partial u_{P_i}} = -\left[\frac{\partial T_{P_i}}{\partial u_{P_i}} \sin i_{P_i} + \frac{\partial N_{P_i}}{\partial u_{P_i}} \cos i_{P_i} \right]$$

$$Z_{\alpha_{P_i}} = \frac{\partial (Z)_{P_i}}{\partial \alpha_{P_i}} = -\left[\frac{\partial T_{P_i}}{\partial \alpha_{P_i}} \sin i_{P_i} + \frac{\partial N_{P_i}}{\partial \alpha_{P_i}} \cos i_{P_i} \right]$$

7.1.3.2 Z_V

$$Z_V = (Z_V)_F + (Z_V)_R + (Z_V)_{FUS} + (Z_V)_W + (Z_V)_T + (Z_V)_{VT} + (Z_V)_{TR} + \sum_{i=1}^{n} (Z_V)_{P_i} - \frac{W}{g} p$$

where

$$(Z_v)_F = \text{[illegible]}$$

$$(Z_v)_R = 0$$

$$(Z_v)_{FUS} = \frac{\partial (Z)_{FUS}}{\partial v} = \frac{1}{V_0}\frac{\partial (Z)_{FUS}}{\partial \beta_s} = -\frac{1}{V_0}\left[\frac{\partial D_{FUS}}{\partial \beta_s}\sin(\alpha - \epsilon_{FUS}) + \frac{\partial L_{FUS}}{\partial \beta_s}\cos(\alpha - \epsilon_{FUS})\right]$$

$$(Z_v)_W = 0$$

$$(Z_v)_T = 0$$

$$(Z_v)_{VT} = \frac{\partial (Z)_{VT}}{\partial v} = \frac{1}{V_0}\frac{\partial (Z)_{VT}}{\partial \beta_s} = -\frac{1}{V_0}\left[\frac{\partial D_{VT}}{\partial \beta_s}\sin(\alpha - \epsilon_{VT})\right]$$

$$(Z_v)_{TR} = \frac{\partial (Z)_{TR}}{\partial v} = \frac{1}{V_0}\frac{\partial (Z)_{TR}}{\partial \beta_s} = -\frac{1}{V_0}\left[\frac{\partial D_{TR}}{\partial \beta_s}\sin(\alpha - \epsilon_{TR}) + \frac{\partial Y_{TR}}{\partial \beta_s}\cos(\alpha - \epsilon_{TR})\right]$$

$$(Z_v)_{P_i} = \frac{\partial (Z)_{P_i}}{\partial v} = \frac{1}{V_0}\frac{\partial (Z)_{P_i}}{\partial \beta_s} = -\frac{1}{V_0}\left[\frac{\partial T_{P_i}}{\partial \beta_s}\sin i_{P_i} + \frac{\partial N_{P_i}}{\partial \beta_s}\cos i_{P_i}\right]$$

7.1.3.3 Z_w

$$Z_w = (Z_w)_F + (Z_w)_R + (Z_w)_{FUS} + (Z_w)_W + (Z_w)_T + (Z_w)_{VT} + (Z_w)_{TR} + \sum_{i=1}^{n}(Z_w)_{P_i}$$

where

$$(Z_w)_F = \frac{\partial (Z)_F}{\partial w} = Z_{W_F}\frac{\partial \alpha_F}{\partial \alpha}$$

$$Z_{w_F} = \frac{\partial (Z)_F}{\partial w_F} = \frac{1}{V_0} \frac{\partial (Z)_F}{\partial \alpha_F} = \frac{1}{V_0} Z_{\alpha_F}$$

$$(Z_w)_R = \frac{\partial (Z)_R}{\partial w} = Z_{w_R} \frac{\partial \alpha_R}{\partial \alpha}$$

$$Z_{w_R} = \frac{\partial (Z)_R}{\partial w_R} = \frac{1}{V_0} \frac{\partial (Z)_R}{\partial \alpha_R} = \frac{1}{V_0} Z_{\alpha_R}$$

$$(Z_w)_{FUS} = \frac{\partial (Z)_{FUS}}{\partial w} = Z_{w_{FUS}} \frac{\partial \alpha_{FUS}}{\partial \alpha}$$

$$Z_{w_{FUS}} = \frac{\partial (Z)_{FUS}}{\partial w_{FUS}} = \frac{1}{V_0} \frac{\partial (Z)_{FUS}}{\partial \alpha_{FUS}} = \frac{1}{V_0} Z_{\alpha_{FUS}}$$

$$(Z_w)_W = \frac{\partial (Z)_W}{\partial w} = Z_{w_W} \frac{\partial \alpha_W}{\partial \alpha}$$

$$Z_{w_W} = \frac{\partial (Z)_W}{\partial w_W} = \frac{1}{V_0} \frac{\partial (Z)_W}{\partial \alpha_W} = \frac{1}{V_0} Z_{\alpha_W}$$

$$(Z_w)_T = \frac{\partial (Z)_T}{\partial w} = Z_{w_T} \frac{\partial \alpha_T}{\partial \alpha}$$

$$Z_{w_T} = \frac{\partial (Z)_T}{\partial w_T} = \frac{1}{V_0} \frac{\partial (Z)_T}{\partial \alpha_T} = \frac{1}{V_0} Z_{\alpha_T}$$

$$(Z_w)_{VT} = \frac{\partial (Z)_{VT}}{\partial w} = Z_{w_{VT}} \frac{\partial \alpha_{VT}}{\partial \alpha}$$

$$Z_{w_{VT}} = \frac{\partial (Z)_{VT}}{\partial w_{VT}} = \frac{1}{V_0} \frac{\partial (Z)_{VT}}{\partial \alpha_{VT}} = \frac{1}{V_0} Z_{\alpha_{VT}}$$

$$(Z_w)_{TR} = \frac{\partial (Z)_{TR}}{\partial w} = Z_{w_{TR}} \frac{\partial \alpha_{TR}}{\partial \alpha}$$

$$Z_{w_{TR}} = \frac{\partial (Z)_{TR}}{\partial w_{TR}} = \frac{1}{V_0} \frac{\partial (Z)_{TR}}{\partial \alpha_{TR}} = \frac{1}{V_0} Z_{\alpha_{TR}}$$

$$(Z_w)_{P_i} = \frac{\partial (Z)_{P_i}}{\partial w} = Z_{w_{P_i}} \frac{\partial \alpha_{P_i}}{\partial \alpha}$$

$$Z_{w_{P_i}} = \frac{\partial(Z)_{P_i}}{\partial w_{P_i}} = \frac{1}{V_0}\,\frac{\partial(Z)_{P_i}}{\partial \alpha_{P_i}} = \frac{1}{V_0}\,Z_{\alpha_{P_i}}$$

7.1.3.4 $Z_{\dot{w}}$

$$Z_{\dot{w}} = (Z_{\dot{w}})_R + (Z_{\dot{w}})_T + (Z_{\dot{w}})_{VT} + (Z_{\dot{w}})_{TR} - \frac{W}{g}$$

where

$$(Z_{\dot{w}})_R = \frac{\partial(Z)_R}{\partial \dot{w}} = \frac{1}{V_0}\,\frac{\partial(Z)_R}{\partial \dot{\alpha}} = \frac{1}{V_0}\,Z_{\alpha_R}\,\frac{\partial \alpha_R}{\partial \dot{\alpha}}$$

$$(Z_{\dot{w}})_T = \frac{\partial(Z)_T}{\partial \dot{w}} = \frac{1}{V_0}\,\frac{\partial(Z)_T}{\partial \dot{\alpha}} = \frac{1}{V_0}\,Z_{\alpha_T}\,\frac{\partial \alpha_T}{\partial \dot{\alpha}}$$

$$(Z_{\dot{w}})_{VT} = \frac{\partial(Z)_{VT}}{\partial \dot{w}} = \frac{1}{V_0}\,\frac{\partial(Z)_{VT}}{\partial \dot{\alpha}} = \frac{1}{V_0}\,Z_{\alpha_{VT}}\,\frac{\partial \alpha_{VT}}{\partial \dot{\alpha}}$$

$$(Z_{\dot{w}})_{TR} = \frac{\partial(Z)_{TR}}{\partial \dot{w}} = \frac{1}{V_0}\,\frac{\partial(Z)_{TR}}{\partial \dot{\alpha}} = \frac{1}{V_0}\,Z_{\alpha_{TR}}\,\frac{\partial \alpha_{TR}}{\partial \dot{\alpha}}$$

7.1.3.5 Z_θ

$$Z_\theta = -W \sin\theta \cos\phi$$

7.1.3.6 $Z_{\dot{\theta}}$

$$Z_{\dot\theta} = (Z_{\dot\theta})_F + (Z_{\dot\theta})_R + (Z_{\dot\theta})_W + (Z_{\dot\theta})_T + (Z_{\dot\theta})_{VT} + (Z_{\dot\theta})_{TR} + \sum_{i=1}^{n} (Z_{\dot\theta})_{P_i} + \frac{W}{g} V_o$$

where

$$(Z_{\dot\theta})_F = \frac{\partial(Z)_F}{\partial\dot\theta} = Z_{u_F}\,\ell_{z_F} - Z_{w_F}\,\ell_{x_F} + \left(\frac{\partial Z}{\partial a_1}\right)_F \frac{\partial a_{1_F}}{\partial q} + \left(\frac{\partial Z}{\partial b_1}\right)_F \frac{\partial b_{1_F}}{\partial q}$$

$$\left(\frac{\partial Z}{\partial a_1}\right)_F = -\left[\frac{\partial D_F}{\partial a_{1_F}}\sin(\alpha-\epsilon_F) + \left(\frac{\partial L_F}{\partial a_{1_F}}\cos A_{1_F} - \frac{\partial Y_F}{\partial a_{1_F}}\sin A_{1_F}\right)\cos(\alpha-\epsilon_F)\right]$$

$$\left(\frac{\partial Z}{\partial b_1}\right)_F = -\left[\frac{\partial D_F}{\partial b_{1_F}}\sin(\alpha-\epsilon_F) + \left(\frac{\partial L_F}{\partial b_{1_F}}\cos A_{1_F} - \frac{\partial Y_F}{\partial b_{1_F}}\sin A_{1_F}\right)\cos(\alpha-\epsilon_F)\right]$$

$$(Z_{\dot\theta})_R = \frac{\partial(Z)_R}{\partial\dot\theta} = Z_{u_R}\,\ell_{z_R} - Z_{w_R}\,\ell_{x_R} + \left(\frac{\partial Z}{\partial a_1}\right)_R \frac{\partial a_{1_R}}{\partial q} + \left(\frac{\partial Z}{\partial b_1}\right)_R \frac{\partial b_{1_R}}{\partial q}$$

$$\left(\frac{\partial Z}{\partial a_1}\right)_R = -\left[\frac{\partial D_R}{\partial a_{1_R}}\sin(\alpha-\epsilon_R) + \left(\frac{\partial L_R}{\partial a_{1_R}}\cos A_{1_R} + \frac{\partial Y_R}{\partial a_{1_R}}\sin A_{1_R}\right)\cos(\alpha-\epsilon_R)\right]$$

$$\left(\frac{\partial Z}{\partial b_1}\right)_R = -\left[\frac{\partial D_R}{\partial b_{1_R}}\sin(\alpha-\epsilon_R) + \left(\frac{\partial L_R}{\partial b_{1_R}}\cos A_{1_R} + \frac{\partial Y_R}{\partial b_{1_R}}\sin A_{1_R}\right)\cos(\alpha-\epsilon_R)\right]$$

$$(Z_{\dot\theta})_W = \frac{\partial(Z)_W}{\partial\dot\theta} = Z_{u_W}\,\ell_{z_W} - Z_{w_W}\,\ell_{x_W}$$

$$(Z_{\dot\theta})_T = \frac{\partial(Z)_T}{\partial\dot\theta} = Z_{u_T}\,\ell_{z_T} - Z_{w_T}\,\ell_{x_T}$$

$$(Z_{\dot\theta})_{VT} = \frac{\partial(Z)_{VT}}{\partial\dot\theta} = Z_{u_{VT}}\,\ell_{z_{VT}} - Z_{w_{VT}}\,\ell_{x_{VT}}$$

$$(Z_{\dot\theta})_{TR} = \frac{\partial(Z)_{TR}}{\partial\dot\theta} = Z_{u_{TR}}\,\ell_{z_{TR}} - Z_{w_{TR}}\,\ell_{x_{TR}}$$

$$(Z_{\dot\theta})_{P_i} = \frac{\partial(Z)_{P_i}}{\partial\dot\theta} = Z_{u_{P_i}}\,\ell_{z_{P_i}} - Z_{w_{P_i}}\,\ell_{x_{P_i}}$$

7.1.3.7 $Z_{\dot\phi}$

$$Z_{\dot\phi} = (Z_{\dot\phi})_F + (Z_{\dot\phi})_R + (Z_{\dot\phi})_W + (Z_{\dot\phi})_T + (Z_{\dot\phi})_{VT} + (Z_{\dot\phi})_{TR} + \sum_{i=1}^{n} (Z_{\dot\phi})_{P_i}$$

where

$$(Z_{\dot\phi})_F = \frac{\partial (Z)_F}{\partial \dot\phi} = Z_{w_F}\, \ell_{Y_F} - Z_{v_F}\, \ell_{Z_F} + \left(\frac{\partial Z}{\partial a_1}\right)_F \frac{\partial a_{1_F}}{\partial p} + \left(\frac{\partial Z}{\partial b_1}\right)_F \frac{\partial b_{1_F}}{\partial p}$$

$$(Z_{\dot\phi})_R = \frac{\partial (Z)_R}{\partial \dot\phi} = Z_{w_R}\, \ell_{Y_R} - Z_{v_R}\, \ell_{Z_R} + \left(\frac{\partial Z}{\partial a_1}\right)_R \frac{\partial a_{1_R}}{\partial p} + \left(\frac{\partial Z}{\partial b_1}\right)_R \frac{\partial b_{1_R}}{\partial p}$$

$$(Z_{\dot\phi})_W = \frac{\partial (Z)_W}{\partial \dot\phi} = Z_{w_W}\, \ell_{Y_W} - Z_{v_W}\, \ell_{Z_W}$$

$$(Z_{\dot\phi})_T = \frac{\partial (Z)_T}{\partial \dot\phi} = Z_{w_T}\, \ell_{Y_T} - Z_{v_T}\, \ell_{Z_T}$$

$$(Z_{\dot\phi})_{VT} = \frac{\partial (Z)_{VT}}{\partial \dot\phi} = Z_{w_{VT}}\, \ell_{Y_{VT}} - Z_{v_{VT}}\, \ell_{Z_{VT}}$$

$$(Z_{\dot\phi})_{TR} = \frac{\partial (Z)_{TR}}{\partial \dot\phi} = Z_{w_{TR}}\, \ell_{Y_{TR}} - Z_{v_{TR}}\, \ell_{Z_{TR}}$$

$$(Z_{\dot\phi})_{P_i} = \frac{\partial (Z)_{P_i}}{\partial \dot\phi} = Z_{w_{P_i}}\, \ell_{Y_{P_i}} - Z_{v_{P_i}}\, \ell_{Z_{P_i}}$$

7.1.3.8 Z_ψ

$$Z_\psi = 0$$

7.1.3.9 $Z_{\dot\psi}$

$$Z_{\dot\psi} = (Z_{\dot\psi})_F + (Z_{\dot\psi})_R + (Z_{\dot\psi})_W + (Z_{\dot\psi})_T + (Z_{\dot\psi})_{VT} + (Z_{\dot\psi})_{TR} + \sum_{i=1}^{n} (Z_{\dot\psi})_{P_i}$$

where

$$(Z_{\dot\psi})_F = \frac{\partial (Z)_F}{\partial \dot\psi} = Z_{v_F}\, \ell_{X_F} - Z_{u_F}\, \ell_{Y_F} + \left(\frac{\partial Z}{\partial a_1}\right)_F \frac{\partial a_{1_F}}{\partial r} + \left(\frac{\partial Z}{\partial b_1}\right)_F \frac{\partial b_{1_F}}{\partial r}$$

$$(Z_{\dot\psi})_R = \frac{\partial (Z)_R}{\partial \dot\psi} = Z_{V_R}\, \ell_{X_R} - Z_{U_R}\, \ell_{Y_R} + \left(\frac{\partial Z}{\partial a_1}\right)_R \frac{\partial a_{1_R}}{\partial r} + \left(\frac{\partial Z}{\partial b_1}\right)_R \frac{\partial b_{1_R}}{\partial r}$$

$$(Z_{\dot\psi})_W = \frac{\partial (Z)_W}{\partial \dot\psi} = Z_{V_W}\, \ell_{X_W} - Z_{U_W}\, \ell_{Y_W}$$

$$(Z_{\dot\psi})_T = \frac{\partial (Z)_T}{\partial \dot\psi} = Z_{V_T}\, \ell_{X_T} - Z_{U_T}\, \ell_{Y_T}$$

$$(Z_{\dot\psi})_{VT} = \frac{\partial (Z)_{VT}}{\partial \dot\psi} = Z_{V_{VT}}\, \ell_{X_{VT}} - Z_{U_{VT}}\, \ell_{Y_{VT}}$$

$$(Z_{\dot\psi})_{TR} = \frac{\partial (Z)_{TR}}{\partial \dot\psi} = Z_{V_{TR}}\, \ell_{X_{TR}} - Z_{U_{TR}}\, \ell_{Y_{TR}}$$

$$(Z_{\dot\psi})_{P_i} = \frac{\partial (Z)_{P_i}}{\partial \dot\psi} = Z_{V_{P_i}}\, \ell_{X_{P_i}} - Z_{U_{P_i}}\, \ell_{Y_{P_i}}$$

7.1.4 The Rolling Moment ($\mathcal{L}$) Derivatives

The rolling moment (about body X-axis) can be written in its abbreviated form as

$$\mathcal{L} = \sum_{i=1}^{n} (\mathcal{L})_i = \sum_{i=1}^{n} \left[(Z)_i\, \ell_{Y_i} - (Y)_i\, \ell_{Z_i} + (\mathcal{L}_0)_i \right] + \mathcal{L}_I$$

where

$(Y)_i$ and $(Z)_i$ are forces in the Y and Z directions of body axes, respectively, due to i^{th} aircraft components, and ℓ_{Y_i} and ℓ_{Z_i} are respective moment arms.

$(\mathcal{L}_0)_i$ is the steady aerodynamic rolling moment about aircraft C.G. due to i^{th} aircraft components, and $\mathcal{L}_I$ is the inertia rolling moment.

7.1.4.1 $\mathcal{L}_u$

$$\mathcal{L}_u = (Z_u)_F \ell_{Y_F} - (Y_u)_F \ell_{Z_F} + (Z_u)_R \ell_{Y_R} - (Y_u)_R \ell_{Z_R}$$

$$+ (Z_u)_W \ell_{Y_W} - (Y_u)_W \ell_{Z_W} + (Z_u)_T \ell_{Y_T} - (Y_u)_T \ell_{Z_T}$$

$$+ (Z_u)_{VT} \ell_{Y_{VT}} - (Y_u)_{VT} \ell_{Z_{VT}} + (Z_u)_{TR} \ell_{Y_{TR}} - (Y_u)_{TR} \ell_{Z_{TR}}$$

$$+ \sum_{i=1}^{n} \left[(Z_u)_{P_i} \ell_{Y_{P_i}} - (Y_u)_{P_i} \ell_{Z_{P_i}} + \frac{\partial Q_{P_i}}{\partial u} \right] + \frac{\partial \mathcal{L}_{FUS}}{\partial u} + \frac{\partial \mathcal{L}_{HUB_F}}{\partial u} - \frac{\partial \mathcal{L}_{HUB_R}}{\partial u}$$

where

$$\frac{\partial \mathcal{L}_{FUS}}{\partial u} = \frac{\partial \mathcal{L}_{FUS}}{\partial u_{FUS}} + \frac{\partial \mathcal{L}_{FUS}}{\partial \alpha_{FUS}} \frac{\partial \alpha_{FUS}}{\partial u}$$

$$\frac{\partial \mathcal{L}_{HUB_F}}{\partial u} = \frac{\partial \mathcal{L}_{HUB_F}}{\partial u_F} + \frac{\partial \mathcal{L}_{HUB_F}}{\partial \alpha_F} \frac{\partial \alpha_F}{\partial u}$$

$$\frac{\partial \mathcal{L}_{HUB_R}}{\partial u} = \frac{\partial \mathcal{L}_{HUB_R}}{\partial u_R} + \frac{\partial \mathcal{L}_{HUB_R}}{\partial \alpha_R} \frac{\partial \alpha_R}{\partial u}$$

7.1.4.2 $\mathcal{L}_v$

$$\mathcal{L}_v = (Z_v)_F \ell_{Y_F} - (Y_v)_F \ell_{Z_F} + (Z_v)_R \ell_{Y_R} - (Y_v)_R \ell_{Z_R}$$

$$+ (Z_v)_W \ell_{Y_W} - (Y_v)_W \ell_{Z_W} + (Z_v)_T \ell_{Y_T} - (Y_v)_T \ell_{Z_T}$$

$$+ (Z_v)_{VT} \ell_{Y_{VT}} - (Y_v)_{VT} \ell_{Z_{VT}} + (Z_v)_{TR} \ell_{Y_{TR}} - (Y_v)_{TR} \ell_{Z_{TR}}$$

$$+ \sum_{i=1}^{n} \left[(Z_v)_{P_i} \ell_{Y_{P_i}} - (Y_v)_{P_i} \ell_{Z_{P_i}} + \frac{1}{V_0} \frac{\partial Q_{P_i}}{\partial \beta_s} \right]$$

$$+\frac{1}{V_0}\left(\frac{\partial \mathcal{L}_{FUS}}{\partial \beta_S}+\frac{\partial \mathcal{L}_{HUB_F}}{\partial \beta_S}-\frac{\partial \mathcal{L}_{HUB_R}}{\partial \beta_S}\right)$$

7.1.4.3 $\mathcal{L}_w$

$$\mathcal{L}_w = (Z_w)_F \ell_{Y_F} - (Y_w)_F \ell_{Z_F} + (Z_w)_R \ell_{Y_R} - (Y_w)_R \ell_{Z_R}$$

$$+ (Z_w)_W \ell_{Y_W} - (Y_w)_W \ell_{Z_W} + (Z_w)_T \ell_{Y_T} - (Y_w)_T \ell_{Z_T}$$

$$+ (Z_w)_{VT} \ell_{Y_{VT}} - (Y_w)_{VT} \ell_{Z_{VT}} + (Z_w)_{TR} \ell_{Y_{TR}} - (Y_w)_{TR} \ell_{Z_{TR}}$$

$$+ \sum_{i=1}^{n}\left[(Z_w)_{P_i} \ell_{Y_{P_i}} - (Y_w)_{P_i} \ell_{Z_{P_i}} + \frac{1}{V_0}\frac{\partial Q_{P_i}}{\partial \alpha}\right]$$

$$+ \frac{1}{V_0}\left[\frac{\partial \mathcal{L}_{FUS}}{\partial \alpha}+\frac{\partial \mathcal{L}_{HUB_F}}{\partial \alpha}-\frac{\partial \mathcal{L}_{HUB_R}}{\partial \alpha}\right]$$

where

$$\frac{\partial \mathcal{L}_{FUS}}{\partial \alpha} = \frac{\partial \mathcal{L}_{FUS}}{\partial \alpha_{FUS}} \frac{\partial \alpha_{FUS}}{\partial \alpha}$$

$$\frac{\partial \mathcal{L}_{HUB_F}}{\partial \alpha} = \frac{\partial \mathcal{L}_{HUB_F}}{\partial \alpha_F} \frac{\partial \alpha_F}{\partial \alpha}$$

$$\frac{\partial \mathcal{L}_{HUB_R}}{\partial \alpha} = \frac{\partial \mathcal{L}_{HUB_R}}{\partial \alpha_R} \frac{\partial \alpha_R}{\partial \alpha}$$

7.1.4.4 $\mathcal{L}_{\dot{w}}$

$$\mathcal{L}_{\dot{w}} = (Z_{\dot{w}})_R \ell_{Y_R} + (Z_{\dot{w}})_T \ell_{Y_T} + (Z_{\dot{w}})_{VT} \ell_{Y_{VT}} + (Z_{\dot{w}})_{TR} \ell_{Y_{TR}}$$

7.1.4.5 $\mathcal{L}_{\dot{\theta}}$

$$\mathcal{L}_{\dot{\theta}} = (Z_{\dot{\theta}})_F \ell_{Y_F} - (Y_{\dot{\theta}})_F \ell_{Z_F} + (Z_{\dot{\theta}})_R \ell_{Y_R} - (Y_{\dot{\theta}})_R \ell_{Z_R}$$

$$+ (Z_{\dot{\theta}})_W \ell_{Y_W} - (Y_{\dot{\theta}})_W \ell_{Z_W} + (Z_{\dot{\theta}})_T \ell_{Y_T} - (Y_{\dot{\theta}})_T \ell_{Z_T}$$

$$+ (Z_{\dot{\theta}})_{VT} \ell_{Y_{VT}} - (Y_{\dot{\theta}})_{VT} \ell_{Z_{VT}} + (Z_{\dot{\theta}})_{TR} \ell_{Y_{TR}} - (Y_{\dot{\theta}})_{TR} \ell_{Z_{TR}}$$

$$+ \sum_{i=1}^{n} \left[(Z_{\dot{\theta}})_{P_i} \ell_{Y_{P_i}} - (Y_{\dot{\theta}})_{P_i} \ell_{Z_{P_i}} + \frac{\partial Q_{P_i}}{\partial q} \right] + \frac{\partial \mathcal{L}_{HUB_F}}{\partial q} - \frac{\partial \mathcal{L}_{HUB_R}}{\partial q}$$

$$+ I_{XZ}\, p + r(I_{YY} - I_{ZZ}) + 2 I_{YZ}\, q$$

where

$$\frac{\partial \mathcal{L}_{HUB_F}}{\partial q} = \frac{\partial \mathcal{L}_{HUB_F}}{\partial u} \ell_{Z_F} - \frac{1}{V_0} \frac{\partial \mathcal{L}_{HUB_F}}{\partial \alpha} \ell_{X_F} + \frac{eb\Omega^2 M_S}{2} \left(\frac{\partial b_{i_F}}{\partial q}\right)$$

$$\frac{\partial \mathcal{L}_{HUB_R}}{\partial q} = \frac{\partial \mathcal{L}_{HUB_R}}{\partial u} \ell_{Z_R} - \frac{1}{V_0} \frac{\partial \mathcal{L}_{HUB_R}}{\partial \alpha} \ell_{X_R} + \frac{eb\Omega^2 M_S}{2} \left(\frac{\partial b_{i_R}}{\partial q}\right)$$

7.1.4.6 $\mathcal{L}_{\ddot{\theta}}$

$$\mathcal{L}_{\ddot{\theta}} = I_{XY}$$

7.1.4.7 $\mathcal{L}_{\dot{\phi}}$

$$\mathcal{L}_{\dot\phi} = (Z_{\dot\phi})_F \ell_{Y_F} - (Y_{\dot\phi})_F \ell_{Z_F} + (Z_{\dot\phi})_R \ell_{Y_R} - (Y_{\dot\phi})_R \ell_{Z_R}$$

$$+ (Z_{\dot\phi})_W \ell_{Y_W} - (Y_{\dot\phi})_W \ell_{Z_W} + (Z_{\dot\phi})_T \ell_{Y_T} - (Y_{\dot\phi})_T \ell_{Z_T}$$

$$+ (Z_{\dot\phi})_{VT} \ell_{Y_{VT}} - (Y_{\dot\phi})_{VT} \ell_{Z_{VT}} + (Z_{\dot\phi})_{TR} \ell_{Y_{TR}} - (Y_{\dot\phi})_{TR} \ell_{Z_{TR}}$$

$$+ \sum_{i=1}^{n} \left[(Z_{\dot\phi})_{P_i} \ell_{Y_{P_i}} - (Y_{\dot\phi})_{P_i} \ell_{Z_{P_i}} + \frac{\partial Q_{P_i}}{\partial p} \right] + \frac{\partial \mathcal{L}_{HUB_F}}{\partial p} - \frac{\partial \mathcal{L}_{HUB_R}}{\partial p}$$

$$+ I_{XZ}\, q - I_{XY}\, r$$

where

$$\frac{\partial \mathcal{L}_{HUB_F}}{\partial p} = \frac{1}{V_O} \left[\frac{\partial \mathcal{L}_{HUB_F}}{\partial \alpha} \ell_{Y_F} - \frac{\partial \mathcal{L}_{HUB_F}}{\partial \beta_S} \ell_{Z_F} \right] + \frac{eb\Omega^2 M_S}{2} \left(\frac{\partial b_{1_F}}{\partial p} \right)$$

$$\frac{\partial \mathcal{L}_{HUB_R}}{\partial p} = \frac{1}{V_O} \left[\frac{\partial \mathcal{L}_{HUB_R}}{\partial \alpha} \ell_{Y_R} - \frac{\partial \mathcal{L}_{HUB_R}}{\partial \beta_S} \ell_{Z_R} \right] + \frac{eb\Omega^2 M_S}{2} \left(\frac{\partial b_{1_R}}{\partial p} \right)$$

7.1.4.8 $\mathcal{L}_{\ddot\phi}$

$$\mathcal{L}_{\ddot\phi} = -I_{xx}$$

7.1.4.9 $\mathcal{L}_{\dot\psi}$

$$\mathcal{L}_{\dot\psi} = (Z_{\dot\psi})_F \ell_{Y_F} - (Y_{\dot\psi})_F \ell_{Z_F} + (Z_{\dot\psi})_R \ell_{Y_R} - (Y_{\dot\psi})_R \ell_{Z_R}$$

$$+ (Z_{\dot\psi})_W \ell_{Y_W} - (Y_{\dot\psi})_W \ell_{Z_W} + (Z_{\dot\psi})_T \ell_{Y_T} - (Y_{\dot\psi})_T \ell_{Z_T}$$

$$+(Z_{\dot{\psi}})_{VT}\ell_{Y_{VT}}-(Y_{\dot{\psi}})_{VT}\ell_{Z_{VT}}+(Z_{\dot{\psi}})_{TR}\ell_{Y_{TR}}-(Y_{\dot{\psi}})_{TR}\ell_{Z_{TR}}$$

$$+\sum_{i=1}^{n}\left[(Z_{\dot{\psi}})_{P_i}\ell_{YP_i}-(Y_{\dot{\psi}})_{P_i}\ell_{ZP_i}+\frac{\partial Q_{P_i}}{\partial r}\right]+\frac{\partial \mathcal{L}_{HUB_F}}{\partial r}-\frac{\partial \mathcal{L}_{HUB_R}}{\partial r}$$

$$+(I_{YY}-I_{ZZ})q-I_{XY}p-2I_{YZ}r$$

where

$$\frac{\partial \mathcal{L}_{HUB_F}}{\partial r}=\frac{1}{V_O}\frac{\partial \mathcal{L}_{HUB_F}}{\partial \beta_S}\ell_{X_F}-\frac{\partial \mathcal{L}_{HUB_F}}{\partial u}\ell_{Y_F}+\frac{eb\Omega^2 M_S}{2}\left(\frac{\partial b_{1_F}}{\partial r}\right)$$

$$\frac{\partial \mathcal{L}_{HUB_R}}{\partial r}=\frac{1}{V_O}\frac{\partial \mathcal{L}_{HUB_R}}{\partial \beta_S}\ell_{X_R}-\frac{\partial \mathcal{L}_{HUB_R}}{\partial u}\ell_{Y_R}+\frac{eb\Omega^2 M_S}{2}\left(\frac{\partial b_{1_R}}{\partial r}\right)$$

7.1.4.10 $\mathcal{L}_{\ddot{\psi}}$

$$\mathcal{L}_{\ddot{\psi}}=I_{XZ}$$

7.1.5 The Pitching Moment (M) Derivatives

The pitching moment (about body Y-axis) can be written in its abbreviated form as

$$M=\sum_{i=1}^{n}(M)_i=\sum_{i=1}^{n}\left[(X)_i\ell_{Z_i}-(Z)_i\ell_{X_i}+(M_o)_i\right]+M_I$$

where

$(X)_i$ and $(Z)_i$ are forces in the X and Z directions of body axes, respectively, due to i^{th} aircraft components, and ℓ_{X_i} and ℓ_{Z_i} are their respective moment arms.

$(M_0)_i$ is the steady aerodynamic pitching moment about aircraft C. G. due to i^{th} aircraft components, and M_I is the inertia pitching moment.

7.1.5.1 M_u

$$M_u = (X_u)_F \ell_{z_F} - (Z_u)_F \ell_{x_F} + (X_u)_R \ell_{z_R} - (Z_u)_R \ell_{x_R}$$

$$+ (X_u)_W \ell_{z_W} - (Z_u)_W \ell_{x_W} + (X_u)_T \ell_{z_T} - (Z_u)_T \ell_{x_T}$$

$$+ (X_u)_{VT} \ell_{z_{VT}} - (Z_u)_{VT} \ell_{x_{VT}} + (X_u)_{TR} \ell_{z_{TR}} - (Z_u)_{TR} \ell_{x_{TR}}$$

$$+ \sum_{i=1}^{n} \left[(X_u)_{P_i} \ell_{z_{P_i}} - (Z_u)_{P_i} \ell_{x_{P_i}} + \frac{\partial M_{P_i}}{\partial u} \right] + \frac{\partial M_{FUS}}{\partial u} + \frac{\partial M_{HUB_F}}{\partial u}$$

$$+ \frac{\partial M_{HUB_R}}{\partial u} + \frac{\partial Q_{TR}}{\partial u}$$

where

$$\frac{\partial M_{FUS}}{\partial u} = \frac{\partial M_{FUS}}{\partial u_{FUS}} + \frac{\partial M_{FUS}}{\partial \alpha_{FUS}} \frac{\partial \alpha_{FUS}}{\partial u}$$

$$\frac{\partial M_{HUB_F}}{\partial u} = \frac{\partial M_{HUB_F}}{\partial u_F} + \frac{\partial M_{HUB_F}}{\partial \alpha_F} \frac{\partial \alpha_F}{\partial u}$$

$$\frac{\partial M_{HUB_R}}{\partial u} = \frac{\partial M_{HUB_R}}{\partial u_R} + \frac{\partial M_{HUB_R}}{\partial \alpha_R} \frac{\partial \alpha_R}{\partial u}$$

$$\frac{\partial Q_{TR}}{\partial u} = \frac{\partial Q_{TR}}{\partial u_{TR}} + \frac{\partial Q_{TR}}{\partial \alpha_{TR}} \frac{\partial \alpha_{TR}}{\partial u}$$

7.1.5.2 M_v

$$M_V = (X_V)_F \ell_{z_F} - (Z_V)_F \ell_{x_F} + (X_V)_R \ell_{z_R} - (Z_V)_R \ell_{x_R}$$

$$+ (X_V)_W \ell_{z_W} - (Z_V)_W \ell_{x_W} + (X_V)_T \ell_{z_T} - (Z_V)_T \ell_{x_T}$$

$$+ (X_V)_{VT} \ell_{z_{VT}} - (Z_V)_{VT} \ell_{x_{VT}} + (X_V)_{TR} \ell_{z_{TR}} - (Z_V)_{TR} \ell_{x_{TR}}$$

$$+ \sum_{i=1}^{n} \left[(X_V)_{P_i} \ell_{z_{P_i}} - (Z_V)_{P_i} \ell_{x_{P_i}} + \frac{1}{V_0} \frac{\partial M_{P_i}}{\partial \beta_s} \right]$$

$$+ \frac{1}{V_0} \left(\frac{\partial M_{FUS}}{\partial \beta_s} + \frac{\partial M_{HUB_F}}{\partial \beta_s} + \frac{\partial M_{HUB_R}}{\partial \beta_s} + \frac{\partial Q_{TR}}{\partial \beta_s} \right)$$

7.1.5.3 M_W

$$M_W = (X_W)_F \ell_{z_F} - (Z_W)_F \ell_{x_F} + (X_W)_R \ell_{z_R} - (Z_W)_R \ell_{x_R}$$

$$+ (X_W)_W \ell_{z_W} - (Z_W)_W \ell_{x_W} + (X_W)_T \ell_{z_T} - (Z_W)_T \ell_{x_T}$$

$$+ (X_W)_{VT} \ell_{z_{VT}} - (Z_W)_{VT} \ell_{x_{VT}} + (X_W)_{TR} \ell_{z_{TR}} - (Z_W)_{TR} \ell_{x_{TR}}$$

$$+ \sum_{i=1}^{n} \left[(X_W)_{P_i} \ell_{z_{P_i}} - (Z_W)_{P_i} \ell_{x_{P_i}} + \frac{1}{V_0} \frac{\partial M_{P_i}}{\partial \alpha} \right]$$

$$+ \frac{1}{V_0} \left(\frac{\partial M_{FUS}}{\partial \alpha} + \frac{\partial M_{HUB_F}}{\partial \alpha} + \frac{\partial M_{HUB_R}}{\partial \alpha} + \frac{\partial Q_{TR}}{\partial \alpha} \right)$$

where

$$\frac{\partial M_{FUS}}{\partial \alpha} = \frac{\partial M_{FUS}}{\partial \alpha_{FUS}} \frac{\partial \alpha_{FUS}}{\partial \alpha}$$

$$\frac{\partial M_{HUB_F}}{\partial \alpha} = \frac{\partial M_{HUB_F}}{\partial \alpha_F} \frac{\partial \alpha_F}{\partial \alpha}$$

$$\frac{\partial M_{HUB_R}}{\partial \alpha} = \frac{\partial M_{HUB_R}}{\partial \alpha_R} \frac{\partial \alpha_R}{\partial \alpha}$$

$$\frac{\partial Q_{TR}}{\partial \alpha} = \frac{\partial Q_{TR}}{\partial \alpha_{TR}} \frac{\partial \alpha_{TR}}{\partial \alpha}$$

7.1.5.4 $M_{\dot{w}}$

$$M_{\dot{w}} = (X_{\dot{w}})_R \ell_{z_R} - (Z_{\dot{w}})_R \ell_{x_R} + (X_{\dot{w}})_T \ell_{z_T} - (Z_{\dot{w}})_T \ell_{x_T}$$

$$+ (X_{\dot{w}})_{VT} \ell_{z_{VT}} - (Z_{\dot{w}})_{VT} \ell_{x_{VT}} + (X_{\dot{w}})_{TR} \ell_{z_{TR}} - (Z_{\dot{w}})_{TR} \ell_{x_{TR}}$$

7.1.5.5 $M_{\dot{\theta}}$

$$M_{\dot{\theta}} = (X_{\dot{\theta}})_F \ell_{z_F} - (Z_{\dot{\theta}})_F \ell_{x_F} + (X_{\dot{\theta}})_R \ell_{z_R} - (Z_{\dot{\theta}})_R \ell_{x_R}$$

$$+ (X_{\dot{\theta}})_W \ell_{z_W} - (Z_{\dot{\theta}})_W \ell_{x_W} + (X_{\dot{\theta}})_T \ell_{z_T} - (Z_{\dot{\theta}})_T \ell_{x_T}$$

$$+ (X_{\dot{\theta}})_{VT} \ell_{z_{VT}} - (Z_{\dot{\theta}})_{VT} \ell_{x_{VT}} + (X_{\dot{\theta}})_{TR} \ell_{z_{TR}} - (Z_{\dot{\theta}})_{TR} \ell_{x_{TR}}$$

$$+ \sum_{i=1}^{n} \left[(X_{\dot{\theta}})_{P_i} \ell_{z_{P_i}} - (Z_{\dot{\theta}})_{P_i} \ell_{x_{P_i}} + \frac{\partial M_{P_i}}{\partial q} \right] + \frac{\partial M_{HUB_F}}{\partial q} + \frac{\partial M_{HUB_R}}{\partial q}$$

$$+ I_{XY} r - I_{YZ} p$$

where

$$\frac{\partial M_{HUB_F}}{\partial q} = \frac{\partial M_{HUB_F}}{\partial u}\ell_{Z_F} - \frac{1}{V_0}\frac{\partial M_{HUB_F}}{\partial \alpha}\ell_{X_F} + \frac{eb\Omega^2 M_S}{2}\left(\frac{\partial a_{1_F}}{\partial q}\right)$$

$$\frac{\partial M_{HUB_R}}{\partial q} = \frac{\partial M_{HUB_R}}{\partial u}\ell_{Z_R} - \frac{1}{V_0}\frac{\partial M_{HUB_R}}{\partial \alpha}\ell_{X_R} + \frac{eb\Omega^2 M_S}{2}\left(\frac{\partial a_{1_R}}{\partial q}\right)$$

7.1.5.6 $M_{\ddot{\theta}}$

$$M_{\ddot{\theta}} = -I_{YY}$$

7.1.5.7 $M_{\dot{\phi}}$

$$\begin{aligned}
M_{\dot{\phi}} = {} & (X_{\dot{\phi}})_F \ell_{Z_F} - (Z_{\dot{\phi}})_F \ell_{X_F} + (X_{\dot{\phi}})_R \ell_{Z_R} - (Z_{\dot{\phi}})_R \ell_{X_R} \\
& + (X_{\dot{\phi}})_W \ell_{Z_W} - (Z_{\dot{\phi}})_W \ell_{X_W} + (X_{\dot{\phi}})_T \ell_{Z_T} - (Z_{\dot{\phi}})_T \ell_{X_T} \\
& + (X_{\dot{\phi}})_{VT} \ell_{Z_{VT}} - (Z_{\dot{\phi}})_{VT} \ell_{X_{VT}} + (X_{\dot{\phi}})_{TR} \ell_{Z_{TR}} - (Z_{\dot{\phi}})_{TR} \ell_{X_{TR}} \\
& + \sum_{i=1}^{n}\left[(X_{\dot{\phi}})_{P_i} \ell_{Z_{P_i}} - (Z_{\dot{\phi}})_{P_i} \ell_{X_{P_i}} + \frac{\partial M_{P_i}}{\partial p}\right] + \frac{\partial M_{HUB_F}}{\partial p} + \frac{\partial M_{HUB_R}}{\partial p} \\
& - 2I_{XZ}p - (I_{XX} - I_{ZZ})r - I_{YZ}\,q
\end{aligned}$$

where

$$\frac{\partial M_{HUB_F}}{\partial p} = \frac{1}{V_0}\left[\frac{\partial M_{HUB_F}}{\partial \alpha}\ell_{Y_F} - \frac{\partial M_{HUB_F}}{\partial \beta_S}\ell_{Z_F}\right] + \frac{eb\Omega^2 M_S}{2}\left(\frac{\partial a_{1_F}}{\partial p}\right)$$

$$\frac{\partial M_{HUB_R}}{\partial p} = \frac{1}{V_0}\left[\frac{\partial M_{HUB_R}}{\partial \alpha}\ell_{Y_R} - \frac{\partial M_{HUB_R}}{\partial \mu_s}\ell_{Z_R}\right] + \frac{eb\Omega^2 M_S}{2}\left(\frac{\partial a_{1_R}}{\partial p}\right)$$

7.1.5.8 $M\ddot{\phi}$

$$M\ddot{\phi} = I_{XY}$$

7.1.5.9 $M\dot{\psi}$

$$\begin{aligned} M\dot{\psi} = {} & (X\dot{\psi})_F \ell_{Z_F} - (Z\dot{\psi})_F \ell_{X_F} + (X\dot{\psi})_R \ell_{Z_R} - (Z\dot{\psi})_R \ell_{X_R} \\ & + (X\dot{\psi})_W \ell_{Z_W} - (Z\dot{\psi})_W \ell_{X_W} + (X\dot{\psi})_T \ell_{Z_T} - (Z\dot{\psi})_T \ell_{X_T} \\ & + (X\dot{\psi})_{VT} \ell_{Z_{VT}} - (Z\dot{\psi})_{VT} \ell_{X_{VT}} + (X\dot{\psi})_{TR} \ell_{Z_{TR}} - (Z\dot{\psi})_{TR} \ell_{X_{TR}} \\ & + \sum_{i=1}^{n}\left[(X\dot{\psi})_{P_i} \ell_{Z_{P_i}} - (Z\dot{\psi})_{P_i} \ell_{X_{P_i}} + \frac{\partial M_{P_i}}{\partial r}\right] + \frac{\partial M_{HUB_F}}{\partial r} + \frac{\partial M_{HUB_R}}{\partial r} \\ & + 2I_{XZ} r - p\,(I_{XX} - I_{ZZ}) + I_{XY} q \end{aligned}$$

where

$$\frac{\partial M_{HUB_F}}{\partial r} = \frac{1}{V_0}\,\frac{\partial M_{HUB_F}}{\partial \beta_S}\ell_{X_F} - \frac{\partial M_{HUB_F}}{\partial u}\ell_{Y_F} + \frac{eb\Omega^2 M_S}{2}\left(\frac{\partial a_{1_F}}{\partial r}\right)$$

$$\frac{\partial M_{HUB_R}}{\partial r} = \frac{1}{V_0}\,\frac{\partial M_{HUB_R}}{\partial \beta_S}\ell_{X_R} - \frac{\partial M_{HUB_R}}{\partial u}\ell_{Y_R} + \frac{eb\Omega^2 M_S}{2}\left(\frac{\partial a_{1_R}}{\partial r}\right)$$

7.1.5.10 $M_{\ddot{\psi}}$

$$M_{\ddot{\psi}} = I_{YZ}$$

7.1.6 The Yawing Moment (N) Derivatives

The yawing moment (about body Z-axis) can be written in its abbreviated form as

$$N = \sum_{i=1}^{n} (N)_i = \sum_{i=1}^{n} \left[(Y)_i \ell_{X_i} - (X)_i \ell_{Y_i} + (N_o)_i \right] + N_I$$

where

$(X)_i$ and $(Y)_i$ are forces in the X and Y directions of body axes, respectively, due to i^{th} aircraft components, and ℓ_{X_i} and ℓ_{Y_i} are their respective moment arms.

$(N_o)_i$ is the steady aerodynamic yawing moment about aircraft C.G. due to i^{th} aircraft components, and N_I is the inertia yawing moment.

7.1.6.1 N_u

$$N_u = (Y_u)_F \ell_{X_F} - (X_u)_F \ell_{Y_F} + (Y_u)_R \ell_{X_R} - (X_u)_R \ell_{Y_R}$$

$$+ (Y_u)_W \ell_{X_W} - (X_u)_W \ell_{Y_W} + (Y_u)_T \ell_{X_T} - (X_u)_T \ell_{Y_T}$$

$$+ (Y_u)_{VT} \ell_{X_{VT}} - (X_u)_{VT} \ell_{Y_{VT}} + (Y_u)_{TR} \ell_{X_{TR}} - (X_u)_{TR} \ell_{Y_{TR}}$$

$$+ \sum_{i=1}^{n} \left[(Y_u)_{P_i} \ell_{X_{P_i}} - (X_u)_{P_i} \ell_{Y_{P_i}} \right] + \frac{\partial N_{FUS}}{\partial u} + \frac{\partial Q_F}{\partial u} - \frac{\partial Q_R}{\partial u}$$

where

$$\frac{\partial N_{FUS}}{\partial u} = \frac{\partial N_{FUS}}{\partial u_{FUS}} + \frac{\partial N_{FUS}}{\partial \alpha_{FUS}} \frac{\partial \alpha_{FUS}}{\partial u}$$

$$\frac{\partial Q_F}{\partial u} = \frac{\partial Q_F}{\partial u_F} + \frac{\partial Q_F}{\partial \alpha_F} \frac{\partial \alpha_F}{\partial u}$$

$$\frac{\partial Q_R}{\partial u} = \frac{\partial Q_R}{\partial u_R} + \frac{\partial Q_R}{\partial \alpha_R} \frac{\partial \alpha_R}{\partial u}$$

<u>7.1.6.2 N_V</u>

$$\begin{aligned} N_V = {} & (Y_V)_F \ell_{X_F} - (X_V)_F \ell_{Y_F} + (Y_V)_R \ell_{X_R} - (X_V)_R \ell_{Y_R} \\ & + (Y_V)_W \ell_{X_W} - (X_V)_W \ell_{Y_W} + (Y_V)_T \ell_{X_T} - (X_V)_T \ell_{Y_T} \\ & + (Y_V)_{VT} \ell_{X_{VT}} - (X_V)_{VT} \ell_{Y_{VT}} + (Y_V)_{TR} \ell_{X_{TR}} - (X_V)_{TR} \ell_{Y_{TR}} \\ & + \sum_{i=1}^{n} \left[(Y_V)_{P_i} \ell_{X_{P_i}} - (X_V)_{P_i} \ell_{Y_{P_i}} \right] + \frac{1}{V_0} \left(\frac{\partial N_{FUS}}{\partial \beta_S} + \frac{\partial Q_F}{\partial \beta_S} - \frac{\partial Q_R}{\partial \beta_S} \right) \end{aligned}$$

<u>7.1.6.3 N_W</u>

$$\begin{aligned} N_W = {} & (Y_W)_F \ell_{X_F} - (X_W)_F \ell_{Y_F} + (Y_W)_R \ell_{X_R} - (X_W)_R \ell_{Y_R} \\ & + (Y_W)_W \ell_{X_W} - (X_W)_W \ell_{Y_W} + (Y_W)_T \ell_{X_T} - (X_W)_T \ell_{Y_T} \end{aligned}$$

$$+(Y_{\dot{w}})_{VT}\ell_{X_{VT}}-(X_{\dot{w}})_{VT}\ell_{Y_{VT}}+(Y_{\dot{w}})_{TR}\ell_{X_{TR}}-(X_{\dot{w}})_{TR}\ell_{Y_{TR}}$$

$$+\sum_{i=1}^{n}\left[(Y_{\dot{w}})_{P_i}\ell_{X_{P_i}}-(X_{\dot{w}})_{P_i}\ell_{Y_{P_i}}\right]+\frac{1}{V_0}\left(\frac{\partial N_{FUS}}{\partial\alpha}+\frac{\partial Q_F}{\partial\alpha}-\frac{\partial Q_R}{\partial\alpha}\right)$$

where

$$\frac{\partial N_{FUS}}{\partial\alpha}=\frac{\partial N_{FUS}}{\partial\alpha_{FUS}}\;\frac{\partial\alpha_{FUS}}{\partial\alpha}$$

$$\frac{\partial Q_F}{\partial\alpha}=\frac{\partial Q_F}{\partial\alpha_F}\;\frac{\partial\alpha_F}{\partial\alpha}$$

$$\frac{\partial Q_R}{\partial\alpha}=\frac{\partial Q_R}{\partial\alpha_R}\;\frac{\partial\alpha_R}{\partial\alpha}$$

7.1.6.4 $N_{\dot{w}}$

$$N_{\dot{w}}=-(X_{\dot{w}})_R\ell_{Y_R}-(X_{\dot{w}})_T\ell_{Y_T}-(X_{\dot{w}})_{VT}\ell_{Y_{VT}}-(X_{\dot{w}})_{TR}\ell_{Y_{TR}}$$

7.1.6.5 $N_{\dot{\theta}}$

$$N_{\dot{\theta}}=(Y_{\dot{\theta}})_F\ell_{X_F}-(X_{\dot{\theta}})_F\ell_{Y_F}+(Y_{\dot{\theta}})_R\ell_{X_R}-(X_{\dot{\theta}})_R\ell_{Y_R}$$

$$+(Y_{\dot{\theta}})_W\ell_{X_W}-(X_{\dot{\theta}})_W\ell_{Y_W}+(Y_{\dot{\theta}})_T\ell_{X_T}-(X_{\dot{\theta}})_T\ell_{Y_T}$$

$$+(Y_{\dot{\theta}})_{VT}\ell_{X_{VT}}-(X_{\dot{\theta}})_{VT}\ell_{Y_{VT}}+(Y_{\dot{\theta}})_{TR}\ell_{X_{TR}}-(X_{\dot{\theta}})_{TR}\ell_{Y_{TR}}$$

$$+\sum_{i=1}^{n}\left[(Y_{\dot\theta})_{P_i}\ell_{X_{P_i}}-(X_{\dot\theta})_{P_i}\ell_{Y_{P_i}}\right]+\frac{\partial Q_F}{\partial q}-\frac{\partial Q_R}{\partial q}$$

$$-I_{XZ}\,r-p\,(I_{YY}-I_{XX})-2I_{XY}\,q$$

where

$$\frac{\partial Q_F}{\partial q}=\frac{\partial Q_F}{\partial u}\ell_{Z_F}-\frac{1}{V_0}\frac{\partial Q_F}{\partial \alpha}\ell_{X_F}+\left(\frac{\partial Q_F}{\partial a_{1_F}}\right)\left(\frac{\partial a_{1_F}}{\partial q}\right)+\left(\frac{\partial Q_F}{\partial b_{1_F}}\right)\left(\frac{\partial b_{1_F}}{\partial q}\right)$$

$$\frac{\partial Q_R}{\partial q}=\frac{\partial Q_R}{\partial u}\ell_{Z_R}-\frac{1}{V_0}\frac{\partial Q_R}{\partial \alpha}\ell_{X_R}+\left(\frac{\partial Q_R}{\partial a_{1_R}}\right)\left(\frac{\partial a_{1_R}}{\partial q}\right)+\left(\frac{\partial Q_R}{\partial b_{1_R}}\right)\left(\frac{\partial b_{1_R}}{\partial q}\right)$$

7.1.6.6 $N_{\ddot\theta}$

$$N_{\ddot\theta}=I_{YZ}$$

7.1.6.7 $N_{\dot\phi}$

$$N_{\dot\phi}=(Y_{\dot\phi})_F\ell_{X_F}-(X_{\dot\phi})_F\ell_{Y_F}+(Y_{\dot\phi})_R\ell_{X_R}-(X_{\dot\phi})_R\ell_{Y_R}$$

$$+(Y_{\dot\phi})_W\ell_{X_W}-(X_{\dot\phi})_W\ell_{Y_W}+(Y_{\dot\phi})_T\ell_{X_T}-(X_{\dot\phi})_T\ell_{Y_T}$$

$$+(Y_{\dot\phi})_{VT}\ell_{X_{VT}}-(X_{\dot\phi})_{VT}\ell_{Y_{VT}}+(Y_{\dot\phi})_{TR}\ell_{X_{TR}}-(X_{\dot\phi})_{TR}\ell_{Y_{TR}}$$

$$+\sum_{i=1}^{n}\left[(Y_{\dot\phi})_{P_i}\ell_{X_{P_i}}-(X_{\dot\phi})_{P_i}\ell_{Y_{P_i}}\right]+\frac{\partial Q_F}{\partial p}-\frac{\partial Q_R}{\partial p}$$

$$-q\,(I_{YY}-I_{XX})+2p\,I_{XY}+I_{YZ}\,r$$

where

$$\frac{\partial Q_F}{\partial p} = \frac{1}{V_0}\left(\frac{\partial Q_F}{\partial \alpha}\ell_{Y_F} - \frac{\partial Q_F}{\partial \beta_S}\ell_{Z_F}\right) + \left(\frac{\partial Q_F}{\partial a_{1_F}}\right)\left(\frac{\partial a_{1_F}}{\partial p}\right) + \left(\frac{\partial Q_F}{\partial b_{1_F}}\right)\left(\frac{\partial b_{1_F}}{\partial p}\right)$$

$$\frac{\partial Q_R}{\partial p} = \frac{1}{V_0}\left(\frac{\partial Q_R}{\partial \alpha}\ell_{Y_R} - \frac{\partial Q_R}{\partial \beta_S}\ell_{Z_R}\right) + \left(\frac{\partial Q_R}{\partial a_{1_R}}\right)\left(\frac{\partial a_{1_R}}{\partial p}\right) + \left(\frac{\partial Q_R}{\partial b_{1_R}}\right)\left(\frac{\partial b_{1_R}}{\partial p}\right)$$

7.1.6.8 $N_{\ddot{\phi}}$

$$N_{\ddot{\phi}} = I'_{XZ}$$

7.1.6.9 $N_{\dot{\psi}}$

$$\begin{aligned} N_{\dot{\psi}} = {} & (Y_{\dot{\psi}})_F \ell_{X_F} - (X_{\dot{\psi}})_F \ell_{Y_F} + (Y_{\dot{\psi}})_R \ell_{X_R} - (X_{\dot{\psi}})_R \ell_{Y_R} \\ & + (Y_{\dot{\psi}})_W \ell_{X_W} - (X_{\dot{\psi}})_W \ell_{Y_W} + (Y_{\dot{\psi}})_T \ell_{X_T} - (X_{\dot{\psi}})_T \ell_{Y_T} \\ & + (Y_{\dot{\psi}})_{VT} \ell_{X_{VT}} - (X_{\dot{\psi}})_{VT} \ell_{Y_{VT}} + (Y_{\dot{\psi}})_{TR} \ell_{X_{TR}} - (X_{\dot{\psi}})_{TR} \ell_{Y_{TR}} \\ & + \sum_{i=1}^{n} \left[(Y_{\dot{\psi}})_{P_i} \ell_{X_{P_i}} - (X_{\dot{\psi}})_{P_i} \ell_{Y_{P_i}} \right] + \frac{\partial Q_F}{\partial r} - \frac{\partial Q_R}{\partial r} \\ & - q I_{XZ} + p I_{YZ} \end{aligned}$$

where

$$\frac{\partial Q_F}{\partial r} = \frac{1}{V_a}\,\frac{\partial Q_F}{\partial \beta_S}\ell_{X_F} - \frac{\partial Q_F}{\partial u}\ell_{Y_F} + \left(\frac{\partial Q_F}{\partial a_{1_F}}\right)\left(\frac{\partial a_{1_F}}{\partial r}\right) + \left(\frac{\partial Q_F}{\partial b_{1_F}}\right)\left(\frac{\partial b_{1_F}}{\partial r}\right)$$

$$\frac{\partial Q_R}{\partial r} = \frac{1}{V_a}\frac{\partial Q_R}{\partial \beta_s}\ell_{X_R} - \frac{\partial Q_R}{\partial u}\ell_{Y_R} + \left(\frac{\partial Q_R}{\partial a_{1_R}}\right)\left(\frac{\partial a_{1_R}}{\partial r}\right) + \left(\frac{\partial Q_R}{\partial b_{1_R}}\right)\left(\frac{\partial b_{1_R}}{\partial r}\right)$$

7.1.6.10 $N_{\ddot{\psi}}$

$$N_{\ddot{\psi}} = -I_{zz}$$

LITERATURE CITED

1. Kisielowski, E., Perlmutter, A. A., and Tang, J., STABILITY AND CONTROL HANDBOOK FOR HELICOPTERS, USAAVLABS Technical Report 67-63, U. S. Army Aviation Material Laboratories, Fort Eustis, Virginia, August 1967, AD 662259.

7.2 CONTROL DERIVATIVES

In response calculations, particularly when stability augmentation devices are used, it is necessary to determine the control derivatives.

For some high-performance compound helicopters, the control system may consist of a mixture of conventional helicopter and fixed-wing aircraft controls. These controls may be automatically or manually switched to operate either in the helicopter or aircraft control modes, or integrated to work together in a coupled system. The mathematical procedures given below for generalized compound helicopter controls can be readily modified to suit any of the above control variations by excluding the nonapplicable control terms.

The generalized compound helicopter controls consist of:

(a) Pilot Longitudinal Cyclic Control (B_{1_C})

The longitudinal control, B_{1_C} , is applied through a forward or aft control stick motion. This control gives rise to a pitch moment about the aircraft center of gravity. For single-rotor helicopters, the stick motion actuates the longitudinal cyclic pitch, B_{1_F} . For tandem-rotor helicopters, this control, which in some cases may also activate the cyclic controls of both rotors (B_{1_F} and B_{1_R}), always applies differential collective pitch. Differential collective pitch is achieved by reducing the collective pitch on one rotor head and increasing it on the other. With fixed-wing aircraft controls, the stick motion actuates the elevator angle, δ_e , or the horizontal tail incidence, i_T .

Mathematically, the longitudinal control of a generalized compound helicopter can be expressed as

$$B_{1_C} = d_1 B_{1_F} + e_1 B_{1_R} - f_1 \Delta\theta_{0_F} + g \, \Delta\theta_{0_R} + h_1 \delta_e + i_1 i_T$$

where d_1 , e_1 , f_1 , g_1 , h_1 , and i_1 are the appropriate linkage ratios between the stick motion and the actual control motion. In the case of single-rotor pure helicopters, the linkage ratios e_1 , f_1 , g_1 , h_1 , and i_1 are zero. For tandem-rotor helicopters, generally $d_1 = e_1$ (or both d_1 and e_1 may be zero for some modern tandem helicopters) and $f_1 = g_1$. Thus, the

longitudinal control for tandem-rotor helicopters without fixed-wing controls becomes

$$B_{1_C} = d_1(B_{1_F} + B_{1_R}) - f_1(\Delta\theta_{0_F} - \Delta\theta_{0_R})$$

For a single-rotor compound helicopter, the linkage ratios e_1, f_1, and g_1 are zero. Thus, the longitudinal control for such an aircraft can be expressed as:

$$B_{1_C} = d_1 B_{1_F} + h_1 \delta_e + i_1 i_T$$

(b) Pilot Lateral Cyclic Control (A_{1_C})

The lateral control is applied through a lateral stick motion (right or left) which activates lateral cyclic pitch control at the front and rear rotor (A_{1_F} and A_{1_R}) in the same direction as the stick motion and/or deflects the ailerons antisymetrically to produce a rolling motion in the same sense as the stick motion.

The lateral control for a generalized compound helicopter can be expressed as:

$$A_{1_C} = d_2 A_{1_F} + e_2 A_{1_R} + f_2 \delta_a$$

where d_2, e_2, and f_2 are the control linkage ratios.

For single-rotor helicopters, $e_2 = f_2 = 0$, and for tandem-rotor helicopters, $d_2 = e_2$ and $f_2 = 0$, thus

$$A_{1_C} = d_2(A_{1_F} + A_{1_R})$$

For a conventional compound helicopter configuration, the lateral control can be expressed as

$$A_{1_C} = d_2 A_{1_F} + f_2 \delta_a$$

(c) Pilot Directional Control (δ_{r_C})

Directional control is applied through a pedal movement. For a tandem-rotor helicopter, the right pedal forward applies the lateral cyclic to the right on the front rotor head (A_{1_F}) and to the left on the rear rotor (A_{1_R}). In the case of a single-rotor helicopter, the right pedal forward increases the thrust of the tail rotor to the left, through a change of tail rotor collective pitch ($\Delta\theta_{0_{TR}}$). With fixed-wing controls, the right pedal forward defects the rudder to the right through an angle δ_e about the rudder hinge.

In general, the directional control can be expressed as:

$$\delta_{r_C} = d_3 A_{1_F} - e_3 A_{1_R} - f_3 \Delta\theta_{0_{TR}} - g_3 \delta_r$$

For a single-rotor configuration, the linkage ratios $d_3 = e_3 = g_3 = 0$. For a tandem-rotor configuration, $f_3 = g_3 = 0$ and $d_3 = e_3$. Hence, for tandem-rotor helicopters,

$$\delta_{r_C} = d_3 (A_{1_F} - A_{1_R})$$

For a single-rotor compound helicopter, $d_3 = e_3 = 0$. Hence, the direction control is given by

$$\delta_{r_C} = - f_3 \Delta\theta_{0_{TR}} - g_3 \delta_r$$

(d) Pilot Vertical Control (θ_C)

Vertical control which is achieved through a change in rotor thrust is applied through a collective pitch lever, which activates the collective pitch of the front and rear rotor in the same direction. In addition, the wing incidence (i_W) can be coupled to the collective control to maintain a more constant rotor-wing loading ratio in order to reduce the problems with rotor speed and roll control in autorotation, caused by high wing loadings. Thus,

$$\theta_C = d_4 \Delta\theta_{0_F} + e_4 \Delta\theta_{0_R} + f_4 i_W$$

For a single-rotor helicopter, the linkage ratios $f_4 = e_4 = 0$, and in the case of a tandem configuration, $d_4 = e_4$ and $f_4 = 0$. Thus

$$\theta_C = d_4 (\Delta\theta_{0_F} + \Delta\theta_{0_R})$$

For a single-rotor compound helicopter, $e_4 = 0$, therefore the vertical control can be expressed as

$$\theta_C = d_4 \Delta\theta_{0_F} + f_4 i_W$$

(e) Stability Augmentation Systems

Stability augmentation systems are used to introduce corrective control inputs automatically into the helicopter control system. These inputs are generally mixed with pilot control inputs. The total control motion can be written as a superposition of inputs from the pilot control and from the stability augmentation system as follows:

Longitudinal Control

$$B_1 = J_1 B_{1_C} + B_{1_S}$$

Lateral Control

$$A_1 = J_2 A_{1_C} + A_{1_S}$$

Directional Control

$$\delta_r = J_3 \delta_{r_C} + \delta_{r_S}$$

Vertical Control

$$\Theta = J_4 \theta_C + \theta_S$$

In the above expressions, J_1 to J_4 are the pilot authority ratios for longitudinal, lateral, directional, and vertical controls, respectively.

7.2.1 The Longitudinal Control (B_{1C}) Derivatives

7.2.1.1 X_{B1C}

$$X_{B_{1_C}} = \frac{\partial X}{\partial B_{1_F}} \frac{\partial B_{1_F}}{\partial B_{1_C}} + \frac{\partial X}{\partial \theta_{0_F}} \frac{\partial \theta_{0_F}}{\partial B_{1_C}} + \frac{\partial X}{\partial B_{1_R}} \frac{\partial B_{1_R}}{\partial B_{1_C}} + \frac{\partial X}{\partial \theta_{0_R}} \frac{\partial \theta_{0_R}}{\partial B_{1_C}} + \frac{\partial X}{\partial \delta_e} \frac{\partial \delta_e}{\partial B_{1_C}} + \frac{\partial X}{\partial i_T} \frac{\partial i_T}{\partial B_{1_C}}$$

$$= \frac{1}{d_1}\left[\frac{\partial X}{\partial B_{1_F}} + \frac{\partial X}{\partial B_{1_R}}\right] - \frac{1}{f_1}\left[\frac{\partial X}{\partial \theta_{0_F}} - \frac{\partial X}{\partial \theta_{0_R}}\right] + \frac{1}{h_1}\left[\frac{\partial X}{\partial \delta_e}\right] + \frac{1}{i_1}\left[\frac{\partial X}{\partial i_T}\right]$$

where

$$\frac{\partial X}{\partial B_{1_F}} = \frac{\partial D_F}{\partial \alpha_F} \cos(\alpha - \epsilon_F) - \left(\frac{\partial L_F}{\partial \alpha_F} \cos A_{1_F} - \frac{\partial Y_F}{\partial \alpha_F} \sin A_{1_F}\right) \sin(\alpha - \epsilon_F)$$

$$\frac{\partial X}{\partial \theta_{0_F}} = -\frac{\partial D_F}{\partial \theta_{0_F}} \cos(\alpha - \epsilon_F) + \left(\frac{\partial L_F}{\partial \theta_{0_F}} \cos A_{1_F} - \frac{\partial Y_F}{\partial \theta_{0_F}} \sin A_{1_F}\right) \sin(\alpha - \epsilon_F)$$

$$\frac{\partial X}{\partial B_{1_R}} = \frac{\partial D_R}{\partial \alpha_R} \cos(\alpha - \epsilon_R) - \left(\frac{\partial L_R}{\partial \alpha_R} \cos A_{1_R} + \frac{\partial Y_R}{\partial \alpha_R} \sin A_{1_R}\right) \sin(\alpha - \epsilon_R)$$

$$\frac{\partial X}{\partial \theta_{0_R}} = -\frac{\partial D_R}{\partial \theta_{0_R}} \cos(\alpha - \epsilon_R) + \left(\frac{\partial L_R}{\partial \theta_{0_R}} \cos A_{1_R} + \frac{\partial Y_R}{\partial \theta_{0_R}} \sin A_{1_R}\right) \sin(\alpha - \epsilon_R)$$

$$\frac{\partial X}{\partial \delta_e} = \frac{\partial L_T}{\partial \delta_e} \sin(\alpha - \epsilon_T) - \frac{\partial D_T}{\partial \delta_e} \cos(\alpha - \epsilon_T)$$

$$\frac{\partial X}{\partial i_T} = (\frac{\partial L_T}{\partial \alpha_T} + D_T) \sin(\alpha - \epsilon_T) + (L_T - \frac{\partial D_T}{\partial \alpha_T}) \cos(\alpha - \epsilon_T)$$

7.2.1.2 $Y_{B_{I_C}}$

$$Y_{B_{I_C}} = \frac{1}{d_I}\left[\frac{\partial Y}{\partial B_{I_F}} + \frac{\partial Y}{\partial B_{I_R}}\right] - \frac{1}{f_I}\left[\frac{\partial Y}{\partial \theta_{0_F}} - \frac{\partial Y}{\partial \theta_{0_R}}\right] + \frac{1}{h_I}\left[\frac{\partial Y}{\partial \delta e}\right] + \frac{1}{i_I}\left[\frac{\partial Y}{\partial i_T}\right]$$

where

$$\frac{\partial Y}{\partial B_{I_F}} = -(\frac{\partial L_F}{\partial \alpha_F} \sin A_{I_F} + \frac{\partial Y_F}{\partial \alpha_F} \cos A_{I_F})$$

$$\frac{\partial Y}{\partial \theta_{0_F}} = \frac{\partial L_F}{\partial \theta_{0_F}} \sin A_{I_F} + \frac{\partial Y_F}{\partial \theta_{0_F}} \cos A_{I_F}$$

$$\frac{\partial Y}{\partial B_{I_R}} = -(\frac{\partial L_R}{\partial \alpha_R} \sin A_{I_R} - \frac{\partial Y_R}{\partial \alpha_R} \cos A_{I_R})$$

$$\frac{\partial Y}{\partial \theta_{0_R}} = \frac{\partial L_R}{\partial \theta_{0_R}} \sin A_{I_R} - \frac{\partial Y_R}{\partial \theta_{0_R}} \cos A_{I_R}$$

$$\frac{\partial Y}{\partial \delta_e} = \frac{\partial Y}{\partial i_T} = 0$$

7.2.1.3 $Z_{B_{I_C}}$

$$Z_{B_{I_C}} = \frac{1}{d_I}\left[\frac{\partial Z}{\partial B_{I_F}} + \frac{\partial Z}{\partial B_{I_R}}\right] - \frac{1}{f_I}\left[\frac{\partial Z}{\partial \theta_{0_F}} - \frac{\partial Z}{\partial \theta_{0_R}}\right] + \frac{1}{h_I}\left[\frac{\partial Z}{\partial \delta e}\right] + \frac{1}{i_I}\left[\frac{\partial Z}{\partial i_T}\right]$$

where

$$\frac{\partial Z}{\partial B_{1_F}} = \frac{\partial D_F}{\partial \alpha_F}\sin(\alpha-\epsilon_F) + \left(\frac{\partial L_F}{\partial \alpha_F}\cos A_{1_F} - \frac{\partial Y_F}{\partial \alpha_F}\sin A_{1_F}\right)\cos(\alpha-\epsilon_F)$$

$$\frac{\partial Z}{\partial \theta_{0_F}} = -\left[\frac{\partial D_F}{\partial \theta_{0_F}}\sin(\alpha-\epsilon_F) + \left(\frac{\partial L_F}{\partial \theta_{0_F}}\cos A_{1_F} - \frac{\partial Y_F}{\partial \theta_{0_F}}\sin A_{1_F}\right)\cos(\alpha-\epsilon_F)\right]$$

$$\frac{\partial Z}{\partial B_{1_R}} = \frac{\partial D_R}{\partial \alpha_R}\sin(\alpha-\epsilon_R) + \left(\frac{\partial L_R}{\partial \alpha_R}\cos A_{1_R} + \frac{\partial Y_R}{\partial \alpha_R}\sin A_{1_R}\right)\cos(\alpha-\epsilon_R)$$

$$\frac{\partial Z}{\partial \theta_{0_R}} = -\left[\frac{\partial D_R}{\partial \theta_{0_R}}\sin(\alpha-\epsilon_R) + \left(\frac{\partial L_R}{\partial \theta_{0_R}}\cos A_{1_R} + \frac{\partial Y_R}{\partial \theta_{0_R}}\sin A_{1_R}\right)\cos(\alpha-\epsilon_R)\right]$$

$$\frac{\partial Z}{\partial \delta_e} = -\left[\frac{\partial D_T}{\partial \delta_e}\sin(\alpha-\epsilon_T) + \frac{\partial L_T}{\partial \delta_e}\cos(\alpha-\epsilon_T)\right]$$

$$\frac{\partial Z}{\partial i_T} = -\left[\left(\frac{\partial D_T}{\partial i_T} - L_T\right)\sin(\alpha-\epsilon_T) + \left(\frac{\partial L_T}{\partial i_T} + D_T\right)\cos(\alpha-\epsilon_T)\right]$$

7.2.1.4 $\mathcal{L}_{B_{1_C}}$

$$\mathcal{L}_{B_{1_C}} = \frac{1}{d_1}\left[\frac{\partial \mathcal{L}}{\partial B_{1_F}} + \frac{\partial \mathcal{L}}{\partial B_{1_R}}\right] - \frac{1}{f_1}\left[\frac{\partial \mathcal{L}}{\partial \theta_{0_F}} - \frac{\partial \mathcal{L}}{\partial \theta_{0_F}}\right] + \frac{1}{h_1}\left[\frac{\partial \mathcal{L}}{\partial \delta_e}\right] + \frac{1}{i_1}\left[\frac{\partial \mathcal{L}}{\partial i_T}\right]$$

where

$$\frac{\partial \mathcal{L}}{\partial B_{1_F}} = \frac{\partial Z}{\partial B_{1_F}}\ell_{Y_F} - \frac{\partial Y}{\partial B_{1_F}}\ell_{Z_F} + \frac{\partial \mathcal{L}_{HUB_F}}{\partial B_{1_F}}$$

$$\frac{\partial \mathcal{L}}{\partial \theta_{0_F}} = \frac{\partial Z}{\partial \theta_{0_F}}\ell_{Y_F} - \frac{\partial Y}{\partial \theta_{0_F}}\ell_{Z_F} \div \frac{\partial \mathcal{L}_{HUB_F}}{\partial \theta_{0_F}}$$

$$\frac{\partial \mathcal{L}}{\partial B_{1_R}} = \frac{\partial Z}{\partial B_{1_R}} \ell_{Y_R} - \frac{\partial Y}{\partial B_{1_R}} \ell_{Z_R} + \frac{\partial \mathcal{L}_{HUB_R}}{\partial B_{1_R}}$$

$$\frac{\partial \mathcal{L}}{\partial \theta_{0_R}} = \frac{\partial Z}{\partial \theta_{0_R}} \ell_{Y_R} - \frac{\partial Y}{\partial \theta_{0_R}} \ell_{Z_R} + \frac{\partial \mathcal{L}_{HUB_R}}{\partial \theta_{0_R}}$$

$$\frac{\partial \mathcal{L}}{\partial \delta_e} = \frac{\partial Z}{\partial \delta_e} \ell_{Y_T}$$

$$\frac{\partial \mathcal{L}}{\partial i_T} = \frac{\partial Z}{\partial i_T} \ell_{Y_T}$$

and

$$\frac{\partial \mathcal{L}_{HUB_F}}{\partial B_{1_F}} = -\left(\frac{eb\Omega^2 M_S}{2}\right)_F \frac{\partial b_{1_F}}{\partial a_F}$$

$$\frac{\partial \mathcal{L}_{HUB_R}}{\partial B_{1_R}} = -\left(\frac{eb\Omega^2 M_S}{2}\right)_R \frac{\partial b_{1_R}}{\partial a_R}$$

7.2.1.5 $M_{B_{1_C}}$

$$M_{B_{1_C}} = \frac{1}{d_1}\left[\frac{\partial M}{\partial B_{1_F}} + \frac{\partial M}{\partial B_{1_R}}\right] - \frac{1}{f_1}\left[\frac{\partial M}{\partial \theta_{0_F}} - \frac{\partial M}{\partial \theta_{0_R}}\right] + \frac{1}{h_1}\left[\frac{\partial M}{\partial \delta_e}\right] + \frac{1}{i_1}\left[\frac{\partial M}{\partial i_T}\right]$$

where

$$\frac{\partial M}{\partial B_{1_F}} = \frac{\partial X}{\partial B_{1_F}} \ell_{Z_F} - \frac{\partial Z}{\partial B_{1_F}} \ell_{X_F} + \frac{\partial M_{HUB_F}}{\partial B_{1_F}}$$

$$\frac{\partial M}{\partial \theta_{0_F}} = \frac{\partial X}{\partial \theta_{0_F}} \ell_{Z_F} - \frac{\partial Z}{\partial \theta_{0_F}} \ell_{X_F} + \frac{\partial M_{HUB_F}}{\partial \theta_{0_F}}$$

$$\frac{\partial M}{\partial B_{1_R}} = \frac{\partial X}{\partial B_{1_R}} \ell_{Z_R} - \frac{\partial Z}{\partial B_{1_R}} \ell_{X_R} + \frac{\partial M_{HUB_R}}{\partial B_{1_R}}$$

$$\frac{\partial M}{\partial \theta_{O_R}} = \frac{\partial X}{\partial \theta_{O_R}} \ell_{Z_R} - \frac{\partial Z}{\partial \theta_{O_R}} \ell_{X_R} + \frac{\partial M_{HUB_R}}{\partial \theta_{O_R}}$$

$$\frac{\partial M}{\partial \delta_e} = \frac{\partial X}{\partial \delta_e} \ell_{Z_T} - \frac{\partial Z}{\partial \delta_e} \ell_{X_T}$$

$$\frac{\partial M}{\partial i_T} = \frac{\partial X}{\partial i_T} \ell_{Z_T} - \frac{\partial Z}{\partial i_T} \ell_{X_T}$$

and

$$\frac{\partial M_{HUB_F}}{\partial B_{1_F}} = \left(\frac{e b \Omega^2 M_S}{2}\right)_F \left(1 - \frac{\partial a_{1_F}}{\partial \alpha_F}\right)$$

$$\frac{\partial M_{HUB_R}}{\partial B_{1_R}} = \left(\frac{e b \Omega^2 M_S}{2}\right)_R \left(1 - \frac{\partial a_{1_R}}{\partial \alpha_R}\right)$$

7.2.1.6 $N_{B_{1_C}}$

$$N_{B_{1_C}} = \frac{1}{d_1}\left(\frac{\partial N}{\partial B_{1_F}} + \frac{\partial N}{\partial B_{1_R}}\right) - \frac{1}{f_1}\left(\frac{\partial N}{\partial \theta_{O_F}} - \frac{\partial N}{\partial \theta_{O_R}}\right) + \frac{1}{h_1}\left[\frac{\partial N}{\partial \delta_e}\right] + \frac{1}{i_1}\left[\frac{\partial N}{\partial i_T}\right]$$

where

$$\frac{\partial N}{\partial B_{1_F}} = \frac{\partial Y}{\partial B_{1_F}} \ell_{X_F} - \frac{\partial X}{\partial B_{1_F}} \ell_{Y_F} + \frac{\partial Q_F}{\partial B_{1_F}}$$

$$\frac{\partial N}{\partial \theta_{O_F}} = \frac{\partial Y}{\partial \theta_{O_F}} \ell_{X_F} - \frac{\partial X}{\partial \theta_{O_F}} \ell_{Y_F} + \frac{\partial Q_F}{\partial \theta_{O_F}}$$

$$\frac{\partial N}{\partial B_{1_R}} = \frac{\partial Y}{\partial B_{1_R}} \ell_{X_R} \quad \frac{\partial X}{\partial B_{1_R}} \ell_{Y_R} - \frac{\partial Q_R}{\partial B_{1_R}}$$

$$\frac{\partial N}{\partial \theta_{0_R}} = \frac{\partial Y}{\partial \theta_{0_R}} \ell_{X_R} - \frac{\partial X}{\partial \theta_{0_R}} \ell_{Y_R} - \frac{\partial Q_R}{\partial \theta_{0_R}}$$

$$\frac{\partial N}{\partial \delta_e} = -\frac{\partial X}{\partial \delta_e} \ell_{Y_T}$$

$$\frac{\partial N}{\partial i_T} = \frac{\partial X}{\partial i_T} \ell_{Y_T}$$

and

$$\frac{\partial Q_F}{\partial B_{1_F}} = -\Big[(T.F.)\,\sigma R\Big]_F \left[\frac{\partial \frac{C_Q}{\sigma}}{\partial \alpha_C}\right]_F$$

$$\frac{\partial Q}{\partial B_{1_R}} = -\Big[(T.F.)\,\sigma R\Big]_R \left[\frac{\partial \frac{C_Q}{\sigma}}{\partial \alpha_C}\right]_R$$

7.2.1.7 Stability Augmentation System (B_{1_S}) Derivatives

All required (B_{1_S}) derivatives for stability augmentation systems are identical to the control derivatives (B_{1_C}) presented above. Thus,

$$X_{B_{1_S}} = X_{B_{1_C}} \qquad \mathcal{L}_{B_{1_S}} = \mathcal{L}_{B_{1_C}}$$

$$Y_{B_{1_S}} = Y_{B_{1_C}} \qquad M_{B_{1_S}} = M_{B_{1_C}}$$

$$Z_{B_{1_S}} = Z_{B_{1_C}} \qquad N_{B_{1_S}} = N_{B_{1_C}}$$

NOTE: In order to obtain the longitudinal control derivative (B_{1_C}) or (B_{1_S}) for a single-rotor helicopter, all derivatives with respect to θ_{0_F}, B_{1_R}, and θ_{0_R} are eliminated.

7.2.1.8 Rate Derivatives ($\dot{B}_{1_C}$ and $\dot{B}_{1_S}$)

The rate derivatives, $\dot{B}_{1_C}$ and $\dot{B}_{1_S}$, are considered to be small and are herein neglected.

7.2.2 The Lateral Control (A_{1_C}) Derivatives

7.2.2.1 $X_{A_{1_C}}$

$$X_{A_{1_C}} = \frac{\partial X}{\partial A_{1_F}} \frac{\partial A_{1_F}}{\partial A_{1_C}} + \frac{\partial X}{\partial A_{1_R}} \frac{\partial A_{1_R}}{\partial A_{1_C}} + \frac{\partial X}{\partial \delta_a} \frac{\partial \delta_a}{\partial A_{1_C}}$$

$$= \frac{1}{d_2} \left(\frac{\partial X}{\partial A_{1_F}} + \frac{\partial X}{\partial A_{1_R}} \right) + \frac{1}{f_2} \frac{\partial X}{\partial \delta_a}$$

where

$$\frac{\partial X}{\partial A_{1_F}} = -(L_F \sin A_{1_F} + Y_F \cos A_{1_F}) \sin(\alpha - \epsilon_F)$$

$$\frac{\partial X}{\partial A_{1_R}} = -(L_R \sin A_{1_R} - Y_R \cos A_{1_R}) \sin(\alpha - \epsilon_R)$$

$$\frac{\partial X}{\partial \delta_a} = \frac{\partial L_W}{\partial \delta_a} \sin(\alpha - \epsilon_W) - \frac{\partial D_W}{\partial \delta_a} \cos(\alpha - \epsilon_W)$$

7.2.2.2 $Y_{A_{1_C}}$

$$Y_{A_{1_C}} = \frac{1}{d_2}\left(\frac{\partial Y}{\partial A_{1_F}} + \frac{\partial Y}{\partial A_{1_R}}\right) + \frac{1}{f_2}\frac{\partial Y}{\partial \delta_a}$$

where

$$\frac{\partial Y}{\partial A_{1_F}} = L_F \cos A_{1_F} - Y_F \sin A_{1_F}$$

$$\frac{\partial Y}{\partial A_{1_R}} = L_R \cos A_{1_R} + Y_R \sin A_{1_R}$$

$$\frac{\partial Y}{\partial \delta_a} = 0$$

7.2.2.3 $Z_{A_{1_C}}$

$$Z_{A_{1_C}} = \frac{1}{d_2}\left(\frac{\partial Z}{\partial A_{1_F}} + \frac{\partial Z}{\partial A_{1_R}}\right) + \frac{1}{f_2}\frac{\partial Z}{\partial \delta_a}$$

where

$$\frac{\partial Z}{\partial A_{1_F}} = (L_F \sin A_{1_F} + Y_F \cos A_{1_F}) \cos(\alpha - \epsilon_F)$$

$$\frac{\partial Z}{\partial A_{1_R}} = (L_R \sin A_{1_R} - Y_R \cos A_{1_R}) \cos(\alpha - \epsilon_R)$$

$$\frac{\partial Z}{\partial \delta_a} = -\left[\frac{\partial D_W}{\partial \delta_a} \sin(\alpha - \epsilon_W) + \frac{\partial L_W}{\partial \delta_a} \cos(\alpha - \epsilon_W)\right]$$

7.2.2.4 $\mathcal{L}_{A_{1_C}}$

$$\mathcal{L}_{A_{1_C}} = \frac{1}{d_2}\left(\frac{\partial \mathcal{L}}{\partial A_{1_F}} + \frac{\partial \mathcal{L}}{\partial A_{1_R}}\right) + \frac{1}{f_2}\frac{\partial \mathcal{L}}{\partial \delta_a}$$

where

$$\frac{\partial \mathcal{L}}{\partial A_{1_F}} = \frac{\partial Z}{\partial A_{1_F}}\ell_{Y_F} - \frac{\partial Y}{\partial A_{1_F}}\ell_{Z_F} + \frac{\partial \mathcal{L}_{HUB_F}}{\partial A_{1_F}}$$

$$\frac{\partial \mathcal{L}}{\partial A_{1_R}} = \frac{\partial Z}{\partial A_{1_R}}\ell_{Y_R} - \frac{\partial Y}{\partial A_{1_R}}\ell_{Z_R} - \frac{\partial \mathcal{L}_{HUB_R}}{\partial A_{1_R}}$$

$$\frac{\partial \mathcal{L}_{HUB_F}}{\partial A_{1_F}} = -\left(\frac{eb\Omega^2 M_S}{2}\right)_F$$

$$\frac{\partial \mathcal{L}_{HUB_R}}{\partial A_{1_R}} = -\left(\frac{eb\Omega^2 M_S}{2}\right)_R$$

$$\frac{\partial \mathcal{L}}{\partial \delta_a} = \frac{\partial Z}{\partial \delta_a}\ell_{Y_W}$$

7.2.2.5 $M_{A_{1_C}}$

$$M_{A_{1_C}} = \frac{1}{d_2}\left(\frac{\partial M}{\partial A_{1_F}} + \frac{\partial M}{\partial A_{1_R}}\right) + \frac{1}{f_2}\frac{\partial M}{\partial \delta_a}$$

where

$$\frac{\partial M}{\partial A_{1_F}} = \frac{\partial X}{\partial A_{1_F}}\ell_{Z_F} - \frac{\partial Z}{\partial A_{1_F}}\ell_{X_F}$$

$$\frac{\partial M}{\partial A_{1_R}} = \frac{\partial X}{\partial A_{1_R}}\ell_{Z_R} - \frac{\partial Z}{\partial A_{1_R}}\ell_{X_R}$$

$$\frac{\partial M}{\partial \delta_a} = \frac{\partial X}{\partial \delta_a} \ell_{Z_W} - \frac{\partial Z}{\partial \delta_a} \ell_{X_W}$$

7.2.2.6 $N_{A_{1C}}$

$$N_{A_{1C}} = \frac{1}{d_2}\left(\frac{\partial N}{\partial A_{1_F}} + \frac{\partial N}{\partial A_{1_R}}\right) + \frac{1}{f_2} \frac{\partial N}{\partial \delta_a}$$

where

$$\frac{\partial N}{\partial A_{1_F}} = \frac{\partial Y}{\partial A_{1_F}} \ell_{X_F} - \frac{\partial X}{\partial A_{1_F}} \ell_{Y_F}$$

$$\frac{\partial N}{\partial A_{1_R}} = \frac{\partial Y}{\partial A_{1_R}} \ell_{X_R} - \frac{\partial X}{\partial A_{1_R}} \ell_{Y_R}$$

$$\frac{\partial N}{\partial \delta_a} = \frac{\partial X}{\partial \delta_a} \ell_{Y_W}$$

7.2.2.7 Stability Augmentation System (A_{1_S}) Derivatives

All required (A_{1_S}) derivatives for stability augmentation systems are identical to the control derivatives (A_{1_C}) presented above. Thus,

$X_{A_{1_S}} = X_{A_{1_C}}$ $\qquad$ $\mathcal{L}_{A_{1_S}} = \mathcal{L}_{A_{1_C}}$

$Y_{A_{1_S}} = Y_{A_{1_C}}$ $\qquad$ $M_{A_{1_S}} = M_{A_{1_C}}$

$Z_{A_{1_S}} = Z_{A_{1_C}}$ $\qquad$ $N_{A_{1_S}} = N_{A_{1_C}}$

NOTE: In order to obtain the lateral control derivatives (A_{1_C}) or (A_{1_S}) for a single-rotor helicopter, all derivatives with respect to A_{1_R} are eliminated.

7.2.2.8 Rate Derivatives $(\dot{A}_{1_C}$ and $\dot{A}_{1_S})$

The rate derivatives $(\dot{A}_{1_C}$ and $\dot{A}_{1_S})$ are considered to be small and are herein neglected.

7.2.3 The Directional Control (δ_{r_C}) Derivatives

7.2.3.1 $X_{\delta_{r_C}}$

$$X_{\delta_{r_C}} = \frac{\partial X}{\partial A_{1_F}} \frac{\partial A_{1_F}}{\partial \delta_{r_C}} + \frac{\partial X}{\partial A_{1_R}} \frac{\partial A_{1_R}}{\partial \delta_{r_C}} + \frac{\partial X}{\partial \theta_{0_{TR}}} \frac{\partial \theta_{0_{TR}}}{\partial \delta_{r_C}} + \frac{\partial X}{\partial \delta_r} \frac{\partial \delta_r}{\partial \delta_{r_C}}$$

$$= \frac{1}{d_3}\left(\frac{\partial X}{\partial A_{1_F}} - \frac{\partial X}{\partial A_{1_R}}\right) - \frac{1}{f_3} \frac{\partial X}{\partial \theta_{0_{TR}}} - \frac{1}{g_3} \frac{\partial X}{\partial \delta_r}$$

where

$$\frac{\partial X}{\partial \theta_{C_{TR}}} = \frac{\partial Y_{TR}}{\partial \theta_{0_{TR}}} \sin(\alpha - \epsilon_{TR}) - \frac{\partial D_{TR}}{\partial \theta_{0_{TR}}} \cos(\alpha - \epsilon_{TR})$$

$$\frac{\partial X}{\partial \delta_r} = \frac{\partial D_{VT}}{\partial \delta_r} \cos(\alpha - \epsilon_{VT})$$

7.2.3.2 $Y_{\delta_{r_c}}$

$$Y_{\delta_{r_c}} = \frac{1}{d_3}\left(\frac{\partial Y}{\partial A_{1_F}} - \frac{\partial Y}{\partial A_{1_R}}\right) - \frac{1}{f_3}\frac{\partial Y}{\partial \theta_{0_{TR}}} - \frac{1}{g_3}\frac{\partial Y}{\partial \delta_r}$$

where

$$\frac{\partial Y}{\partial \theta_{C_{TR}}} = \frac{\partial T_{TR}}{\partial \theta_{0_{TR}}}$$

$$\frac{\partial Y}{\partial \delta_r} = -\frac{\partial L_{VT}}{\partial \delta_r}\cos(\alpha - \epsilon_{VT})$$

7.2.3.3 $Z_{\delta_{r_c}}$

$$Z_{\delta_{r_c}} = \frac{1}{d_3}\left(\frac{\partial Z}{\partial A_{1_F}} - \frac{\partial Z}{\partial A_{1_R}}\right) - \frac{1}{f_3}\frac{\partial Z}{\partial \theta_{0_{TR}}} - \frac{1}{g_3}\frac{\partial Z}{\partial \delta_r}$$

where

$$\frac{\partial Z}{\partial \theta_{0_{TR}}} = -\left[\frac{\partial Y_{TR}}{\partial \theta_{0_{TR}}}\cos(\alpha - \epsilon_{TR}) + \frac{\partial D_{TR}}{\partial \theta_{0_{TR}}}\sin(\alpha - \epsilon_{TR})\right]$$

$$\frac{\partial Z}{\partial \delta_r} = -\frac{\partial D_{VT}}{\partial \delta_r}\sin(\alpha - \epsilon_{VT})$$

7.2.3.4 $\mathcal{L}_{\delta_{r_c}}$

$$\mathcal{L}_{\delta_{r_c}} = \frac{1}{d_3}\left(\frac{\partial \mathcal{L}}{\partial A_{1_F}} - \frac{\partial \mathcal{L}}{\partial A_{1_R}}\right) - \frac{1}{f_3}\frac{\partial \mathcal{L}}{\partial \theta_{0_{TR}}} - \frac{1}{g_3}\frac{\partial \mathcal{L}}{\partial \delta_r}$$

where

$$\frac{\partial \mathcal{L}}{\partial \theta_{0_{TR}}} = \frac{\partial Z}{\partial \theta_{0_{TR}}} \ell_{Y_{TR}} - \frac{\partial Y}{\partial \theta_{0_{TR}}} \ell_{Z_{TR}}$$

$$\frac{\partial \mathcal{L}}{\partial \delta_r} = \frac{\partial Z}{\partial \delta_r} \ell_{Y_{VT}} - \frac{\partial Y}{\partial \delta_r} \ell_{Z_{VT}}$$

7.2.3.5 $M_{\delta_{r_c}}$

$$M_{\delta_{r_c}} = \frac{1}{d_3}\left(\frac{\partial M}{\partial A_{1_F}} - \frac{\partial M}{\partial A_{1_R}}\right) - \frac{1}{f_3} \frac{\partial M}{\partial \theta_{0_{TR}}} - \frac{1}{g_3} \frac{\partial M}{\partial \delta_r}$$

where

$$\frac{\partial M}{\partial \theta_{0_{TR}}} = \frac{\partial X}{\partial \theta_{0_{TR}}} \ell_{Z_{TR}} - \frac{\partial Z}{\partial \theta_{0_{TR}}} \ell_{X_{TR}} + \frac{\partial Q_{TR}}{\partial \theta_{0_{TR}}}$$

$$\frac{\partial M}{\partial \delta_r} = \frac{\partial X}{\partial \delta_r} \ell_{Z_{VT}} - \frac{\partial Z}{\partial \delta_r} \ell_{X_{VT}}$$

7.2.3.6 $N_{\delta_{r_c}}$

$$N_{\delta_{r_c}} = \frac{1}{d_3}\left(\frac{\partial N}{\partial A_{1_F}} - \frac{\partial N}{\partial A_{1_R}}\right) - \frac{1}{f_3} \frac{\partial N}{\partial \theta_{0_{TR}}} - \frac{1}{g_3} \frac{\partial N}{\partial \delta_r}$$

where

$$\frac{\partial N}{\partial \theta_{0_{TR}}} = \frac{\partial Y}{\partial \theta_{0_{TR}}} \ell_{X_{TR}} - \frac{\partial X}{\partial \theta_{0_{TR}}} \ell_{Y_{TR}}$$

$$\frac{\partial N}{\partial \delta_r} = \frac{\partial Y}{\partial \delta_r} \ell_{X_{VT}} - \frac{\partial X}{\partial \delta_r} \ell_{Y_{VT}}$$

7.2.3.7 Stability Augmentation System (δ_{r_s}) Derivatives

All required (δ_{r_s}) derivatives for stability augmentation systems are identical to the control derivatives (δ_{r_c}) presented above. Thus,

$$X_{\delta_{r_s}} = X_{\delta_{r_c}} \qquad \mathcal{L}_{\delta_{r_s}} = \mathcal{L}_{\delta_{r_c}}$$

$$Y_{\delta_{r_s}} = Y_{\delta_{r_c}} \qquad M_{\delta_{r_s}} = M_{\delta_{r_c}}$$

$$Z_{\delta_{r_s}} = Z_{\delta_{r_c}} \qquad N_{\delta_{r_s}} = N_{\delta_{r_c}}$$

NOTE: In order to obtain the directional control derivatives (δ_{r_c}) or (δ_{r_s}) for a tandem-rotor helicopter, eliminate all derivatives with respect to $(\theta_{0_{TR}})$. In the case of a single-rotor helicopter, eliminate all derivatives with respect to (A_{1_R}).

7.2.3.8 Rate Derivatives $(\dot{\delta}_{r_c}$ and $\dot{\delta}_{r_s})$

The rate derivatives $\dot{\delta}_{r_c}$ and $\dot{\delta}_{r_s}$ are considered to be small and are herein neglected.

7.2.4 The Vertical Control (θ_c) Derivatives

7.2.4.1 X_{θ_c}

$$X_{\theta_c} = \frac{\partial X}{\partial \theta_{0_F}} \frac{\partial \theta_{0_F}}{\partial \theta_c} + \frac{\partial X}{\partial \theta_{0_R}} \frac{\partial \theta_{0_R}}{\partial \theta_c} + \frac{\partial X}{\partial i_w} \frac{\partial i_w}{\partial \theta_c}$$

$$= \frac{1}{d_4}\left(\frac{\partial X}{\partial \theta_{0_F}} + \frac{\partial X}{\partial \theta_{0_R}}\right) + \frac{1}{f_4} \frac{\partial X}{\partial i_w}$$

where

$$\frac{\partial X}{\partial \theta_{0_F}} = -\frac{\partial D_F}{\partial \theta_{0_F}} \cos(\alpha - \epsilon_F) + \left(\frac{\partial L_F}{\partial \theta_{0_F}} \cos A_{1_F} - \frac{\partial Y_F}{\partial \theta_{0_F}} \sin A_{1_F}\right) \sin(\alpha - \epsilon_F)$$

$$\frac{\partial X}{\partial \theta_{0_R}} = -\frac{\partial D_R}{\partial \theta_{0_R}} \cos(\alpha - \epsilon_R) + \left(\frac{\partial L_R}{\partial \theta_{0_R}} \cos A_{1_R} + \frac{\partial Y_R}{\partial \theta_{0_R}} \sin A_{1_R}\right) \sin(\alpha - \epsilon_R)$$

$$\frac{\partial X}{\partial i_w} = \left(\frac{\partial L_w}{\partial \alpha_w} + D_w\right) \sin(\alpha - \epsilon_w) + \left(L_w - \frac{\partial D_w}{\partial \alpha_w}\right) \cos(\alpha - \epsilon_w)$$

7.2.4.2 Y_{θ_c}

$$Y_{\theta_c} = \frac{1}{d_4}\left(\frac{\partial Y}{\partial \theta_{0_F}} + \frac{\partial Y}{\partial \theta_{0_R}}\right) + \frac{1}{f_4} \frac{\partial Y}{\partial i_w}$$

where

$$\frac{\partial Y}{\partial \theta_{0_F}} = \frac{\partial L_F}{\partial \theta_{0_F}} \sin A_{1_F} + \frac{\partial Y_F}{\partial \theta_{0_F}} \cos A_{1_F}$$

$$\frac{\partial Y}{\partial \theta_{0_R}} = \frac{\partial L_R}{\partial \theta_{0_R}} \sin A_{I_R} - \frac{\partial Y_R}{\partial \theta_{0_R}} \cos A_{I_R}$$

$$\frac{\partial Y}{\partial i_W} = 0$$

7.2.4.3 Z_{θ_C}

$$Z_{\theta_C} = \frac{1}{d_4}\left(\frac{\partial Z}{\partial \theta_{0_F}} + \frac{\partial Z}{\partial \theta_{0_R}}\right) + \frac{1}{f_4}\frac{\partial Z}{\partial i_W}$$

where

$$\frac{\partial Z}{\partial \theta_{0_F}} = -\left[\frac{\partial D_F}{\partial \theta_{0_F}} \sin(\alpha - \epsilon_F) + \left(\frac{\partial L_F}{\partial \theta_{0_F}} \cos A_{I_F} - \frac{\partial Y_F}{\partial \theta_{0_F}} \sin A_{I_F}\right) \cos(\alpha - \epsilon_F)\right]$$

$$\frac{\partial Z}{\partial \theta_{0_R}} = -\left[\frac{\partial D_R}{\partial \theta_{0_R}} \sin(\alpha - \epsilon_R) + \left(\frac{\partial L_R}{\partial \theta_{0_R}} \cos A_{I_R} + \frac{\partial Y_R}{\partial \theta_{0_R}} \sin A_{I_R}\right) \cos(\alpha - \epsilon_R)\right]$$

$$\frac{\partial Z}{\partial i_W} = -\left[\left(\frac{\partial D_W}{\partial \alpha_W} - L_W\right) \sin(\alpha - \epsilon_W) + \left(D_W + \frac{\partial L_W}{\partial \alpha_W}\right) \cos(\alpha - \epsilon_W)\right]$$

7.2.4.4 $\mathcal{L}_{\theta_C}$

$$\mathcal{L}_{\theta_C} = \frac{1}{d_4}\left(\frac{\partial \mathcal{L}}{\partial \theta_{0_F}} + \frac{\partial \mathcal{L}}{\partial \theta_{0_R}}\right) + \frac{1}{f_4}\frac{\partial \mathcal{L}}{\partial i_W}$$

where

$$\frac{\partial \mathcal{L}}{\partial \theta_{0_F}} = \frac{\partial Z}{\partial \theta_{0_F}} \ell_{Y_F} - \frac{\partial Y}{\partial \theta_{0_F}} \ell_{Z_F} + \frac{\partial \mathcal{L}_{HUB_F}}{\partial \theta_{0_F}}$$

$$\frac{\partial \mathcal{L}}{\partial \theta_{0_R}} = \frac{\partial Z}{\partial \theta_{0_R}} \ell_{Y_R} - \frac{\partial Y}{\partial \theta_{0_R}} \ell_{Z_R} - \frac{\partial \mathcal{L}_{HUB_R}}{\partial \theta_{0_R}}$$

$$\frac{\partial \mathcal{L}}{\partial i_W} = \frac{\partial Z}{\partial i_W} \ell_{Y_W}$$

7.2.4.5 M_{θ_c}

$$M_{\theta_c} = \frac{1}{d_4}\left(\frac{\partial M}{\partial \theta_{0_F}} + \frac{\partial M}{\partial \theta_{0_R}}\right) + \frac{1}{f_4}\frac{\partial M}{\partial i_W}$$

where

$$\frac{\partial M}{\partial \theta_{0_F}} = \frac{\partial X}{\partial \theta_{0_F}} \ell_{Z_F} - \frac{\partial Z}{\partial \theta_{0_F}} \ell_{X_F} + \frac{\partial M_{HUB_F}}{\partial \theta_{0_F}}$$

$$\frac{\partial M}{\partial \theta_{0_R}} = \frac{\partial X}{\partial \theta_{0_R}} \ell_{Z_R} - \frac{\partial Z}{\partial \theta_{0_R}} \ell_{X_R} + \frac{\partial M_{HUB_R}}{\partial \theta_{0_R}}$$

$$\frac{\partial M}{\partial i_W} = \frac{\partial X}{\partial i_W} \ell_{Z_W} - \frac{\partial Z}{\partial i_W} \ell_{X_W}$$

7.2.4.6 N_{θ_c}

$$N_{\theta_c} = \frac{1}{d_4}\left(\frac{\partial N}{\partial \theta_{0_F}} + \frac{\partial N}{\partial \theta_{0_R}}\right) + \frac{1}{f_4}\frac{\partial N}{\partial i_W}$$

where

$$\frac{\partial N}{\partial \theta_{0_F}} = \frac{\partial Y}{\partial \theta_{0_F}} \ell_{X_F} - \frac{\partial X}{\partial \theta_{0_F}} \ell_{Y_F} + \frac{\partial Q_F}{\partial \theta_{0_F}}$$

$$\frac{\partial N}{\partial \theta_{O_R}} = \frac{\partial Y}{\partial \theta_{O_R}} \ell_{X_R} - \frac{\partial X}{\partial \theta_{O_R}} \ell_{Y_R} - \frac{\partial Q_R}{\partial \theta_{O_R}}$$

$$\frac{\partial N}{\partial i_W} = - \frac{\partial X}{\partial i_W} \ell_{Y_W}$$

7.2.4.7 Stability Augmentation System (θ_s) Derivatives

All required (θ_s) derivatives for a stability augmentation system are identical to the vertical control derivatives (θ_c) given above. Thus,

$X_{\theta_s} = X_{\theta_c}$ $\qquad$ $\mathcal{L}_{\theta_s} = \mathcal{L}_{\theta_c}$

$Y_{\theta_s} = Y_{\theta_c}$ $\qquad$ $M_{\theta_s} = M_{\theta_c}$

$Z_{\theta_s} = Z_{\theta_c}$ $\qquad$ $N_{\theta_s} = N_{\theta_c}$

NOTE: In order to obtain vertical control derivatives for a single-rotor helicopter, it is necessary to eliminate all the derivatives with respect to (θ_{O_R})

7.2.4.8 The Rate Derivatives $(\dot{\theta}_c$ and $\dot{\theta}_s)$

The rate derivatives $(\dot{\theta}_c)$ and $(\dot{\theta}_s)$ are considered to be small and are herein neglected.

7.3 LOCAL DERIVATIVES

The local stability derivatives contained in this section are presented as partial differentials of local forces and moments of aerodynamic components with respect to local wind conditions. These derivatives are expressed in a suitable nondimensional form and are obtained for the following aircraft components:

(a) Main Rotor (or Rotors)
(b) Fuselage
(c) Wing
(d) Horizontal and Vertical Tailplanes
(e) Tail Rotor
(f) Propulsion System

7.3.1 Single Rotor (or Front Rotor of a Tandem Rotor Helicopter)

The rotor local stability derivatives must be evaluated at the required rotor solidity (σ). These derivatives are obtained by using the values corresponding to rotor solidity of $\sigma = 0.1$ and by applying the appropriate solidity correction factors presented in Section 7.4. The rotor derivatives for $\sigma = 0.1$ were obtained from the theoretical results of Reference 1 and are presented in the form of nondimensionalized charts in Section 7.5

Some of the rotor derivatives, such a Y-force and coning angle (a_0), for which the numerical data were not available, were determined analytically using the classical rotor theory. Wherever possible, these derivatives are expressed in terms of rotor parameters for which the performance data of Reference 1 could be used.

7.3.1.1 The Longitudinal Speed (u_F) Derivatives

$$\frac{\partial L_F}{\partial u_F} = \left[\frac{(\mathrm{T.F.})\,\sigma}{\Omega R}\right]_F \left[\frac{\partial(\frac{C_L'}{\sigma})}{\partial \mu}\right]_F$$

$$\frac{\partial D_F}{\partial u_F} = \left[\frac{(\mathrm{T.F.})\,\sigma}{\Omega R}\right]_F \left[\frac{\partial(\frac{C_D'}{\sigma})}{\partial \mu}\right]_F$$

$$\frac{\partial Y_F}{\partial u_F} = \left[\frac{(\mathrm{T.F.})\,\sigma}{\Omega R}\right]_F \left[\frac{\partial(\frac{C_Y}{\sigma})}{\partial \mu}\right]_F$$

$$\frac{\partial Q_F}{\partial u_F} = \left[\frac{(\mathrm{T.F.})\,\sigma}{\Omega}\right]_F \left[\frac{\partial(\frac{C_Q}{\sigma})}{\partial \mu}\right]_F$$

$$\frac{\partial a_{1_F}}{\partial u_F} = \left(\frac{1}{\Omega R}\right)_F \left(\frac{\partial a_1}{\partial \mu}\right)_F$$

$$\frac{\partial b_{1_F}}{\partial u_F} = \left(\frac{1}{\Omega R}\right)_F \left(\frac{\partial b_1}{\partial \mu}\right)_F$$

$$\frac{\partial \mathcal{L}_{HUB_F}}{\partial u_F} = \left(\frac{e b \Omega^2 M_s}{2}\right)_F \left(\frac{\partial b_{1_F}}{\partial u_F}\right)$$

$$\frac{\partial M_{HUB_F}}{\partial u_F} = \left(\frac{e b \Omega^2 M_s}{2}\right)_F \left(\frac{\partial a_{1_F}}{\partial u_F}\right)$$

7.3.1.2 The Angle of Attack (α_F) Derivatives

$$\frac{\partial L_F}{\partial \alpha_F} = \left[(\mathrm{T.F.})\,\sigma\right]_F \left[\frac{\partial(\frac{C_L'}{\sigma})}{\partial \alpha_C}\right]_F$$

$$\frac{\partial D_F}{\partial \alpha_F} = \left[(\mathrm{T.F.})\,\sigma\right]_F \left[\frac{\partial(\frac{C_D'}{\sigma})}{\partial \alpha_C}\right]_F$$

$$\frac{\partial Y_F}{\partial \alpha_F} = \left[(\mathrm{T.F.})\,\sigma\right]_F \left[\frac{\partial(\frac{C_Y}{\sigma})}{\partial \alpha_C}\right]_F$$

$$\frac{\partial Q_F}{\partial \alpha_F} = \Big[(T.F.)\,\sigma R\Big]_F \left[\frac{\partial (\frac{C_Q}{\sigma})}{\partial \alpha_C}\right]_F$$

$$\frac{\partial a_{1_F}}{\partial \alpha_F} = \left(\frac{\partial a_1}{\partial \alpha_C}\right)_F$$

$$\frac{\partial b_{1_F}}{\partial \alpha_F} = \left(\frac{\partial b_1}{\partial \alpha_C}\right)_F$$

$$\frac{\partial \mathcal{L}_{HUB_F}}{\partial \alpha_F} = \left(\frac{eb\Omega^2 M_S}{2}\right)_F \left(\frac{\partial b_{1_F}}{\partial \alpha_F}\right)$$

$$\frac{\partial M_{HUB_F}}{\partial \alpha_F} = \left(\frac{eb\Omega^2 M_S}{2}\right)_F \left(\frac{\partial a_{1_F}}{\partial \alpha_F}\right)$$

7.3.1.3 The Side Slip (β_S) Derivatives

$$\frac{\partial a_{1_F}}{\partial \beta_S} = b_{1_F}$$

$$\frac{\partial b_{1_F}}{\partial \beta_S} = -a_{1_F}$$

$$\frac{\partial Q_F}{\partial \beta_S} = \left(\frac{\partial Q_F}{\partial a_{1_F}}\right)\left(\frac{\partial a_{1_F}}{\partial \beta_S}\right) + \left(\frac{\partial Q_F}{\partial b_{1_F}}\right)\left(\frac{\partial b_{1_F}}{\partial \beta_S}\right)$$

$$\frac{\partial \mathcal{L}_{HUB_F}}{\partial \beta_S} = -M_{HUB_F}$$

$$\frac{\partial M_{HUB_F}}{\partial \beta_S} = \mathcal{L}_{HUB_F}$$

7.3.1.4 The Angular Pitching Velocity (q) Derivatives

$$\frac{\partial a_{1_F}}{\partial q} = \left(\frac{\partial a_1}{\partial q}\right)_F = -\left[\frac{34}{\gamma\Omega(1.883-\mu^2)}\right]_F$$

$$\frac{\partial b_{1_F}}{\partial q} = \left(\frac{\partial b_1}{\partial q}\right)_F = -\left[\frac{1.883}{\Omega(1.883+\mu^2)}\right]_F$$

7.3.1.5 The Angular Rolling Velocity (p) Derivatives

$$\frac{\partial a_{1_F}}{\partial p} = \left(\frac{\partial a_1}{\partial p}\right)_F = \left[\frac{1.883}{\Omega(1.883-\mu^2)}\right]_F$$

$$\frac{\partial b_{1_F}}{\partial p} = \left(\frac{\partial b_1}{\partial p}\right)_F = -\left[\frac{34}{\gamma\Omega(1.883+\mu^2)}\right]_F$$

7.3.1.6 The Angular Yawing Velocity (r) Derivatives

$$\frac{\partial a_{1_F}}{\partial r} = \left(\frac{\partial a_1}{\partial r}\right)_F = -\frac{\partial a_{1_F}}{\partial \Omega} = \left(\frac{\partial a_1}{\partial \mu}\right)_F \left(\frac{\mu}{\Omega}\right)_F$$

$$\frac{\partial b_{1_F}}{\partial r} = \left(\frac{\partial b_1}{\partial \mu}\right)_F \left(\frac{\mu}{\Omega}\right)_F$$

7.3.1.7 The Longitudinal Flapping Angle (a_{1_F}) Derivatives

$$\frac{\partial L_F}{\partial a_{1_F}} = -D_F$$

$$\frac{\partial D_F}{\partial a_{1_F}} = L_F$$

$$\frac{\partial Y_F}{\partial a_{1_F}} = 0$$

$$\left[\frac{\partial(\frac{C_Q}{\sigma})}{\partial a_1}\right]_F = -\frac{a}{2}\left[a_1\left(\frac{1}{4}+\frac{3}{8}\mu^2\right)+\frac{1}{2}\mu\lambda\right]_F$$

$$\frac{\partial Q_F}{\partial a_{1_F}} = \left[(T.F.)\sigma R\right]_F \left[\frac{\partial(\frac{C_Q}{\sigma})}{\partial a_1}\right]_F$$

7.3.1.8 The Lateral Flapping Angle (b_{1_F}) Derivatives

$$\frac{\partial L_F}{\partial b_{1_F}} = -Y_F$$

$$\frac{\partial D_F}{\partial b_{1_F}} = 0$$

$$\frac{\partial Y_F}{\partial b_{1_F}} = L_F$$

$$\left[\frac{\partial(\frac{C_Q}{\sigma})}{\partial b_1}\right]_F = -\frac{a}{2}\left[b_1\left(\frac{1}{4}+\frac{1}{8}\mu^2\right)-\frac{1}{3}\mu a_0\right]_F$$

$$\frac{\partial Q_F}{\partial b_{1_F}} = \left[(T.F.)\sigma R\right]_F \left[\frac{\partial(\frac{C_Q}{\sigma})}{\partial b_1}\right]_F$$

7.3.1.9 Rotor Collective Pitch (θ_{0_F}) Derivatives

$$\frac{\partial L_F}{\partial \theta_{0_F}} = \left[(T.F.)\sigma\right]_F \left[\frac{\partial(\frac{C_L'}{\sigma})}{\partial \theta_{.75}}\right]_F$$

$$\frac{\partial D_F}{\partial \theta_{0F}} = \left[(T.F.)\sigma\right]_F \left[\frac{\partial(\frac{C_D'}{\sigma})}{\partial \theta_{.75}}\right]_F$$

$$\frac{\partial Y_F}{\partial \theta_{0F}} = \left[(T.F.)\sigma\right]_F \left[\frac{\partial(\frac{C_Y}{\sigma})}{\partial \theta_{.75}}\right]_F$$

$$\frac{\partial Q_F}{\partial \theta_{0F}} = \left[(T.F.)\sigma R\right]_F \left[\frac{\partial(\frac{C_Q}{\sigma})}{\partial \theta_{.75}}\right]_F$$

$$\frac{\partial \mathcal{L}_{HUB_F}}{\partial \theta_{0F}} = \left(\frac{eb\Omega^2 M_S}{2}\right)_F \left(\frac{\partial b_1}{\partial \theta_{.75}}\right)_F$$

$$\frac{\partial M_{HUB_F}}{\partial \theta_{0F}} = \left(\frac{eb\Omega^2 M_S}{2}\right)_F \left(\frac{\partial a_1}{\partial \theta_{.75}}\right)_F$$

7.3.2 Rear Rotor of a Tandem Rotor Configuration

The local derivatives for the rear rotor of a tandem rotor helicopter can be obtained in exactly the same manner as those for the single rotor presented in Subsection 7.3.1. However, to avoid duplication, the majority of the rear rotor derivatives can be formulated by changing suffix (F) to suffix (R) in the equations of Subsection 7.3.1 with the exception of the following:

$$\frac{\partial b_{1_R}}{\partial q} = \left[\frac{1.883}{\Omega(1.883+\mu^2)}\right]_R$$

$$\frac{\partial b_{1_R}}{\partial p} = \left[\frac{34}{\gamma\Omega(1.883+\mu^2)}\right]_R$$

$$\frac{\partial a_{1_R}}{\partial r} = -\left(\frac{\partial a_1}{\partial \mu}\right)_R \left(\frac{\mu}{\Omega}\right)_R$$

$$\frac{\partial b_{1_R}}{\partial r} = -\left(\frac{\partial b_1}{\partial \mu}\right)_R \left(\frac{\mu}{\Omega}\right)_R$$

$$\frac{\partial a_{1_R}}{\partial \beta_s} = -b_{1_R}$$

$$\frac{\partial b_{1_R}}{\partial \beta_s} = a_{1_R}$$

$$\frac{\partial \mathcal{L}_{HUB_R}}{\partial \beta_s} = M_{HUB_R}$$

$$\frac{\partial M_{HUB_R}}{\partial \beta_s} = -\mathcal{L}_{HUB_R}$$

7.3.3 Fuselage Derivatives

The required local fuselage derivatives are obtained by taking slopes of the appropriate fuselage data. It is recommended that actual test data such as presented in Section 5.3 for various fuselage shapes be used for this purpose.

7.3.3.1 The Forward Speed (u_{FUS}) Derivatives

$$\frac{\partial L_{FUS}}{\partial u_{FUS}} = \frac{2}{V_o} L_{FUS}$$

$$\frac{\partial D_{FUS}}{\partial u_{FUS}} = \frac{2}{V_o} D_{FUS}$$

$$\frac{\partial Y_{FUS}}{\partial u_{FUS}} = \frac{2}{V_o} Y_{FUS}$$

$$\frac{\partial \mathcal{L}_{FUS}}{\partial u_{FUS}} = \frac{2}{V_o} \mathcal{L}_{FUS}$$

$$\frac{\partial M_{FUS}}{\partial u_{FUS}} = \frac{2}{V_o} M_{FUS}$$

$$\frac{\partial N_{FUS}}{\partial u_{FUS}} = \frac{2}{V_o} N_{FUS}$$

7.3.3.2 The Angle of Attack (α_{FUS}) Derivatives

$$\frac{\partial L_{FUS}}{\partial \alpha_{FUS}} = q_o A_{Z_{FUS}} \left(\frac{\partial C_{L_{FUS}}}{\partial \alpha_{FUS}}\right)$$

$$\frac{\partial D_{FUS}}{\partial \alpha_{FUS}} = q_o A_{X_{FUS}} \left(\frac{\partial C_{D_{FUS}}}{\partial \alpha_{FUS}}\right)$$

$$\frac{\partial Y_{FUS}}{\partial \alpha_{FUS}} = q_o A_{Y_{FUS}} \left(\frac{\partial C_{Y_{FUS}}}{\partial \alpha_{FUS}}\right)$$

$$\frac{\partial \mathcal{L}_{FUS}}{\partial \alpha_{FUS}} = q_o A_{X_{FUS}} \ell_{FUS} \left(\frac{\partial C_{\mathcal{L}_{FUS}}}{\partial \alpha_{FUS}}\right)$$

$$\frac{\partial M_{FUS}}{\partial \alpha_{FUS}} = q_o A_{X_{FUS}} \ell_{FUS} \left(\frac{\partial C_{M_{FUS}}}{\partial \alpha_{FUS}}\right)$$

$$\frac{\partial N_{FUS}}{\partial \alpha_{FUS}} = q_o A_{X_{FUS}} \ell_{FUS} \left(\frac{\partial C_{N_{FUS}}}{\partial \alpha_{FUS}}\right)$$

7.3.3.3 The Sideslip Angle (β_S) Derivatives

$$\frac{\partial L_{FUS}}{\partial \beta_S} = q_o A_{Z_{FUS}} \left(\frac{\partial C_{L_{FUS}}}{\partial \beta_S}\right)$$

$$\frac{\partial D_{FUS}}{\partial \beta_S} = q_o A_{X_{FUS}} \left(\frac{\partial C_{D_{FUS}}}{\partial \beta_S}\right)$$

$$\frac{\partial Y_{FUS}}{\partial \beta_S} = q_o A_{Y_{FUS}} \left(\frac{\partial C_{Y_{FUS}}}{\partial \beta_S}\right)$$

$$\frac{\partial \mathcal{L}_{FUS}}{\partial \beta_S} = q_o A_{X_{FUS}} \ell_{FUS} \left(\frac{\partial C_{\mathcal{L}_{FUS}}}{\partial \beta_S}\right)$$

$$\frac{\partial M_{FUS}}{\partial \beta_S} = q_o A_{X_{FUS}} \ell_{FUS} \left(\frac{\partial C_{M_{FUS}}}{\partial \beta_S}\right)$$

$$\frac{\partial N_{FUS}}{\partial \beta_s} = q_o A_{x_{FUS}} \ell_{FUS} \left(\frac{\partial C_{N_{FUS}}}{\partial \beta_s}\right)$$

NOTE: The remaining fuselage derivatives can be neglected

7.3.4 Wing Derivatives

7.3.4.1 The Forward Speed (u_W) Derivatives

$$\frac{\partial L_W}{\partial u_W} = \frac{2}{V_o} L_W$$

$$\frac{\partial D_W}{\partial u_W} = \frac{2}{V_o} D_W$$

For deflected ailerons also calculate:

$$\frac{\partial \mathcal{L}_W}{\partial u_W} = \frac{4}{V_o} C_{\mathcal{L}_{\delta_a}} \delta_a q_o S_W b_W$$

7.3.4.2 The Angle of Attack (α_W) Derivatives

$$\frac{\partial L_W}{\partial \alpha_W} = q_o a_W S_W$$

$$\frac{\partial D_W}{\partial \alpha_W} = \frac{2 L_W}{\pi (AR)_W} a_W$$

The remaining wing derivatives may be neglected. However, if required, the additional wing derivatives can be obtained from Reference 2.

7.3.5 Horizontal Tail Derivatives

The horizontal tailplane derivatives can be obtained in exactly the same way as for the wing by changing suffix (W) to suffix (T).

7.3.6 Vertical Tail (Fin) Derivatives

7.3.6.1 The Forward Speed (u_{VT}) Derivatives

$$\frac{\partial L_{VT}}{\partial u_{VT}} = \frac{2}{V_0} L_{VT}$$

$$\frac{\partial D_{VT}}{\partial u_{VT}} = \frac{2}{V_0} D_{VT}$$

7.3.6.2 The Angle of Attack (α_{VT}) Derivatives

$$\frac{\partial L_{VT}}{\partial \alpha_{VT}} = \frac{\partial D_{VT}}{\partial \alpha_{VT}} = 0$$

7.3.6.3 The Sideslip Angle (β_S) Derivatives

$$\frac{\partial L_{VT}}{\partial \beta_S} = q_0 a_{VT} S_{VT}$$

$$\frac{\partial D_{VT}}{\partial \beta_S} = \frac{2L_{VT}}{\pi (AR)_{VT}} a_{VT}$$

7.3.7 Tail Rotor Derivatives

7.3.7.1 The Forward Speed (u_{TR}) Derivatives

$$\frac{\partial T_{TR}}{\partial u_{TR}} = \left[\frac{(T.F.)\sigma}{\Omega R}\right]_{TR} \left[\frac{\partial (\frac{C_L'}{\sigma})}{\partial \mu}\right]_{TR}$$

$$\frac{\partial D_{TR}}{\partial u_{TR}} = \left[\frac{(T.F.)\sigma}{\Omega R}\right]_{TR} \left[\frac{\partial (\frac{C_D'}{\sigma})}{\partial \mu}\right]_{TR}$$

$$\frac{\partial Y_{TR}}{\partial u_{TR}} = \left[\frac{(T.F.)\sigma}{\Omega R}\right]_{TR} \left[\frac{\partial (\frac{C_Y}{\sigma})}{\partial \mu}\right]_{TR}$$

$$\frac{\partial Q_{TR}}{\partial u_{TR}} = \left[\frac{(T.F.)\sigma}{\Omega}\right]_{TR} \left[\frac{\partial (\frac{C_Q}{\sigma})}{\partial \mu}\right]_{TR}$$

7.3.7.2 The Angle of Attack (α_{TR}) Derivatives

$$\frac{\partial T_{TR}}{\partial \alpha_{TR}} = \frac{\partial D_{TR}}{\partial \alpha_{TR}} = \frac{\partial Y_{TR}}{\partial \alpha_{TR}} = \frac{\partial Q_{TR}}{\partial \alpha_{TR}} = 0$$

7.3.7.3 The Sideslip Angle (β_S) Derivatives

$$\frac{\partial T_{TR}}{\partial \beta_S} = -\left[(T.F.)\sigma\right]_{TR} \left[\frac{\partial (\frac{C_L'}{\sigma})}{\partial \alpha_C}\right]_{TR}$$

$$\frac{\partial D_{TR}}{\partial \beta_s} = -\left[(T.F.)\sigma\right]_{TR}\left[\frac{\partial(\frac{C_D'}{\sigma})}{\partial a_C}\right]_{TR}$$

$$\frac{\partial Y_{TR}}{\partial \beta_s} = -\left[(T.F.)\sigma\right]_{TR}\left[\frac{\partial(\frac{C_Y'}{\sigma})}{\partial a_C}\right]_{TR}$$

$$\frac{\partial Q_{TR}}{\partial \beta_s} = -\left[(T.F.)\sigma R\right]_{TR}\left[\frac{\partial(\frac{C_Q}{\sigma})}{\partial a_C}\right]_{TR}$$

7.3.7.4 The Tail Rotor Collective (θ_{0TR}) Derivatives

$$\frac{\partial T_{TR}}{\partial \theta_{0TR}} = \left[(T.F.)\sigma\right]_{TR}\left[\frac{\partial(\frac{C_L'}{\sigma})}{\partial \theta_{.75}}\right]_{TR}$$

$$\frac{\partial D_{TR}}{\partial \theta_{0TR}} = \left[(T.F.)\sigma\right]_{TR}\left[\frac{\partial(\frac{C_D'}{\sigma})}{\partial \theta_{.75}}\right]_{TR}$$

$$\frac{\partial Y_{TR}}{\partial \theta_{0TR}} = \left[(T.F.)\sigma\right]_{TR}\left[\frac{\partial(\frac{C_Y}{\sigma})}{\partial \theta_{.75}}\right]_{TR}$$

$$\frac{\partial Q_{TR}}{\partial \theta_{0TR}} = \left[(T.F.)\sigma R\right]_{TR}\left[\frac{\partial(\frac{C_Q}{\sigma})}{\partial \theta_{.75}}\right]_{TR}$$

The remaining tail rotor derivatives, if any, can be neglected.

7.3.8 Auxiliary Propulsion Derivatives

7.3.8.1 Propeller Derivatives

The required propeller derivatives are evaluated by obtaining appropriate slopes from the performance data presented in References 1 through 14 of Section 5.7. or from specific test data.

7.3.8.1.1 The Longitudinal Speed (u_P) Derivatives

$$\frac{\partial T_{P_i}}{\partial u_{P_i}} = \left[\rho n D^3 \left(\frac{\partial C_T}{\partial J}\right)\right]_{P_i}$$

$$\frac{\partial N_{P_i}}{\partial u_{P_i}} = \left[\rho n D^3 \left(\frac{\partial C_N}{\partial J}\right)\right]_{P_i}$$

$$\frac{\partial Y_{P_i}}{\partial u_{P_i}} = \left[\rho n D^3 \left(\frac{\partial C_S}{\partial J}\right)\right]_{P_i}$$

$$\frac{\partial Q_{P_i}}{\partial u_{P_i}} = \left[2\pi \rho n D^4 \left(\frac{\partial C_P}{\partial J}\right)\right]_{P_i}$$

$$\frac{\partial M_{P_i}}{\partial u_{P_i}} = \left[\rho n D^4 \left(\frac{\partial C_M}{\partial J}\right)\right]_{P_i}$$

7.3.8.1.2 The Angle of Attack (α_P) Derivatives

$$\frac{\partial T_{P_i}}{\partial \alpha_{P_i}} = \left[\rho n D^4 \left(\frac{\partial C_T}{\partial \alpha}\right)\right]_{P_i}$$

$$\frac{\partial N_{P_i}}{\partial \alpha_{P_i}} = \left[\rho n D^4 \left(\frac{\partial C_N}{\partial \alpha}\right)\right]_{P_i}$$

$$\frac{\partial Y_{P_i}}{\partial \alpha_{P_i}} = 0$$

$$\frac{\partial Q_{P_i}}{\partial \alpha_{P_i}} = \left[2\pi \rho n D^5 \left(\frac{\partial C_P}{\partial \alpha}\right)\right]_{P_i}$$

$$\frac{\partial M_{P_i}}{\partial \alpha_{P_i}} = \left[\rho n D^5 \left(\frac{\partial C_M}{\partial \alpha}\right)\right]_{P_i}$$

7.3.8.1.3 The Sideslip (β_S) Derivatives

$$\frac{\partial T_{P_i}}{\partial \beta_S} = \left[\rho n^2 D^4 \left(\frac{\partial C_T}{\partial \beta_S}\right)\right]_{P_i}$$

$$\frac{\partial N_{P_i}}{\partial \beta_S} = 0$$

$$\frac{\partial Y_{P_i}}{\partial \beta_S} = \left[\rho n^2 D^4 \left(\frac{\partial C_S}{\partial \beta_S}\right)\right]_{P_i}$$

$$\frac{\partial Q_{P_i}}{\partial \beta_S} = \left[2\pi \rho n^2 D^5 \left(\frac{\partial C_P}{\partial \beta_S}\right)\right]_{P_i}$$

$$\frac{\partial M_{P_i}}{\partial \beta_S} = \left[\rho n^2 D^5 \left(\frac{\partial C_M}{\partial \beta_S}\right)\right]_{P_i}$$

7.3.8.1.4 The Angular Pitching Velocity (q) Derivatives

$$\frac{\partial M_{P_i}}{\partial q} = -\frac{\partial M_{P_i}}{\partial u_{P_i}} Z_{P_i} - \frac{\partial M_{P_i}}{\partial \alpha_{P_i}} \frac{X_{P_i}}{V_0}$$

7.3.8.1.5 The Angular Rolling Velocity (p) Derivatives

$$\frac{\partial Q_{P_i}}{\partial p} = \frac{Z_{P_i}}{V_0}\left(\frac{\partial Q_{P_i}}{\partial \alpha_{P_i}}\right)$$

7.3.8.1.6 The Angular Yawing Velocity (r) Derivatives

$$\frac{\partial Q_{P_i}}{\partial r} = -Y_{P_i}\left(\frac{\partial Q_{P_i}}{\partial u_{P_i}}\right)$$

The remaining propeller derivatives can be neglected.

7.3.8.2 Ducted Propeller Derivatives

The required ducted propeller derivatives are evaluated in a similar manner to the propeller derivatives above by using appropriate performance data cited in Section 5.7.2.

7.3.8.3 Jet Engine Derivatives

7.3.8.3.1 The Longitudinal Speed (u_P) Derivatives

The jet engine derivative $(\partial T/\partial u_{P_i})$ can be obtained graphically from the performance data presented in Figure 1 of Section 5.7.3.

$$\frac{\partial N_{P_i}}{\partial u_{P_i}} = \frac{2 q_0 A_i}{V_0}\left[2 \sin \alpha_{P_i} - K_{FP_i}\left(\frac{\lambda}{\mu} - \frac{\partial \lambda}{\partial \mu}\right)_F \cos \alpha_{P_i}\right]$$

7.3.8.3.2 The Angle of Attack (α_P) Derivatives

$$\frac{\partial T_{P_i}}{\partial \alpha_{P_i}} = 0$$

$$\frac{\partial N_{P_i}}{\partial \alpha_{P_i}} = 57.3\, A_{i_i}\left(\frac{\partial (N/A_{i_i})}{\partial \alpha}\right)_{P_i}$$

The jet engine derivative $(\partial(N/A_{i_i})/\partial\alpha)_{P_i}$ can be obtained graphically from the performance data presented in Figure 2 of Section 5.7.3.

LITERATURE CITED

1. Tanner, W. H., CHARTS FOR ESTIMATING ROTARY WING PERFORMANCE IN HOVER AND AT HIGH FOFWARD SPEEDS, United Aircraft Corporation, NASA Contractor Report CR-114, National Aeronautics and Space Administration, Washington, D. C., November 1964.

2. Ellison, D. E., and Malthan, L. V., USAF STABILITY AND CONTROL DATCOM, McDonnell Douglas Corporation, Douglas Aircraft Division, Flight Control Division, Air Force Flight Dynamics Laboratory, Wright-Patterson Air Force Base, Ohio, October 1960 (Revised to June 1969).

7.4 CORRECTIONS OF ISOLATED ROTOR DERIVATIVES FOR VARIATION OF ROTOR SOLIDITY (σ)

The isolated rotor stability derivatives presented as charts in Section 7.5 apply only for a rotor solidity of $\sigma = 0.1$. In order to evaluate the required stability derivatives for rotors having solidity $\sigma \neq 0.1$, the following solidity corrections must be applied:

7.4.1 Solidity Corrections for (μ) Derivatives

$$\frac{\partial(\frac{C_L'}{\sigma})}{\partial\mu} = K_1 \left\{ \left[\frac{\partial(\frac{C_L'}{\sigma})}{\partial\mu}\right]_{0.1} + \frac{\Delta\sigma}{\mu^3}\left(\frac{C_L'}{\sigma}\right)\left[\frac{\partial(\frac{C_L'}{\sigma})}{\partial\alpha_C}\right]_{0.1} \right\}$$

where

$$\Delta\sigma = \sigma - 0.1$$

$$K_1 = \frac{1}{1 + \frac{\Delta\sigma}{2\mu^2}\left[\frac{\partial(\frac{C_L'}{\sigma})}{\partial\alpha_C}\right]_{0.1}}$$

$(\ )_{0.1}$ - denotes stability derivatives for rotor solidity $\sigma = 0.1$. These values can be directly obtained from the charts of Section 7.5.

$$\frac{\partial(\frac{C_D'}{\sigma})}{\partial\mu} = \left[\frac{\partial(\frac{C_D'}{\sigma})}{\partial\mu}\right]_{0.1} + K_2\left[\frac{\partial(\frac{C_D'}{\sigma})}{\partial\alpha_C}\right]_{0.1} - \left(\frac{C_L'}{\sigma}\right)\left\{K_2 - \frac{\Delta\sigma}{2\mu^2}\left[\frac{\partial(\frac{C_L'}{\sigma})}{\partial\mu}\right]\right\}$$

where

$$K_2 = \frac{\Delta\sigma}{2\mu^2}\left[\frac{2}{\mu}\left(\frac{C_L'}{\sigma}\right) - \frac{\partial(\frac{C_L'}{\sigma})}{\partial\mu}\right]$$

$$\frac{\partial(\frac{C_Q}{\sigma})}{\partial\mu} = \left[\frac{\partial(\frac{C_Q}{\sigma})}{\partial\mu}\right]_{0.1} + K_2\left[\frac{\partial(\frac{C_Q}{\sigma})}{\partial\alpha_C}\right]_{0.1}$$

$$\frac{\partial a_1}{\partial \mu} = \left(\frac{\partial a_1}{\partial \mu}\right)_{0.1} + K_2\left(\frac{\partial a_1}{\partial \alpha_c}\right)_{0.1}$$

$$\frac{\partial b_1}{\partial \mu} = \left(\frac{\partial b_1}{\partial \mu}\right)_{0.1} + K_2\left(\frac{\partial b_1}{\partial \alpha_c}\right)_{0.1}$$

$$\frac{\partial \lambda}{\partial \mu} = \left(\frac{\partial \lambda}{\partial \mu}\right)_{0.1} + K_2\left(\frac{\partial \lambda}{\partial \alpha_c}\right)_{0.1}$$

7.4.2 Solidity Corrections for (α_c) Derivatives

$$\frac{\partial\left(\frac{C_L'}{\sigma}\right)}{\partial \alpha_c} = K_1\left[\frac{\partial\left(\frac{C_L'}{\sigma}\right)}{\partial \alpha_c}\right]_{0.1}$$

$$\frac{\partial\left(\frac{C_D'}{\sigma}\right)}{\partial \alpha_c} = K_1\left\{\left[\frac{\partial\left(\frac{C_D'}{\sigma}\right)}{\partial \alpha_c}\right]_{0.1} - \frac{\Delta\sigma}{\mu^2}\left(\frac{C_L'}{\sigma}\right)\left[\frac{\partial\left(\frac{C_L'}{\sigma}\right)}{\partial \alpha_c}\right]_{0.1}\right\}$$

$$\frac{\partial\left(\frac{C_Q}{\sigma}\right)}{\partial \alpha_c} = K_1\left[\frac{\partial\left(\frac{C_Q}{\sigma}\right)}{\partial \alpha_c}\right]_{0.1}$$

$$\frac{\partial a_1}{\partial \alpha_c} = K_1\left(\frac{\partial a_1}{\partial \alpha_c}\right)_{0.1}$$

$$\frac{\partial b_1}{\partial \alpha_c} = K_1\left(\frac{\partial b_1}{\partial \alpha_c}\right)_{0.1}$$

$$\frac{\partial \lambda}{\partial \alpha_c} = K_1\left(\frac{\partial \lambda}{\partial \alpha_c}\right)_{0.1}$$

7.4.3 Solidity Corrections for $(\theta_{.75})$ Derivatives

$$\frac{\partial\left(\frac{C_L'}{\sigma}\right)}{\partial \theta_{.75}} = K_1\left[\frac{\partial\left(\frac{C_L'}{\sigma}\right)}{\partial \theta_{.75}}\right]_{0.1}$$

$$\frac{\partial(\frac{C_D'}{\sigma})}{\partial\theta_{.75}} = \left[\frac{\partial(\frac{C_D'}{\sigma})}{\partial\theta_{.75}}\right]_{0.1} + K_3\left\{2\left(\frac{C_L'}{\sigma}\right) - \left[\frac{\partial(\frac{C_D'}{\sigma})}{\partial\alpha_i}\right]_{0.1}\right\}$$

where

$$K_3 = \frac{\Delta\sigma}{2\mu^2}\left[\frac{\partial(\frac{C_L'}{\sigma})}{\partial\theta_{.75}}\right]$$

$$\frac{\partial(\frac{C_Q}{\sigma})}{\partial\theta_{.75}} = \left[\frac{\partial(\frac{C_Q}{\sigma})}{\partial\theta_{.75}}\right]_{0.1} - K_3\left[\frac{\partial(\frac{C_Q}{\sigma})}{\partial\alpha_c}\right]_{0.1}$$

$$\frac{\partial a_1}{\partial\theta_{.75}} = \left(\frac{\partial a_1}{\partial\theta_{.75}}\right)_{0.1} - K_3\left(\frac{\partial a_1}{\partial\alpha_c}\right)_{0.1}$$

$$\frac{\partial b_1}{\partial\theta_{.75}} = \left(\frac{\partial b_1}{\partial\theta_{.75}}\right)_{0.1} - K_3\left(\frac{\partial b_1}{\partial\alpha_c}\right)_{0.1}$$

$$\frac{\partial\lambda}{\partial\theta_{.75}} = \left(\frac{\partial\lambda}{\partial\theta_{.75}}\right)_{0.1} - K_3\left(\frac{\partial\lambda}{\partial\alpha_c}\right)_{0.1}$$

7.5 ISOLATED ROTOR DERIVATIVES FOR ROTOR SOLIDITY σ = 0.1

The changes of rotor aerodynamic parameters with respect to the basic variables, μ, a_c, and $\theta_{.75}$, are defined here as isolated rotor derivatives. These are functions of the trim values a_c, μ, $\theta_{.75}$, and M_T, as well as of the design variables σ, θ_1, and γ.

The isolated rotor derivatives presented in this section apply to rotor solidity of σ = 0.1, blade twist of $\theta_1 = 0^\circ$, advancing tip Mach number of M_T = 0.8, and a range of Lock inertia number varying between γ = 2.0 and γ = 25.0.

One of the prime parameters affecting these derivatives is rotor solidity σ. In order to obtain the required values of the derivatives for rotor solidities other than σ = 0.1, appropriate solidity corrections must be applied. Such corrections may be obtained by using the equations presented in Section 7.4. The effect of blade twist and advancing tip Mach number may be obtained from the charts presented in Reference 1. The Lock inertia number γ, although generally negligible in performance work, primarily affects rotor flapping motion. This effect of γ on rotor flapping derivatives can be easily accounted for, since the parameters such as coning angle a_0, lateral flapping angle b_1, and higher harmonic flapping terms are essentially proportional to γ.

The isolated rotor derivatives have been extracted from the theoretical rotor performance data presented in Reference 2, by using the graphical slope method. The data of Reference 2 include the effects of compressibility, stall, and reverse flow. The assumptions of classical theory, such as uniform induced velocity, rigid blades, no radial flow, and two-dimensional steady aerodynamic effects are retained. These derivatives cover the range of tip speed ratios between μ = 0.3 and μ = 1.0. The derivatives for the low μ values, $\mu \leq 0.2$, were obtained from Reference 3 and were converted into the same form used for the derivatives of $\mu \geq 0.3$. The results of Reference 3 are based on classical Bailey theory with all its assumptions and limitations.

7.5.1 Isolated Rotor Derivatives With Respect to Rotor Tip Speed Ratio (μ)

7.5.1.1 $\frac{\partial(\frac{C_L'}{\sigma})}{\partial\mu}$ for $\sigma = 0.1$, $\theta_1 = 0°$, and $M_T = 0.8$

Figures 1(a) through 1(i) present the isolated rotor derivative $\partial(C_L'/\sigma)/\partial\mu$ as a function of C_L'/σ for constant values of $\theta_{.75}$, covering the range of tip speed ratios from $\mu = 0.1$ through $\mu = 1.0$. The values of $\partial(C_L'/\sigma)\partial\mu$ for $\mu = 0.1$ and 0.2 (Figures 1(a) and 1(b)) were obtained from Reference 3 by using the following equation:

$$\frac{\partial(\frac{C_L'}{\sigma})}{\partial\mu} = \frac{\partial(\frac{C_T}{\sigma})}{\partial\mu}\cos\alpha_C - \frac{\partial(\frac{C_H}{\sigma})}{\partial\mu}\sin\alpha_C$$

Values of the $\partial(C_L'/\sigma)\partial\mu$ for $\mu \geq 0.3$ were extracted from the theoretical rotor performance data of Reference 2, as slopes of the C_L'/σ versus μ relationships for constant values of $\theta_{.75}$ and α_C .

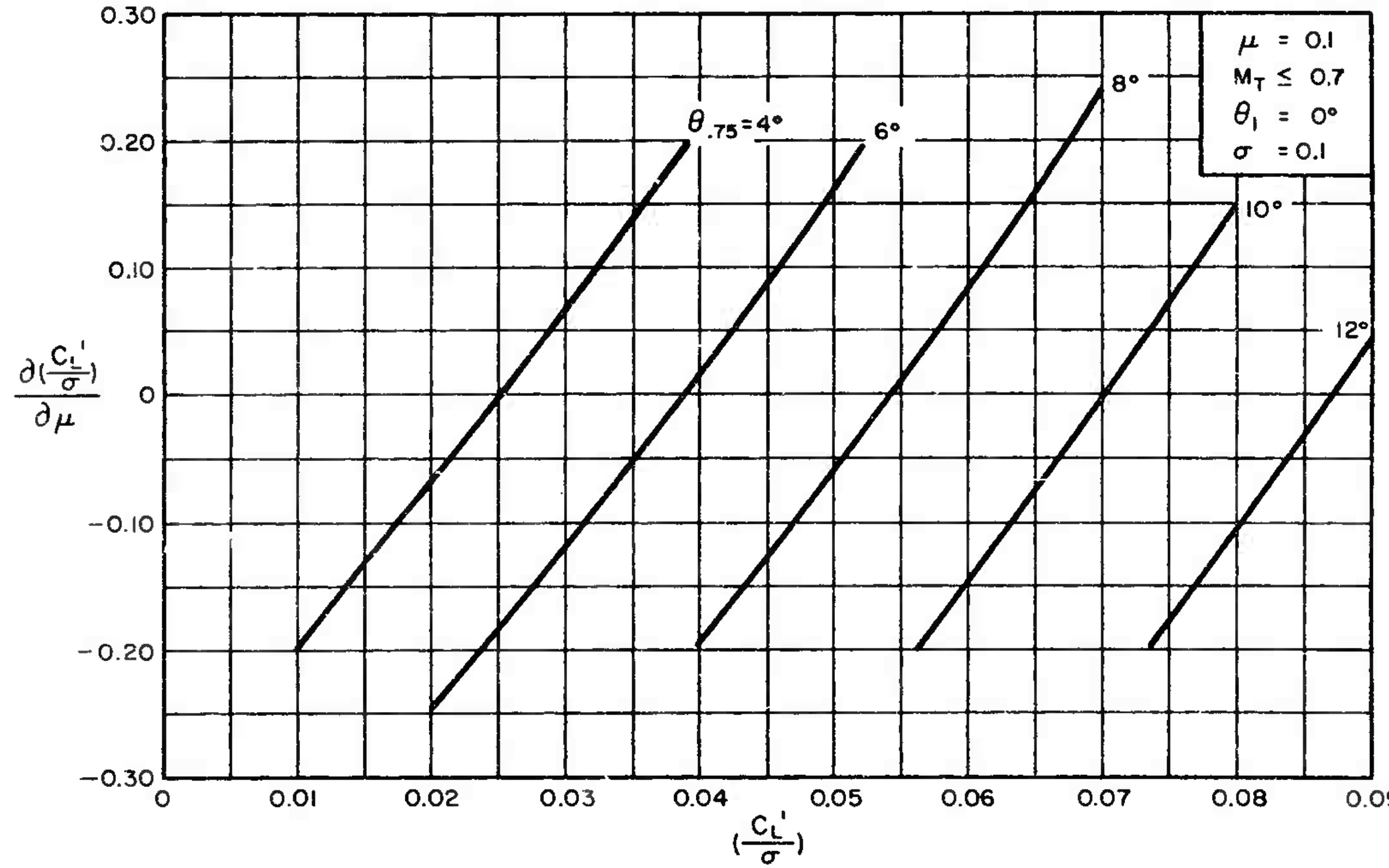

(a) μ = 0.1

Figure 1. Variation of $\frac{\partial(\frac{C_L'}{\sigma})}{\partial\mu}$ With $\frac{C_L'}{\sigma}$ for Constant Values of $\theta_{.75}$.

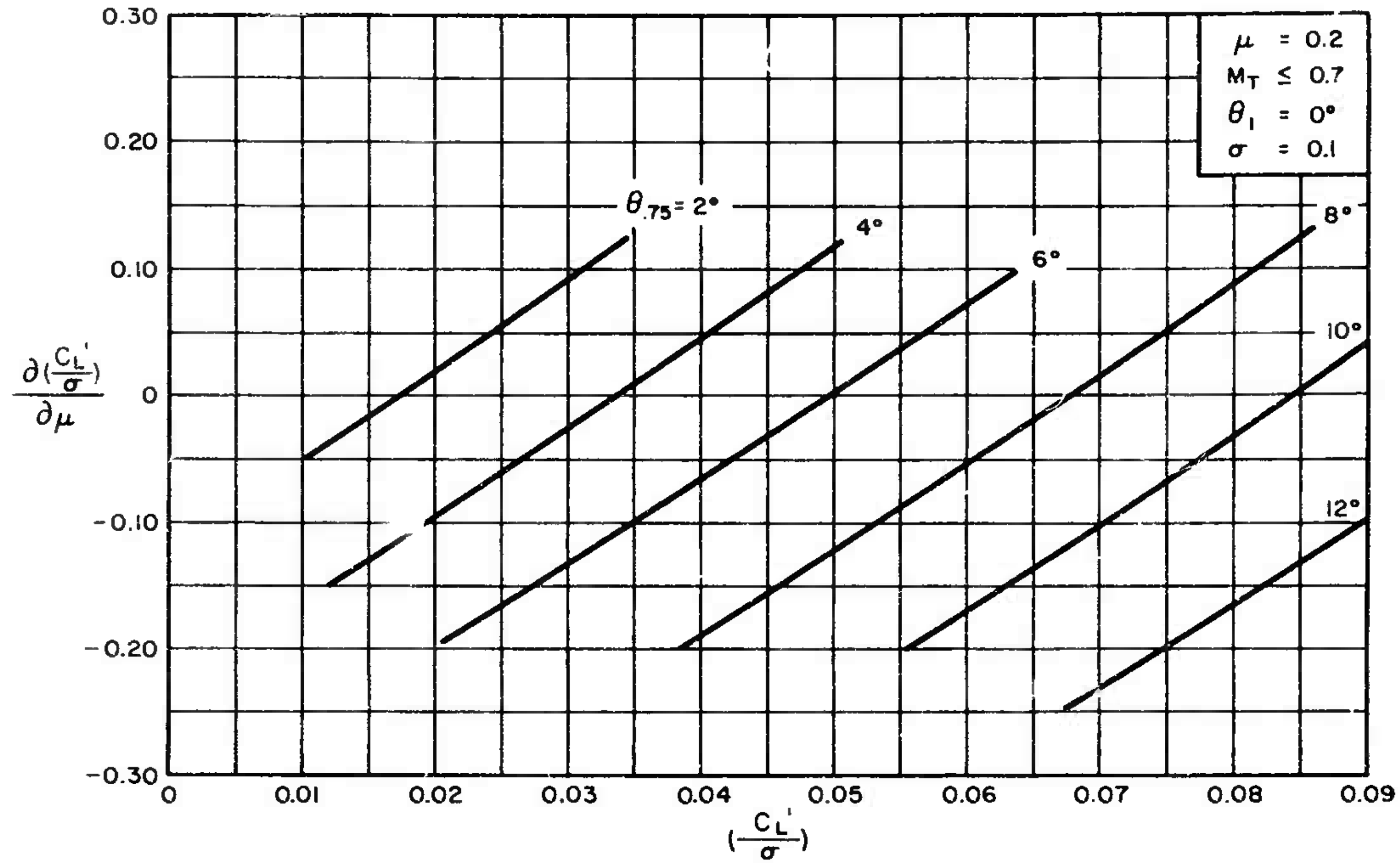

(b) μ = 0.2

Figure 1. Continued.

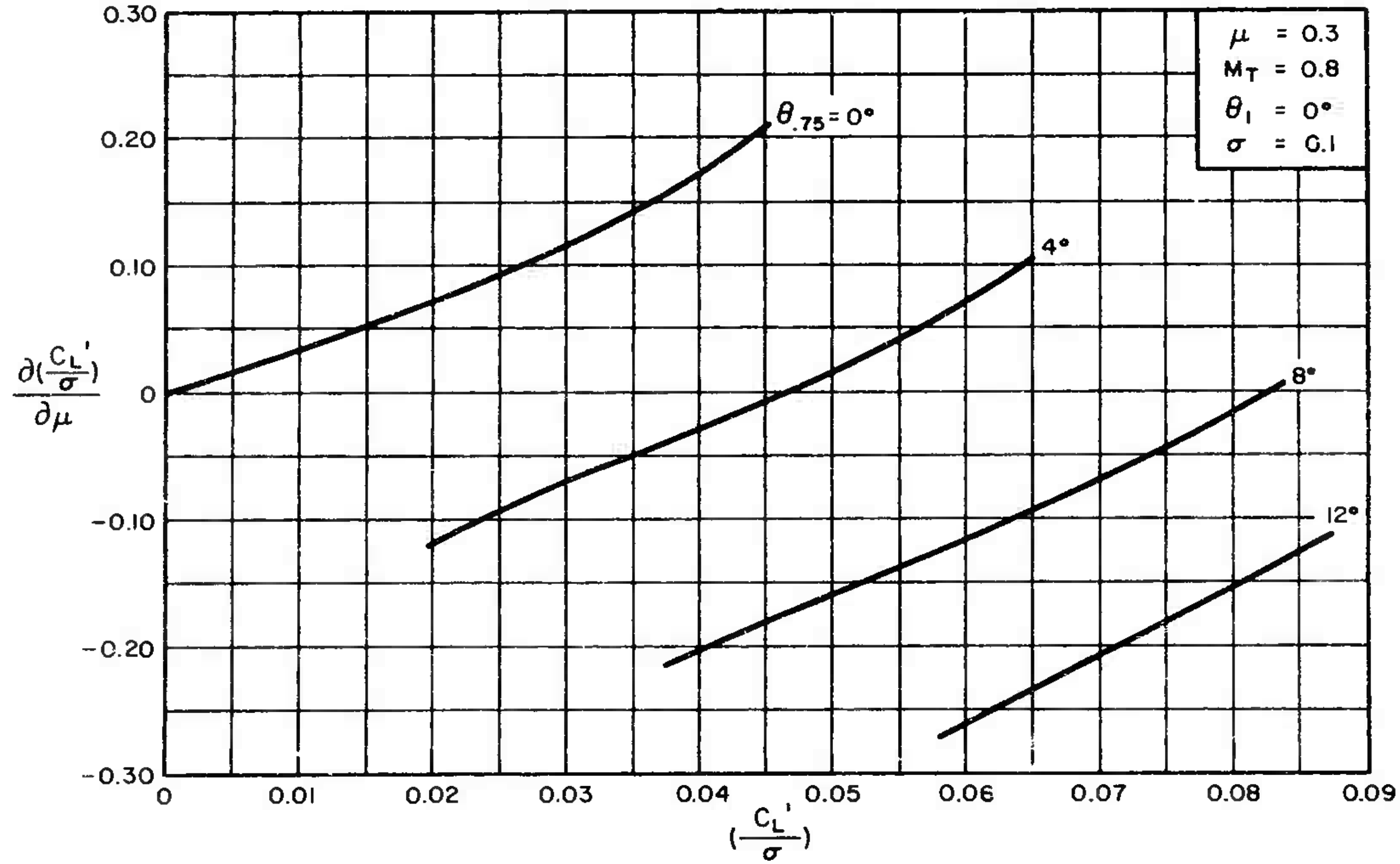

(c) μ = 0.3

Figure 1. Continued.

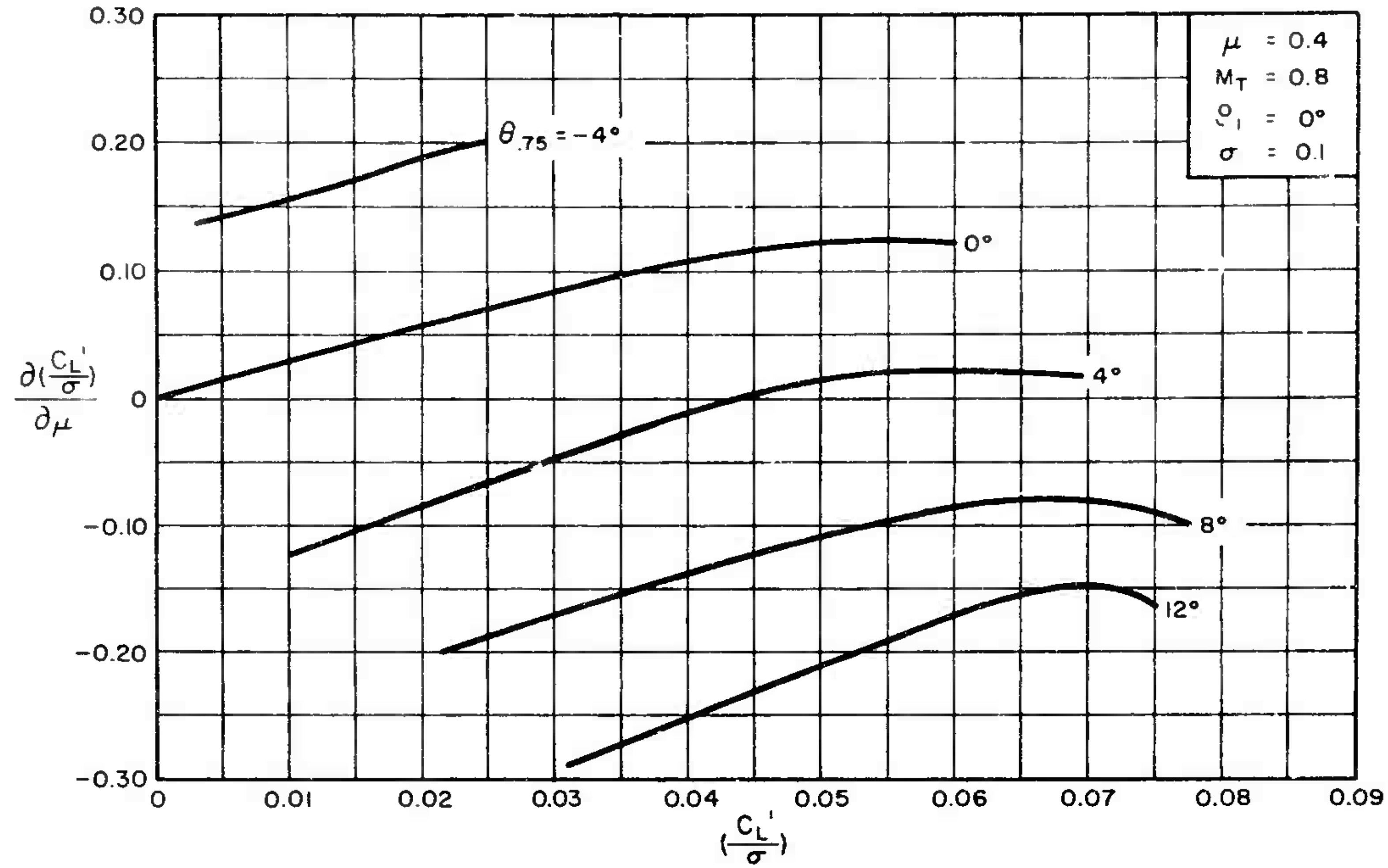

(d) $\mu = 0.4$

Figure 1. Continued.

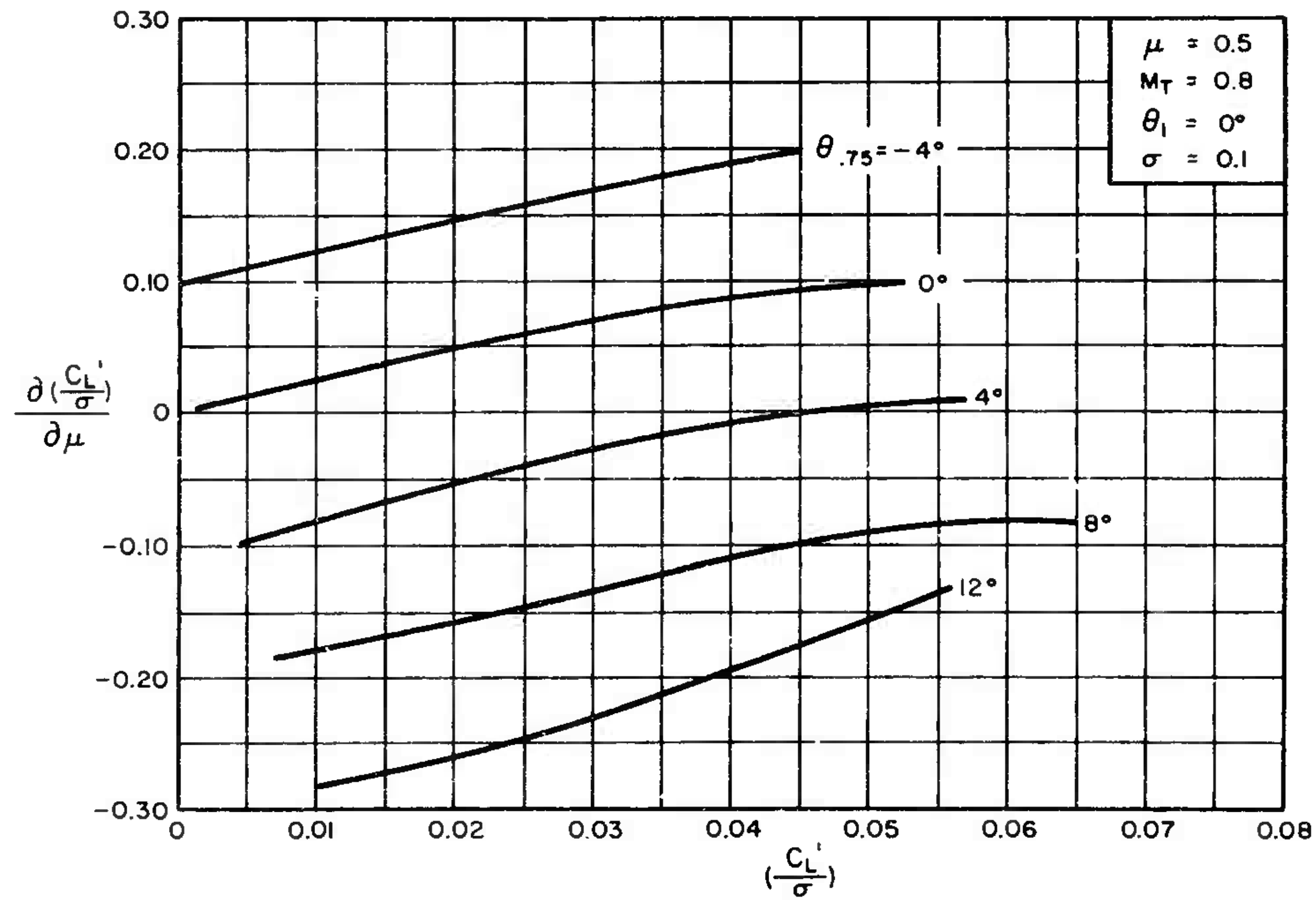

(e) $\mu = 0.5$

Figure 1. Continued.

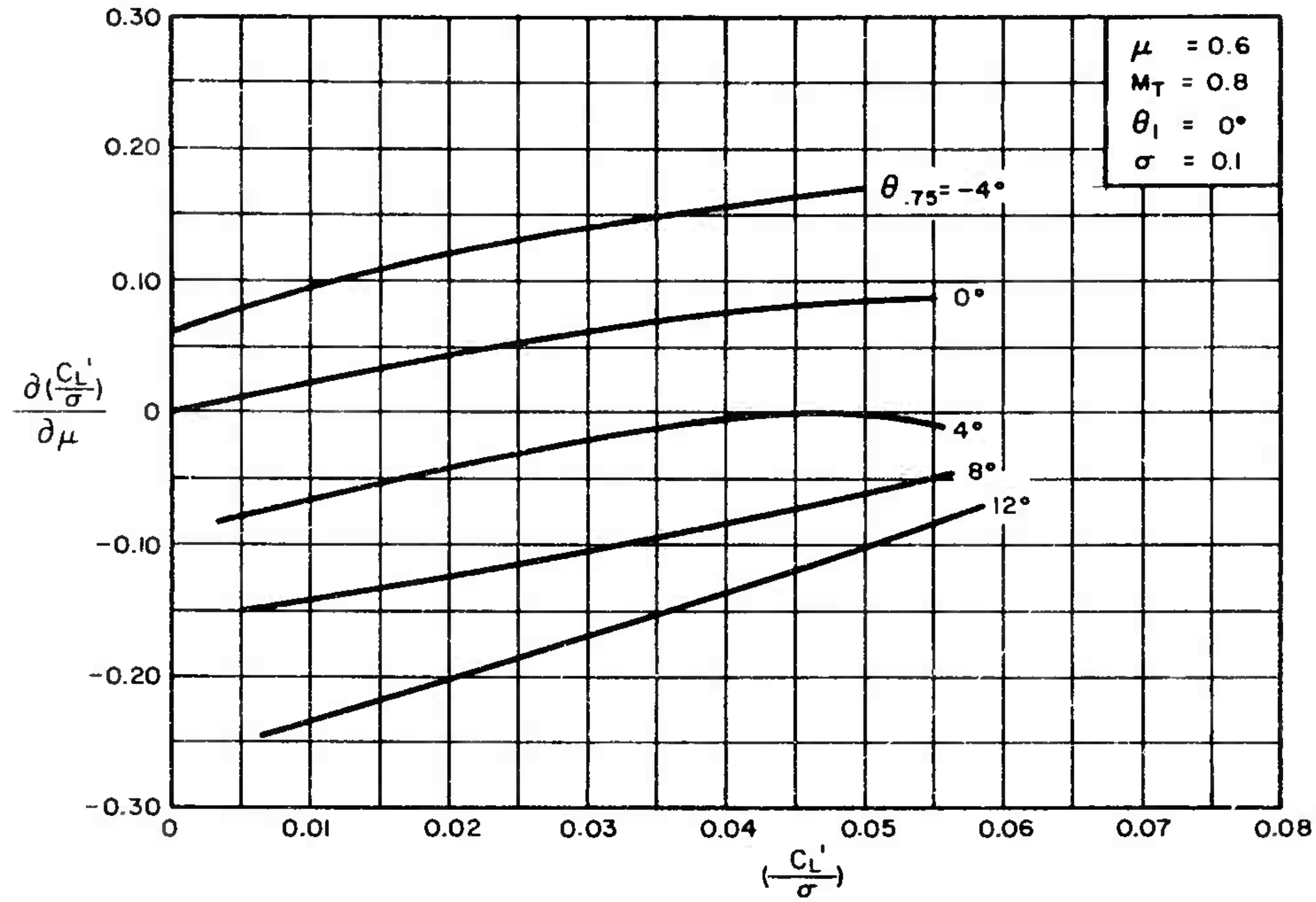

(f) $\mu = 0.6$

Figure 1. Continued.

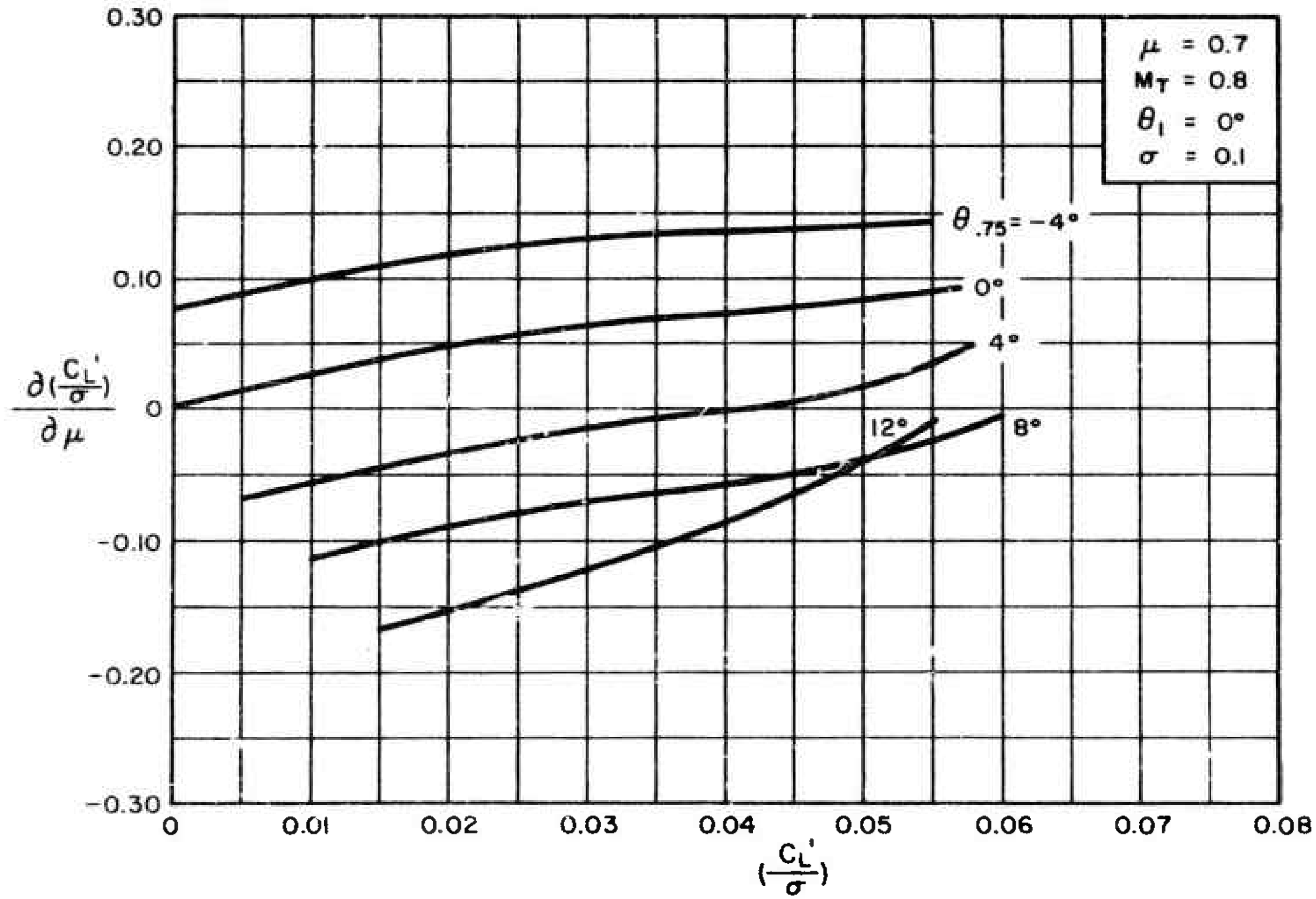

(g) μ = 0.7

Figure 1. Continued.

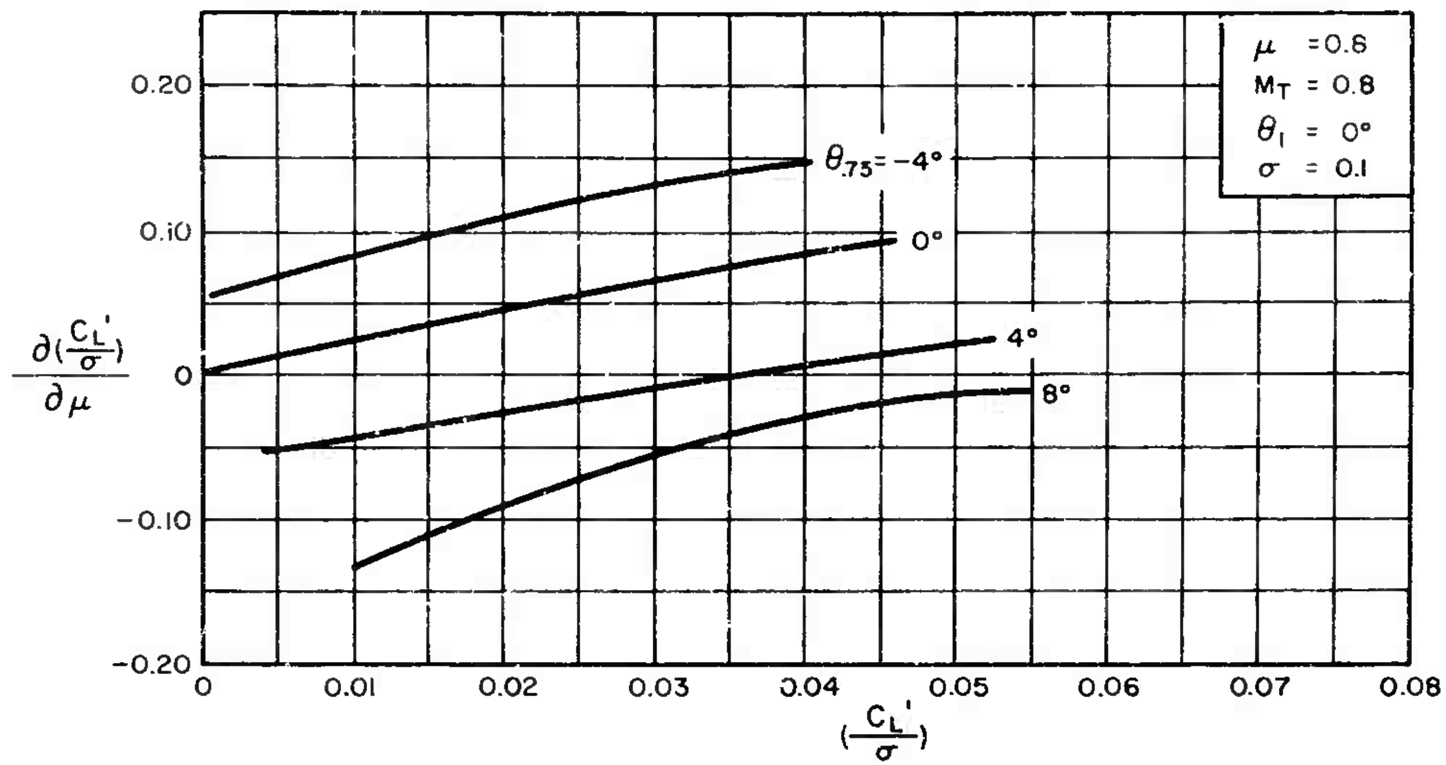

(h) μ = 0.8

Figure 1. Continued.

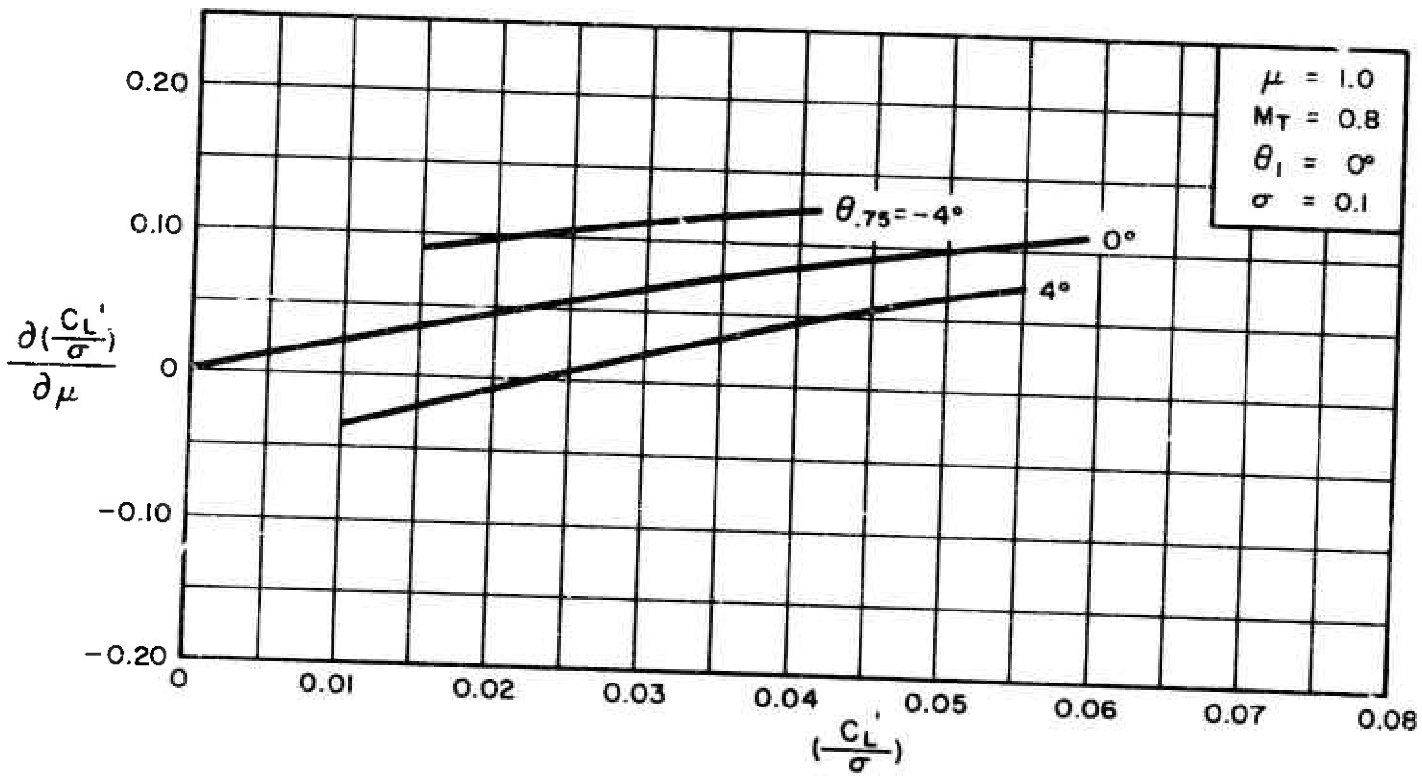

(i) μ = 1.0

Figure 1. Concluded.

7.5.1.2 $\frac{\partial(\frac{C_D'}{\sigma})}{\partial\mu}$ for $\sigma = 0.1$, $\theta = 0°$, and $M_T = 0.8$

Figures 2(a) through 2(e) present the isolated rotor derivative $\partial(C_D'/\sigma)/\partial\mu$ as a function of C_L'/σ for constant values of μ covering the collective pitch range ($\theta_{.75}$) between -4° and +12°. The values of the above derivatives for $\mu \geq 0.3$ were extracted from rotor performance data of Reference 2 by graphically obtaining the slopes of the C_D'/σ versus μ relationships for constant values of $\theta_{.75}$ and α_c. The derivatives for $\mu \leq 0.2$ can be obtained from the data of Reference 3 by using the following expression:

$$\frac{\partial(\frac{C_D'}{\sigma})}{\partial\mu} = \frac{\partial(\frac{C_H}{\sigma})}{\partial\mu}\cos\alpha_C + \frac{\partial(\frac{C_T}{\sigma})}{\partial\mu}\sin\alpha_C$$

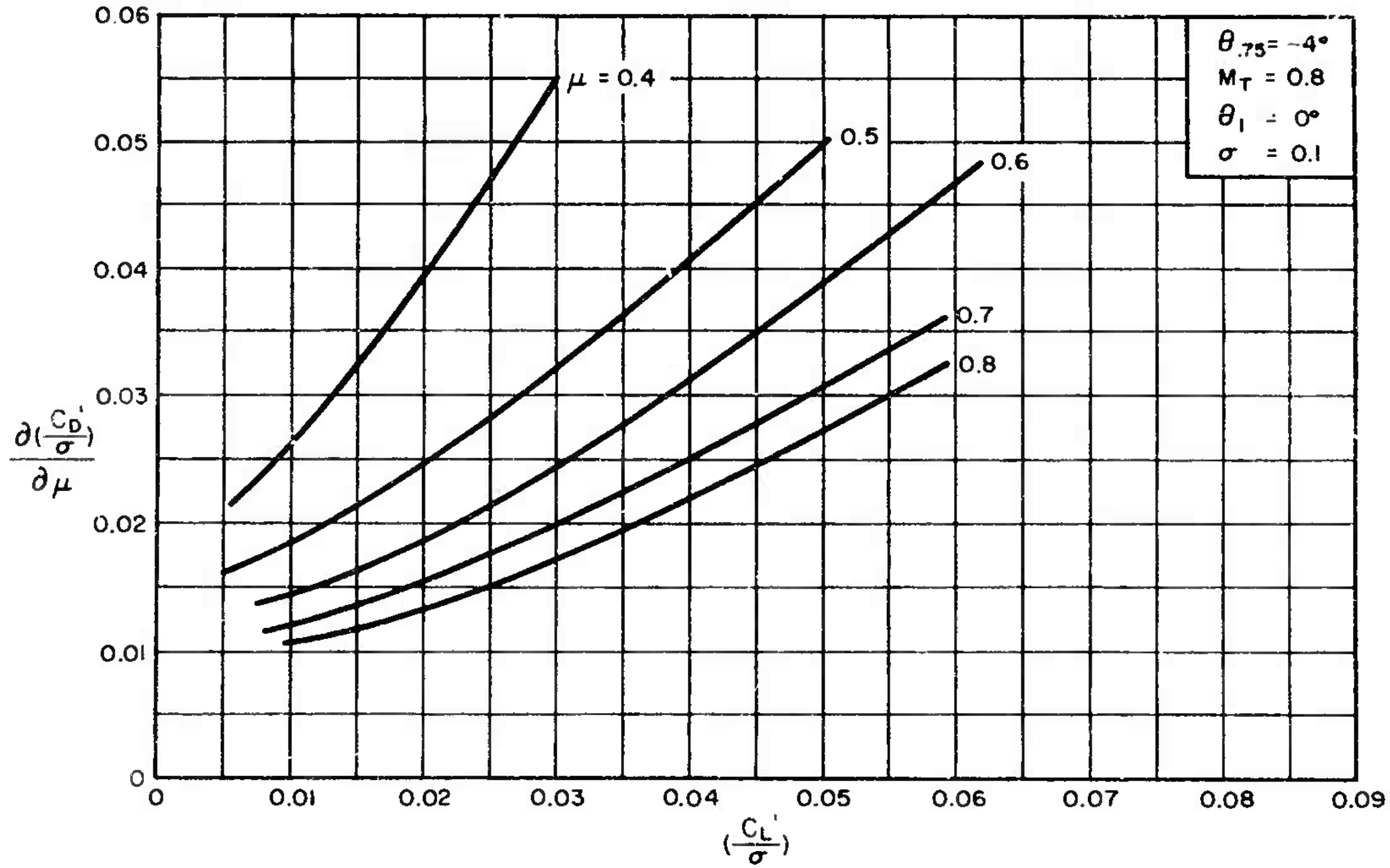

(a) $\theta_{.75} = -4°$

Figure 2. Variation of $\frac{\partial(\frac{C_D'}{\sigma})}{\partial\mu}$ With $\frac{C_L'}{\sigma}$ for Constant Values of μ .

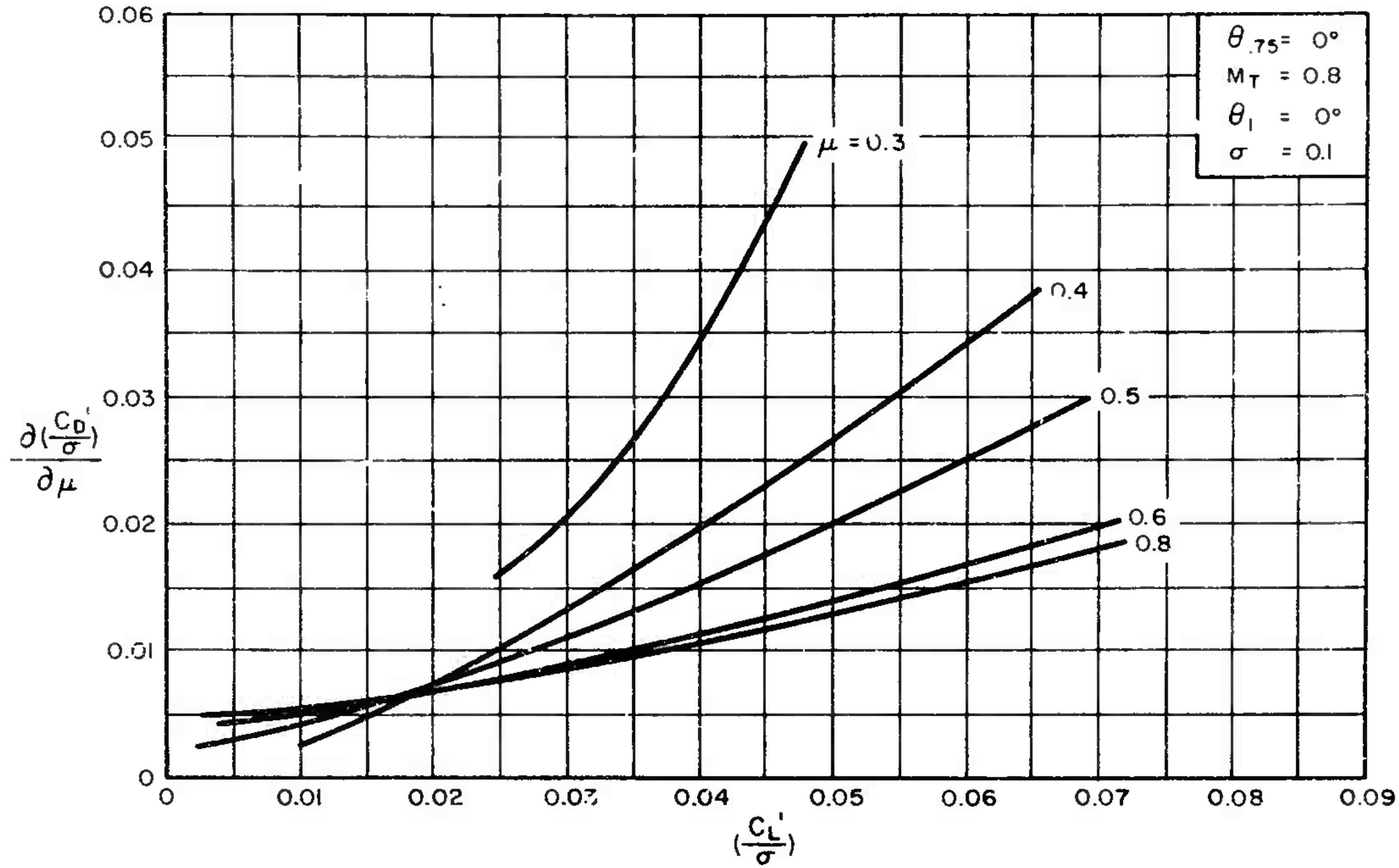

(b) $\theta_{.75} = 0°$

Figure 2. Continued.

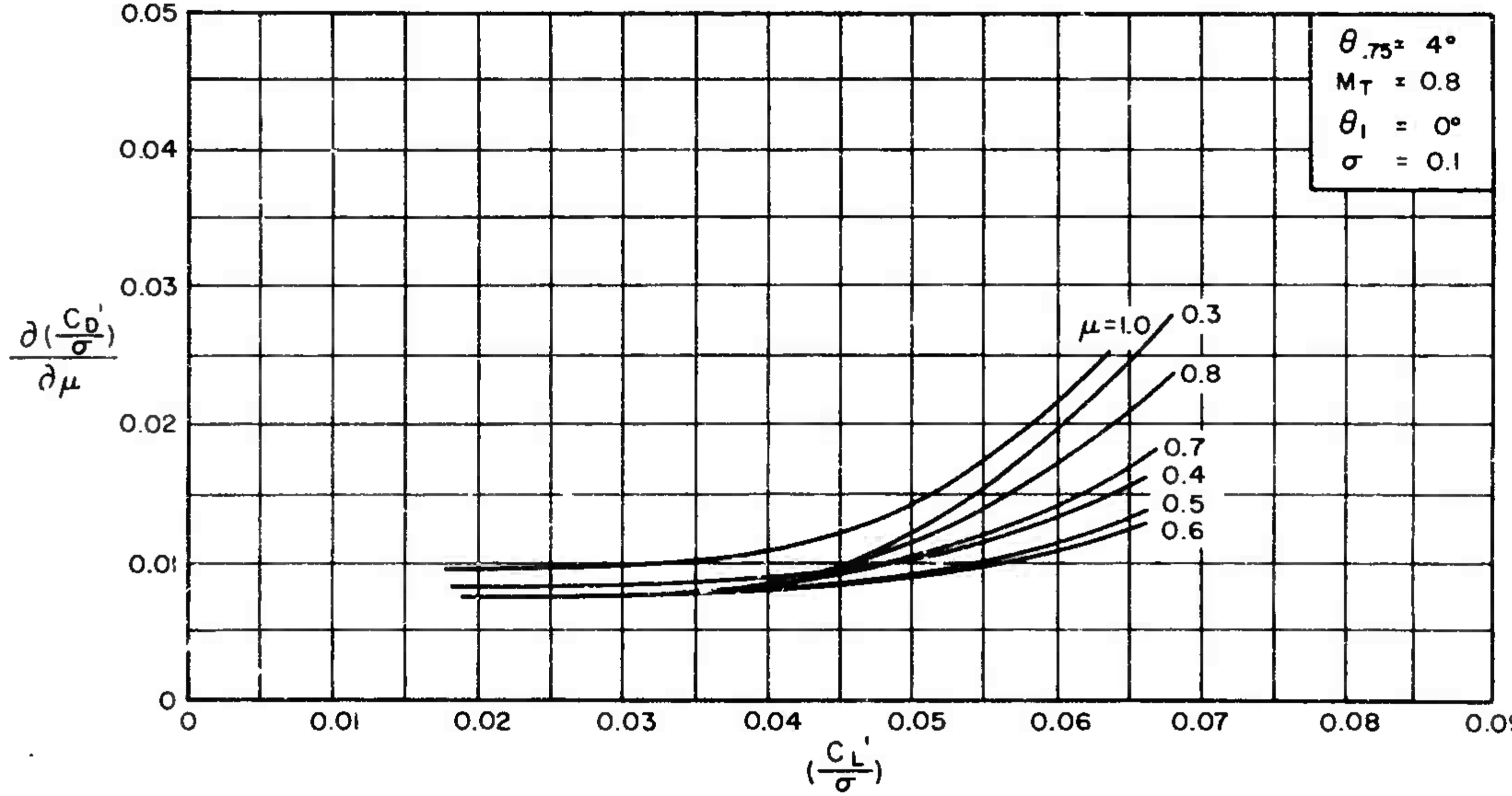

(c) $\theta_{.75} = 4°$

Figure 2. Continued.

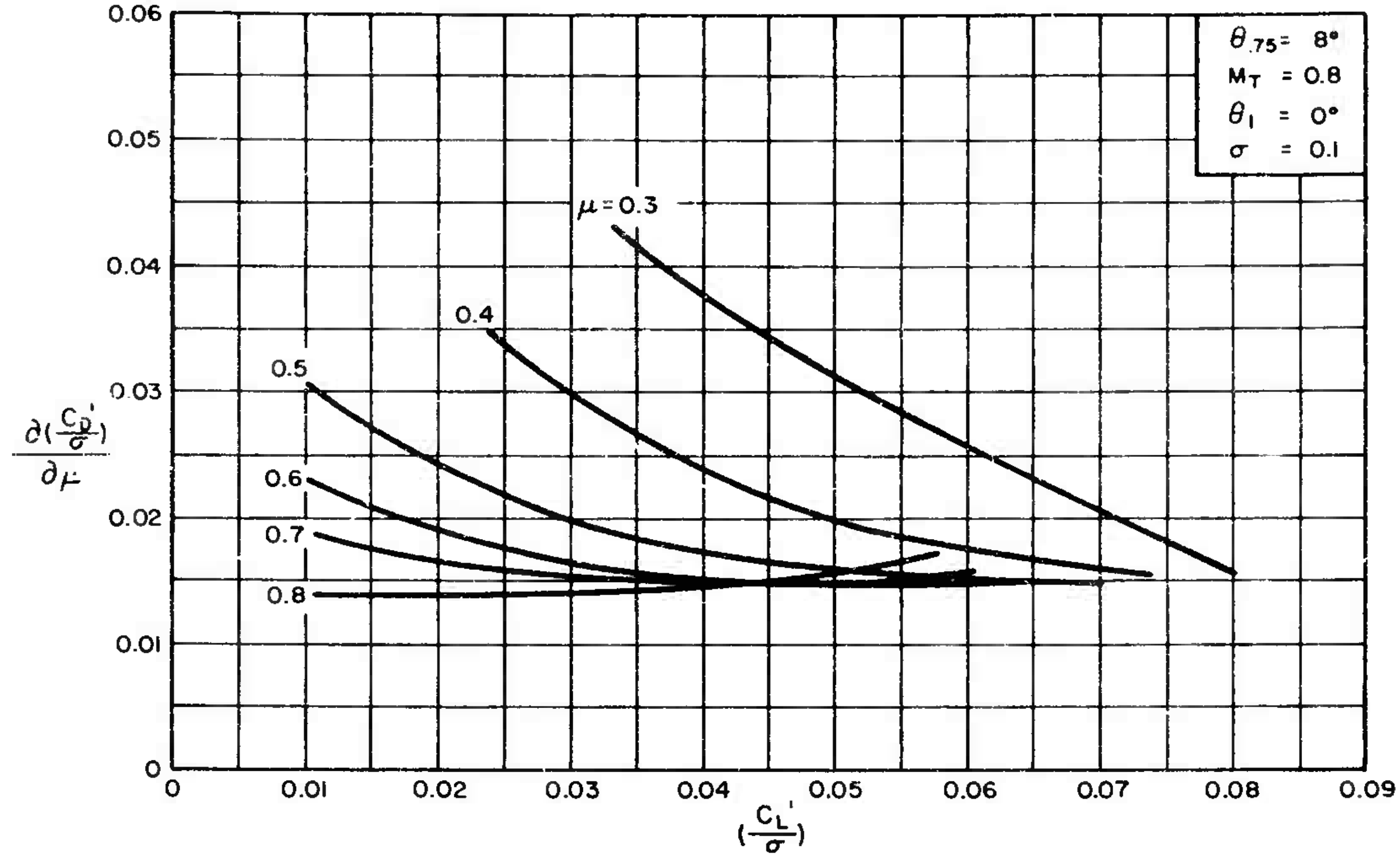

(d) $\theta_{.75} = 8°$

Figure 2. Continued.

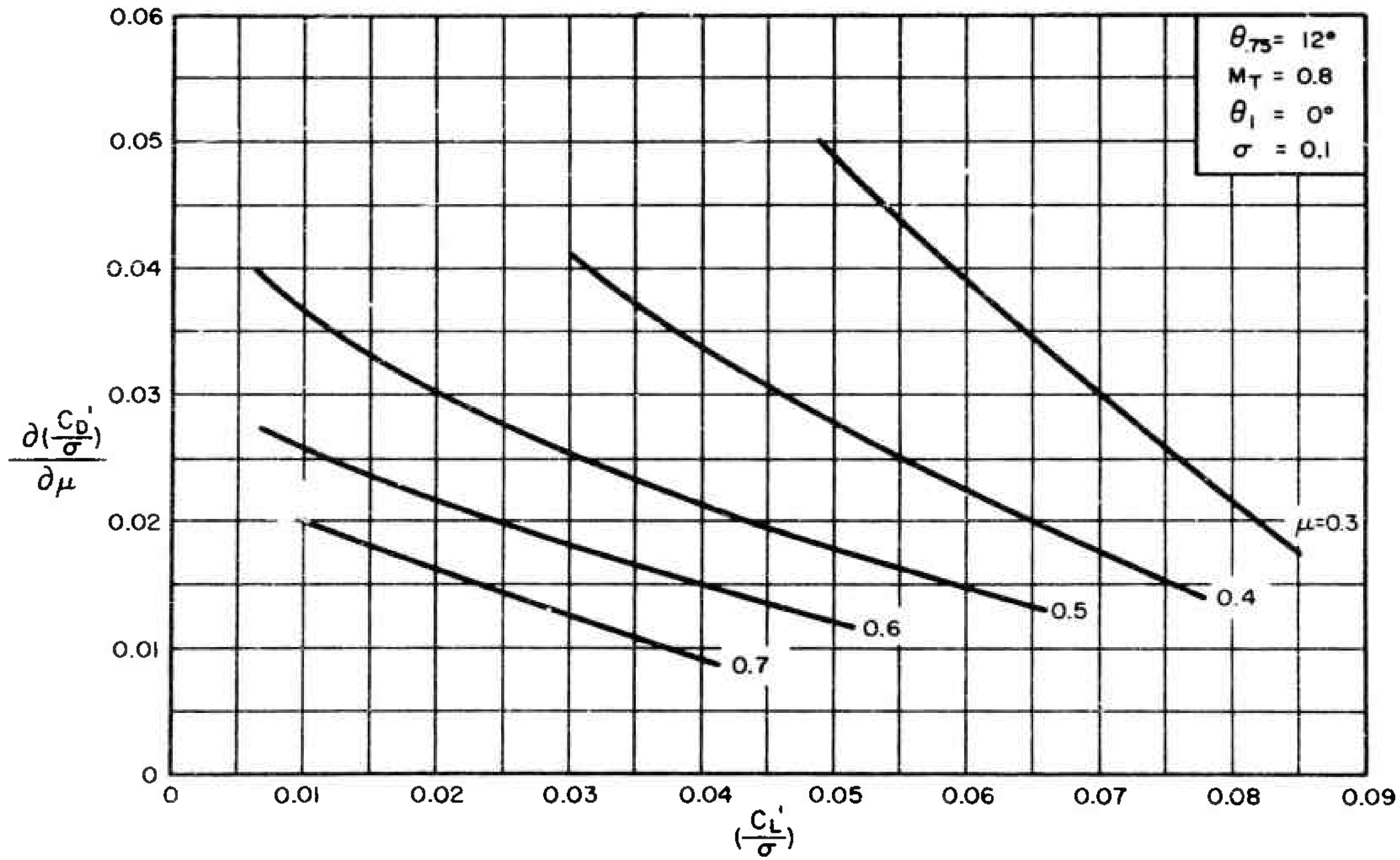

(e) $\theta_{.75} = 12°$

Figure 2. Concluded.

7.5.1.3 $\dfrac{\partial(\frac{C_Q}{\sigma})}{\partial\mu}$ for $\sigma = 0.1$, $\theta_1 = 0°$, and $M_T = 0.8$

Figures 3(a) through 3(e) present the isolated rotor derivative $\partial(C_Q/\sigma)/\partial\mu$ as a function of C_L'/σ for constant values of μ for the collective pitch range from $\theta_{.75} = -4°$ to $\theta_{.75} = 12°$. The values of the derivatives for $\mu \geq 0.3$ were extracted from the rotor performance data of Reference 1 by graphically obtaining the slopes of the C_Q/σ versus μ relationships for constant values of $\theta_{.75}$ and α_c. For values of $\mu \leq 0.2$, the following expression may be used:

$$\frac{\partial(\frac{C_Q}{\sigma})}{\partial\mu} = \frac{1}{2}\left\{\frac{\delta_0\mu}{2} + \frac{\delta_1\mu\theta_{.75}}{2} + \lambda^2\left[\delta_2\frac{\partial t_{55}}{\partial\mu} - a\frac{\partial t_{41}}{\partial\mu}\right]\right.$$

$$+\lambda\theta_{.75}\left[\frac{\partial t_{56}}{\partial\mu} - a\frac{\partial t_{42}}{\partial\mu}\right] + \theta_{.75}^2\left[\delta_2\frac{\partial t_{58}}{\partial\mu} - a\frac{\partial t_{44}}{\partial\mu}\right]$$

$$\left.+\frac{\partial\lambda}{\partial\mu}\left[\delta_1 t_{52} + 2\lambda(\delta_2 t_{55} - a_1 t_{41}) + \theta_{.75}(\delta_2 t_{56} - a\, t_{42})\right]\right\}$$

where

$$\frac{\partial t_{55}}{\partial\mu} = 2\mu\left[1.3776 - 0.000648\,\gamma^2\right]$$

$$\frac{\partial t_{41}}{\partial\mu} = 2\mu\left[1.250 + 0.000605\,\gamma^2\right]$$

$$\frac{\partial t_{56}}{\partial\mu} = 2\mu\left[2.835 + 0.000942\,\gamma^2\right] + 0.424\,\mu^2$$

$$\frac{\partial t_{42}}{\partial\mu} = 2\mu\left[0.2587 + 0.00088\,\gamma^2\right] + 0.212\,\mu^2$$

$$\frac{\partial t_{58}}{\partial\mu} = 2\mu\left[1.195 + 0.000343\,\gamma^2\right]$$

$$\frac{\partial t_{44}}{\partial \mu} = 2\mu\left[0.836 + 0.00032\,\gamma^2\right]$$

The value of $\partial\lambda/\partial\mu$ can be obtained from Subsection 7.5.1.6. The parameters δ_0, δ_1 ,and δ_2 are given on page 82 of Reference 4. The parameters t_{41} ,and t_{42} can be obtained from Table 8-4, page 208 of Reference 4, and the parameters t_{52} , t_{55} , and t_{56} can be obtained from Table 8-5, page 209 of Reference 4.

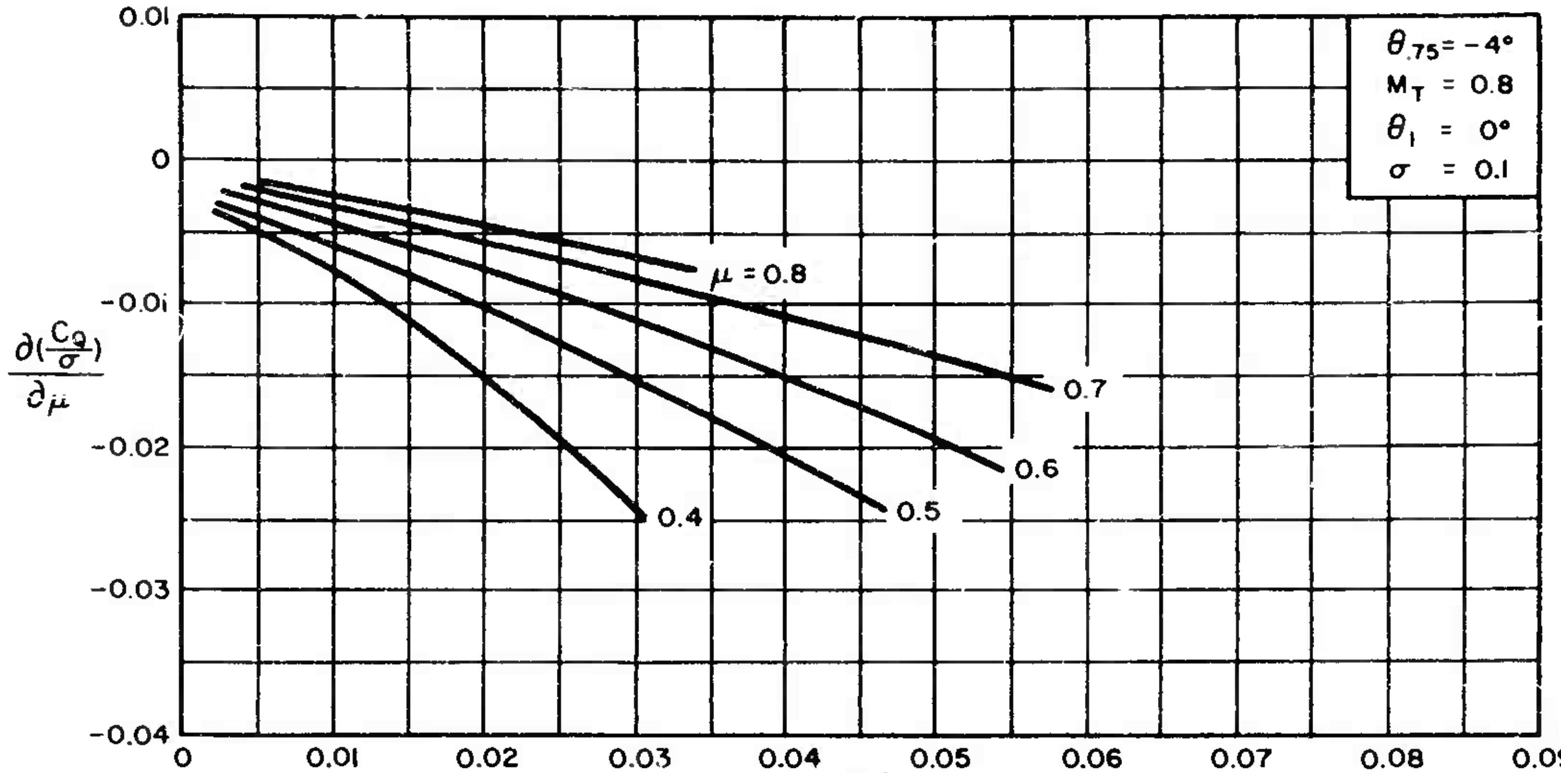

(a) $\theta_{.75} = -4°$

Figure 3. Variation of $\frac{\partial(\frac{C_Q}{\sigma})}{\partial\mu}$ With $\frac{C_L'}{\sigma}$ for Constant Values of μ .

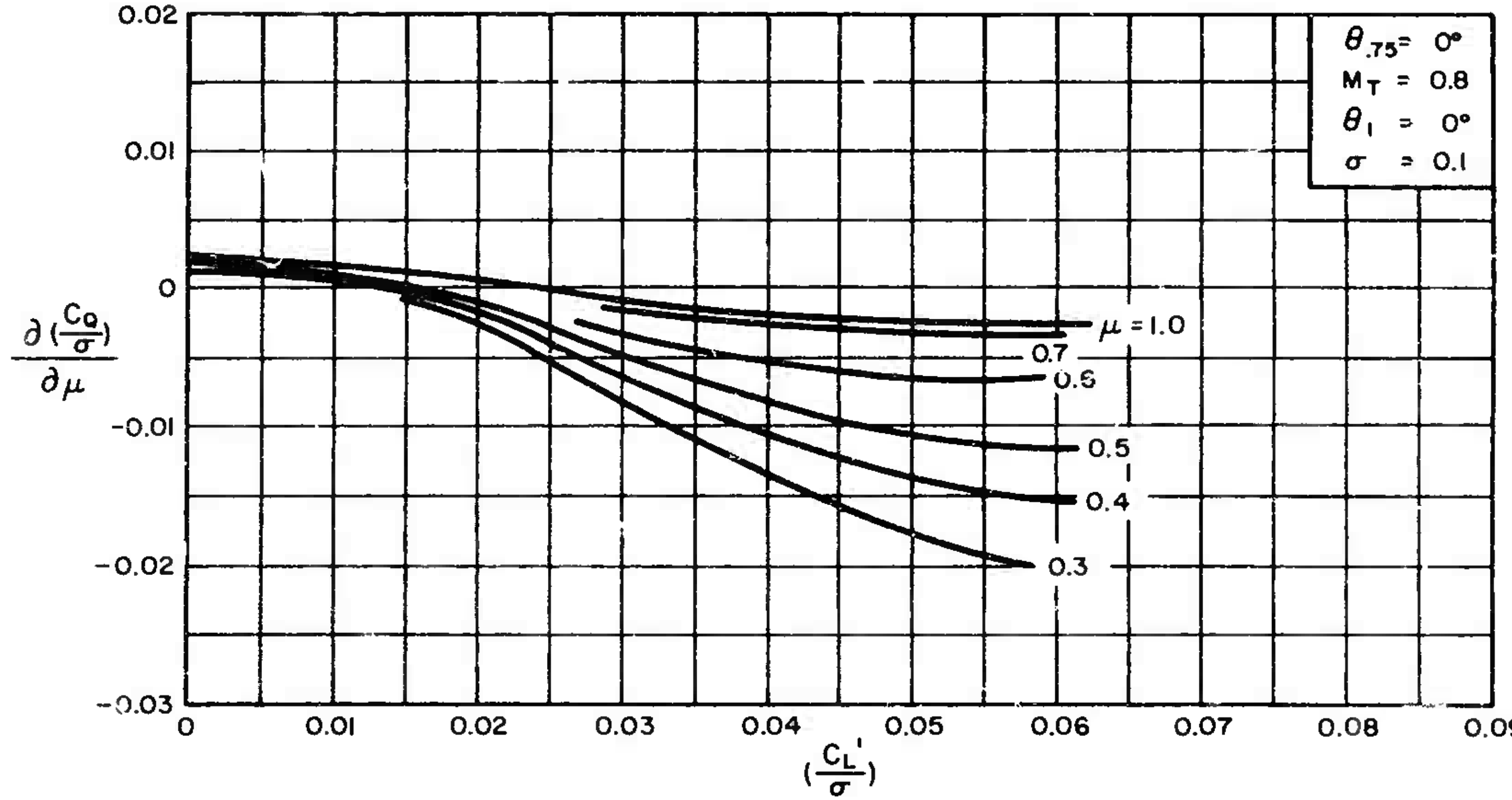

(b) $\theta_{.75} = 0°$

Figure 3. Continued.

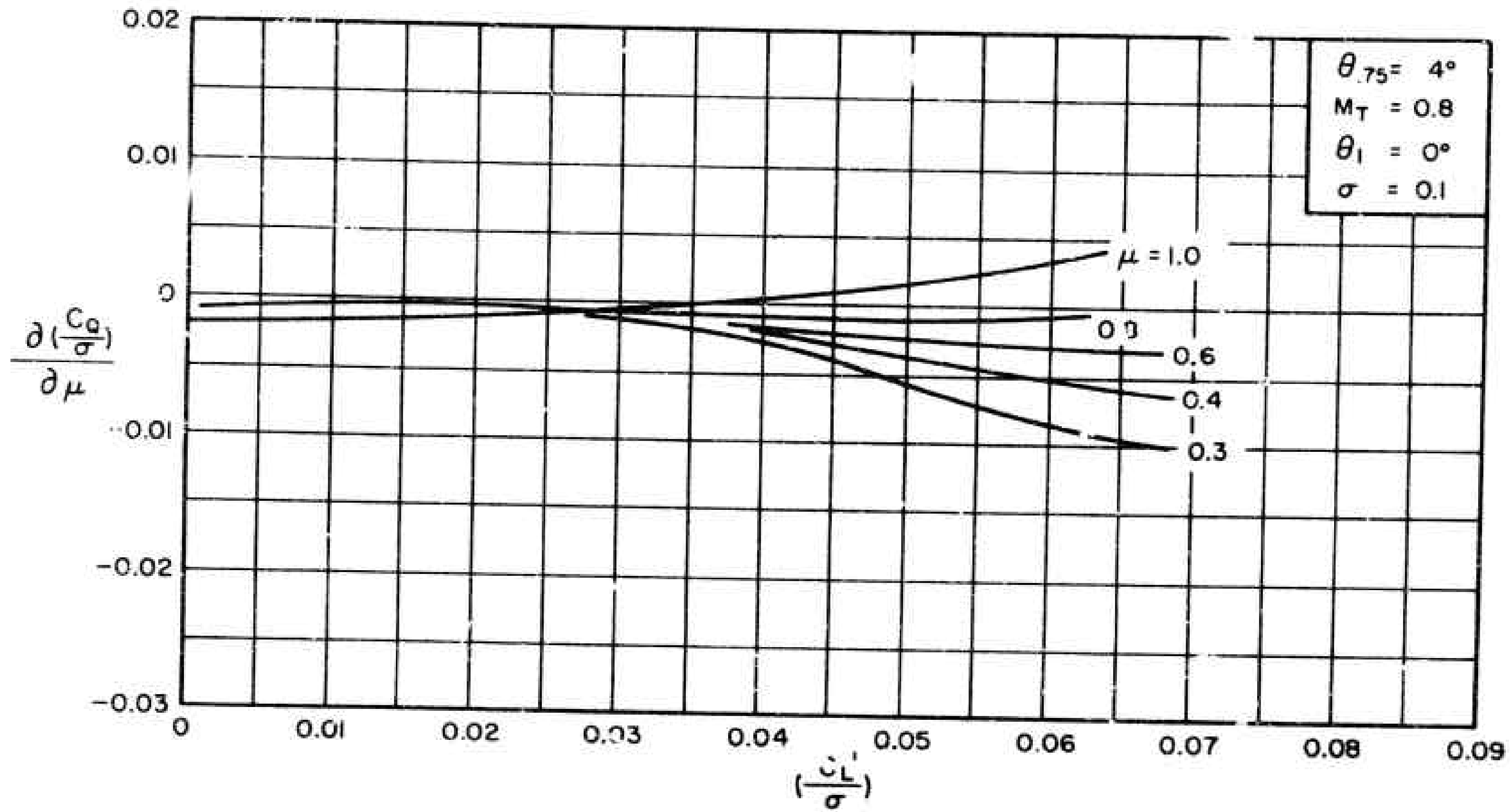

(c) $\theta_{.75} = 4°$

Figure 3. Continued.

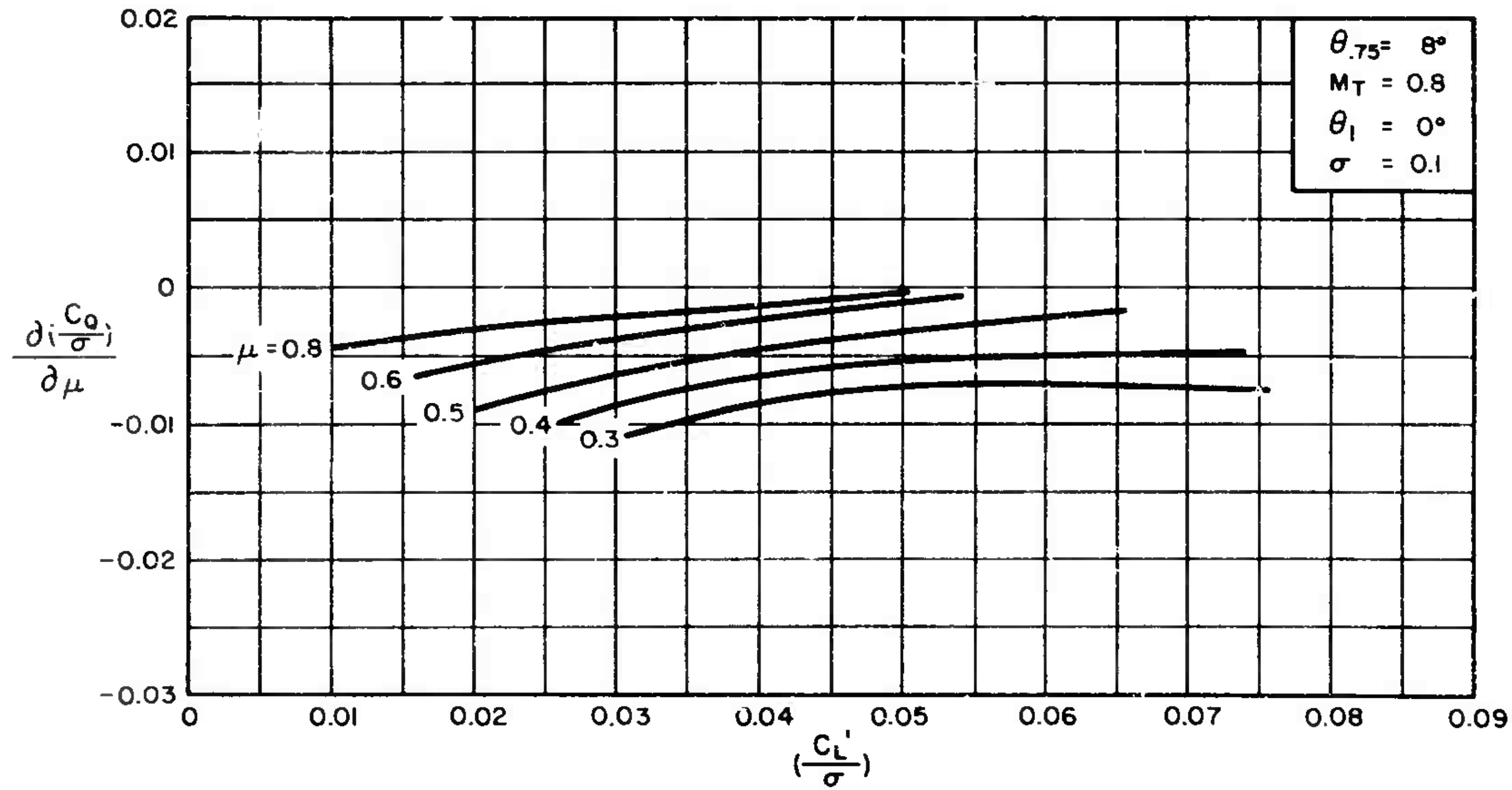

(d) $\theta_{.75}$ = 8°

F gure 3. Continued.

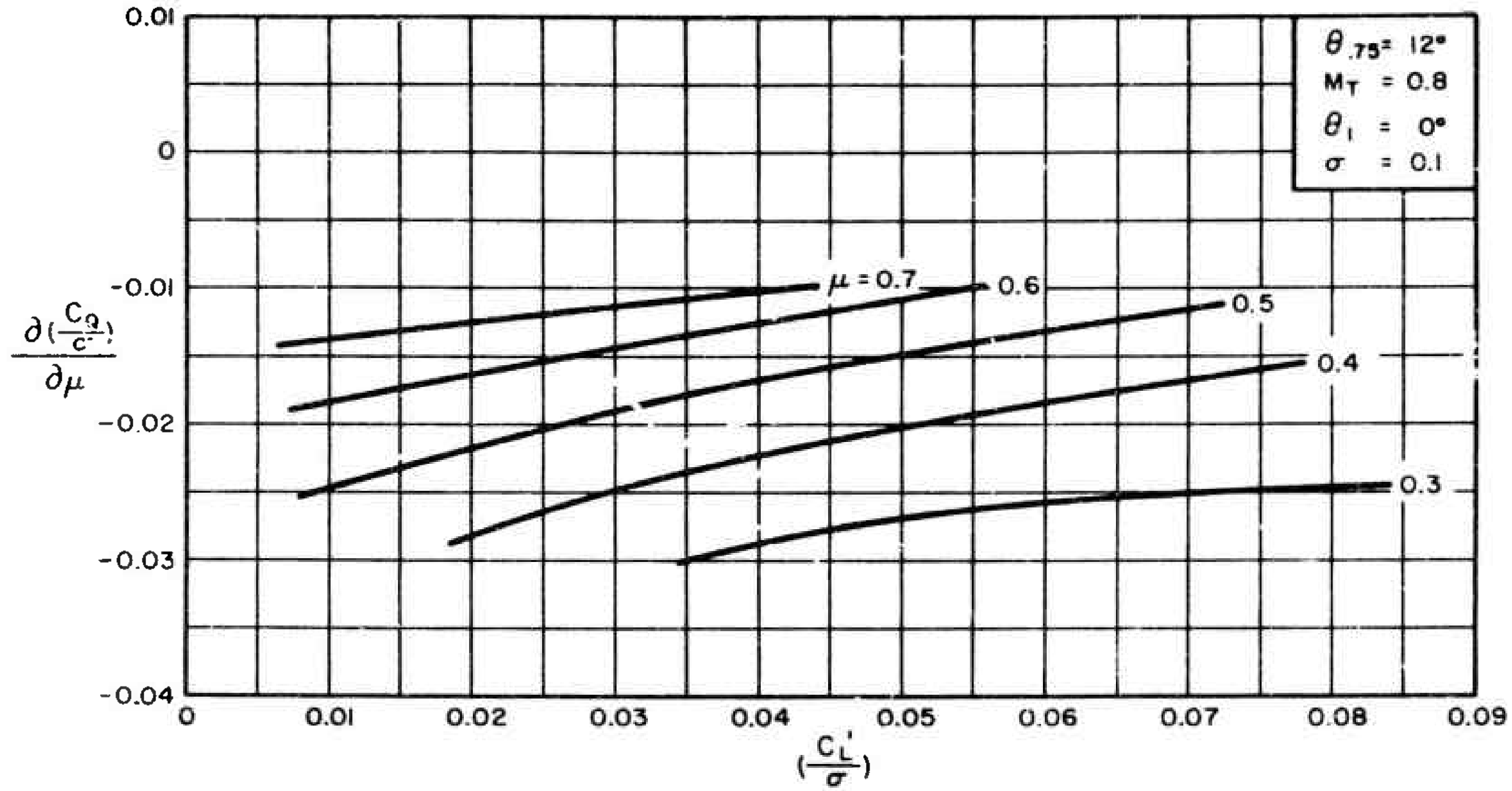

(e) $\theta_{.75} = 12°$

Figure 3. Concluded.

7.5.1.4 $\frac{\partial a_1}{\partial \mu}$ for $\sigma = 0.1$, $\theta_1 = 0°$ and $M_T = 0.8$

Figure 4 presents the rotor isolated derivative $\partial a_1/\partial \mu$ as a function of C_L'/σ for all values of $\theta_{.75}$ and $\mu = 0.1$ and 0.2. These derivatives for $\mu \geq 0.3$ are presented in Figures 5(a) through 5(g) as functions of C_L'/σ for constant values of $\theta_{.75}$.

The derivatives $\partial a_1/\partial \mu$ for the values of $\mu \leq 0.2$ were obtained directly from Reference 3. The values for $\mu \geq 0.3$ were extracted from the theoretical rotor performance data of Reference 2 by obtaining the slopes of the a_1 versus μ relationships for constant values of $\theta_{.75}$ and α_c.

The data of Reference 3, presented herein as Figure 4, show that the derivative of the longitudinal flapping angle a_1 with respect to μ is independent of $\theta_{.75}$ variation and is only a function of μ. However, for high μ values ($\mu \geq 0.3$) the results of Reference 2 indicate a substantial variation of the $(\partial a_1/\partial \mu)$ derivative with $\theta_{.75}$ as well as μ.

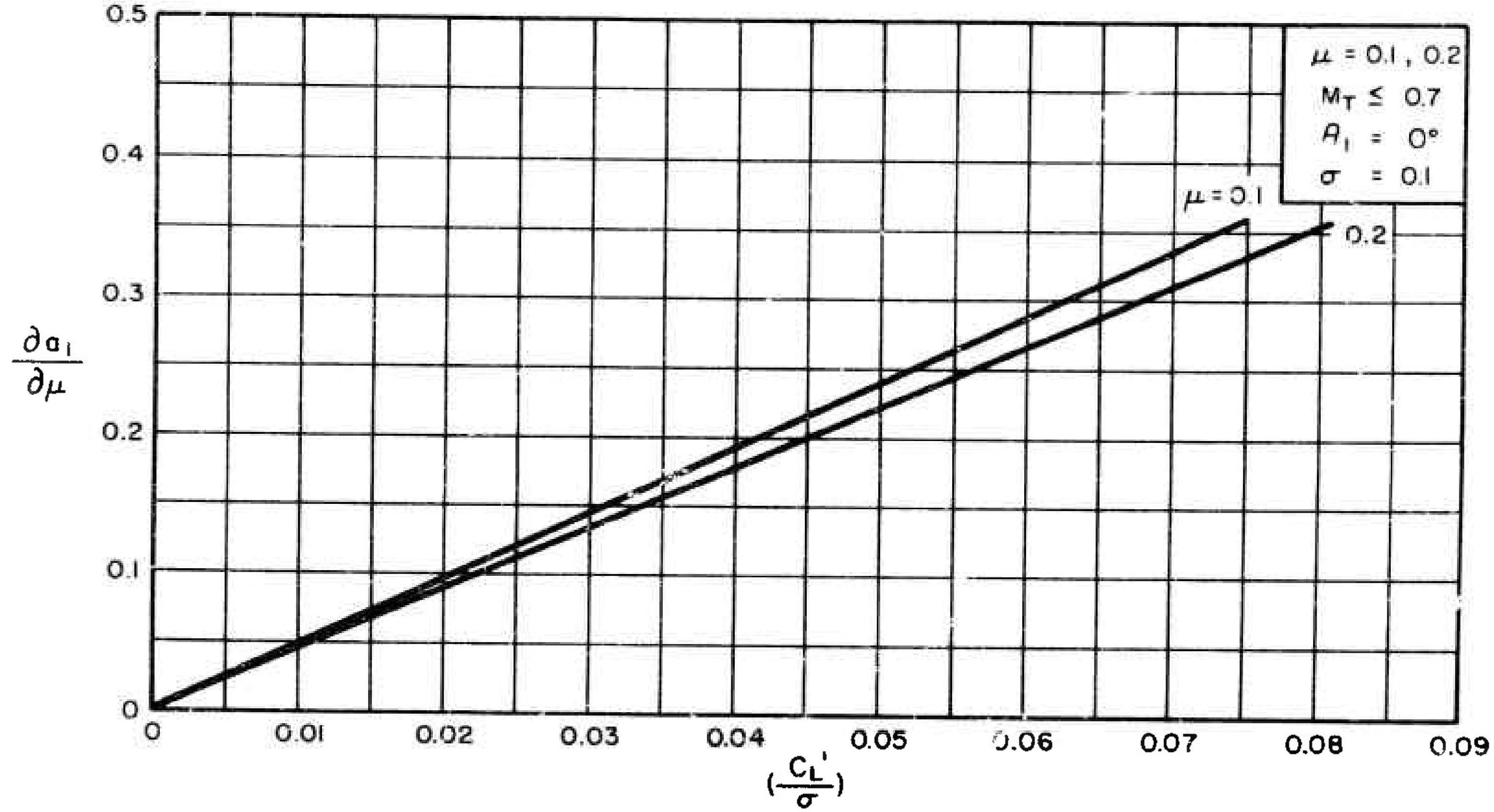

Figure 4. Variation of $\frac{\partial a_1}{\partial \mu}$ With $\frac{C_L'}{\sigma}$ for μ = 0.1 and 0.2, and All Values of $\theta_{.75}$.

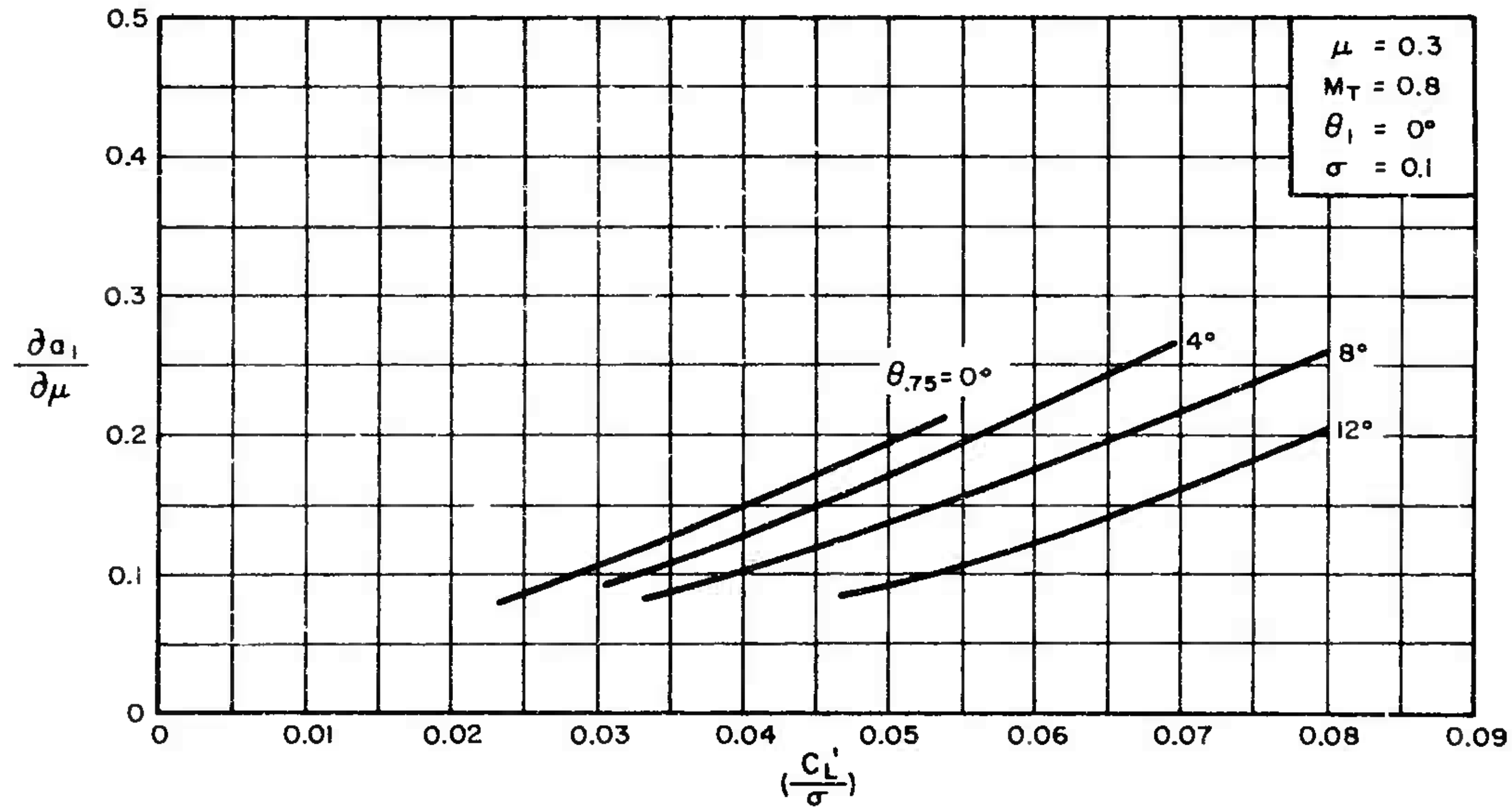

(a) $\mu = 0.3$

Figure 5. Variation of $\frac{\partial a_1}{\partial \mu}$ With $\frac{C_L'}{\sigma}$ for Constant Values of $\theta_{.75}$.

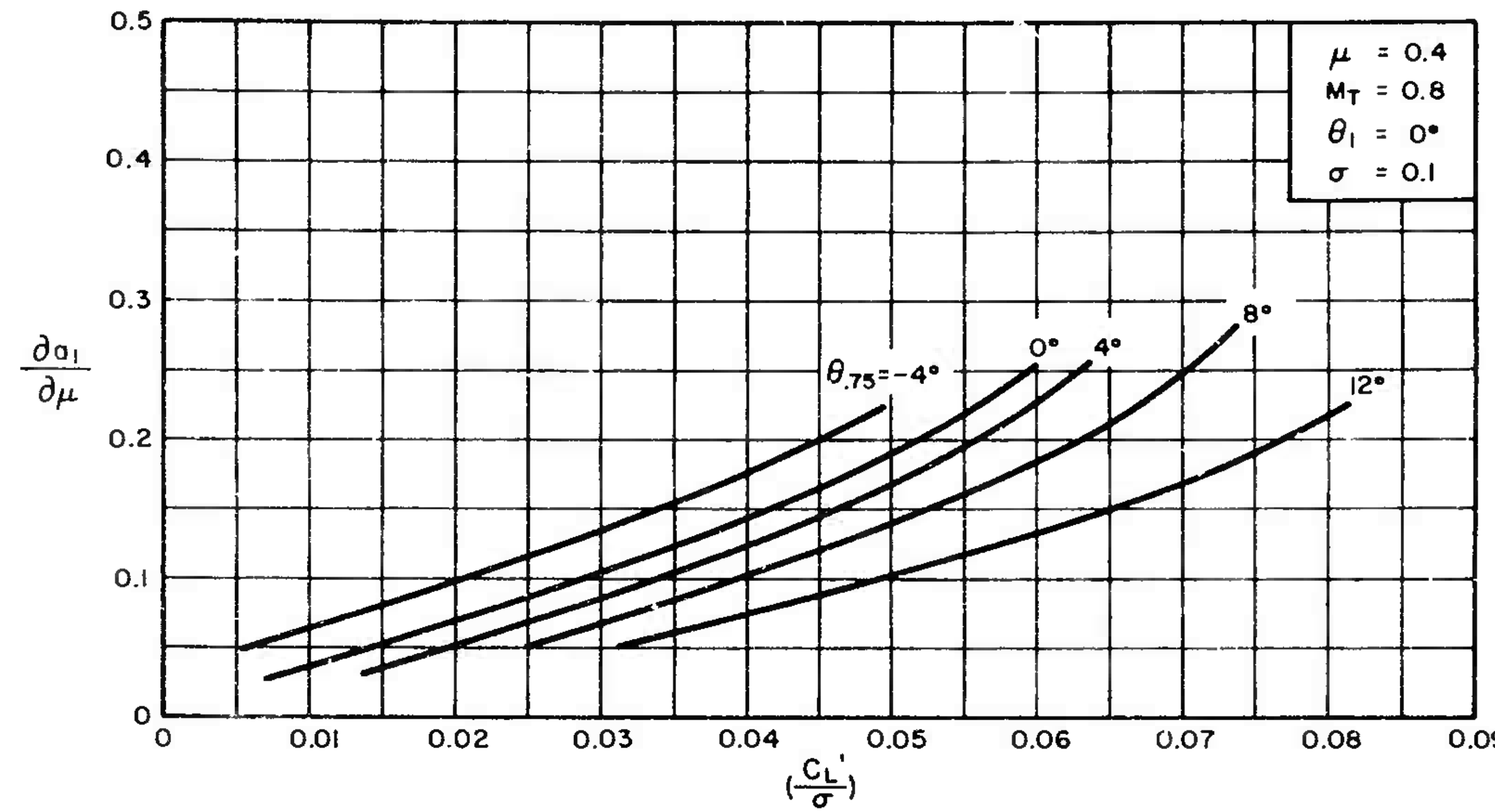

(b) $\mu = 0.4$

Figure 5. Continued.

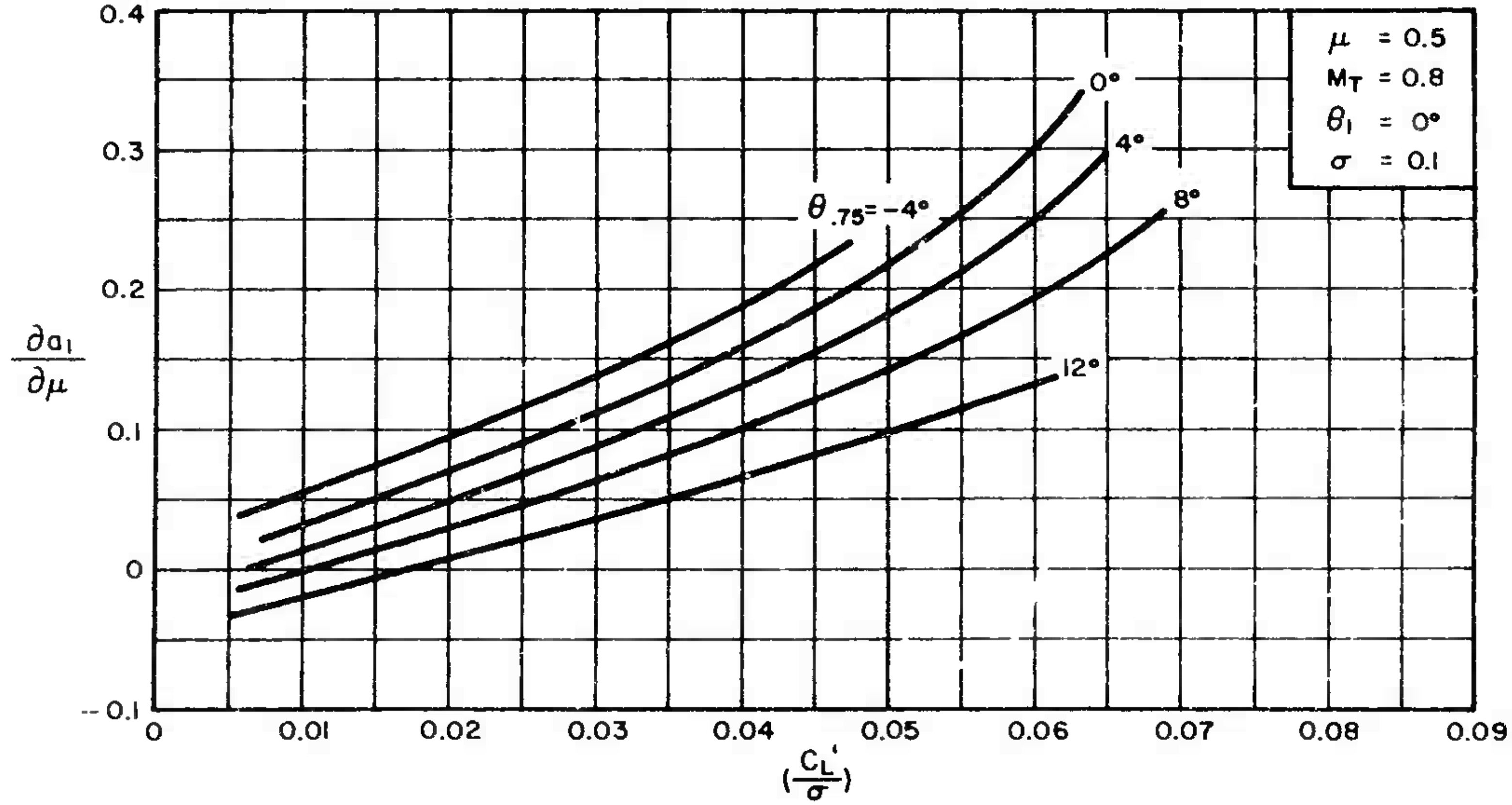

(c) $\mu = 0.5$

Figure 5. Continued.

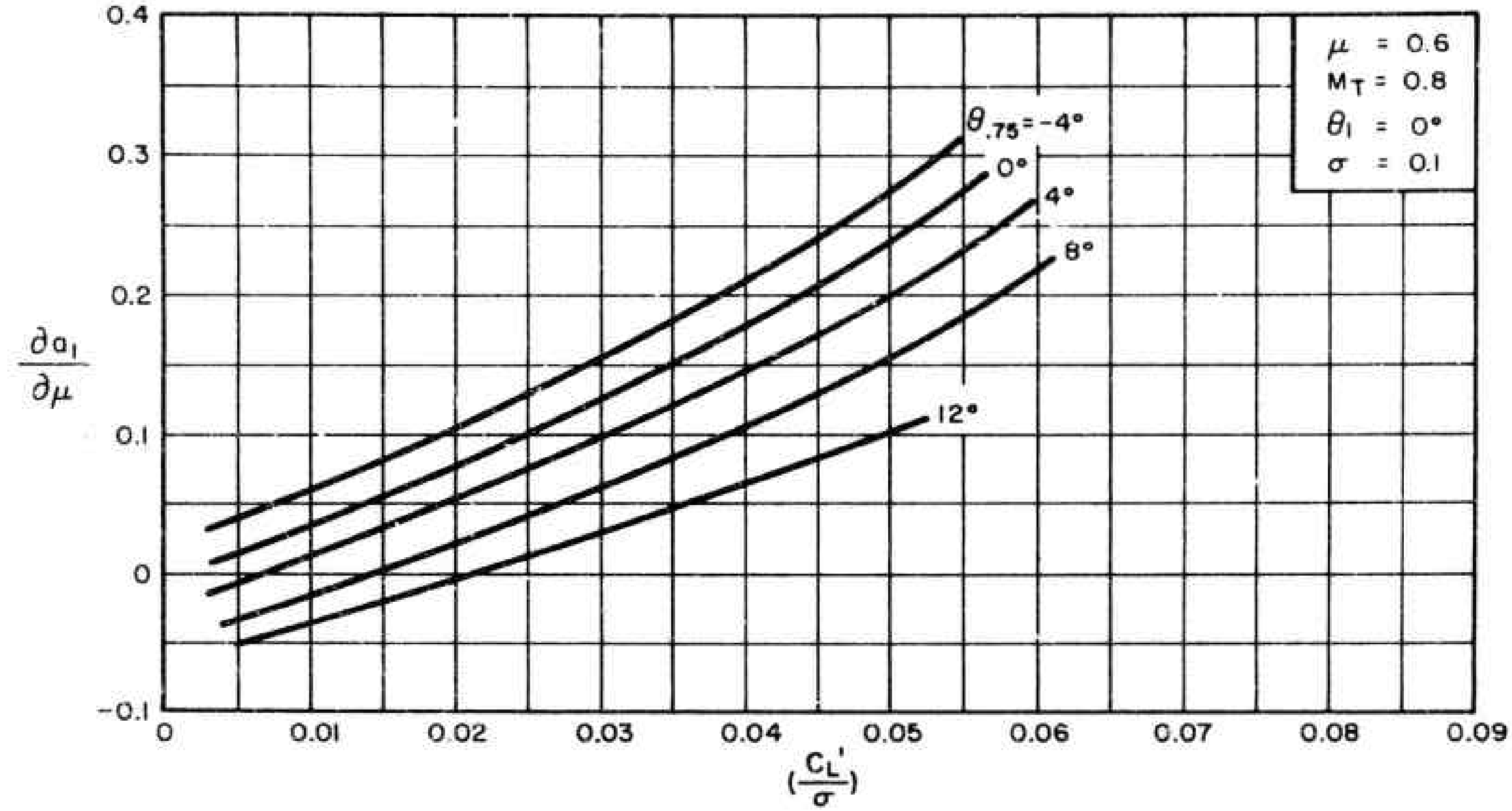

(d) $\mu = 0.6$

Figure 5. Continued.

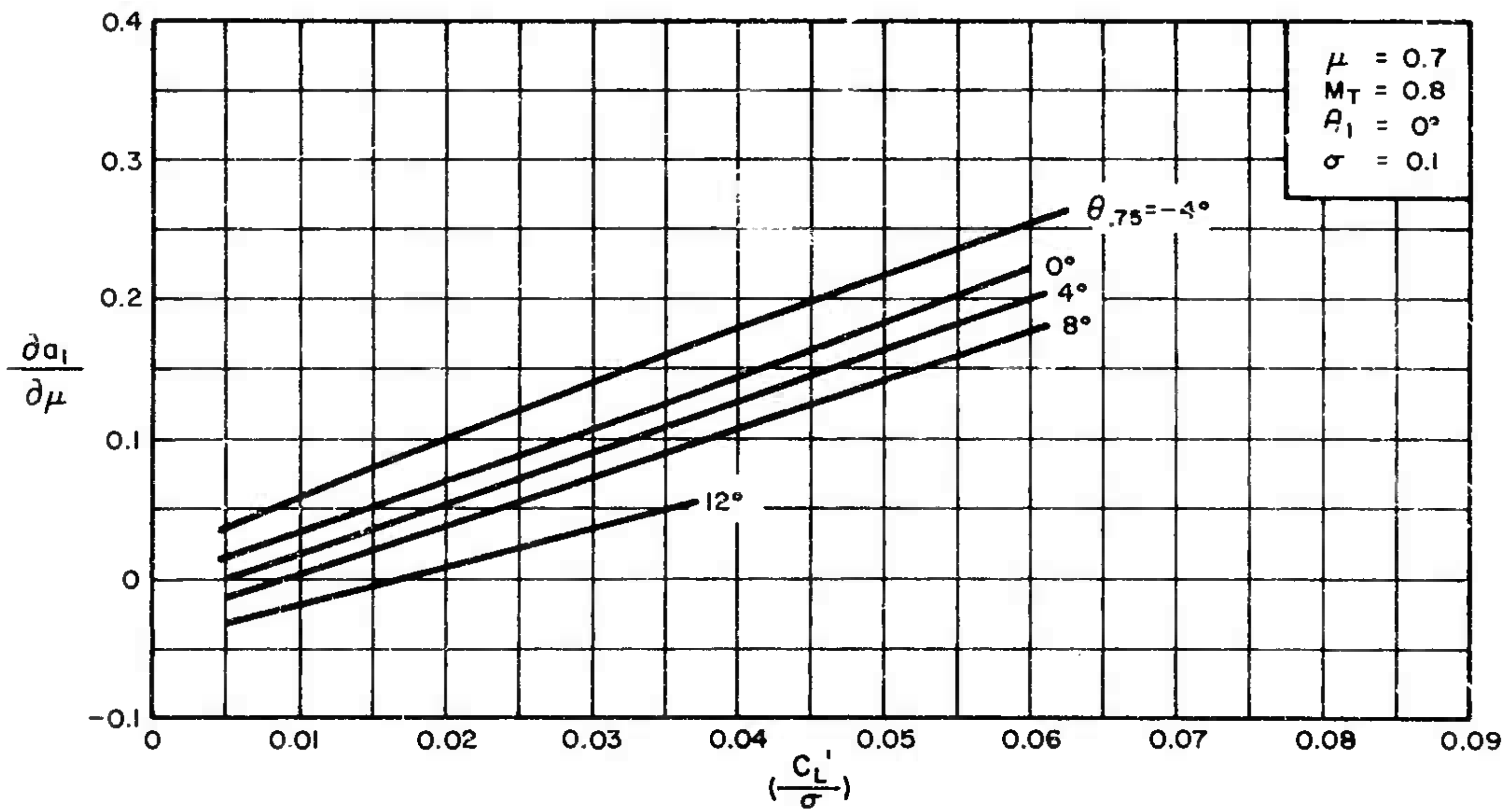

(e) $\mu = 0.7$

Figure 5. Continued.

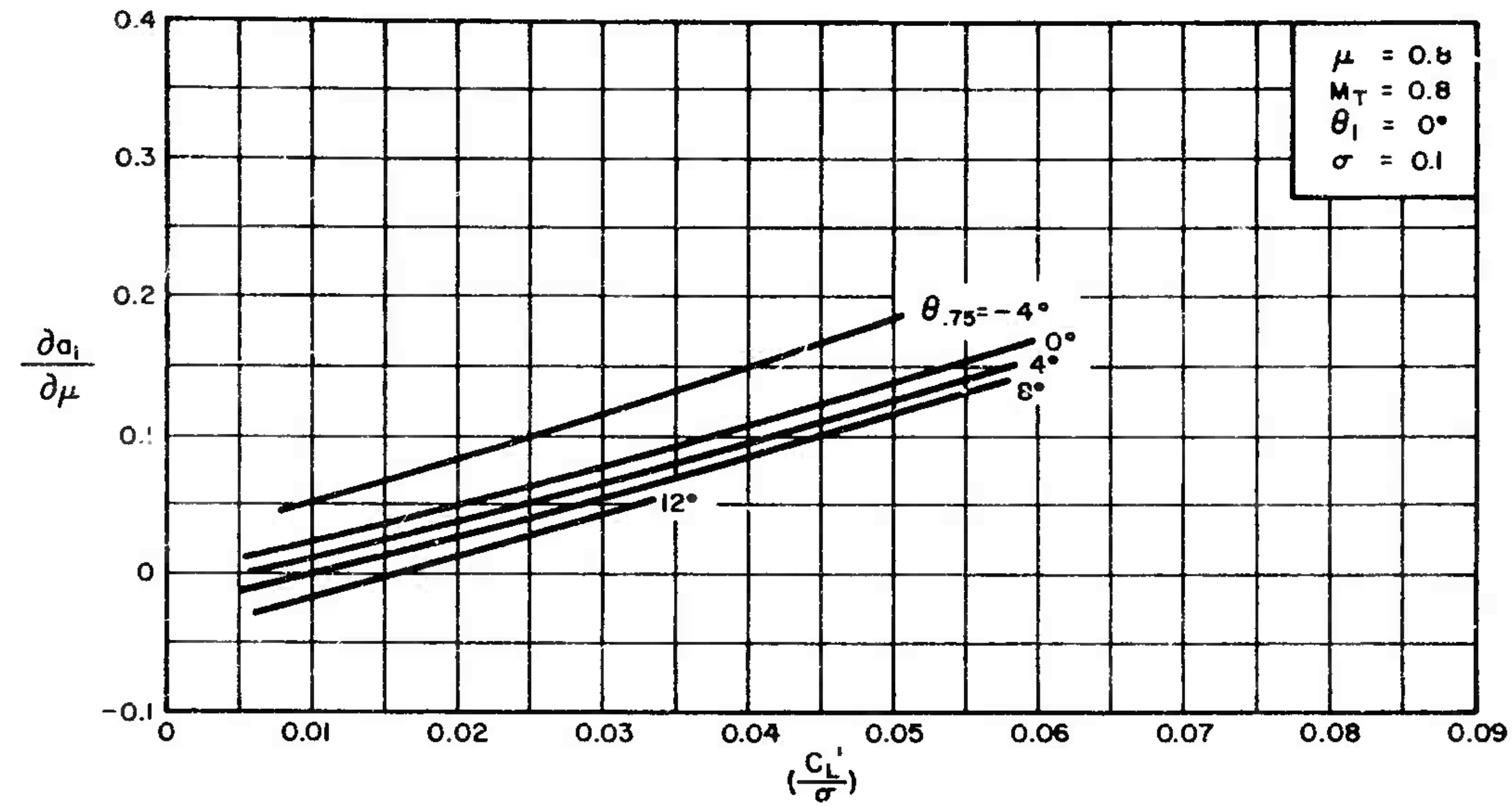

(f) μ = 0.8

Figure 5. Continued.

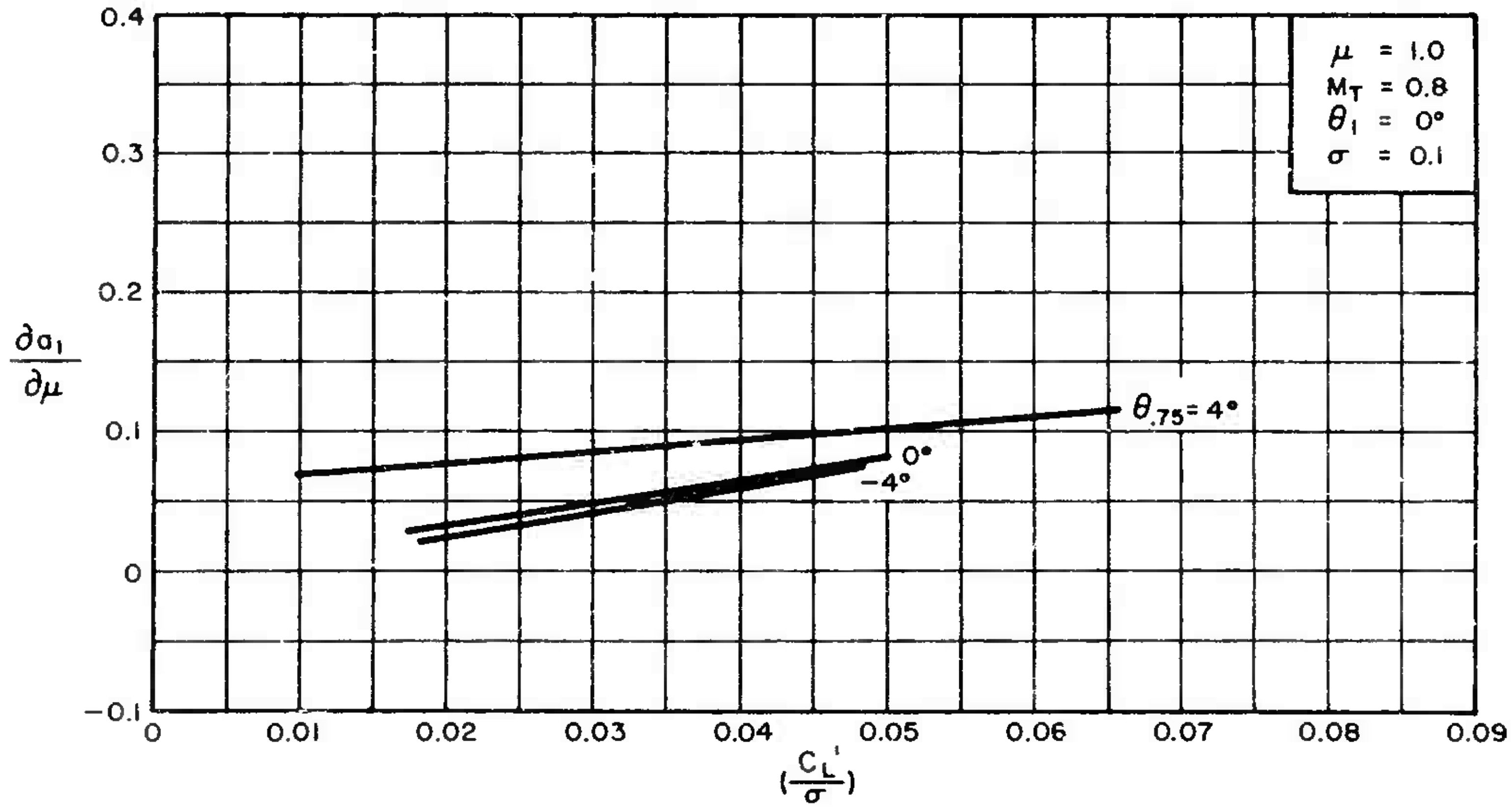

(g) $\mu = 1.0$

Figure 5. Concluded.

7.5.1.5 $\frac{\partial b_1}{\partial \mu}$ for $\sigma = 0.1$, $\theta_1 = 0°$, and $M_T = 0.8$

Figures 6(a) through 6(g) present the isolated rotor derivative $\partial b_1/\partial \mu$ as a function of C_L'/σ for constant values of $\theta_{.75}$ and a range of tip speed ratios from $\mu = 0.3$ through $\mu = 1.0$. The values of the above derivatives were extracted from the theoretical rotor performance data of Reference 2 by graphically obtaining the slopes of the b_1 versus μ relationships for constant values of $\theta_{.75}$ and a_C. These derivatives are specifically applicable to rotors having Lock inertia number $\gamma = 8.0$. However, since the lateral flapping angle b_1 is essentially proportional to γ, a correction factor of $\gamma/8.0$ may be used to compute $\partial b_1/\partial \mu$ derivatives applicable to rotors having γ values other than 8.0. Thus:

$$\left(\frac{\partial b_1}{\partial \mu}\right)_{\gamma} = \frac{\gamma}{8.0}\left(\frac{\partial b_1}{\partial \mu}\right)_{\gamma = 8.0}$$

The $\frac{\partial b_1}{\partial \mu}$ derivatives for $\mu \leq 0.2$ can be computed by using the following equation:

$$\frac{\partial b_1}{\partial \mu} = \gamma\left[\lambda\left(0.2091 - \frac{\mu^2}{3}\right) + \frac{\partial \lambda}{\partial \mu}(t_{17}) + \theta_{.75}(0.1388 + 0.2425\mu^2)\right]$$

where $\frac{\partial \lambda}{\partial \mu}$ can be obtained from Subsection 7.5.1.6 and where values of t_{17} can be obtained from Table 8-1, page 205 of Reference 4.

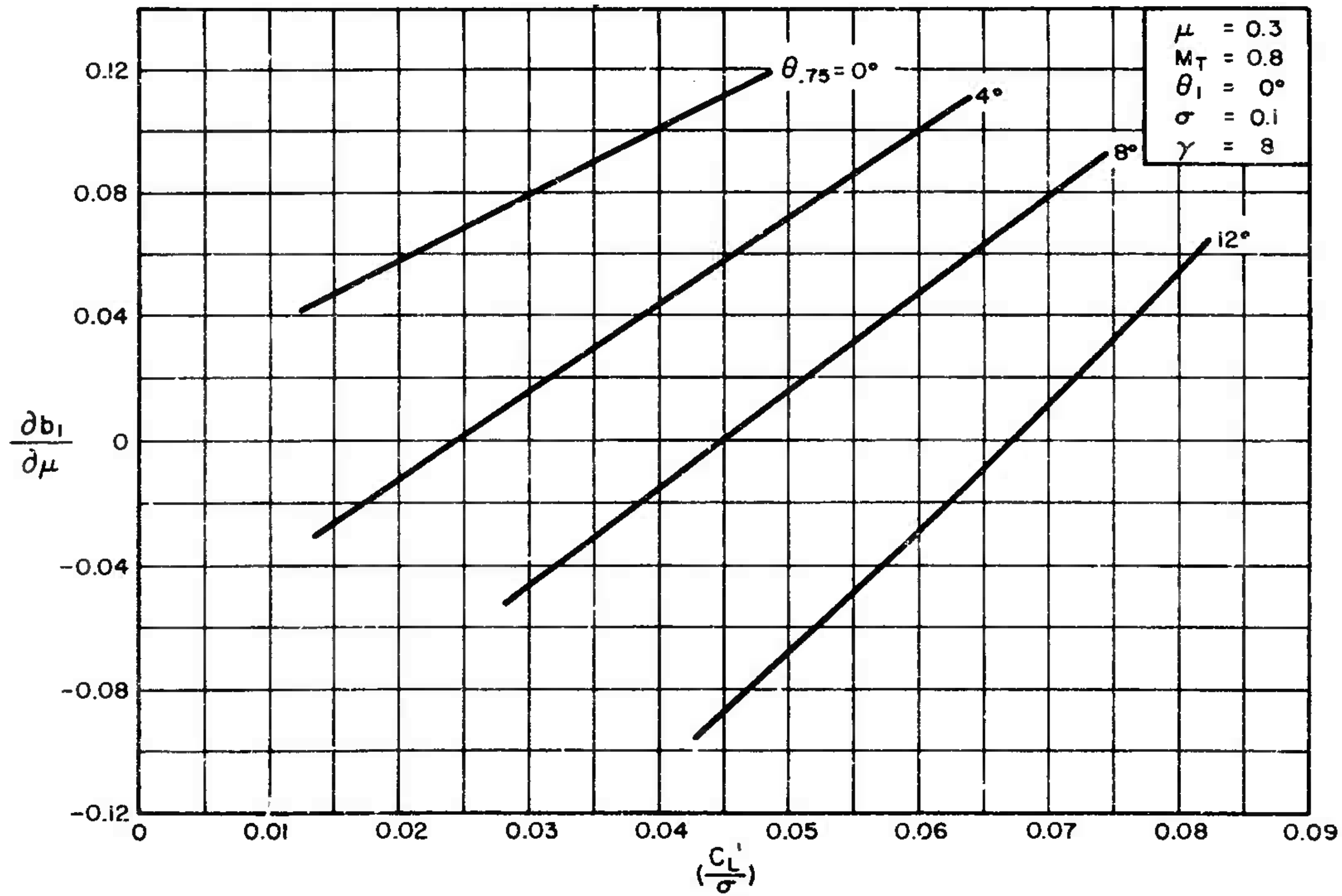

(a) $\mu = 0.3$

Figure 6. Variation of $\frac{\partial b_1}{\partial \mu}$ With $\frac{C_L'}{\sigma}$ for Constant Values of $\theta_{.75}$.

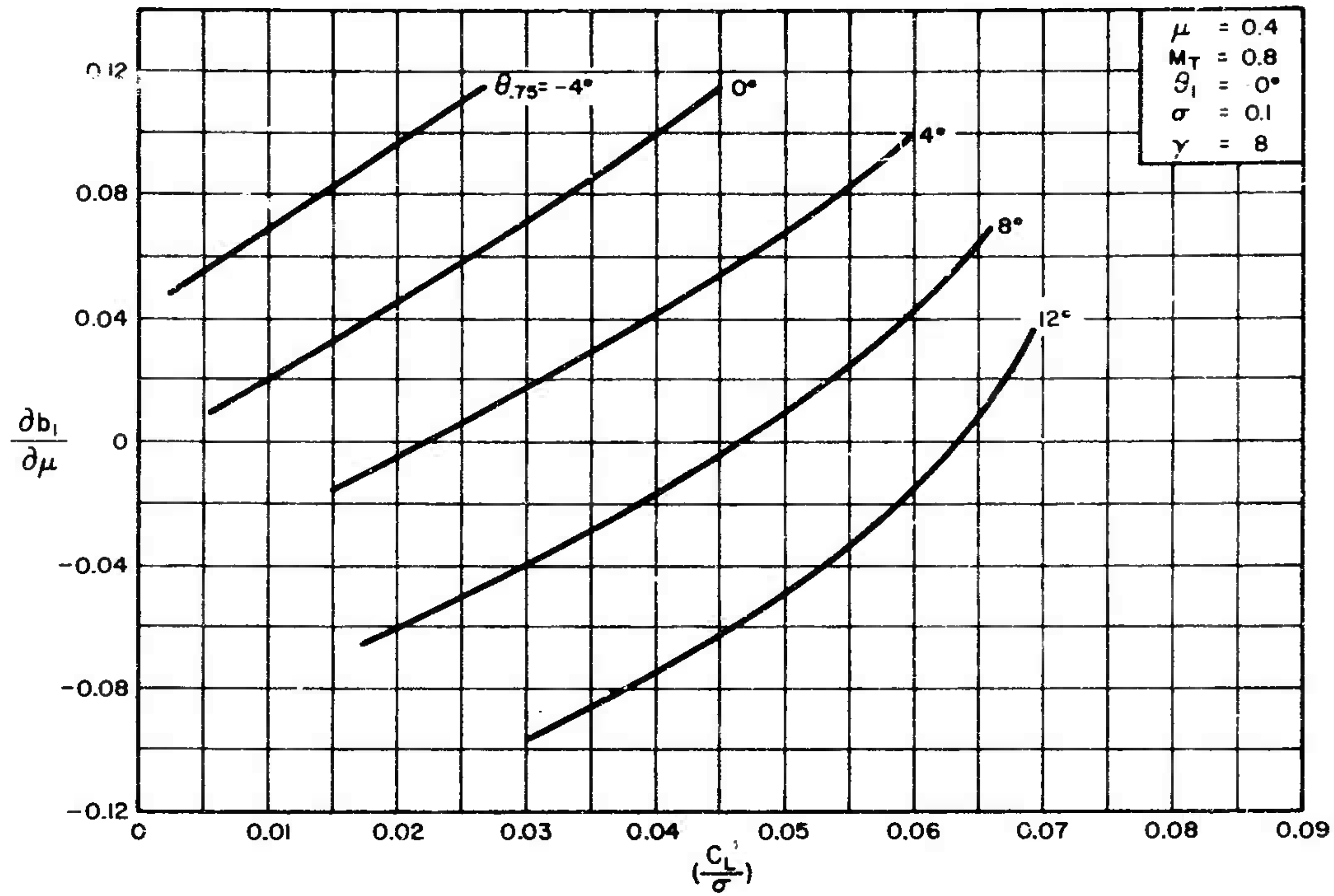

(b) $\mu = 0.4$

Figure 6. Continued.

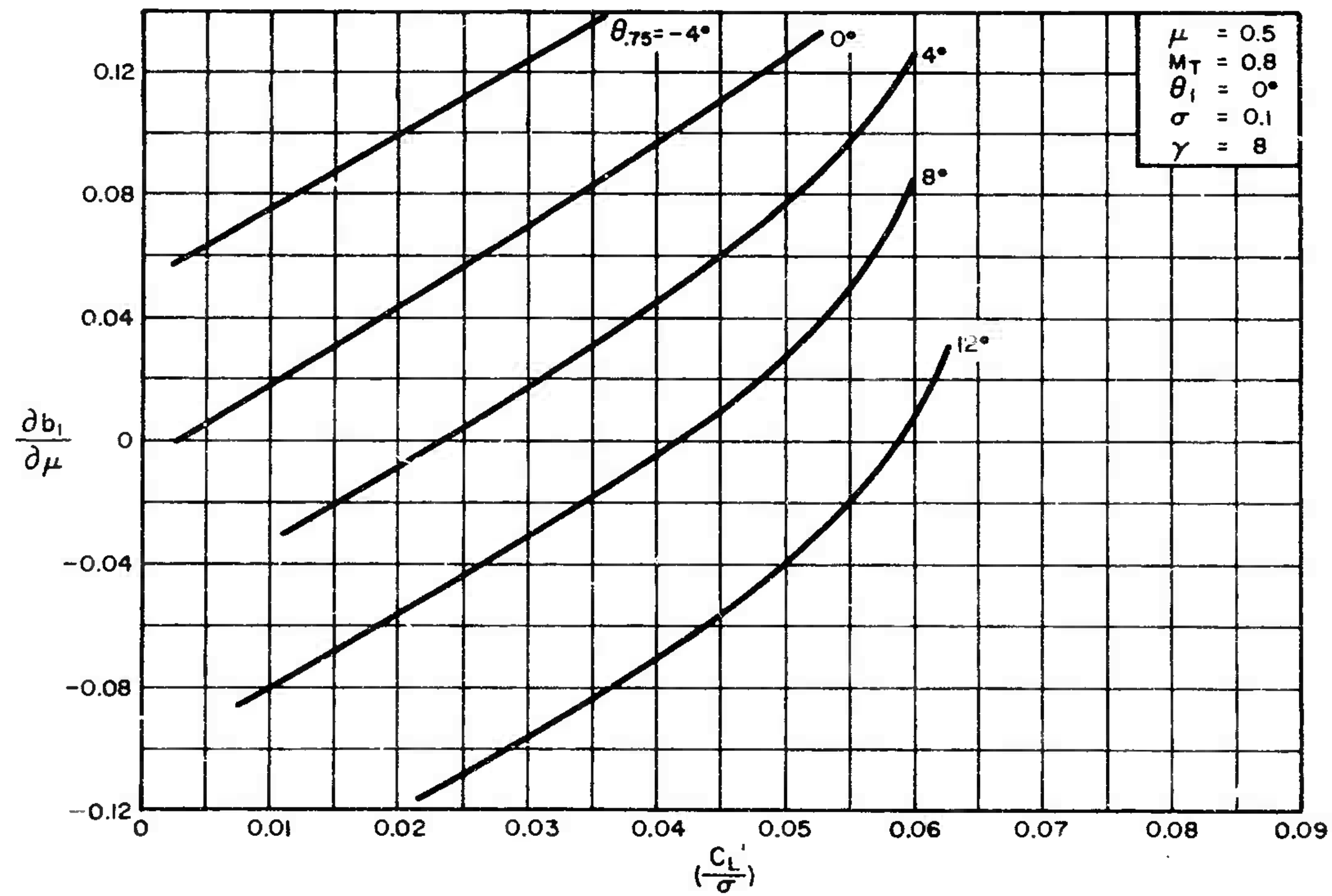

(c) $\mu = 0.5$

Figure 6. Continued.

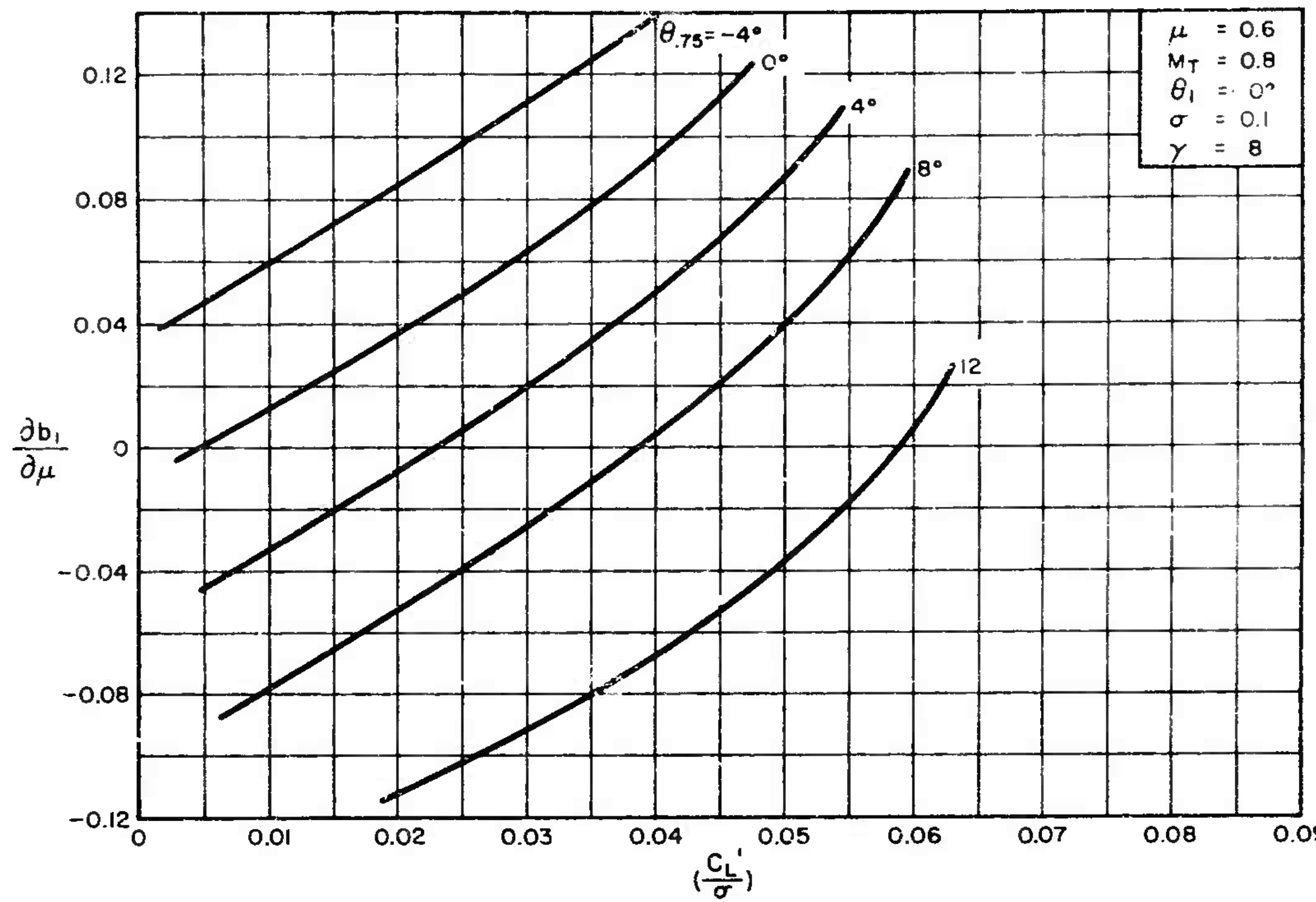

(d) $\mu = 0.6$

Figure 6. Continued.

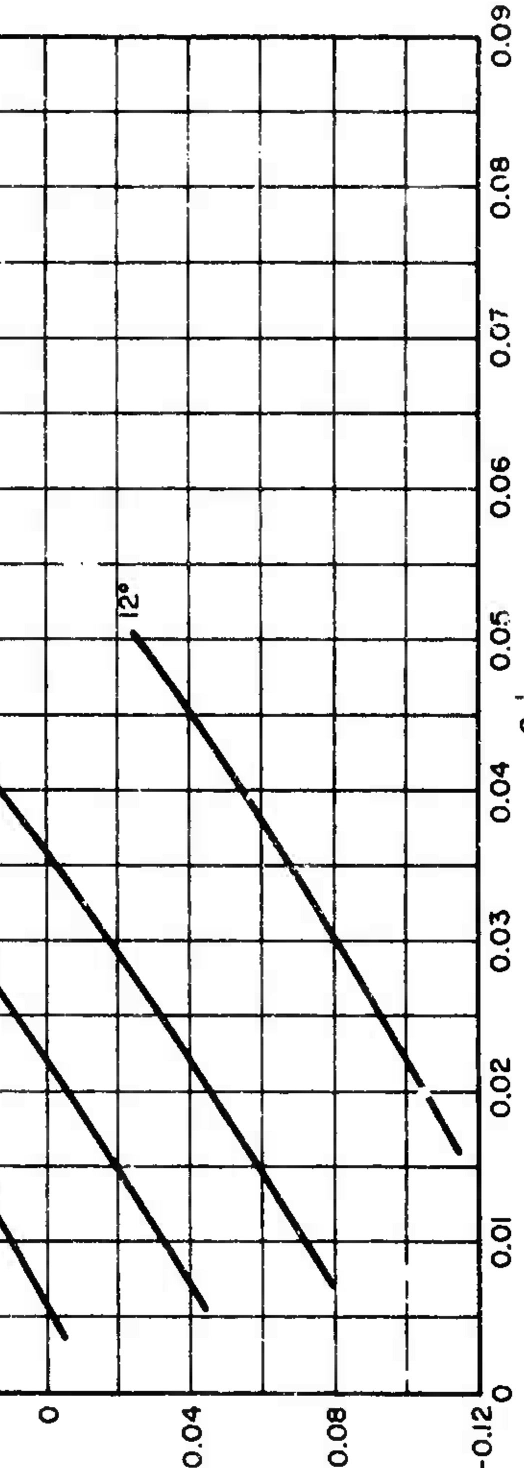

(e) $\mu = 0.7$

Figure 6. Continued.

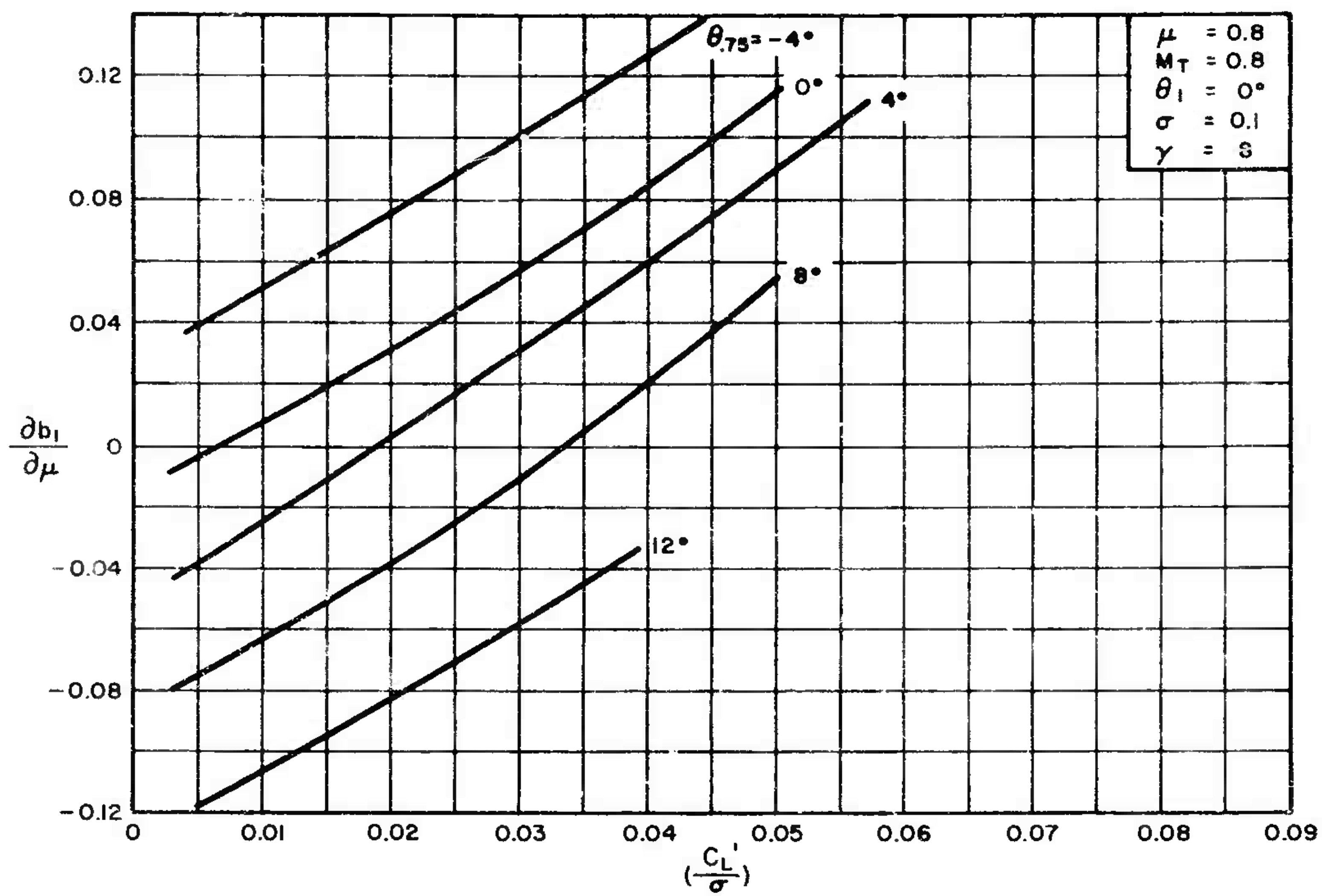

(f) μ = 0.8

Figure 6. Continued.

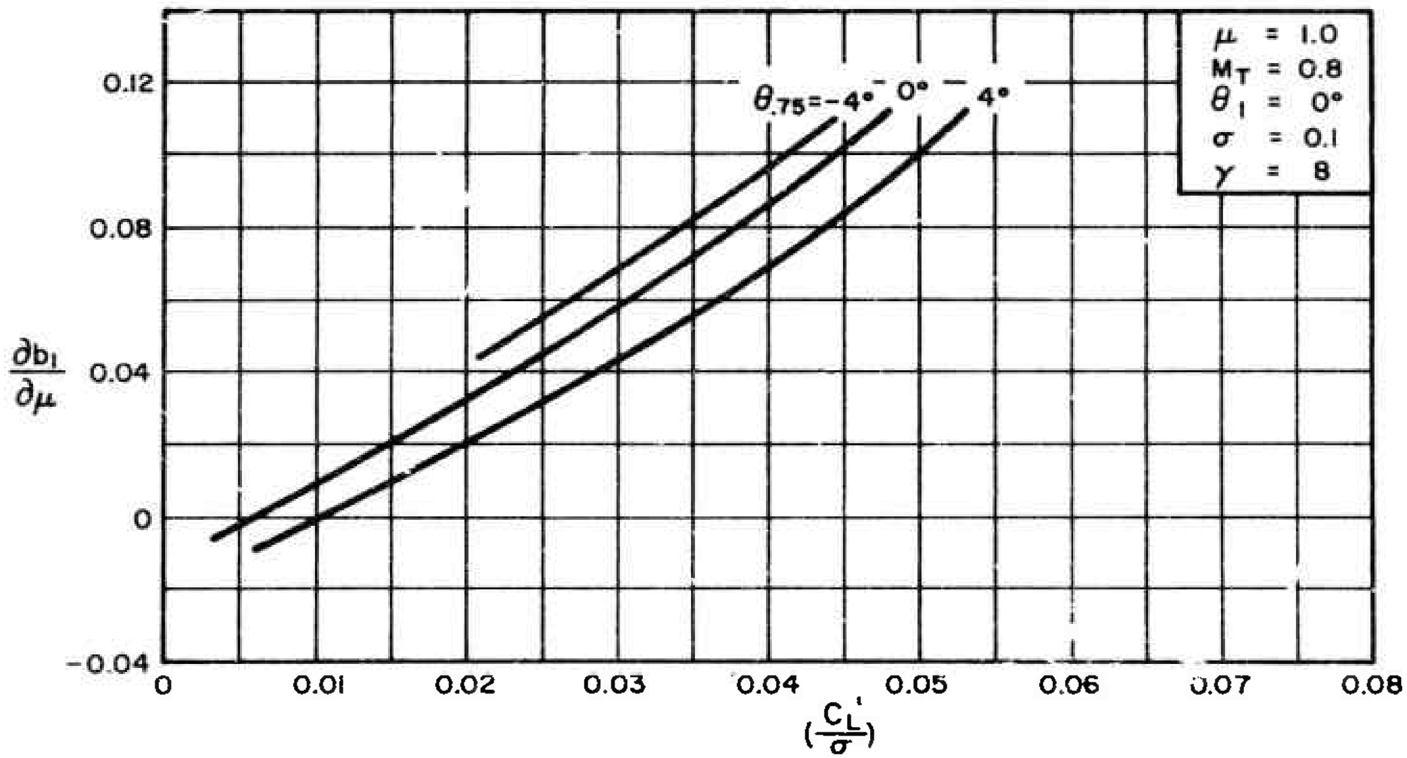

(g) μ = 1.0

Figure 6. Concluded.

7.5.1.6 $\frac{\partial \lambda}{\partial \mu}$ for $\sigma = 0.1$, $\theta_1 = 0°$, and $M_T = 0.8$

Figures 7(a) through 7(i) present the isolated rotor derivative $\partial\lambda/\partial\mu$ as a function of C_L'/σ for constant values of $\theta_{.75}$ for a range of μ values of $\mu = 0.1$ through $\mu = 1.0$. The values of $\partial\lambda/\partial\mu$ for $\mu = 0.1$ and 0.2 were obtained directly from Reference 3. The values for $\mu \geq 0.3$ were extracted from the theoretical rotor performance data of Reference 2 by graphically obtaining the slopes of the λ versus μ relationships for constant values of $\theta_{.75}$ and α_c.

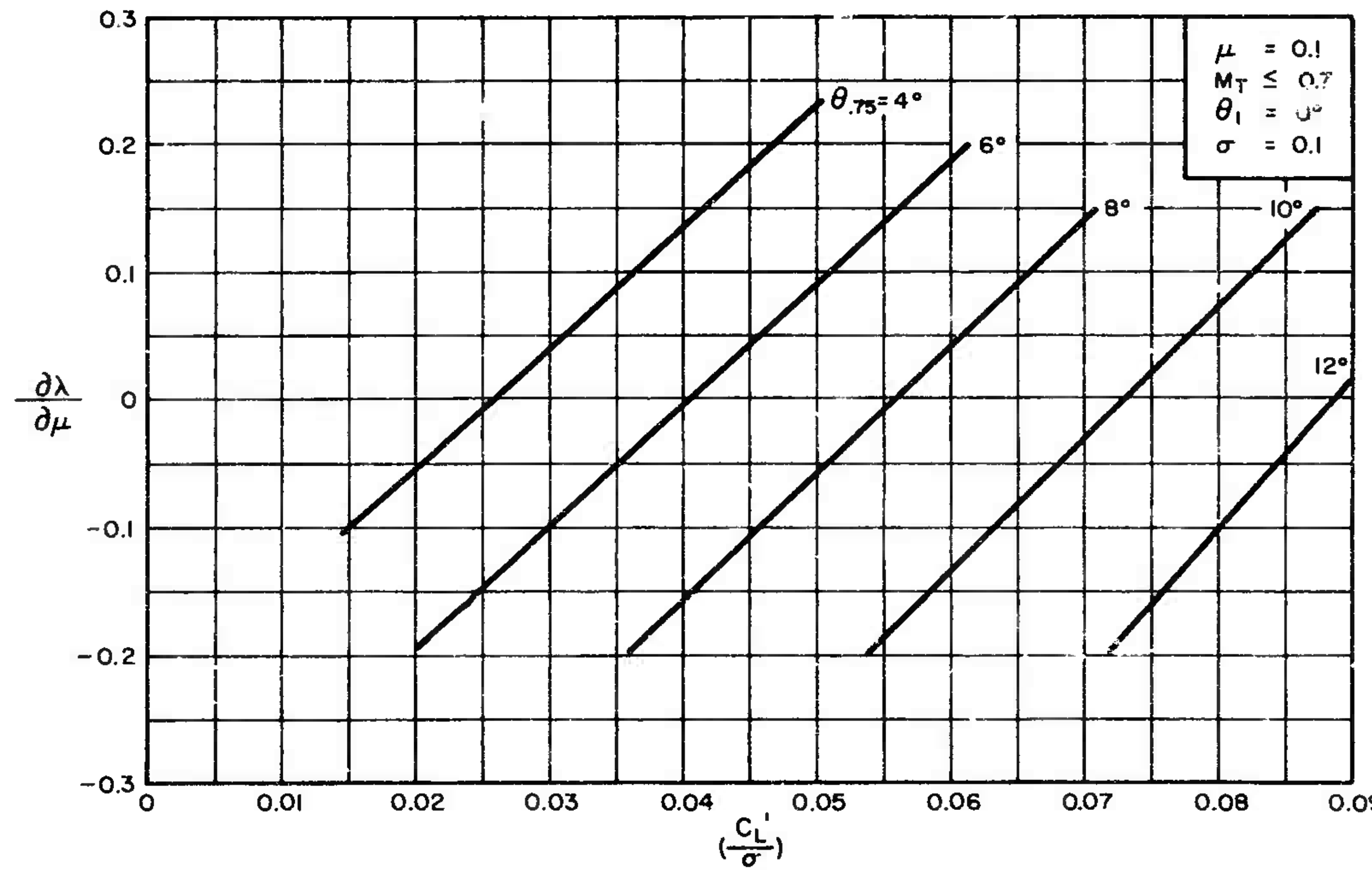

(a) $\mu = 0.1$

Figure 7. Variation of $\frac{\partial \lambda}{\partial \mu}$ With $\frac{C_L'}{\sigma}$ for Constant Values of $\theta_{.75}$.

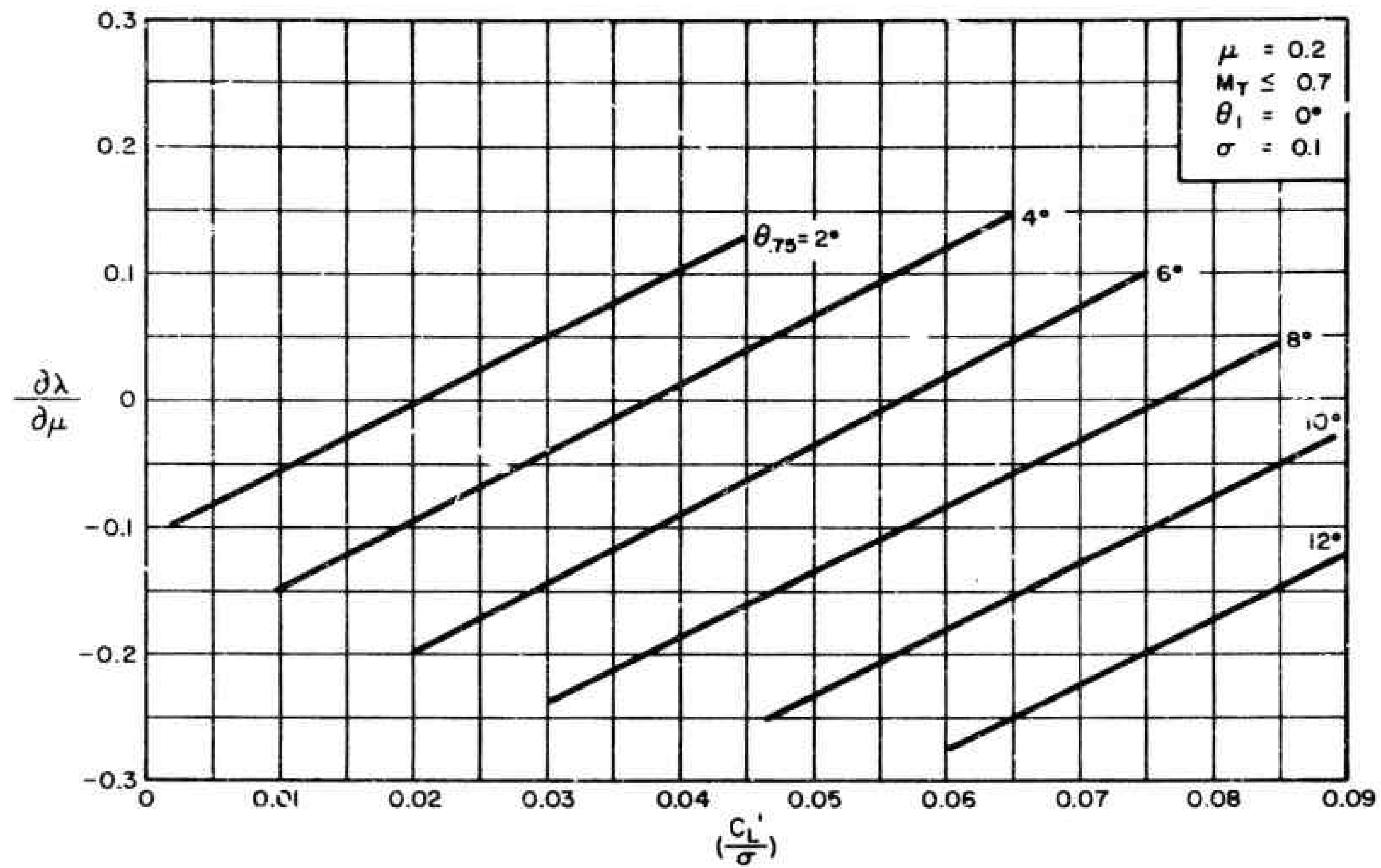

(b) μ = 0.2

Figure 7. Continued.

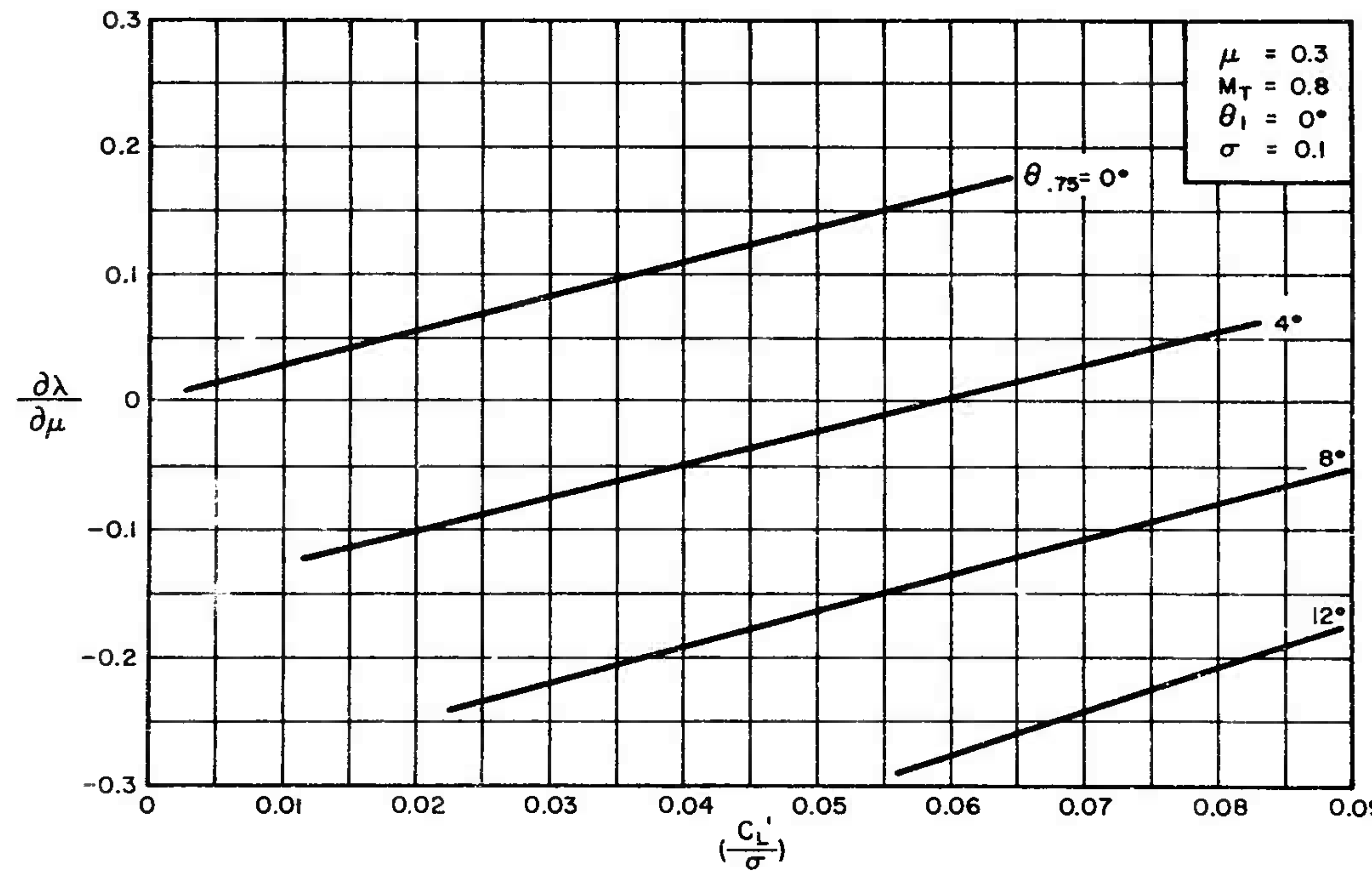

(c) $\mu = 0.3$

Figure 7. Continued.

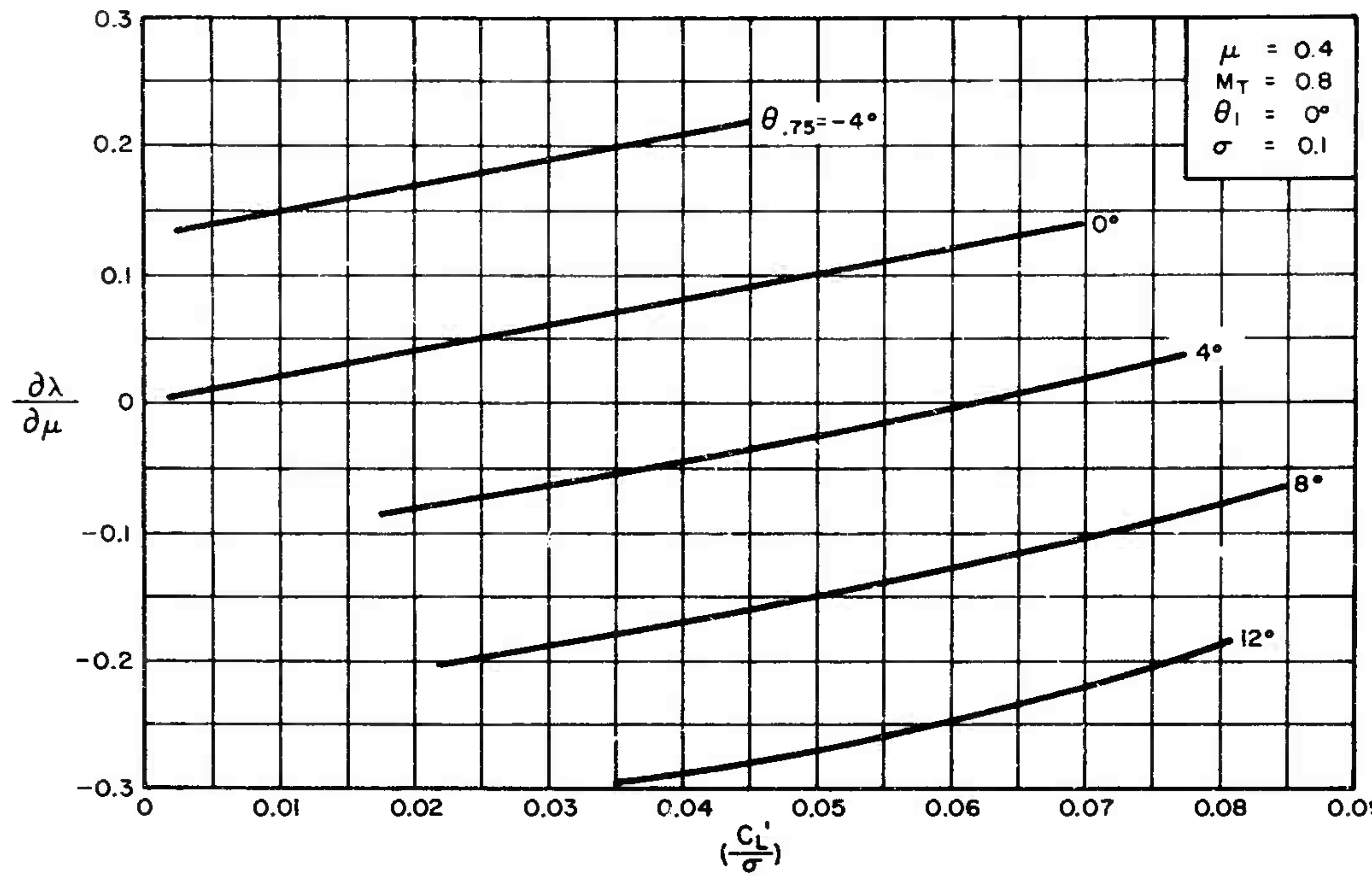

(d) μ = 0.4

Figure 7. Continued.

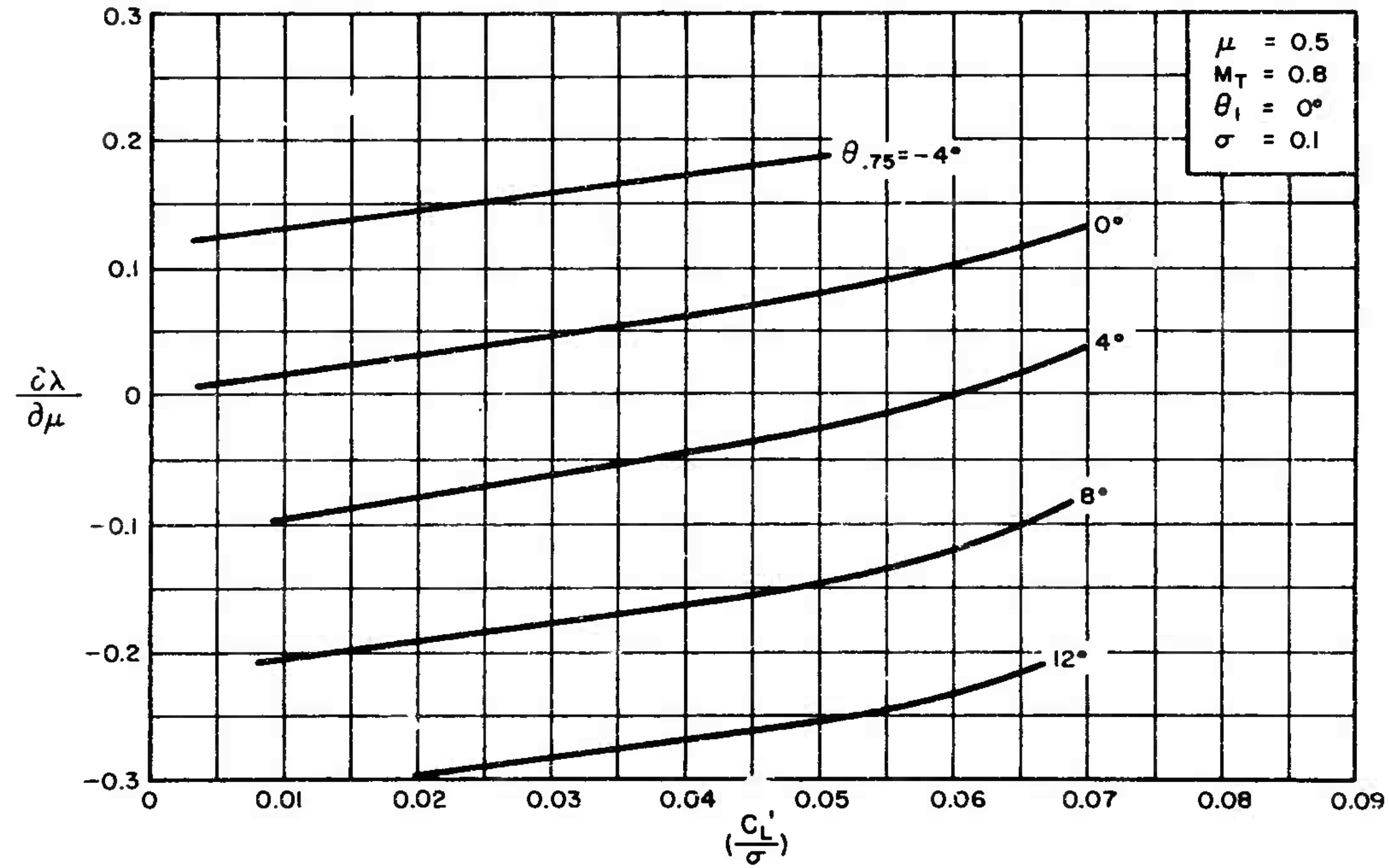

(e) $\mu = 0.5$

Figure 7. Continued.

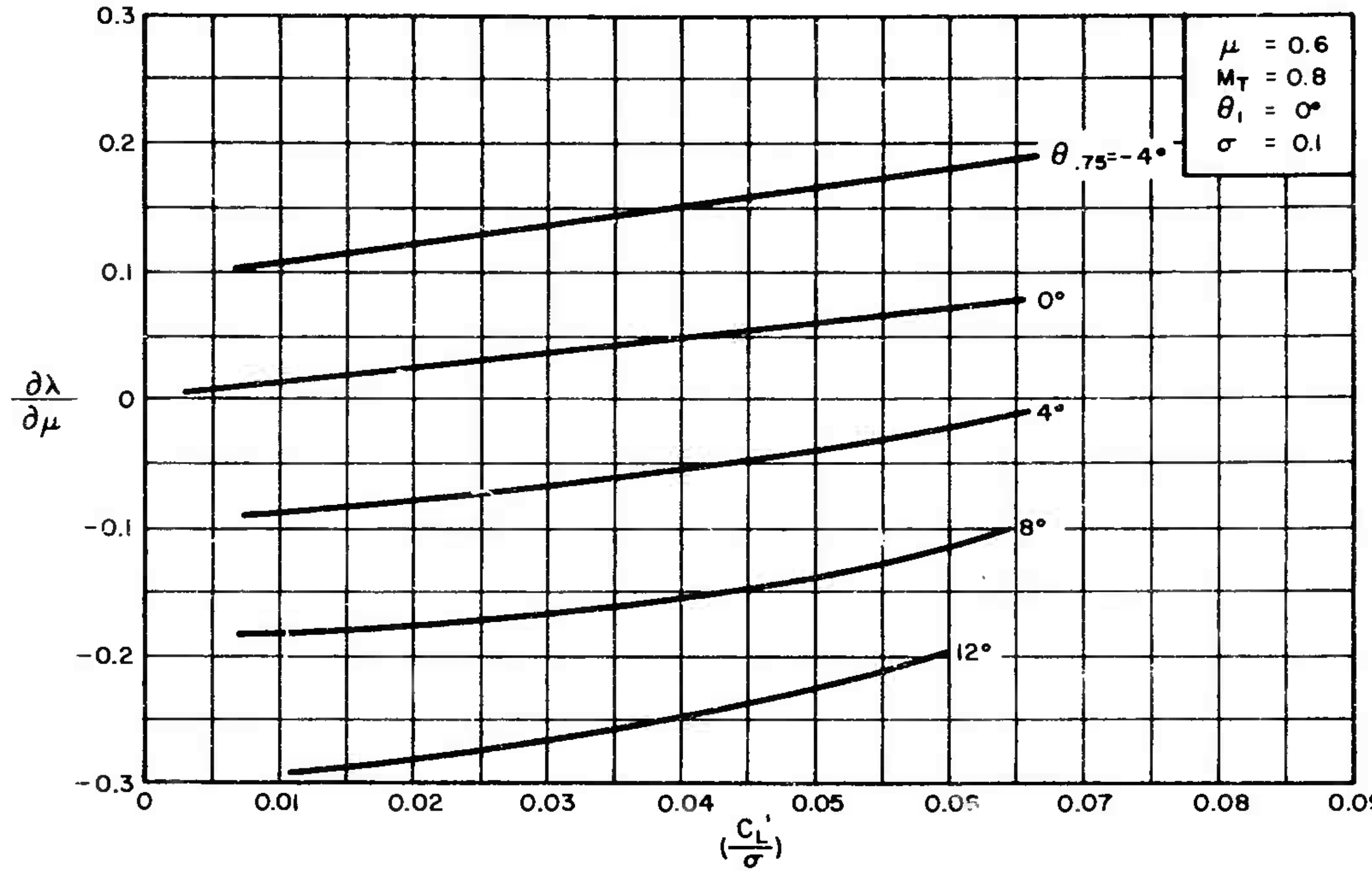

(f) $\mu = 0.6$

Figure 7. Continued.

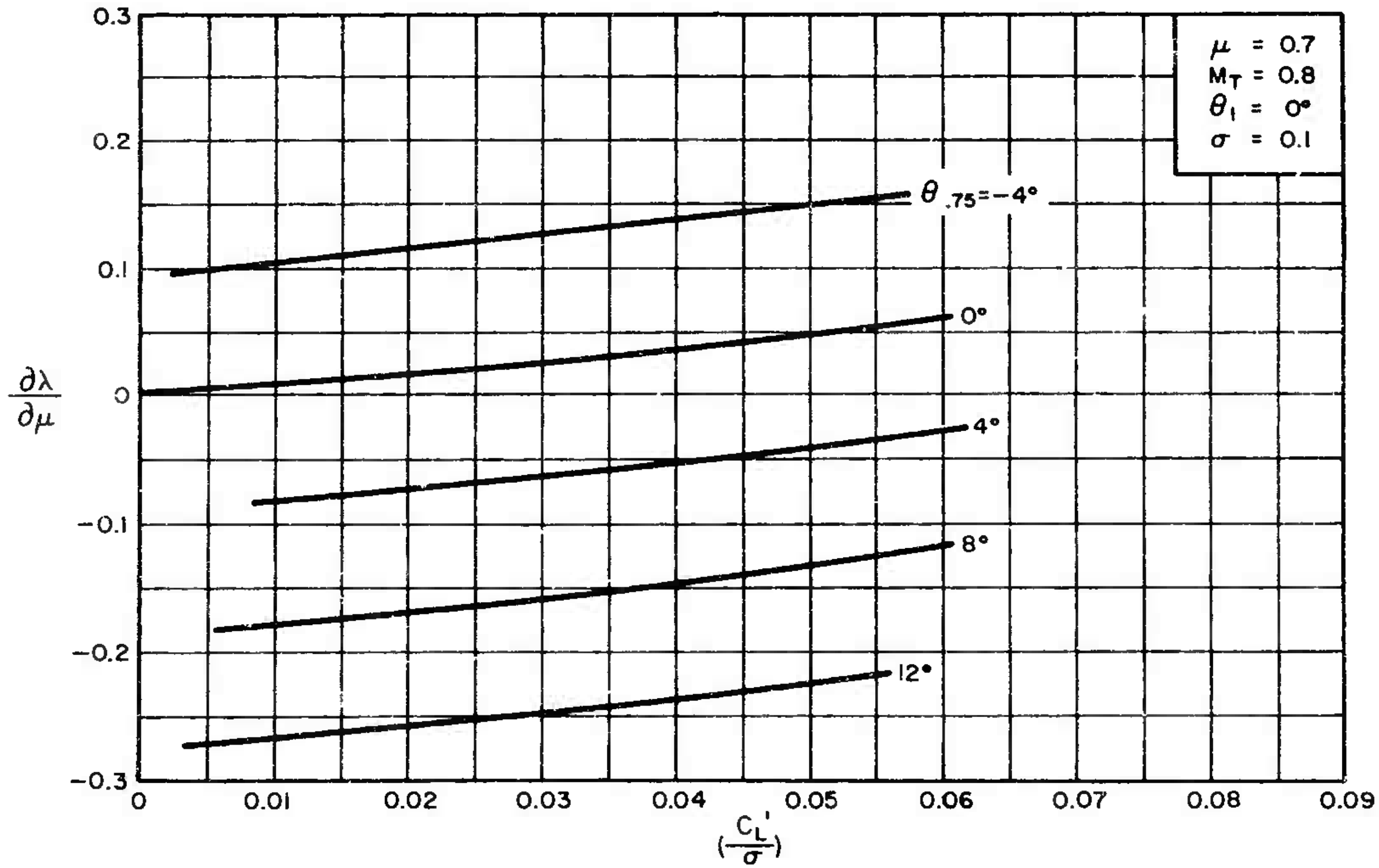

(g) μ = 0.7

Figure 7. Continued.

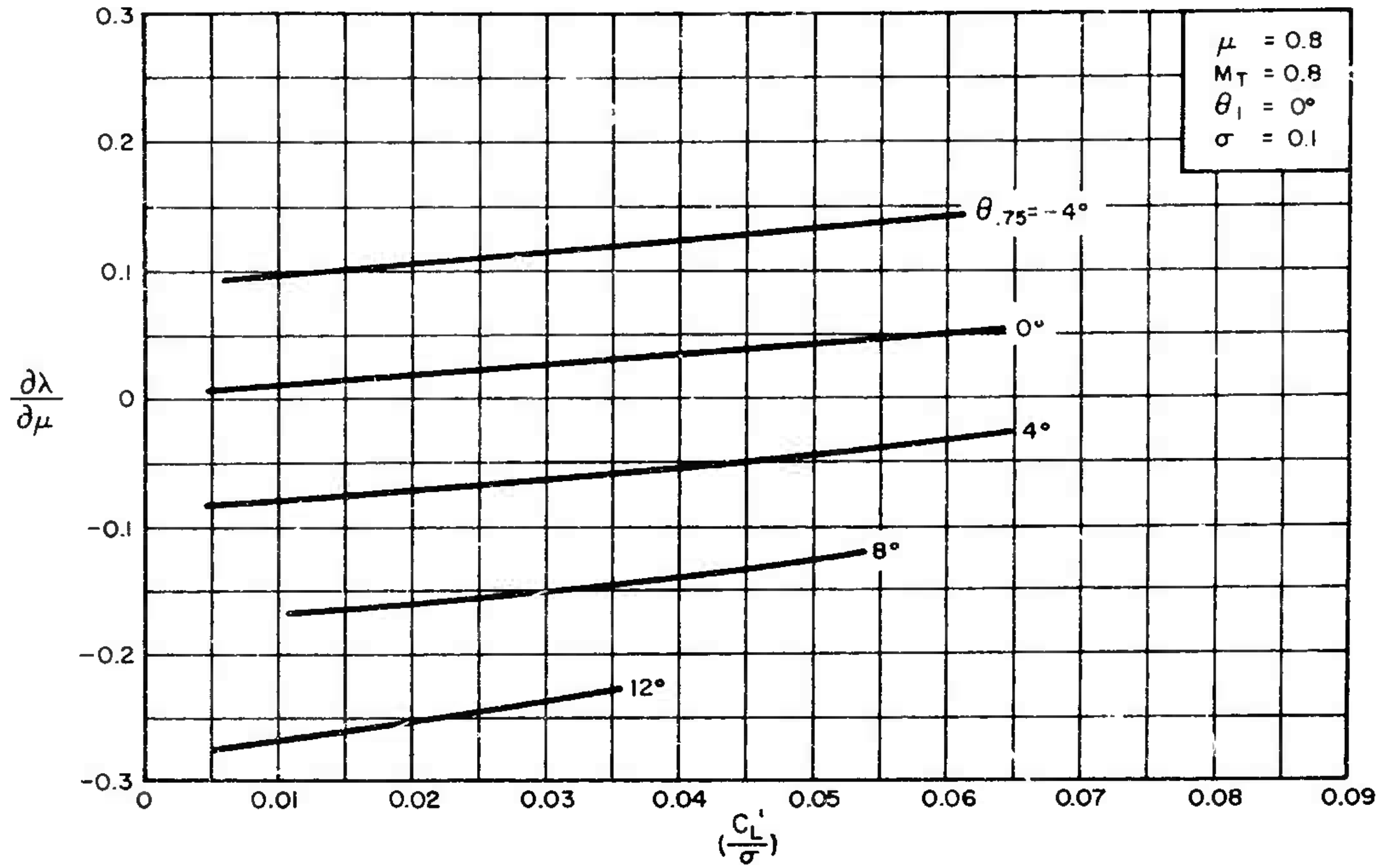

(h) $\mu = 0.8$

Figure 7. Continued.

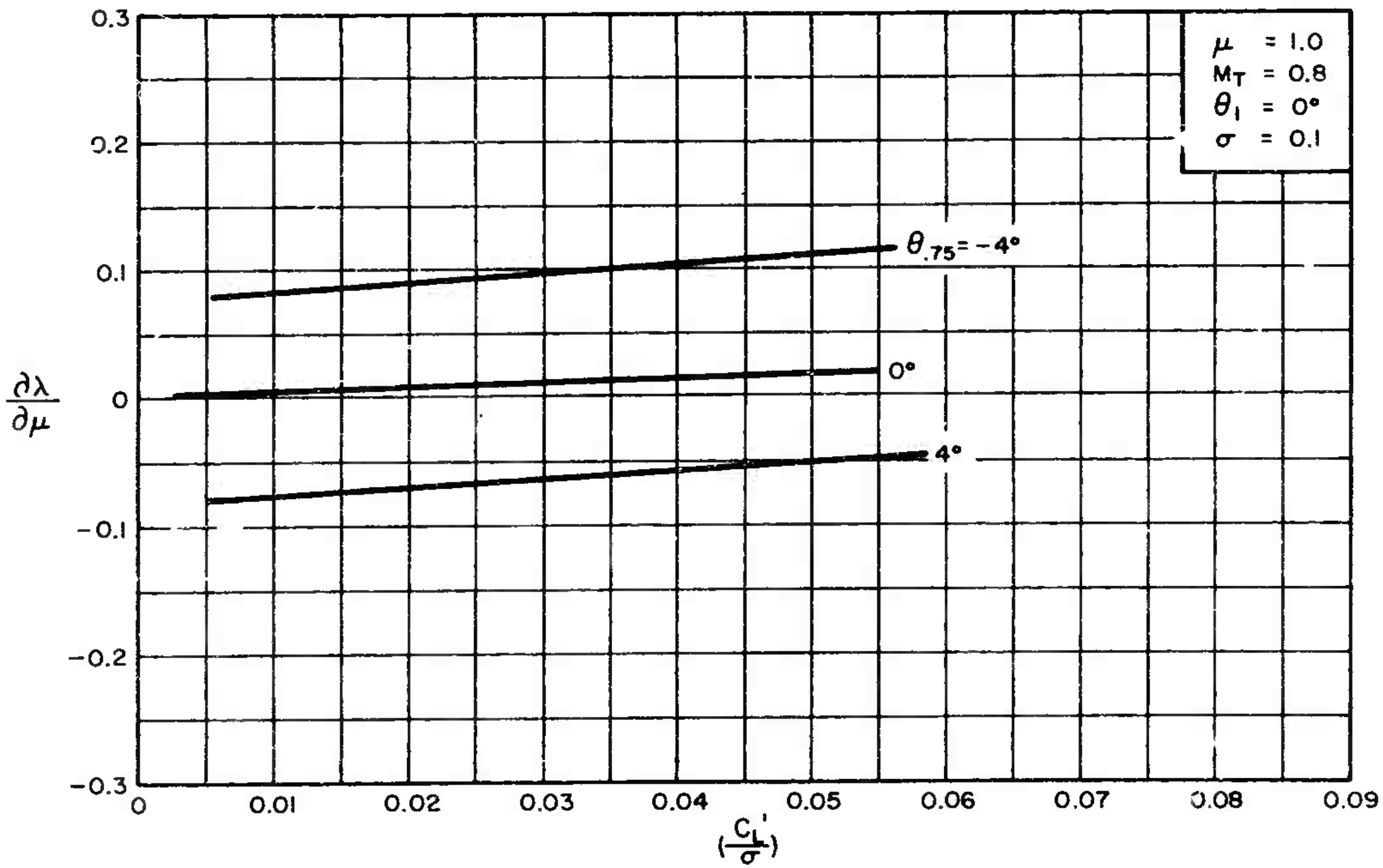

(i) $\mu = 1.0$

Figure 7. Concluded.

7.5.1.7 $\frac{\partial(C_Y'/\sigma)}{\partial\mu}$ for All Values of σ, θ_1, and M_T

Reference 2 and other reviewed reports do not include the calculated data required to determine the rotor Y-force derivatives. It is therefore suggested that the classical Bailey theory be used for this purpose. If the above theory is used, the following expression for $\partial(C_Y'/\sigma)/\partial\mu$ can be derived:

$$
\begin{aligned}
\frac{\partial(\frac{C_Y'}{\sigma})}{\partial\mu} = \frac{a}{2}\Bigg\{ & \frac{\partial a_0}{\partial\mu}\left[a_1\left(\frac{1}{6}-\mu^2\right)-\frac{3}{4}\mu(\theta_{.75}+2\lambda)\right] \\
& + \frac{\partial a_1}{\partial\mu}\left[a_0\left(\frac{1}{6}-\mu^2\right)+\frac{1}{4}\mu b_1\right] \\
& + \frac{\partial b_1}{\partial\mu}\left[\theta_{.75}\left(\frac{1}{3}+\frac{3}{8}\mu^2\right)+\lambda\left(\frac{3}{4}+\frac{1}{8}\mu^2\right)+\frac{1}{4}\mu a_1\right] \\
& + \frac{\partial\lambda}{\partial\mu}\left[b_1\left(\frac{3}{4}+\frac{1}{8}\mu^2\right)-\frac{3}{2}\mu a_0\right] \\
& + \frac{1}{4}b_1\left[\mu(3\theta_{.75}+\lambda)+a_1\right]-a_0\left[\frac{3}{4}\theta_{.75}+\frac{2}{3}\lambda-2\mu a_1\right]\Bigg\}
\end{aligned}
$$

where

$$
\frac{\partial a_0}{\partial\mu} = \frac{\gamma}{2}\left[\frac{\theta_{.75}}{2}\mu+\frac{1}{3}\frac{\partial\lambda}{\partial\mu}\right]
$$

and where $\partial a_1/\partial\mu$, $\partial b_1/\partial\mu$, and $\partial\lambda/\partial\mu$ are given in Subsections 7.5.1.4, 7.5.1.5, and 7.5.1.6, respectively.

The above derivative is applicable to all values of σ, θ_1, and M_T, provided that the pertinent rotor parameters comprising it are evaluated at the required condition.

7.5.2 Isolated Rotor Derivatives With Respect to Rotor Angle of Attack (α_C)

7.5.2.1 $\dfrac{\partial(\frac{C_L'}{\sigma})}{\partial\alpha_C}$ for $\sigma = 0.1$, $\theta_1 = 0°$ and $M_T = 0.8$

Figures 8(a) through 8(d) present the isolated rotor derivative $\partial(C_L'/\sigma)/\partial\alpha_C$ as a function of C_L'/σ for constant values of μ covering a range of collective pitch settings from $\theta_{.75} = 0$ to $\theta_{.75} = 12°$.

The derivatives for $\mu \leq 0.2$ were extracted from the data of Reference 3 by using the following expression:

$$\frac{\partial(\frac{C_L'}{\sigma})}{\partial\alpha_C} = \left[\frac{\partial(\frac{C_T}{\sigma})}{\partial\alpha_C} - \frac{C_H}{\sigma}\right]\cos\alpha_C - \left[\frac{\partial(\frac{C_H}{\sigma})}{\partial\alpha_C} + \frac{C_T}{\sigma}\right]\sin\alpha_C$$

The values of $\partial(C_T/\sigma)/\partial\alpha_C$ and $\partial(C_H/\sigma)/\partial\alpha_C$ obtained from Reference 3 are found to be practically independent of $\theta_{.75}$ and C_L'/σ variations.

The values of $\partial(C_L'/\sigma)/\partial\alpha_C$ for $\mu \geq 0.3$ were extracted from the theoretical data of Reference 2 by graphically obtaining slopes of the C_L'/σ vs. α_C relationships for constant values of μ and $\theta_{.75}$.

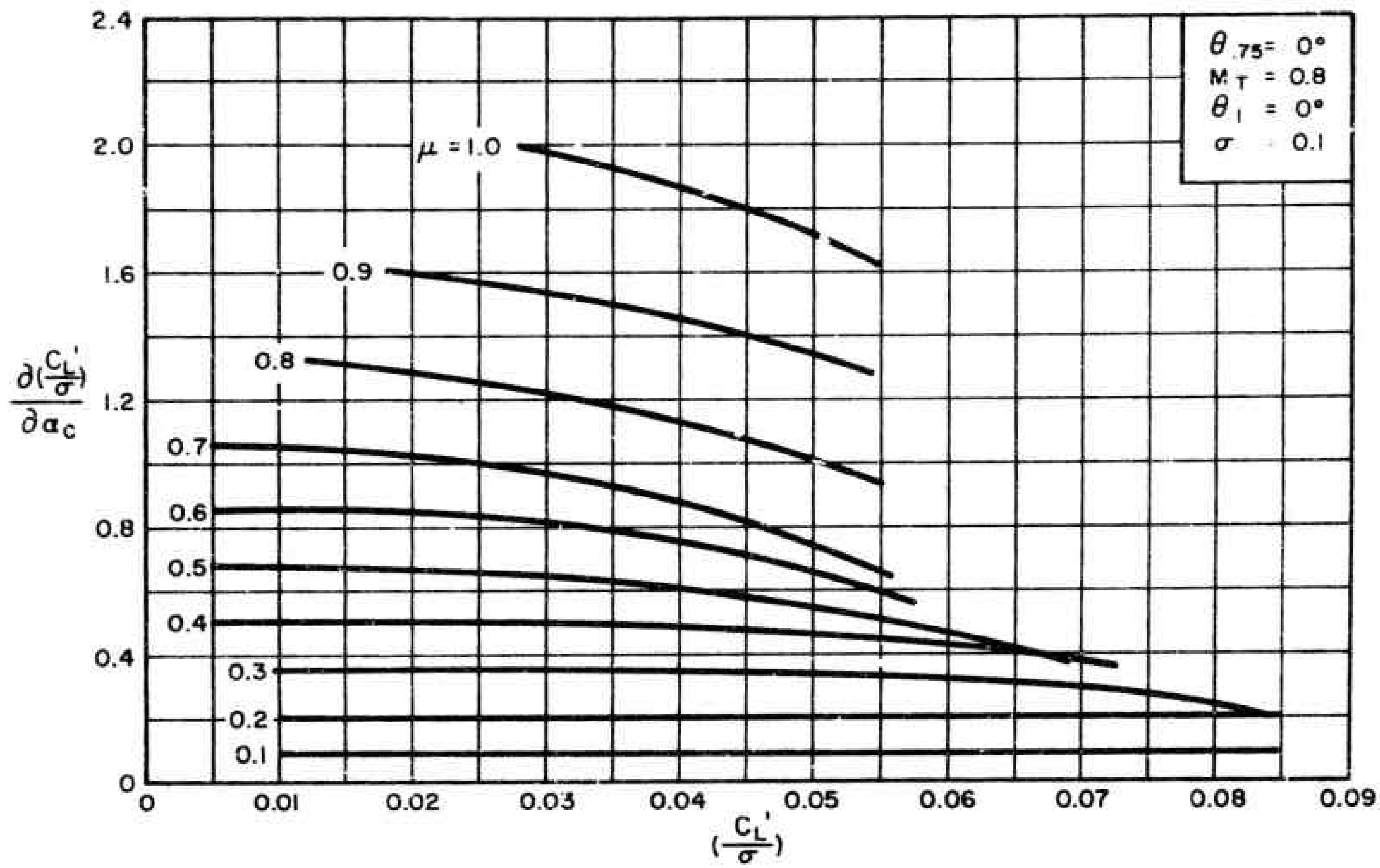

(a) $\theta_{.75} = 0°$

Figure 8. Variation of $\frac{\partial(\frac{C_L'}{\sigma})}{\partial \alpha_c}$ With $\frac{C_L'}{\sigma}$ for Constant Values of μ .

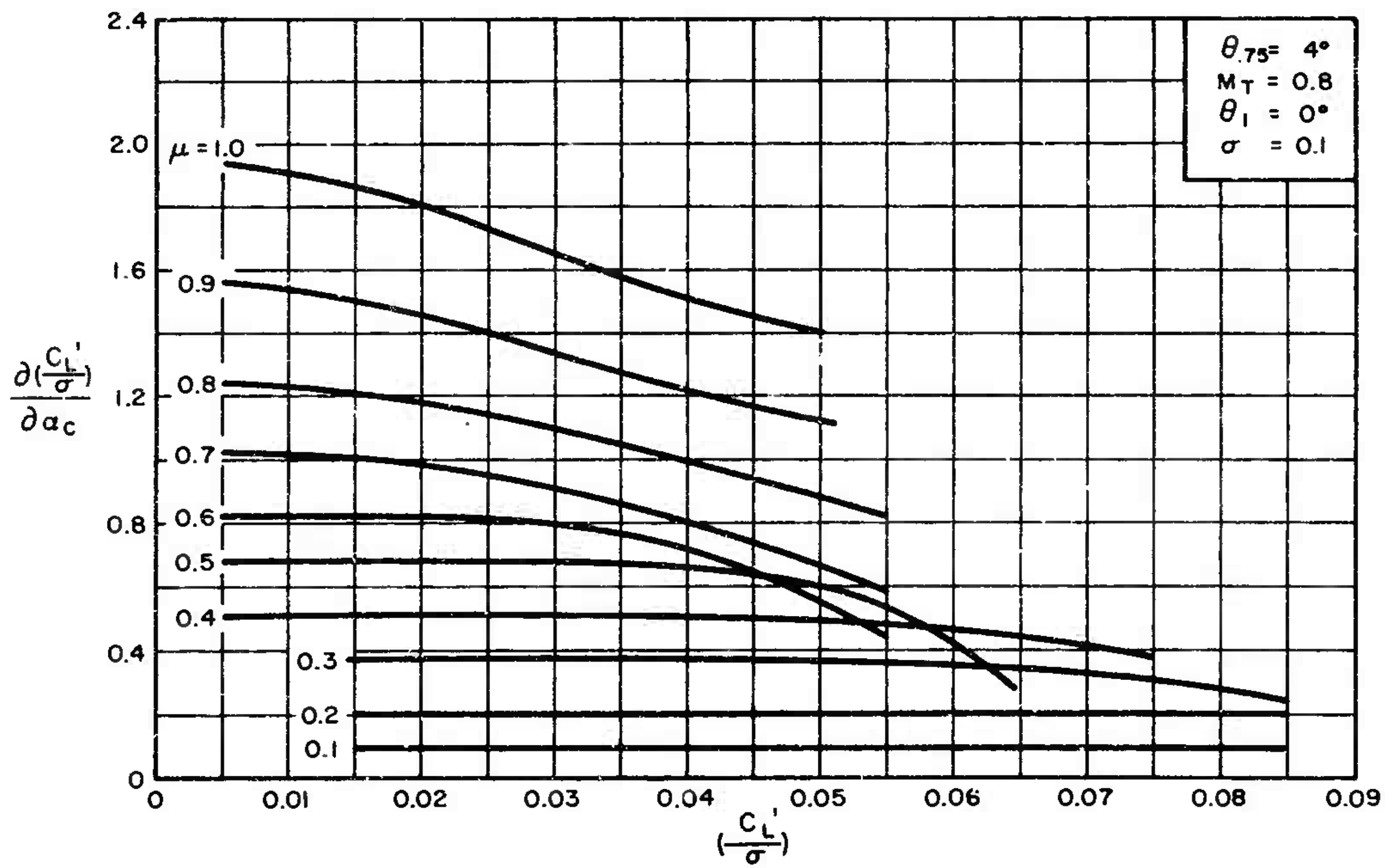

(b) $\theta_{.75} = 4°$

Figure 8. Continued.

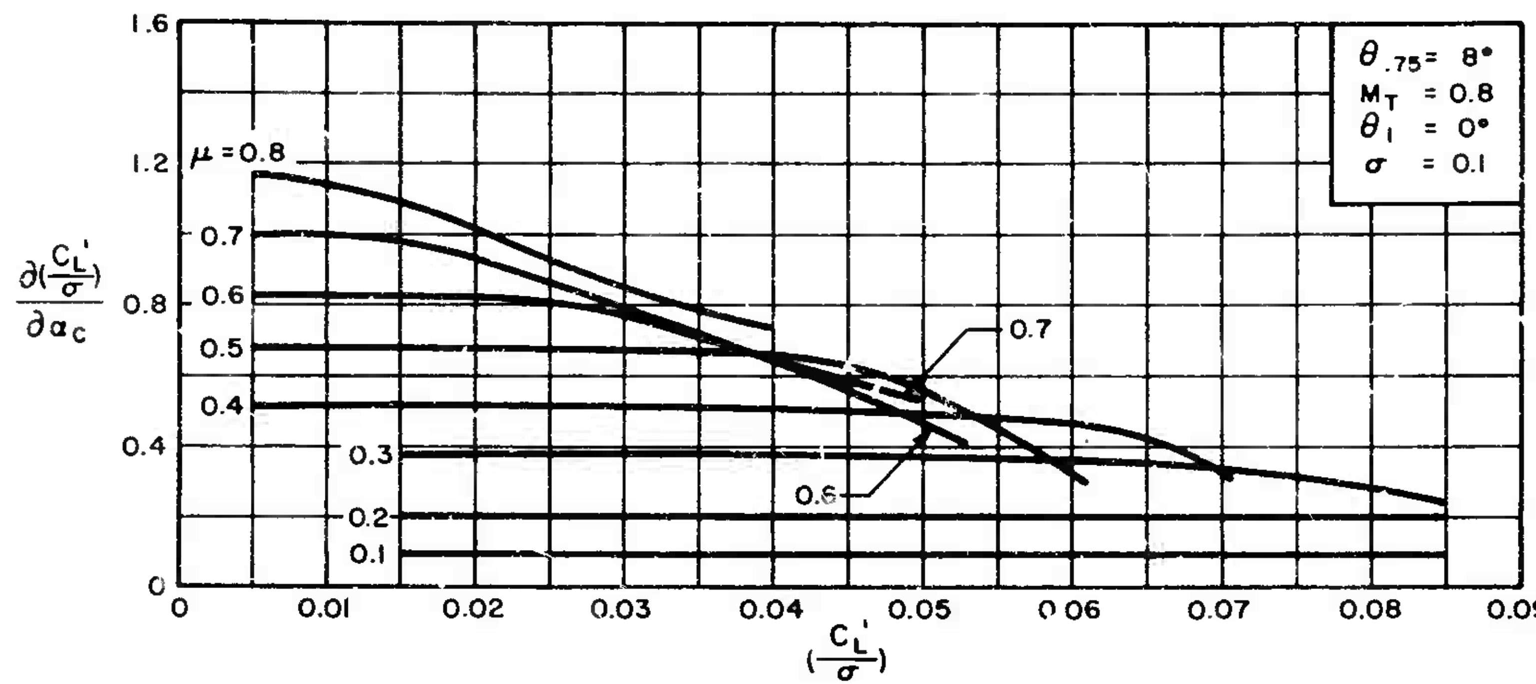

(c) $\theta_{.75} = 8°$

Figure 8. Continued.

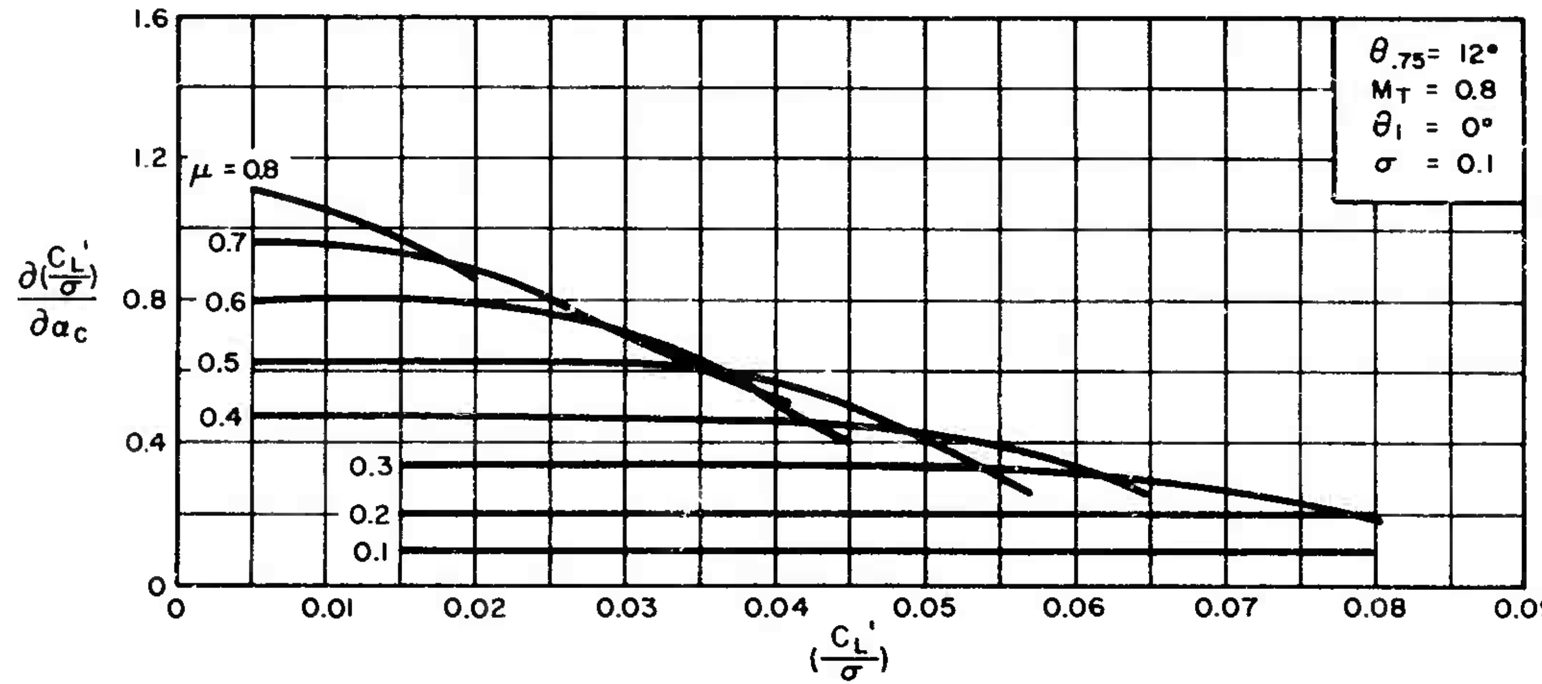

(d) $\theta_{.75} = 12°$

Figure 8. Concluded.

7.5.2.2 $\dfrac{\partial(\frac{C_D'}{\sigma})}{\partial\alpha_C}$ for $\sigma = 0.1$, $\theta_1 = 0°$, and $M_T = 0.8$

Figures 9(a) through 9(i) present the isolated rotor derivative $\partial(C_D'/\sigma)/\partial\alpha_C$ as a function of C_L'/σ for constant values of $\theta_{.75}$ and a range of μ from $\mu = 0.1$ through $\mu = 1.0$.

The values of $\partial(C_D'/\sigma)/\partial\alpha_C$ for $\mu = 0.1$ and $\mu = 0.2$ were obtained from Reference 3 by using the following equation:

$$\frac{\partial(\frac{C_D'}{\sigma})}{\partial\alpha_C} = \left[\frac{\partial(\frac{C_H}{\sigma})}{\partial\alpha_C} + \frac{C_T}{\sigma}\right]\cos\alpha_C + \left[\frac{\partial(\frac{C_T}{\sigma})}{\partial\alpha_C} - \frac{C_H}{\sigma}\right]\sin\alpha_C$$

where $\partial(C_T/\sigma)/\partial\alpha_C$ and $\partial(C_H/\sigma)/\partial\alpha_C$ were obtained directly from Reference 3.

The values of $\partial(C_D'/\sigma)/\partial\alpha_C$ for $\mu \geq 0.3$ were extracted from the theoretical rotor performance data of Reference 2 by graphically obtaining slopes of the C_D'/σ vs. α_C relationships for constant values of μ and $\theta_{.75}$.

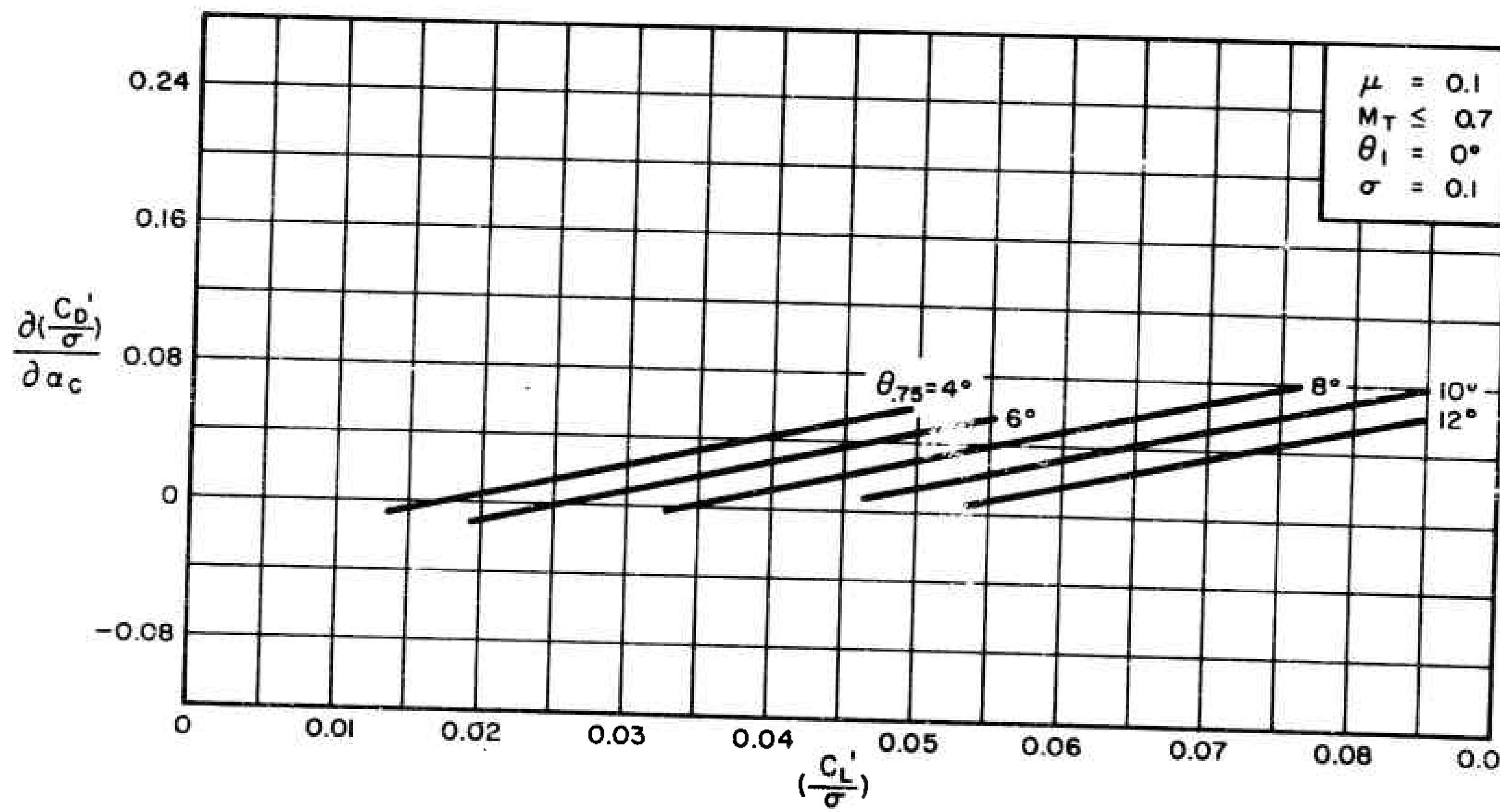

(a) μ = 0.1

Figure 9. Variation of $\frac{\partial(\frac{C_D'}{\sigma})}{\partial \alpha_c}$ With $\frac{C_L'}{\sigma}$ for Constant Values of $\theta_{.75}$.

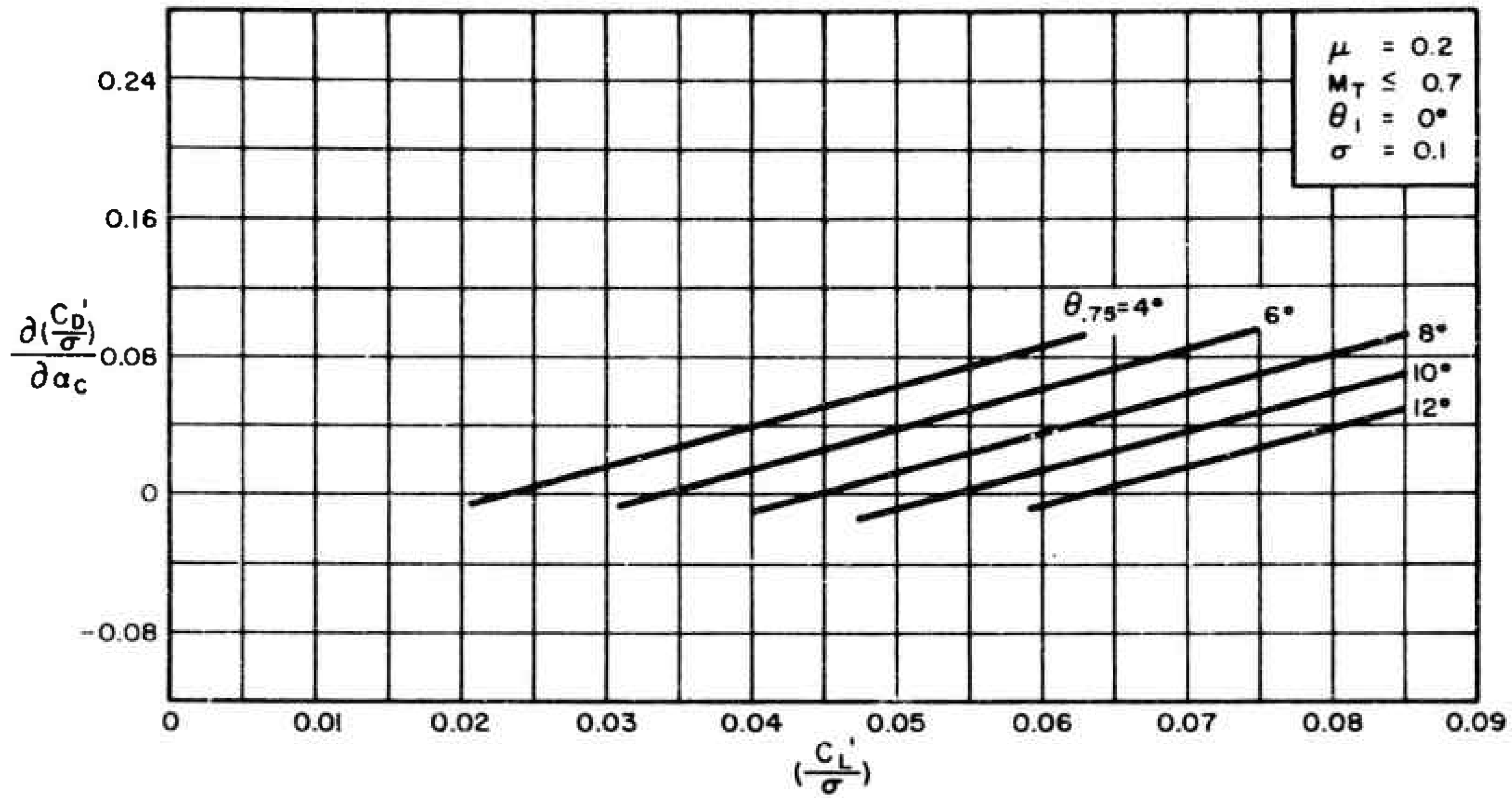

(b) μ = 0.2

Figure 9. Continued.

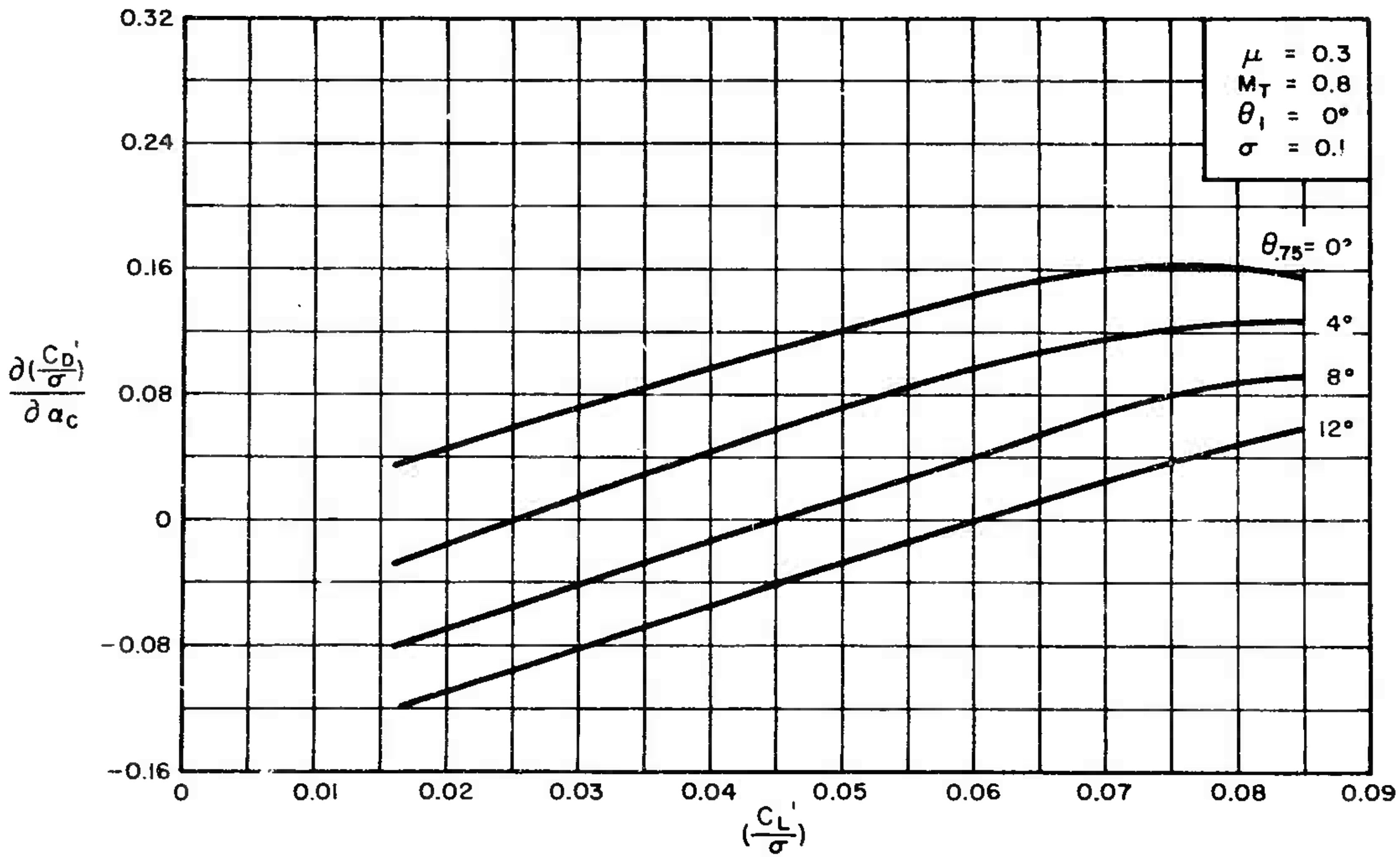

(c) μ = 0.3

Figure 9. Continued.

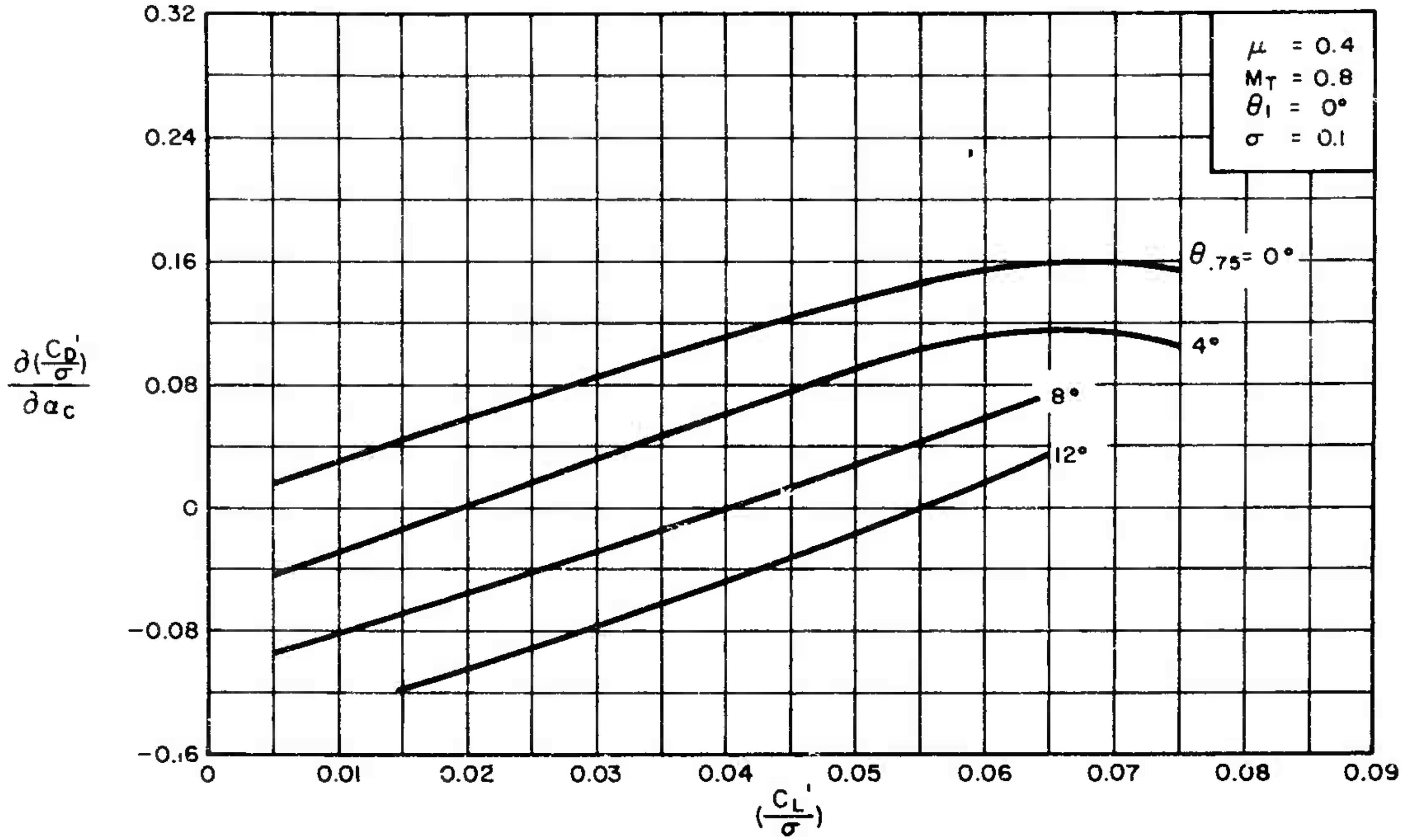

(d) μ = 0.4

Figure 9. Continued.

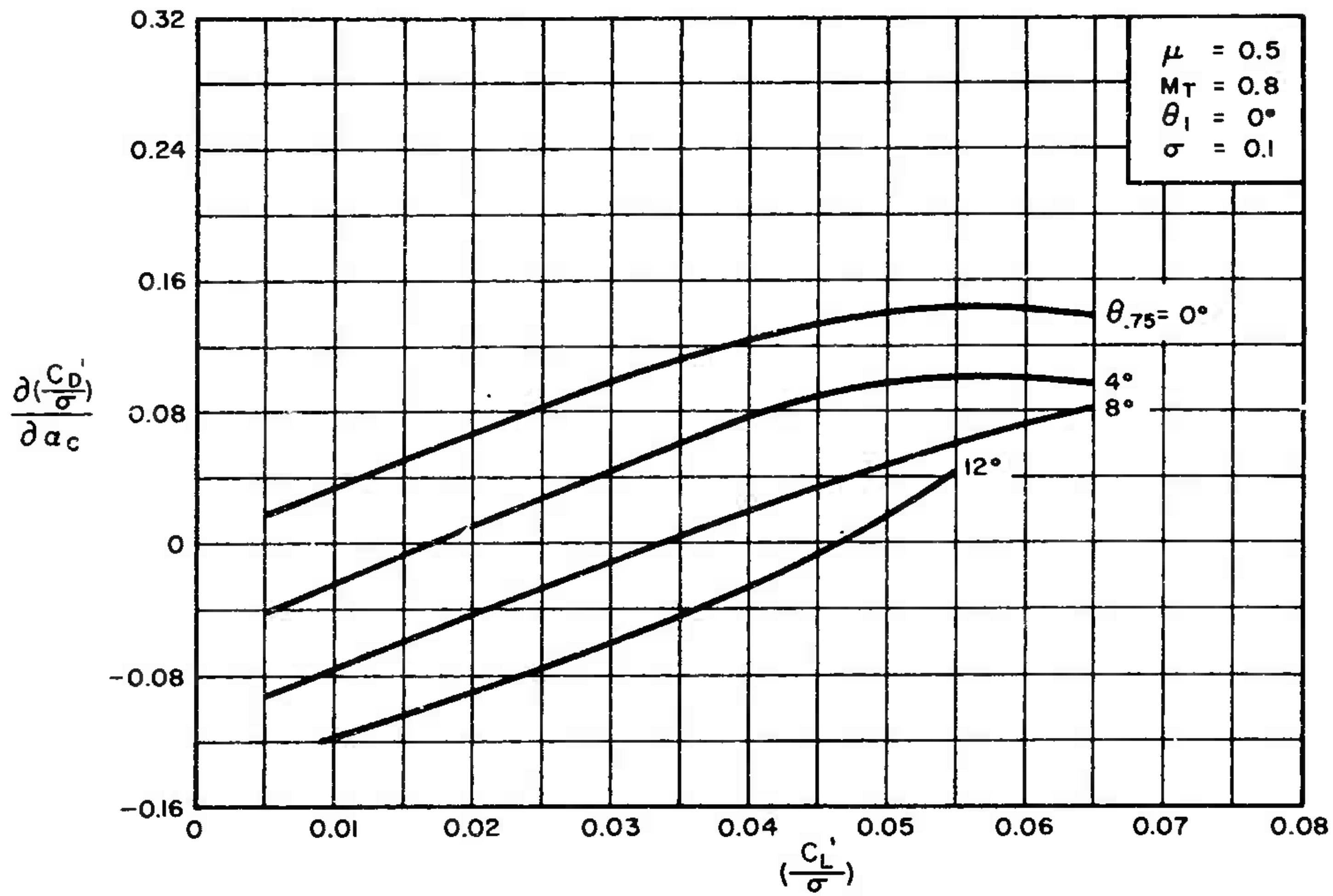

(e) μ = 0.5

Figure 9. Continued.

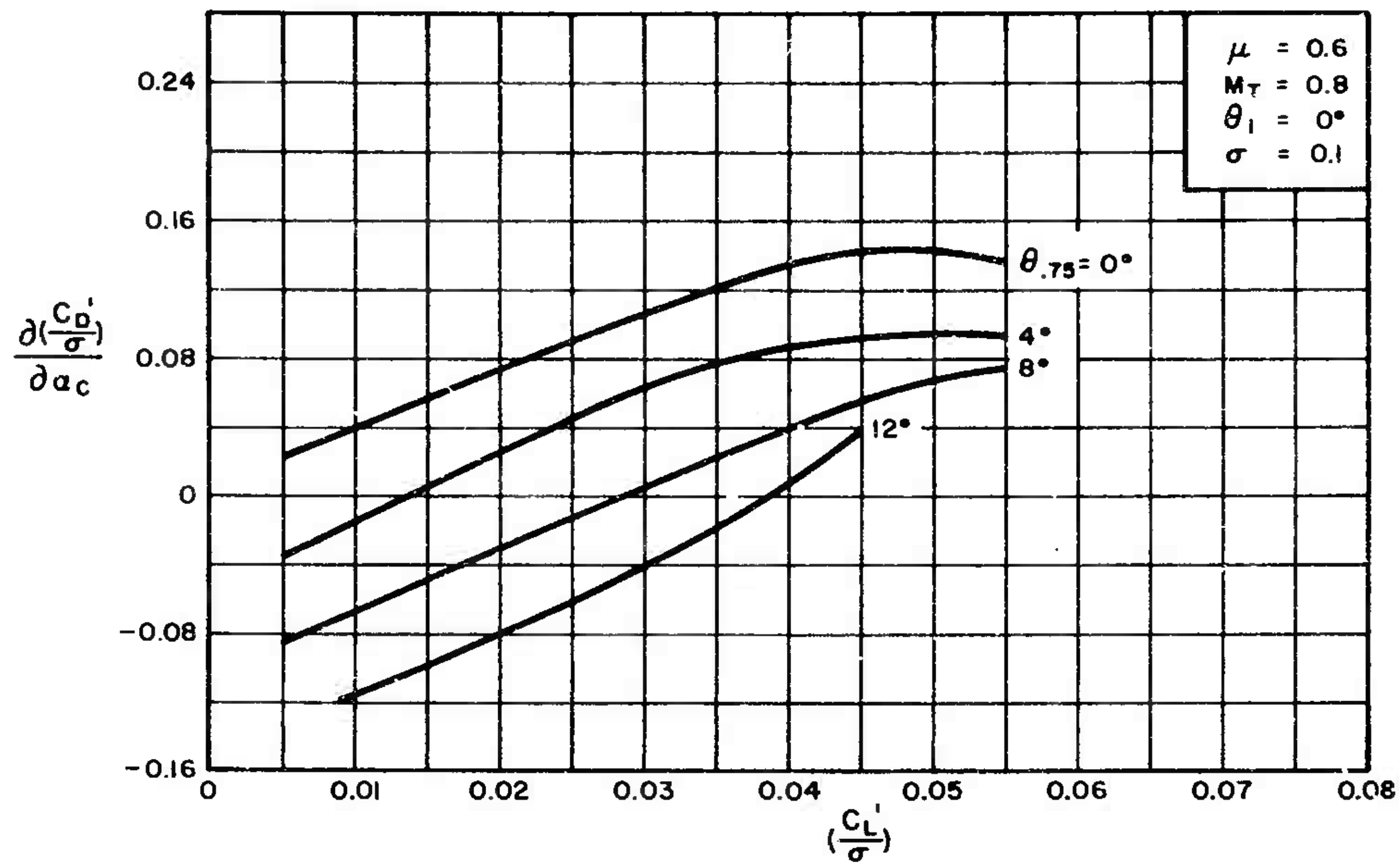

(f) $\mu = 0.6$

Figure 9. Continued.

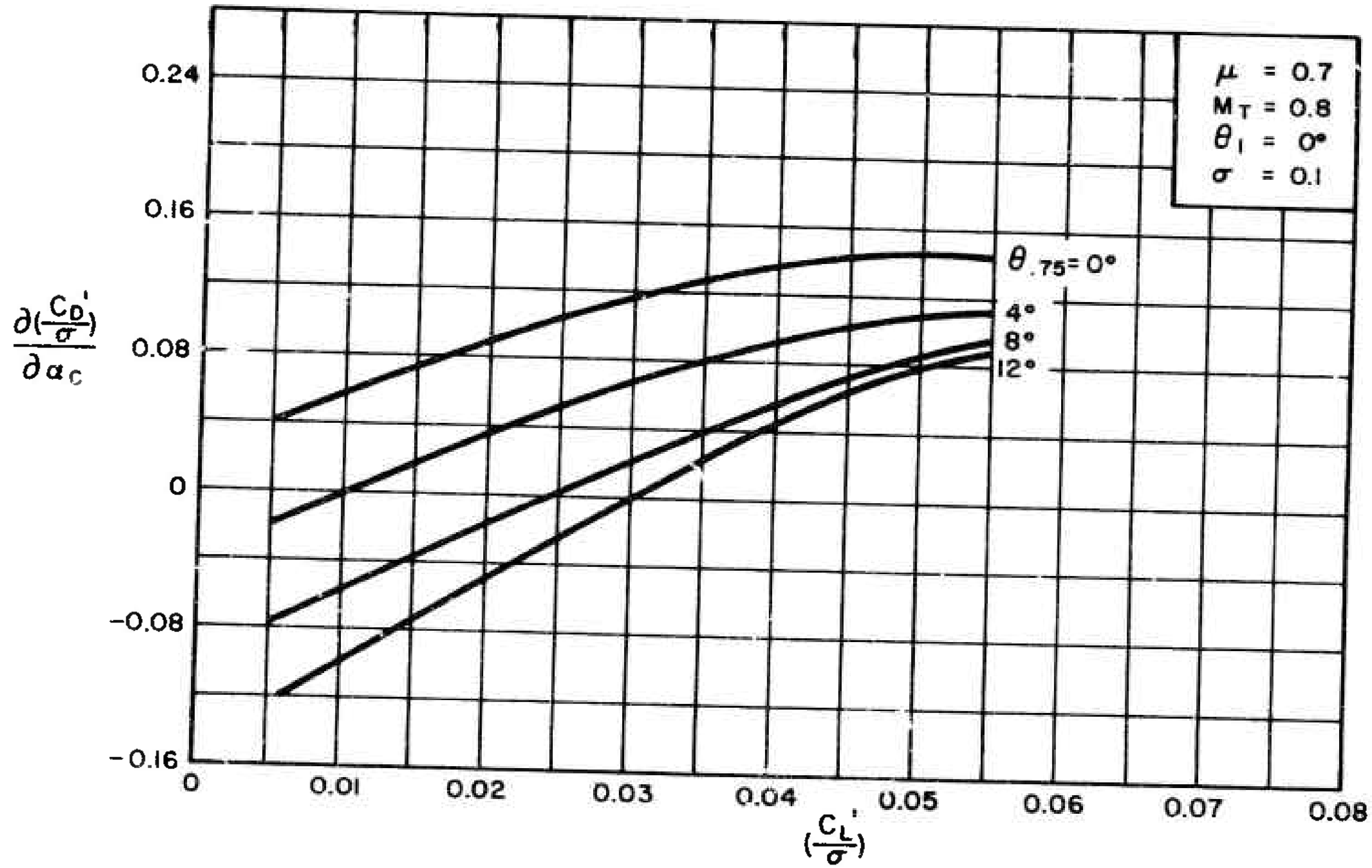

(g) $\mu = 0.7$

Figure 9. Continued.

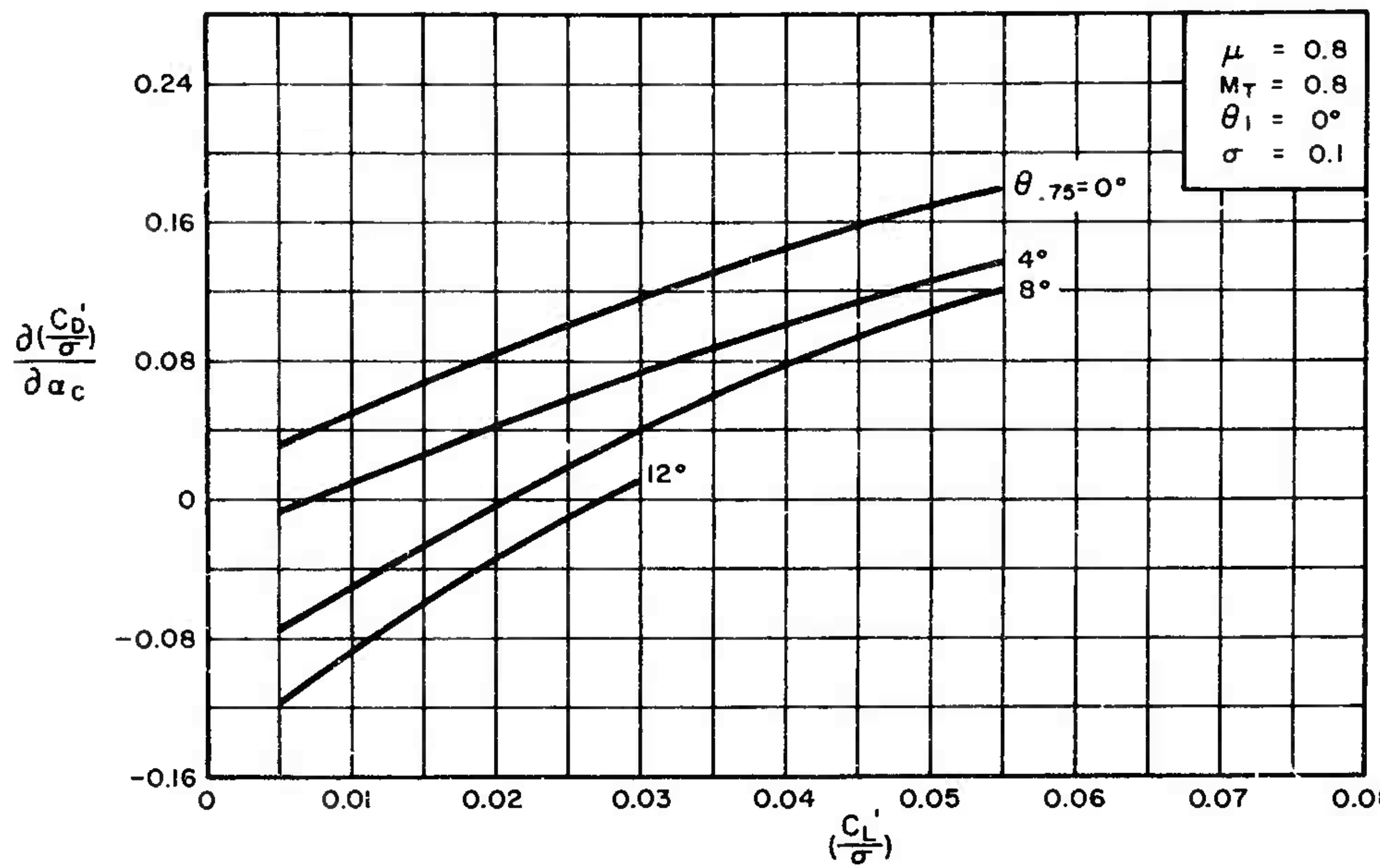

(h) μ = 0.8

Figure 9. Continued.

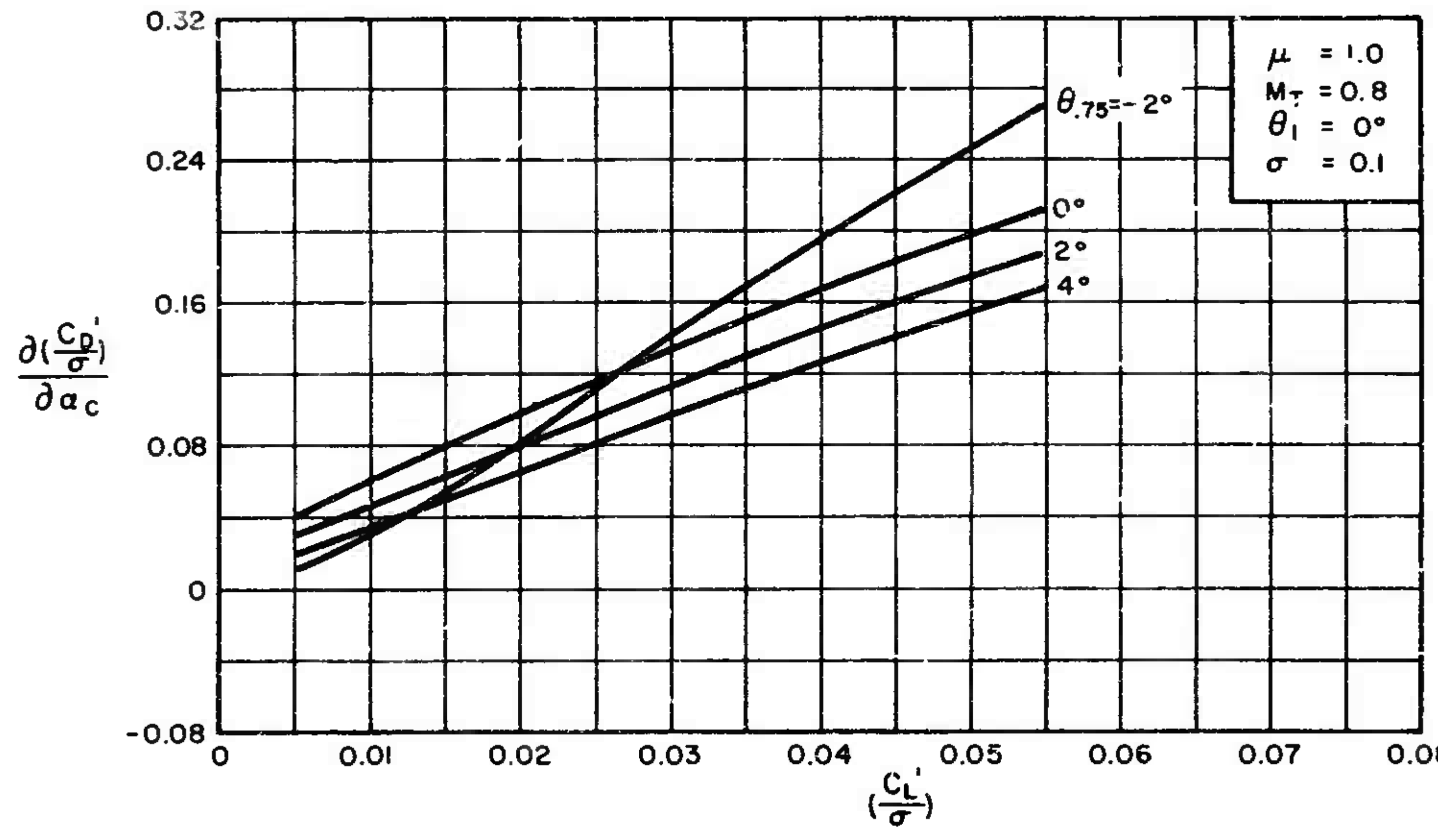

(i) μ = 1.0

Figure 9. Concluded.

7.5.2.3 $\frac{\partial(\frac{C_Q}{\sigma})}{\partial \alpha_c}$ for $\sigma = 0.1$, $\theta_1 = 0°$, and $M_T = 0.8$

Figures 10(a) through 10(g) present the isolated derivative $\partial(C_Q/\sigma)/\partial\alpha_c$ as a function of C_L'/σ for constant values of $\theta_{.75}$ and a range of μ values from $\mu = 0.3$ through $\mu = 1.0$. These were obtained from performance data of Reference 2 as slopes of the C_Q/σ vs. α_c relationships for constant values of μ and $\theta_{.75}$.

For the values of $\mu \leq 0.2$, the following expression may be used:

$$\frac{\partial(\frac{C_Q}{\sigma})}{\partial \alpha_c} = \left[\frac{\partial(\frac{C_Q}{\sigma})}{\partial \mu}\right]\left(\frac{\partial \mu}{\partial \alpha_c}\right) + \left[\frac{\partial(\frac{C_Q}{\sigma})}{\partial \lambda}\right]\left(\frac{\partial \lambda}{\partial \alpha_c}\right)$$

where $\partial(C_Q/\sigma)/\partial\mu$ and $\partial\lambda/\partial\alpha_c$ are obtained from Subsections 7.5.1.3 and 7.5.2.6, respectively, and

$$\frac{\partial \mu}{\partial \alpha_c} = -\mu \tan \alpha_c$$

$$\frac{\partial(\frac{C_Q}{\sigma})}{\partial \lambda} = \frac{1}{2}\left[(\delta_1 t_{52} + 2\lambda t_{55} + \delta_2 t_{56}\theta_{.75} - a(2\lambda t_{41} + t_{42}\theta_{.75})\right]$$

Values for δ_1 , and δ_2 are givan on page 82 of Reference 4. Values for the parameters t_{41} , and t_{42} may be obtained from Table 8-4, page 208 of Reference 4, and values for t_{52} , t_{55} , and t_{56} may be obtained from Table 8-5, page 209 of Reference 4.

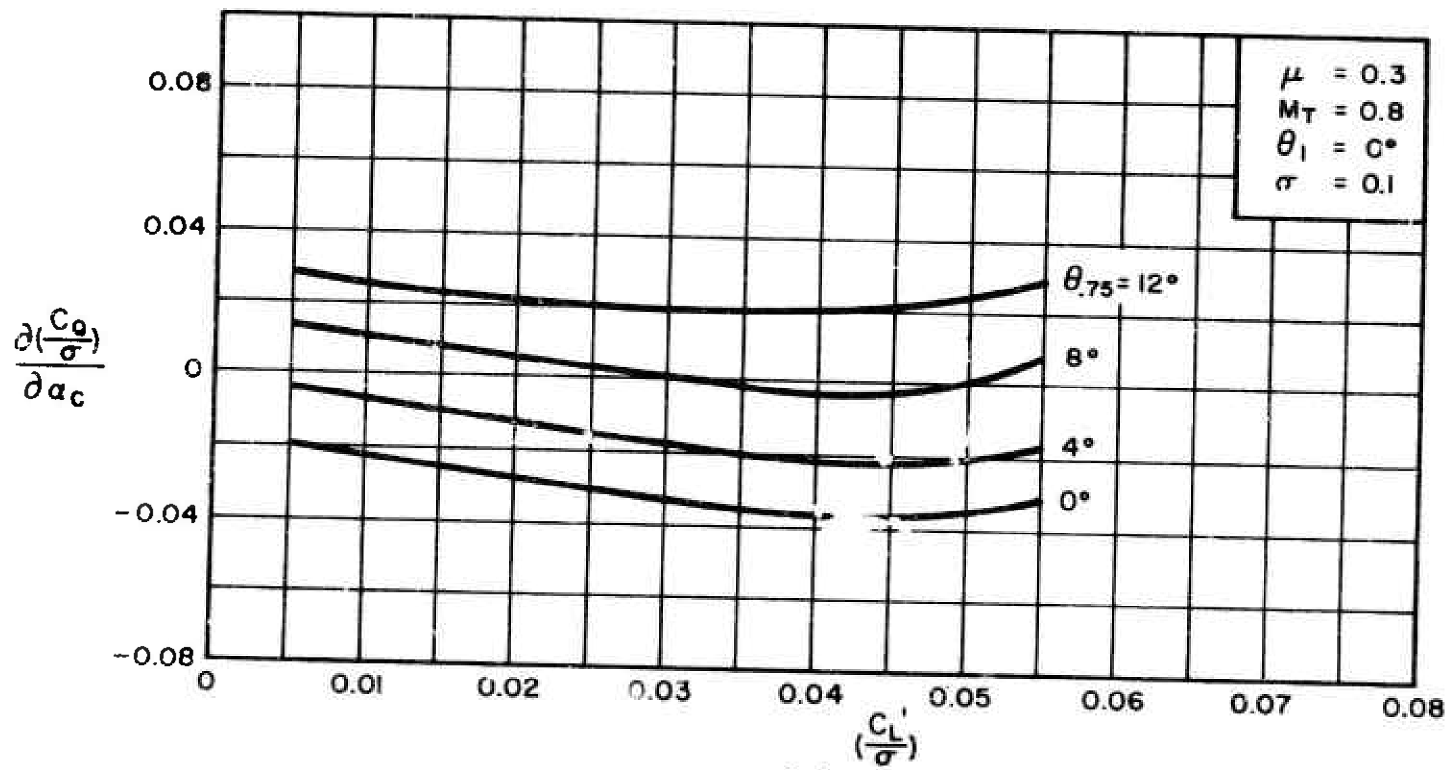

(a) μ = 0.3

Figure 10. Variation of $\frac{\partial(\frac{C_Q}{\sigma})}{\partial a_c}$ With $\frac{C_L'}{\sigma}$ for Constant Values of $\theta_{.75}$.

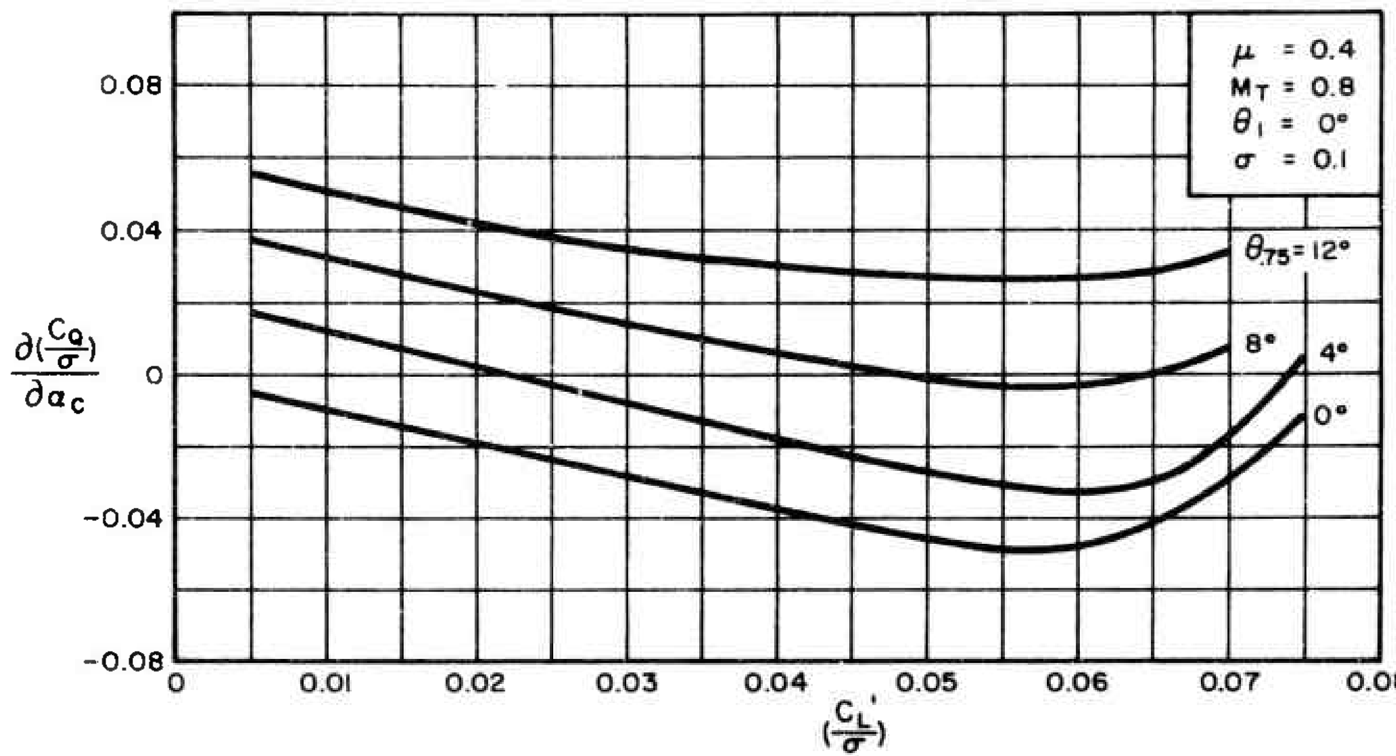

(b) $\mu = 0.4$

Figure 10. Continued.

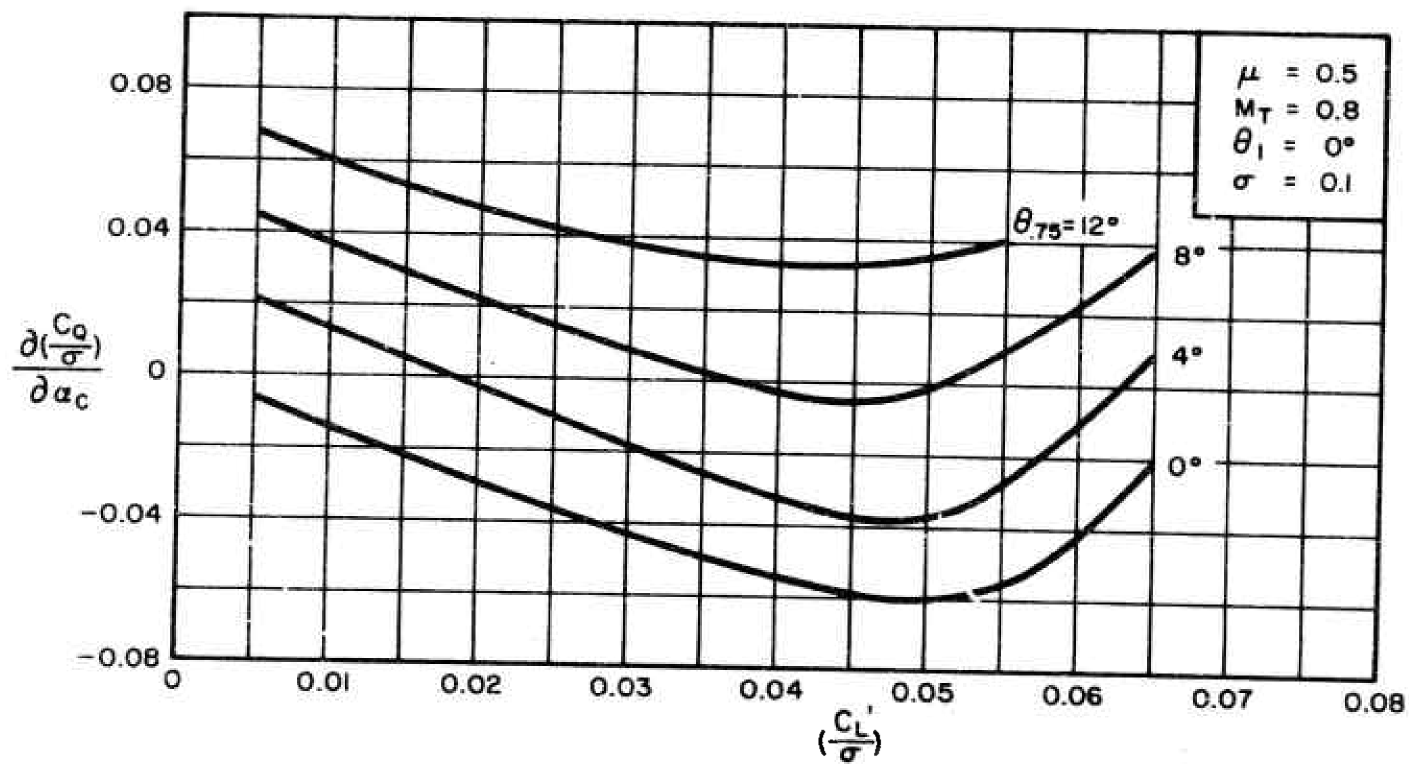

(c) $\mu = 0.5$

Figure 10. Continued.

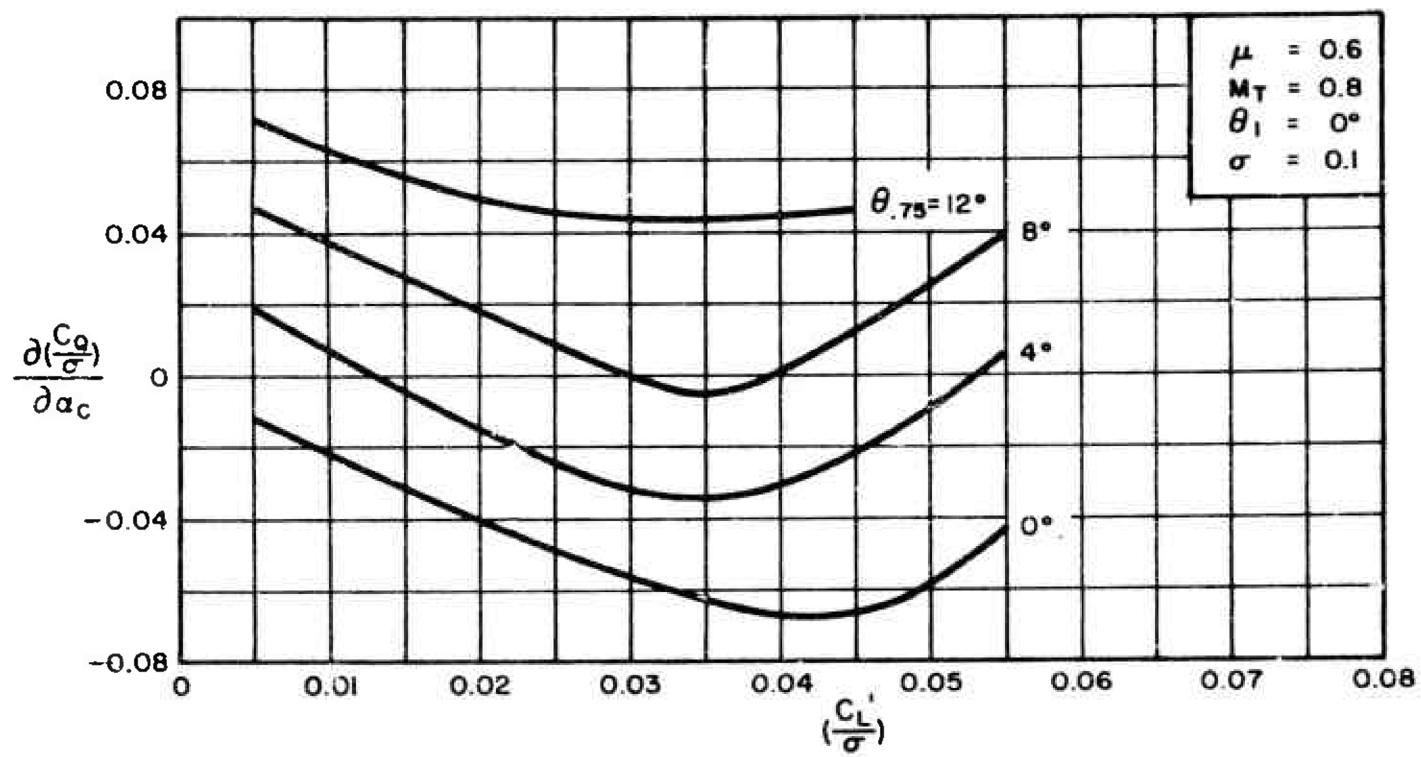

(d) μ = 0.6

Figure 10. Continued.

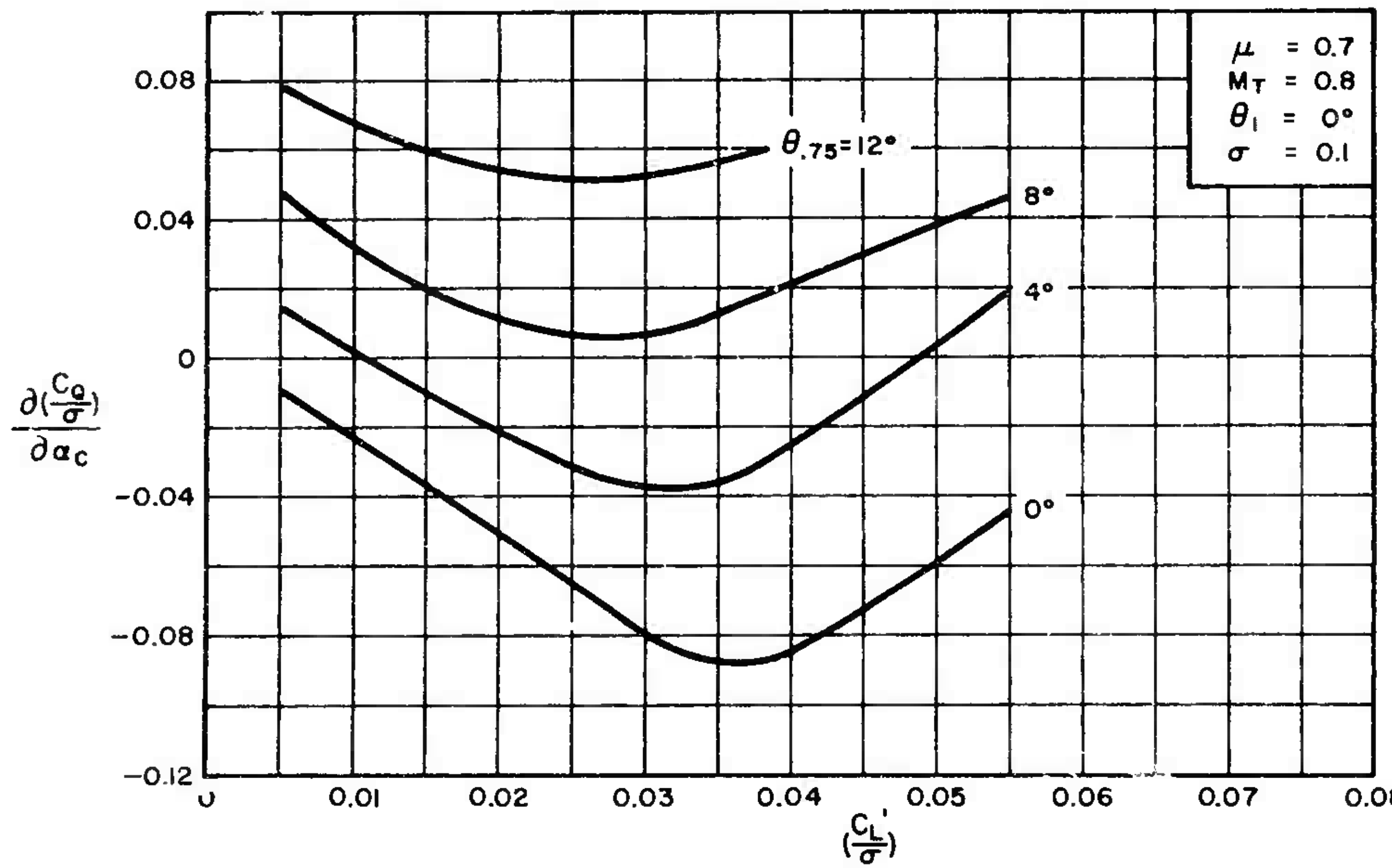

(e) $\mu = 0.7$

Figure 10. Continued.

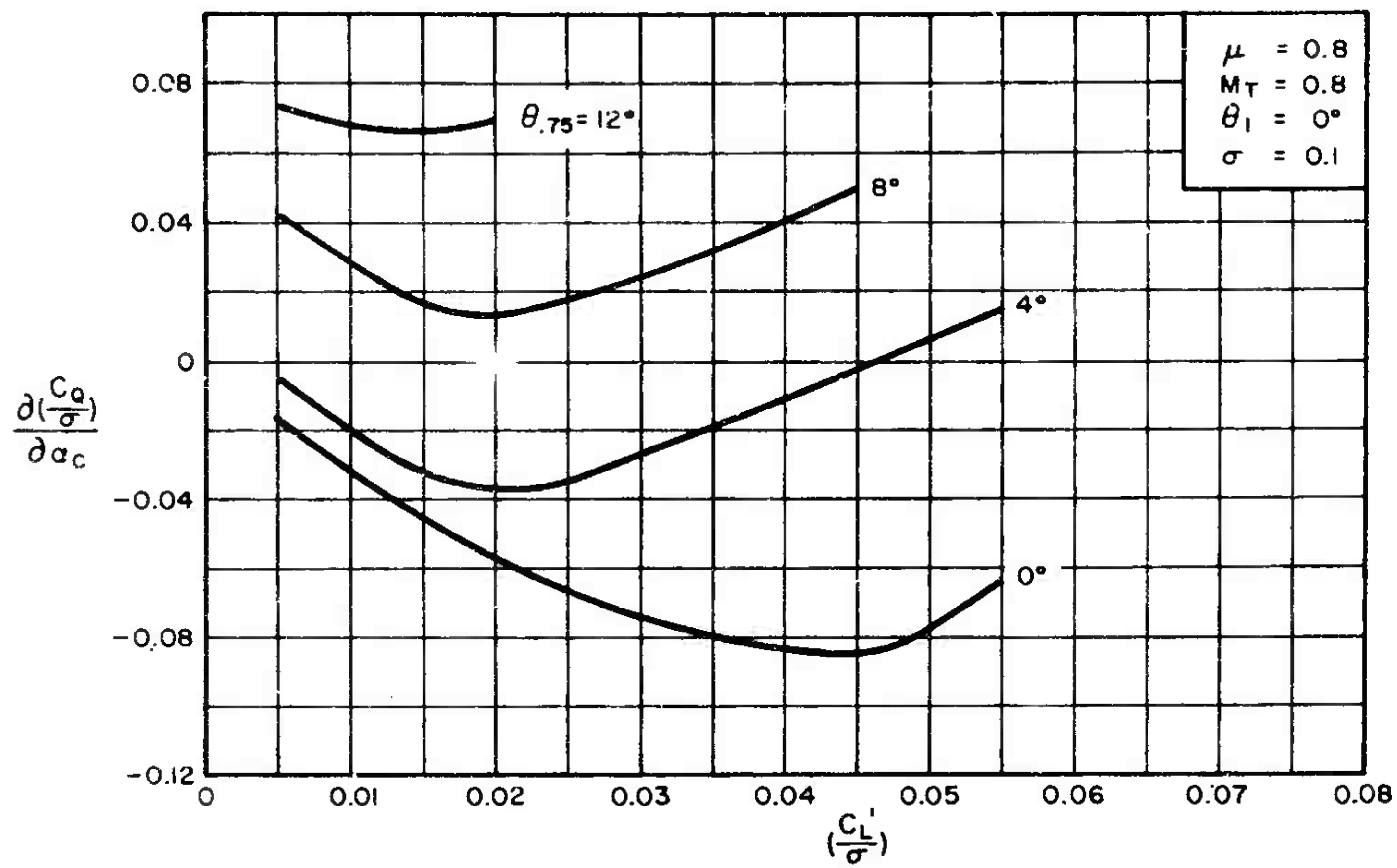

(f) $\mu = 0.8$

Figure 10. Continued.

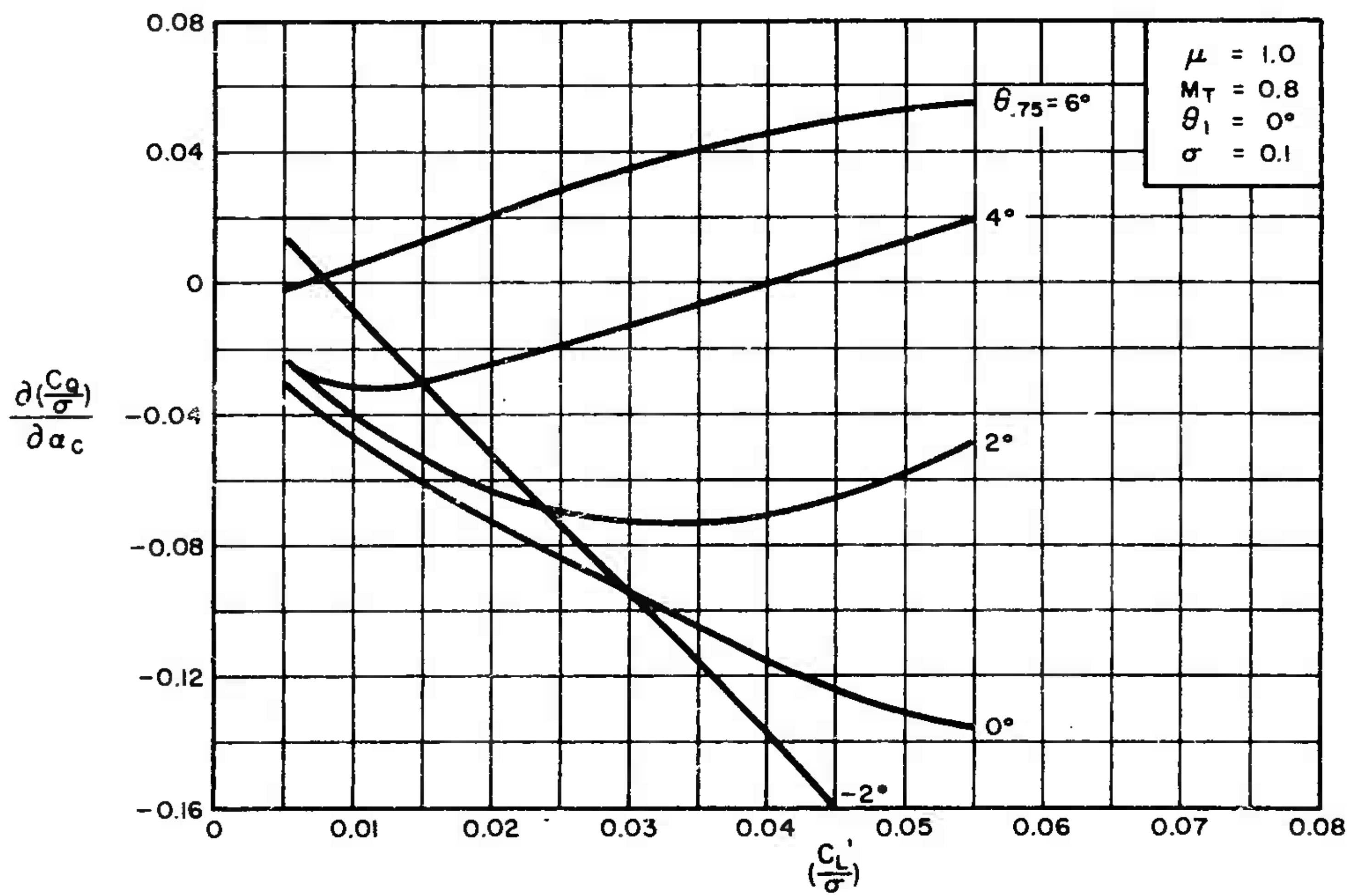

(g) μ = 1.0

Figure 10. Concluded.

7.5.2.4 $\frac{\partial a_1}{\partial \alpha_c}$ for $\sigma = 0.1$, $\theta_1 = 0°$, and $M_T = 0.8$

Figures 11(a) through 11(d) present the isolated rotor derivative $\partial a_1/\partial \alpha_c$ as a function of C_L'/σ for constant values of μ and a range of $\theta_{.75}$ values from $\theta_{.75} = 0°$ through $\theta_{.75} = 12°$.

The values of $\partial a_1/\partial \alpha_c$ for $\mu = 0.1$ and $\mu = 0.2$ were obtained directly from Reference 3.

The values of $\partial a_1/\partial \alpha_c$ for $\mu \geq 0.3$ were obtained from the theoretical rotor performance data of Reference 2 by graphically obtaining slopes of the a_1 versus α_c relationships for constant values of μ and $\theta_{.75}$.

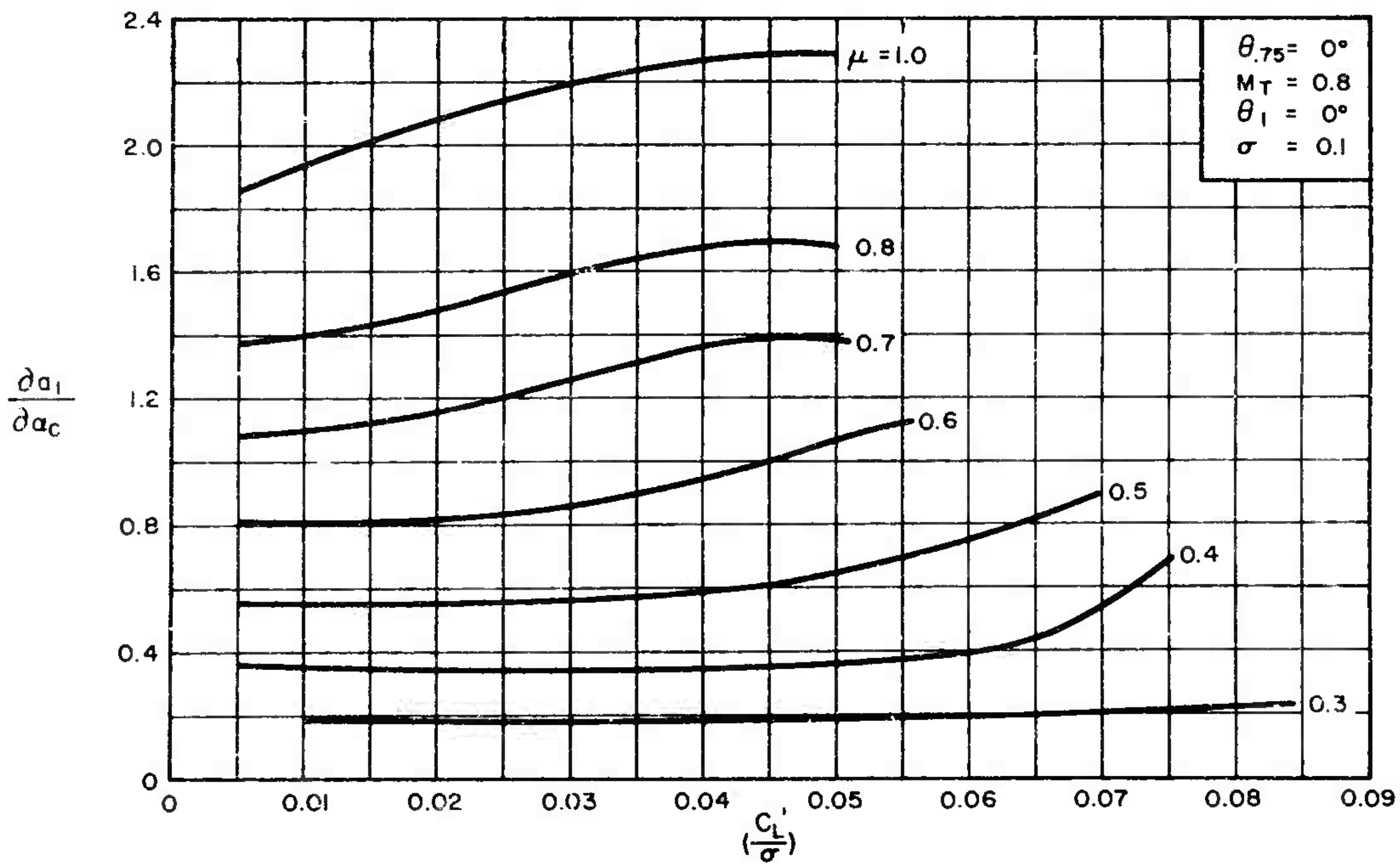

(a) $\theta_{.75} = 0°$

Figure 11. Variation of $\frac{\partial a_1}{\partial a_c}$ With $\frac{C_L'}{\sigma}$ for Constant Values of μ.

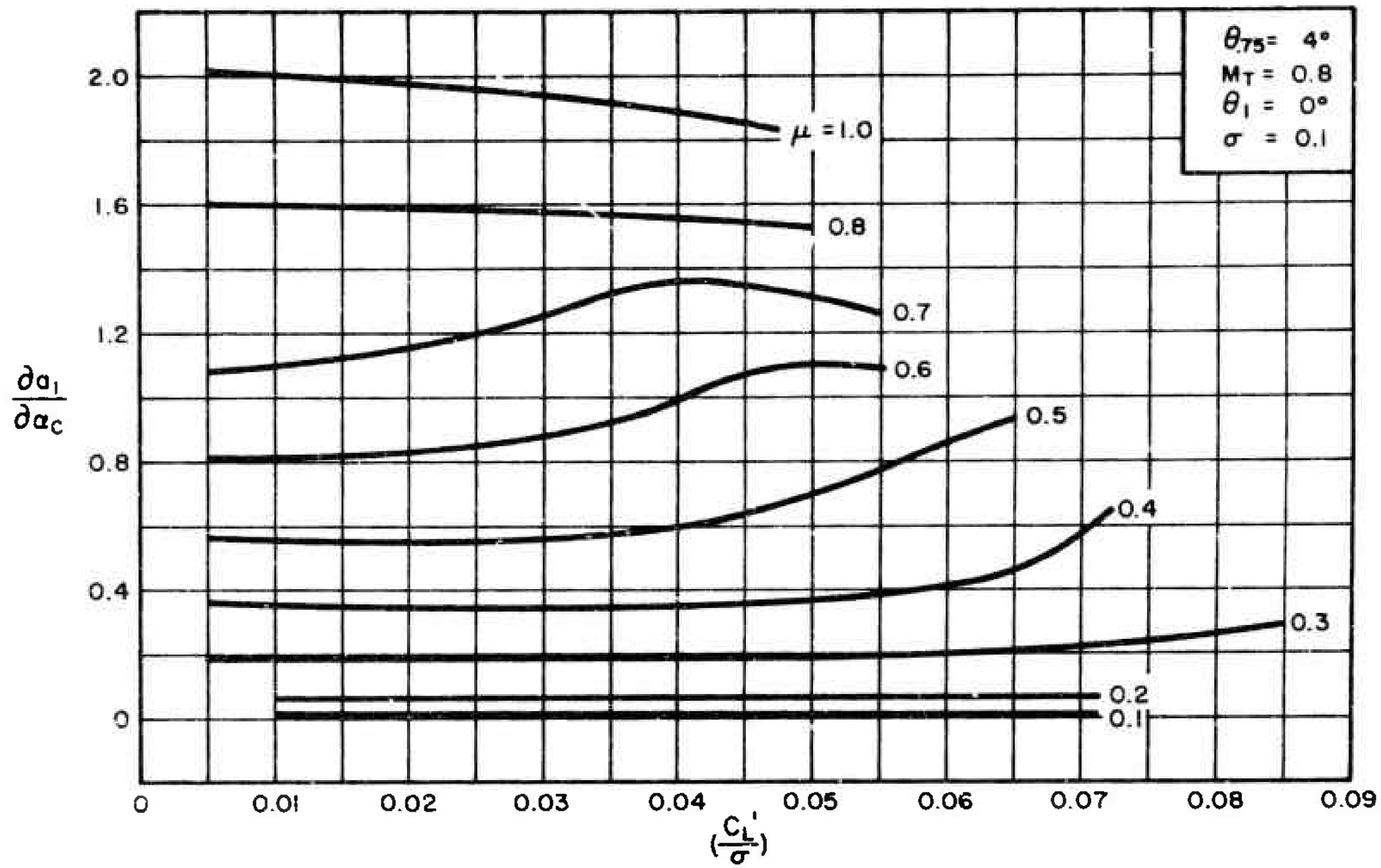

(b) $\theta_{.75} = 4°$

Figure 11. Continued.

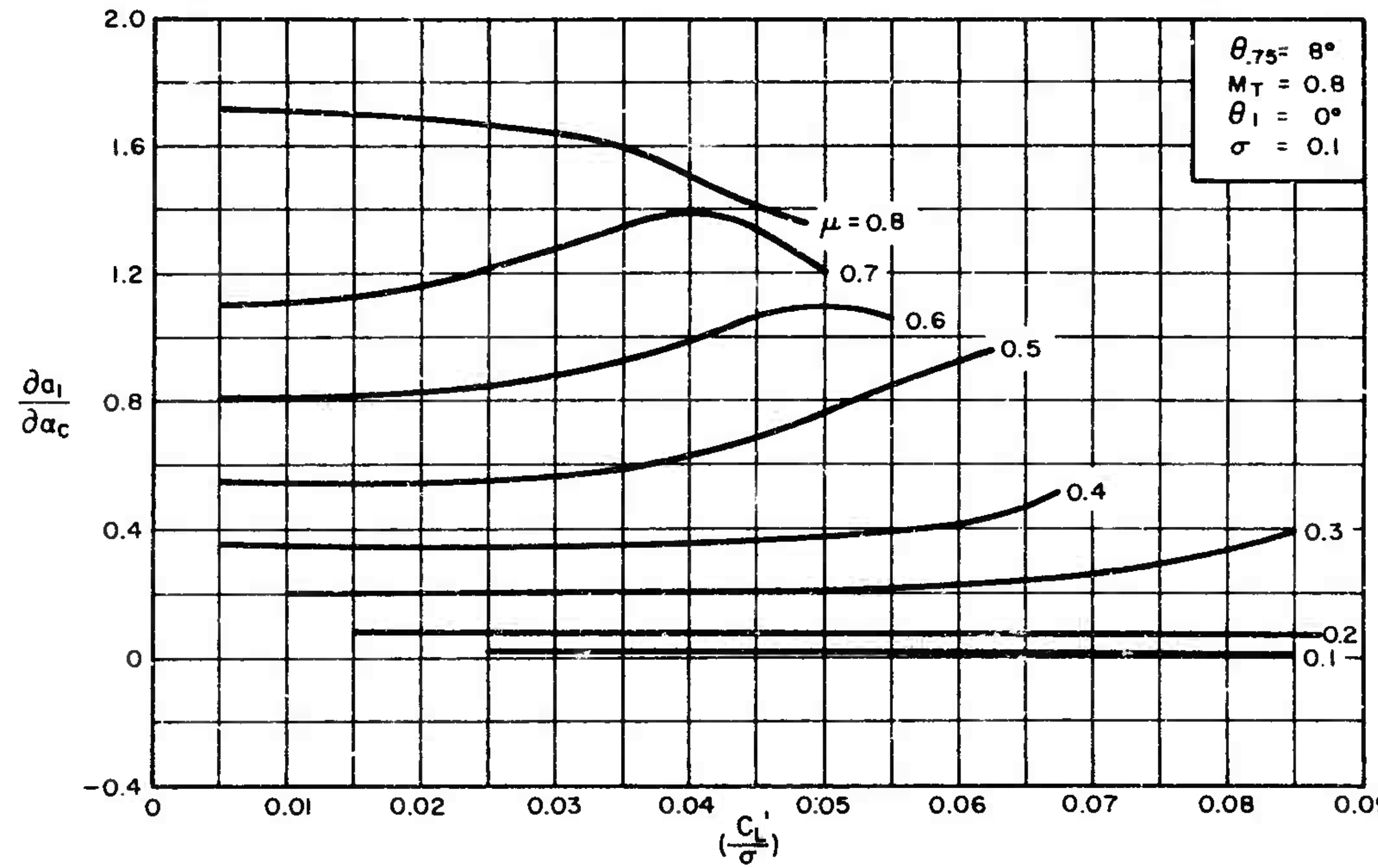

(c) $\theta_{.75} = 8°$

Figure 11. Continued.

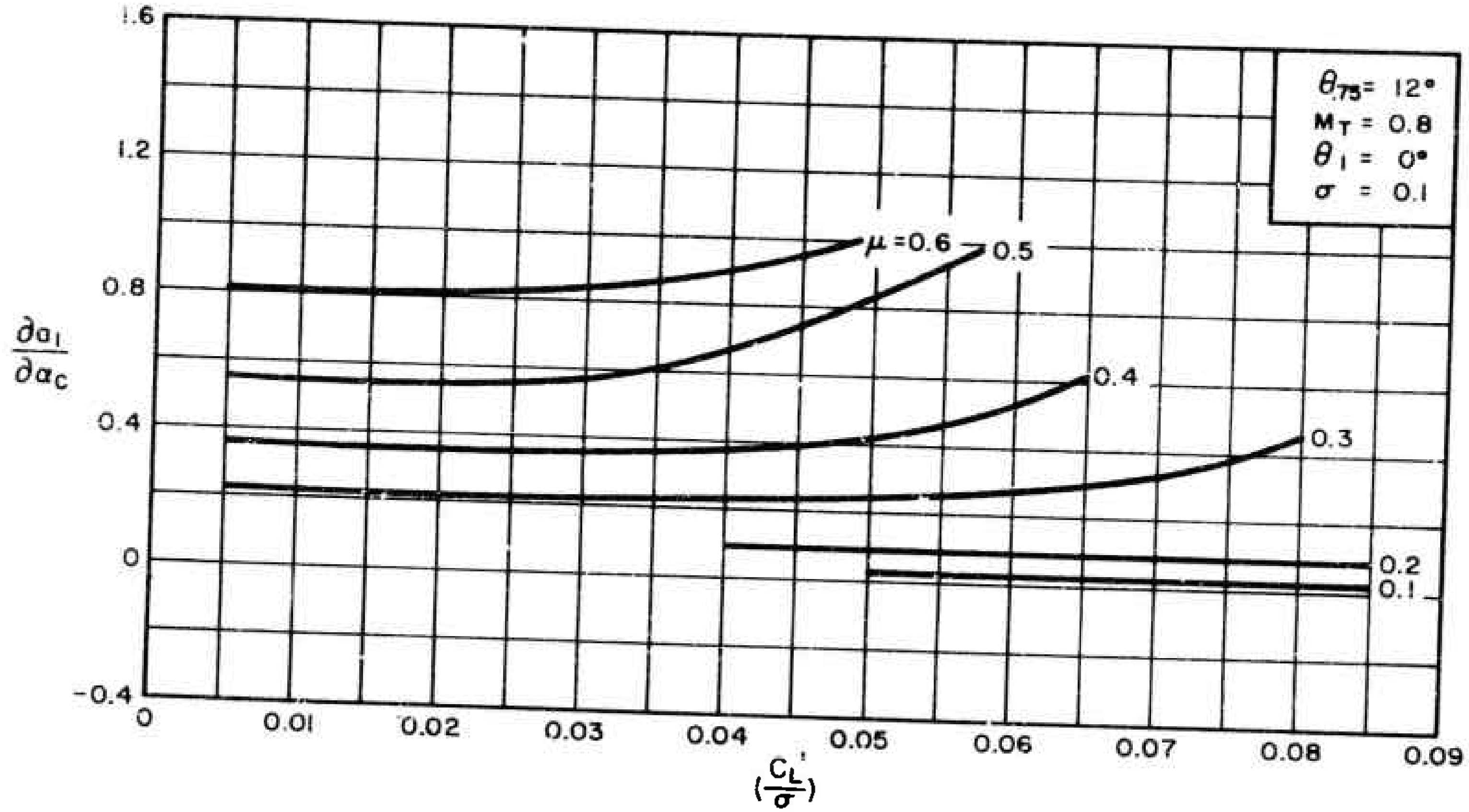

(d) $\theta_{.75} = 12°$

Figure 11. Concluded.

7.5.2.5 $\frac{\partial b_1}{\partial \alpha_c}$ for $\sigma = 0.1$, $\theta_1 = 0°$, and $M_T = 0.8$

Figures 12(a) through 12(d) present the isolated rotor derivative $\partial b_1/\partial \alpha_c$ as a function of C_L'/σ for constant values of μ and a range of $\theta_{.75}$ values from $\theta_{.75} = 0$ through $\theta_{.75} = 12°$. These derivatives were obtained from the theoretical data of Reference 2 by graphically obtaining slopes of the b_1 versus α_c relationships for constant values of μ and $\theta_{.75}$. These derivatives are specifically applicable to rotors having Lock inertia number $\gamma = 8.0$. However, since the lateral flapping angle b_1 is essentially proportional to γ, a correction factor of $\gamma/8.0$ may be used to compute $\partial b_1/\partial \alpha_c$ derivatives for rotors having γ values other than 8.0. Thus:

$$\left(\frac{\partial b_1}{\partial \alpha_c}\right)_\gamma = \frac{\gamma}{8.0}\left(\frac{\partial b_1}{\partial \alpha_c}\right)_{\gamma=8.0}$$

The $\partial b_1/\partial \alpha_c$ derivatives for $\mu \leq 0.2$ can be computed by using the following expression:

$$\left(\frac{\partial b_1}{\partial \alpha_c}\right) = \gamma\left[\left(\frac{2}{9}B^2 - \frac{1}{3}\mu^2\right)\lambda + \frac{\partial \lambda}{\partial \mu}(t_{17}) + \left(\frac{B^3}{6} + \frac{B\mu^2}{4}\right)\theta_{.75}\right]$$

where $\partial \lambda/\partial \mu$ is presented in Subsection 7.5.1.6, and where values of t_{17} can be obtained from Table 8-1, page 205 of Reference 4.

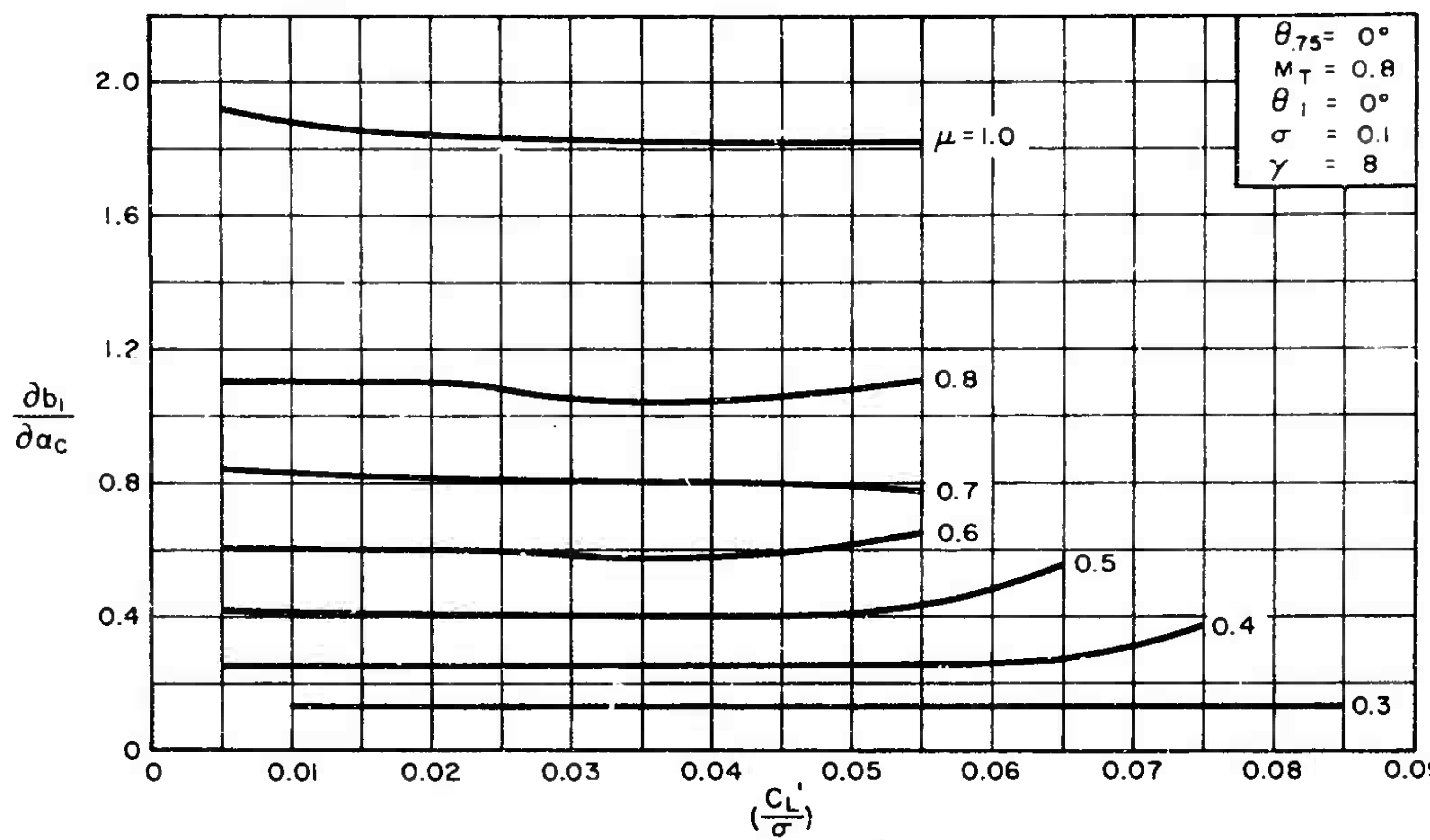

(a) $\theta_{.75} = 0°$

Figure 12. Variation of $\frac{\partial b_1}{\partial a_c}$ With $\frac{C_L'}{\sigma}$ for Constant Values of μ.

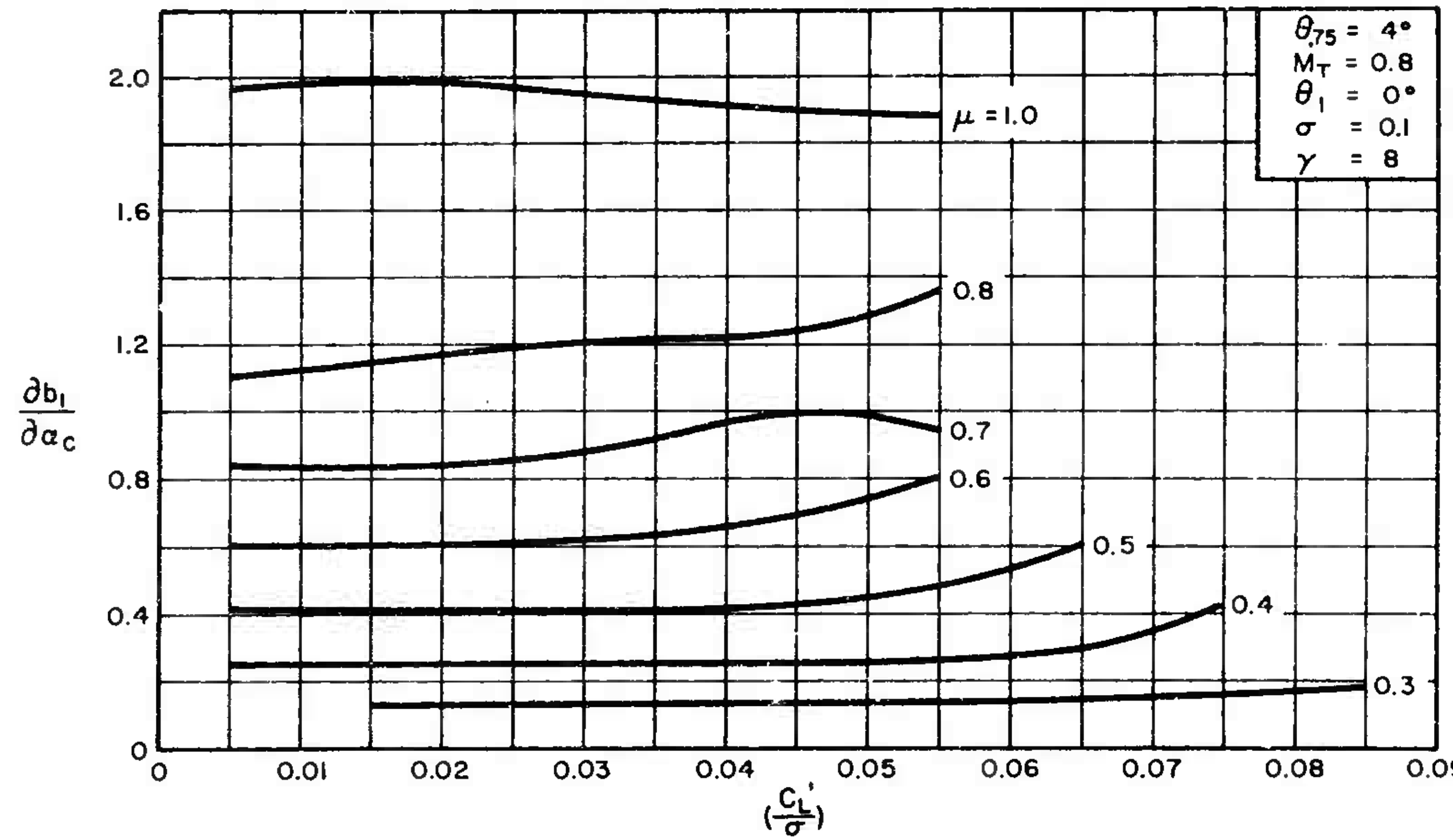

(b) $\theta_{.75} = 4°$

Figure 12. Continued.

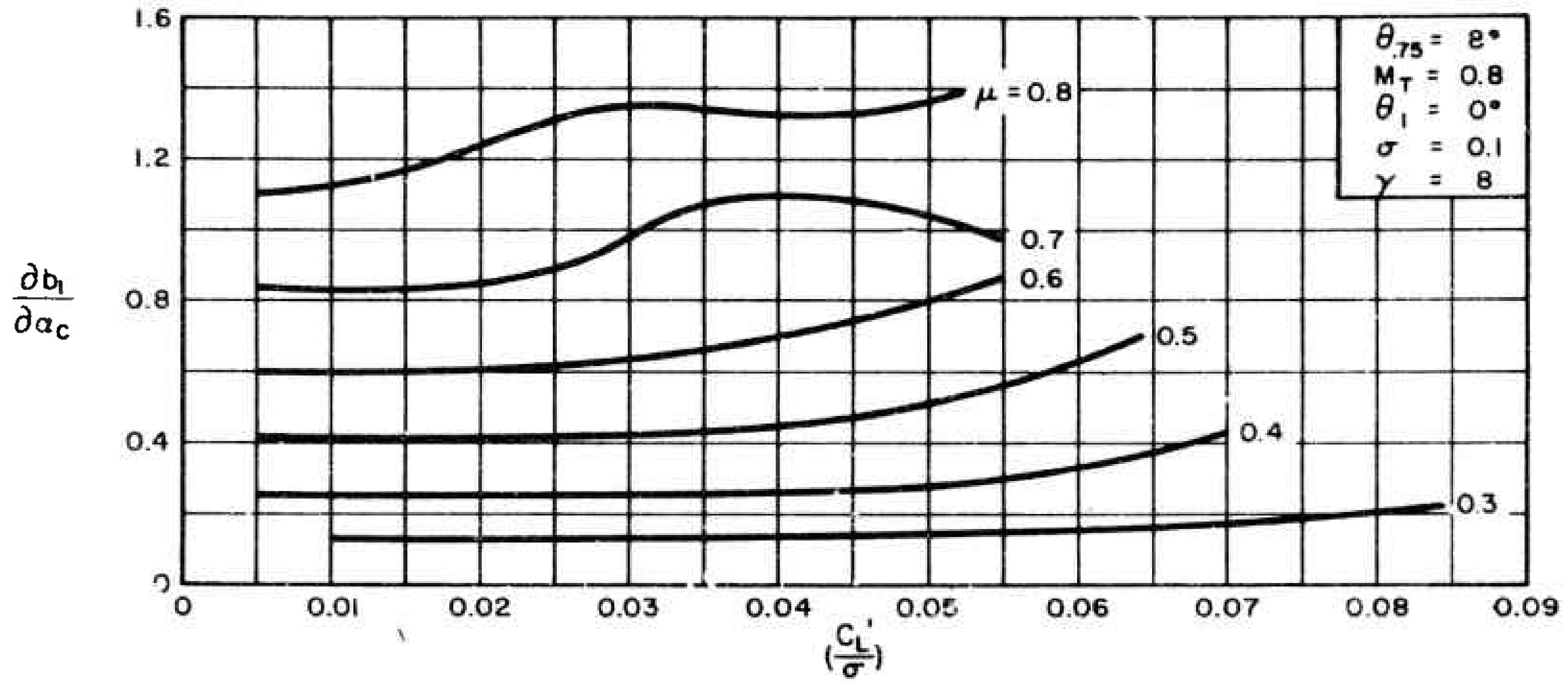

(c) $\theta_{.75} = 8°$

Figure 12. Continued.

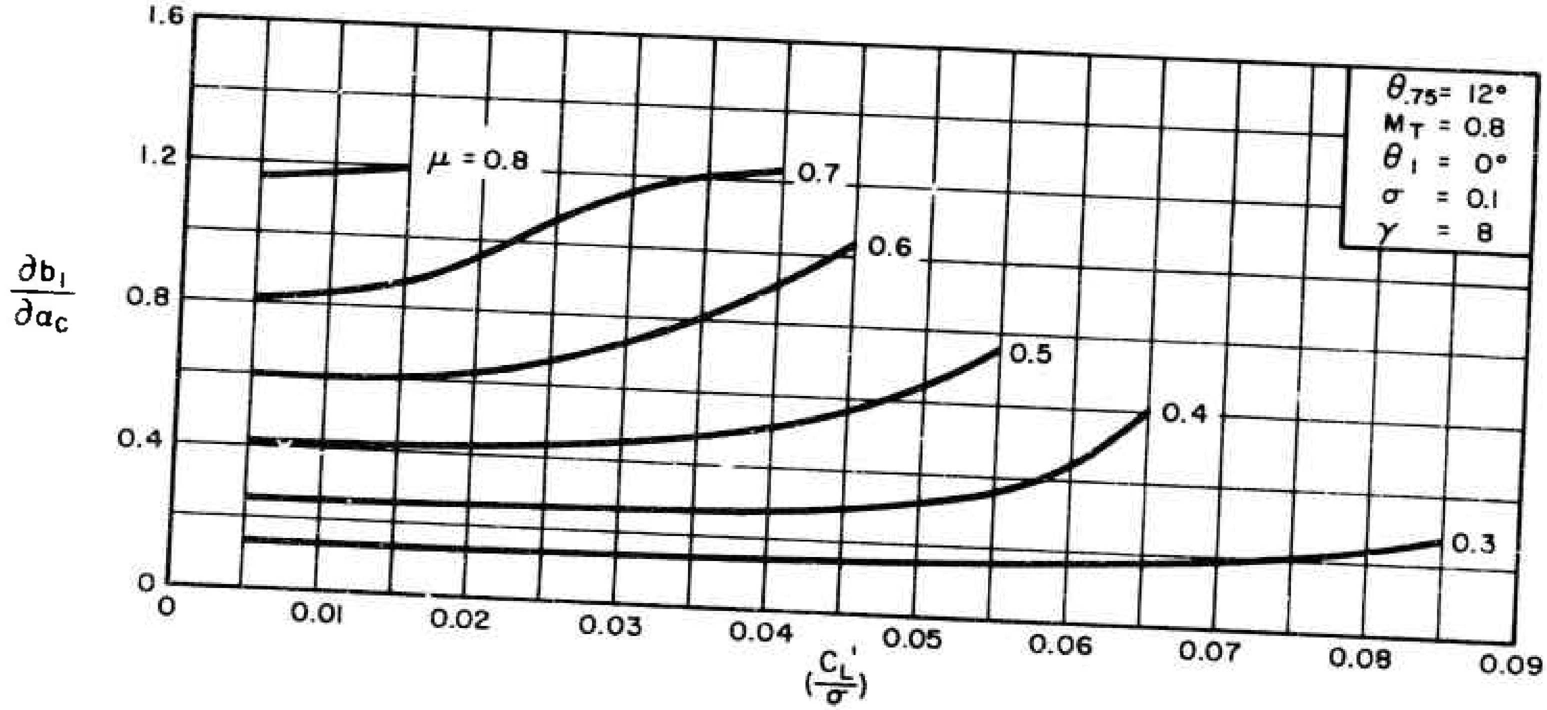

(d) $\theta_{.75} = 12°$

Figure 12. Concluded.

7.5.2.6 $\dfrac{\partial \lambda}{\partial \alpha_c}$ for $\sigma = 0.1$, $\theta_1 = 0°$, and $M_T = 0.8$

The derivative $\partial\lambda/\partial\alpha_C$ is plotted in Figure 13 as a function of μ and is applicable for all values of $\theta_{.75}$ and C_L'/σ. The values of $\partial\lambda/\partial\alpha_C$ for $\mu = 0.1$ and $\mu = 0.2$ were obtained directly from Reference 3 For $\mu \geq 0.3$, the values were extracted graphically from the theoretical rotor performance data of Reference 2. The results obtained are applicable for all values of $\theta_{.75}$, C_L'/σ, and α_C.

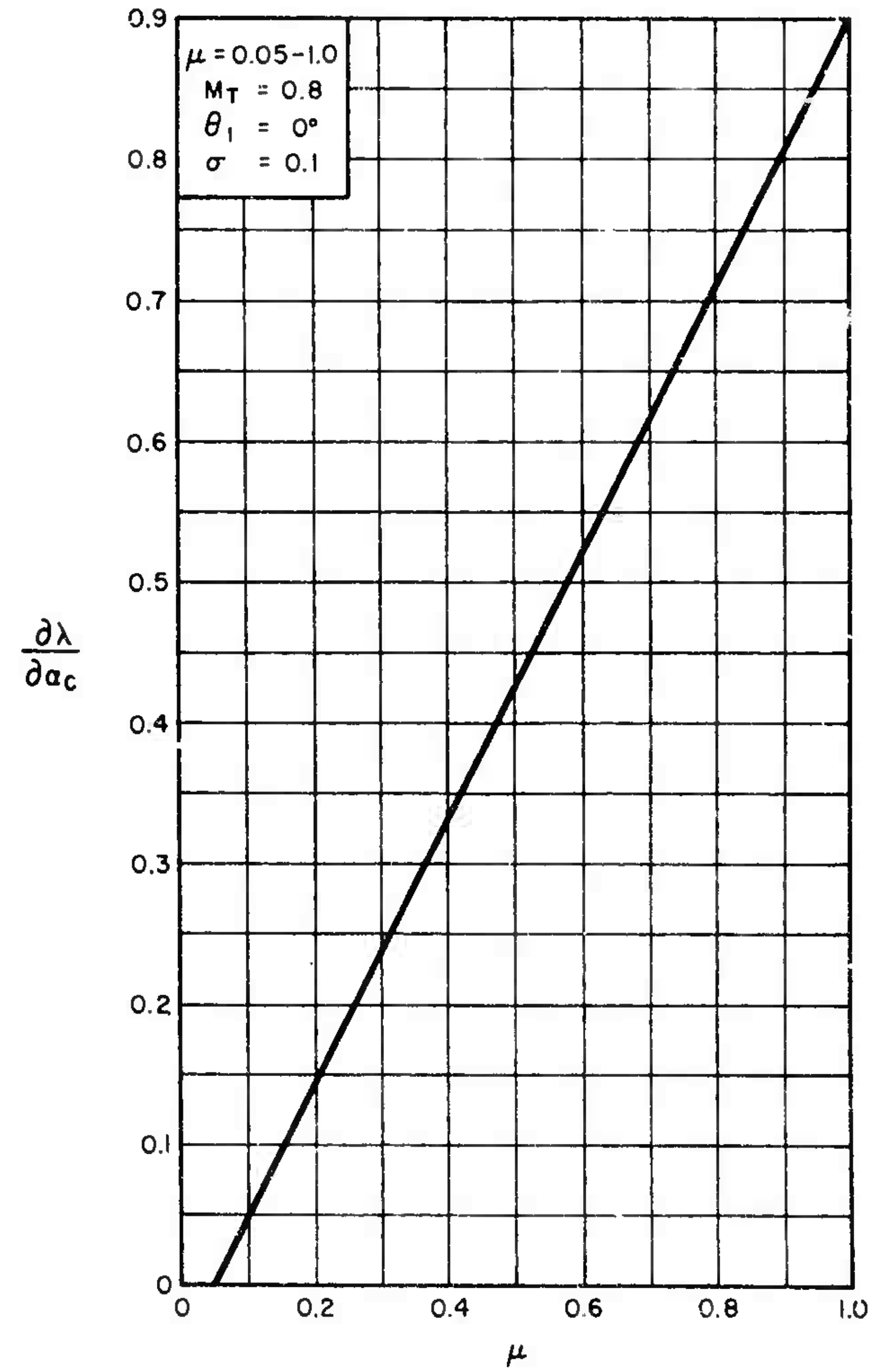

Figure 13. Variation of $\frac{\partial \lambda}{\partial \alpha_c}$ With μ for All Values of $\theta_{.75}$ and $\frac{C_L'}{\sigma}$.

7.5.2.7 $\dfrac{\partial(\frac{C_Y'}{\sigma})}{\partial \alpha_c}$ for All Values of σ, θ_1, and M_T

Reference 2 and other reviewed reports do not include the calculated data required to obtain the rotor Y-force derivatives.

It is therefore suggested that the classical Bailey theory be utilized for this purpose. If the above theory is used, the following expression for $\partial(C_Y'/\sigma)/\partial\alpha_c$ can be derived:

$$\frac{\partial(\frac{C_Y'}{\sigma})}{\partial \alpha_c} = \frac{a}{2}\left\{\frac{\partial a_0}{\partial \alpha_c}\left[a_1\left(\frac{1}{6}-\mu^2\right)-\frac{3}{4}\mu(\theta_{.75}+2\lambda)\right]\right.$$

$$+\frac{\partial a_1}{\partial \alpha_c}\left[a_0\left(\frac{1}{6}-\mu^2\right)+\frac{1}{4}\mu b_1\right]$$

$$+\frac{\partial b_1}{\partial \alpha_c}\left[\theta_{.75}\left(\frac{1}{3}+\frac{3}{8}\mu^2\right)+\lambda\left(\frac{3}{4}+\frac{1}{8}\mu^2\right)+\frac{1}{4}\mu a_1\right]$$

$$\left.+\frac{\partial \lambda}{\partial \alpha_c}\left[b_1\left(\frac{3}{4}+\frac{1}{8}\mu^2\right)-\frac{3}{2}\mu a_0\right]\right\}$$

where

$$\frac{\partial a_0}{\partial \alpha_c} = \frac{\gamma}{2}\left[-\frac{\theta_{.75}}{4}\mu^2\sin 2\alpha_c+\frac{1}{3}\frac{\partial\lambda}{\partial\alpha_c}\right]$$

and where $\partial a_1/\partial\alpha_c$, $\partial b_1/\partial\alpha_c$, and $\partial\lambda/\partial\alpha_c$ are given in Subsections 7.5.2.4, 7.5.2.5, and 7.5.2.6, respectively.

The expression for the isolated rotor derivative $\partial(C_Y'/\sigma)/\partial\alpha_c$ as given above is applicable for all values of σ, θ_1, and M_T, provided that the pertinent rotor parameters comprising the derivative are evaluated at the required conditions.

7.5.3 Isolated Rotor Derivatives With Respect to Rotor Collective Pitch at 75% Rotor Radius (θ_{75})

7.5.3.1 $\dfrac{\partial(\frac{C_L'}{\sigma})}{\partial\theta_{.75}}$ for $\sigma = 0.1$, $\theta_1 = 0°$, and $M_T = 0.8$

Figures 14 through 15(g) present the isolated rotor derivative $\partial(C_L'/\sigma)/\partial\theta_{.75}$ as functions of C_L'/σ and α_C for $\mu = 0.1$ through 1.0.

The derivatives for low μ values, i.e., $\mu \leq 0.2$, were obtained by using the following equation:

$$\frac{\partial(\frac{C_L'}{\sigma})}{\partial\theta_{.75}} = \frac{\partial(\frac{C_T}{\sigma})}{\partial\theta_{.75}} \cos\alpha_C - \frac{\partial(\frac{C_H}{\sigma})}{\partial\theta_{.75}} \sin\alpha_C$$

where $\partial(C_T/\sigma)/\partial\theta_{.75}$ and $\partial(C_H/\sigma)/\partial\theta_{.75}$ were obtained from Reference 3. Values of $\partial(C_L'/\sigma)/\partial\theta_{.75}$ for $\mu \geq 0.3$ were extracted graphically from rotor performance data of Reference 2 by obtaining slopes of the C_L'/σ vs. $\theta_{.75}$ relationships for constant values of μ and α_C.

Figure 14 indicates that for $\mu \leq 0.2$ the derivatives are practically independent of α_C and C_L'/σ variations, whereas these for $\mu \geq 0.3$ presented in Figures 15(a) through 15(g) are functions of α_C and C_L'/σ.

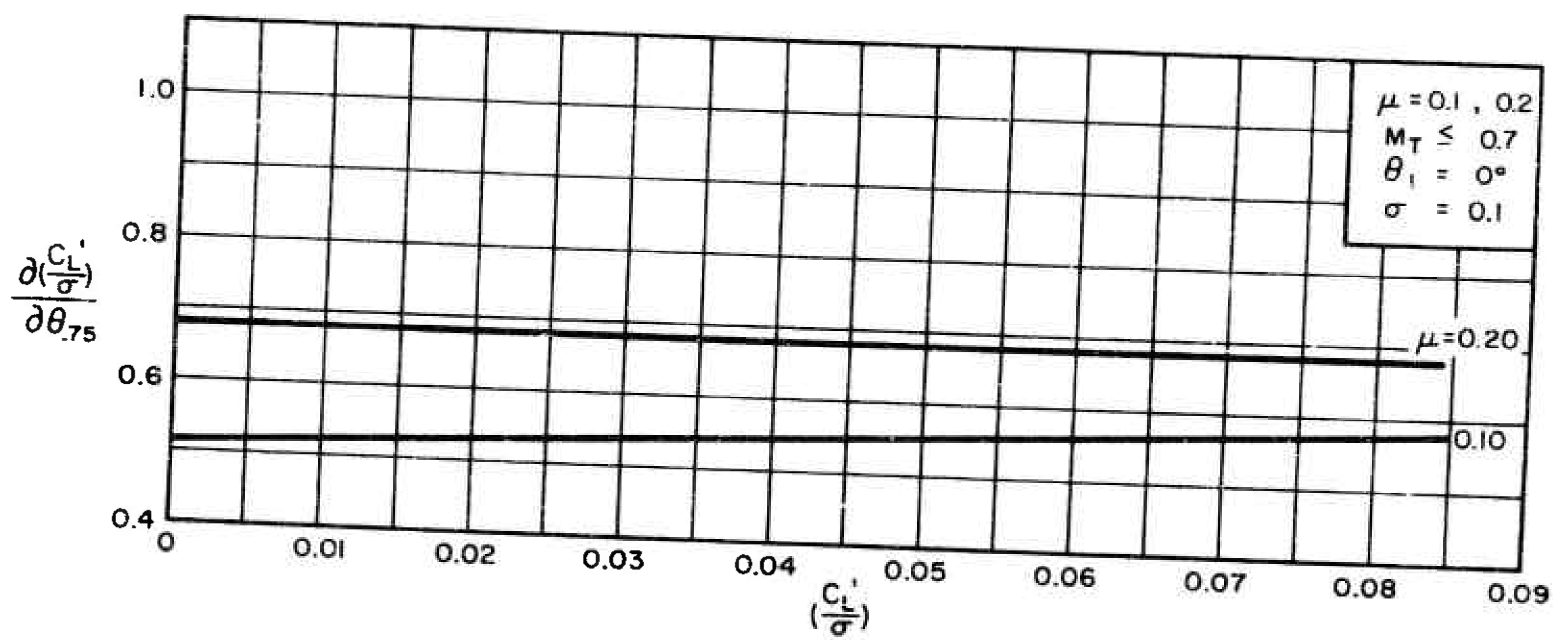

Figure 14. Variation of $\frac{\partial(\frac{C_L'}{\sigma})}{\partial\theta_{.75}}$ With $\frac{C_L'}{\sigma}$ for $\mu = 0.1$ and 0.2.

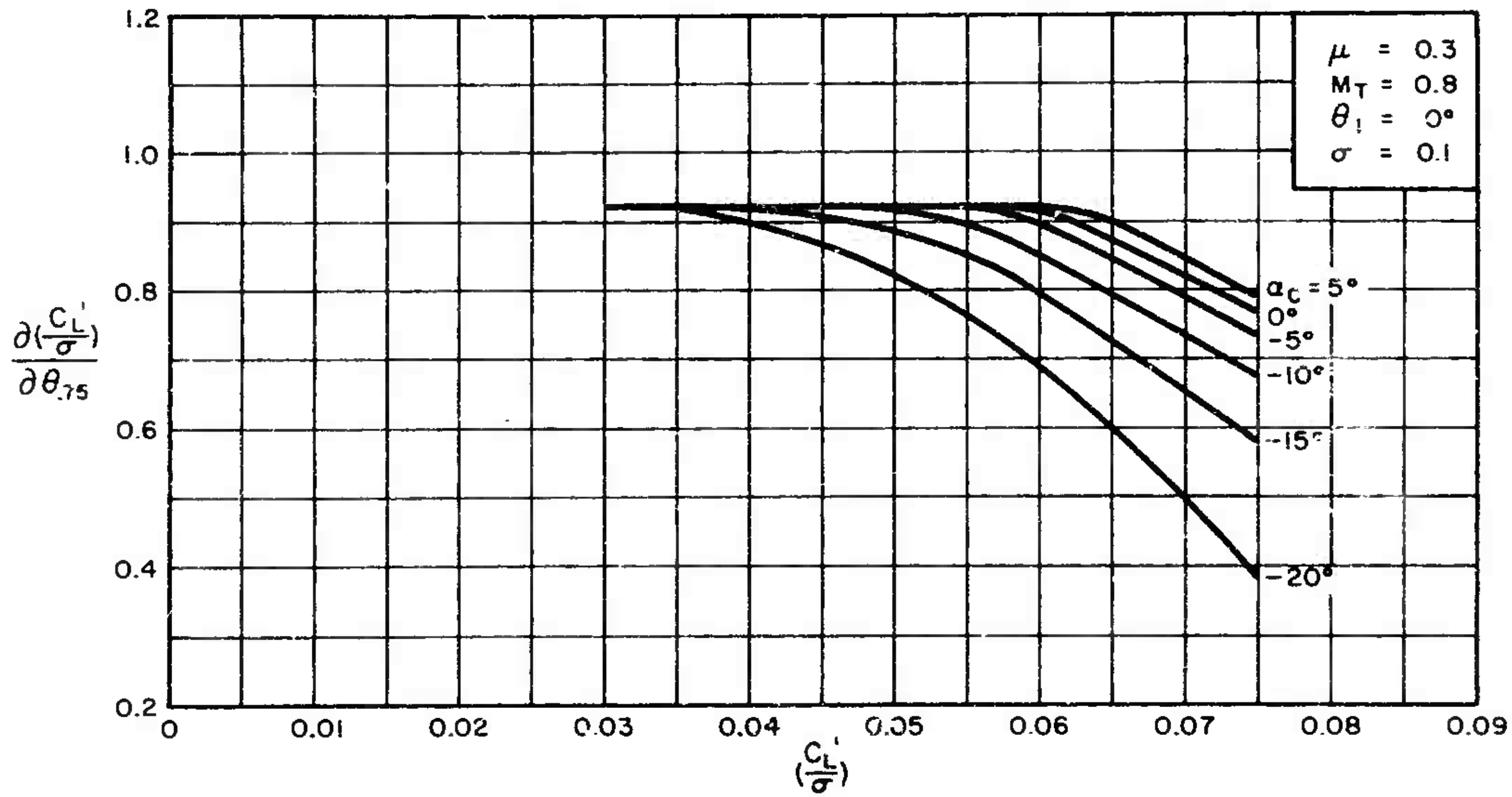

(a) $\mu = 0.3$

Figure 15. Variation of $\frac{\partial(\frac{C_L'}{\sigma})}{\partial \theta_{.75}}$ With $\frac{C_L'}{\sigma}$ for Constant Values of α_c.

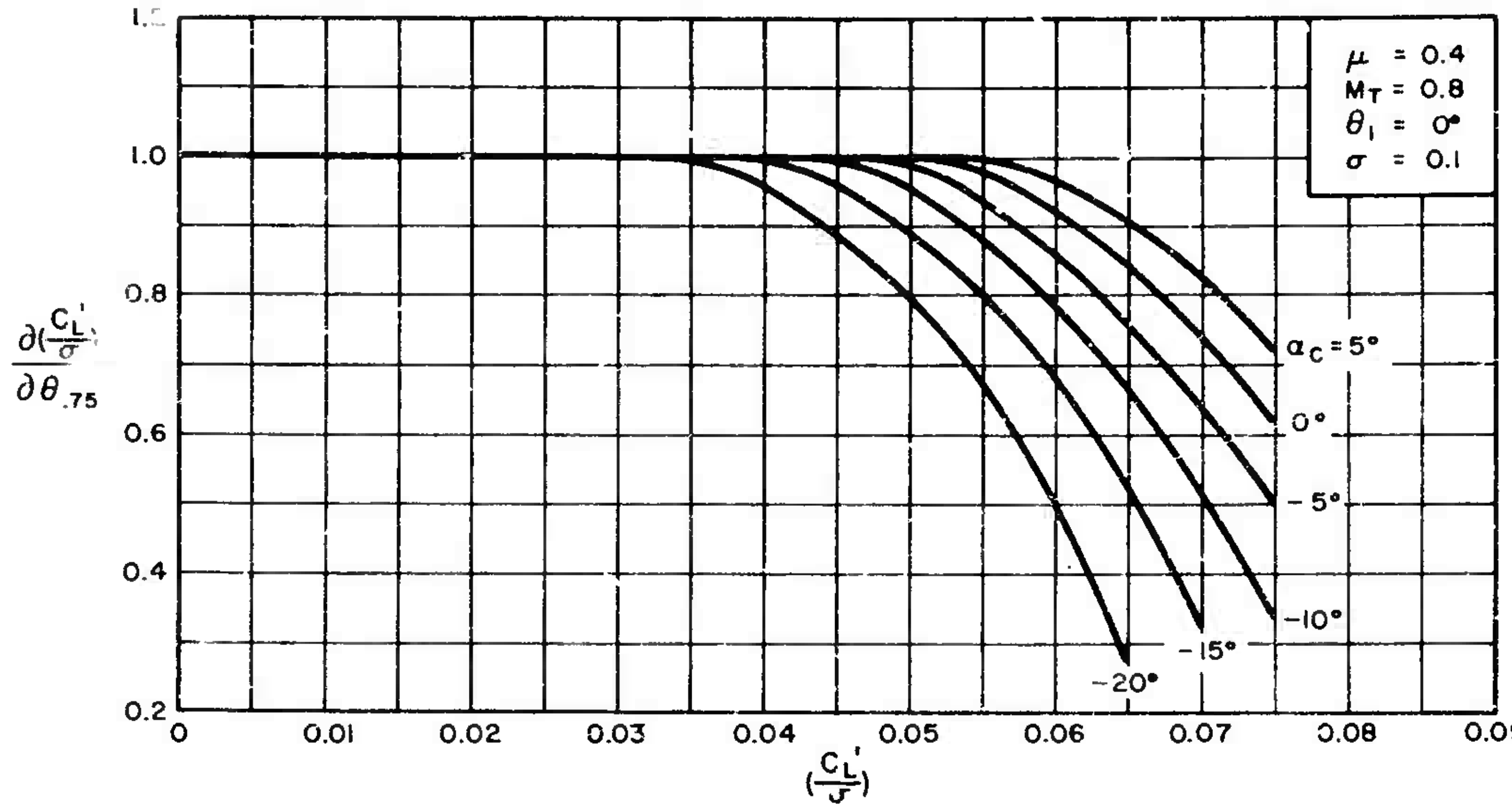

(b) $\mu = 0.4$

Figure 15. Continued.

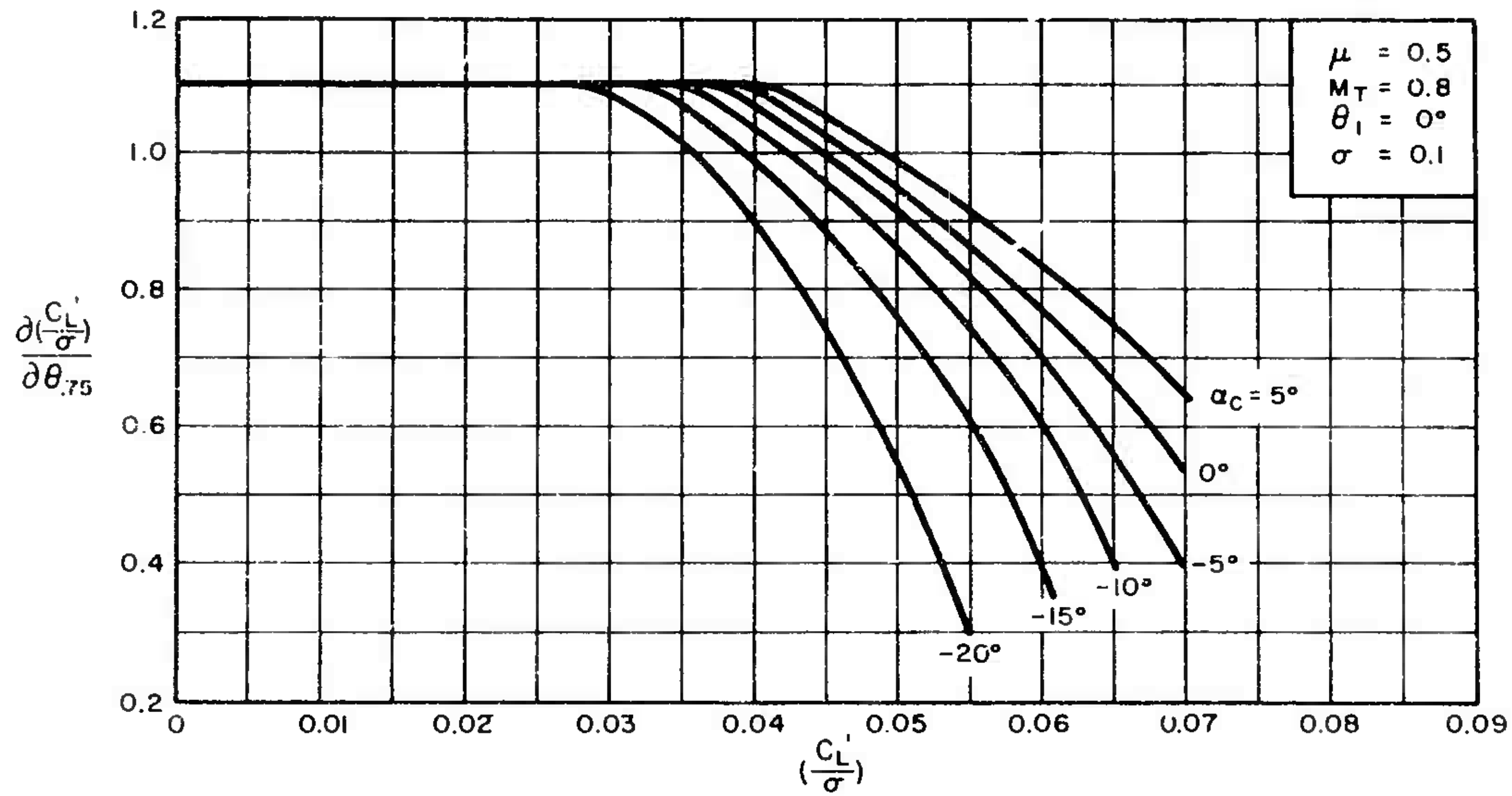

(c) $\mu = 0.5$

Figure 15. Continued.

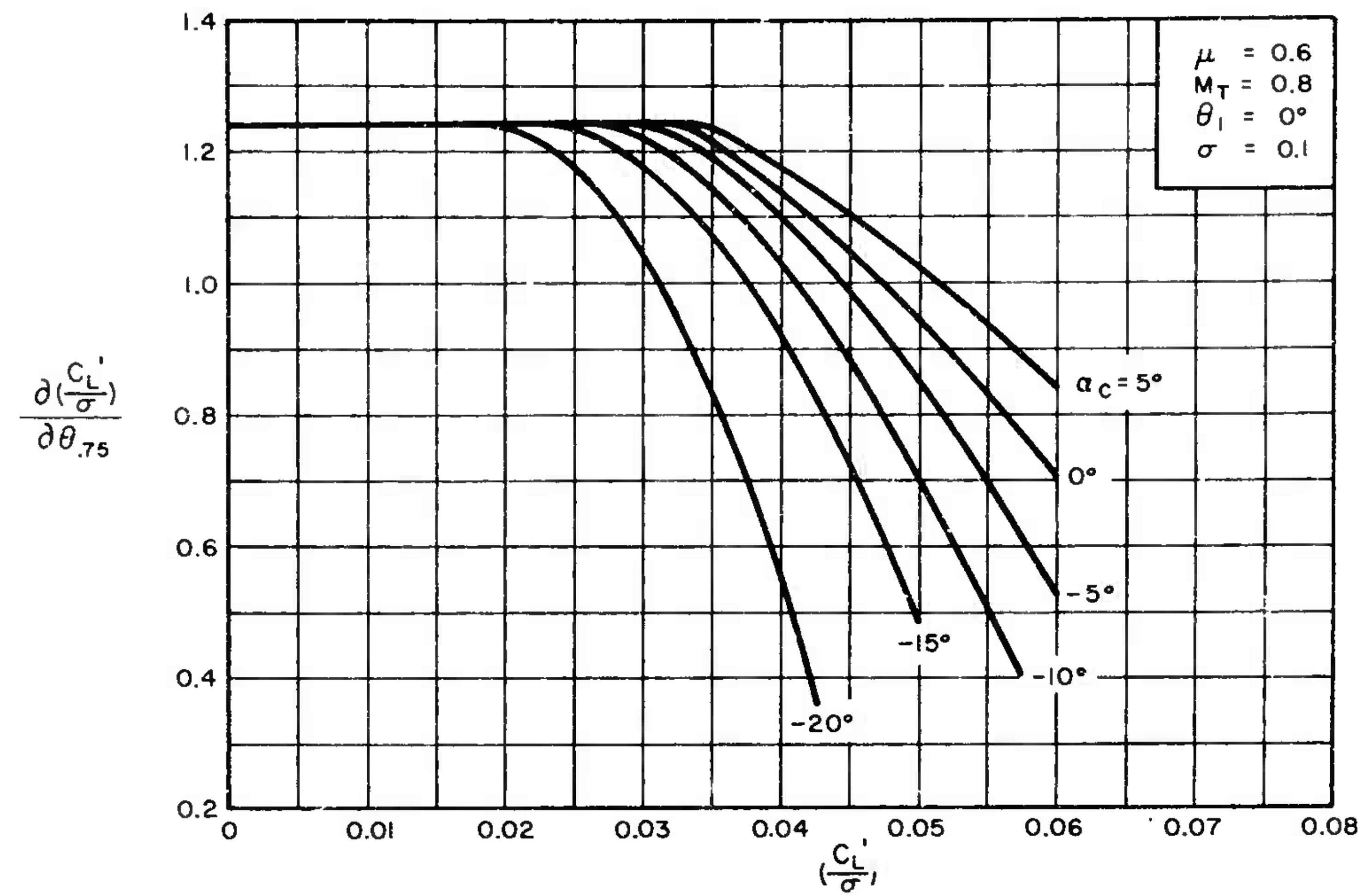

(d) $\mu = 0.6$

Figure 15. Continued.

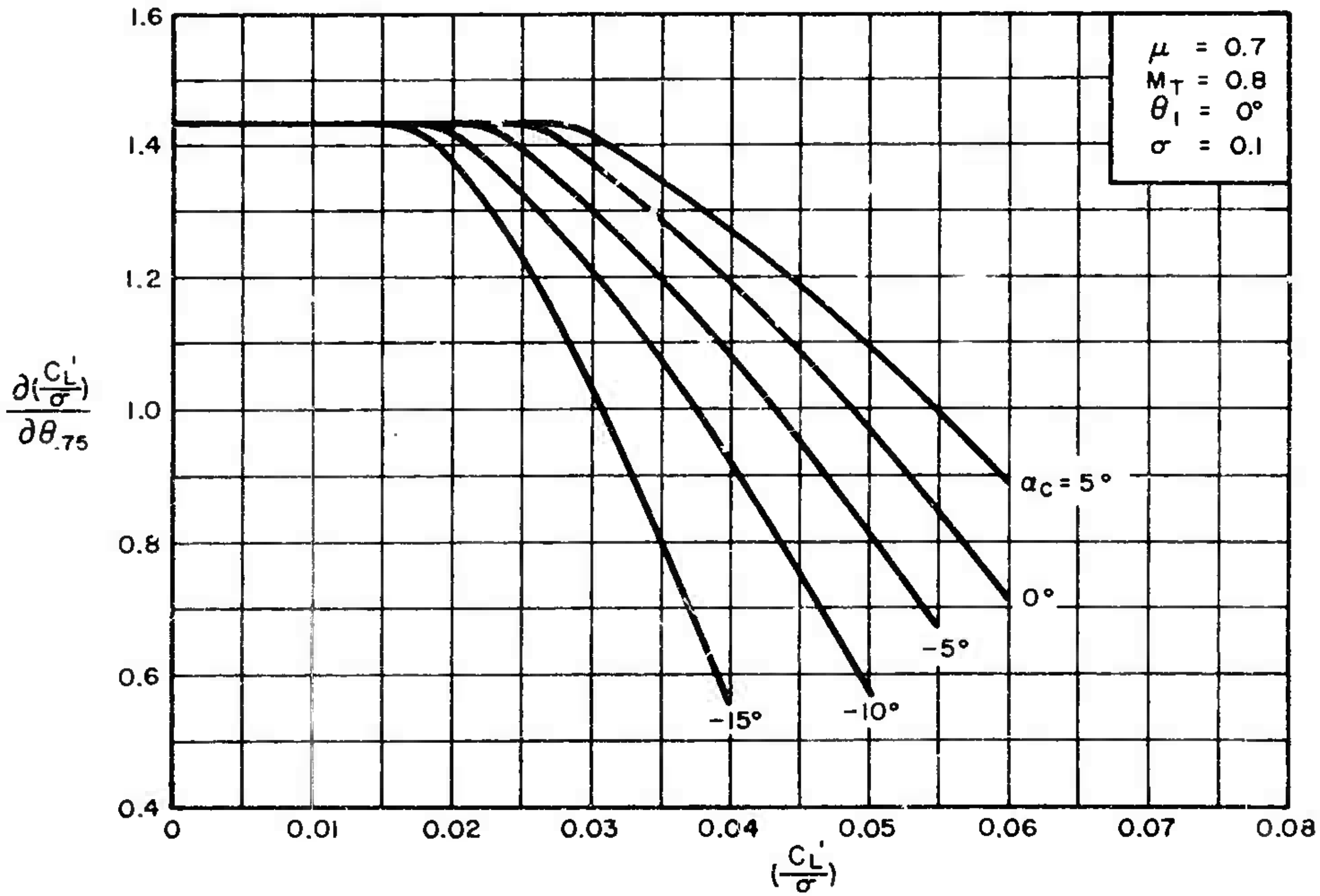

(e) $\mu = 0.7$

Figure 15. Continued.

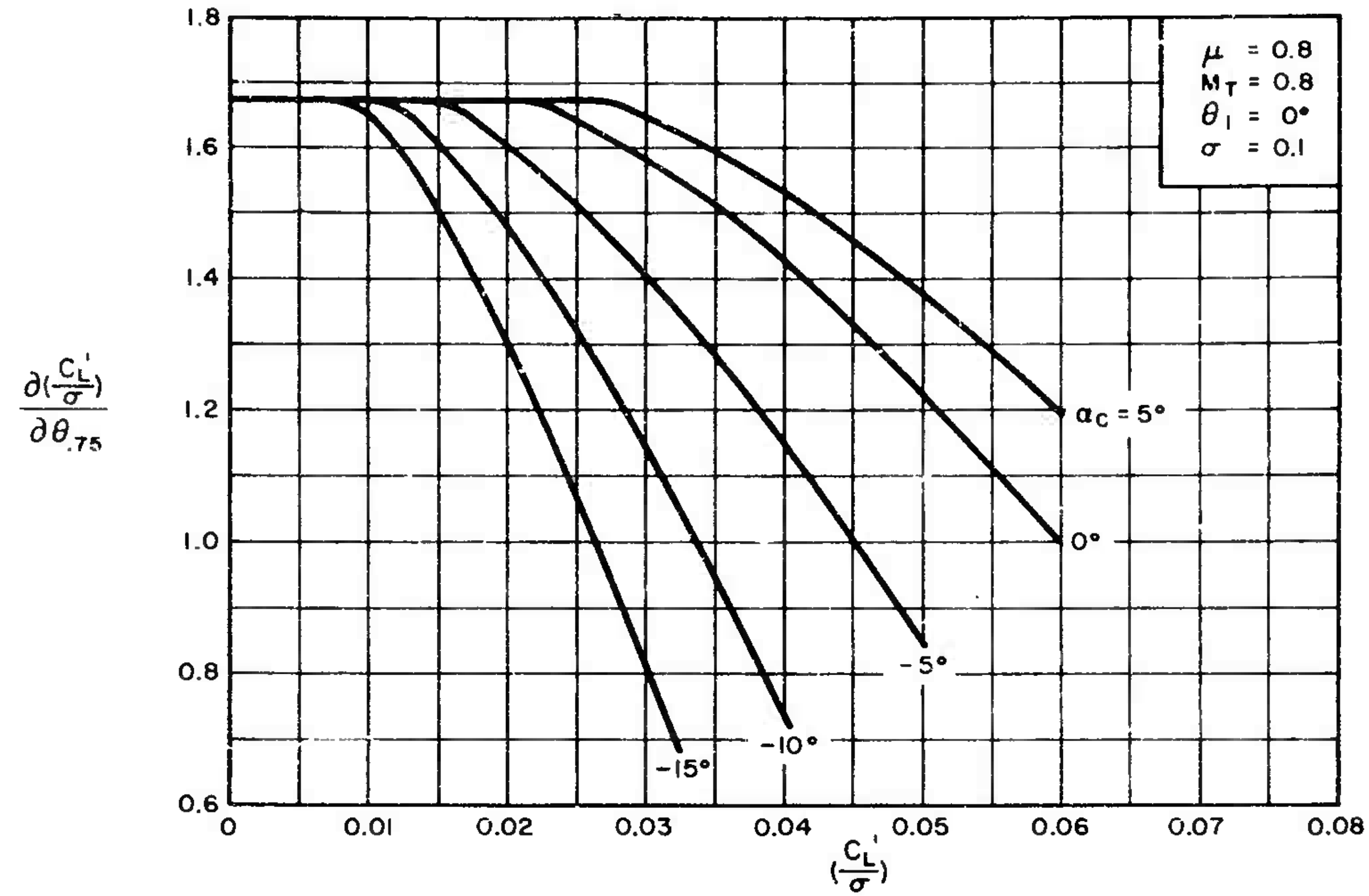

(f) $\mu = 0.8$

Figure 15. Continued.

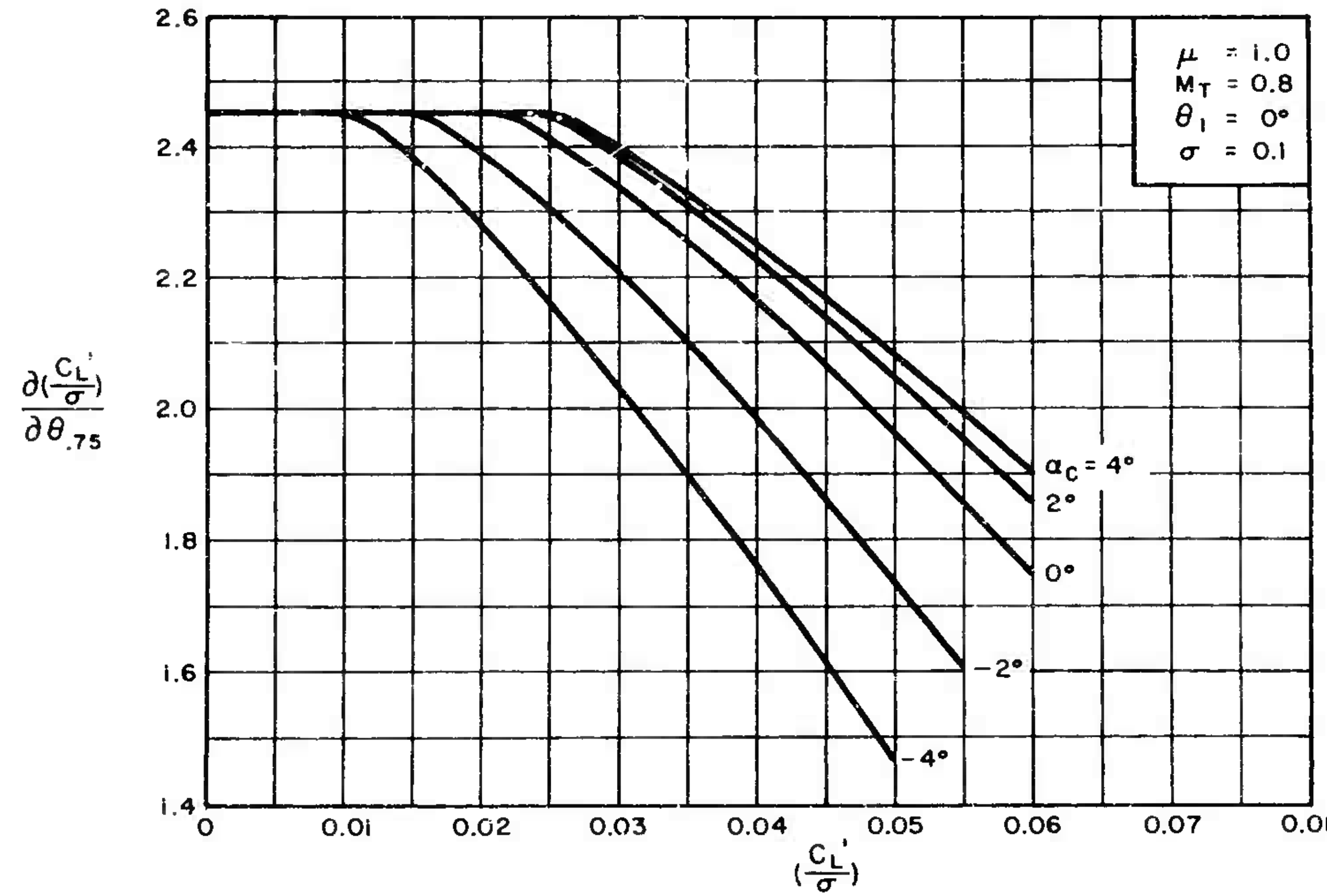

(g) $\mu = 1.0$

Figure 15. Concluded.

7.5.3.2 $\dfrac{\partial(\frac{C_D'}{\sigma})}{\partial\theta_{.75}}$ for $\sigma = 0.1$, $\theta_1 = 0°$, and $M_T = 0.8$

Figures 16(a) through 16(i) present the isolated rotor derivative $\partial(C_D'/\sigma)/\partial\theta_{.75}$ as a function of C_L'/σ for constant values of α_C and a range of μ from $\mu = 0.1$ through $\mu = 1.0$.

The above derivatives for $\mu \leq 0.2$ were obtained by using the following equation:

$$\frac{\partial(\frac{C_D'}{\sigma})}{\partial\theta_{.75}} = \frac{\partial(\frac{C_T}{\sigma})}{\partial\theta_{.75}} \sin\alpha_C + \frac{\partial(\frac{C_H}{\sigma})}{\partial\theta_{.75}} \cos\alpha_C$$

where $\partial(C_T/\sigma)/\partial\theta_{.75}$ and $\partial(C_H'/\sigma)/\partial\theta_{.75}$ were obtained from Reference 3. For $\mu \geq 0.3$, $\partial(C_D'/\sigma)/\partial\theta_{.75}$ was extracted graphically from the theoretical rotor performance data of Reference 2.

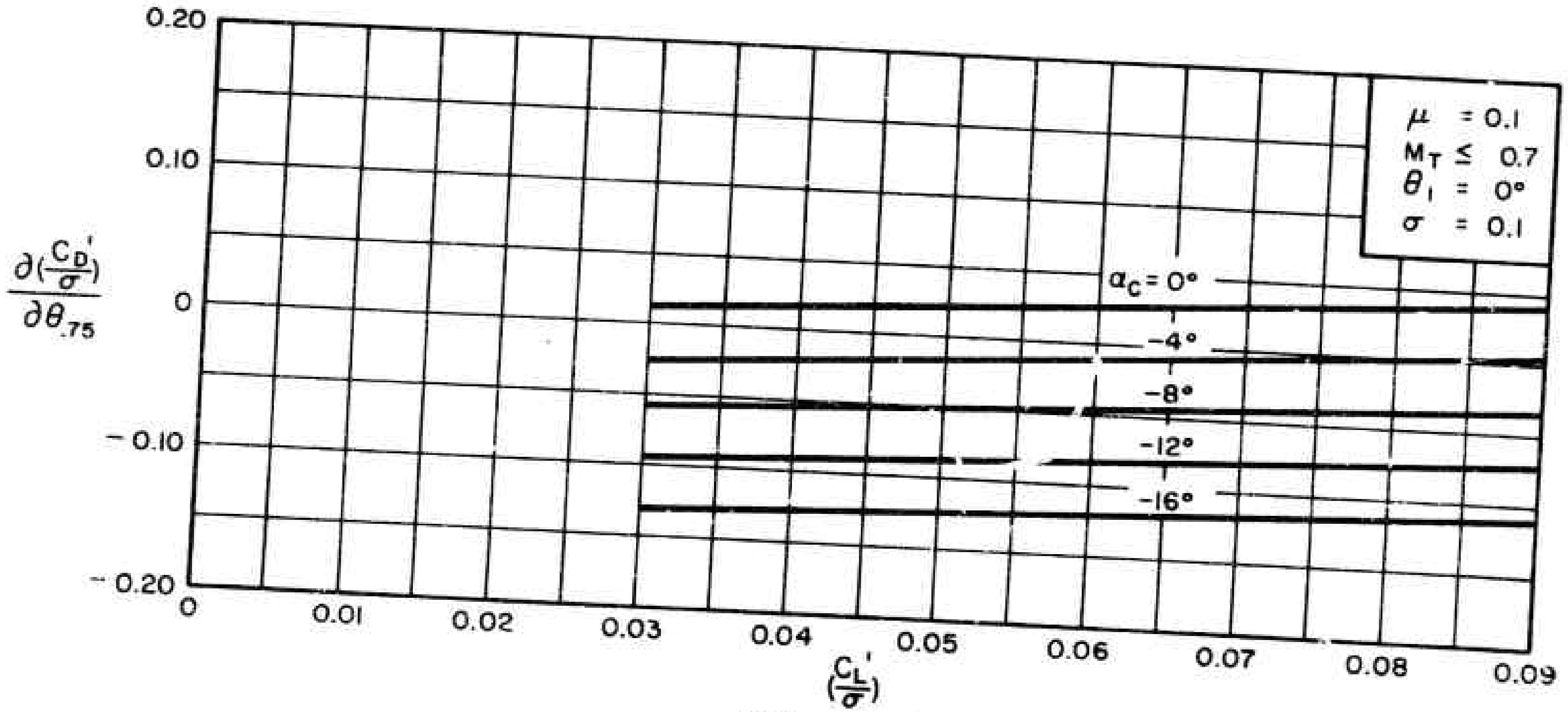

(a) $\mu = 0.1$

Figure 16. Variation of $\frac{\partial(\frac{C_D'}{\sigma})}{\partial\theta_{.75}}$ With $\frac{C_L'}{\sigma}$ for Constant Values of α_c.

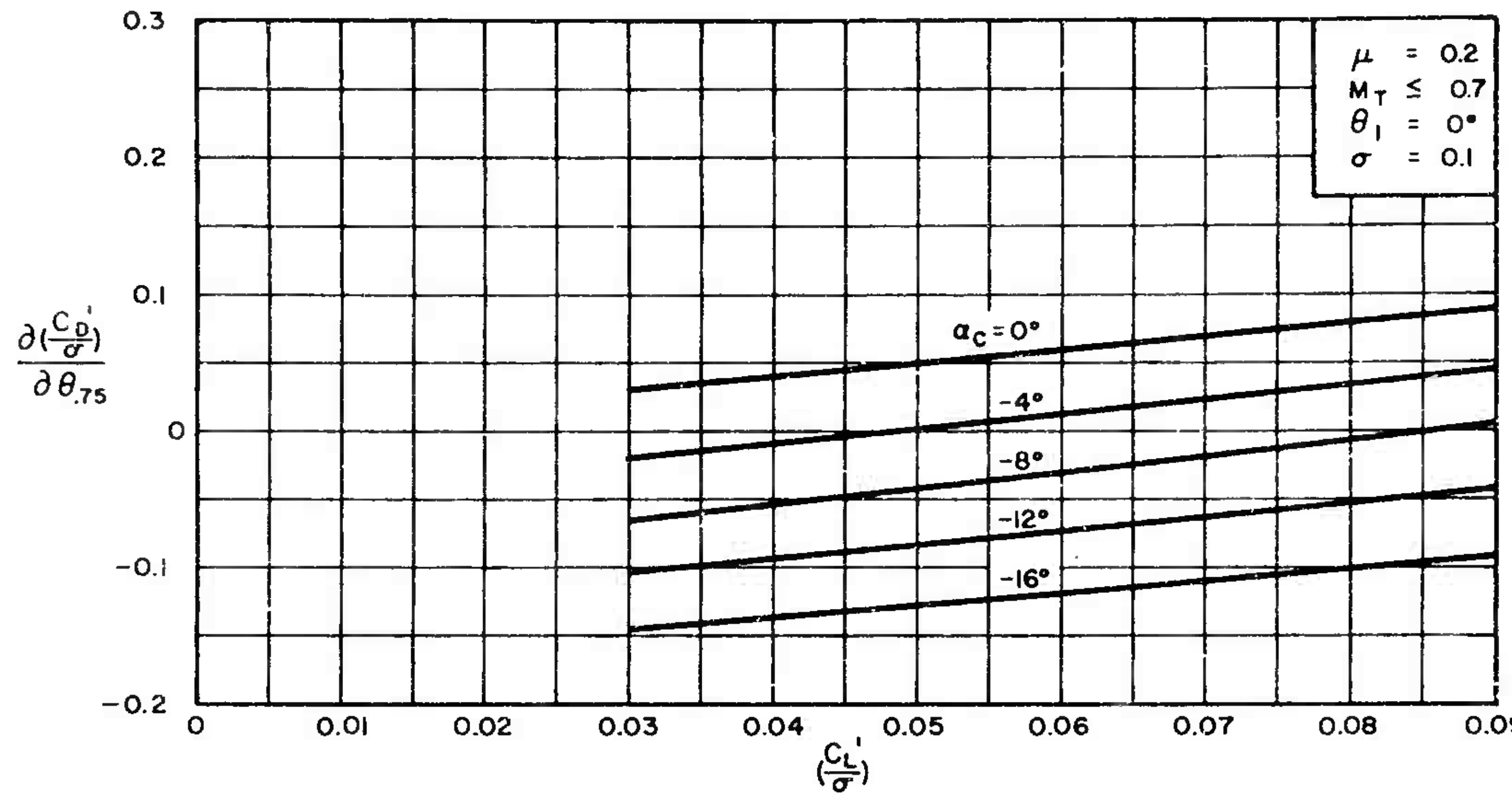

(b) μ = 0.2

Figure 16. Continued.

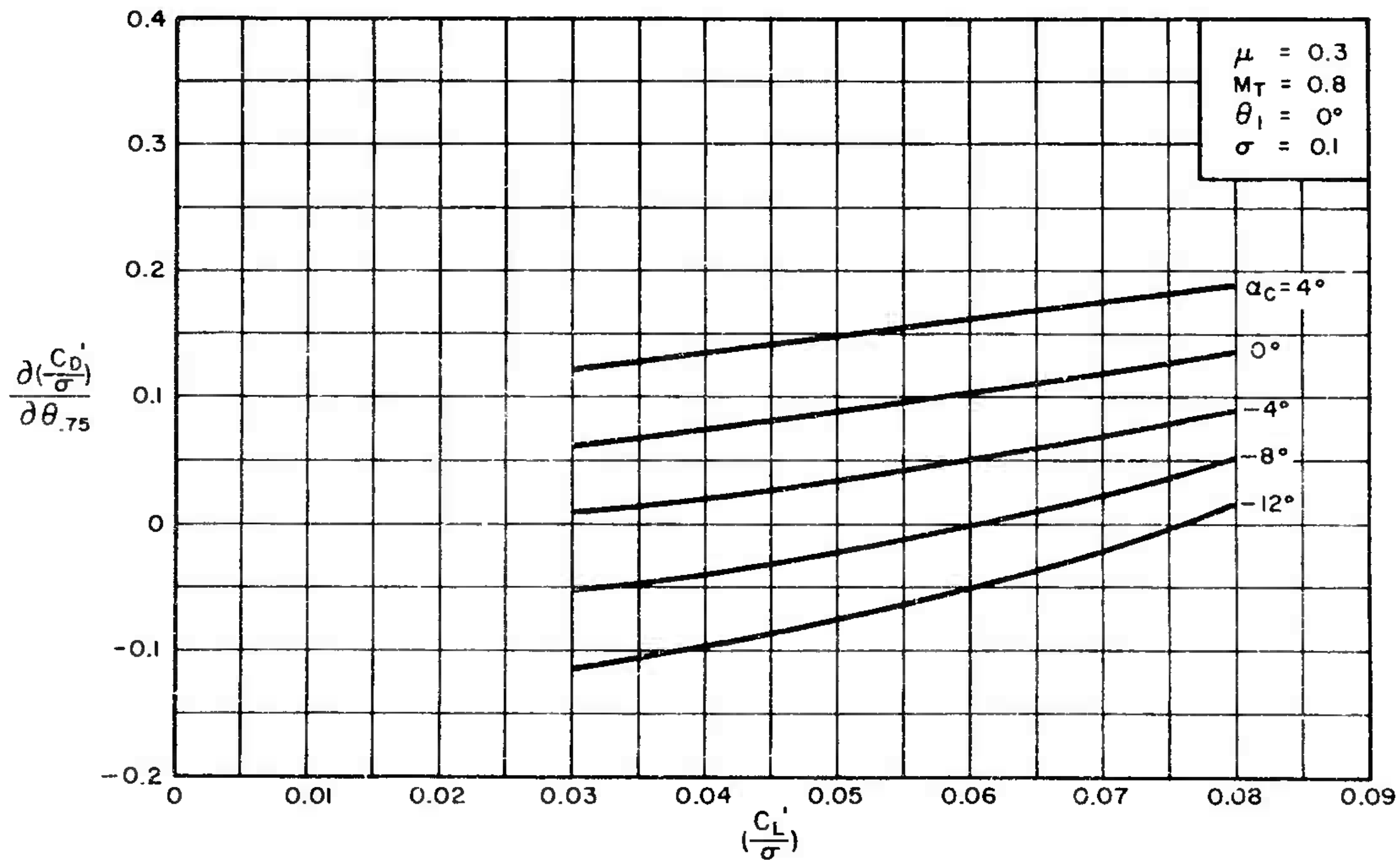

(c) μ = 0.3

Figure 16. Continued.

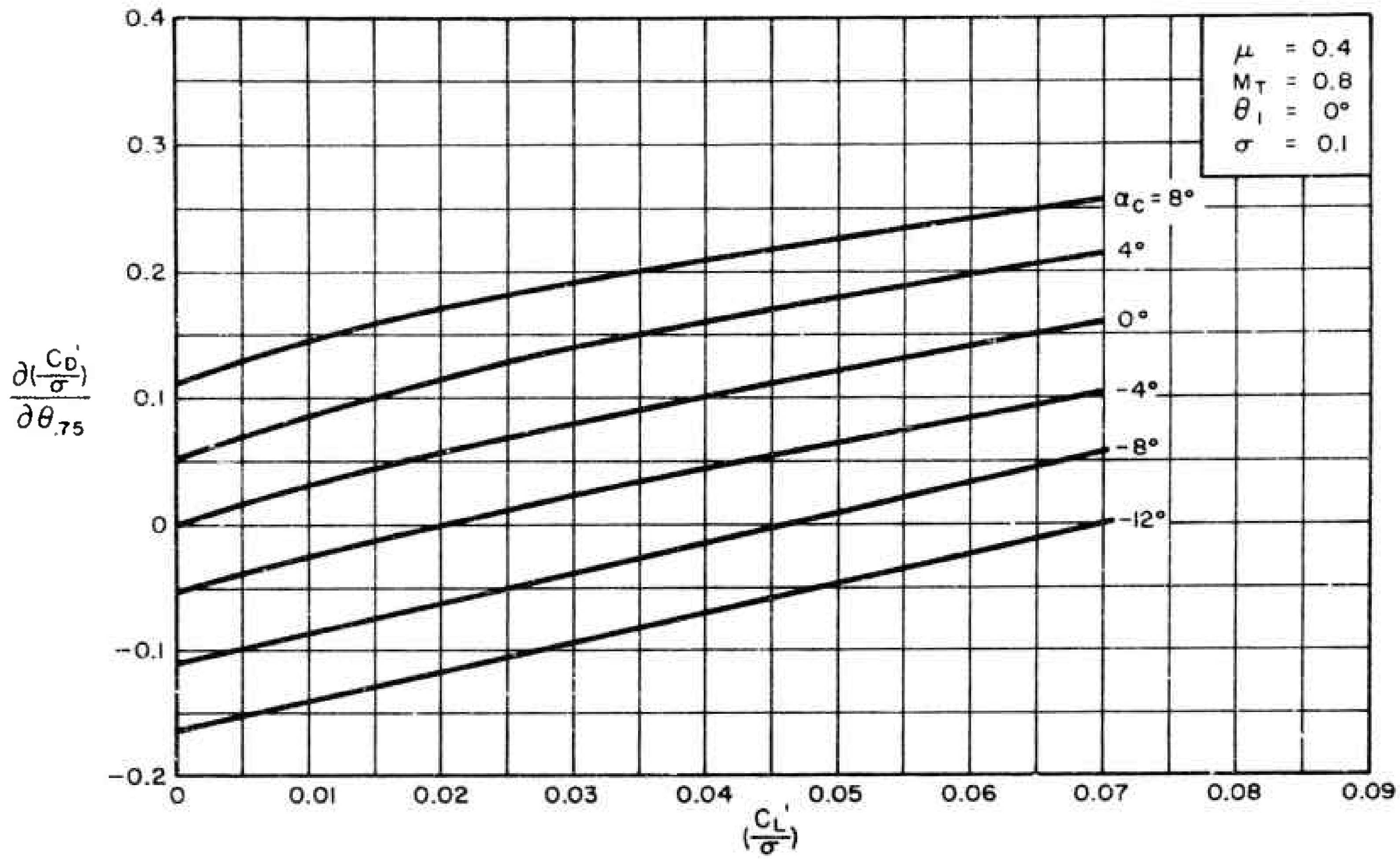

(d) $\mu = 0.4$

Figure 16. Continued.

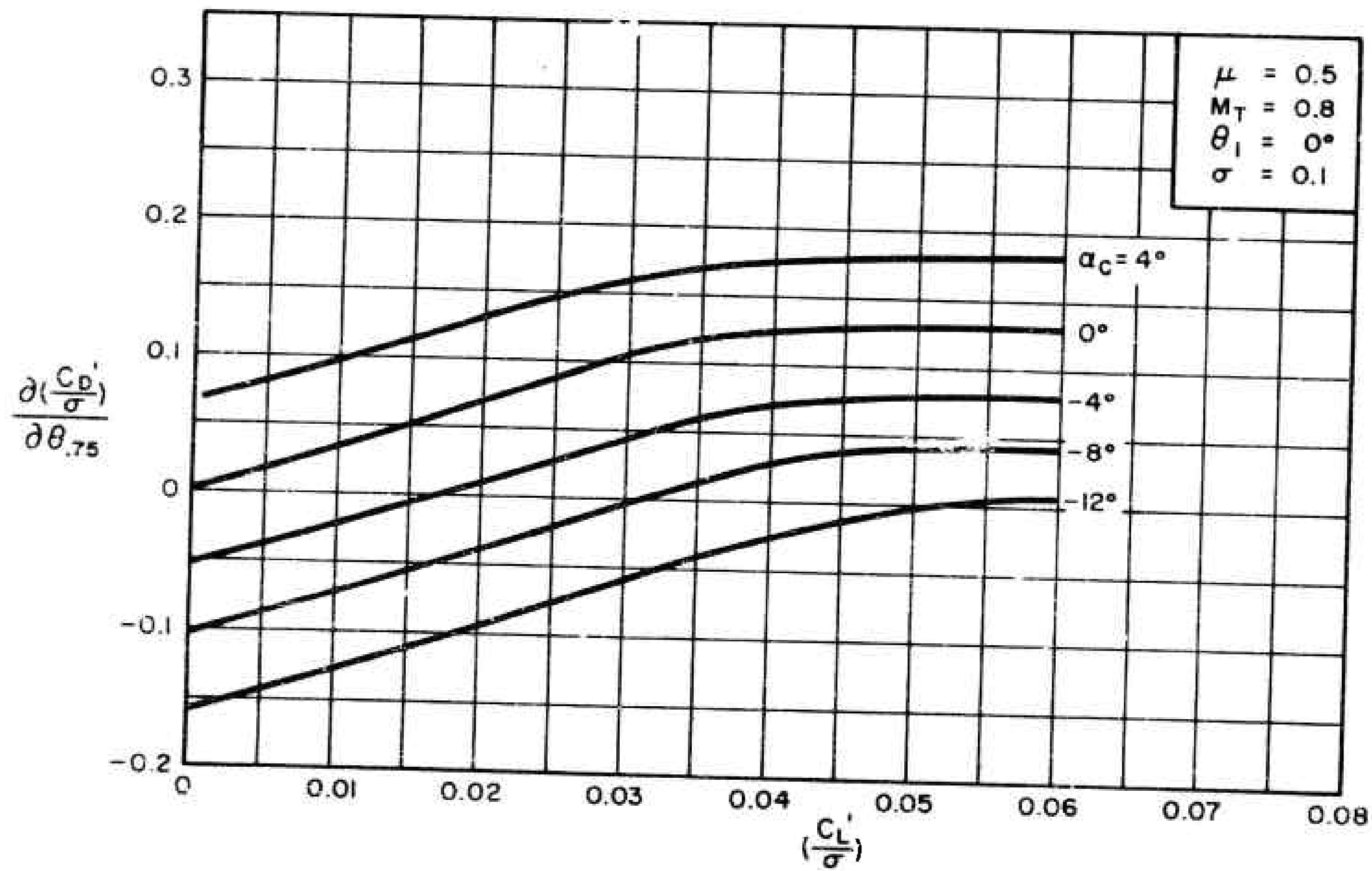

(e) $\mu = 0.5$

Figure 16. Continued.

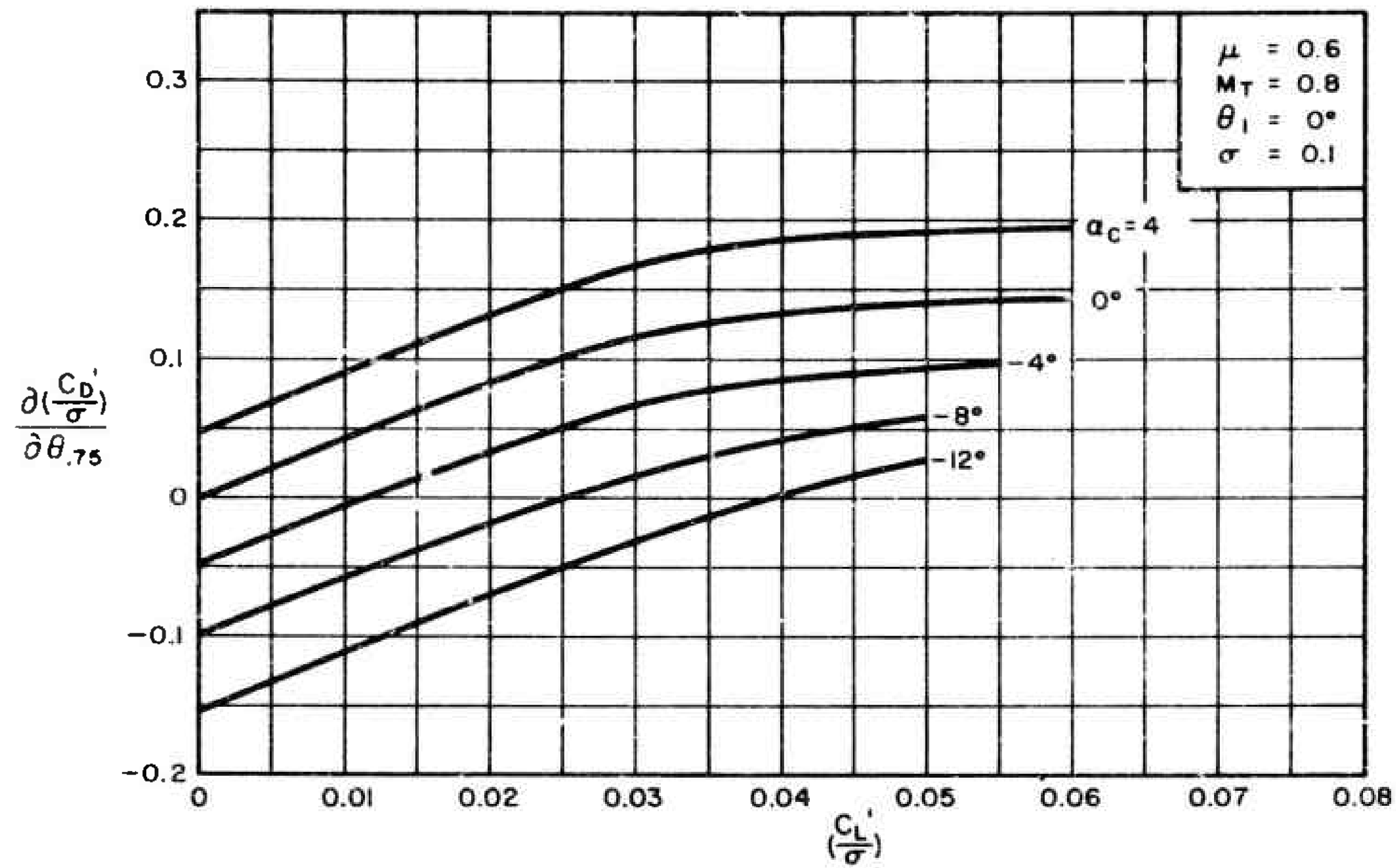

(f) $\mu = 0.6$

Figure 16. Continued.

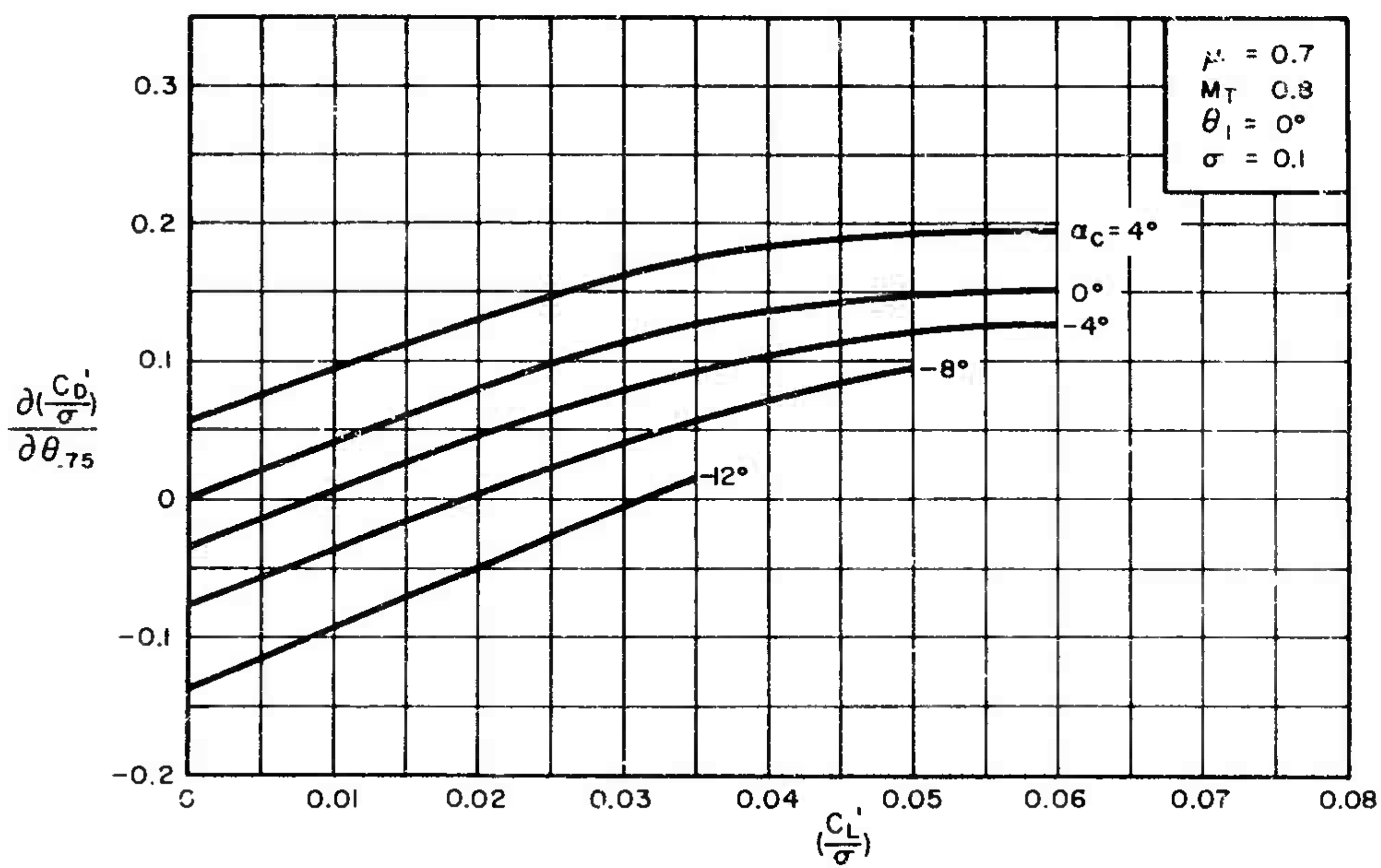

(g) $\mu = 0.7$

Figure 16. Continued.

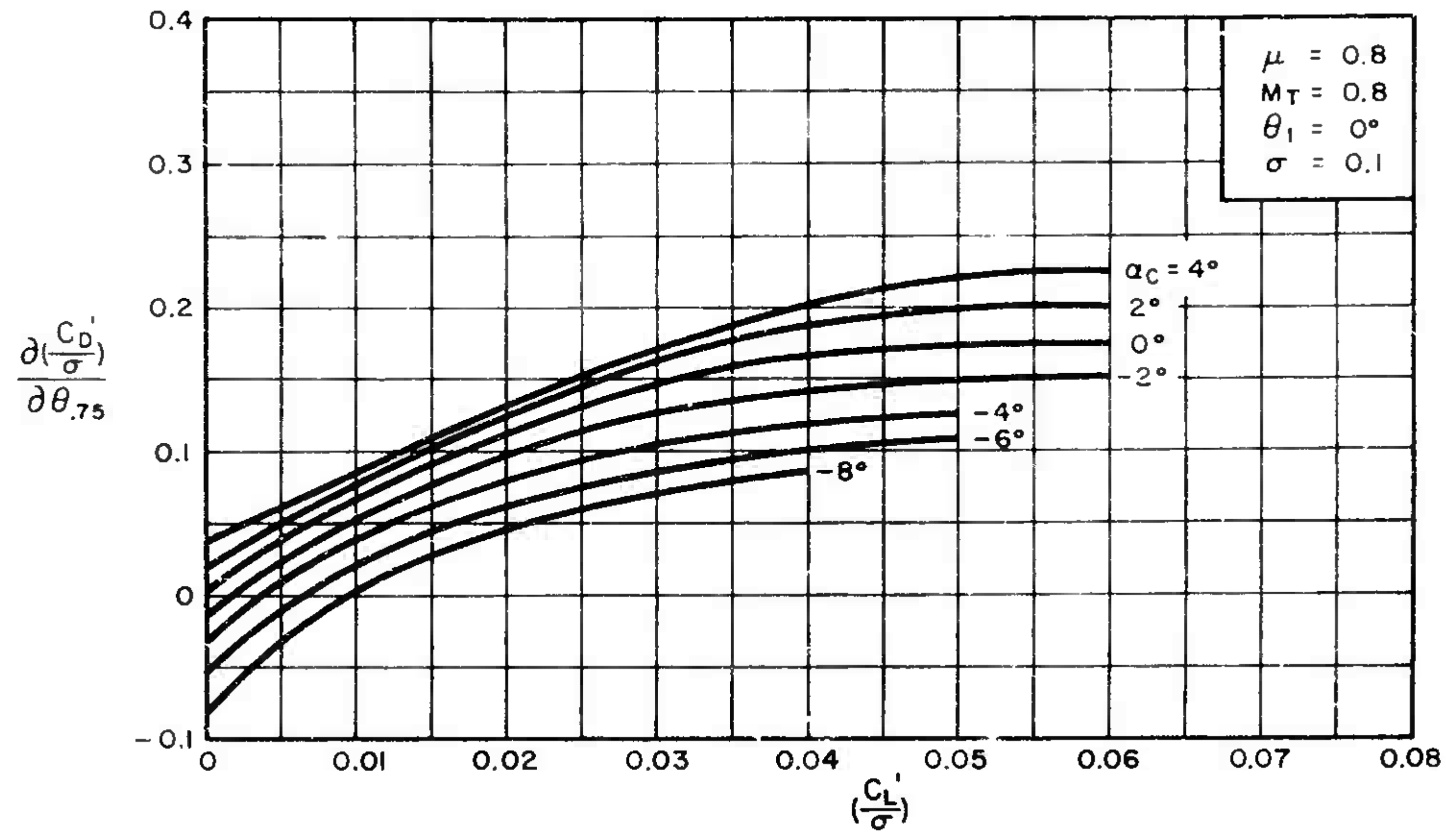

(h) μ = 0.8

Figure 16. Continued.

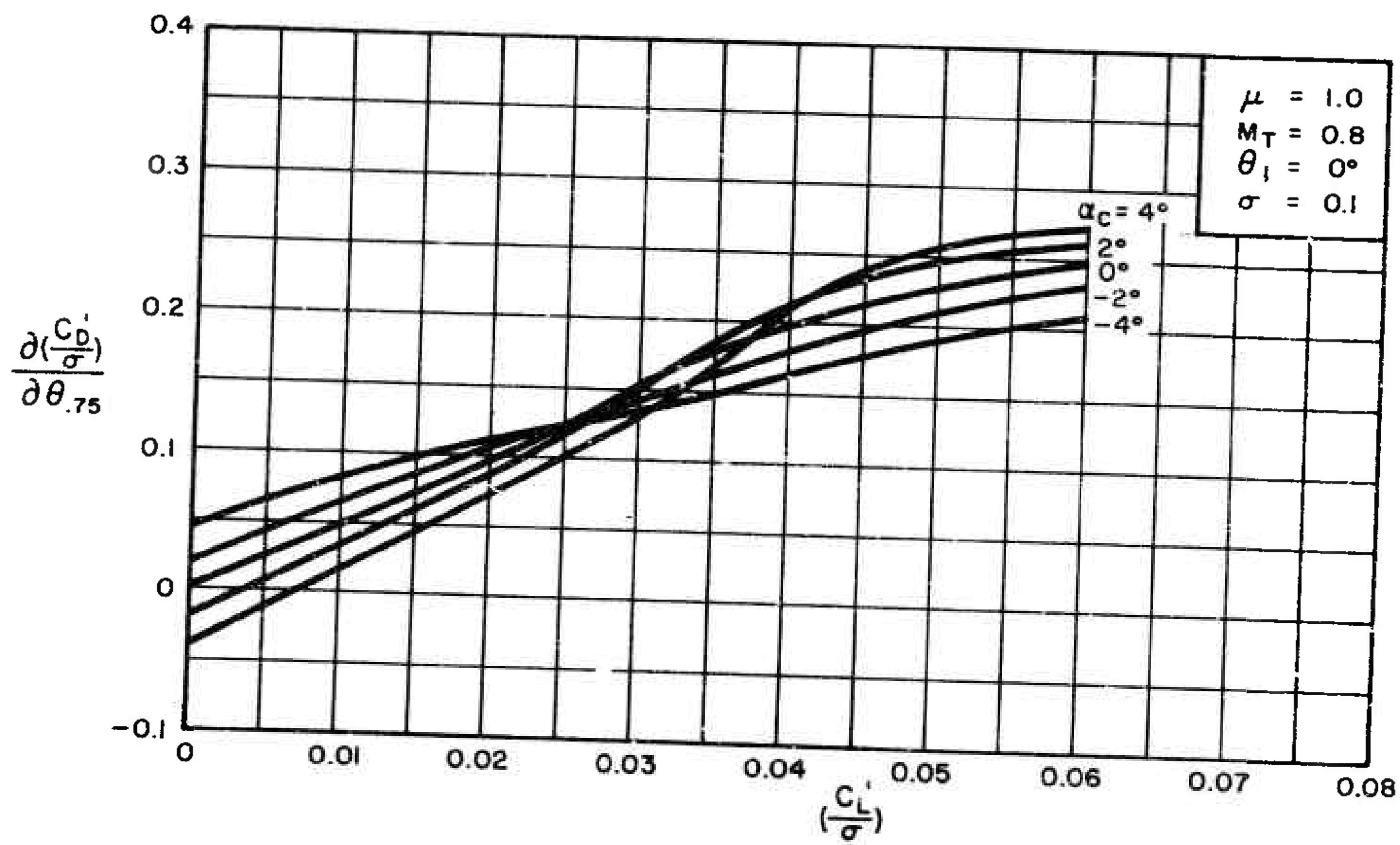

(i) $\mu = 1.0$

Figure 16. Concluded.

7.5.3.3 $\dfrac{\partial(\frac{C_Q}{\sigma})}{\partial\theta_{.75}}$ for $\sigma = 0.1$, $\theta_1 = 0°$, and $M_T = 0.8$

Figures 17(a) through 17(g) present the isolated rotor derivative $\partial(C_Q/\sigma)/\partial\theta_{.75}$ as a function of C_L'/σ for constant values of α_C and a range of tip speed ratios from $\mu = 0.3$ through $\mu = 1.0$. The values of the above derivatives for $\mu \geq 0.3$ were extracted graphically from the theoretical rotor performance data of Reference 2.

For $\mu \leq 0.2$, the following expression was used:

$$\frac{\partial(\frac{C_Q}{\sigma})}{\partial\theta_{.75}} = \frac{1}{2}\left\{\left[\delta_1 t_{53} + \lambda(\delta_2 t_{56} - a t_{42}) + 2\theta_{.75}(\delta_2 t_{58} - a t_{44})\right]\right.$$

$$\left. + \frac{\partial\lambda}{\partial\theta_{.75}}\left[\delta_1 t_{52} + 2\lambda(\delta_2 t_{55} - a t_{41}) + \theta_{.75}(\delta_2 t_{56} - a t_{42})\right]\right\}$$

where $\partial\lambda/\partial\theta_{.75}$ is presented in Subsection 7.5.3.6, and where δ_1, and δ_2 are given on page 82 of Reference 4. Values for the parameters t_{41}, t_{42}, and t_{44} can be obtained from Table 8-4, page 208 of Reference 4, and t_{52}, t_{53}, t_{55}, t_{56}, and t_{58} can be obtained from Table 8-5, page 209 of Reference 4.

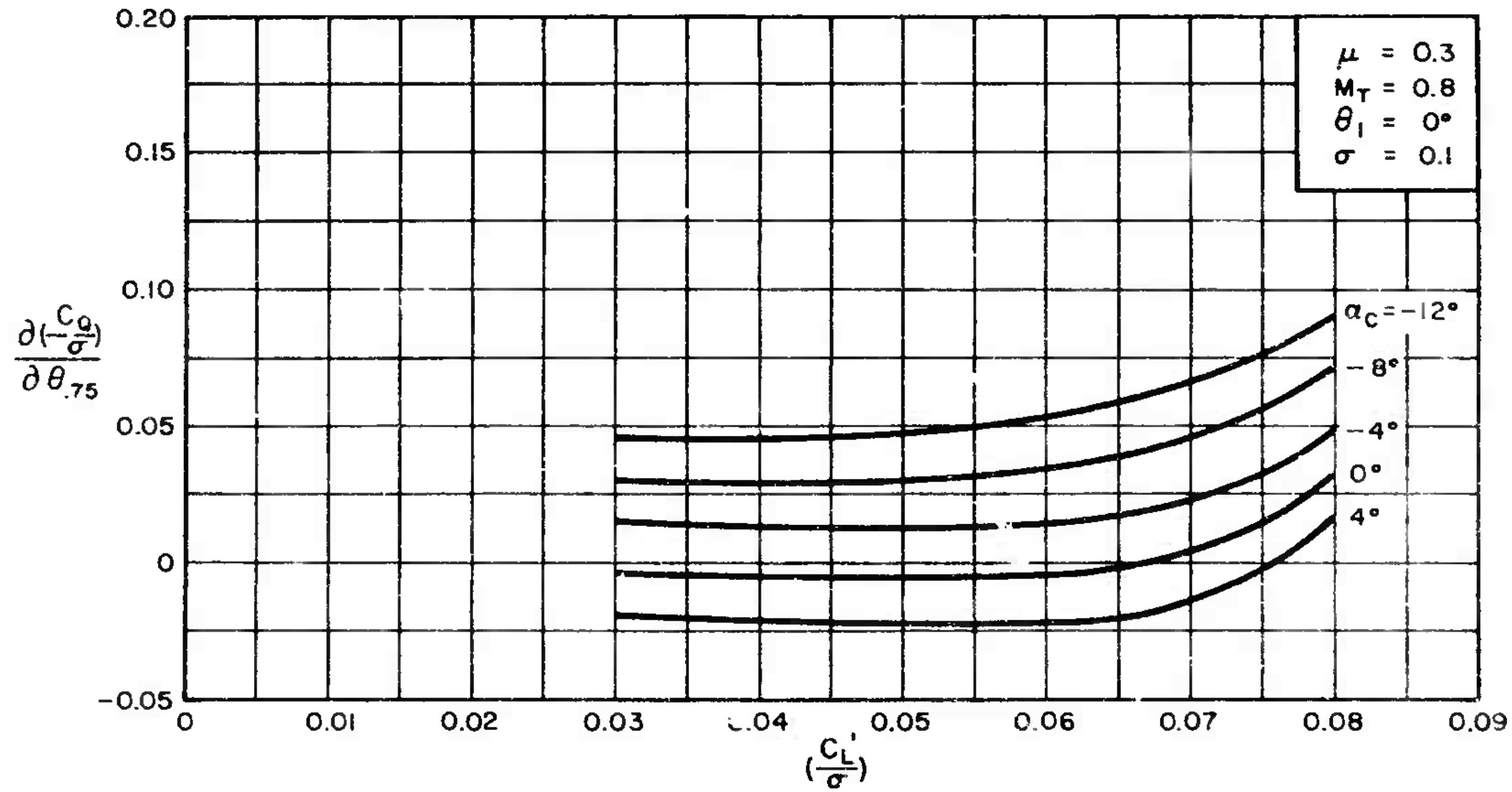

(a) $\mu = 0.3$

Figure 17. Variation of $\frac{\partial(\frac{C_Q}{\sigma})}{\partial\theta_{.75}}$ With $\frac{C_L'}{\sigma}$ for Constant Values of α_c .

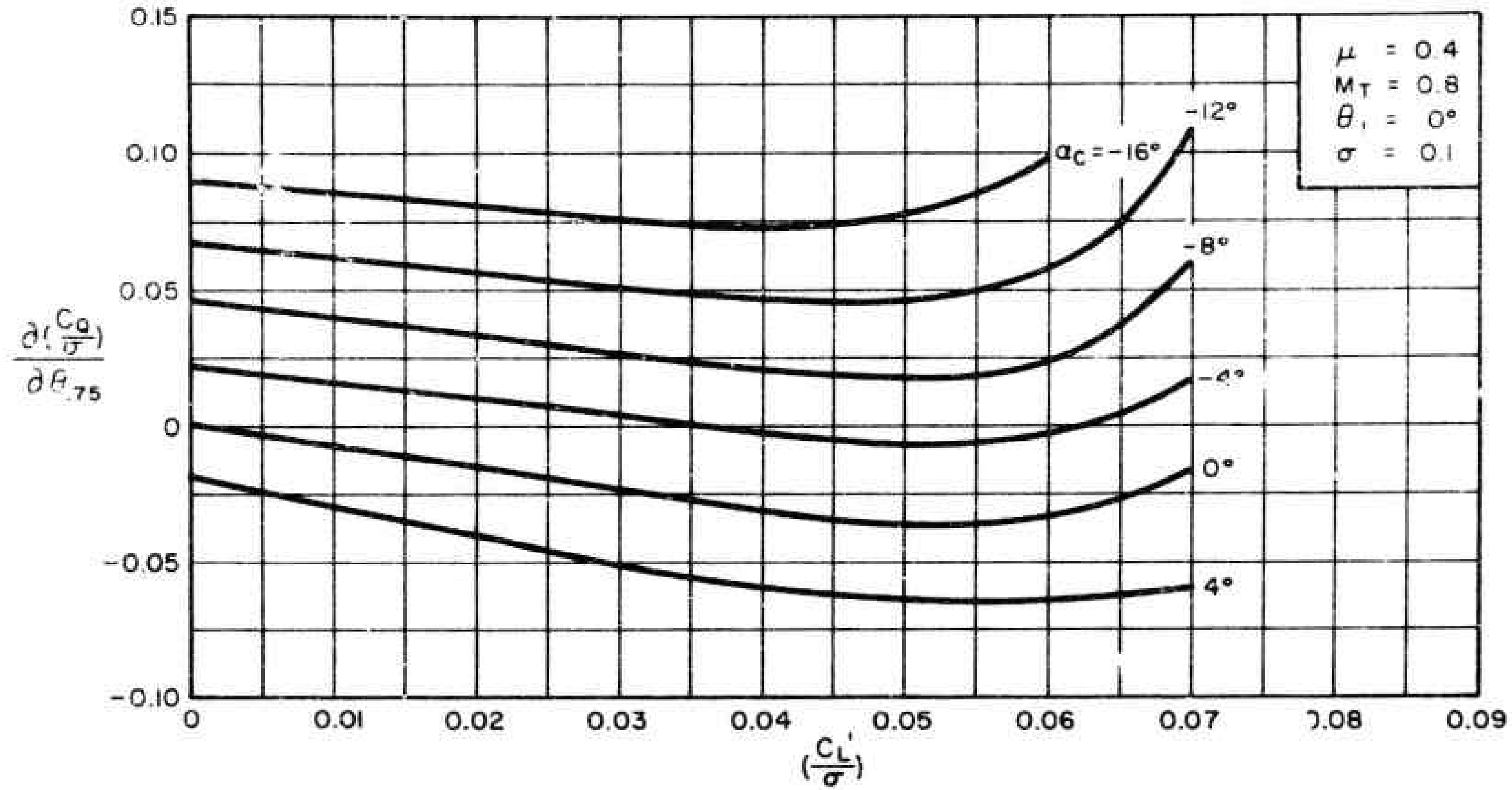

(b) $\mu = 0.4$

Figure 17. Continued.

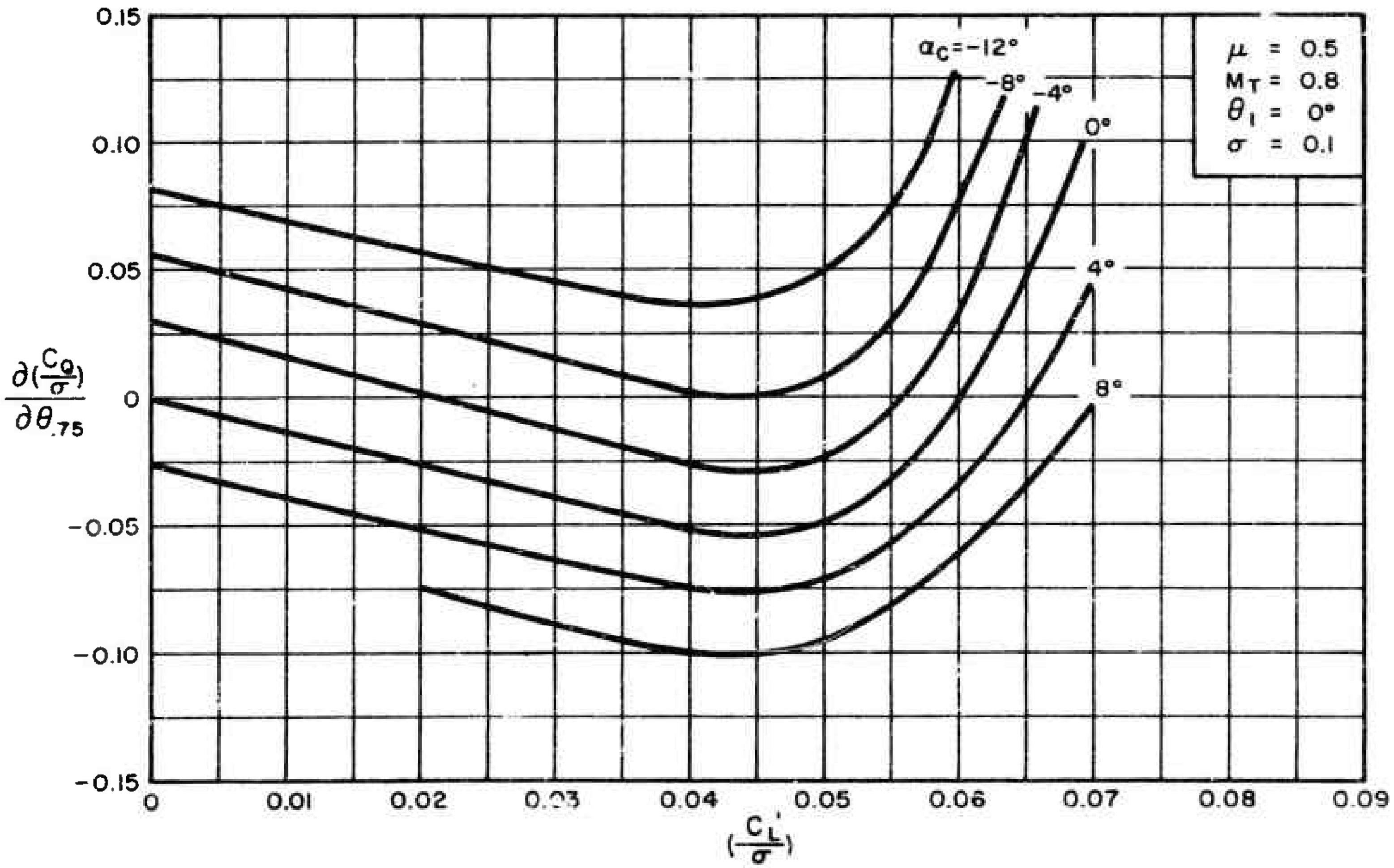

(c) μ = 0.5

Figure 17. Continued.

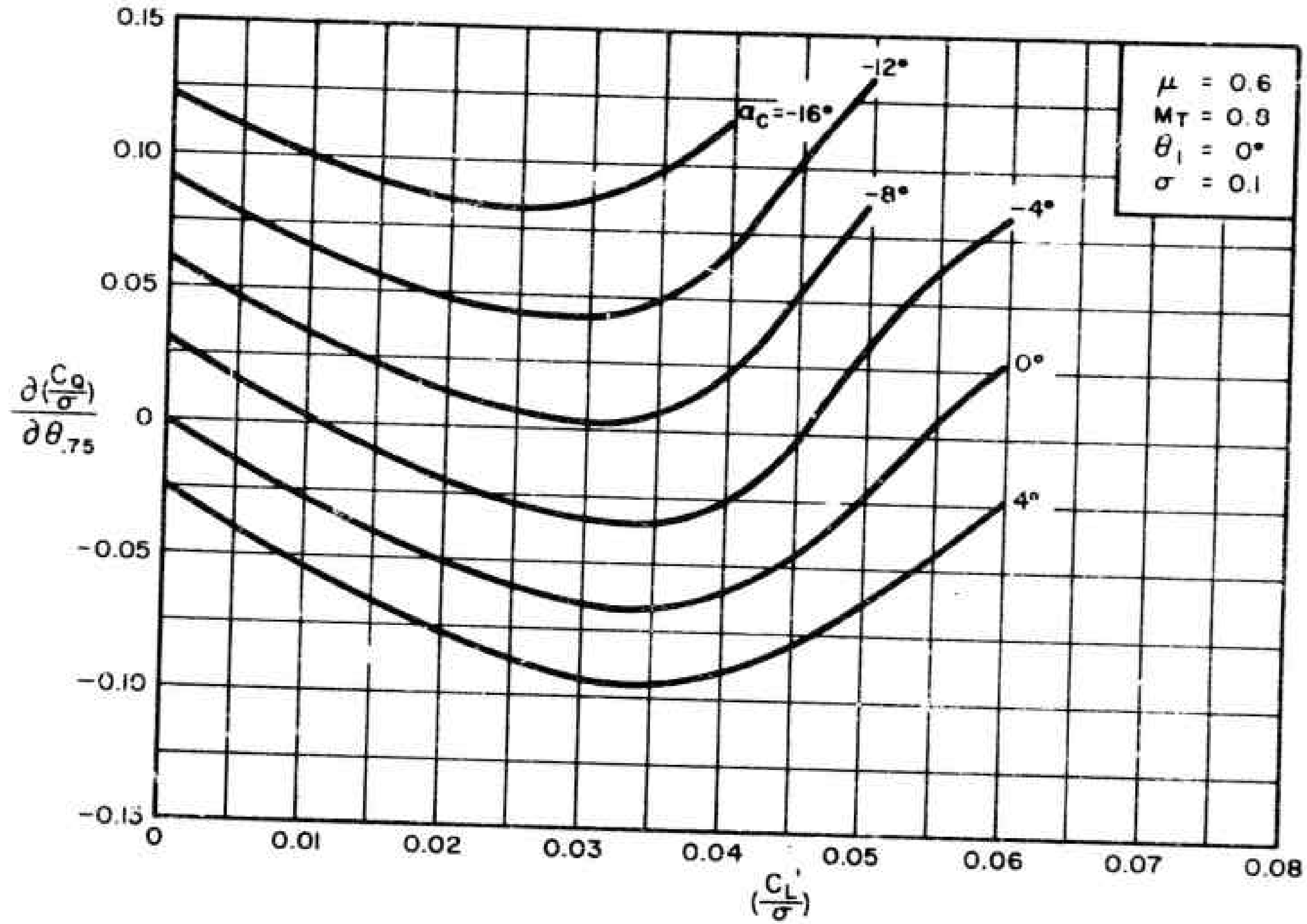

(d) μ = 0.6

Figure 17. Continued.

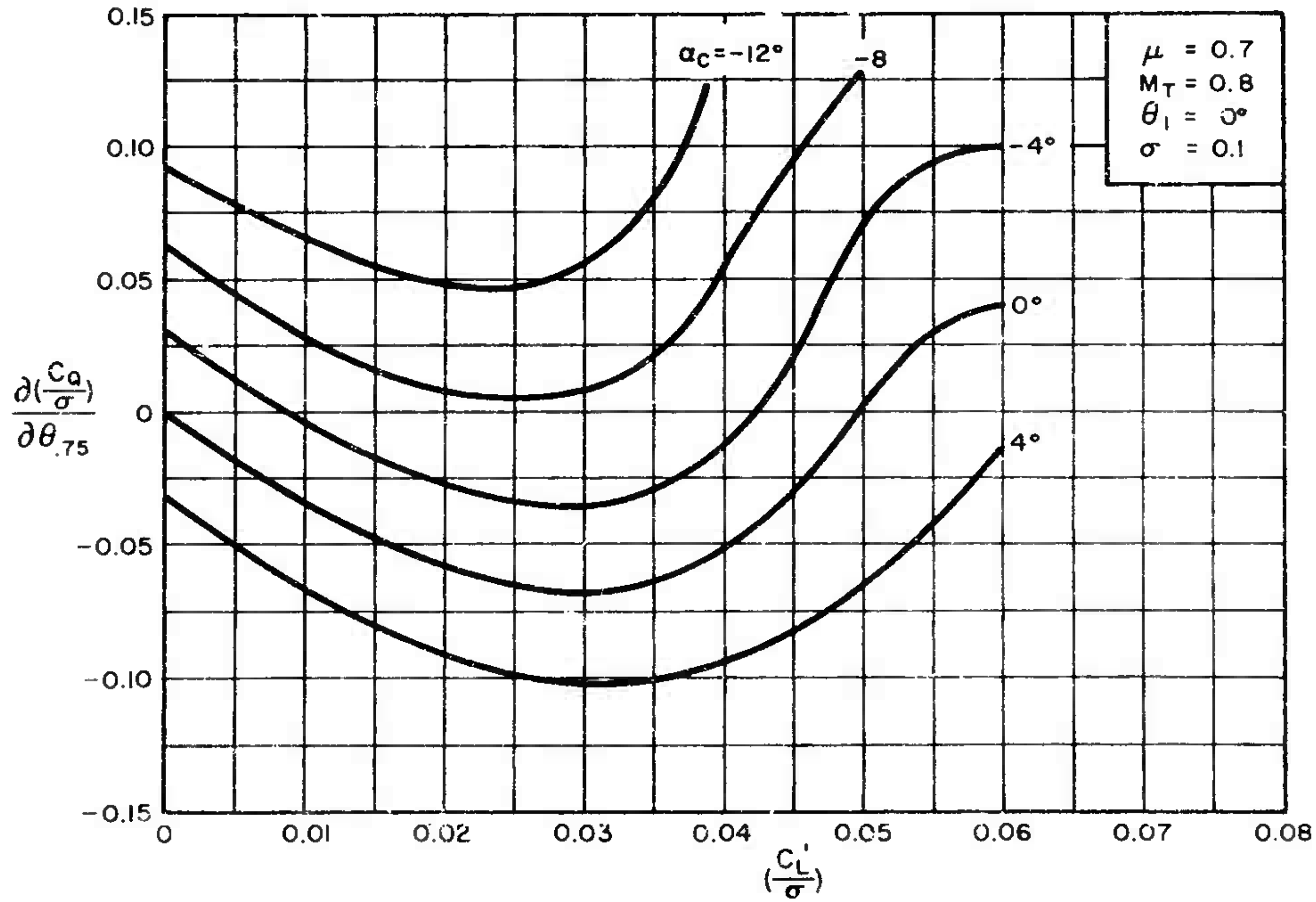

(e) μ = 0.7

Figure 17. Continued.

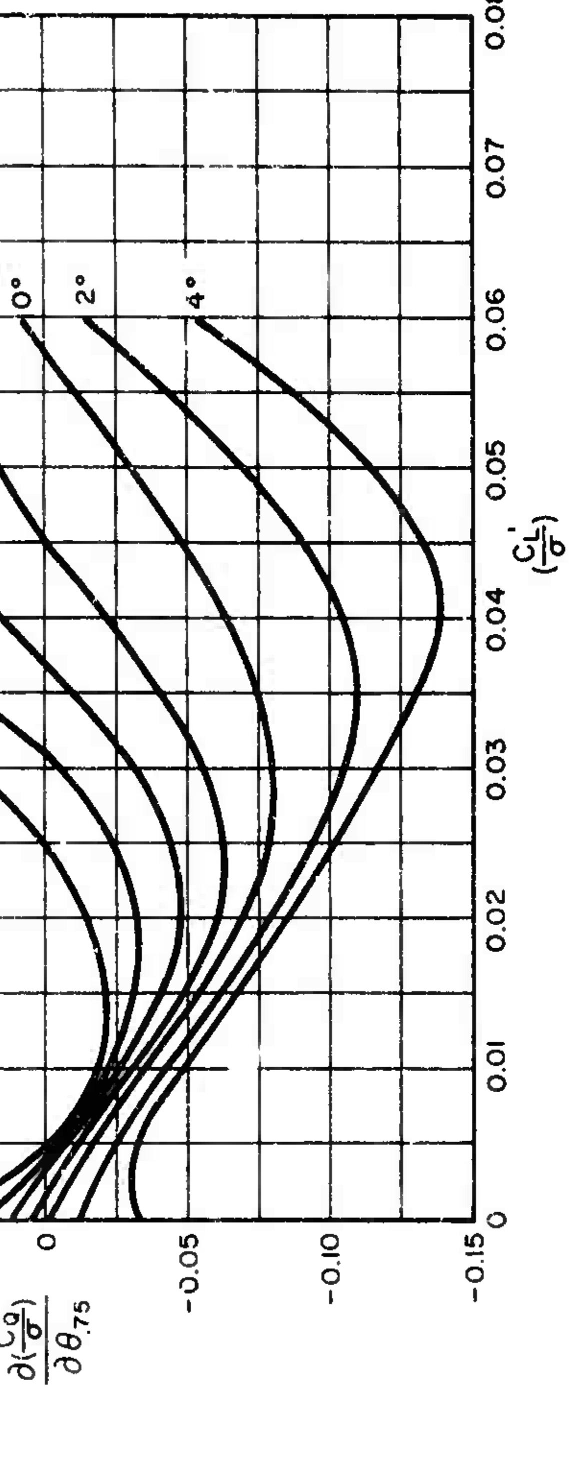

(f) μ = 0.8

Figure 17. Continued.

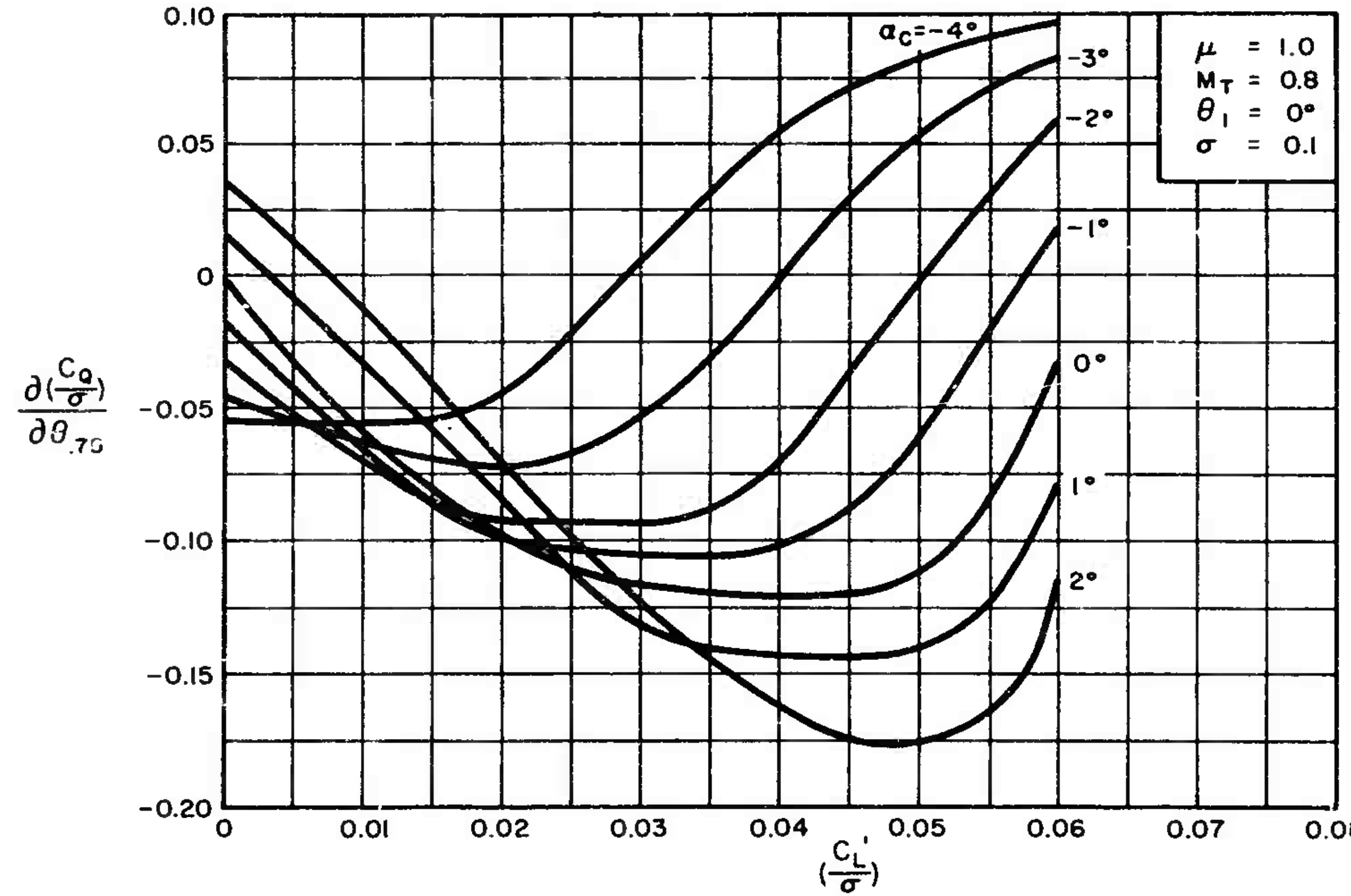

(g) $\mu = 1.0$

Figure 17. Concluded.

7.5.3.4 $\frac{\partial a_1}{\partial \theta_{.75}}$ for $\sigma = 0.1$, $\theta_1 = 0°$, and $M_T = 0.8$

Figure 18 presents the variation of the isolated rotor derivative $\partial a_1/\partial \theta_{.75}$ as a function of rotor tip speed ratio μ .

For values of $\mu \leq 0.2$, the above derivative was obtained by using the following expression:

$$\frac{\partial a_1}{\partial \theta_{.75}} = t_{14} \frac{\partial \lambda}{\partial \theta_{.75}} + (t_{15})$$

where $\partial \lambda/\partial \theta_{75}$ is presented in Subsection 7.5.3.6 and where t_{14} , t_{15} can be obtained from Table 8-1, page 205 of Reference 4.

For values of $\mu \geq 0.3$, the $\partial a_1/\partial \theta_{.75}$ derivative was obtained graphically by using the theoretical data of Reference 2.

The results obtained are applicable for all values of $\theta_{.75}$, C_L'/σ and α_C.

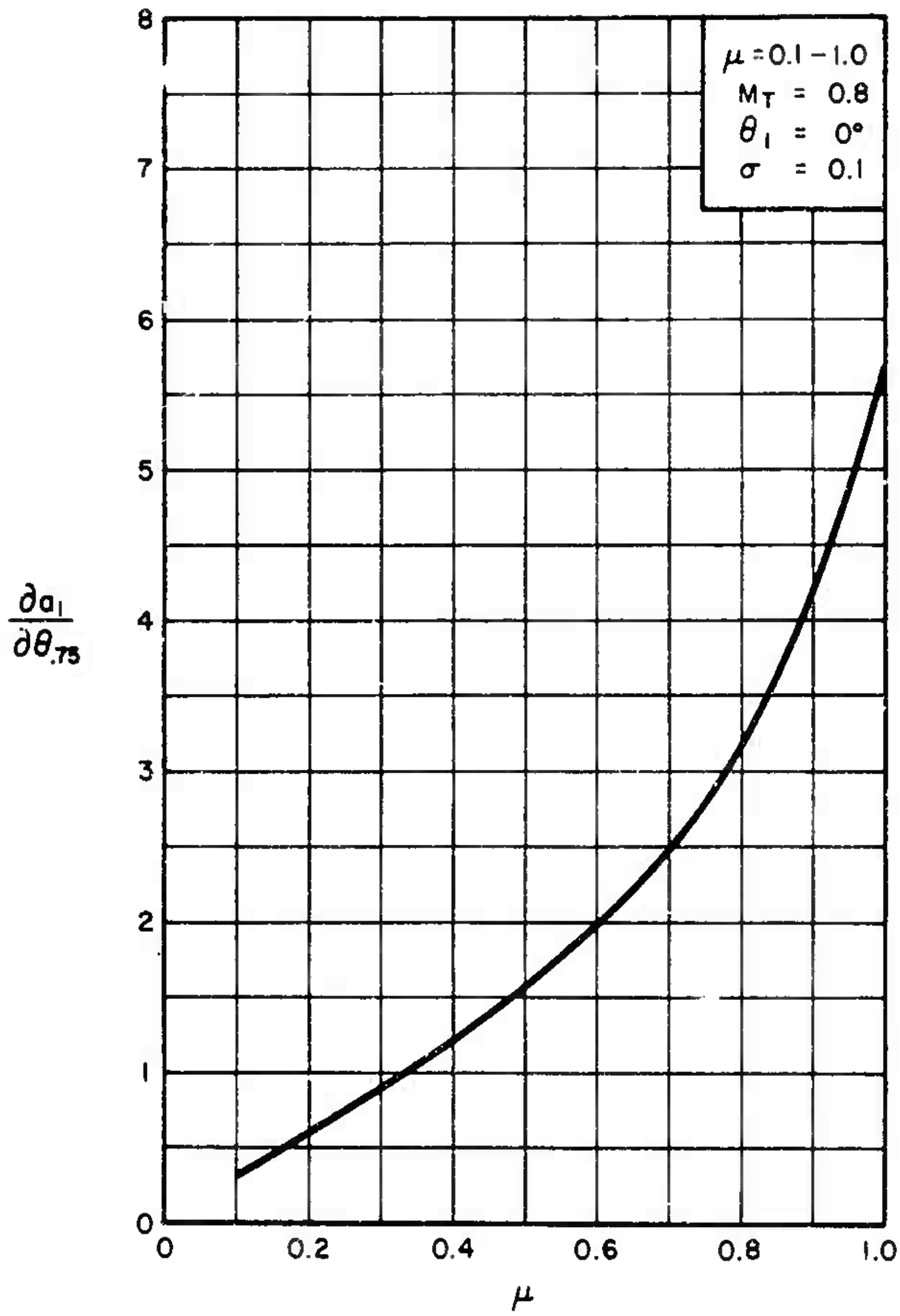

Figure 18. Variation of $\frac{\partial a_1}{\partial \theta_{.75}}$ W..th μ for All Values of $\theta_{.75}$, $\frac{C_L{}'}{\sigma}$, and α_C.

7.5.3.5 $\frac{\partial b_1}{\partial \theta_{.75}}$ for $\sigma = 0.1$, $\theta_1 = 0°$, and $M_T = 0.8$

Figure 19 presents the variation of the isolated rotor derivative $\partial b_1/\partial \theta_{.75}$ as a function of rotor tip speed ratio μ .

For values of $\mu \leq 0.2$, the above derivative was obtained by using the following expression:

$$\frac{\partial b_1}{\partial \theta_{.75}} = \gamma \left[t_{17} \frac{\partial \lambda}{\partial \theta} + t_{18} \right]$$

where $\partial \lambda/\partial \theta_{.75}$ is presented in Subsection 7.5.3.6 and where t_{17} , t_{18} can be obtained from Table 8-1, page 205 of Reference 4.

For values of $\mu \geq 0.3$, the values of $\partial b_1/\partial \theta_{.75}$ were extracted graphically from the theoretical data of Reference 2.

The results cbtained are applicable for all values of $\theta_{.75}$, C_L/σ, α_C, and $\gamma = 8.0$.

As explained previously for γ values other than 8.0, the $\partial b_1/\partial \theta_{.75}$ derivatives can be obtained as follows:

$$\left(\frac{\partial b_1}{\partial \theta_{.75}}\right)_{\gamma} = \frac{\gamma}{8.0} \left(\frac{\partial b_1}{\partial \theta_{.75}}\right)_{\gamma = 8.0}$$

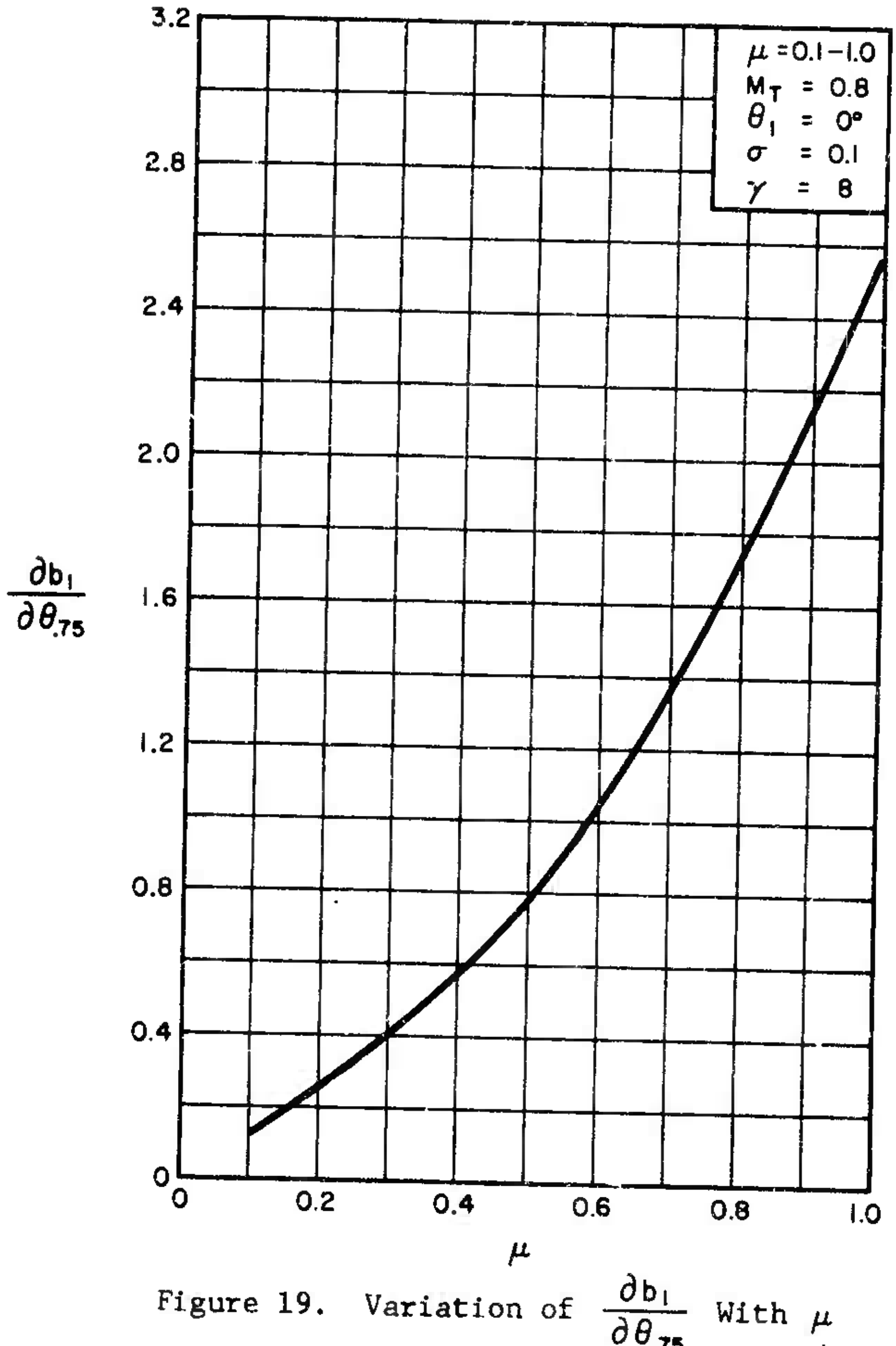

Figure 19. Variation of $\frac{\partial b_1}{\partial \theta_{.75}}$ With μ for All Values of $\theta_{.75}$, $\frac{C_L'}{\sigma}$, and α_C.

7.5.3.6 $\frac{\partial \lambda}{\partial \theta_{.75}}$ for $\sigma = 0.1$, $\theta_1 = 0°$, and $M_T = 0.8$

Figure 20 presents the variation of the isolated rotor derivative $\partial\lambda/\partial\theta_{.75}$ as a function of rotor tip speed ratio μ .

For values of $\mu \leq 0.2$, the above derivative was obtained by using the following expression:

$$\frac{\partial \lambda}{\partial \theta_{.75}} = \frac{\frac{2}{a}\left[\frac{\partial(\frac{C_L'}{\sigma})}{\partial \theta_{.75}}\right] - t_{32}}{t_{31}}$$

where $\partial(C_L'/\sigma)/\partial\theta_{.75}$ is presented in Subsection 7.5.3.1 and where t_{31} , t_{32} can be obtained from Table 8-3, page 207 of Reference 4.

For $\mu \geq 0.3$, the values of the $\partial\lambda/\partial\theta_{.75}$ derivative were extracted graphically from the theoretical data of Reference 2.

The results obtained are applicable for all values of $\theta_{.75}$, C_L'/σ, and a_C .

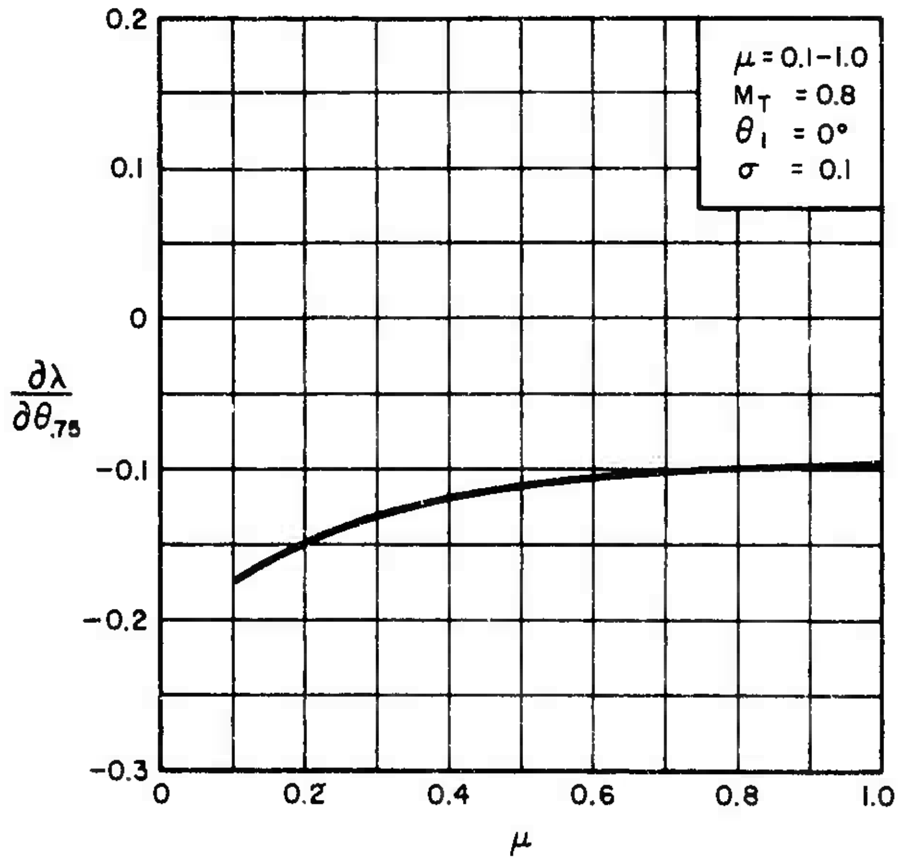

Figure 20. Variation of $\frac{\partial\lambda}{\partial\theta_{.75}}$ With μ for All Values of $\theta_{.75}$, $\frac{C_L'}{\sigma}$, and α_c.

7.5.3.7 $\dfrac{\partial(\frac{C_Y'}{\sigma})}{\partial\theta_{.75}}$ for All Values of σ, θ_1, and M_T

Reference 2 and other reviewed reports do not include the calculated data required to evaluate the rotor Y-force derivatives. It is therefore suggested that the classical Bailey theory be utilized for this purpose. If the above theory is used, the following expression for the isolated rotor derivative $\partial(C_Y'/\sigma)/\partial\theta_{.75}$ can be derived:

$$\begin{aligned}\frac{\partial(\frac{C_Y'}{\sigma})}{\partial\theta_{.75}} = \frac{a}{2}\Bigg\{ & \frac{\partial a_0}{\partial\theta_{.75}}\left[\mu(-\frac{3}{4}\theta_{75}-\frac{3}{2}\lambda-\mu a_1)+\frac{a_1}{6}\right] \\ & +\frac{\partial a_1}{\partial\theta_{.75}}\left[\frac{a_0}{6}+\mu(-\mu a_0+\frac{b_1}{4})\right] \\ & +\frac{\partial b_1}{\partial\theta_{.75}}\left[\theta_{.75}(\frac{1}{3}+\frac{3}{8}\mu^2)+\lambda(\frac{3}{4}+\frac{\mu^2}{8})+\frac{\mu a_1}{4}\right] \\ & +\frac{\partial\lambda}{\partial\theta_{.75}}\left[b_1(\frac{3}{4}+\frac{\mu^2}{8})-\frac{3}{2}\mu a_0\right] \\ & -\frac{3}{4}\mu a_0+b_1(\frac{1}{3}+\frac{3}{8}\mu^2)\Bigg\}\end{aligned}$$

where

$$\frac{\partial a_0}{\partial\theta_{.75}} = \frac{\gamma}{2}\left[\frac{1}{4}(1-\mu^2)+\frac{1}{3}\frac{\partial\lambda}{\partial\theta_{.75}}\right],$$

and where $\partial a_1/\partial\theta_{.75}$, $\partial b_1/\partial\theta_{.75}$, and $\partial\lambda/\partial\theta_{.75}$ are given in Subsections 7.5.3.4, 7.5.3.5, and 7.5.3.6, respectively.

The above derivative is applicable for all values of σ, θ_1, and M_T, provided that the pertinent rotor parameters comprising this derivative are evaluated at the required condition.

LITERATURE CITED

1. Kisielowski, E., Perlmutter, A. A., and Tang, J., STABILITY AND CONTROL HANDBOOK FOR HELICOPTERS, USAAVLABS Technical Report 67-63, U. S. Army Aviation Materiel Laboratories, Fort Eustis Virginia, August 1967, AD 662259.

2. Tanner, W. H., CHARTS FOR ESTIMATING ROTARY WING PERFORMANCE IN HOVER AND AT HIGH FORWARD SPEEDS, NASA Contractor Report CR-114, National Aeronautics and Space Administration, Washington, D. C., November 1964.

3. STABILITY AND CONTROL HANDBOOK FOR HELICOPTERS, TRECOM Report 60-43, U. S. Army Transportation Research Command (presently, U. S. Army Aviation Materiel Laboratories), Fort Eustis, Virginia, August 1960.

4. Gessow, A., and Myers, G. C., Jr., AERODYNAMICS OF THE HELICOPTER, The MacMillan Company, New York, 1962.

SECTION 8. STABILITY CHARACTERISTIC EQUATIONS

The linearized equations of motion given in Section 6 can be represented as a set of homogeneous algebraic equations containing the unknowns $\bar{u}, \bar{v}, \bar{w}, \bar{\theta}, \bar{\phi}, \bar{\psi}$, etc., and the operator Λ. This operator is defined as the time rate of change of the unknowns, thus $\Lambda \equiv d(\ )/dt$ and $\Lambda^2 \equiv d^2(\ )/dt^2$, etc.

The simultaneous solution for the unknowns can be obtained by employing the usual determinant methods which yield

$$\bar{u} = \frac{f_1(\Lambda)}{F(\Lambda)}, \quad \bar{v} = \frac{f_2(\Lambda)}{F(\Lambda)}, \quad \bar{w} = \frac{f_3(\Lambda)}{F(\Lambda)}, \quad \bar{\theta} = \frac{f_4(\Lambda)}{F(\Lambda)}$$

The numerator determinants $f_1(\Lambda)$, $f_2(\Lambda)$, ... $f_4(\Lambda)$ ... are formed by replacing the coefficients of the appropriate unknown variables by the column of constants which pertain to the control inputs. The denominator determinant $F(\Lambda)$ consists of the coefficients of the homogeneous algebraic equations with control inputs fixed at zero. The determinant $F(\Lambda)$ is known as the stability determinant. Expansion of the determinant $F(\Lambda)$ leads to the stability characteristic equation. The property of this type of equation is that there can be nonzero values of the unknowns $(\bar{u}, \bar{v}, \bar{w})$ if, and only if, the determinant $F(\Lambda) = 0$. Setting the determinant equal to zero provides the condition for finding the roots of the characteristic equation $\Lambda_1, \Lambda_2, \ldots \Lambda_n$.

In order to obtain the actual response solution of the unknown variables $(\bar{u}, \bar{v}, \bar{w})$ due to a given forcing function or control input, the Heaviside expansion theorem can be used. The Heaviside expansion method is developed in Reference 1, pages 436 to 438, and will not be duplicated in this section; however, the final response equations are given below.

If it is assumed that the stability characteristic equation $F(\Lambda)=0$ yields n real roots, $\Lambda_1, \Lambda_2, \ldots \Lambda_n$, and m pairs of complex roots, $\Lambda_m = a_m \pm b_m i$, the time history response

of any variable (e.g., variable $\bar{\theta}$) can be expressed as follows:

$$\bar{\theta} = \frac{f_4(\Lambda)}{F(\Lambda)} = \frac{f_4(0)}{F'(0)} + \sum_{\Lambda=\Lambda_1}^{\Lambda_n} \frac{f_4(\Lambda)}{\Lambda F'(\Lambda)} e^{\Lambda t} + \sum_{\Lambda=\Lambda_1}^{\Lambda_m} A e^{a_m t} \sin(b_m t + \Phi)$$

where the constants A and Φ can be obtained by using appropriate boundary conditions.

In the case that one of the real roots of the characteristic equation is zero (i.e., $\Lambda_1 = 0$), the response equation becomes

$$\bar{\theta} = \frac{f_4(\Lambda)}{F(\Lambda)} = \frac{f_4(0)}{F'(0)} t + \sum_{\Lambda=\Lambda_2}^{\Lambda_n} \frac{f_4(\Lambda)}{\Lambda F'(\Lambda)} e^{\Lambda t} + \sum_{\Lambda=\Lambda_1}^{\Lambda_m} A e^{a_m t} \sin(b_m t + \Phi)$$

LITEPATURE CITED

1. Perkins, C. D., and Hage, R. E., AIRPLANE PERFORMANCE STABILITY AND CONTROL, Third Edition, John Wiley and Sons, Inc., New York, Chapman and Hall Ltd., London, England, February 1953.

8.1 COUPLED LONGITUDINAL AND LATERAL MODES, INCLUDING STABILITY AUGMENTATION SYSTEM

In this section, the generalized case of aircraft perturbation motion consisting of 6 degrees of freedom of aircraft motion and 3 degrees of freedom of the motion of the stability augmentation system is considered. The analysis presented herein is suitable for either analog or digital computer work.

The linearized equations of motion presented in Section 6 can be expressed as follows:

(a) The X-Force Equation

$$a_{11}\bar{u} + a_{12}\bar{v} + a_{13}\bar{w} + a_{14}\bar{\theta} + a_{15}\bar{\phi} + a_{16}\bar{\psi} + a_{17}\bar{B}_{1_S} + a_{18}\bar{A}_{1_S} + a_{19}\delta_{r_S} = K_1$$

(b) The Y-Force Equation

$$a_{21}\bar{u} + a_{22}\bar{v} + a_{23}\bar{w} + a_{24}\bar{\theta} + a_{25}\bar{\phi} + a_{26}\bar{\psi} + a_{27}\bar{B}_{1_S} + a_{28}\bar{A}_{1_S} + a_{29}\delta_{r_S} = K_2$$

(c) The Z-Force Equation

$$a_{31}\bar{u} + a_{32}\bar{v} + a_{33}\bar{w} + a_{34}\bar{\theta} + a_{35}\bar{\phi} + a_{36}\bar{\psi} + a_{37}\bar{B}_{1_S} + a_{38}\bar{A}_{1_S} + a_{39}\delta_{r_S} = K_3$$

(d) The Rolling Moment($\mathcal{L}$) Equation

$$a_{41}\bar{u} + a_{42}\bar{v} + a_{43}\bar{w} + a_{44}\bar{\theta} + a_{45}\bar{\phi}$$

$$+ a_{46}\bar{\psi} + a_{47}\bar{B}_{1_S} + a_{48}\bar{A}_{1_S} + a_{49}\bar{\delta}_{r_S} = K_4$$

(e) The Pitching Moment(M) Equation

$$a_{51}\bar{u} + a_{52}\bar{v} + a_{53}\bar{w} + a_{54}\bar{\theta} + a_{55}\bar{\phi}$$

$$+ a_{56}\bar{\psi} + a_{57}\bar{B}_{1_S} + a_{58}\bar{A}_{1_S} + a_{59}\bar{\delta}_{r_S} = K_5$$

(f) The Yawing Moment(N) Equation

$$a_{61}\bar{u} + a_{62}\bar{v} + a_{63}\bar{w} + a_{64}\bar{\theta} + a_{65}\bar{\phi}$$

$$+ a_{66}\bar{\psi} + a_{67}\bar{B}_{1_S} + a_{68}\bar{A}_{1_S} + a_{69}\bar{\delta}_{r_S} = K_6$$

(g) Stability Augmentation System Equations

(i) Longitudinal Control (B_{1_S}) Equation

$$a_{71}\bar{u} + a_{72}\bar{v} + a_{73}\bar{w} + a_{74}\bar{\theta} + a_{75}\bar{\phi}$$

$$+ a_{76}\bar{\psi} + a_{77}\bar{B}_{1_S} + a_{78}\bar{A}_{1_S} + a_{79}\bar{\delta}_{r_S} = K_7$$

(ii) Lateral Control (A_{1_S}) Equation

$$a_{81}\bar{u}+a_{82}\bar{v}+a_{83}\bar{w}+a_{84}\bar{\theta}+a_{85}\bar{\phi}$$

$$+a_{36}\bar{\psi}+a_{87}\bar{B}_{1_S}+a_{88}\bar{A}_{1_S}+a_{89}\bar{\delta}_{r_S}=K_8$$

(iii) Directional Control (δ_{r_S}) Equation

$$a_{91}\bar{u}+a_{92}\bar{v}+a_{93}\bar{w}+a_{94}\bar{\theta}+a_{95}\bar{\phi}$$

$$+a_{96}\bar{\psi}+a_{97}\bar{B}_{1_S}+a_{98}\bar{A}_{1_S}+a_{99}\bar{\delta}_{r_S}=K_9$$

The coefficients $a_{m,n}$ and the control parameters K_n are given in Table I.

The numerator determinant $f_4(\Lambda)$ required to determine the response of variable (θ) is given by

$$f_4(\Lambda)=\begin{vmatrix} a_{11} & a_{12} & a_{13} & K_1 & \cdot & \cdot & \cdot & a_{19} \\ a_{21} & a_{22} & a_{23} & K_2 & \cdot & \cdot & \cdot & a_{29} \\ \cdot & \cdot & \cdot & \cdot & \cdot & \cdot & \cdot & \cdot \\ \cdot & \cdot & \cdot & \cdot & \cdot & \cdot & \cdot & \cdot \\ \cdot & \cdot & \cdot & \cdot & \cdot & \cdot & \cdot & \cdot \\ a_{91} & a_{92} & a_{93} & K_9 & \cdot & \cdot & \cdot & a_{99} \end{vmatrix}$$

The numerator determinants $f_1(\Lambda)$, $f_2(\Lambda)$, $f_3(\Lambda)$, etc., required for response calculations of the perturbation variables $\bar{u}, \bar{v}, \bar{w}$, etc., are obtained by replacing the coefficients of columns 2 and 3 by the set of control coefficients $K_1, K_2, \ldots\ldots\ldots$ K_8, respectively.

TABLE I

THE COEFFICIENTS OF THE DETERMINANT FOR AIRCRAFT RESPONSE ANALYSIS

EQUAT	a	1	2	3	4	5	6	7	8	9	K
X	1	$X_u + X_{\dot{u}}\Lambda$	X_v	$X_w + X_{\dot{w}}\Lambda$	$X_\theta + X_{\dot{\theta}}\Lambda + X_{\ddot{\theta}}\Lambda^2$	$X_{\dot{\phi}}\Lambda$	$X_{\dot{\psi}}\Lambda$	$X_{B_{1s}} + X_{\dot{B}_{1s}}\Lambda$	$X_{A_{1s}} + X_{\dot{A}_{1s}}\Lambda$	$X_{\delta_{rs}} + X_{\dot{\delta}_{rs}}\Lambda$	$-J_1 X_{B_{1c}}\overline{B_{1c}} - J_2 X_{A_{1c}}\overline{A_{1c}} - J_3 X_{\delta_{rc}}\overline{\delta_{rc}} - J_4 X_{\theta_c}\overline{\theta_c}$
Y	2	Y_u	$Y_v + Y_{\dot{v}}\Lambda$	Y_w	$Y_{\dot{\theta}}\Lambda$	$Y_\phi + Y_{\dot{\phi}}\Lambda$	$Y_\psi + Y_{\dot{\psi}}\Lambda$	$Y_{B_{1s}} + Y_{\dot{B}_{1s}}\Lambda$	$Y_{A_{1s}} + Y_{\dot{A}_{1s}}\Lambda$	$Y_{\delta_{rs}} + Y_{\dot{\delta}_{rs}}\Lambda$	$-J_1 Y_{B_{1c}}\overline{B_{1c}} - J_2 Y_{A_{1c}}\overline{A_{1c}} - J_3 Y_{\delta_{rc}}\overline{\delta_{rc}} - J_4 Y_{\theta_c}\overline{\theta_c}$
Z	3	Z_u	Z_v	$Z_w + Z_{\dot{w}}\Lambda$	$Z_\theta + Z_{\dot{\theta}}\Lambda + Z_{\ddot{\theta}}\Lambda^2$	$Z_{\dot{\phi}}\Lambda$	$Z_{\dot{\psi}}\Lambda$	$Z_{B_{1s}} + Z_{\dot{B}_{1s}}\Lambda$	$Z_{A_{1s}} + Z_{\dot{A}_{1s}}\Lambda$	$Z_{\delta_{rs}} + Z_{\dot{\delta}_{rs}}\Lambda$	$-J_1 Z_{B_{1c}}\overline{B_{1c}} - J_2 Z_{A_{1c}}\overline{A_{1c}} - J_3 Z_{\delta_{rc}}\overline{\delta_{rc}} - J_4 Z_{\theta_c}\overline{\theta_c}$
$\mathcal{L}$	4	$\mathcal{L}_u$	$\mathcal{L}_v$	$\mathcal{L}_w + \mathcal{L}_{\dot{w}}\Lambda$	$\mathcal{L}_\theta + \mathcal{L}_{\dot{\theta}}\Lambda + \mathcal{L}_{\ddot{\theta}}\Lambda^2$	$\mathcal{L}_{\dot{\phi}}\Lambda + \mathcal{L}_{\ddot{\phi}}\Lambda^2$	$\mathcal{L}_{\dot{\psi}}\Lambda + \mathcal{L}_{\ddot{\psi}}\Lambda^2$	$\mathcal{L}_{B_{1s}} + \mathcal{L}_{\dot{B}_{1s}}\Lambda$	$\mathcal{L}_{A_{1s}} + \mathcal{L}_{\dot{A}_{1s}}\Lambda$	$\mathcal{L}_{\delta_{rs}} + \mathcal{L}_{\dot{\delta}_{rs}}\Lambda$	$-J_1 \mathcal{L}_{B_{1c}}\overline{B_{1c}} - J_2 \mathcal{L}_{A_{1c}}\overline{A_{1c}} - J_3 \mathcal{L}_{\delta_{rc}}\overline{\delta_{rc}} - J_4 \mathcal{L}_{\theta_c}\overline{\theta_c}$
M	5	M_u	M_v	$M_w + M_{\dot{w}}\Lambda$	$M_{\dot{\theta}}\Lambda + M_{\ddot{\theta}}\Lambda^2$	$M_{\dot{\phi}}\Lambda + M_{\ddot{\phi}}\Lambda^2$	$M_{\dot{\psi}}\Lambda + M_{\ddot{\psi}}\Lambda^2$	$M_{B_{1s}} + M_{\dot{B}_{1s}}\Lambda$	$M_{A_{1s}} + M_{\dot{A}_{1s}}\Lambda$	$M_{\delta_{rs}} + M_{\dot{\delta}_{rs}}\Lambda$	$-J_1 M_{B_{1c}}\overline{B_{1c}} - J_2 M_{A_{1c}}\overline{A_{1c}} - J_3 M_{\delta_{rc}}\overline{\delta_{rc}} - J_4 M_{\theta_c}\overline{\theta_c}$
N	6	N_u	N_v	$N_w + N_{\dot{w}}\Lambda$	$N_{\dot{\theta}}\Lambda + N_{\ddot{\theta}}\Lambda^2$	$N_{\dot{\phi}}\Lambda + N_{\ddot{\phi}}\Lambda^2$	$N_{\dot{\psi}}\Lambda + N_{\ddot{\psi}}\Lambda^2$	$N_{B_{1s}} + N_{\dot{B}_{1s}}\Lambda$	$N_{A_{1s}} + N_{\dot{A}_{1s}}\Lambda$	$N_{\delta_{rs}} + N_{\dot{\delta}_{rs}}\Lambda$	$-J_1 N_{B_{1c}}\overline{B_{1c}} - J_2 N_{A_{1c}}\overline{A_{1c}} - J_3 N_{\delta_{rc}}\overline{\delta_{rc}} - J_4 N_{\theta_c}\overline{\theta_c}$
B_{1s}	7	$-k_3$	0	$-k_4$	$-(k_1\Lambda + k_2\Lambda^2)$	0	0	$\Lambda + D_1 + D_2\overline{B_{1s}}$	0	0	0
A_{1s}	8	0	k_7	0	0	$-k_5\Lambda + k_6\Lambda^2$	0	0	$\Lambda + D_1 + D_2\overline{A_{1s}}$	0	0
δ_{rs}	9	0	k_9	0	0	0	$k_{10}\Lambda$	0	0	$\Lambda + k_8$	0

The stability determinant $F(\Lambda)$ is given by:

$$F(\Lambda) = \begin{vmatrix} a_{11} & a_{12} & a_{13} & \cdot & & \cdot & a_{19} \\ a_{21} & a_{22} & a_{23} & \cdot & \cdot & \cdot & a_{29} \\ \cdot & \cdot & \cdot & \cdot & \cdot & \cdot & \cdot \\ \cdot & \cdot & \cdot & \cdot & \cdot & \cdot & \cdot \\ \cdot & \cdot & \cdot & \cdot & \cdot & \cdot & \cdot \\ a_{91} & a_{92} & a_{93} & \cdot & \cdot & \cdot & a_{99} \end{vmatrix}$$

Expanding the stability determinant $F(\Lambda) = 0$ yields the generalized characteristic equation as follows:

$$A\Lambda^{n} + B\Lambda^{n-1} + C\Lambda^{n-2} + \cdot \quad \cdot \quad \cdot + E = 0$$

where n is an integer denoting the highest order of the stability characteristic equation and A, B, C, ... E are coefficients of the characteristic equation in terms of total stability derivatives.

8.2 UNCOUPLED LONGITUDINAL MODE (Three Degrees of Freedom)

Considering decoupled longitudinal motion as affected by changes in the stability variables u, w, and θ, the corresponding stability determinant $F(\Lambda)$ is obtained by deleting the remaining stability variables v, ϕ, ψ, etc., in the equations for X, Z, and M, thus:

$$F(\Lambda) = \begin{vmatrix} a_{11} & a_{13} & a_{14} \\ a_{31} & a_{33} & a_{34} \\ a_{51} & a_{53} & a_{54} \end{vmatrix} = 0$$

Expanding the stability determinant $F(\Lambda)$ yields

$$F(\Lambda) = a_{11}(a_{33}a_{54} - a_{53}a_{34}) - a_{13}(a_{31}a_{54} - a_{51}a_{34})$$

$$+ a_{14}(a_{31}a_{53} - a_{51}a_{33})$$

Substituting the values for the coefficients from Table I of Section 8.1 yields

$$F(\Lambda) = (X_u + X_{\dot u}\Lambda)\Big[(Z_w + Z_{\dot w}\Lambda)(M_{\dot\theta}\Lambda + M_{\ddot\theta}\Lambda^2)$$

$$-(M_w + M_{\dot w}\Lambda)(Z_\theta + Z_{\dot\theta}\Lambda + Z_{\ddot\theta}\Lambda^2)\Big]$$

$$-(X_w + X_{\dot w}\Lambda)\Big[Z_u(M_{\dot\theta}\Lambda + M_{\ddot\theta}\Lambda^2) - M_u(Z_\theta + Z_{\dot\theta}\Lambda + Z_{\ddot\theta}\Lambda^2)\Big]$$

$$+(X_\theta + X_{\dot\theta}\Lambda + X_{\ddot\theta}\Lambda^2)\Big[Z_u(M_w + M_{\dot w}\Lambda) - M_u(Z_w + Z_{\dot w}\Lambda)\Big]$$

Thus:

$$F(\Lambda) = A\Lambda^4 + B\Lambda^3 + C\Lambda^2 + D\Lambda + E = 0$$

where

$$A = G_1 X_{\dot u}$$

$$B = G_1 X_u + G_2 X_{\dot u} + G_3 X_{\dot w} + G_4 X_{\ddot\theta}$$

$$C = G_2 X_u + G_3 X_w + G_4 X_{\dot\theta} + G_5 X_{\dot u} + G_6 X_{\dot w} + G_7 X_{\ddot\theta}$$

$$D = G_4 X_\theta + G_5 X_u + G_6 X_w + G_7 X_{\dot\theta} + G_8 Z_\theta$$

$$E = G_7 X_\theta + G_9 Z_\theta$$

and

$$G_1 = Z_{\dot w} M_{\ddot\theta} - M_{\dot w} Z_{\ddot\theta}$$

$$G_2 = Z_w M_{\ddot\theta} + Z_{\dot w} M_{\dot\theta} - M_w Z_{\ddot\theta} - M_{\dot w} Z_{\dot\theta}$$

$$G_3 = Z_{\ddot\theta} M_u - Z_u M_{\ddot\theta}$$

$$G_4 = Z_u M_{\dot w} - M_u Z_{\dot w}$$

$$G_5 = Z_w M_{\dot\theta} - M_w Z_{\dot\theta} - Z_\theta M_{\dot w}$$

$$G_6 = M_u Z_{\dot\theta} - Z_u M_{\dot\theta}$$

$$G_7 = Z_u M_w - M_u Z_w$$

$$G_8 = M_u X_{\dot w} - M_w X_{\dot u}$$

$$G_9 = X_w M_u - X_u M_w$$

In order to determine the aircraft response, say, in pitch $[\theta = f_4(\Lambda)/F(\Lambda)]$ due to a step input of the longitudinal control $(\overline{B_{1c}})$, it is necessary to evaluate the numerator determinant $f_4(\Lambda)$. The determinant $f_4(\Lambda)$ is formed by replacing the coefficients of (θ) (namely, a_{14}, a_{34}, and a_{54}) of the stability determinant $F(\Lambda)$ given above by the control input functions K_1, K_3, and K_5.

The function $f_4(\Lambda)$ can be obtained as follows:

$$f_4(\Lambda) = \begin{vmatrix} a_{11} & a_{13} & K_1 \\ a_{31} & a_{33} & K_3 \\ a_{51} & a_{53} & K_5 \end{vmatrix}$$

$$= a_{11}(K_5 a_{33} - K_3 a_{53}) - a_{13}(K_5 a_{31} - K_3 a_{51}) + K_1(a_{31} a_{53} - a_{51} a_{33})$$

Since, in this case, the uncoupled longitudinal motion of 3 degrees of freedom with no stability augmentation system is considered, the stability authority ratios J_1, J_2, J_3 ...., etc., are taken as unity, and all control inputs other than $(\overline{B_{1_C}})$ are taken as zero.

Thus, when the values for the coefficients a_{13}, a_{15} ......, etc., and the appropriate control inputs K_1, K_3, and K_5 from Table I of Section 8.1 are substituted, the function $f_4(\Lambda)$ becomes

$$f_4(\Lambda) = (X_u + X_{\dot{u}}\Lambda)\left[-M_{B_{1_C}}\overline{B_{1_C}}(Z_w + Z_{\dot{w}}\Lambda) + Z_{B_{1_C}}\overline{B_{1_C}}(M_w + M_{\dot{w}}\Lambda)\right]$$
$$-(X_w + X_{\dot{w}}\Lambda)\left[-M_{B_{1_C}}\overline{B_{1_C}}(Z_u) + Z_{B_{1_C}}\overline{B_{1_C}}(M_u)\right]$$
$$-X_{B_{1_C}}\overline{B_{1_C}}\left[Z_u(M_w + M_{\dot{w}}\Lambda) - M_u(Z_w + Z_{\dot{w}}\Lambda)\right]$$

Thus:

$$f_4(\Lambda) = \overline{B_{1_C}}(A\Lambda^2 + B\Lambda + C)$$

where

$$A = X_{\dot{u}}(Z_{B_{1_C}}M_{\dot{w}} - M_{B_{1_C}}Z_{\dot{w}})$$

$$B = X_u(Z_{B_{1_C}}M_{\dot{w}} - M_{B_{1_C}}Z_{\dot{w}}) + X_{\dot{u}}(Z_{B_{1_C}}M_w - M_{B_{1_C}}Z_w)$$
$$+ X_{\dot{w}}(M_{B_{1_C}}Z_u - Z_{B_{1_C}}M_u) + X_{B_{1_C}}(M_u Z_{\dot{w}} - Z_u M_{\dot{w}})$$

$$C = X_u(Z_{B_{1_C}}M_w - M_{B_{1_C}}Z_w) + X_w(M_{B_{1_C}}Z_u - Z_{B_{1_C}}M_u)$$
$$+ X_{B_{1_C}}(M_u Z_w - M_w Z_u)$$

8.3 UNCOUPLED LATERAL MODE (Three Degrees of Freedom)

When the longitudinal stability variables u, v, and θ and longitudinal equations of motion X, Z, M are deleted, the stability determinant for the 3 lateral degrees of freedom becomes

$$F(\Lambda) = \begin{vmatrix} a_{22} & a_{25} & a_{26} \\ a_{42} & a_{45} & a_{46} \\ a_{62} & a_{65} & a_{66} \end{vmatrix} = 0$$

Expanding the above determinant yields

$$F(\Lambda) = a_{22}(a_{45}a_{66} - a_{65}a_{46}) - a_{25}(a_{42}a_{66} - a_{62}a_{46})$$

$$+ a_{26}(a_{42}a_{65} - a_{62}a_{45})$$

Substituting the values for the coefficients a_{mn} from Table I of Section 8.1 yields

$$F(\Lambda) = (Y_u + Y_{\dot{u}}\Lambda)\left[(L_{\dot{\phi}}\Lambda + L_{\ddot{\phi}}\Lambda^2)(N_{\dot{\psi}}\Lambda + N_{\ddot{\psi}}\Lambda^2)\right.$$

$$\left. -(N_{\dot{\phi}}\Lambda + N_{\ddot{\phi}}\Lambda^2)(L_{\dot{\psi}}\Lambda + L_{\ddot{\psi}}\Lambda^2)\right]$$

$$-(Y_{\phi} + Y_{\dot{\phi}}\Lambda)\left[L_v(N_{\dot{\psi}}\Lambda + N_{\ddot{\psi}}\Lambda^2) - N_v(L_{\dot{\psi}}\Lambda + L_{\ddot{\psi}}\Lambda^2)\right]$$

$$-(Y_{\psi} + Y_{\dot{\psi}}\Lambda)\left[L_v(N_{\dot{\phi}}\Lambda + N_{\ddot{\phi}}\Lambda^2) - N_v(L_{\dot{\phi}}\Lambda + L_{\ddot{\phi}}\Lambda^2)\right]$$

Thus:

$$F(\Lambda) = \Lambda\left[A\Lambda^4 + B\Lambda^3 + C\Lambda^2 + D\Lambda + E\right] = 0$$

where

$$A = H_1 Y_{\dot{v}}$$

$$B = H_1 Y_v + H_2 Y_{\dot{v}}$$

$$C = H_2 Y_v + H_3 Y_{\dot{v}} + H_4 Y_{\dot{\phi}} + H_5 Y_{\dot{\psi}}$$

$$D = H_3 Y_v + H_4 Y_{\phi} + H_5 Y_{\psi} + H_6 Y_{\dot{\phi}} + H_7 Y_{\dot{\psi}}$$

$$E = H_6 Y_{\phi} + H_7 Y_{\psi}$$

and

$$H_1 = L_{\ddot{\phi}} N_{\ddot{\psi}} - N_{\ddot{\phi}} L_{\ddot{\psi}}$$

$$H_2 = L_{\dot{\phi}} N_{\ddot{\psi}} + L_{\ddot{\phi}} N_{\ddot{\psi}} - N_{\dot{\phi}} L_{\ddot{\psi}} - N_{\ddot{\phi}} L_{\dot{\psi}}$$

$$H_3 = L_{\dot{\phi}} N_{\dot{\psi}} - N_{\dot{\phi}} L_{\dot{\psi}}$$

$$H_4 = N_v L_{\ddot{\psi}} - L_v N_{\ddot{\psi}}$$

$$H_5 = L_v N_{\ddot{\phi}} - N_v L_{\ddot{\phi}}$$

$$H_6 = N_v L_{\dot{\psi}} - L_v N_{\dot{\psi}}$$

$$H_7 = L_v N_{\dot{\phi}} - N_v L_{\dot{\phi}}$$

8.4 CRITERIA FOR STABILITY

The requirement for positive stability is that there be no positive real root or positive real part of the complex roots of the characteristic equation.

If there are to be no unstable modes, certain conditions pertaining to the coefficients of the characteristic equation must be met. These conditions can be expressed in terms of Routh stability criteria which involve sign tests of the coefficients of the characteristic equation and the magnitude and sign of the Routh discriminant R^*. More detailed information on the subject can be obtained from Reference 1.

The sections below present a summary of the Routh stability criteria for various types of the characteristic equations commonly encountered in stability work.

8.4.1 Routh Criteria for a Cubic

Let the cubic equation be

$$A\Lambda^3 + B\Lambda^2 + C\Lambda + D = 0 \qquad (A > 0)$$

The necessary and sufficient conditions for stability are

(a) The coefficients A, B, C, $D > 0$
(b) $R^* = BC - AD > 0$

8.4.2 Routh Criteria for a Quartic

Let the quartic equation be

$$A\Lambda^4 + B\Lambda^3 + C\Lambda^2 + D\Lambda + E = 0$$

The necessary and sufficient conditions for stability are

(a) The coefficients A, B, C, D, E > 0
(b) $R^{*} = D(BC-AD)-B^{2}E > 0$

8.4.3 Routh Criteria for a Quintic

Let the quintic equation be

$$A\Lambda^{5}+B\Lambda^{4}+C\Lambda^{3}+D\Lambda^{2}+E\Lambda+F=0$$

The necessary and sufficient conditions for stability are

(a) The coefficients A, B, C, D, E, F > 0
(b) $BC-AD > 0$
(c) $R^{*} = D(BC-AD)(BE-AF)-B(BF-AF)^{2}-F(BC-AD)^{2} > 0$

LITERATURE CITED

1. Routh, E. J., DYNAMICS OF A SYSTEM OF RIGID BODIES. 6th Edition, MacMillan and Company, London, England, 1905.

8.5 SOLUTION OF THE CHARACTERISTIC EQUATION

There are many methods in the literature for obtaining the roots of the characteristic equation. The method used will depend on the order of the characteristic equation and particularly on whether the roots are to be extracted by hand or by machine.

Reference 1, pages 2.1.1-167 to 2.1.1-190, gives a fairly detailed review of the most commonly used methods for extracting roots of the characterisitc equation ranging from 3rd to 6th order equations.

Since quartic equations occur most frequently in aircraft stability work, a method is herein given for solution of stability quartics. The method is known as an "Analytical Solution of Quartics" and is based on the Ferrari reducing cubic method. Some of the advantages of this analytical method are that it is independent of the relative magnitude of the coefficients, does not require initial knowledge of the order of magnitudes of the roots, and is particularly useful if no real roots exist. This method is equally as well applicable for hand calculation as it is for machine computation.

The calculation procedure of this method is as follows:

(a) Determine the coefficients B, C, D and E of a given quartic as follows:

$$\Lambda^4 + B\Lambda^3 + C\Lambda^2 + D\Lambda + E = 0$$

(b) Calculate

$$S^* = BD + C^2 - 4E$$

$R^* = BCD - EB^2 - D^2$

(Note that R^* is the usual Routh discriminant discussed in Section 8.4)

(c) Compute

$$h_1 = \frac{1}{3}(3S^* - 4C^2)$$

$$h_2 = \frac{1}{27}(18CS^* - 16C^3 - 27R^*)$$

(d) Evaluate discriminant (Δ)

$$\Delta = \frac{h_2^2}{4} + \frac{h_1^3}{27}$$

(e) Determine (Π_n) as follows:

(i) If $\Delta > 0$, then

$$\Pi_n = \sqrt[3]{-\frac{h_2}{2} + \sqrt{\Delta}} + \sqrt[3]{-\frac{h_2}{2} - \sqrt{\Delta}}$$

(ii) If $\Delta = 0$, then

$$\Pi_1 = 2\sqrt[3]{-\frac{h_2}{2}}$$

$$\Pi_2 = \Pi_3 = -\sqrt[3]{-\frac{h_2}{2}}$$

(iii) If $\Delta < 0$, then calculate

$$\cos\Phi = -\frac{h_2}{2} \Big/ \sqrt{-\frac{h_1^3}{27}}$$

and obtain

$$\Pi_1 = 2\left[\sqrt{-\frac{h_1}{3}}\cos\left(\frac{\Phi}{3}\right)\right]$$

$$\Pi_2 = 2\left[\sqrt{-\frac{h_1}{3}}\cos\left(\frac{\Phi}{3} + 120°\right)\right]$$

$$\Pi_3 = 2\left[\sqrt{-\frac{h_1}{3}}\cos\left(\frac{\Phi}{3} + 240°\right)\right]$$

(f) Select the algebraically smallest value of (Π_n) using step (i), (ii), or (iii), whichever applies, and compute

$$\zeta\eta \equiv \Pi_n + \frac{2C}{3} \leq \frac{B^2}{4}$$

(g) Calculate

$$\varsigma = \frac{C-\zeta\eta}{2} + \sqrt{\left(\frac{C-\zeta\eta}{2}\right)^2 - E}$$

$$\nu = \frac{E}{\varsigma}$$

$$\eta = \frac{D-B\varsigma}{\nu-\varsigma}$$

$$\zeta = B - \eta$$

(h) Finally, determine the four roots of the quartic thus:

$$\Lambda_{1,2} = -\frac{\zeta}{2} \pm \sqrt{\left(\frac{\zeta}{2}\right)^2 - \nu}$$

$$\Lambda_{3,4} = -\frac{\eta}{2} \pm \sqrt{\left(\frac{\eta}{2}\right)^2 - \varsigma}$$

LITERATURE CITED

1. STABILITY AND CONTROL HANDBOOK FOR HELICOPTERS, TRECOM Report 60-43, U. S. Army Transportation Research Command (presently, U. S. Army Aviation Materiel Laboratories), Fort Eustis, Virginia, August 1960.

8.6 ROOTS OF THE CHARACTERISTIC EQUATION

The roots of the characteristic equation can be

(a) Real
(b) Complex
(c) Combination of real and complex

The real roots correspond to a periodic motion, converging in amplitude as time passes if negative, and diverging in amplitude if positive.

The complex roots ($\Lambda_m = a_m \pm b_m i$) always occur in pairs, and each pair corresponds to an oscillatory mode

$$Ae^{a_m t} \sin(b_m t + \Phi)$$

where A is the amplitude of the oscillation and Φ is the phase angle.

The real part a_m of the complex pair of roots determines the converging or diverging behavior of the mode.

If $a_m > 0$, the amplitude of the mode will increase with time (t) , resulting in unstable, divergent oscillation.
If $a_m = 0$, the amplitude remains unchanged (neutral stability).
If $a_m < 0$, the amplitude will decrease with time (t), resulting in a stable or damped oscillation.

The complex part b_m describes the frequency of the mode, in radians/second.

If the real root or real part of the complex root is negative, the time constant τ of the mode is defined as

$$\tau = \begin{cases} \dfrac{1}{-\Lambda} & \text{for real } \Lambda \\[2ex] \dfrac{1}{-a_m} & \text{for complex } \Lambda \end{cases}$$

The time constant τ corresponds to the time required for the motion to reach 36.8% of its original value. If the real root, or real part of the complex root, is positive, it is more convenient to express the characteristics of the mode in terms of the time required to double its initial amplitude $\tau_{2/1}$ where

$$\tau_{2/1} = \begin{cases} \dfrac{0.693}{+\Lambda} & \text{for real } \Lambda \\[2ex] \dfrac{0.693}{a_m} & \text{for complex } \Lambda \end{cases}$$

The converging characteristics of stable modes is sometimes also expressed in terms of the time required to reduce to half its initial amplitude $\tau_{1/2}$ where

$$\tau_{1/2} = \begin{cases} \dfrac{0.693}{-\Lambda} & \text{for real } \Lambda \\[2ex] \dfrac{0.693}{-a_m} & \text{for complex } \Lambda \end{cases}$$

The period P of an oscillatory mode is given by

$$P = \frac{2\pi}{b_m} \text{ seconds}$$

SECTION 9. EFFECT OF DESIGN PARAMETERS ON DYNAMIC STABILITY CHARACTERISTICS OF COMPOUND HELICOPTERS

In this section the effects of varying a number of design parameters on the dynamic stability characteristics of a typical single rotor compound helicopter are examined. The example compound helicopter shown in Figure 1 has a gross weight of 9,000 pounds, a two-bladed teetering type rotor with no stability augmentation system. The design parameters of this sample compound helicopter are those used in the sample calculation in Section 10.1. For convenience, the reference or normal values of some of the pertinent parameters for this compound helicopter are listed below:

$$V_0 = 100 \text{ knots}$$

$$C.G. = 0 \text{ in (neutral)}$$

$$\Omega_F = 33.9 \text{ rad/sec}$$

$$\sum_{i=1}^{2} T_{P_i} = 1200 \text{ lb}$$

$$S_W = 78.4 \text{ ft}^2$$

$$S_T = 40 \text{ ft}^2$$

$$S_{VT} = 22.4 \text{ ft}^2$$

Each particular design parameter is varied independently, with all remaining parameters held constant. The results of each parametric variation are presented in a group of three plots. The first plot presents the period and damping defined as $1/T_{1/2}$ and $1/T_2$ versus specific parameters. This format is chosen so that the neutral dynamic stability corresponds to $1/T_{1/2}$ or $1/T_2$ equal to zero. The remaining figures are conventional root locus plots of the aircraft longitudinal and lateral modes respectively.

Although the quantitative results apply strictly to the sample helicopter, the qualitative conclusions are considered to be valid for most current single rotor compound helicopters. As such, the results may be used for preliminary design purposes of compound helicopters.

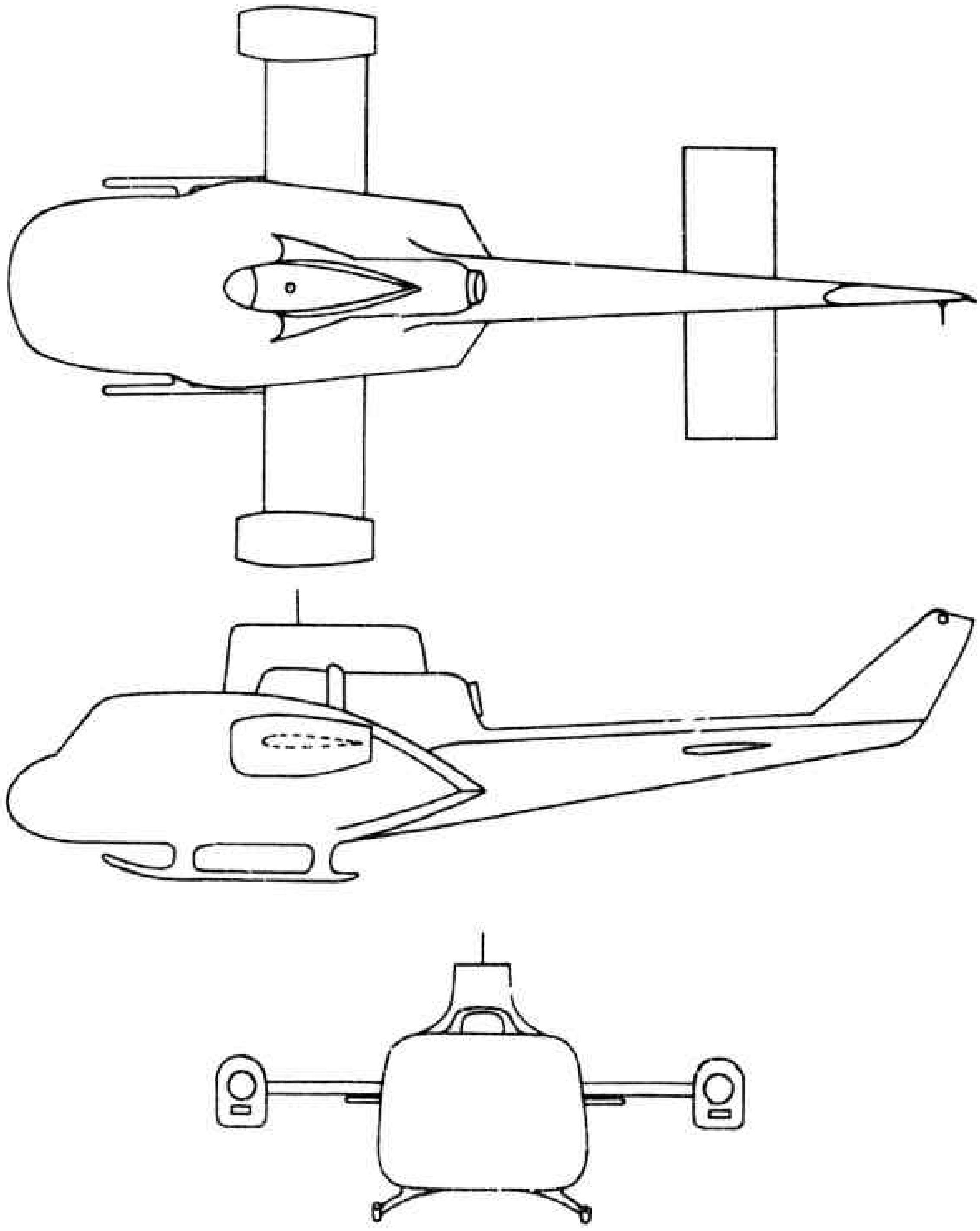

Figure 1. General Arrangement of Sample Teetering Rotor Compound Helicopter.

(a) Effect of Gross Weight

Figures 2, 3, and 4 show the effect of gross weight on the longitudinal and lateral dynamic stability characteristics of the sample compound helicopter. The longitudinal stability modes are characterized by a practically neutral long-period oscillation and a stable short period. The lateral mode consists of two aperiodic modes and a stable, moderately damped high-frequency oscillation.

The effect of gross weight on the aircraft longitudinal dynamic stability is to reduce the period or increase the frequency of the long periodic mode with no change of damping to increase the period with reduction in damping of the short periodic mode. The moderately damped, lateral aperiodic mode becomes more heavily damped with increasing weight. Although the remaining lateral modes show a slight tendency to destabilize, these effects are negligible. Thus it appears that an increase in gross weight does not appreciably affect the dynamic stability of the sample compound helicopter. The maximum gross weight will be limited only by the longitudinal control power available for trim.

(b) Effect of Center-of-Gravity Location

Figures 5, 6, and 7 illustrate the effect of fore-and-aft variation of the center-of-gravity (C.G.) locations on the longitudinal and lateral dynamic stability modes of the sample compound helicopter. The results show that moving the C.G. aft results in large destabilizing effects of both longitudinal and lateral modes whereas a forward shift in C.G. position has little effect on the dynamic stability characteristics.

For center-of-gravity locations ahead of the mid C.G. position, the longitudinal modes are characterized by a long neutrally stable oscillation and a short moderately damped oscillation. Similarly, the lateral modes consist of two stable aperiodic modes and a stable, moderately damped high-frequency oscillation. Over the 8-inch range of forward C.G. shift, no significant changes are noted in either the longitudinal or the lateral stability modes. As the C.G. is shifted rearwards from the mid C.G. position, the neutrally stable long-period oscillation increases in frequency and becomes an unstable or divergent oscillation. The moderately damped, stable longitudinal oscillatory mode rapidly decreases in frequency and splits into a pair of stable aperiodic modes or subsidences. In the lateral mode, the moderately damped high-frequency oscillation reduces in frequency and becomes less stable as the C.G. is moved aft. However, both of the lateral aperiodic modes become more stable with the rearward C.G. shift.

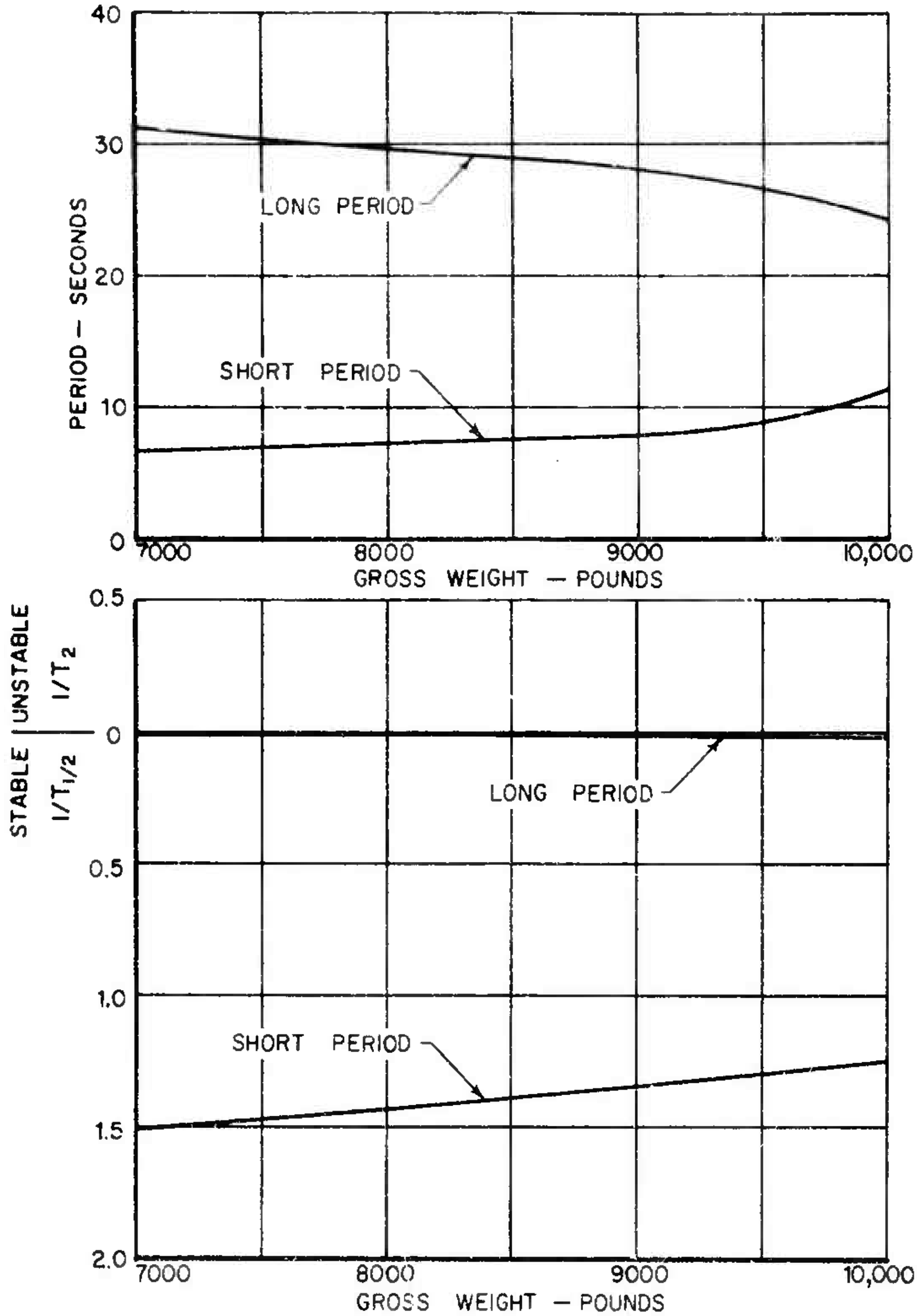

Figure 2. Effect of Gross Weight on Longitudinal Dynamic Stability Characteristics.

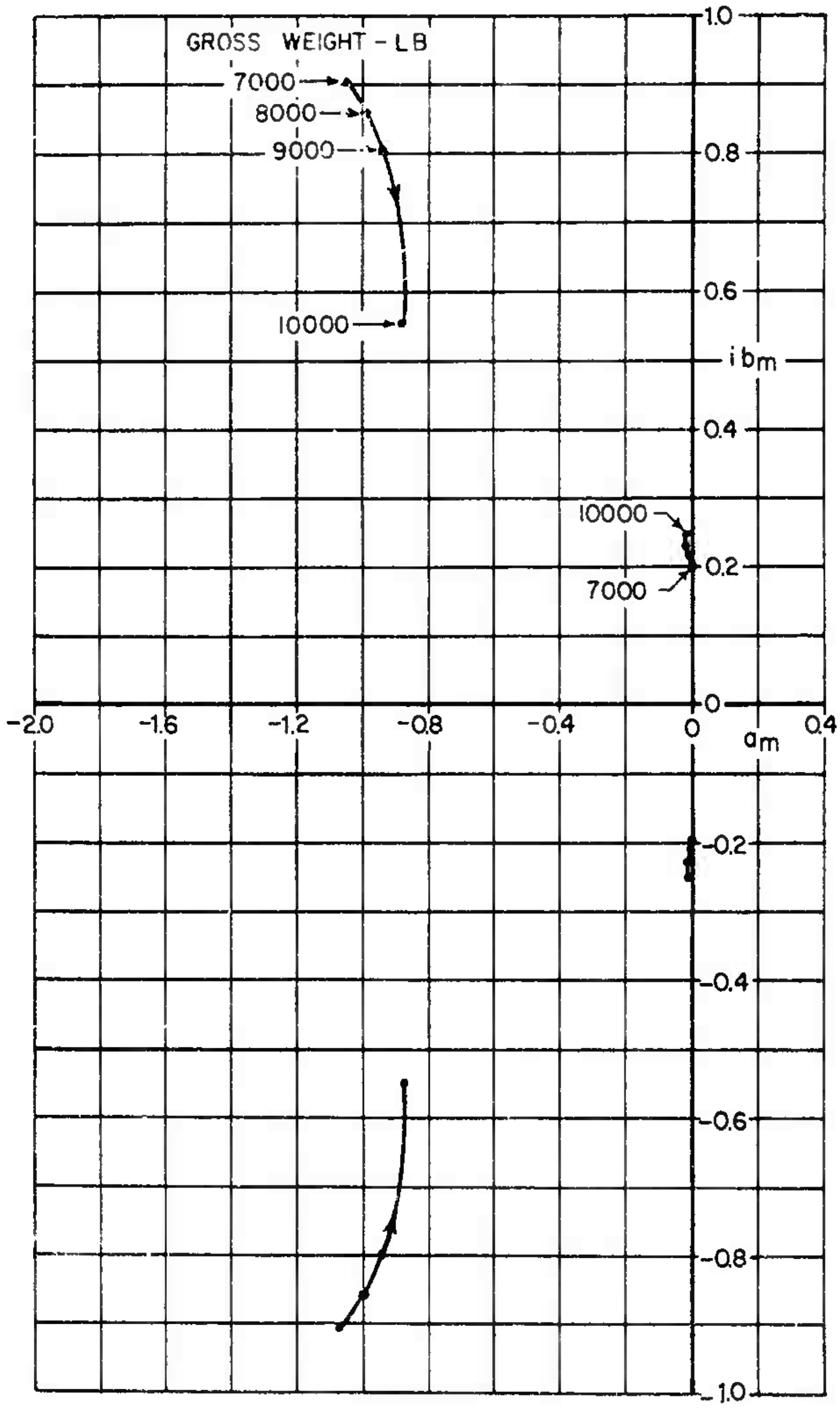

Figure 3. Effect of Gross Weight on Longitudinal Characteristic Roots.

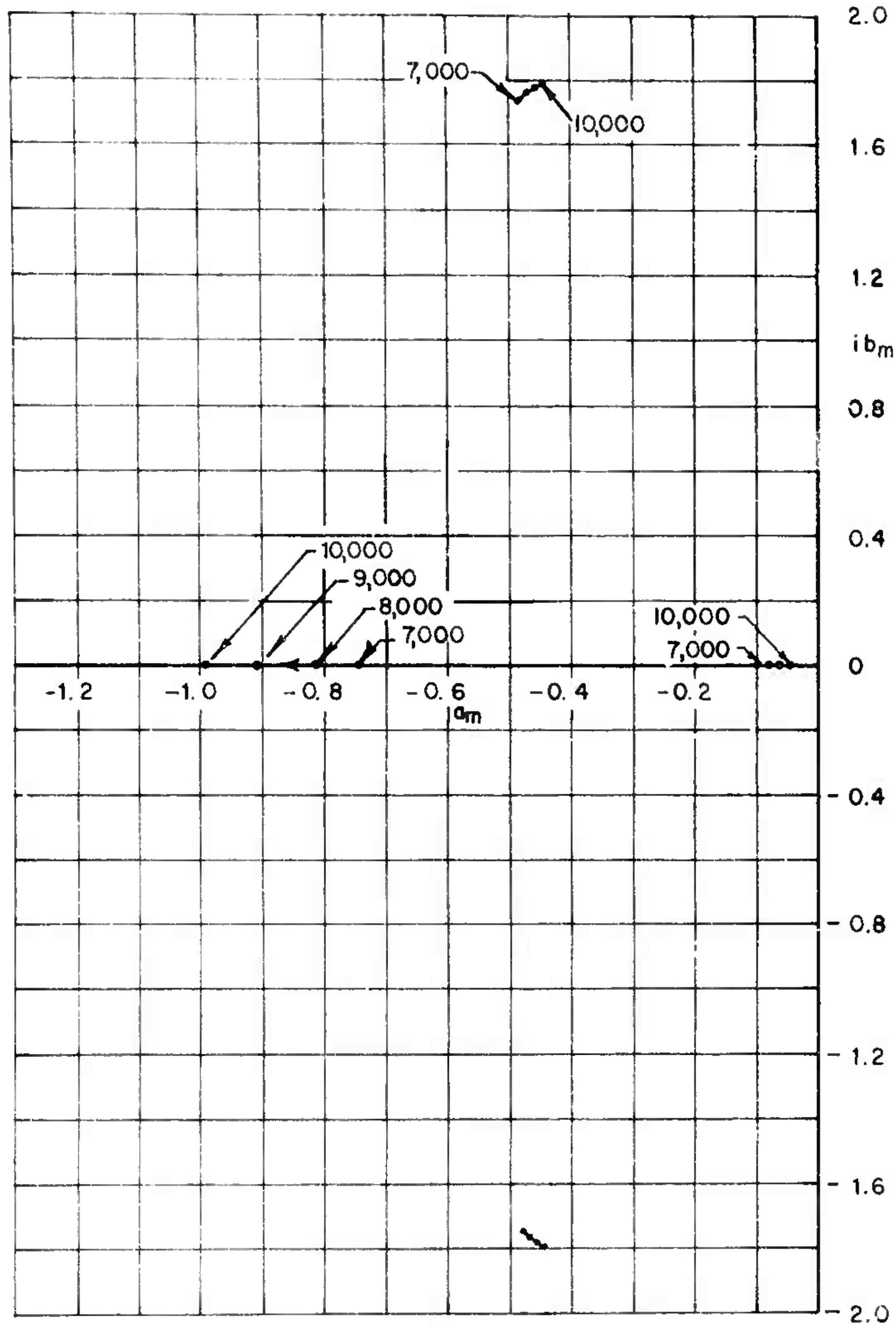

Figure 4. Effect of Gross Weight on Lateral Characteristic Roots.

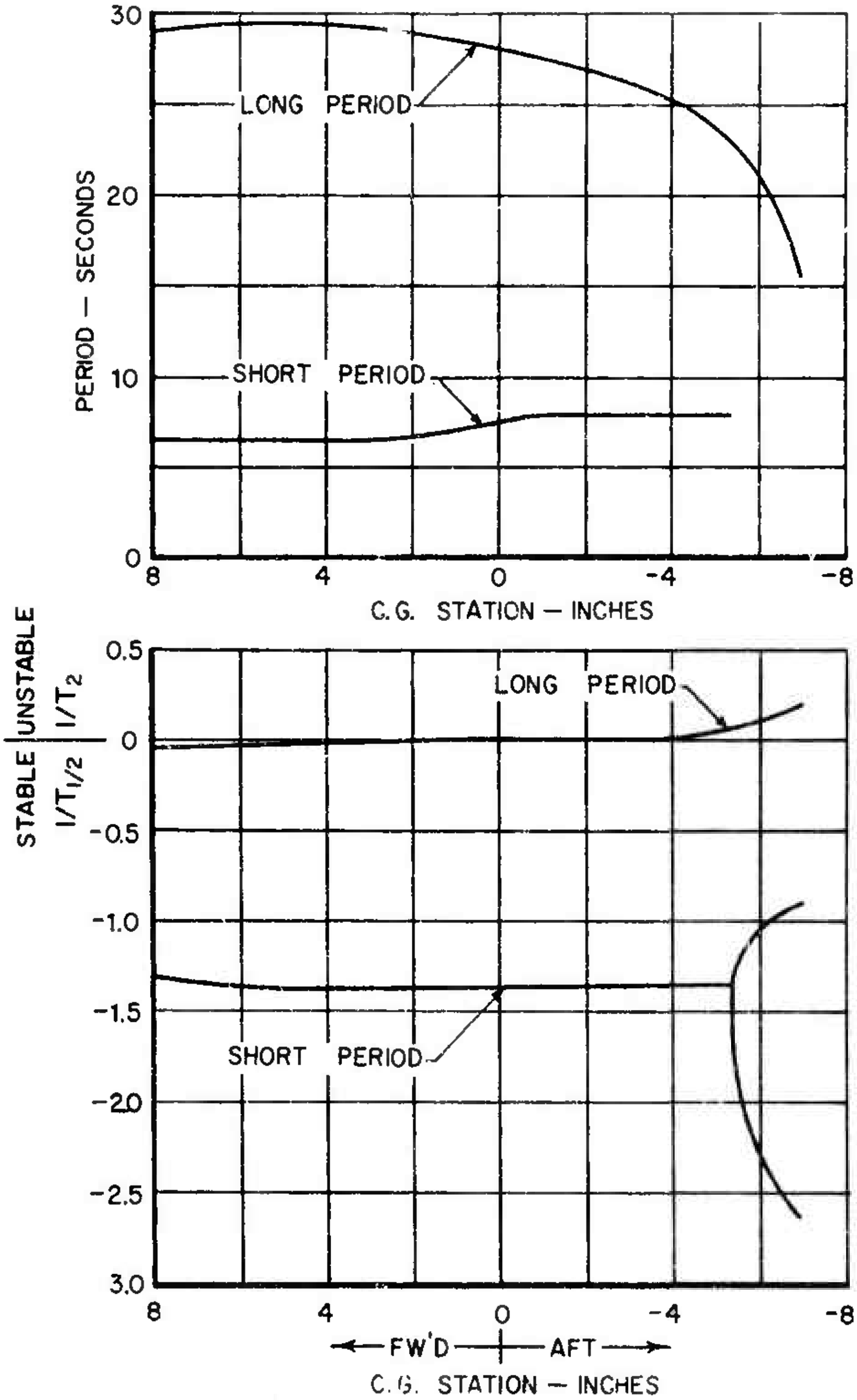

Figure 5. Effect of Center of Gravity on Longitudinal Dynamic Stability Characteristics.

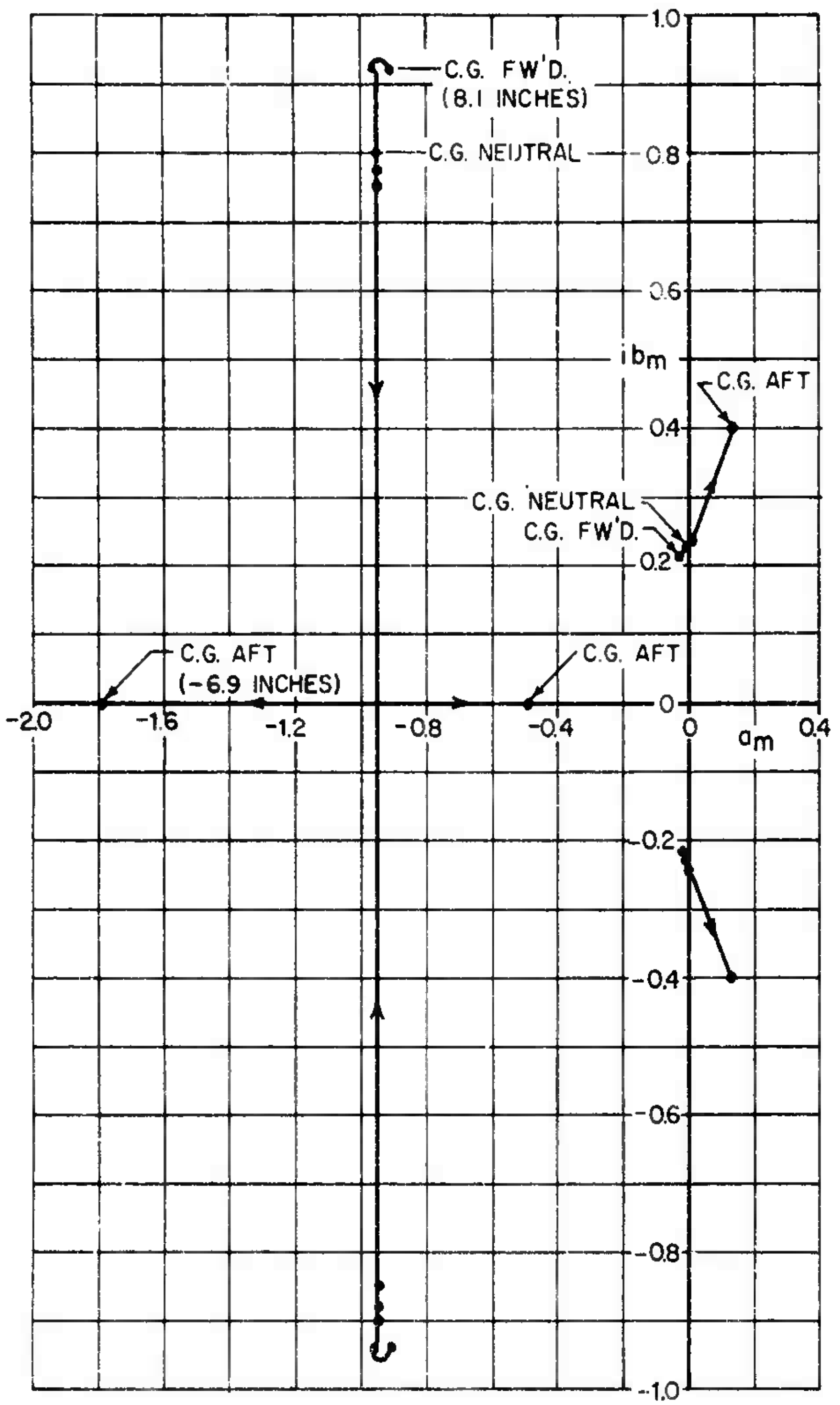

Figure 6. Effect of Center of Gravity on Longitudinal Characteristic Roots.

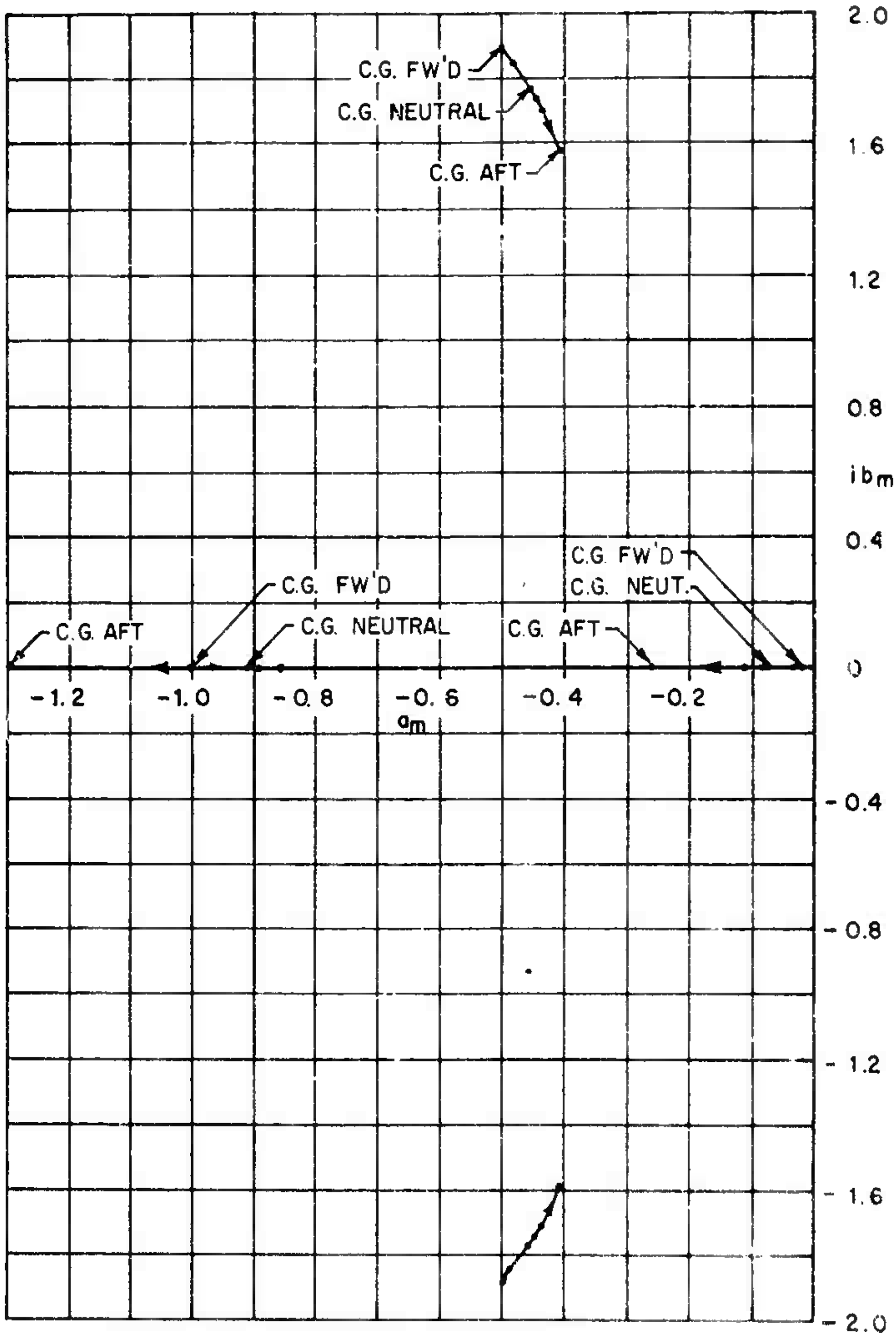

Figure 7. Effect of Center of Gravity on Lateral Characteristic Roots.

Thus, the net effect of a rearward shift of the center of gravity is to reduce both the longitudinal and the lateral dynamic stability of the aircraft. Since this shift in center of gravity also reduces the amount of control power available for longitudinal trim, the aft limit of the center-of-gravity range is an important parameter to be established in the preliminary design phase of a compound helicopter.

(c) Effect of Forward Speed

The effects of forward speed on the longitudinal and lateral dynamic stability characteristics of the sample compound helicopter are shown in Figures 8, 9, and 10. For speeds up to 150 knots, the compound helicopter is flown in the helicopter mode; i.e., only conventional helicopter controls are used for trim. Beyond 150 knots, the compound is flown in the aircraft mode; i.e., conventional airplane controls are used in conjunction with the helicopter controls to increase the available control power.

As can be noted from Figures 8 and 9, the longitudinal modes consist of a neutrally stable long-period oscillation and a moderately damped short-period oscillation. As speed is increased, both of these modes become more stable.

For forward speed up to 200 knots, the lateral modes consist of two stable aperiodic modes and a stable short-period oscillation. Beyond the 200-knot speed, the short-period oscillation decreases in frequency and eventually splits into two aperiodic modes, one of which becomes heavily damped and stable whereas the other becomes unstable. Thus, the principal effect of forward speed especially in the very high-speed range is to reduce the lateral dynamic stability of the compound helicopter.

(d) Effect of Rotor Rotational Speed

The effect of varying the rotational speed of the main rotor on the longitudinal and lateral dynamic stability characteristics of the sample compound helicopter is shown in Figures 11, 12, and 13. These figures show that an increase in rotational speed results in an improvement of both longitudinal and lateral dynamic stability characteristics of the compound helicopter. An increase in rotational speed is particularly beneficial in eliminating the unstable oscillatory mode at low rotational speed as shown in Figures 11 and 12. The low speed boundary for the rotor, although generally established on the basis of performance requirements, should be checked for adequate dynamic stability.

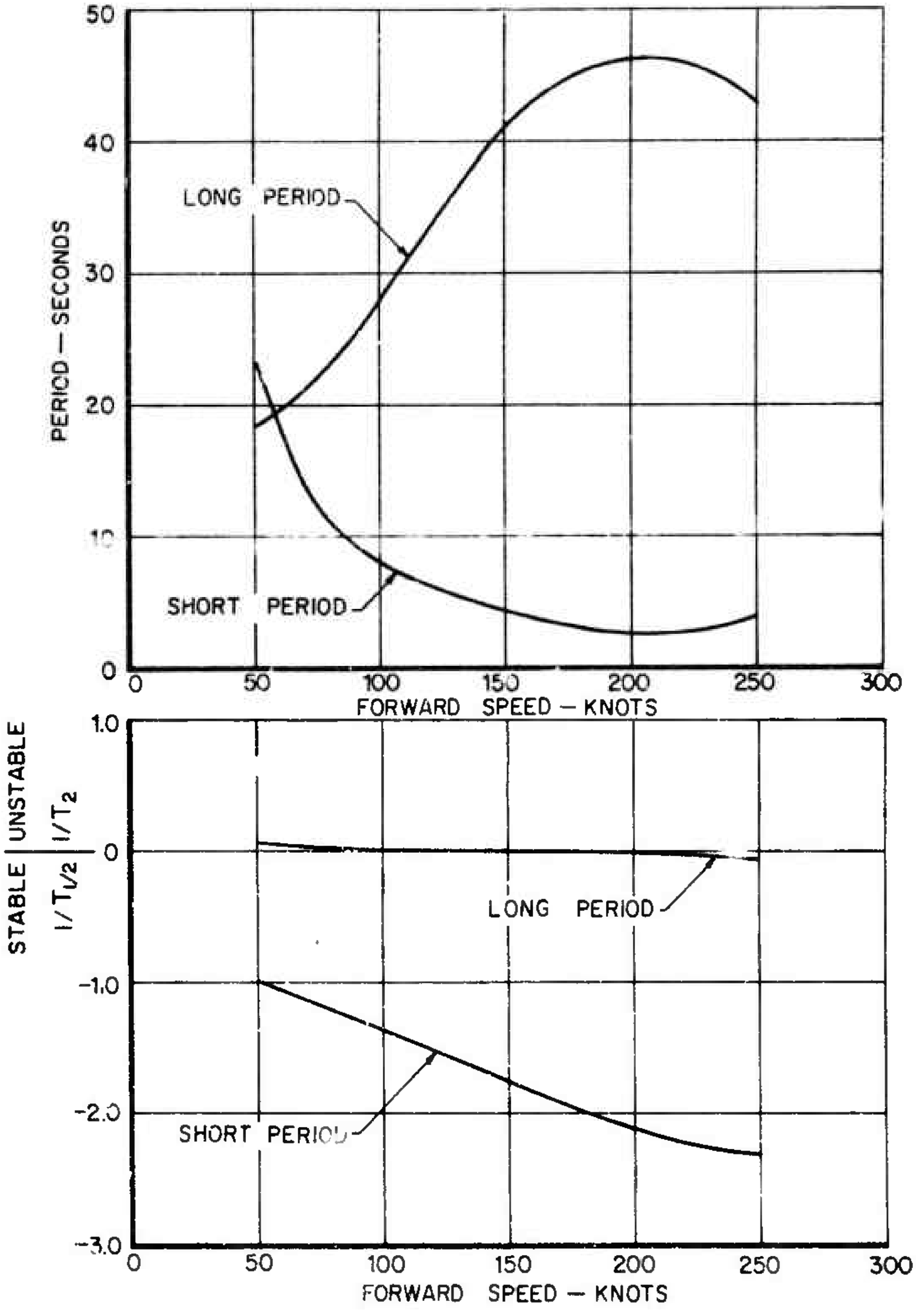

Figure 8. Effect of Forward Speed on Longitudinal Dynamic Stability Characteristics.

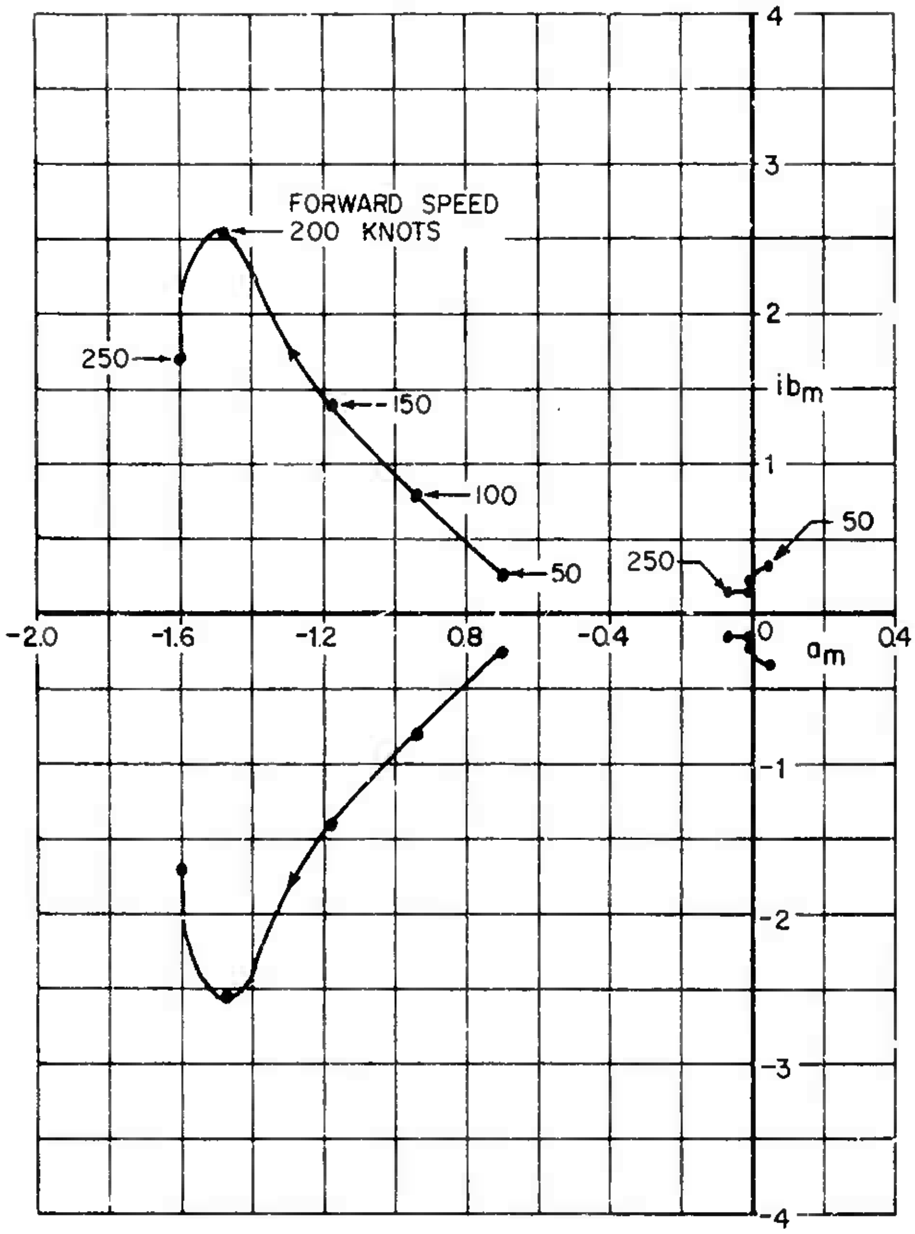

Figure 9. Effect of Forward Speed on Longitudinal Characteristic Roots.

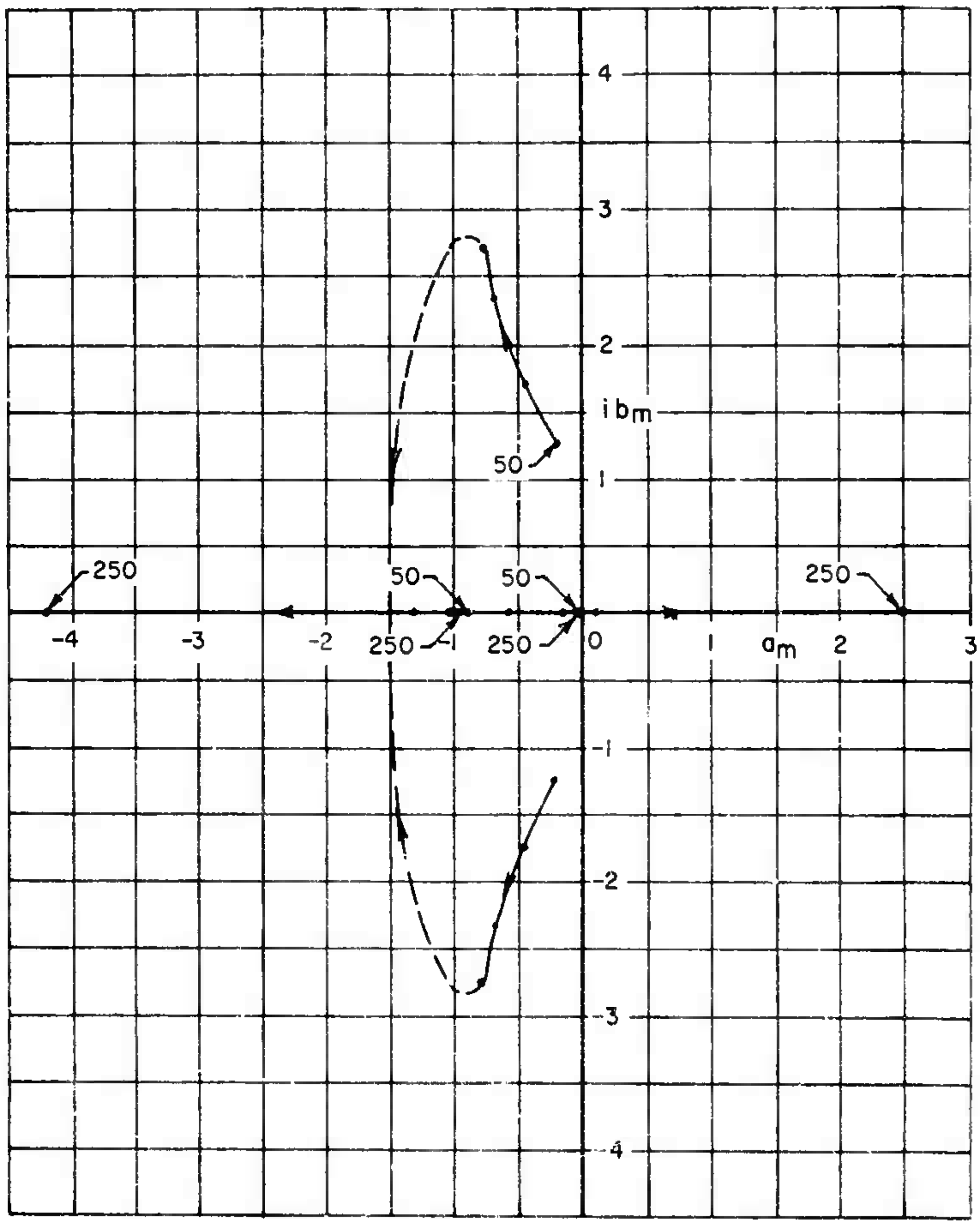

Figure 10. Effect of Forward Speed on Lateral Characteristic Roots.

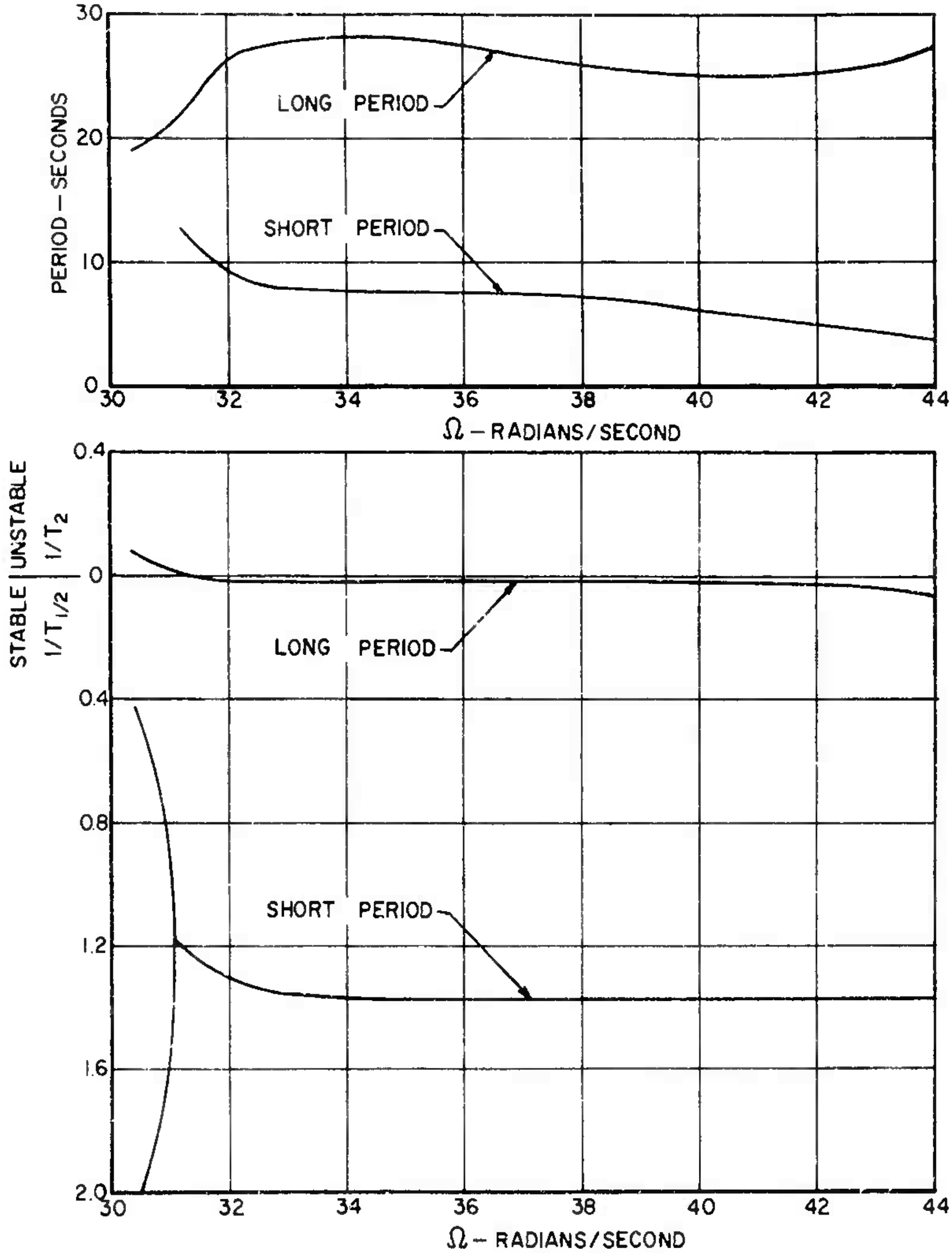

Figure 11. Effect of Rotor Rotational Speed on Longitudinal Dynamic Stability Characteristics.

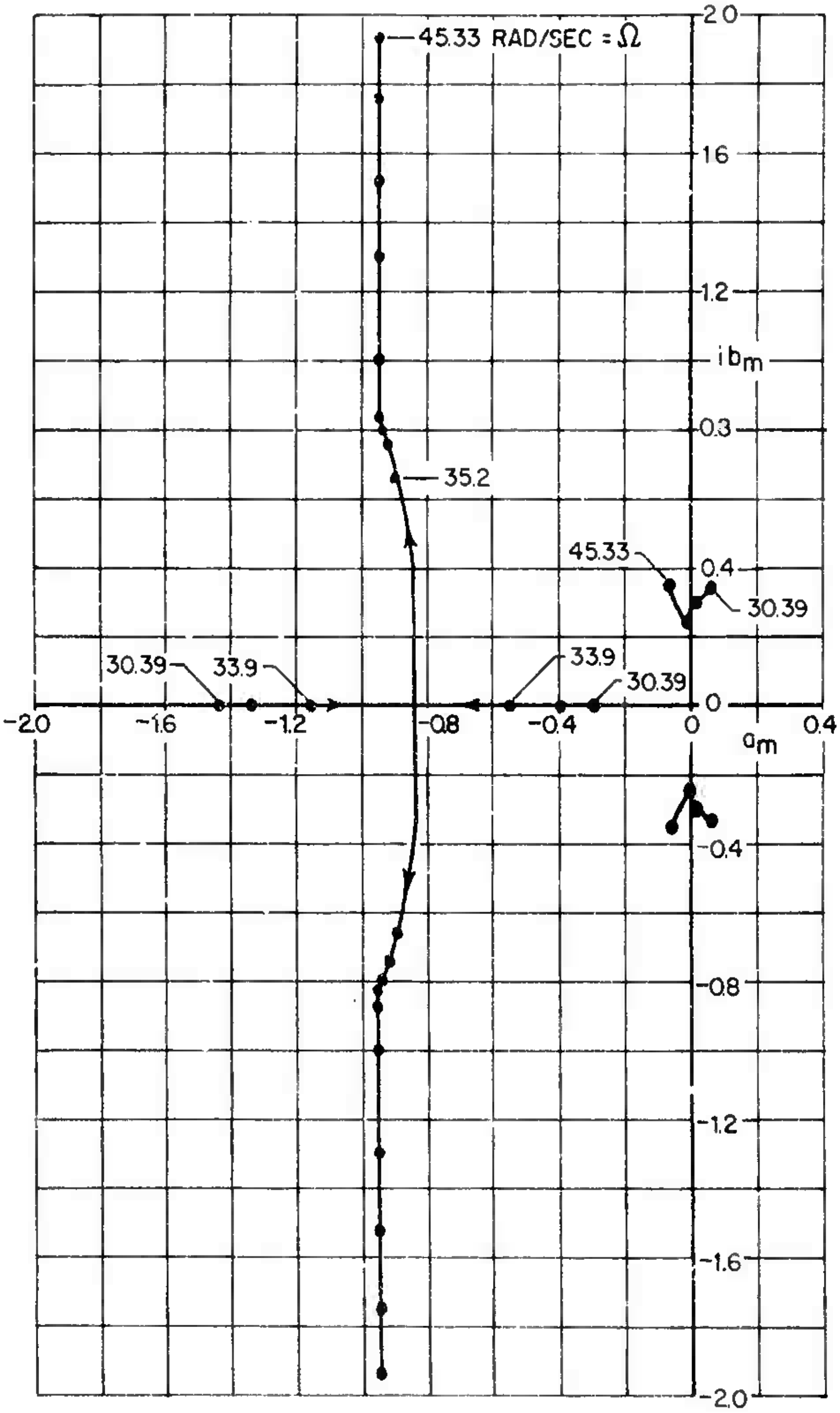

Figure 12. Effect of Rotor Rotational Speed on Longitudinal Characteristic Roots.

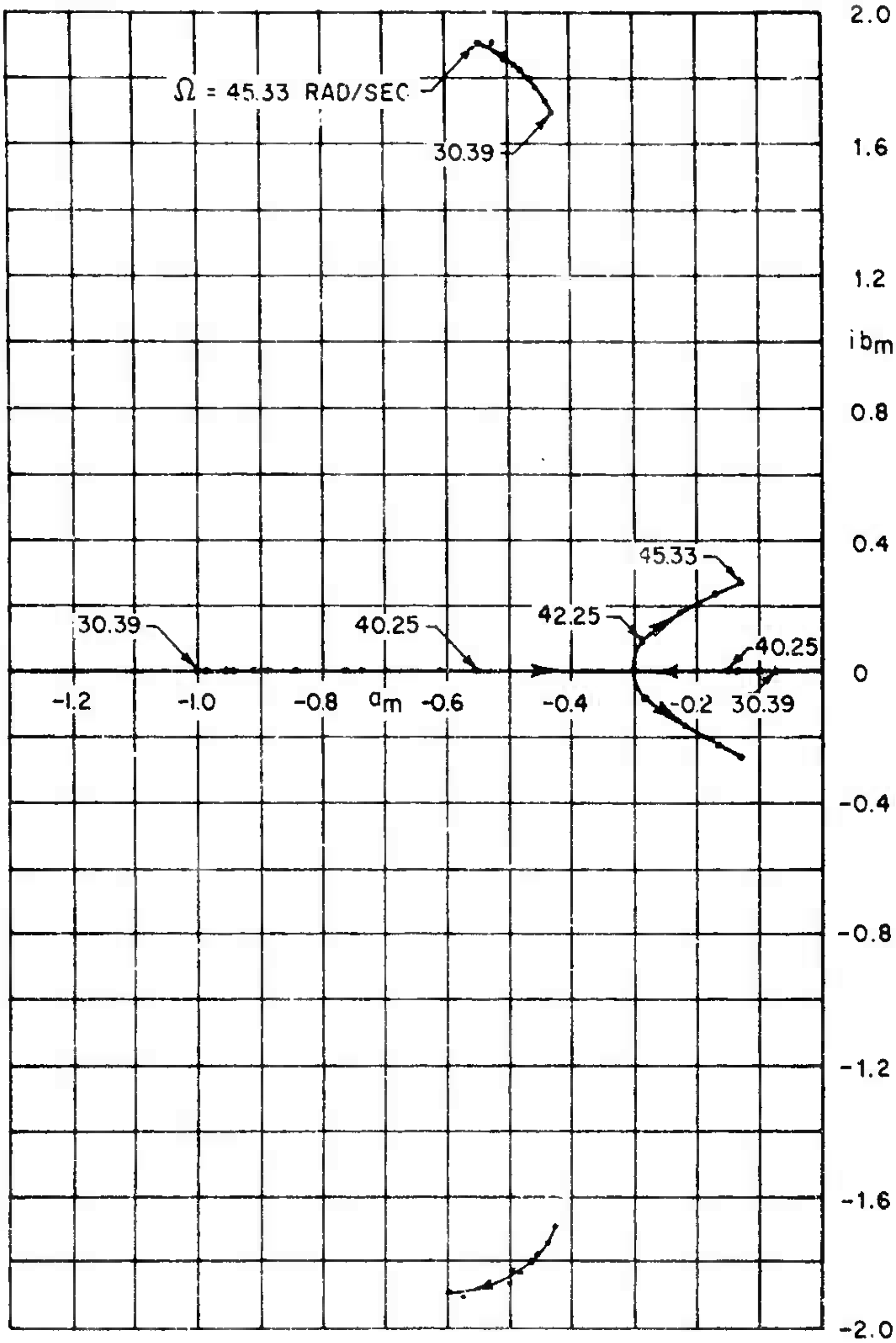

Figure 13. Effect of Rotor Rotational Speed on Lateral Characteristic Roots.

(e) Effect of Lift Distribution Between Rotor and Wing

The effect of unloading the rotor on the longitudinal and lateral dynamic stability characteristics is shown in Figures 14, 15, and 16. The primary effect of loading the wing is to decrease the periods of the two oscillatory modes and slightly increase the period of the lateral oscillatory mode. Increasing the wing to rotor lift ratio seems to have very little effect on the damping of both the longitudinal and lateral modes, all of which are stable. This indicates that a wing can effectively be used to unload a rotor in order to obtain more control power out of the rotor at higher forward speeds without introducing undesirable stability problems.

(f) Effect of Auxiliary Propulsion Thrust

The effects of varying the amount of propulsive thrust provided by the auxiliary propulsion system on the longitudinal and lateral dynamic stability characteristics of the sample helicopter are illustrated in Figures 17, 18, and 19. All three figures show that auxiliary thrust provides beneficial effects for all longitudinal and lateral modes. The main effect of increasing the amount of auxiliary thrust is a mild increase in damping of all the stability modes. In particular, the initial increment of auxiliary thrust removes the instability of the long-period oscillatory mode and causes the two aperiodic longitudinal modes to coalesce into a stable short-period oscillation.

(g) Effect of Wing Area

Figures 20, 21, and 22 illustrate the effect of variation of wing area on the longitudinal and lateral dynamic stability characteristics of the sample compound helicopter. Both longitudinal oscillatory modes increase their period of oscillation with increased wing area. An increase in wing area produces a mild stabilizing effect on the short-period mode whereas the long-period mode tends to become neutrally stable. Also, an increase in wing area results in a very minor increase in frequency of the lateral oscillatory mode, with a rapid increase in damping of one aperiodic mode root and a destabilizing trend for the other aperiodic mode. The predominant effect of increasing wing area thus appears to be an increase in period of the two longitudinal oscillatory modes.

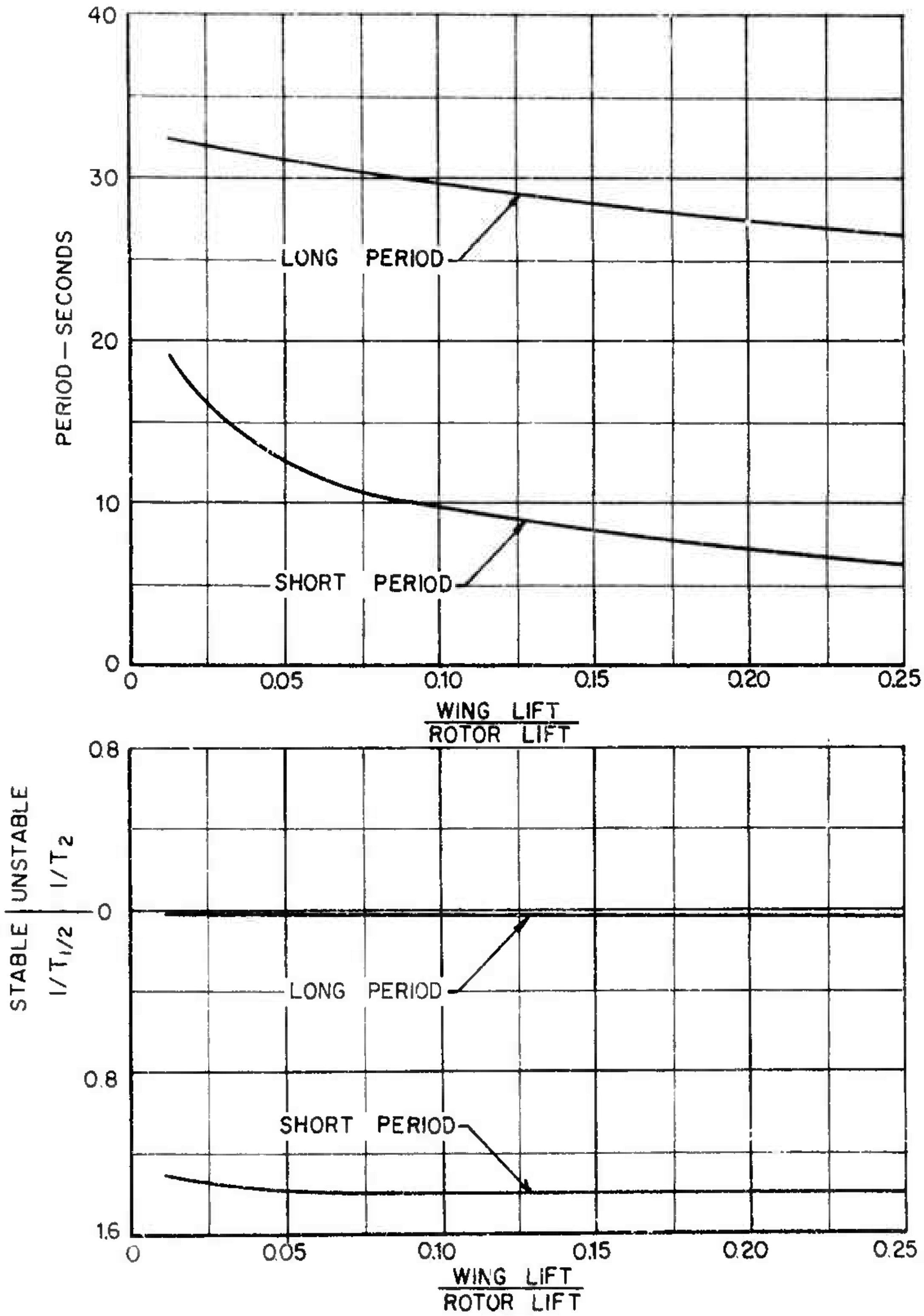

Figure 14. Effect of Wing-Rotor Lift Distribution on Longitudinal Dynamic Stability Characteristics.

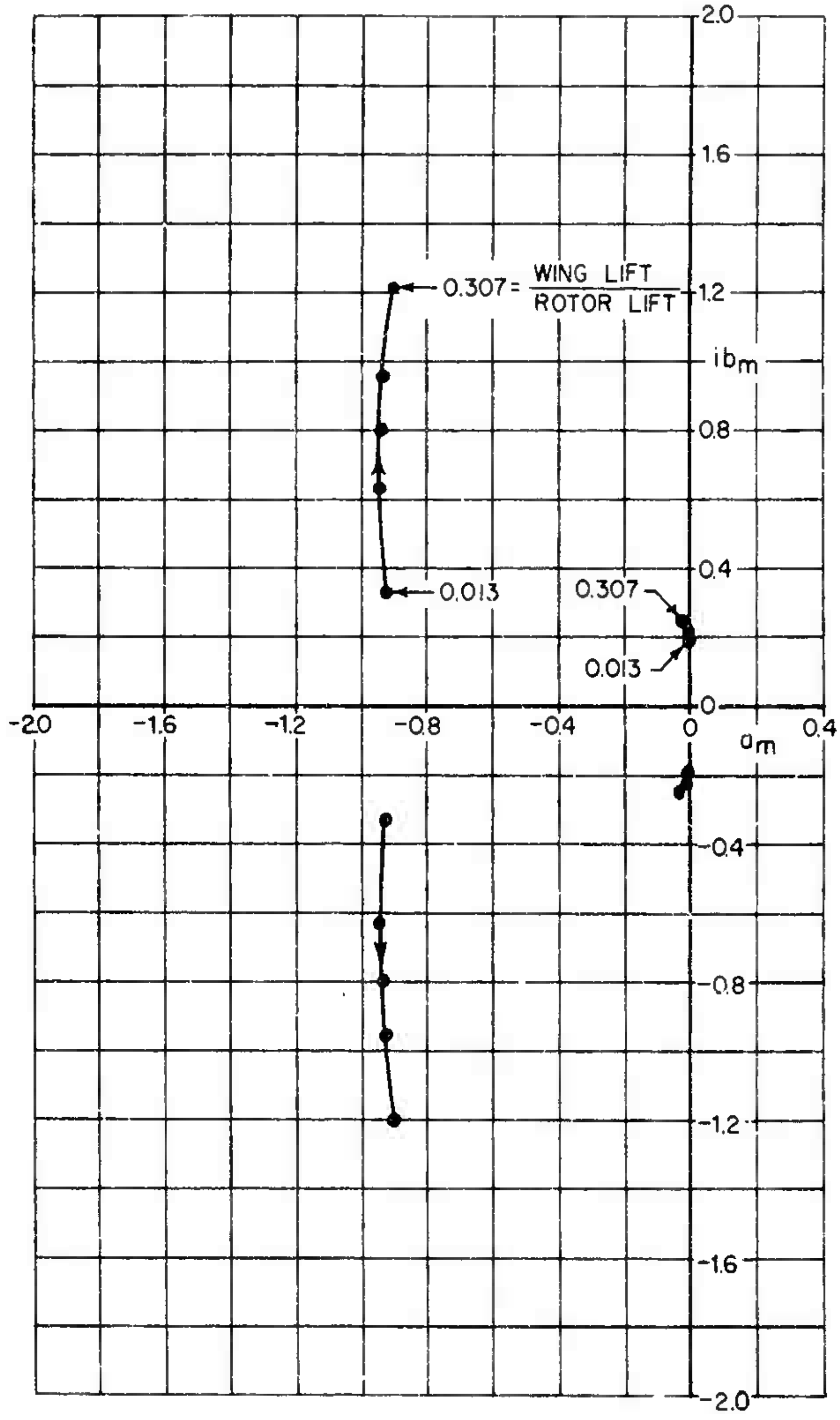

Figure 15. Effect of Wing-Rotor Lift Distribution on Longitudinal Characteristic Roots.

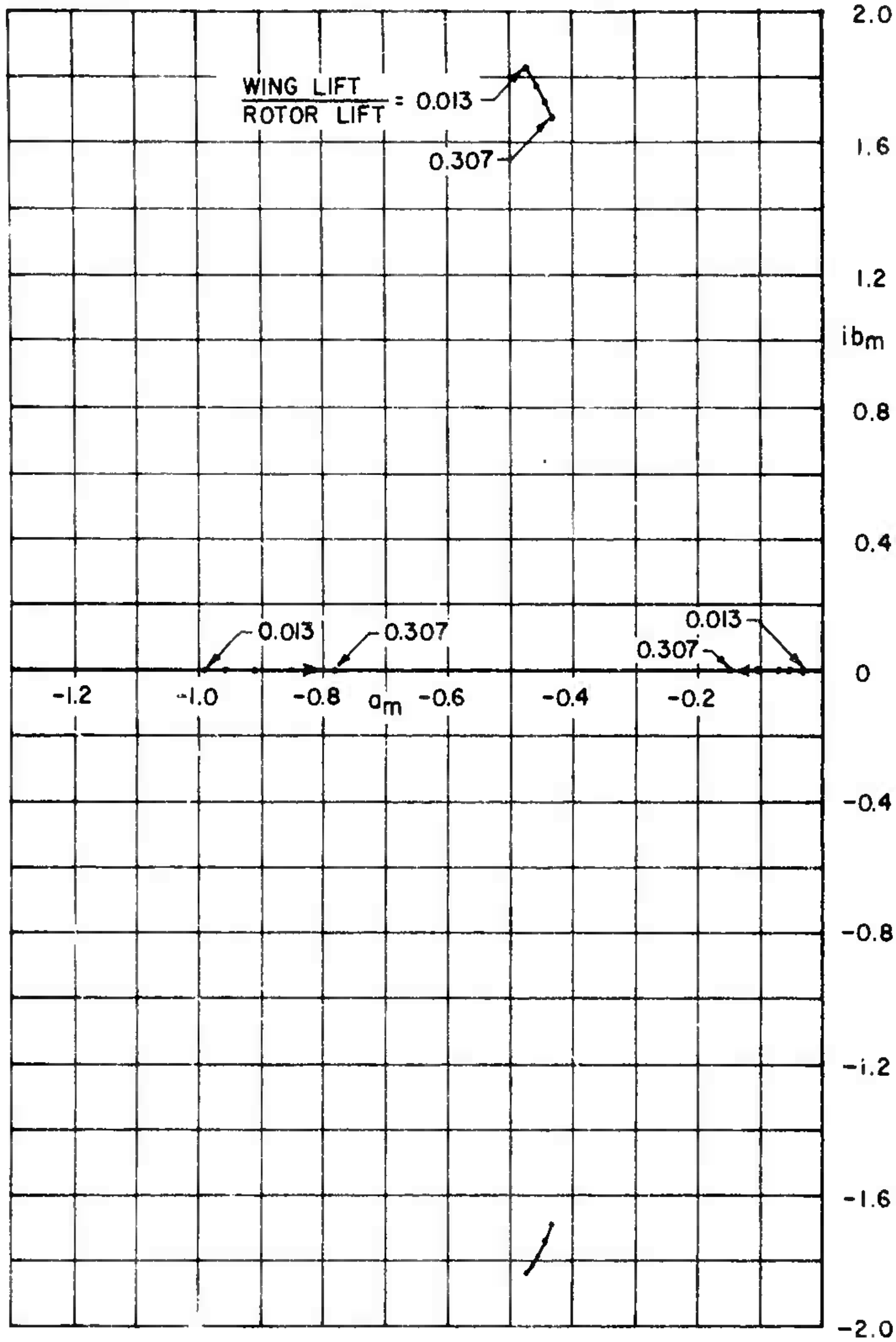

Figure 16. Effect of Wing-Rotor Lift Distribution on Lateral Characteristic Roots.

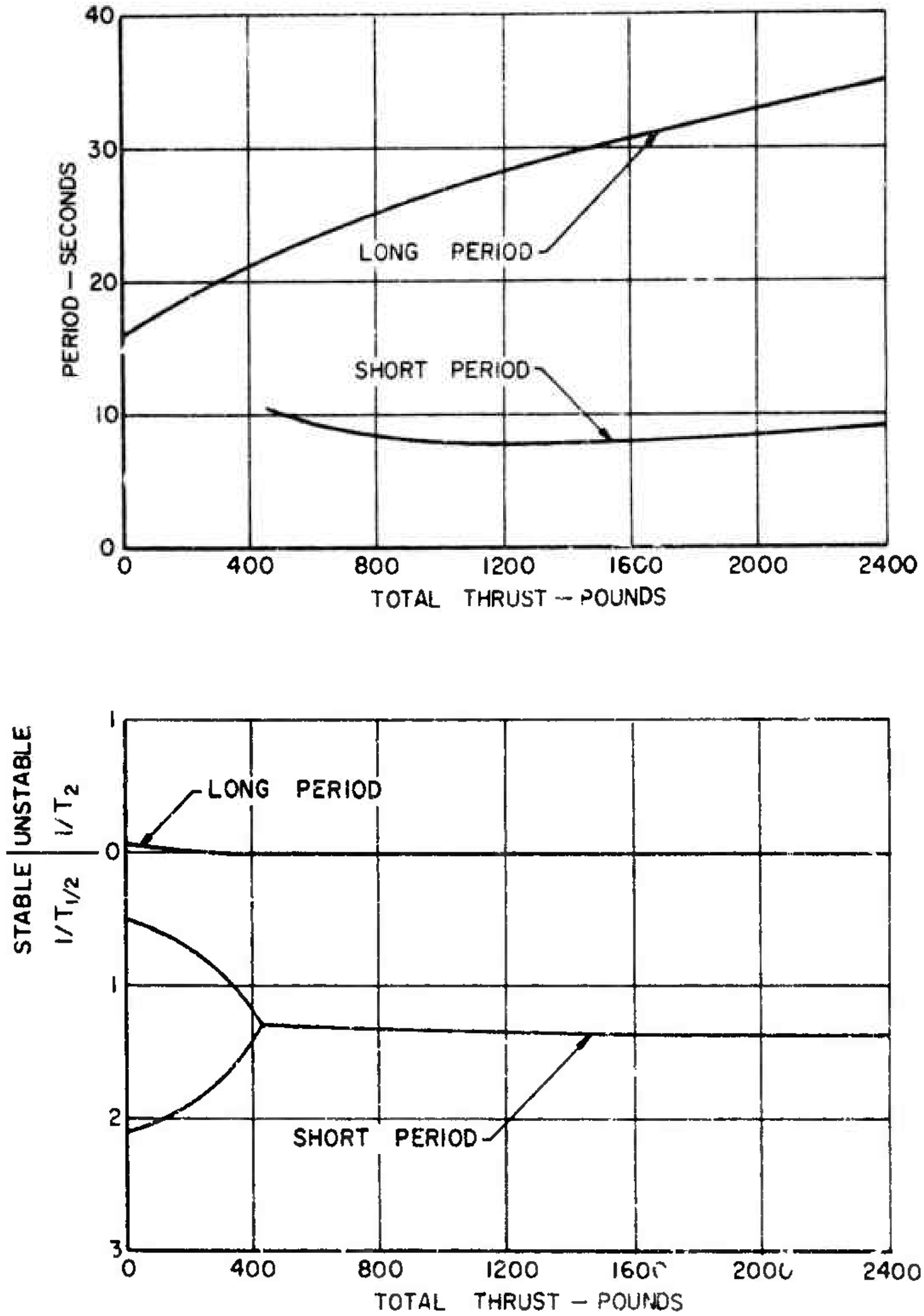

Figure 17. Effect of Auxiliary Thrust on Longitudinal Dynamic Stability Characteristics.

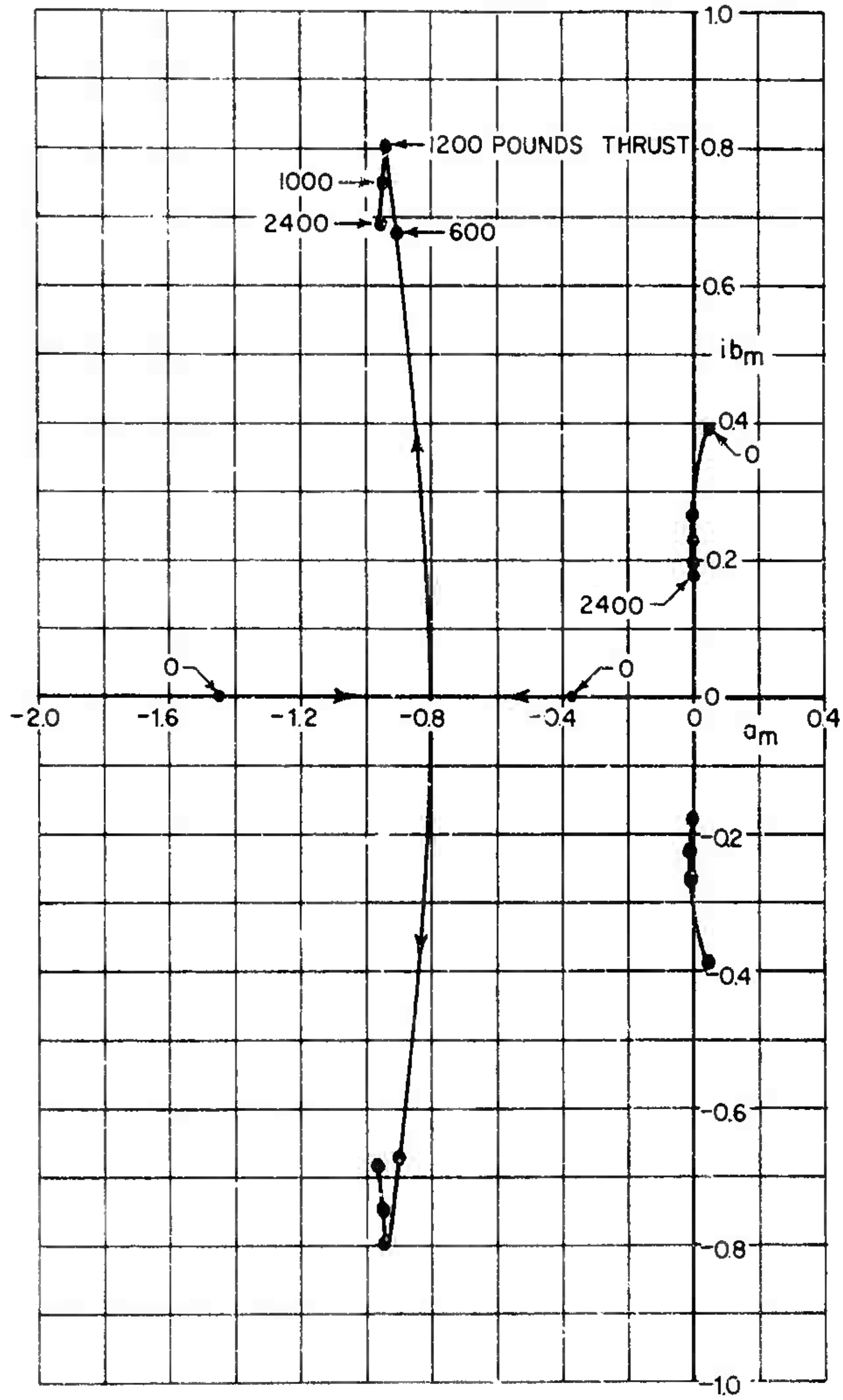

Figure 18. Effect of Auxiliary Thrust on Longitudinal Characteristic Roots.

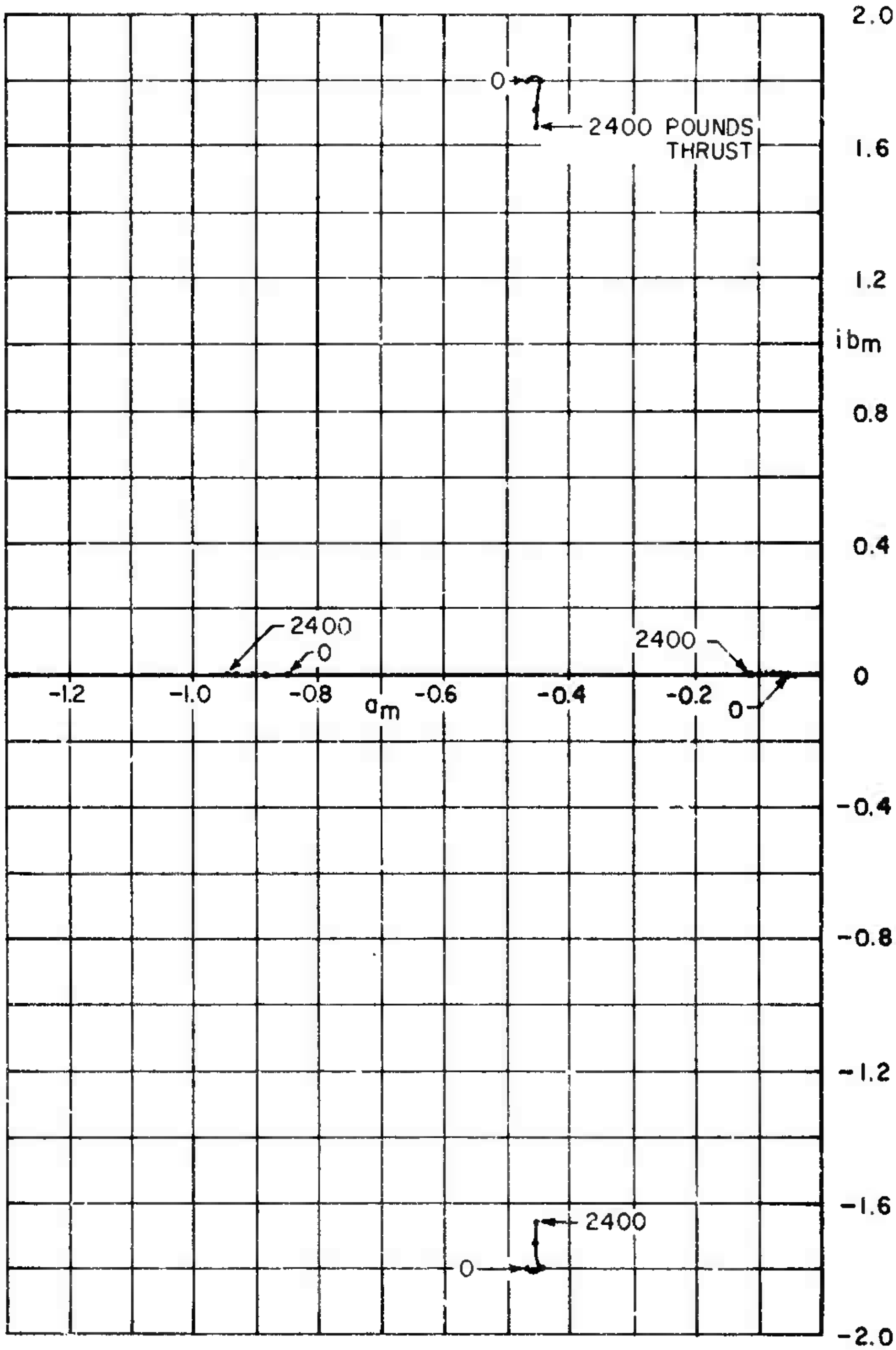

Figure 19. Effect of Auxiliary Thrust on Lateral Characteristic Roots.

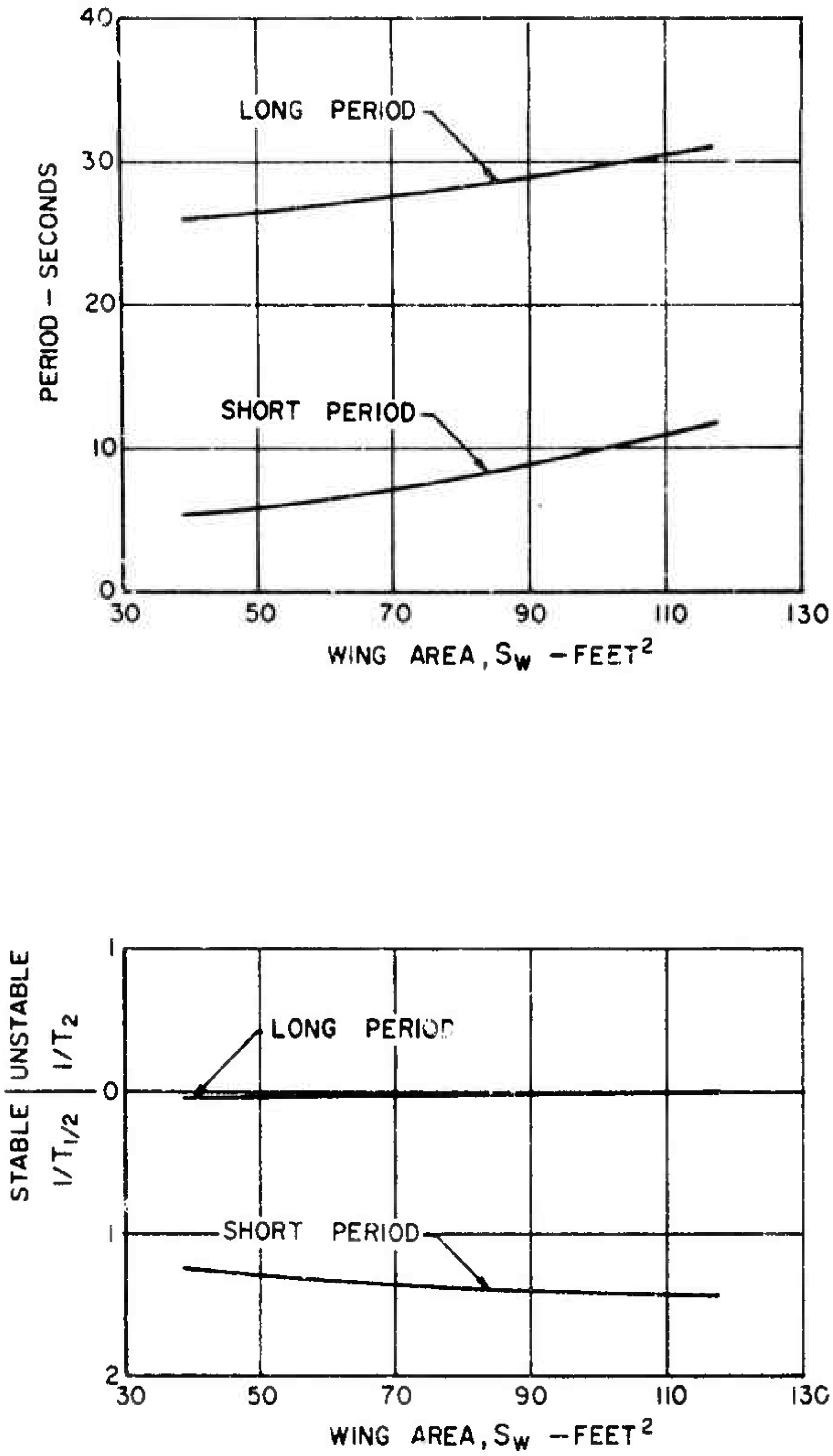

Figure 20. Effect of Wing Area on Longitudinal Dynamic Stability Characteristics.

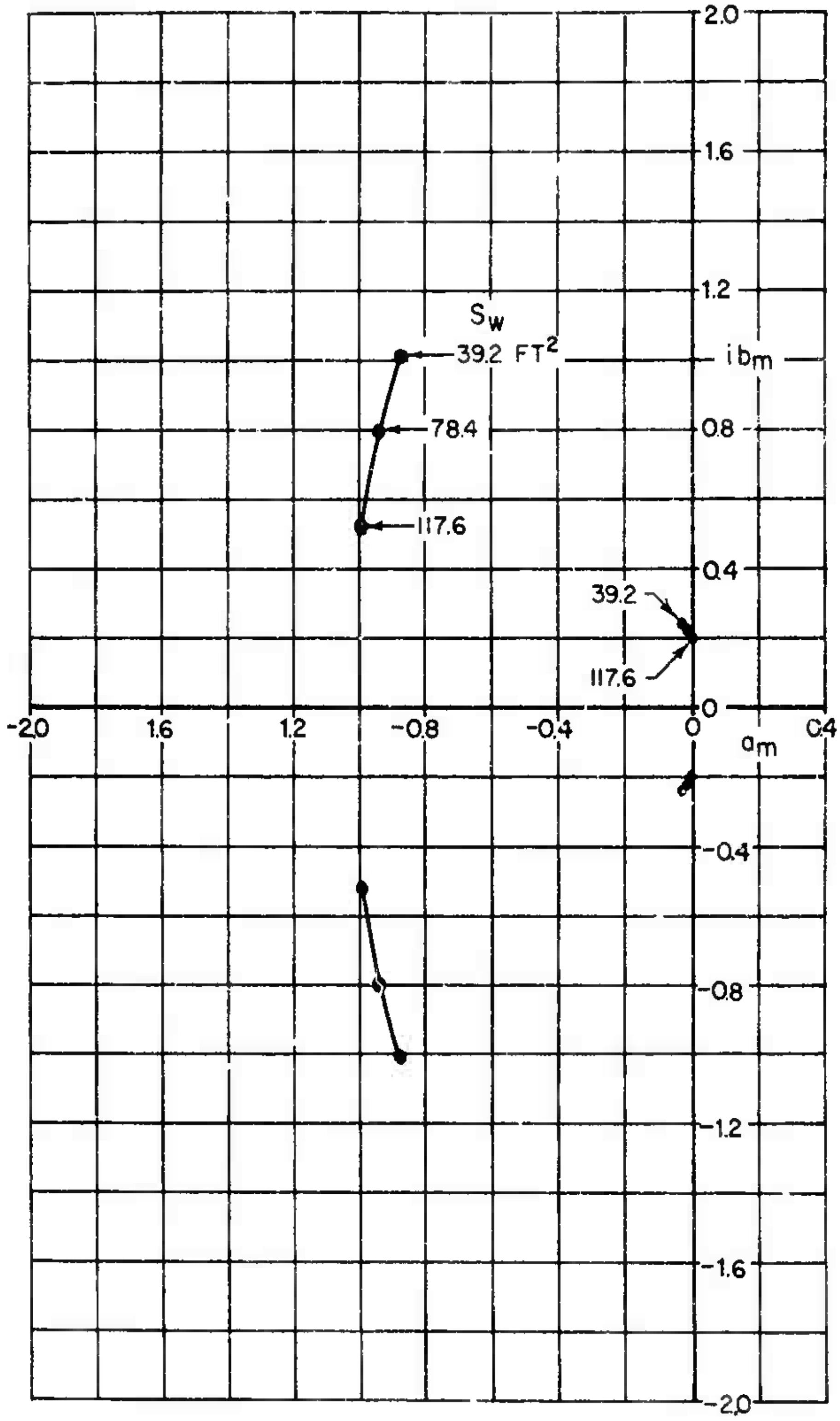

Figure 21. Effect of Wing Area on Longitudinal Characteristic Roots.

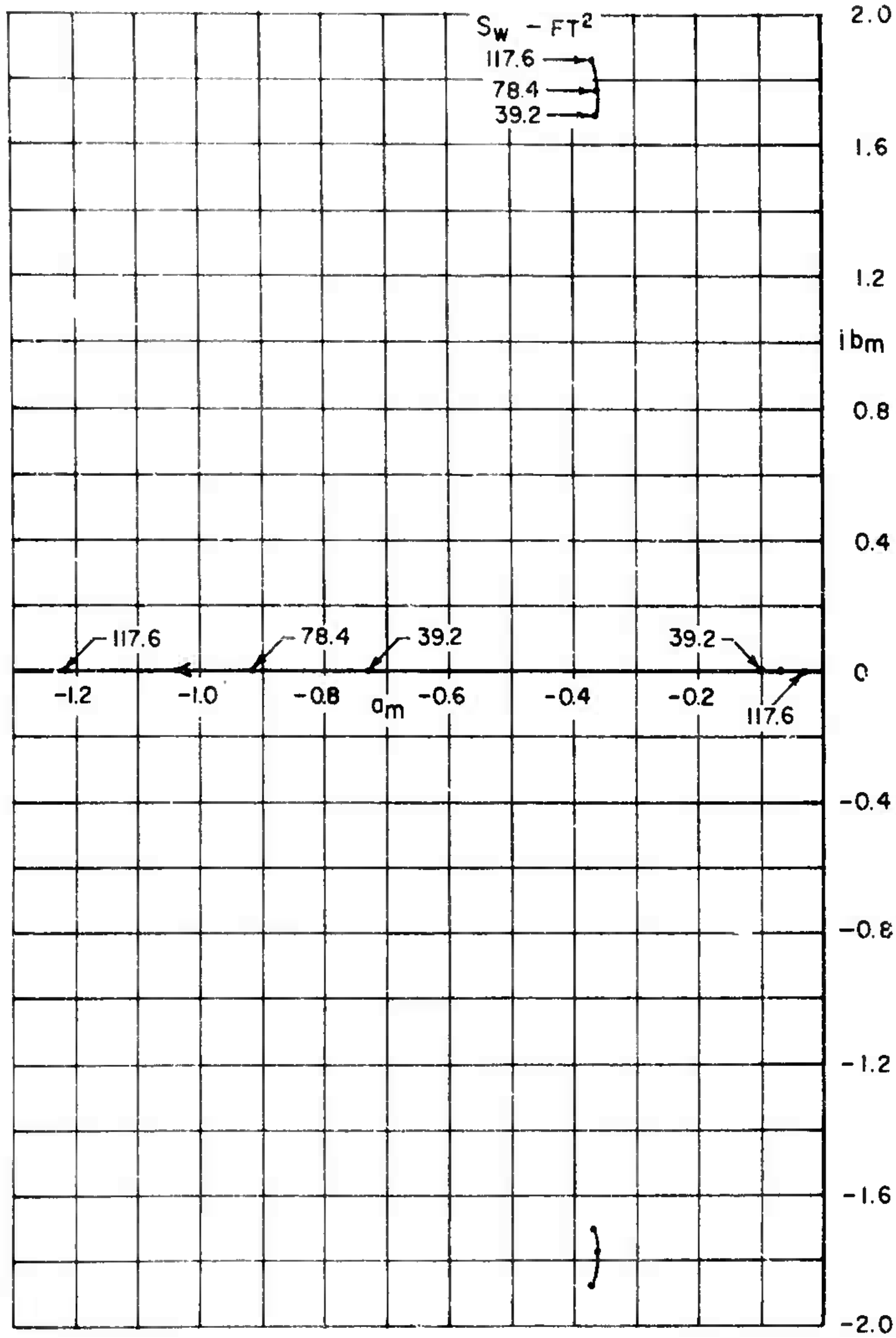

Figure 22. Effect of Wing Area on Lateral Characteristic Roots.

(h) Effect of Horizontal Tailplane Area

The effect of varying the horizontal tailplane area on the longitudinal and lateral dynamic stability characteristics is shown in Figures 23, 24, and 25. Increasing the horizontal tailplane area improves the dynamic stability of the long-period longitudinal mode and also increases the stability of the short-period oscillatory mode. With increasing horizontal tailplane area the dynamics of the compound helicopter approach that of a conventional airplane with its very lightly damped phugoid. Figure 23 also graphically illustrates the appropriate selection of the horizontal tail area of 40 square feet for the sample compound helicopter. With this area, both the long-period instability and the pair of aperiodic roots have been eliminated in favour of two stable oscillatory longitudinal modes.

Furthermore, as can be noted from Figure 25, the variation of the horizontal tailplane area has no effect on the lateral dynamic characteristics of the sample compound helicopter.

(i) Effect of Vertical Tailplane Area

It was found that the variation in vertical tailplane area had no effect on the longitudinal dynamic stability characteristics of the compound helicopters. Therefore, this variation is not presented in this section. The effect of increasing the vertical tailplane area is shown only for the lateral modes in Figures 26 and 27. The lateral stability modes are characterized by a stable short-period oscillatory mode and a pair of stable aperiodic modes. As would be expected, the effect of increasing the vertical tail area is to increase the dynamic lateral stability of the short-period oscillatory mode with only minor changes in the stability of the two aperiodic modes. Choice of a suitable vertical tail area should therefore be made on the basis of handling qualities requirements.

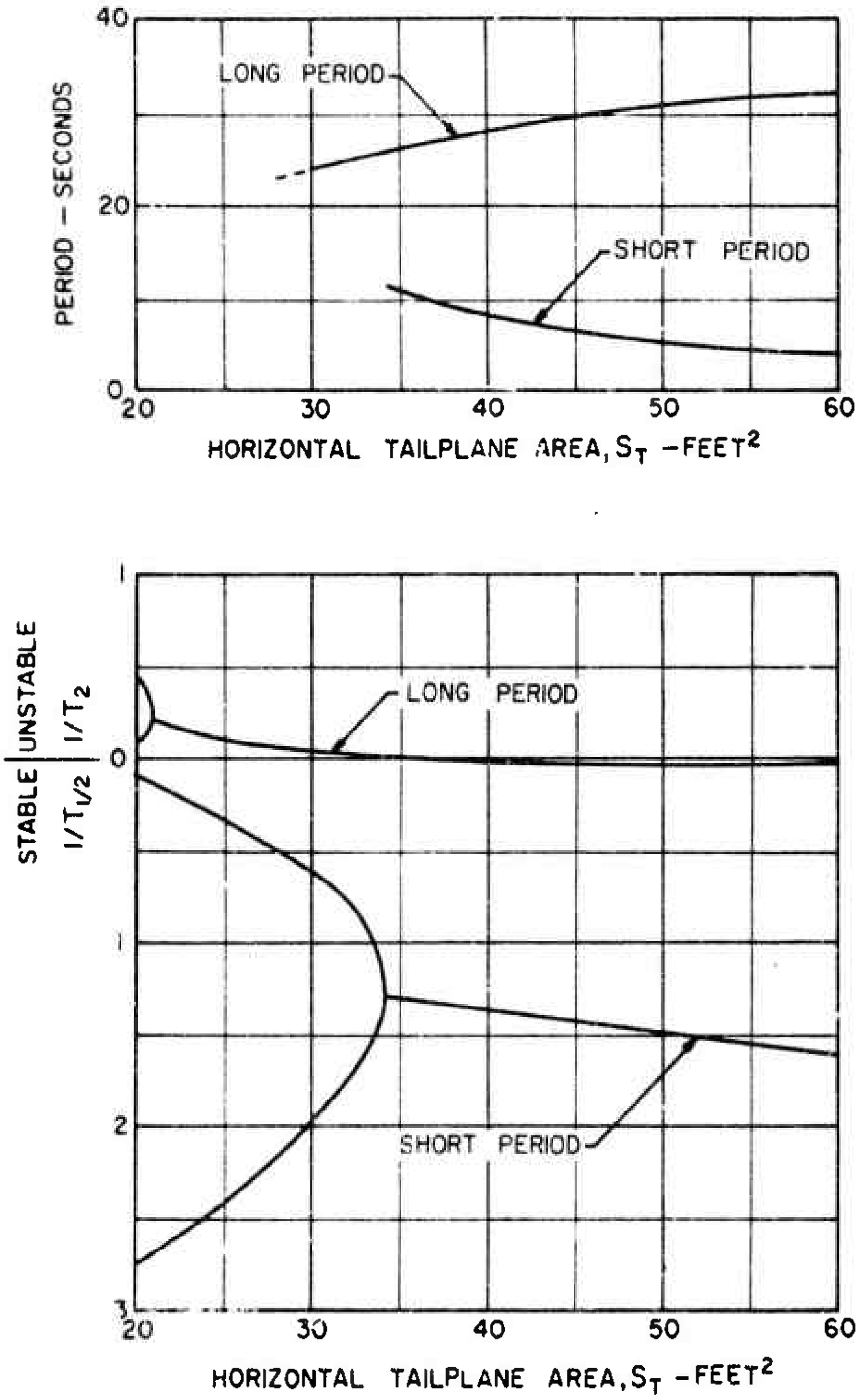

Figure 23. Effect of Horizontal Tailplane Area on Longitudinal Dynamic Stability Characteristics.

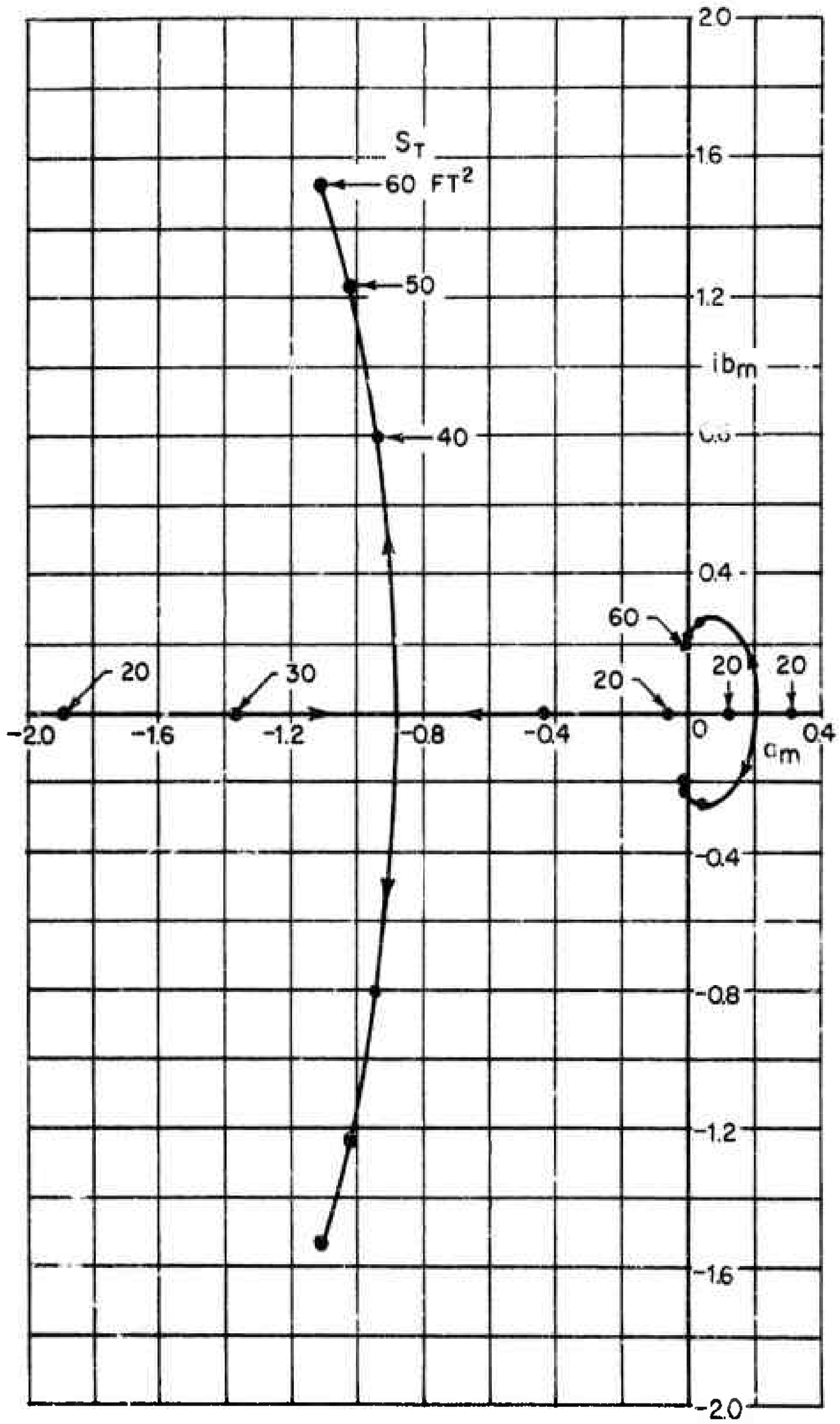

Figure 24. Effect of Horizontal Tailplane Area on Longitudinal Characteristic Roots.

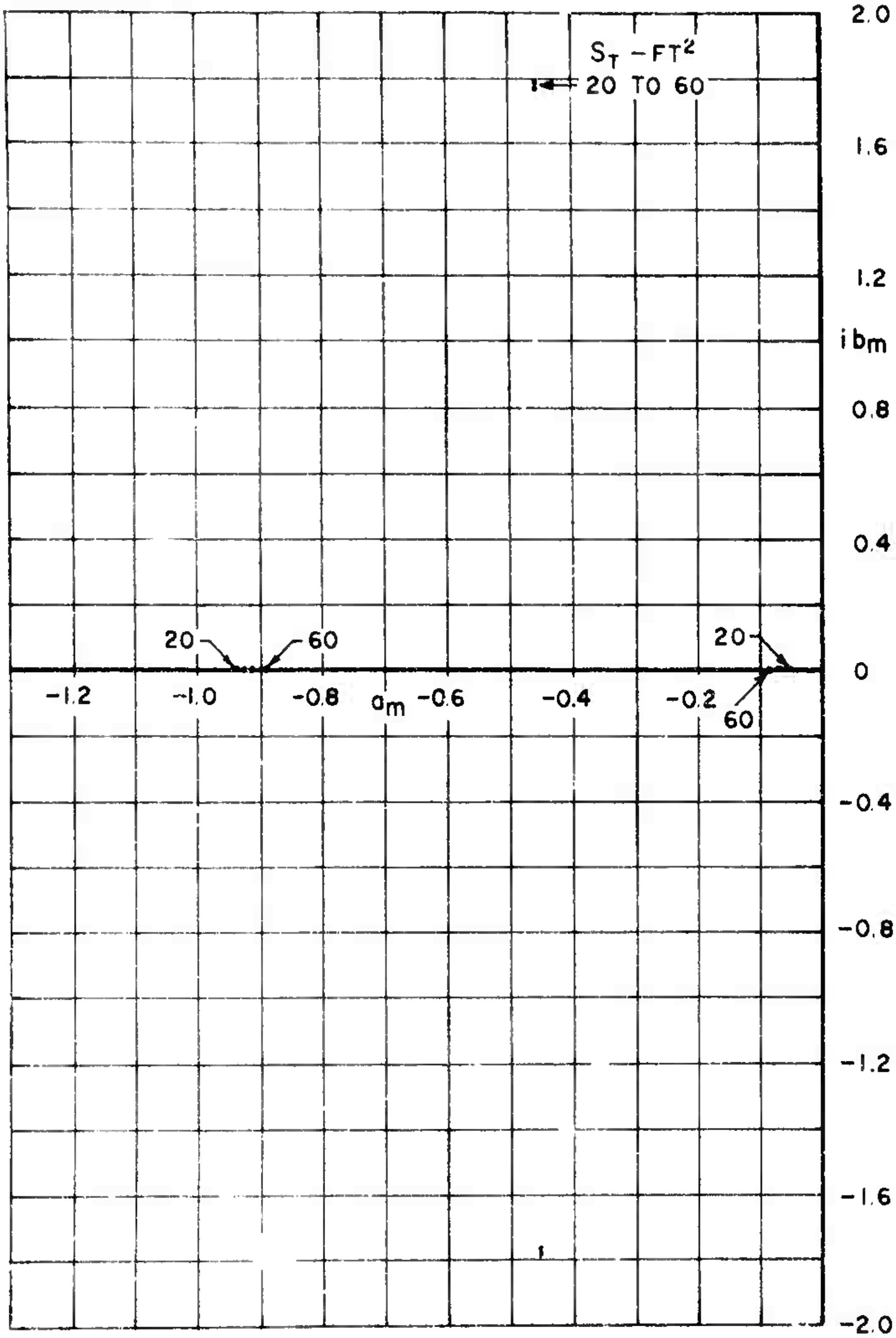

Figure 25. Effect of Horizontal Tailplane Area on Lateral Characteristic Roots.

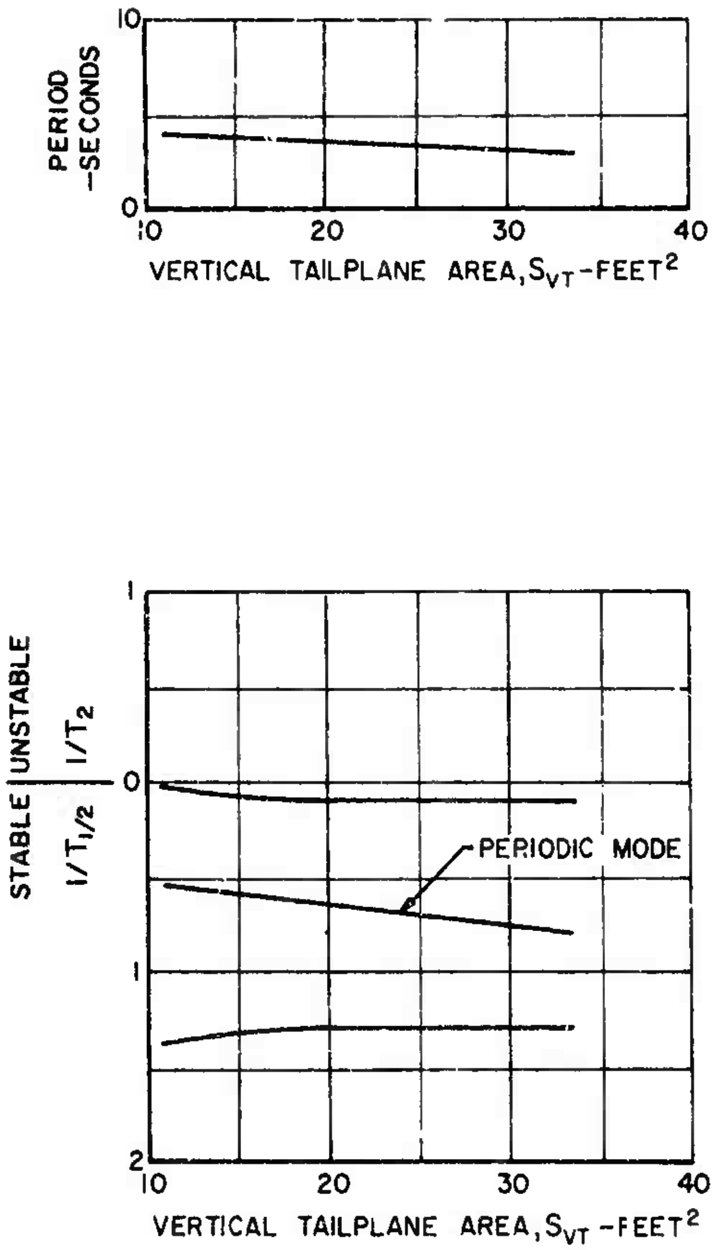

Figure 26. Effect of Vertical Tailplane Area on Lateral Dynamic Stability Characteristics.

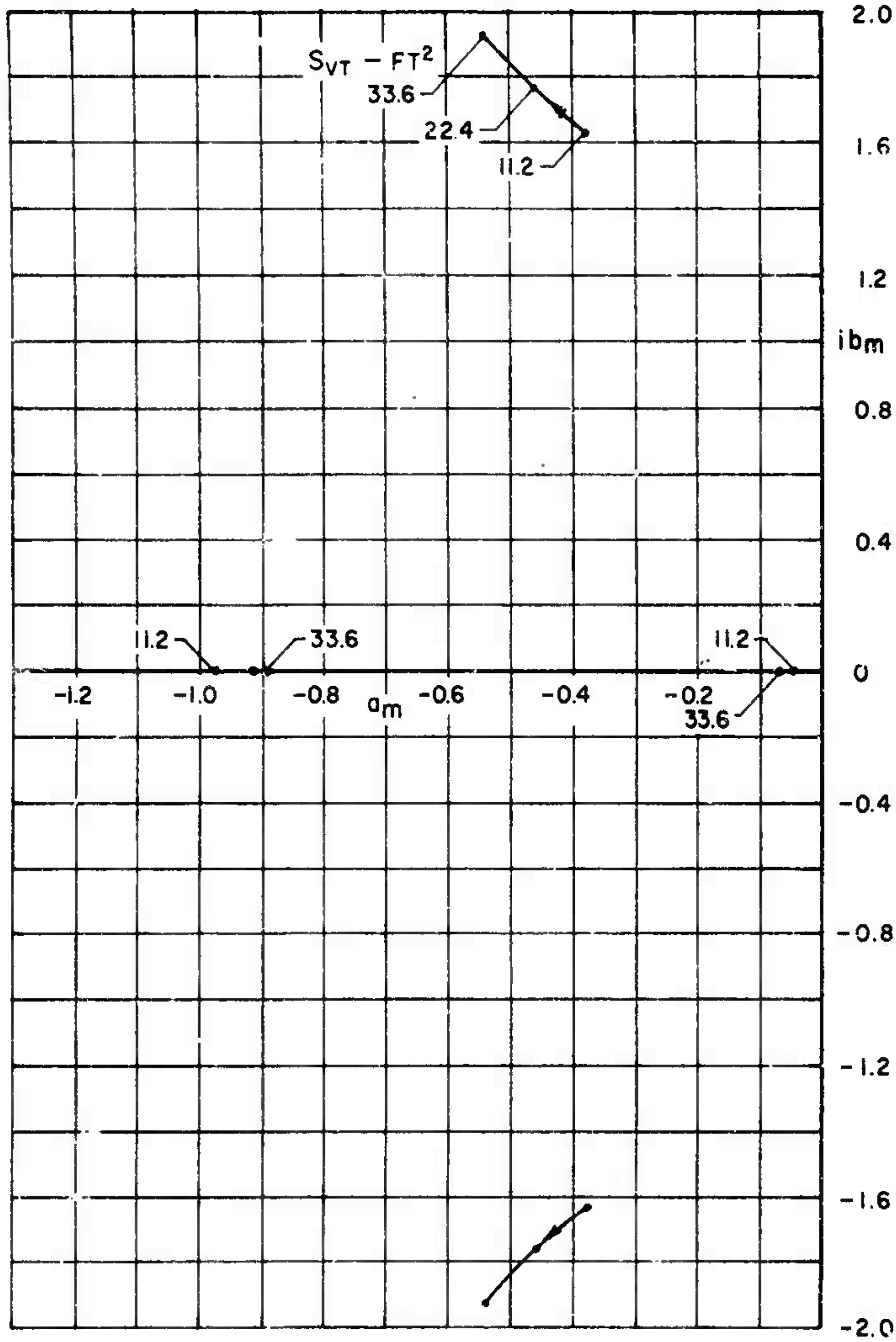

Figure 27. Effect of Vertical Tailplane Area on Lateral Characteristic Roots.

SECTION 10. CORRELATION OF THEORY WITH FLIGHT TEST DATA

In order to appraise the accuracy and applicability of the theoretical methods and procedures presented in this handbook, a comparison between computed stability response data and the corresponding flight test data is presented in this section for three different compound helicopters, each operating at three different flight speeds.

The computation of compound helicopter response to control inputs or externally applied disturbances involving more than three degrees of freedom of aircraft motion is most conveniently performed using an analog computer program. The analog computer is most convenient for preliminary design work because the responses are generated on a real time basis. This enables the dynamic stability characteristics to be immediately assessed, and appropriate adjustments can be made to the stability augmentation system design parameters to optimize the response characteristics with a minimum amount of effort.

Presented in this section are typical computations performed using a Pace 221 R analog computer of the response due to pulsed control inputs for the three compound helicopters under consideration. The computations include six degrees of freedom of aircraft motion and three degrees of freedom of stability augmentation system. The input forcing functions, which are programmed to be activated independently or simultaneously are the pilot's longitudinal cyclic stick, the lateral cyclic stick, and the rudder pedals.

10.1 DYNAMIC STABILITY RESPONSES OF A TEETERING ROTOR COMPOUND HELICOPTER

10.1.1 Description of the Sample Compound Helicopter

The sample teetering rotor compound helicopter considered is the high-speed research vehicle illustrated in Figure 1 of Section 9. This aircraft was developed from a medium utility-type helicopter by the addition of wings, a horizontal tailplane, and two auxiliary jet engines mounted at the wing tips. Both the main and tail rotors have two blades each and teetering type hubs. Although no electronic or mechanical stabilization device is employed on this aircraft, it does have conventional aircraft controls to improve the high-speed handling qualities. These controls are linked with the helicopter controls and are used in the speed range between 140 and 160 knots. A summary of the pertinent design parameters is presented in Table I.

TABLE I

DESIGN PARAMETERS FOR TEETERING ROTOR COMPOUND HELICOPTER

Main Rotor	Tail Rotor	Fuselage	Auxiliary Jets
$\theta_{1_F} = -1.83^\circ$	$\theta_{1_{TR}} = 0^\circ$	$W = 9000$ lb	$n = 2$
$a_F = 5.73$	$a_{TR} = 5.73$	$A_{X_{FUS}} = 48$ ft^2	$i_P = 9^\circ$ @ 100Kn 4° @ 150Kn 4° @ 200Kn
$i_F = -2.57^\circ$	$i_{TR} = 0^\circ$	$A_{Y_{FUS}} = 183.1$ ft^2	
$b_F = 2$	$b_{TR} = 2$	$A_{Z_{FUS}} = 181.9$ ft^2	$A_{ii} = 2$ ft^2
$R_F = 22$ ft	$R_{TR} = 4.25$ ft	$\ell_{FUS} = 37$ ft	$R_{ii} = 0.80$ ft
$e_F = 0$	$e_{TR} = 0$		$\ell_{X_P} = 0.071$ ft
$\sigma_F = 0.0506$	$\sigma_{TR} = 0.105$		$\ell_{Y_P} = \pm 8.66$ ft
$\gamma_F = 5.60$	$\gamma_{TR} = 2.03$		$\ell_{Z_P} = 0$ ft
$\ell_{X_F} = -0.30$ ft	$\ell_{X_{TR}} = -27.05$ ft		
$\ell_{Y_F} = 0$	$\ell_{Y_{TR}} = -1.26$ ft		
$\ell_{Z_F} = -6.78$ ft	$\ell_{Z_{TR}} = -5.33$ ft		
$I_{b_F} = 998$ slug-ft^2	$I_{b_{TR}} = 1.53$ slug-ft^2		

TABLE I - Concluded

Wing	Horizontal Tail	Vertical Tail
$a_W = 3.95$	$a_T = 2.87$	$a_{VT} = 1.30$
$i_W = 6^\circ$ @ 100Kn 3° @ 150Kn 2° @ 200Kn	$i_T = -1.7^\circ$	$i_{VT} = 1^\circ$
$(AR)_W = 4.9$	$(AR)_T = 3.15$	$(AR)_{VT} = 1.9$
$S_W = 78.4$ ft^2	$S_T = 40$ ft^2	$S_{VT} = 22.4$ ft^2
$\ell_{X_W} = 0.071$ ft	$\ell_{X_T} = -17.15$ ft	$\ell_{X_{VT}} = -25.53$ ft
$\ell_{Y_W} = \pm 5.58$ ft	$\ell_{Y_T} = 0$	$\ell_{Y_{VT}} = 0$
$\ell_{Z_W} = 0.083$ ft	$\ell_{Z_T} = 0.38$ ft	$\ell_{Z_{VT}} = -3.75$ ft
$b_W = 19.6$ ft	$b_T = 11.2$ ft	$b_{VT} = 6.5$ ft

The operating conditions assumed in the sample calculations correspond to forward speeds of 100, 150, and 200 knots, all at a constant rotor tip speed of ΩR = 746 ft/sec and a pressure altitude corresponding to sea level standard day. The 100- and 150-knot cases were simulated using only conventional helicopter controls, while the 200-knot case airplane-type controls fully integrated with the helicopter controls were used.

10.1.2 Analog Computer Program

The analog computer program for the sample compound helicopter was developed using the total stability derivatives presented in Tables II, III, and IV. These derivatives were obtained using the design parameters given in Subsection 10.1.1 and the stability data presented in Section 1. The analog computer schematic diagram representing the equations of motion for this aircraft is shown in Figure 1. The settings of potentiometers P and Q shown in Figure 1 are given in Tables V, VI, and VII for the three selected speed conditions. These settings were obtained by first normalizing the total derivatives in Tables II, III, and IV by the coefficient of the highest order variable (e.g., the X equation was divided by $X_{\dot{u}}$, the M equation was divided by $M_{\ddot{\theta}}$, etc) and then by multiplying the normalized derivatives by appropriate scaling factors to prevent any of the amplifiers from exceeding their maximum operating voltage.

10.1.3 Stability Responses of the Teetering Rotor Compound Helicopter

The time history traces of the responses of the selected teetering rotor compound helicopter to pulse inputs of the longitudinal and lateral cyclic controls B_{1_C} and A_{1_C} respectively, and the rudder pedal control δ_{r_C} are shown in Figures 2 through 10 for the three flight speeds considered.

Figures 2, 3, and 4 present the aircraft responses due to pulse inputs of uncoupled longitudinal, lateral, and directional controls, respectively, at a forward speed of 100 knots. Similar data are presented in Figures 5, 6, and 7 for a forward speed of 150 knots and in Figures 8, 9, and 10 for the 200-knot flight condition. Superimposed on these figures are the corresponding flight test data (denoted as dots) which were obtained from the unpublished data supplied by USAAVLABS for the purpose of correlation.

TABLE II

TOTAL STABILITY DERIVATIVES FOR THE TEETERING ROTOR COMPOUND HELICOPTER AT 100 KNOTS

Var. \ Eq.	X	Y	Z	M	N	L
θ	-8990.	0	-418.50	0	0	0
$\dot{\theta}$	-1432.	-224.57	46974.	-12404.	8342.	-1519.
$\ddot{\theta}$	0	0	0	-14202.	0	0
ϕ	0	9000.	0	0	0	0
$\dot{\phi}$	-235.00	1383.	-6.214	1558.	-2663.	-5333.
$\ddot{\phi}$	0	0	0	0	0	-6362.
ψ	0	418.50	0	0	0	0
$\dot{\psi}$	-3.386	-46711.	6.041	217.05	-13158.	2334.
$\ddot{\psi}$	0	0	0	0	-15560.	0
u	-7.225	0.539	-58.365	-46.097	-51.111	3.400
$\dot{u}$	-279.50	0	0	0	0	0
v	-0.239	-46.009	-0.242	-1.990	387.22	-96.495
$\dot{v}$	0	-279.50	0	0	0	0
w	-35.327	1.001	-235.34	99.414	65.216	6.885
$\dot{w}$	0.019	0	-279.022	8.293	0	-0.004
A_1	1.041	7723.	-22.358	-13.678	-2286.	52388.
B_1	14501.	-169.09	27037.	-90357.	-11015.	-1147
δ_r	-116.12	5695.	44.686	1941.	-154221.	30316.

TABLE III

TOTAL STABILITY DERIVATIVES FOR THE TEETERING ROTOR COMPOUND HELICOPTER AT 150 KNOTS

Eq. / Var.	X	Y	Z	M	N	L
θ	-8974.	0	-683.10	0	0	0
$\dot{\theta}$	-4737.	-167.97	70330.	-15000.	10898.	-1135.
$\ddot{\theta}$	0	0	0	-14202.	0	0
ϕ	0	9000.	0	0	0	0
$\dot{\phi}$	-178.95	4721.	-13.355	1128.	-4836.	-4196.
$\ddot{\phi}$	0	0	0	0	0	-6362.
ψ	0	683.10	0	0	0	0
$\dot{\psi}$	-44.397	-70160.	19.263	743.79	-17169.	2988.
$\ddot{\psi}$	0	0	0	0	-15560.	0
u	-11.373	1.754	-70.054	-118.32	-54.415	12.096
$\dot{u}$	-279.50	0	0	0	0	0
v	0.853	-65.458	-0.668	-20.203	494.31	-128.19
$\dot{v}$	0	-279.50	0	0	0	0
w	0.567	2.537	-276.58	-76.980	-349.25	17.308
$\dot{w}$	-0.015	0	-278.60	15.528	0	-0.006
A_1	-18.892	5832.	248.18	201.60	-1726.	39555.
B_1	13806.	-642.71	42118.	-81180.	88483.	-4359.
δ_r	-337.80	7267.	229.98	7847.	-197021.	38465.

TABLE IV

TOTAL STABILITY DERIVATIVES FOR THE TEETERING ROTOR COMPOUND HELICOPTER AT 200 KNOTS

Eq. / Var.	X	Y	Z	M	N	L
θ	-8999.	0	-126.00	0	0	0
$\dot{\theta}$	-538.40	-215.67	93498.	-19274.	22952.	-1445.
$\ddot{\theta}$	0	0	0	-14202.	0	0
ϕ	0	9000.	0	0	0	0
$\dot{\phi}$	-246.07	534.59	23.837	1574.	-12908.	-9359.
$\ddot{\phi}$	0	0	0	0	0	-6362.
ψ	0	126.00	0	0	0	0
$\dot{\psi}$	-10.986	-93631.	26.555	577.93	-20946.	3849.
$\ddot{\psi}$	0	0	0	0	-15560.	0
u	-12.205	2.957	-11.756	-64.226	-42.971	-2.645
$\dot{u}$	-279.50	0	0	0	0	0
v	0.011	-83.365	-0.640	-18.147	557.42	-149.61
$\dot{v}$	0	-279.50	0	0	0	0
w	-6.456	-9.037	-220.86	-164.77	183.29	-54.018
$\dot{w}$	0	0	-278.97	0	0	0
A_1	0.570	7421.	-40.695	-15.910	-2197.	50337.
B_1	10083	3053.	23701.	-61379.	-61445.	20706.
δ_r	-141.41	8056.	249.72	7305.	-218133.	42650.

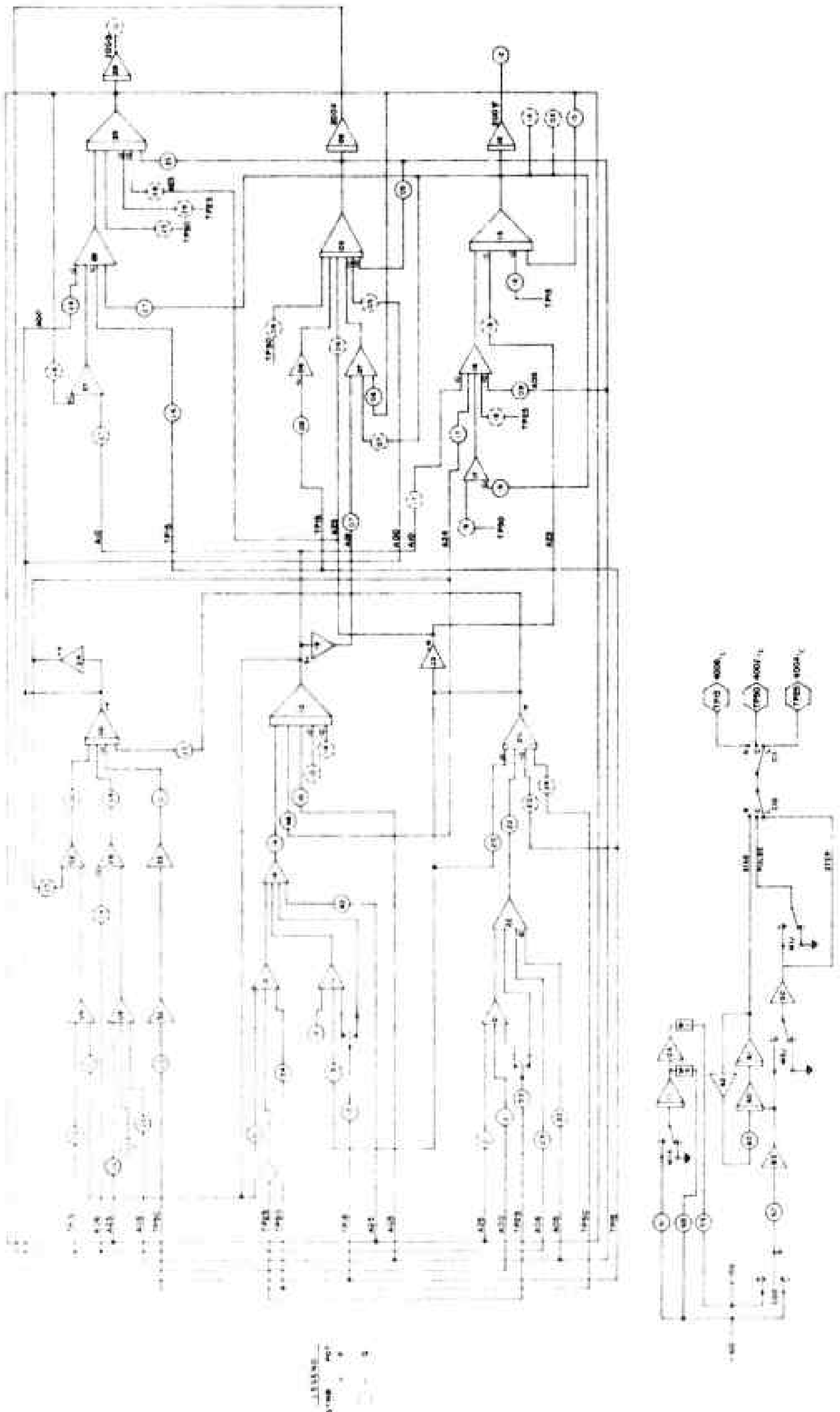

Figure 1. Analog Computer Schematic for the Sample Teetering Rotor Compound Helicopter.

TABLE V

ANALOG COMPUTER POTENTIOMETER SETTINGS FOR THE TEETERING ROTOR COMPOUND HELICOPTER AT 100 KNOTS

Pot. No.	Setting	Pot. No.	Setting	Pot. No.	Setting	Pot. No.	Setting
P00	0.7782	P10	0.0805	P20	0.0242	Q50	—
Q00	0.0010	Q10	0.0201	Q20	0.8434	Q51	0.1975
P01	0.0010	P11	—	P21	0.0003	Q52	—
Q01	0.1000	Q11	0.4145	Q21	0.6275	Q53	0.0006
P02	0.1667	P12	0.1000	P22	0.2525	Q54	0.3056
Q02	0.0252	Q12	0.0449	Q22	0.3333	Q55	—
P03	0.0004	P13	0.0215	P23	0.1551	Q56	—
Q03	0.1537	Q13	0.0091	Q23	0.1264	Q57	—
P04	0.0965	P14	0.4178	P24	0.0004	Q58	—
Q04	0.1667	Q14	0.8333	Q24	0.0225	Q59	0.2000
P05	0.0648	P15	—	P25	0.2382	Q60	1.0000
Q05	0.0873	Q15	0.1711	Q25	0.2387	Q61	0.1000
P06	0.1400	P16	0.4956	P26	0.0838	Q62	—
Q06	0.1097	Q16	—	Q26	0.0090	Q63	0.1485
P07	0.0153	P17	0.0995	P27	0.6064	Q64	—
Q07	0.0056	Q17	0.6560	Q27	0.3668	Q65	—
P08	—	P18	0.0073	P28	0.0216	Q66	—
Q08	0.3181	Q18	0.0354	Q28	0.0106	Q67	0.1000
P09	0.0683	P19	0.0838	P29	0.4117	Q68	0.0096
Q09	0.0536	Q19	0.0846	Q29	—	Q69	0.1000

TABLE VI

ANALOG COMPUTER POTENTIOMETER SETTINGS FOR THE TEETERING ROTOR COMPOUND HELICOPTER AT 150 KNOTS

Pot. No.	Setting	Pot. No.	Setting	Pot. No.	Setting	Pot. No.	Setting
P00	0.7409	P10	0.0805	P20	0.3779	Q50	—
Q00	0.0030	Q10	0.0150	Q20	0.9927	Q51	0.2810
P01	0.0037	P11	—	P21	0.0007	Q52	—
Q01	0.1000	Q11	0.3130	Q21	0.7543	Q53	0.0067
P02	0.1667	P12	0.1000	P22	0.3787	Q54	0.3900
Q02	0.0192	Q12	0.0733	Q22	0.3333	Q55	—
P03	0.0048	P13	0.0544	P23	0.2441	Q56	—
Q03	0.5084	Q13	0.0345	Q23	0.0020	Q57	—
P04	0.0963	P14	0.6275	P24	0.0021	Q58	—
Q04	0.1667	Q14	0.8333	Q24	0.0368	Q59	0.2000
P05	0.1666	P15	—	P25	0.3023	Q60	1.0000
Q05	0.1056	Q15	0.3108	Q25	0.1784	Q61	0.1000
P06	0.1084	P16	0.6331	P26	0.9659	Q62	—
Q06	0.0794	Q16	—	Q26	0.0343	Q63	0.5068
P07	0.0524	P17	0.1270	P27	0.8056	Q64	—
Q07	0.0568	Q17	0.6980	Q27	0.4696	Q65	—
P08	—	P18	0.0055	P28	0.0544	Q66	—
Q08	0.2858	Q18	0.2843	Q28	0.0380	Q67	0.1000
P09	0.2763	P19	0.4488	P29	0.3109	Q68	0.0314
Q09	0.0700	Q19	0.1103	Q29	—	Q69	0.1000

TABLE VII

ANALOG COMPUTER POTENTIOMETER SETTINGS FOR THE TEETERING ROTOR COMPOUND HELICOPTER AT 200 KNOTS

Pot. No.	Setting	Pot. No.	Setting	Pot. No.	Setting	Pot. No.	Setting
P00	0.5411	P10	0.0805	P20	0.0212	Q50	—
Q00	0.0013	Q10	0.0192	Q20	0.7917	Q51	0.3579
P01	—	P11	—	P21	0.0012	Q52	—
Q01	0.1000	Q11	0.3983	Q21	0.1263	Q53	0.0011
P02	0.1667	P12	0.1000	P22	0.5027	Q54	0.4324
Q02	0.0264	Q12	0.0135	Q22	0.3333	Q55	—
P03	0.0011	P13	0.1938	P23	0.2622	Q56	—
Q03	0.0571	Q13	0.1638	Q23	0.0231	Q57	—
P04	0.0965	P14	0.8374	P24	0.0022	Q58	—
Q04	0.1667	Q14	0.8333	Q24	0.0067	Q59	0.2000
P05	0.0900	P15	0.0001	P25	0.3352	Q60	1.0000
Q05	0.1357	Q15	0.8296	Q25	0.2271	Q61	0.1000
P06	0.2320	P16	0.7009	P26	0.1471	Q62	—
Q06	0.1109	Q16	—	Q26	0.1627	Q63	0.0573
P07	0.0407	P17	0.1432	P27	0.9400	Q64	—
Q07	0.0520	Q17	0.5600	Q27	0.6050	Q65	—
P08	—	P18	0.0071	P28	0.1700	Q66	—
Q08	0.2161	Q18	0.1974	Q28	0.0080	Q67	0.1000
P09	0.2572	P19	0.2360	P29	0.3956	Q68	0.0530
Q09	0.1475	Q19	0.1346	Q29	—	Q69	0.1000

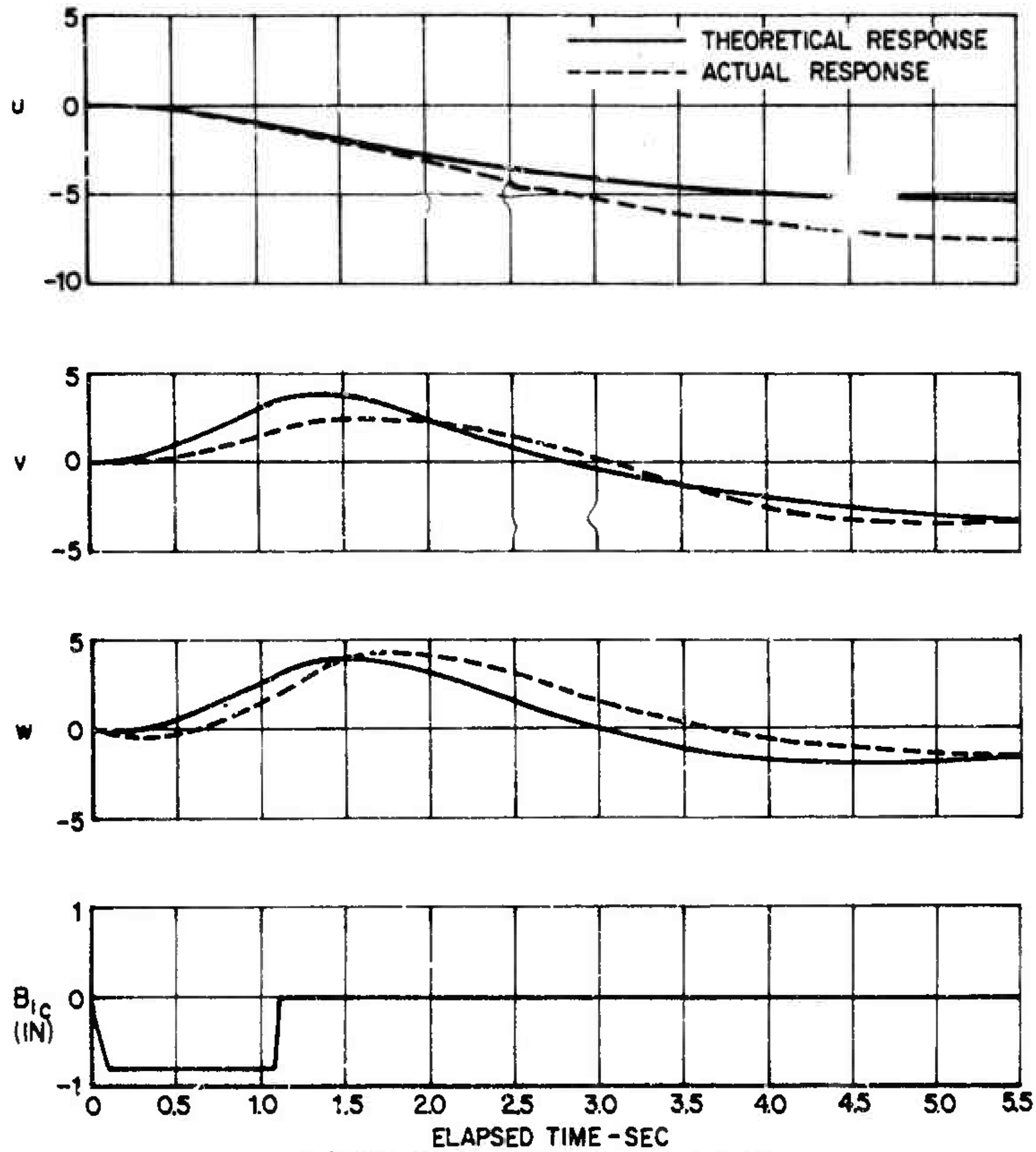

(a) PERTURBATION VELOCITIES, FT/SEC

Figure 2. Response of the Teetering Rotor Compound Helicopter Due to Pulse Input of the Longitudinal Control, $B_{1c} \doteq -0.8"$, V = 100 KTS.

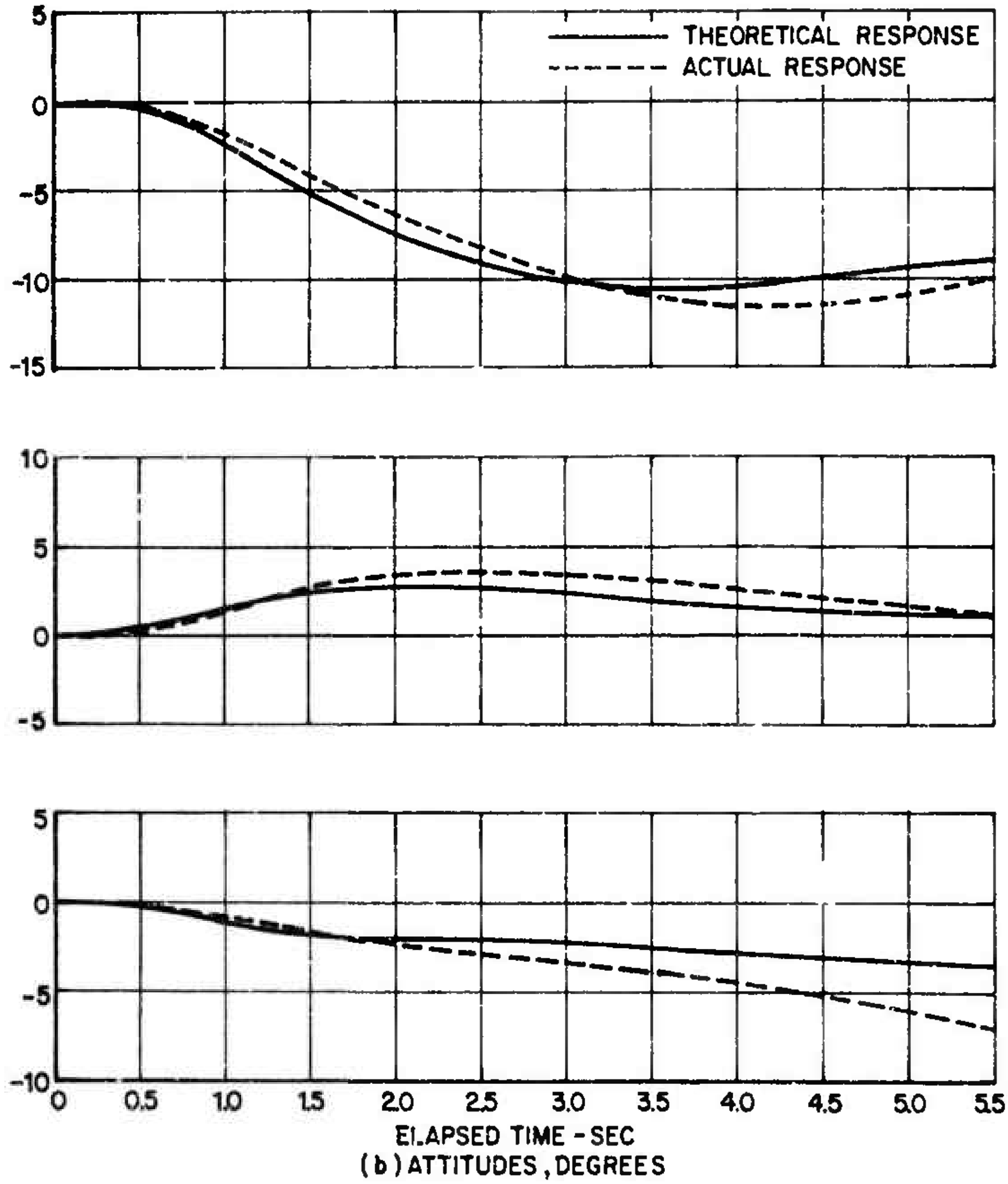

Figure 2. Continued.

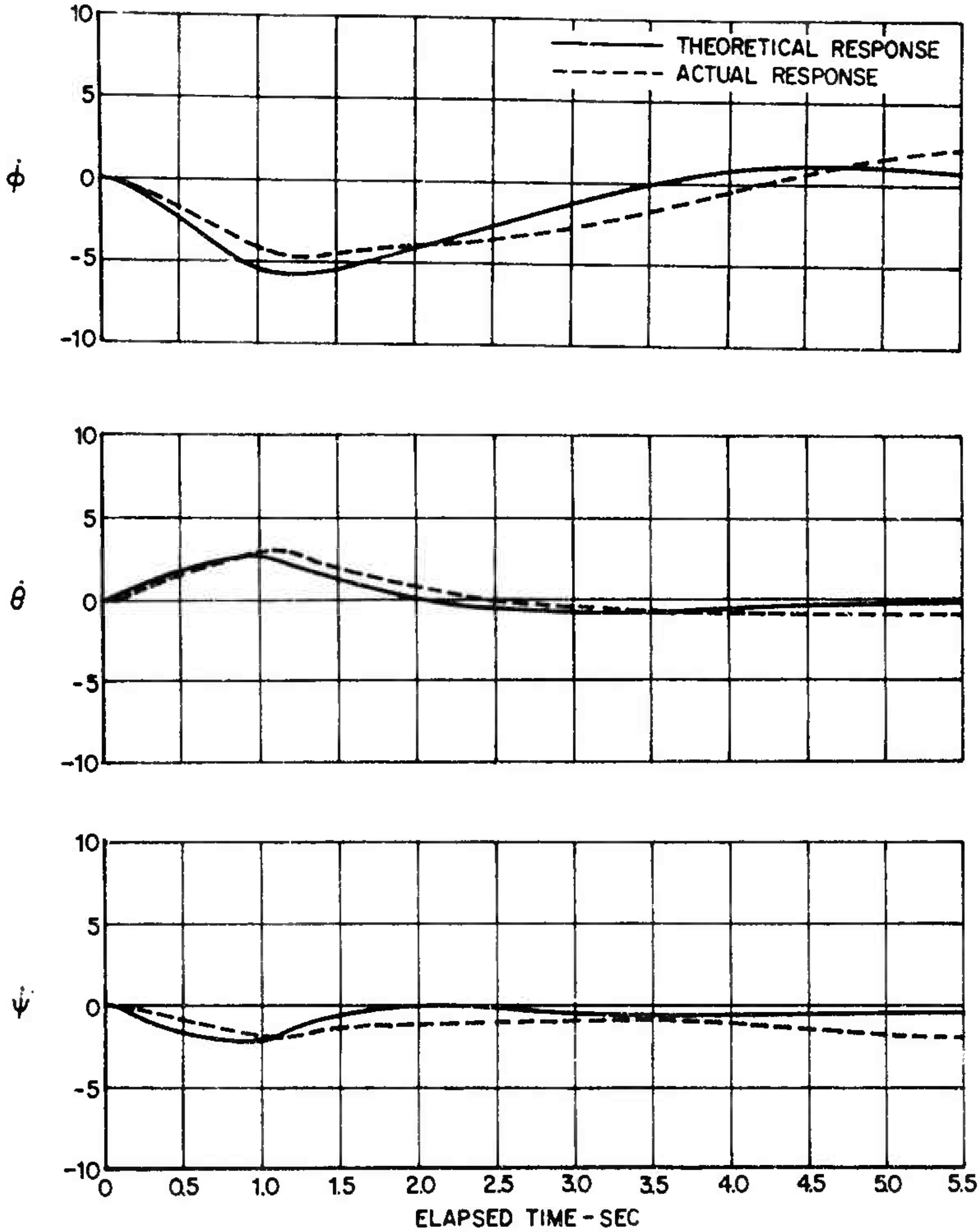

(c) ANGULAR RATES, DEG./SEC

Figure 2. Concluded.

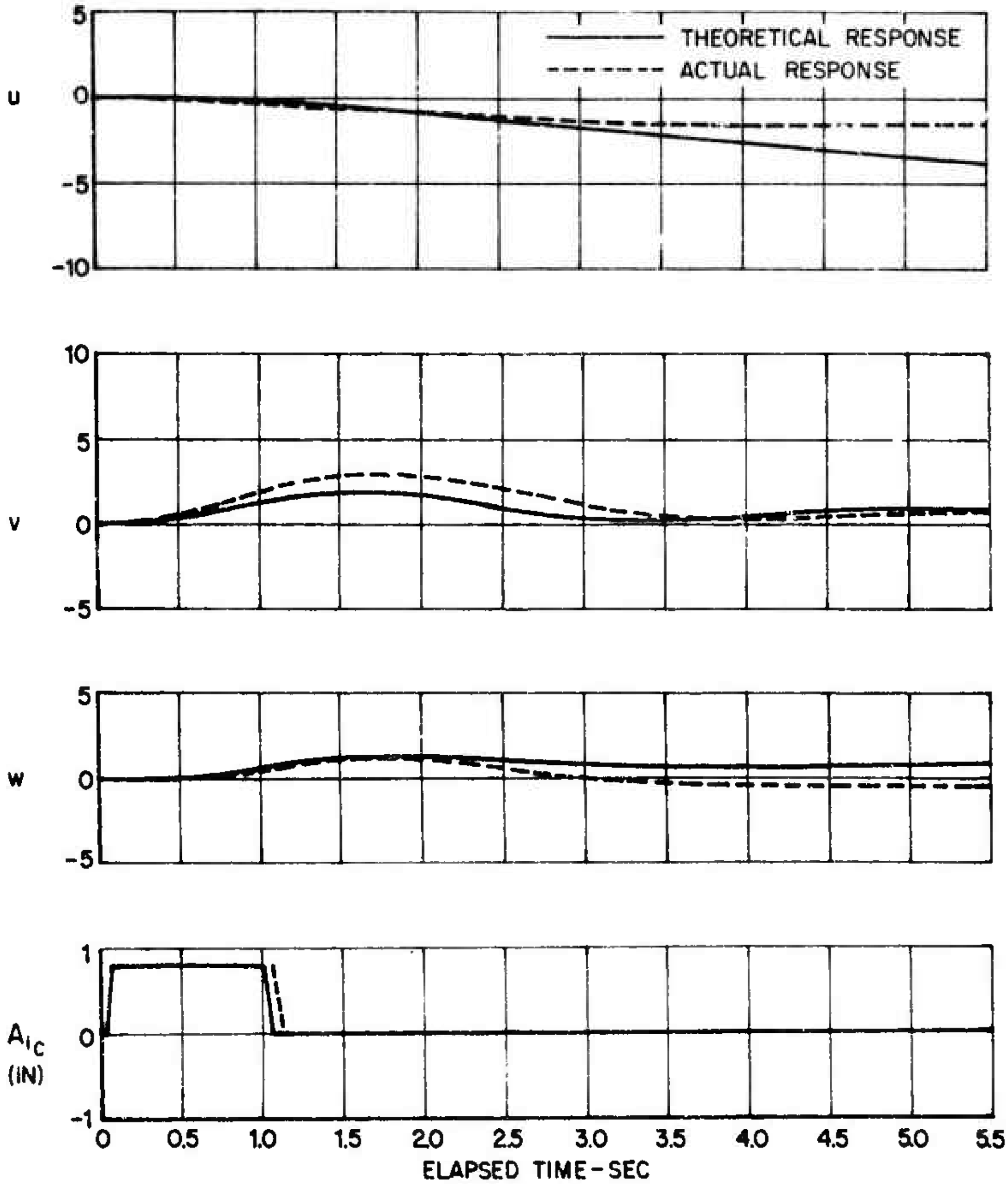

(a) PERTURBATION VELOCITIES, FT/SEC

Figure 3. Response of the Teetering Rotor Compound Helicopter Due to Pulse Input of the Lateral Control, A_{1c} = +0.8", V = 100 KTS.

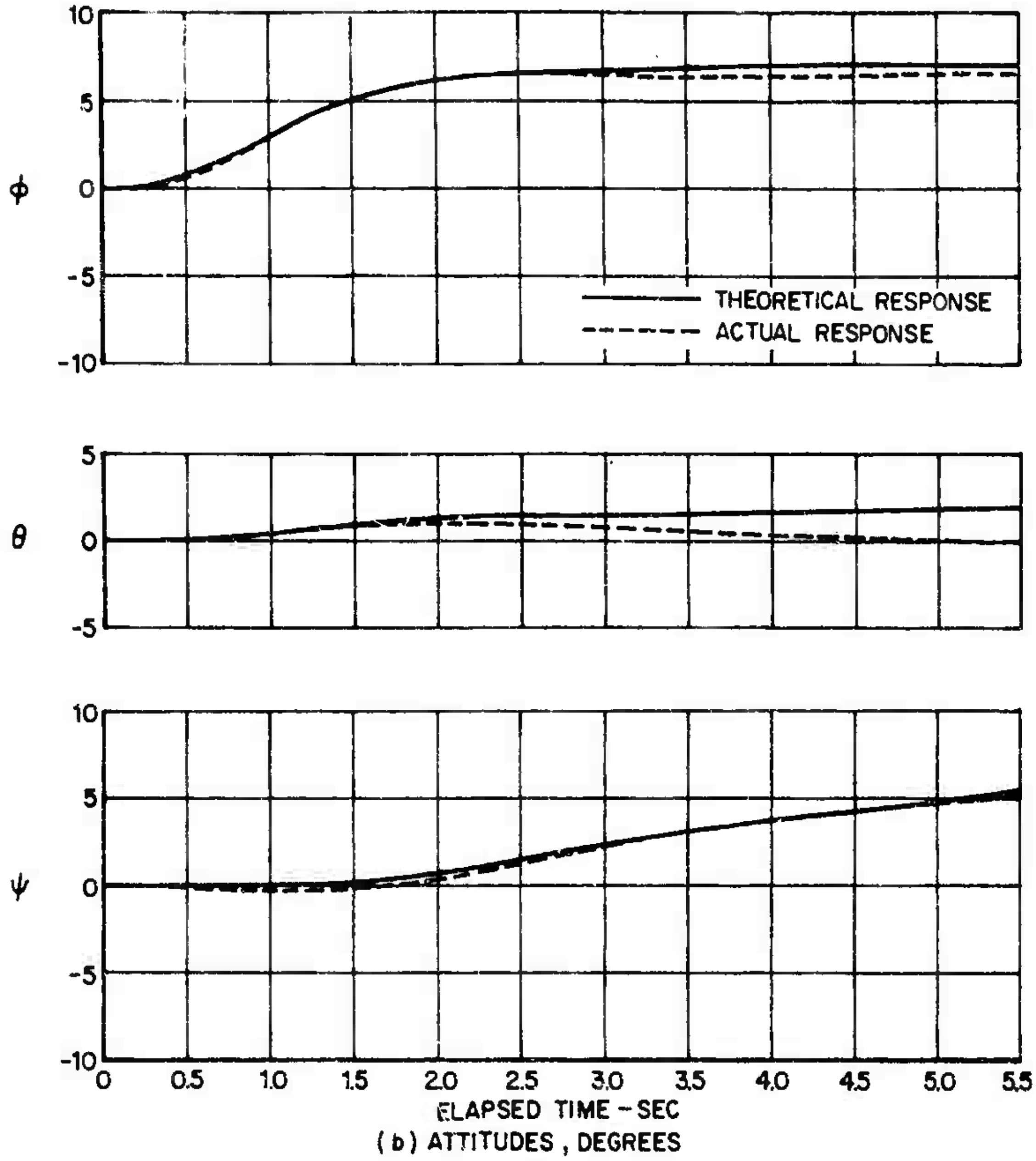

Figure 3. Continued.

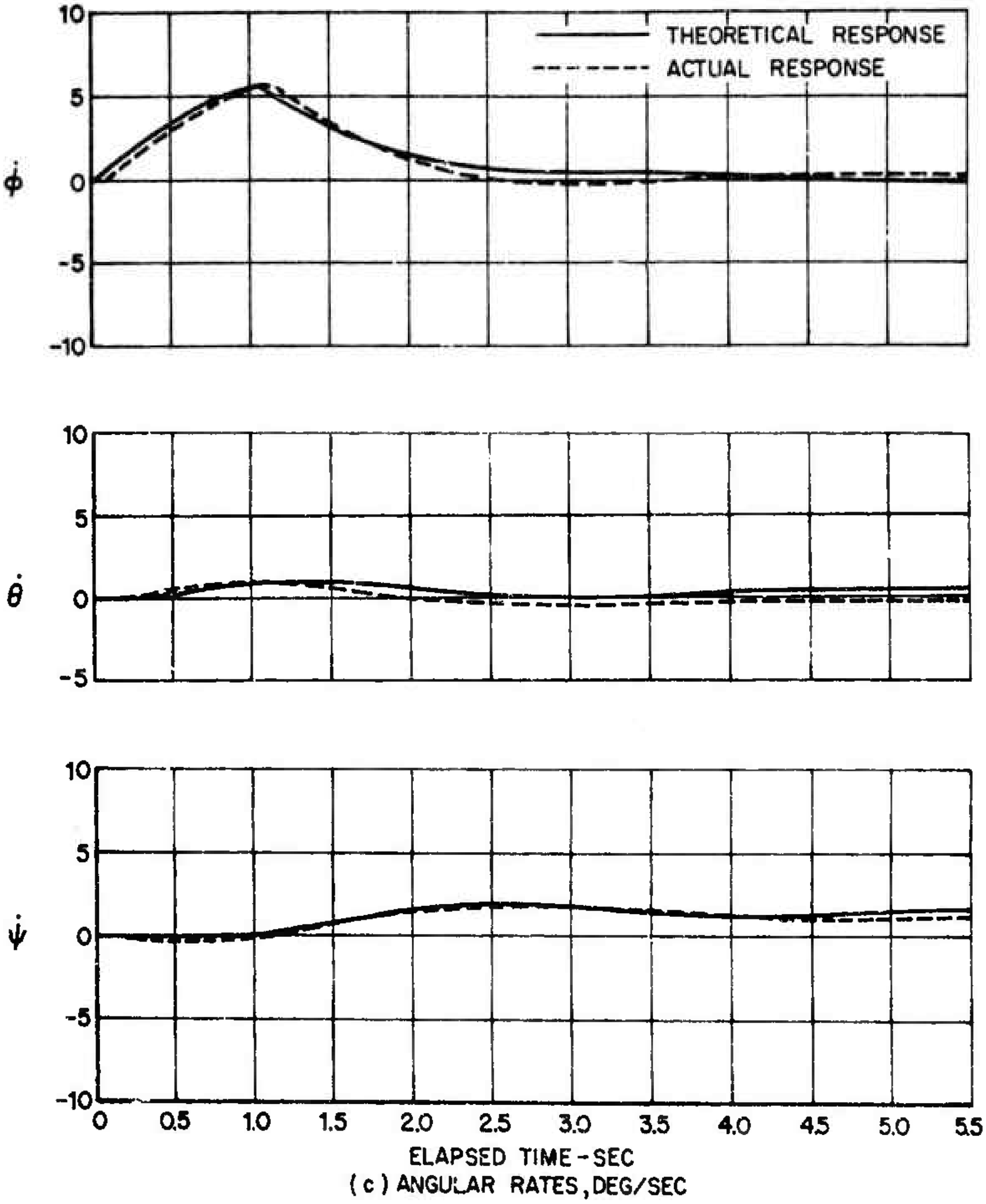

Figure 3. Concluded.

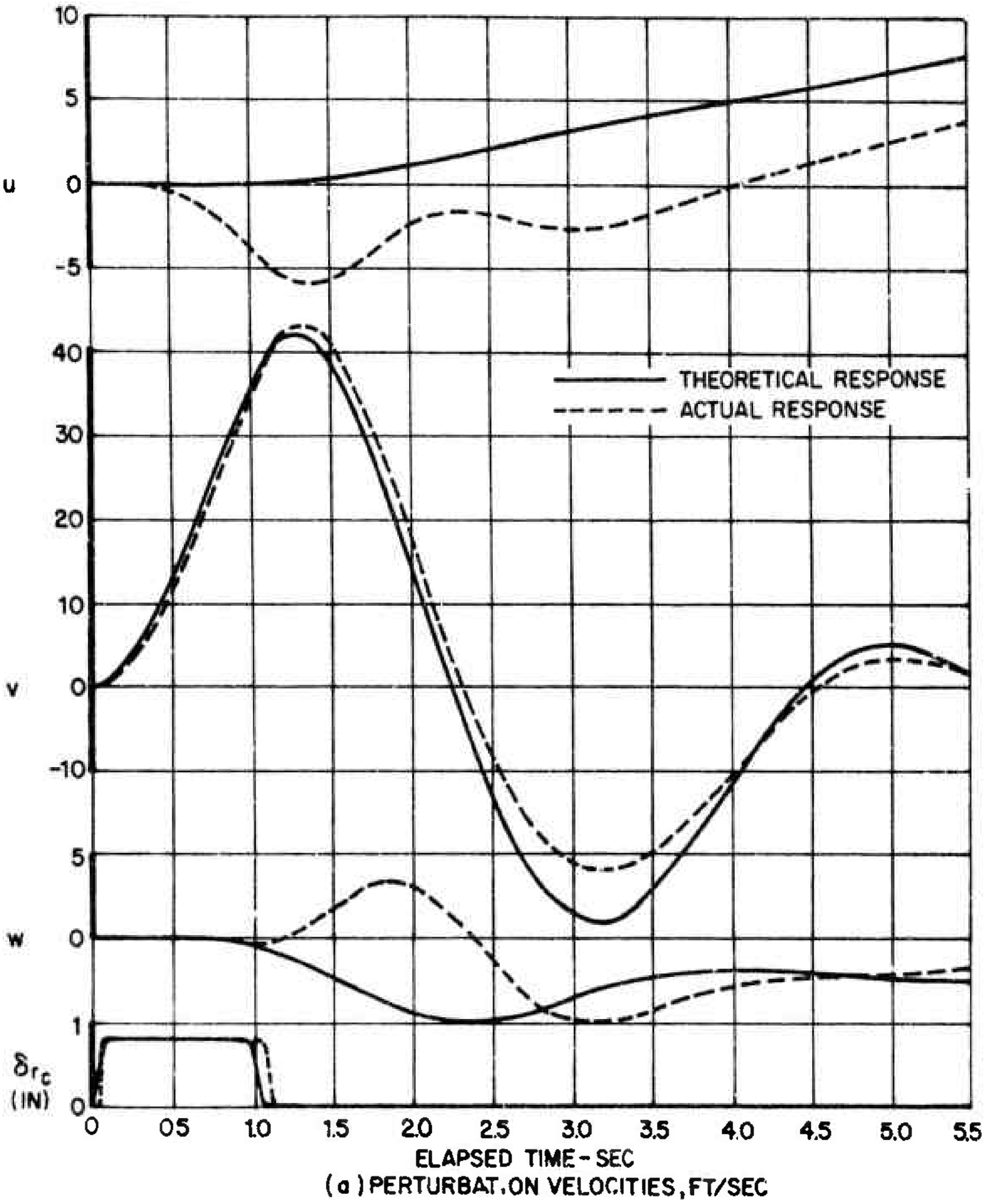

Figure 4. Response of the Teetering Rotor Compound Helicopter Due to Pulse Input of the Directional Control, δ_{r_c} = +0.8', V = 100 KTS.

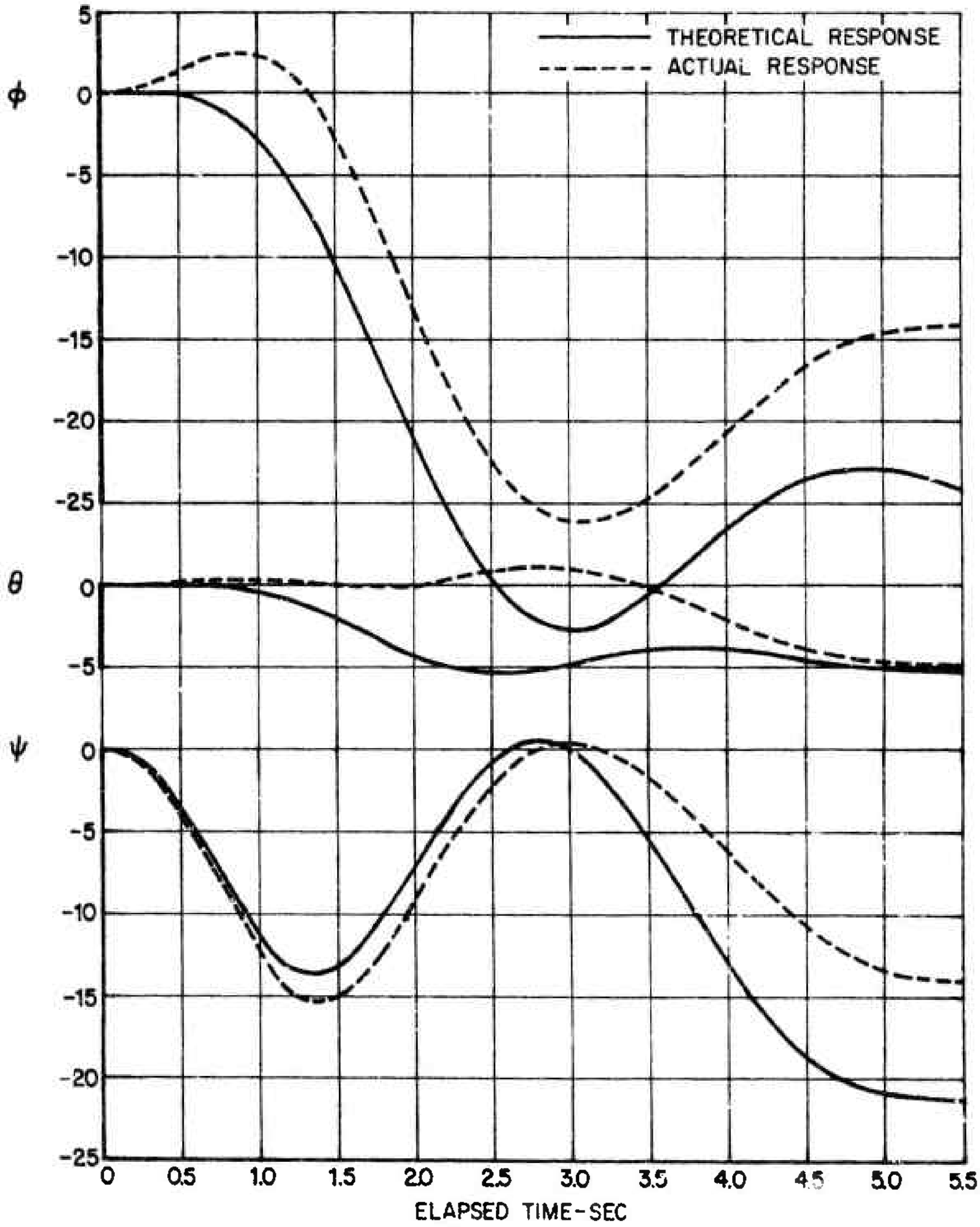

(b) ATTITUDES, DEGREES

Figure 4. Continued.

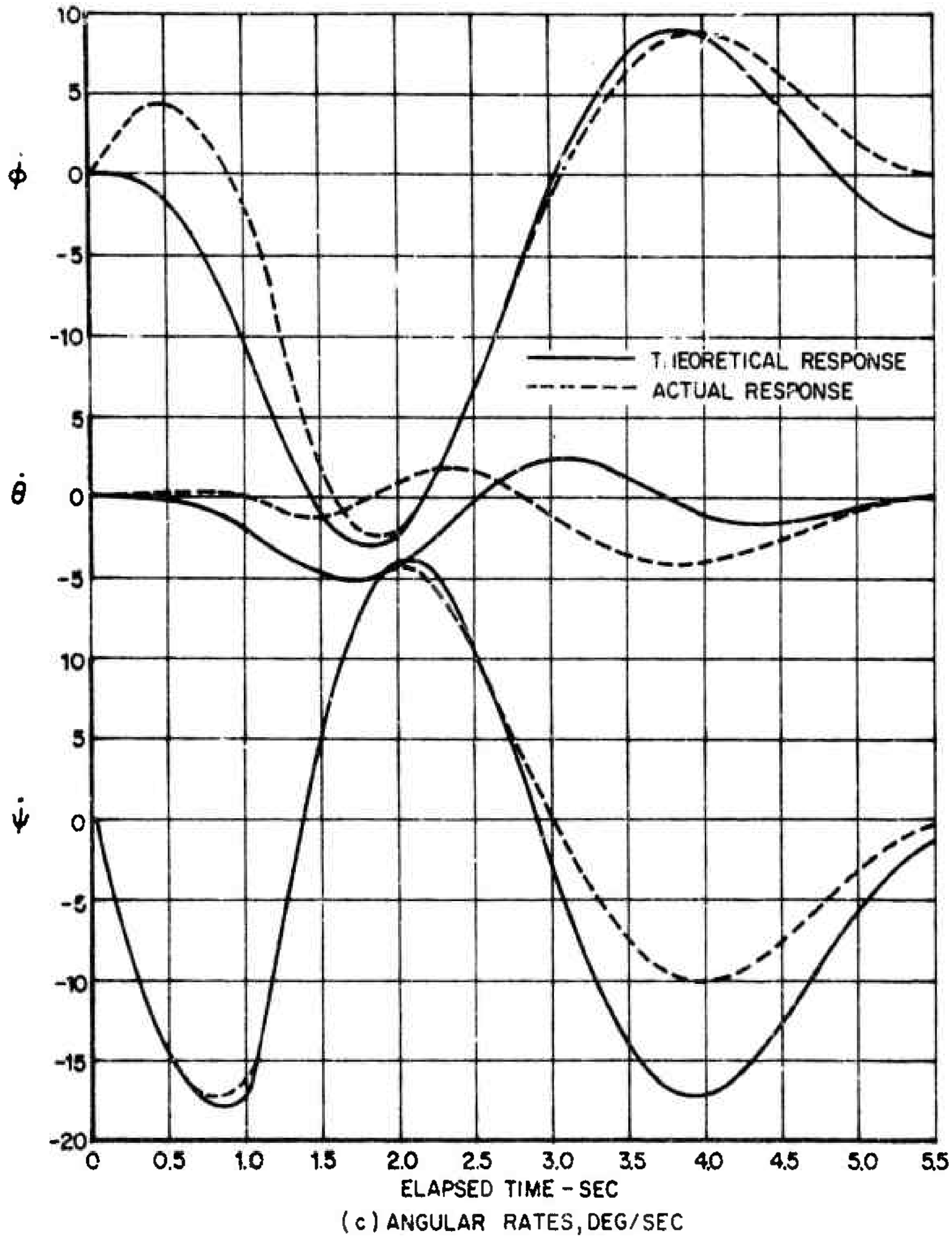

Figure 4. Concluded.

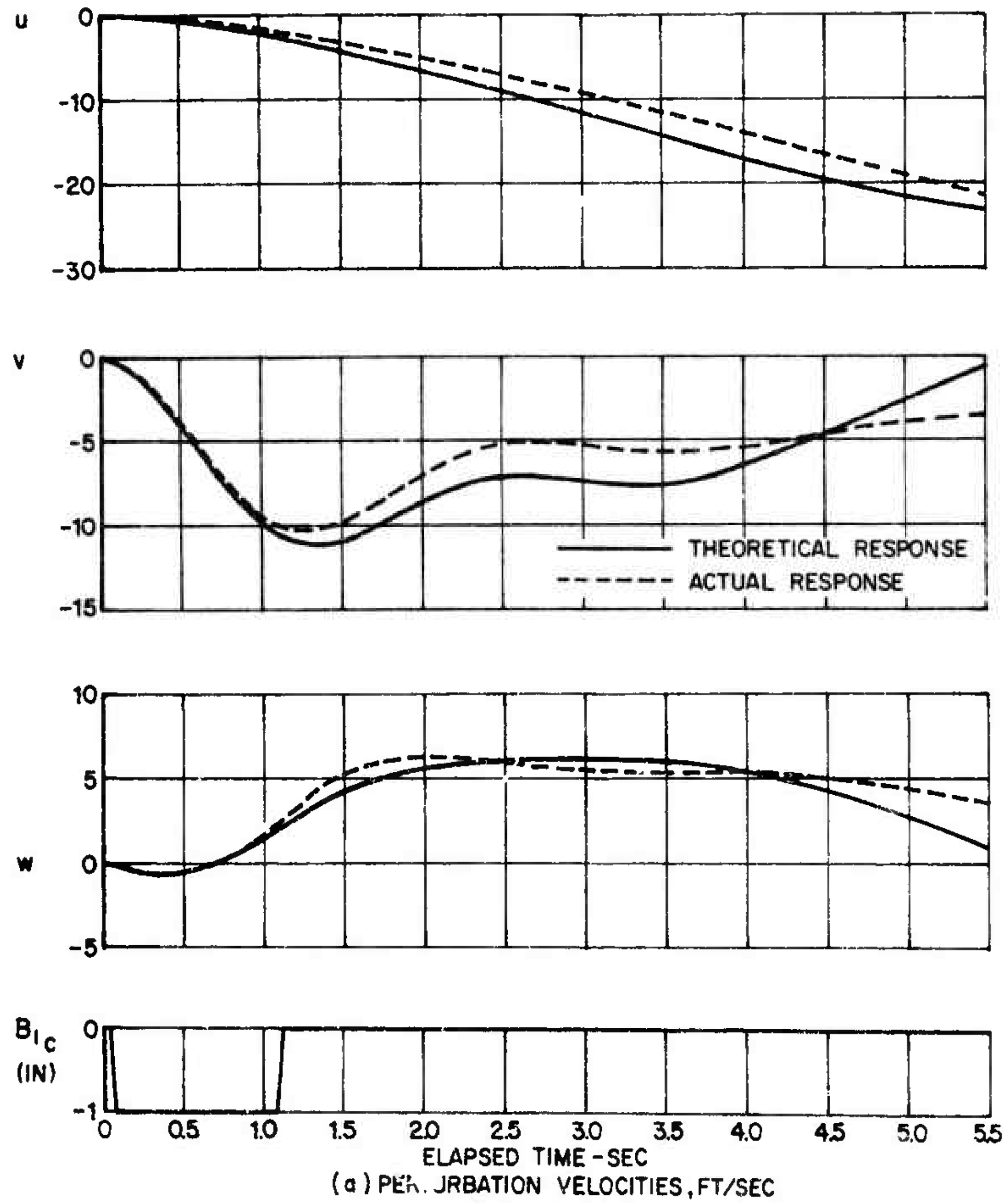

Figure 5. Response of the Teetering Rotor Compound Helicopter Due to Pulse Input of the Longitudinal Control, B_{1_C} = -1", V = 150 KTS.

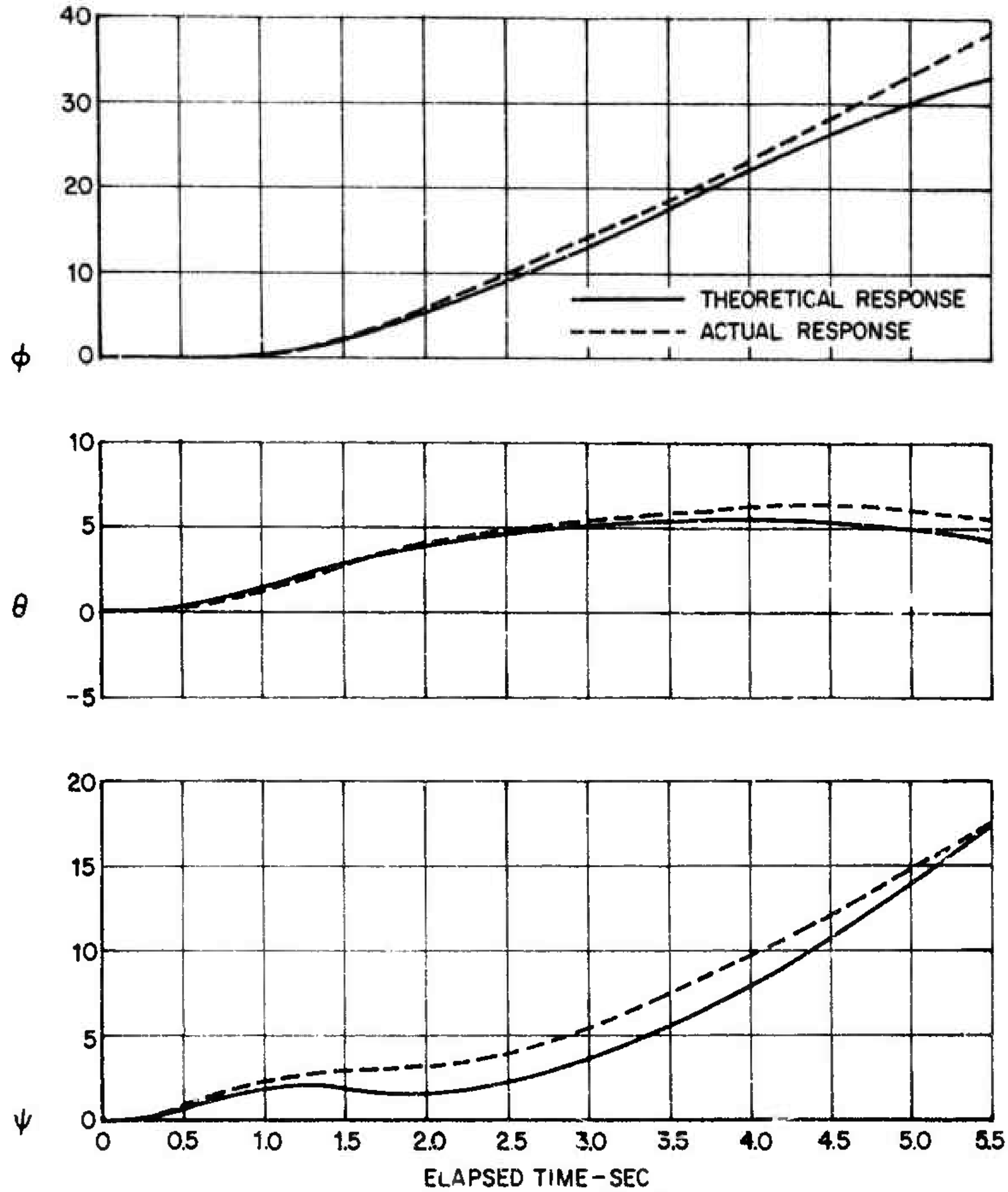

(b) ATTITUDES, DEGREES

Figure 5. Continued.

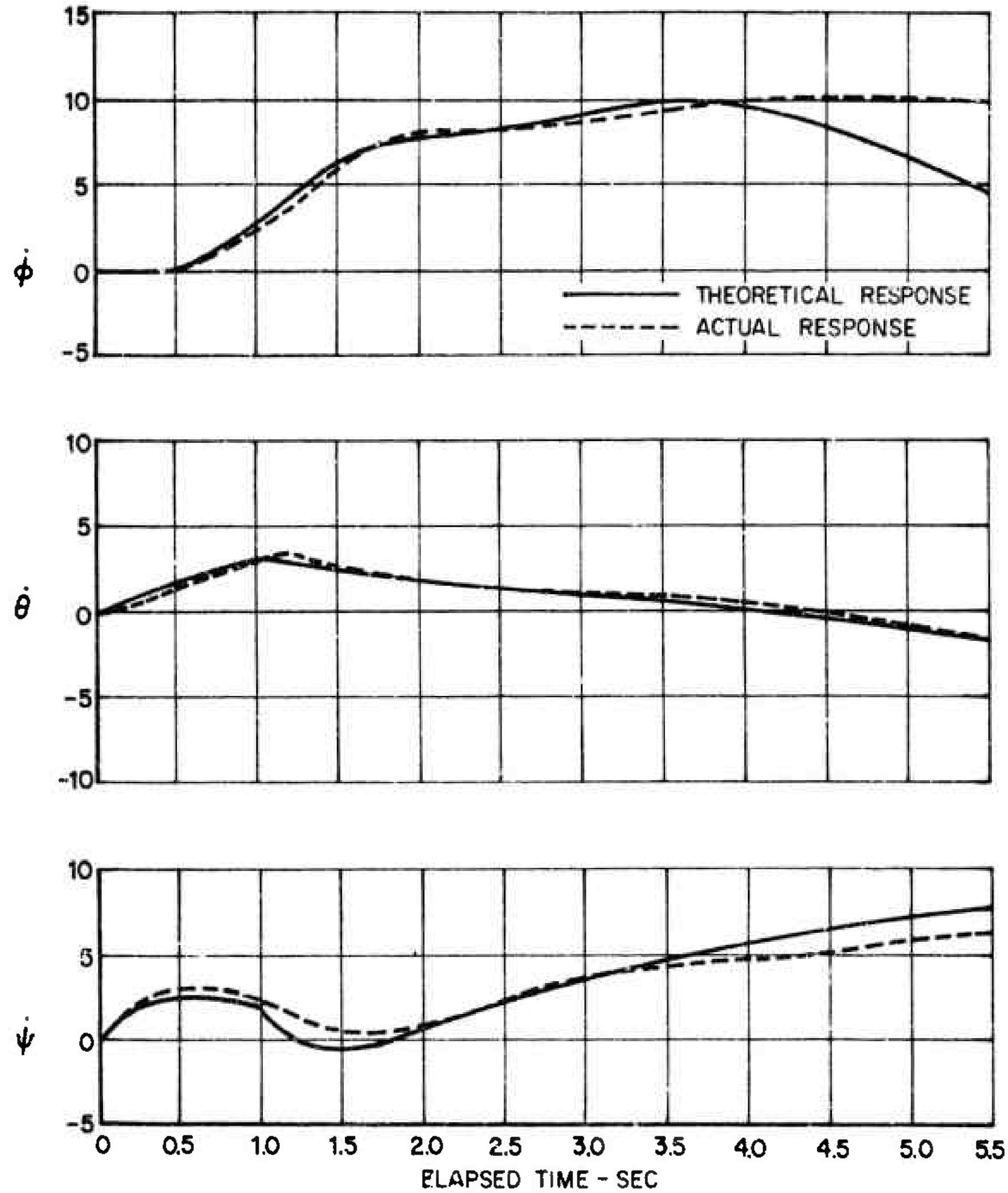

(c) ANGULAR RATES, DEG/SEC

Figure 5. Concluded.

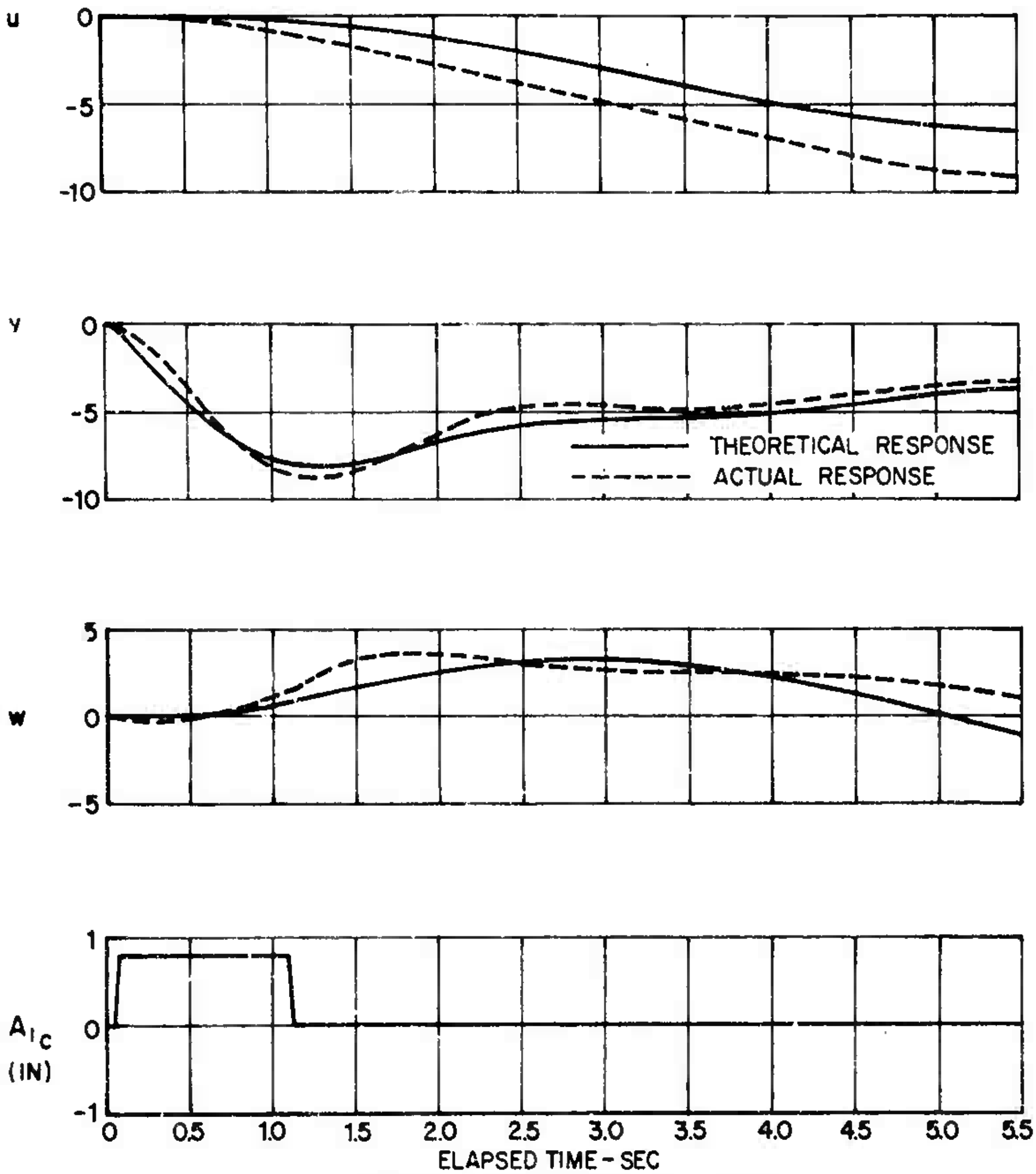

(a) PERTURBATION VELOCITIES, FT/SEC

Figure 6. Response of the Teetering Rotor Compound Helicopter Due to Pulse Input of the Lateral Control. A_{1_C} = +0.8", V = 150 KTS.

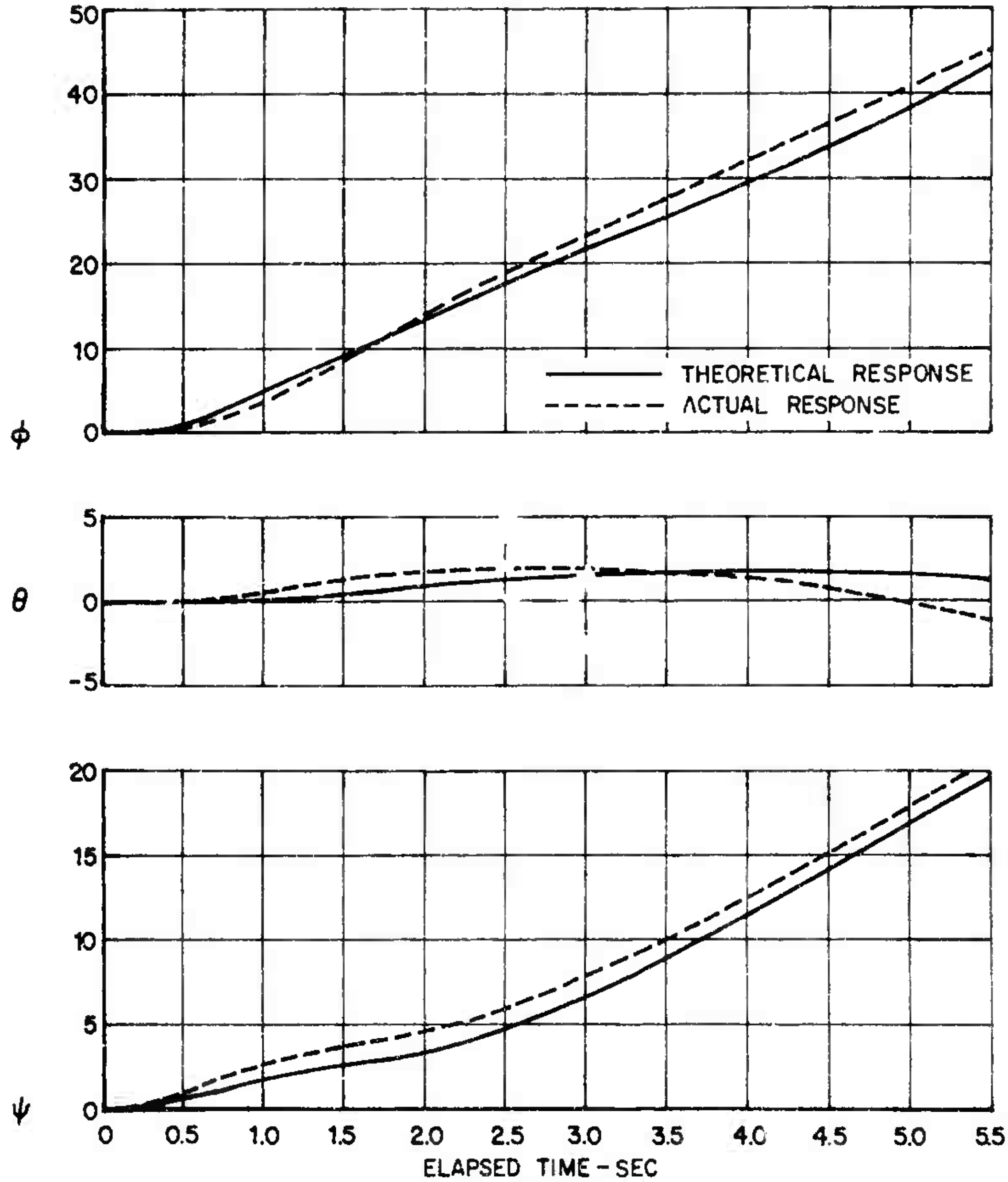

(b) ATTITUDES, DEGREES

Figure 6. Continued.

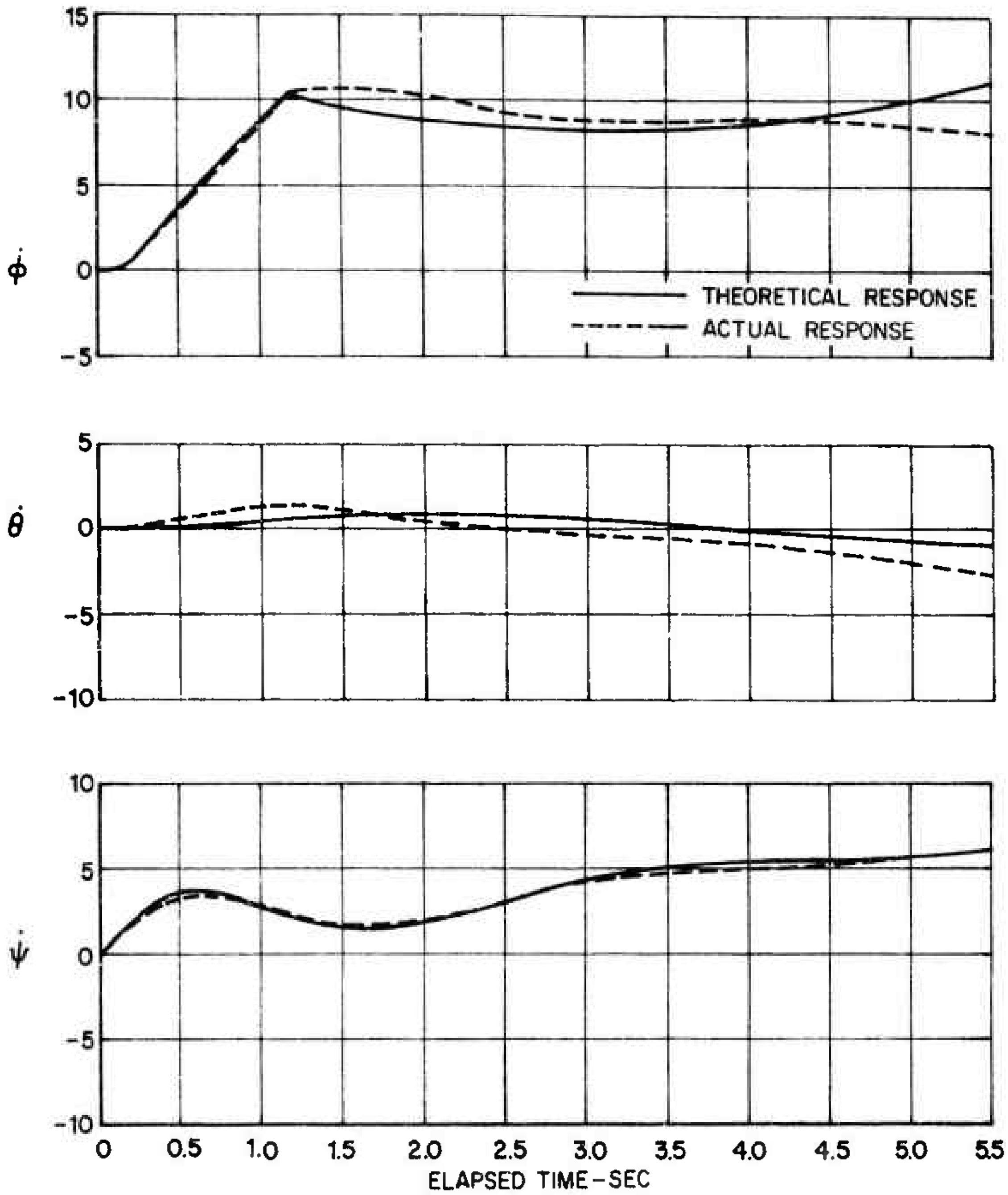

(c) ANGULAR RATES, DEG/SEC

Figure 6. Concluded.

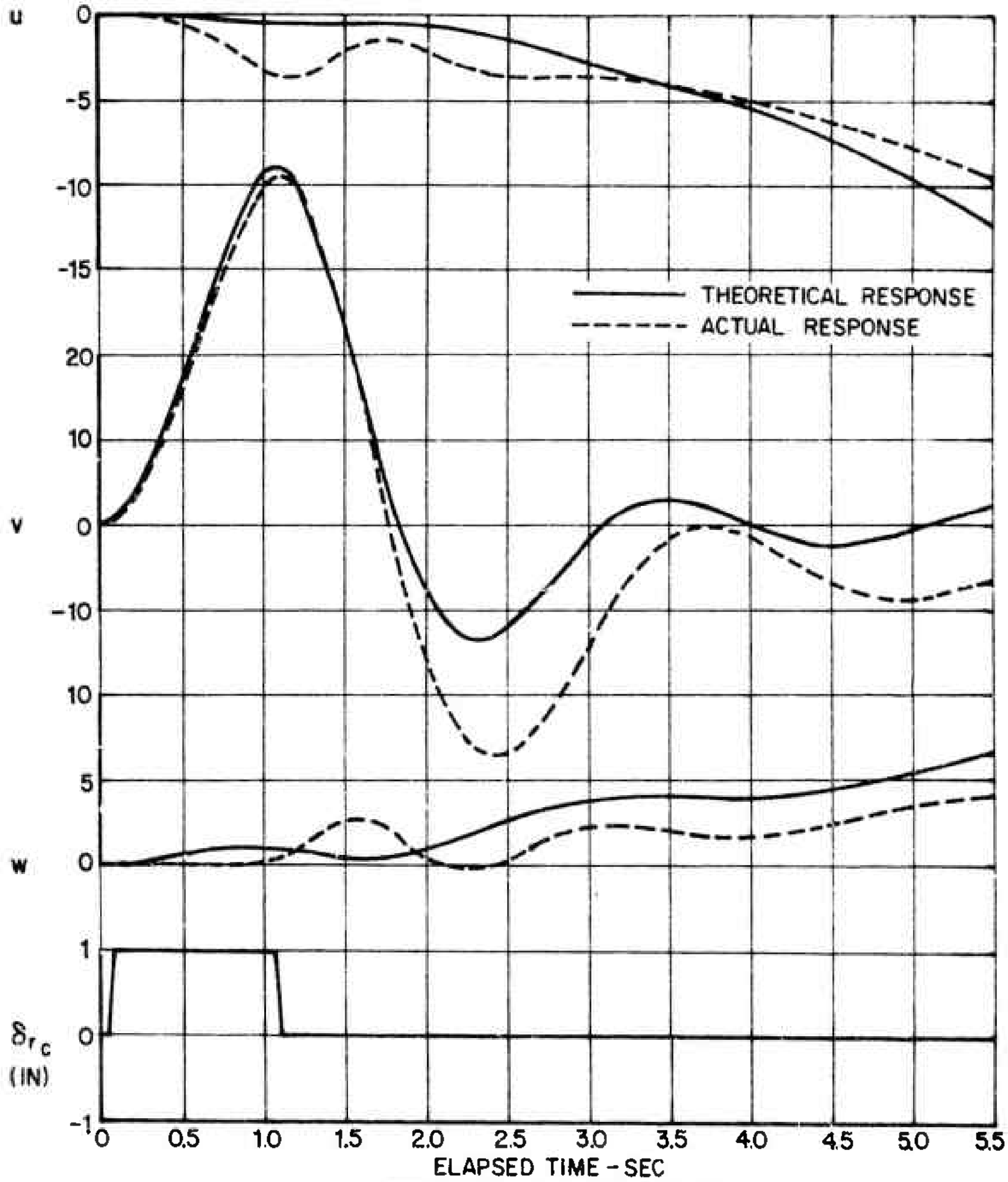

(a) PERTURBATION VELOCITIES, FT/SEC

Figure 7. Response of the Teetering Rotor Compound Helicopter Due to Pulse Input of the Directional Control, δ_{r_c} = +1", V = 150 KTS.

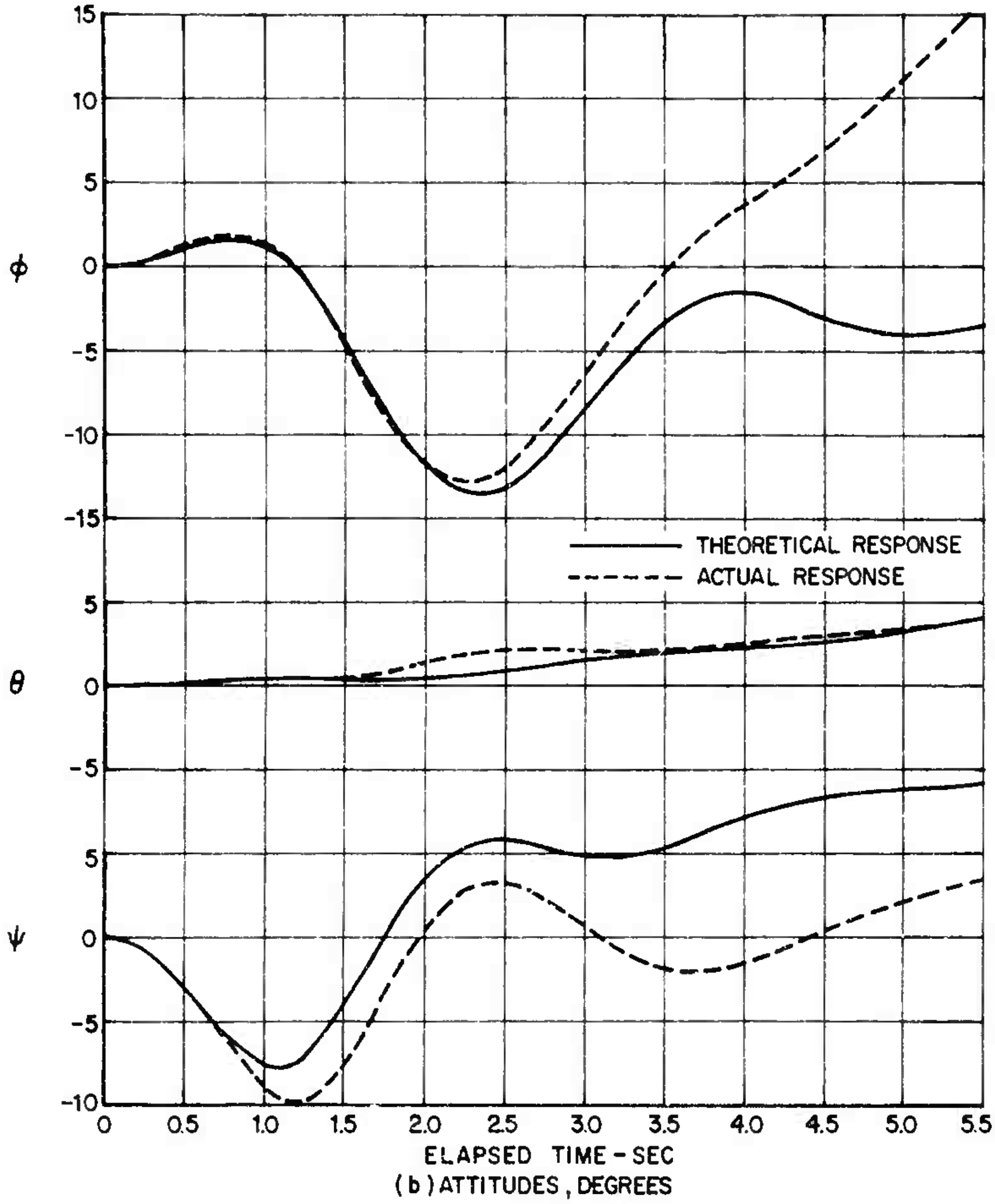

Figure 7. Continued.

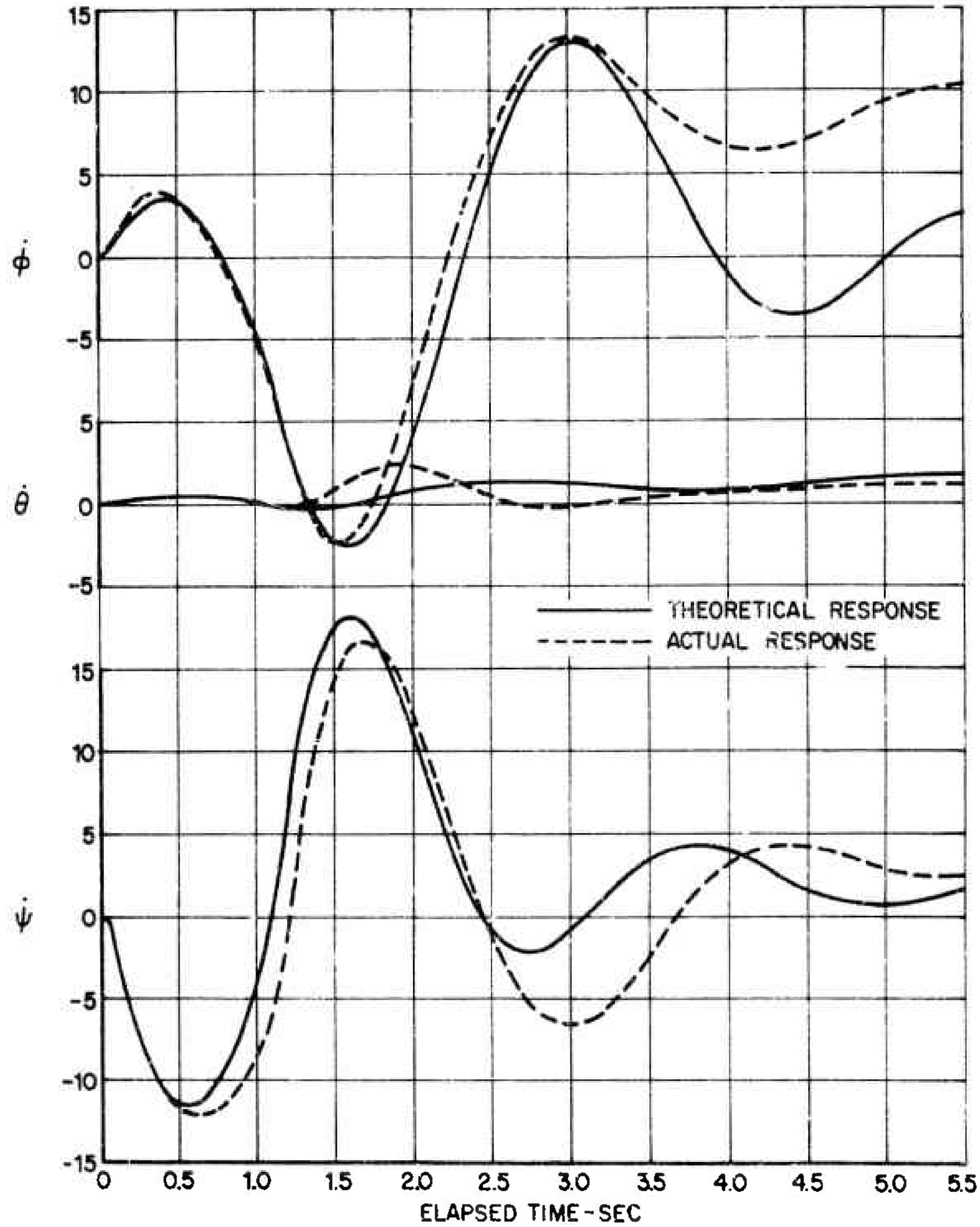

(c) ANGULAR RATES, DEG/SEC

Figure 7. Concluded.

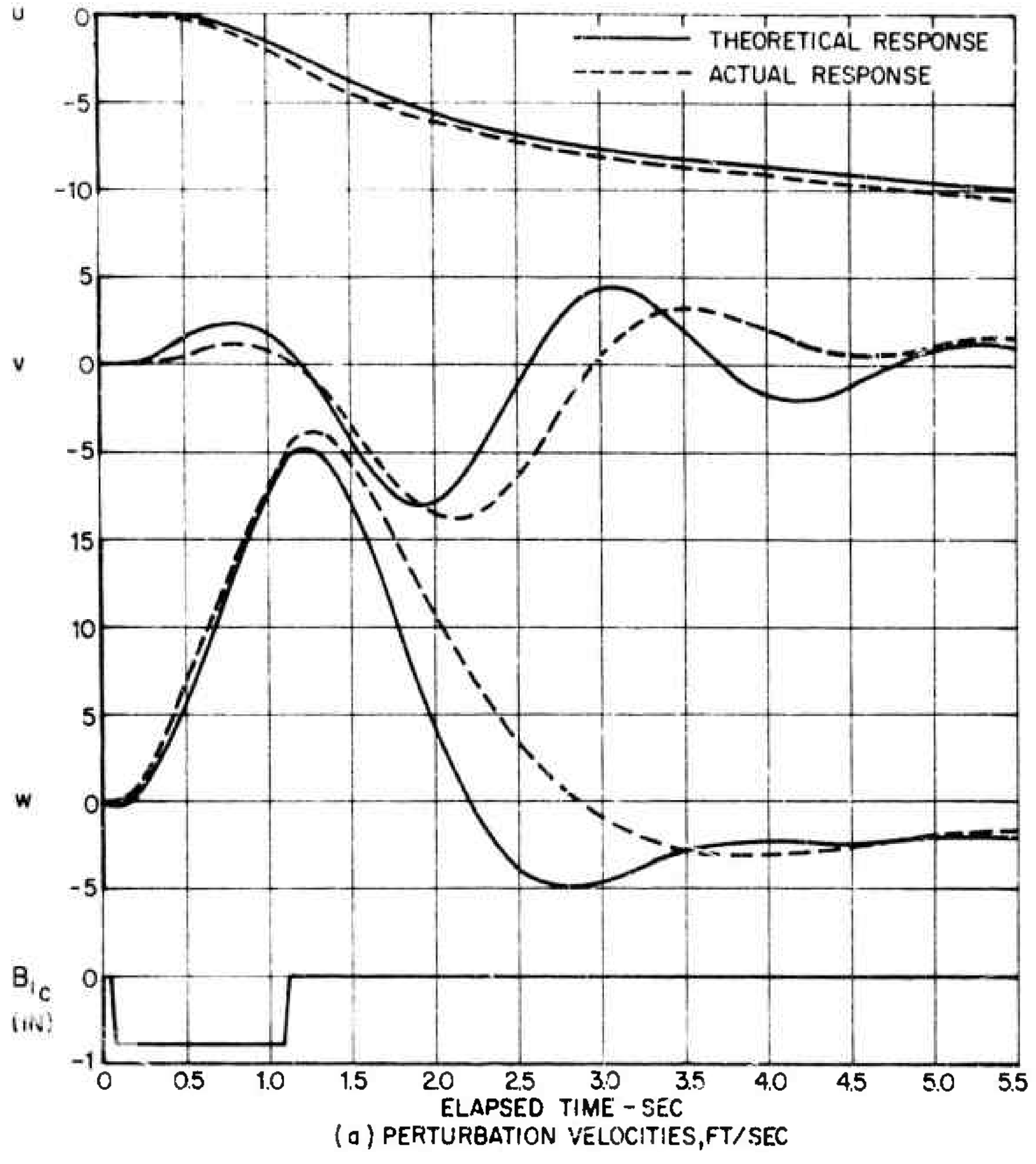

Figure 6. Response of the Teetering Rotor Compound Helicopter Due to Pulse Input of the Longitudinal Control, B_{1_C} = -0.8", V = 200 KTS.

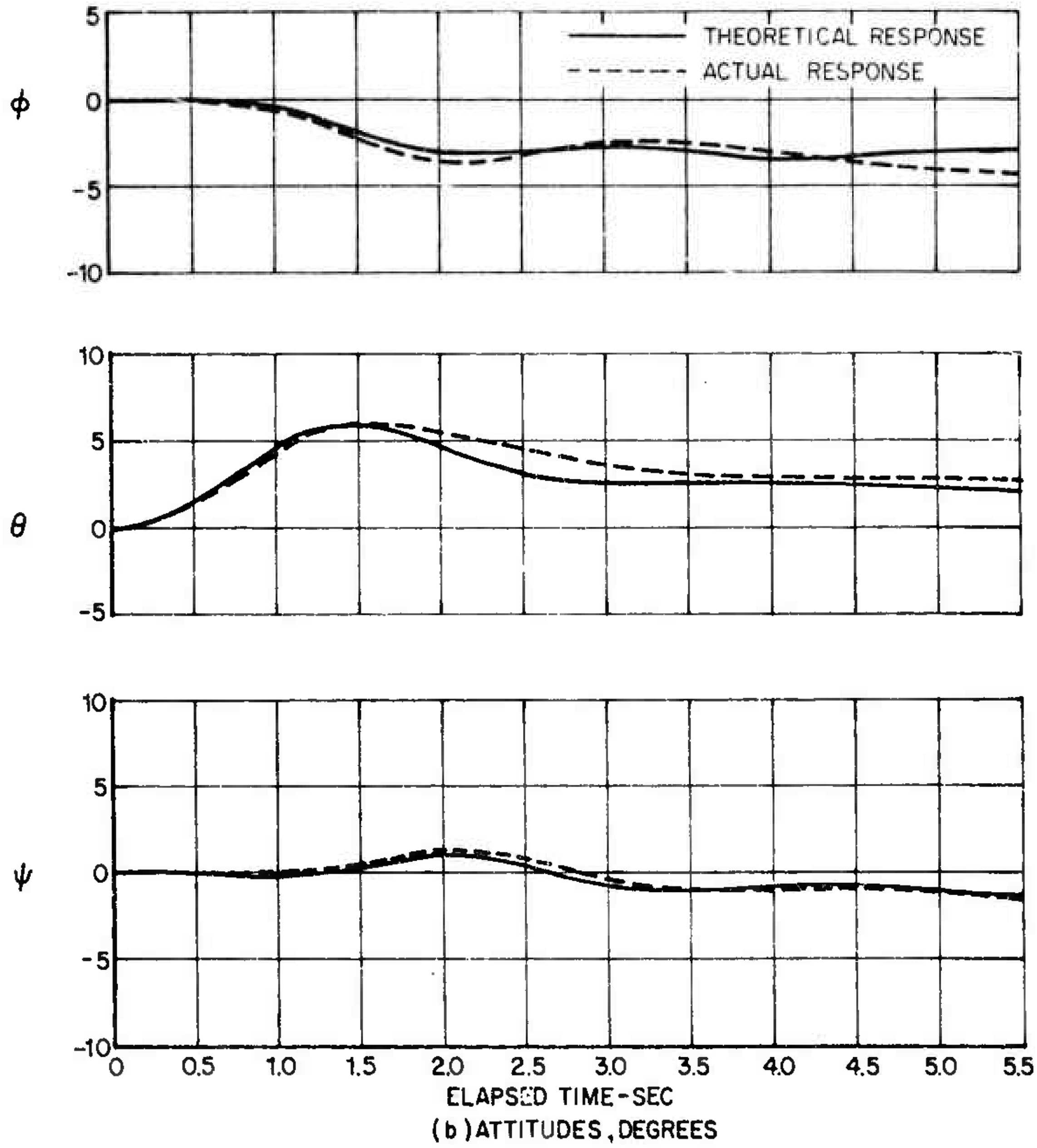

Figure 8. Continued.

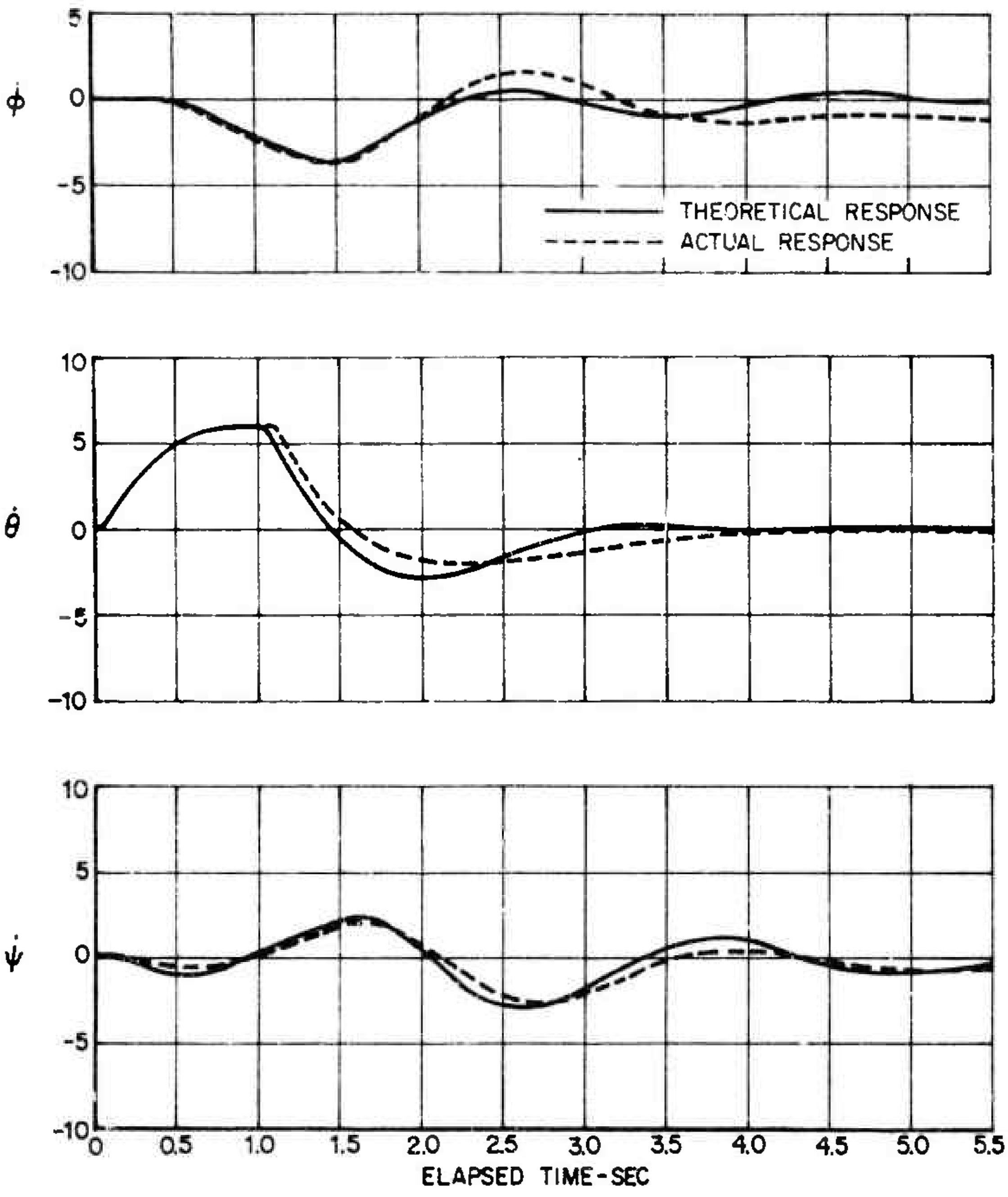

(c) ANGULAR RATES, DEG/SEC

Figure 8. Concluded.

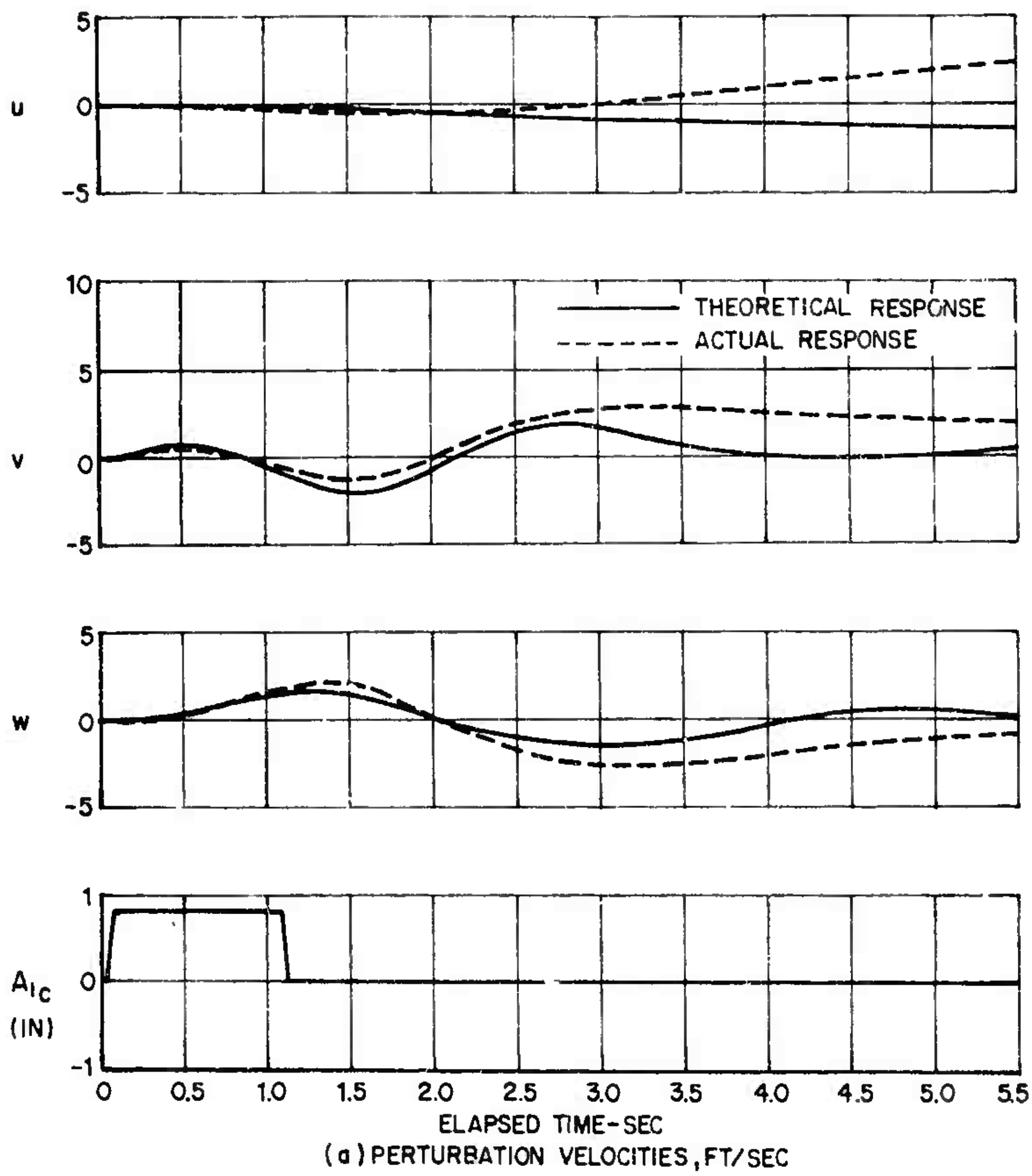

Figure 9. Response of the Teetering Rotor Compound Helicopter Due to Pulse Input of the Lateral Control, A_{1c} = +0.8", V = 200 KTS.

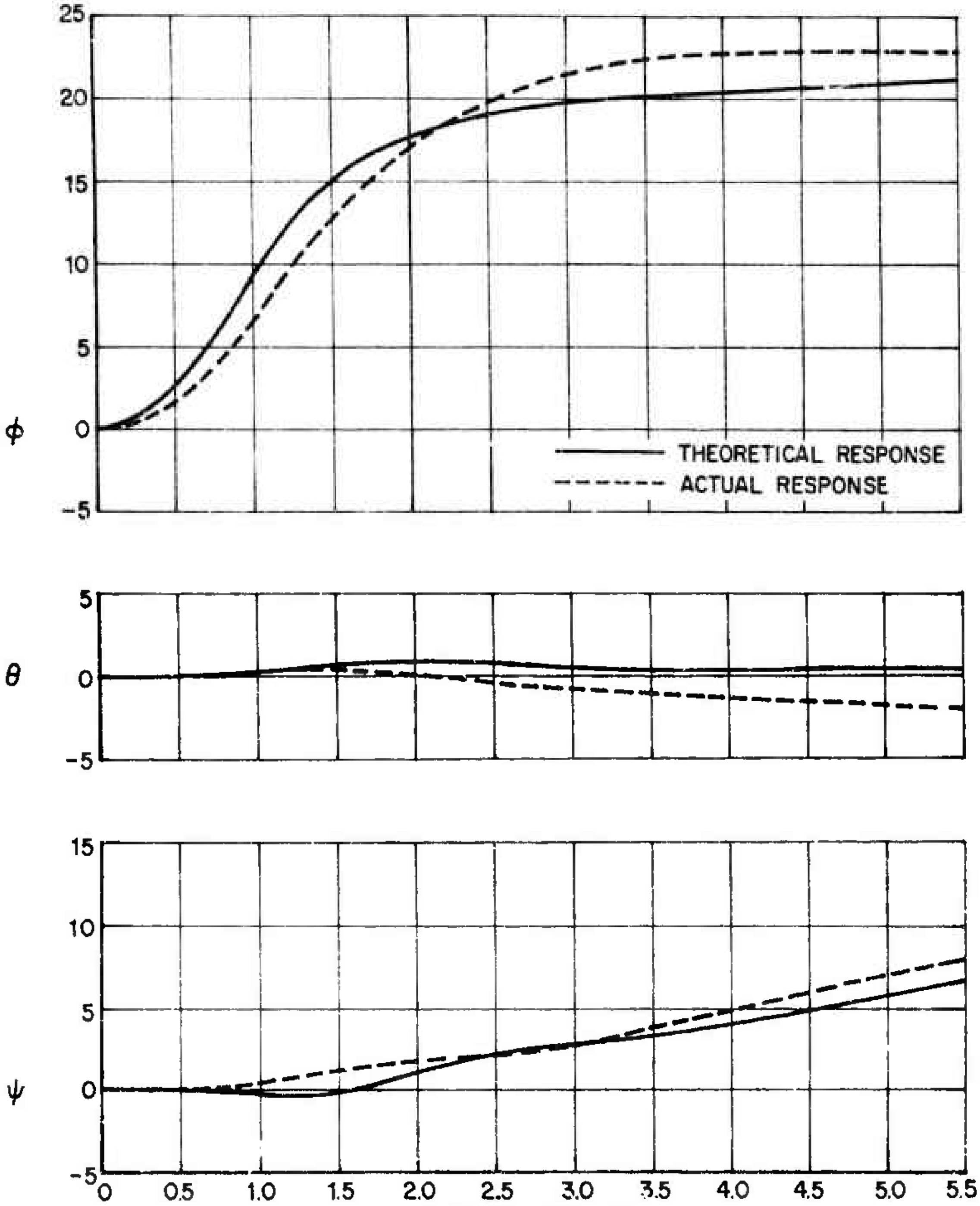

(b) ATTITUDES, DEGREES

Figure 9. Continued.

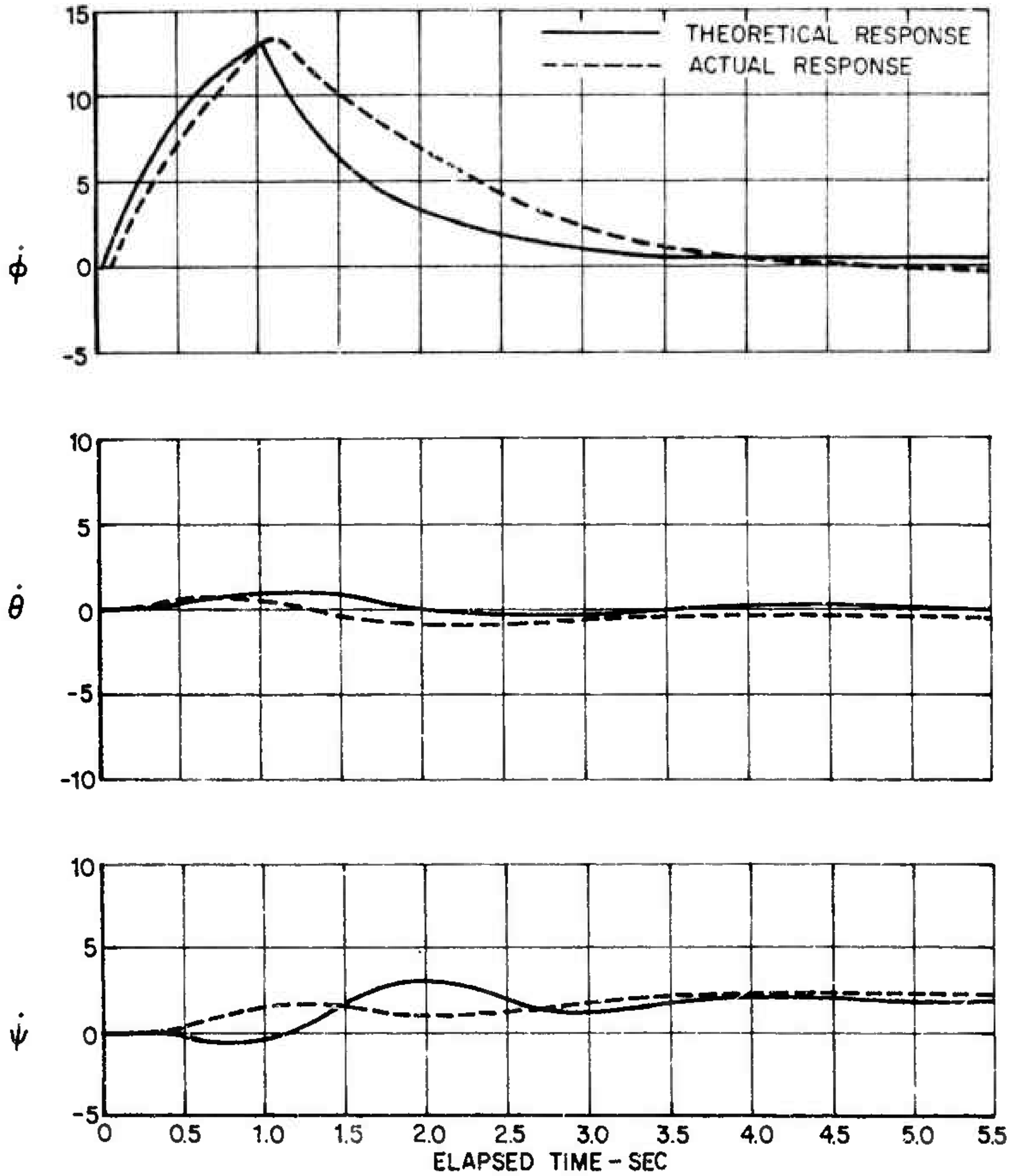

(c) ANGULAR RATES, DEG/SEC

Figure 9. Concluded.

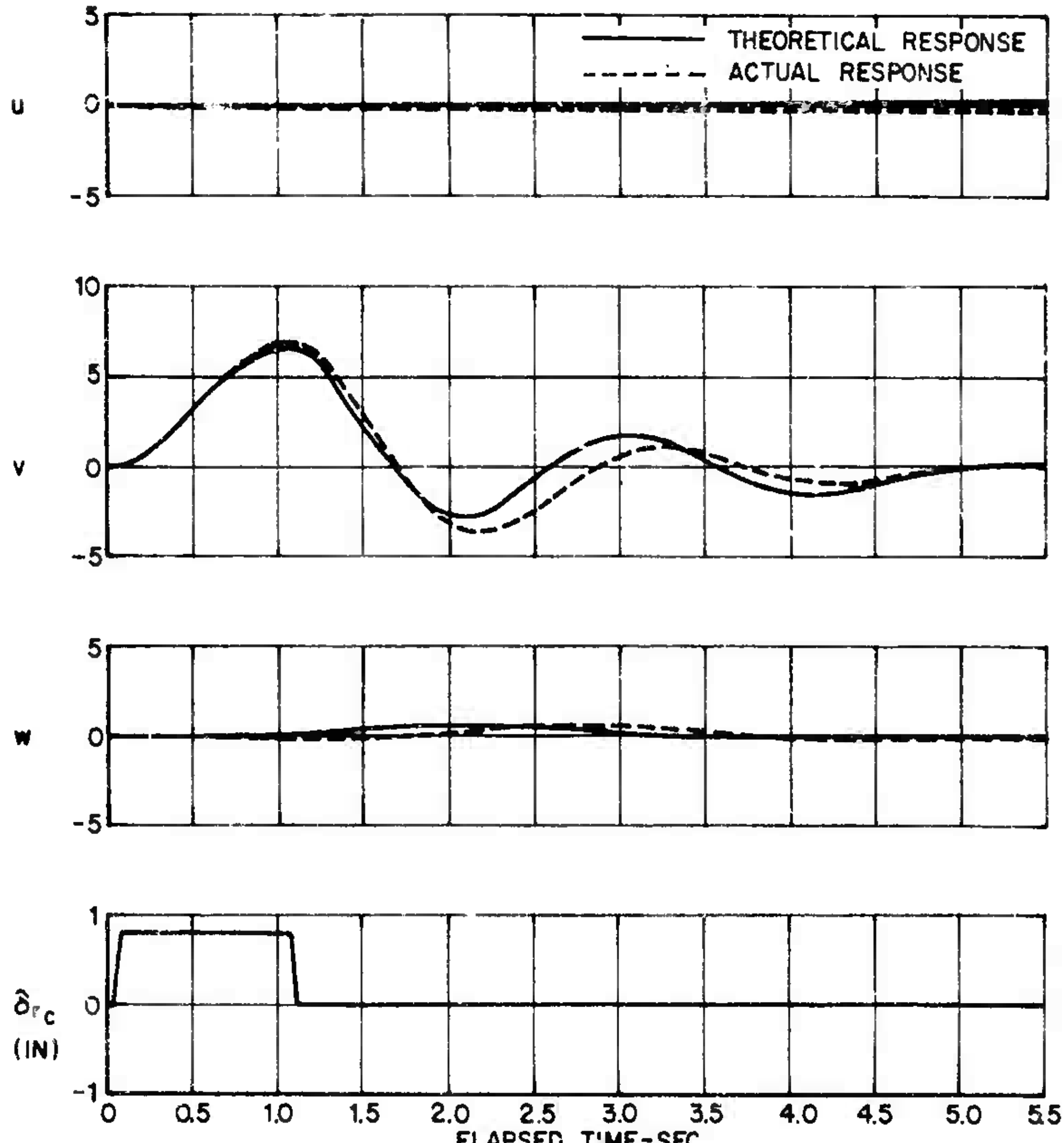

(a) PERTURBATION VELOCITIES, FT/SEC

Figure 10. Response of the Teetering Rotor Compound Helicopter Due to Pulse Input of the Directional Control, δ_{r_c} = +0.8", V = 200 KTS.

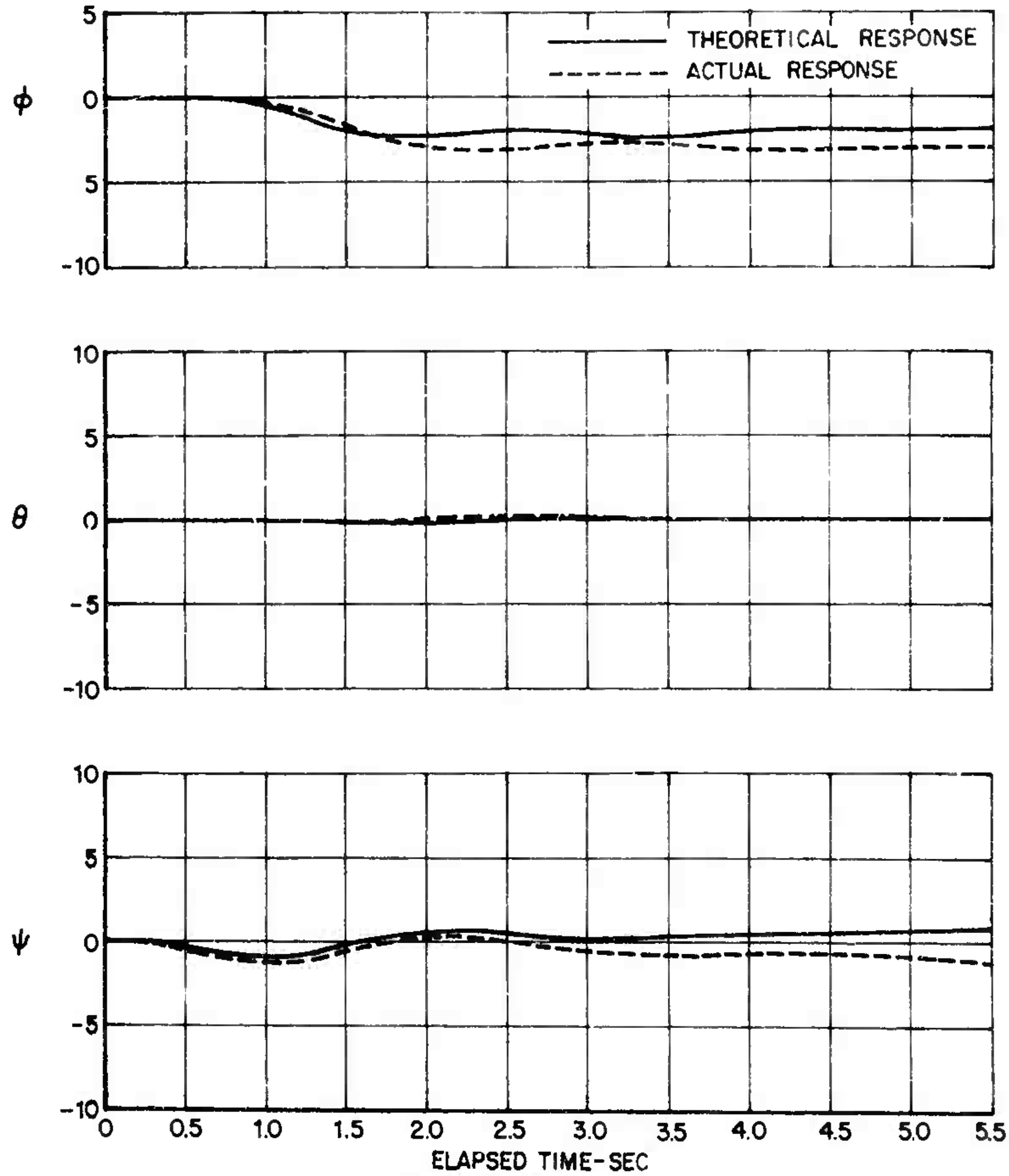

(b) ATTITUDES, DEGREES

Figure 10. Continued.

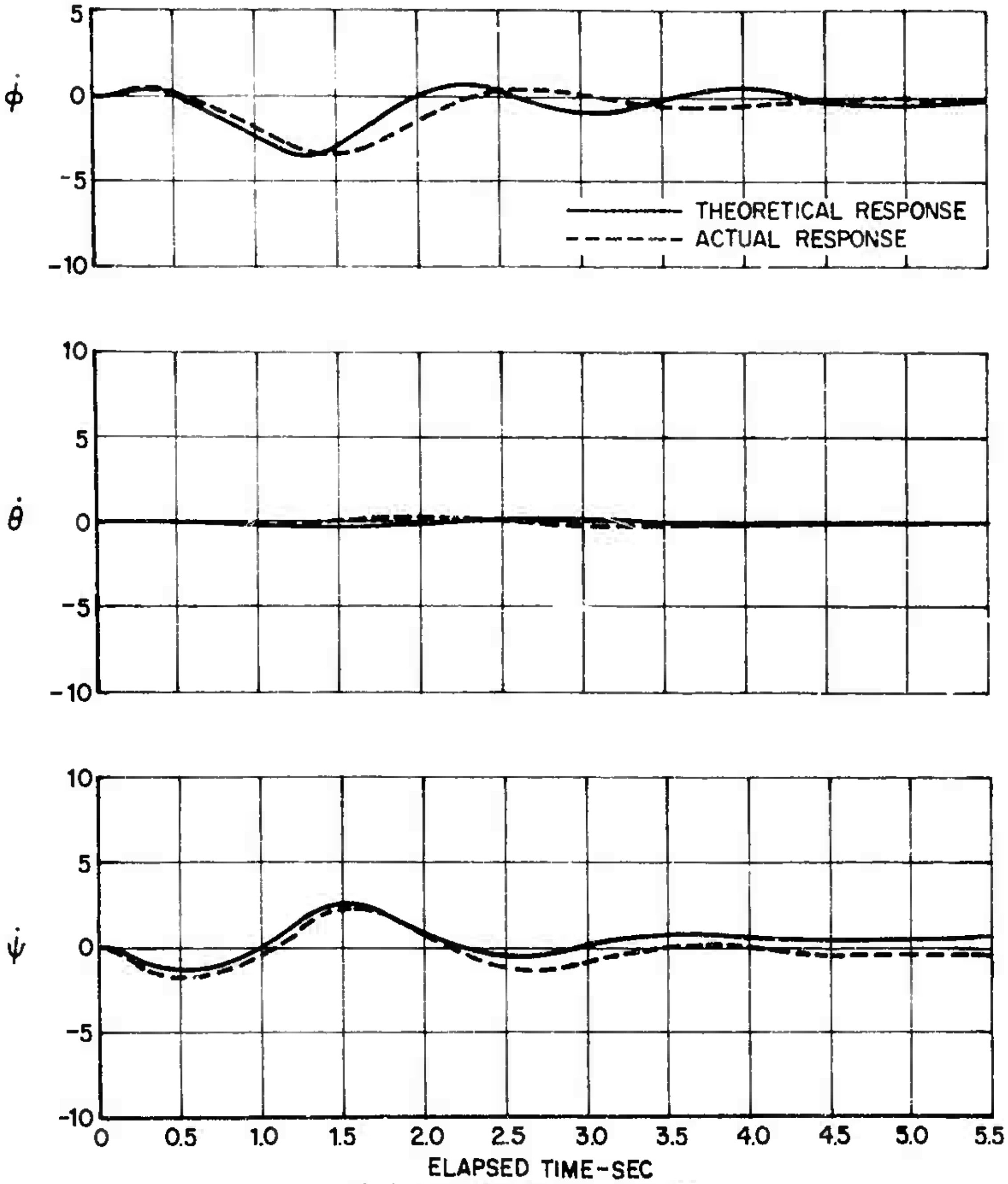

(c) ANGULAR RATES, DEG/SEC

Figure 10. Concluded.

By examining Figures 2 through 10, it can be noted that overall good to very good correlation is achieved between the analytical results obtained using the stability methods presented herein and the corresponding flight test data for the teetering rotor compound helicopter. To facilitate a detailed evaluation of the degree of correlation, a qualitative rating system is introduced.

This system rates the degree of correlation that was achieved between the theoretical and the flight test responses as: excellent (E), very good (VG), good (G), fair (F), and poor (P). The qualitative correlation ratings for the response of each parameter presented in Figures 2 through 10 for the sample teetering rotor compound helicopter are presented in Table VIII.

As can be noted from Table VIII, generally better correlations are achieved for the higher speed cases than for the low speed cases. For a lateral stick pulse (A_{1_C}), the lateral responses of ϕ , $\dot{\phi}$, ψ , $\dot{\psi}$, and v are predicted very well, whereas the prediction of the longitudinal responses of θ , $\dot{\theta}$, u , and w is somewhat poorer, especially at low flight speeds. The responses due to longitudinal stick pulses (B_{1_C}) are all very well predicted except at low speed, where only fair correlation was achieved for w and the directional responses of ψ , $\dot{\psi}$, and v . Very good correlation is obtained for the responses to rudder pedal pulses (δ_{r_C}) except that again at low speed, poor correlation is indicated for the longitudinal flight parameters θ , $\dot{\theta}$, u , and w .

The results discussed above indicate that somewhat poorer correlation exists for the cross-coupled modes, e.g., the responses of the lateral parameters due to longitudinal disturbances and vice versa. This is primarily attributed to the inherent inaccuracies in estimating the cross-products of inertia of the sample compound helicopter. Therefore, it appears that the cross-products of inertia which are generally negligible in the stability analyses of conventional helicopters may be more important in the case of compounds. It is expected, however, that with more accurate input data, including exact similation of aircraft, control motions, the analytical methods presented herein will more than adequately predict the measured responses of a compound helicopter.

TABLE VIII

SUMMARY OF THE CORRELATION OBTAINED BETWEEN THEORETICAL AND TEST RESPONSES FOR THE TEETERING ROTOR COMPOUND HELICOPTER

Control Pulse	Vo (Kn)	Parameter									Figure Number
		u	v	w	ϕ	θ	ψ	$\dot{\phi}$	$\dot{\theta}$	$\dot{\psi}$	
B_{1c}	100	G	F	F	G	VG	F	G	VG	F	2
	150	G	G	G	VG	E	VG	G	E	VG	5
	200	VG	G	G	E	VG	E	VG	VG	E	8
A_{1c}	100	F	G	G	E	F	E	VG	G	E	3
	150	G	VG	G	VG	G	VG	VG	G	E	6
	200	F	G	G	VG	F	VG	VG	VG	VG	9
δ_{r_c}	100	P	VG	P	F	P	G	G	F	VG	4
	150	F	G	F	F	VG	F	G	G	G	7
	200	E	VG	E	VG	E	G	VG	E	VG	10

CORRELATION RATINGS: E-excellent
VG-very good
G-good
F-fair
P-poor

10.2 DYNAMIC STABILITY RESPONSES OF AN ARTICULATED ROTOR COMPOUND HELICOPTER

10.2.1 Description of the Sample Compound Helicopter

The sample compound helicopter is the same aircraft as described in detail in the sample calculations of Section 11. The vehicle is illustrated in Figure 1 of Section 11.1, and the pertinent design parameters are presented in Table I of Section 11.2. This aircraft has no electrical or mechanical stability augmentation system, but it employs integrated airplane and helicopter flight controls throughout its speed regime.

The operating conditions assumed in these sample calculations correspond to forward speeds of 125, 150, and 180 knots, all at a constant rotor tip speed of $\Omega R = 600$ ft/sec and a density altitude corresponding to 3000 feet above sea level.

10.2.2 Analog Computer Program

The analog computer program for this compound helicopter was developed using the total stability derivatives presented in Table I of Section 11.4 for the 125-knot speed case, and Tables I and II in this section for the 150- and 180-knot speed cases respectively. These derivatives were obtained using the design parameters given in Section 11.2 and the methods described earlier in this report. The analog computer schematic diagram representing the equations of motion for this aircraft is shown in Figure 1. The settings of the potentiometers P and Q, shown in Figure 1, are given in Tables III, IV, and V for the 125-, 150-, and 180-knot speed cases respectively. These settings were obtained by normalizing the total derivatives described above and multiplying the normalized derivatives by the appropriate scaling factors required for use on the Pace 221 R computer.

10.2.3 Stability Responses of the Articulated Rotor Compound Helicopter

The time history responses of this articulated rotor compound helicopter to pulse inputs of the longitudinal and lateral cyclic controls B_{1_C} and A_{1_C} respectively and the rudder pedal control δ_{r_C} are shown in Figures 2 through 11 for the three flight speeds considered. Figures 2, 3, and 4 show the aircraft response due to individually applied pulse inputs of the longitudinal, lateral, and directional controls, respectively, at a forward speed of 125 knots.

TABLE I

TOTAL STABILITY DERIVATIVES FOR THE ARTICULATED ROTOR COMPOUND HELICOPTER AT 150 KNOTS

Var. \ Eq.	X	Y	Z	M	N	L
θ	-18868.	0	-1092.	0	0	0
$\dot{\theta}$	-7332.	-563.17	145701.	-140300.	30131.	-9807.
$\ddot{\theta}$	0	0	0	-59800.	0	0
ϕ	0	18900.	0	0	0	0
$\dot{\phi}$	-601.67	-7514.	-39.030	10945.	-11062.	-17430.
$\ddot{\phi}$	0	0	0	0	0	-14920.
ψ	0	1092.	0	0	0	0
$\dot{\psi}$	-127.70	-147623.	-59.894	1104.	-36182.	3633.
$\ddot{\psi}$	0	0	0	0	-56800.	0
u	-33.416	4.773	-44.144	-322.43	-97.728	29.565
$\dot{u}$	-586.96	0	0	0	0	0
v	-1.563	-50.389	-8.220	48.72	707.10	-105.60
$\dot{v}$	0	-586.96	0	0	0	0
w	57.345	-2.837	-805.91	-1178.	-277.70	96.401
$\dot{w}$	-0.129	0	-579.98	249.23	-0.001	-0.042
A_1	-1.321	12267.	22.824	-1.505	5716	91392.
B_1	787.76	1170.	121041.	-230648.	55391.	-24361.
δ_r	1596.	-16511.	335.61	1995.	591736.	-109199.

TABLE II

TOTAL STABILITY DERIVATIVES FOR THE ARTICULATED ROTOR COMPOUND HELICOPTER AT 180 KNOTS

Var. \ Eq.	X	Y	Z	M	N	L
θ	-18894.	0	-842.94	0	0	0
$\dot{\theta}$	-6843.	-440.76	174716.	-163344.	28485.	-8693.
$\ddot{\theta}$	0	0	0	-59800.	0	0
ϕ	0	18900.	0	0	0	0
$\dot{\phi}$	-493.59	7068.	-6.213	10554.	-8779.	-15732.
$\ddot{\phi}$	0	0	0	0	0	-14920.
ψ	0	842.94	0	0	0	0
$\dot{\psi}$	-123.08	-177197.	-83.914	483.67	-41555.	3987.
$\ddot{\psi}$	0	0	0	0	-56800	0
u	-37.51	4.359	-38.332	-342.28	-82.645	21.693
$\dot{u}$	-586.96	0	0	0	0	0
v	-2.396	-63.090	-9.508	73.557	819.56	-159.06
$\dot{v}$	0	-586.96	0	0	0	0
w	60.006	3.217	-918.29	-1639.	-155.36	168.42
$\dot{w}$	-0.177	0	-580.85	218.27	-0.001	-0.039
A_1	-3.939	9731.	88.288	-13.925	4534.	135167.
B_1	-4552.	-311.32	153601.	-341701.	25156.	-51088.
δ_r	1977.	-15178.	556.63	6323.	542586.	-94544.

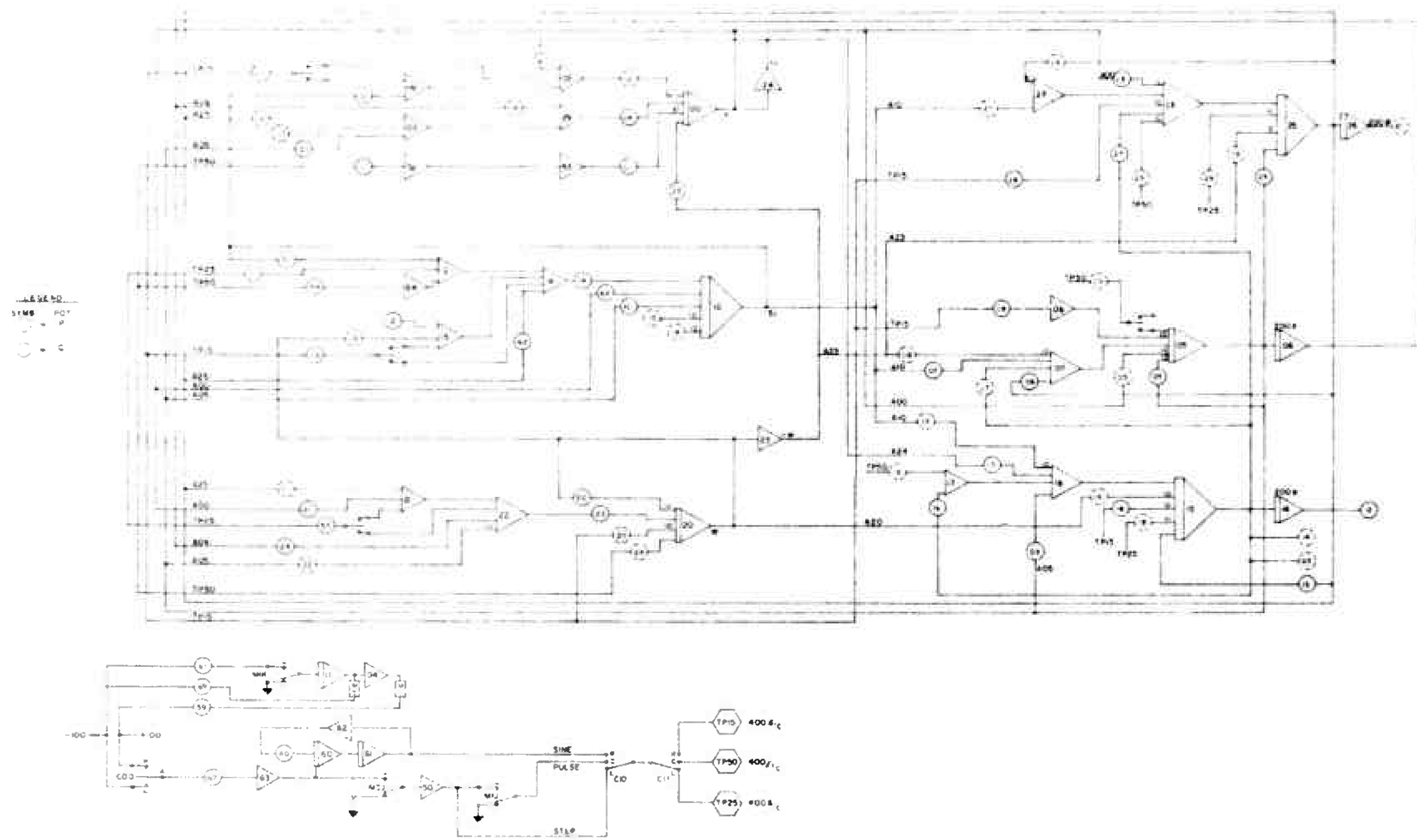

Figure 1. Analog Computer Schematic for the Sample Articulated Rotor Compound Helicopter.

TABLE III

ANALOG COMPUTER POTENTIOMETER SETTINGS FOR THE ARTICULATED ROTOR COMPOUND HELICOPTER AT 125 KNOTS

Pot. No.	Setting	Pot. No.	Setting	Pot. No.	Setting	Pot. No.	Setting
P00	0.0865	P10	0.805	P20	0.0463	Q50	--
Q00	0.0059	Q10	0.0270	Q20	0.1321	Q51	0.0836
P01	0.0022	P11	—	P21	0.0015	Q52	--
Q01	0.1000	Q11	0.3512	Q21	0.2122	Q53	0.0006
P02	0.1667	P12	—	P22	0.3293	Q54	0.3893
Q02	0.0340	Q12	0.0679	Q22	0.3333	Q55	—
P03	0.0060	P13	0.0578	P23	0.3284	Q56	—
Q03	0.3980	Q13	0.0406	Q23	0.0986	Q57	—
P04	0.0964	P14	0.5491	P24	0.0012	Q58	—
Q04	0.1667	Q14	0.8333	Q24	0.0344	Q59	0.1750
P05	0.0896	P15	—	P25	0.3439	Q60	1.0000
Q05	0.2112	Q15	0.1925	Q25	0.6949	Q61	0.1000
P06	0.3130	P16	0.4809	P26	0.1238	Q62	—
Q06	0.1875	Q16	—	Q26	0.0485	Q63	0.4076
P07	0.0177	P17	0.0439	P27	0.1628	Q64	—
Q07	0.0048	Q17	0.3740	Q27	0.2253	Q65	—
P08	—	P18	0.0056	P28	0.0880	Q66	—
Q08	0.1430	Q18	0.0413	Q28	0.0442	Q67	0.0621
P09	—	P19	0.0924	P29	0.2292	Q68	0.0353
Q09	0.5205	Q19	0.5752	Q29	—	Q69	0.1000

TABLE IV

ANALOG COMPUTER POTENTIOMETER SETTINGS FOR THE ARTICULATED ROTOR COMPOUND HELICOPTER AT 150 KNOTS

Pot. No.	Setting	Pot. No.	Setting	Pot. No.	Setting	Pot. No.	Setting
P00	0.0201	P10	0.0805	P20	0.0522	Q50	—
Q00	0.0068	Q10	0.0240	Q20	0.1389	Q51	0.1030
P01	0.0032	P11	—	P21	0.0010	Q52	—
Q01	0.1000	Q11	0.3135	Q21	0.2283	Q53	0.0003
P02	0.1667	P12	—	P22	0.3768	Q54	0.4220
Q02	0.0307	Q12	0.0558	Q22	0.3333	Q55	—
P03	0.0015	P13	0.0290	P23	0.3416	Q56	—
Q03	0.3747	Q13	0.0299	Q23	0.0977	Q57	—
P04	0.0964	P14	0.6288	P24	0.0014	Q58	—
Q04	0.1667	Q14	0.8333	Q24	0.0282	Q59	0.1750
P05	0.1078	P15	—	P25	0.3659	Q60	1.0000
Q05	0.02346	Q15	0.1947	Q25	0.6573	Q61	0.1000
P06	0.3940	P16	0.5209	P26	0.1168	Q62	—
Q06	0.1830	Q16	—	Q26	0.0816	Q63	0.3840
P07	0.0184	P17	0.0498	P27	0.2828	Q64	—
Q07	0.0324	Q17	0.3440	Q27	0.2435	Q65	—
P08	—	P18	0.0030	P28	0.1292	Q66	—
Q08	0.1928	Q18	0.0487	Q28	0.0396	Q67	0.0621
P09	0.0167	P19	0.0976	P29	0.3063	Q68	0.0406
Q09	0.5305	Q19	0.6370	Q29	—	Q69	0.1000

TABLE V

ANALOG COMPUTER POTENTIOMETER SETTINGS FOR THE ARTICULATED ROTOR COMPOUND HELICOPTER AT 180 KNOTS

Pot. No.	Setting	Pot. No.	Setting	Pot. No.	Setting	Pot. No.	Setting
P00	0.1163	P10	0.0805	P20	0.0661	Q50	—
Q00	0.0084	Q10	0.0188	Q20	0.1581	Q51	0.1290
P01	0.0049	P11	—	P21	0.0002	Q52	—
Q01	0.1000	Q11	0.2487	Q21	0.1980	Q53	0.0011
P02	0.1667	P12	—	P22	0.4511	Q54	0.3879
Q02	0.0252	Q12	0.0431	Q22	0.3333	Q55	—
P03	0.0063	P13	0.0329	P23	0.3834	Q56	—
Q03	0.3497	Q13	0.0079	Q23	0.1022	Q57	—
P04	0.0966	P14	0.7547	P24	0.0024	Q58	—
Q04	0.1667	Q14	0.8333	Q24	0.0218	Q59	0.2000
P05	0.1140	P15	—	P25	0.3168	Q60	1.0000
Q05	0.2731	Q15	0.1546	Q25	0.5826	Q61	0.1000
P06	0.5482	P16	0.4776	P26	0.1054	Q62	—
Q06	0.1765	Q16	—	Q26	0.1712	Q63	0.3612
P07	0.0081	P17	0.0577	P27	0.4264	Q64	—
Q07	0.0492	Q17	0.2900	Q27	0.2672	Q65	—
P08	—	P18	0.0040	P28	0.2256	Q66	—
Q08	0.2857	Q18	0.0221	Q28	0.0290	Q67	0.0621
P09	0.0529	P19	0.0546	P29	0.4530	Q68	0.0371
Q09	0.5015	Q19	0.7316	Q29	—	Q69	0.1000

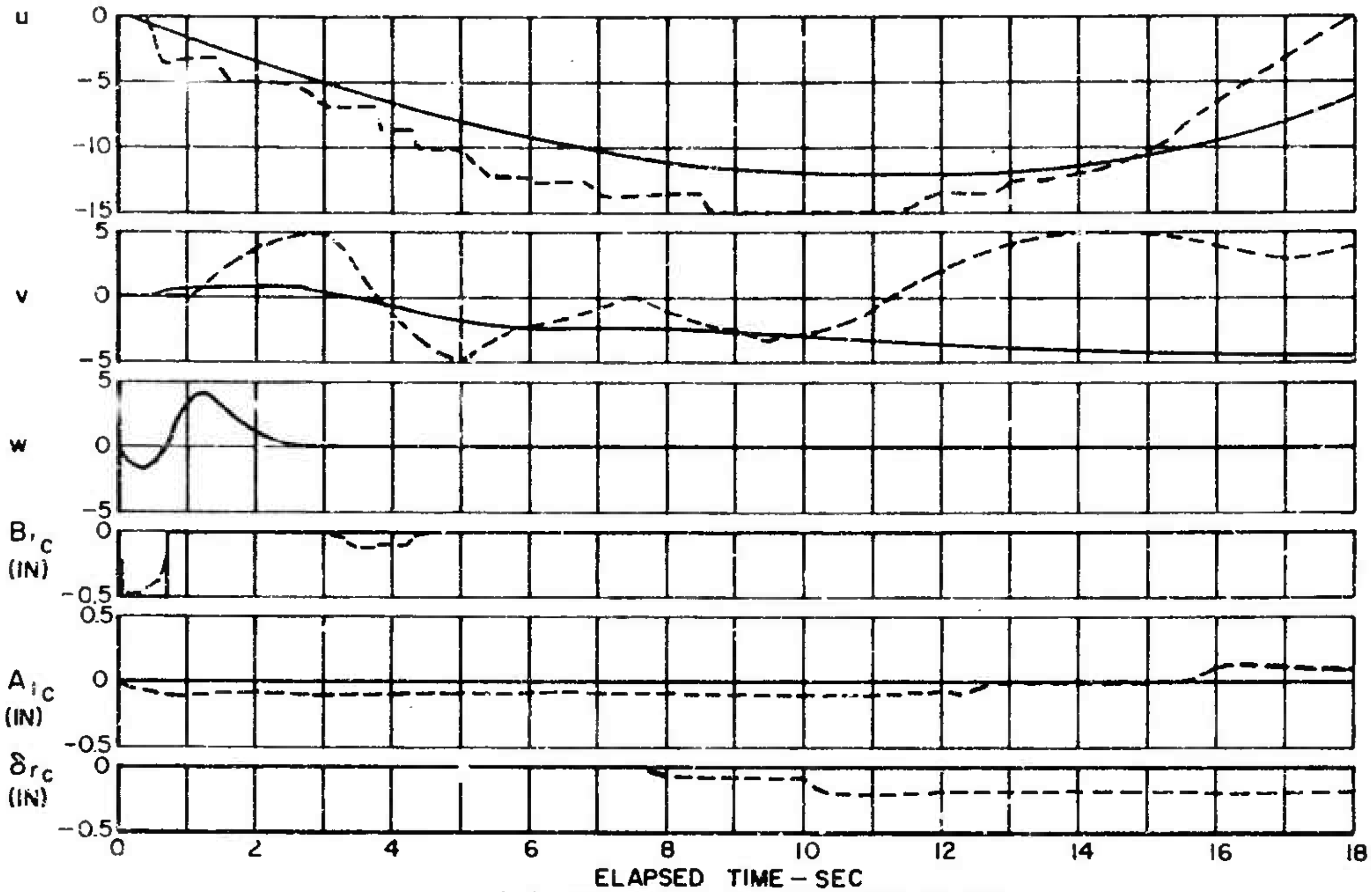

(a) PERTURBATION VELOCITIES, FT/SEC

Figure 2. Response of the Articulated Rotor Compound Helicopter Due to Pulse Input of the Longitudinal Control, B_{1c} = -0.5", V =125 KTS.

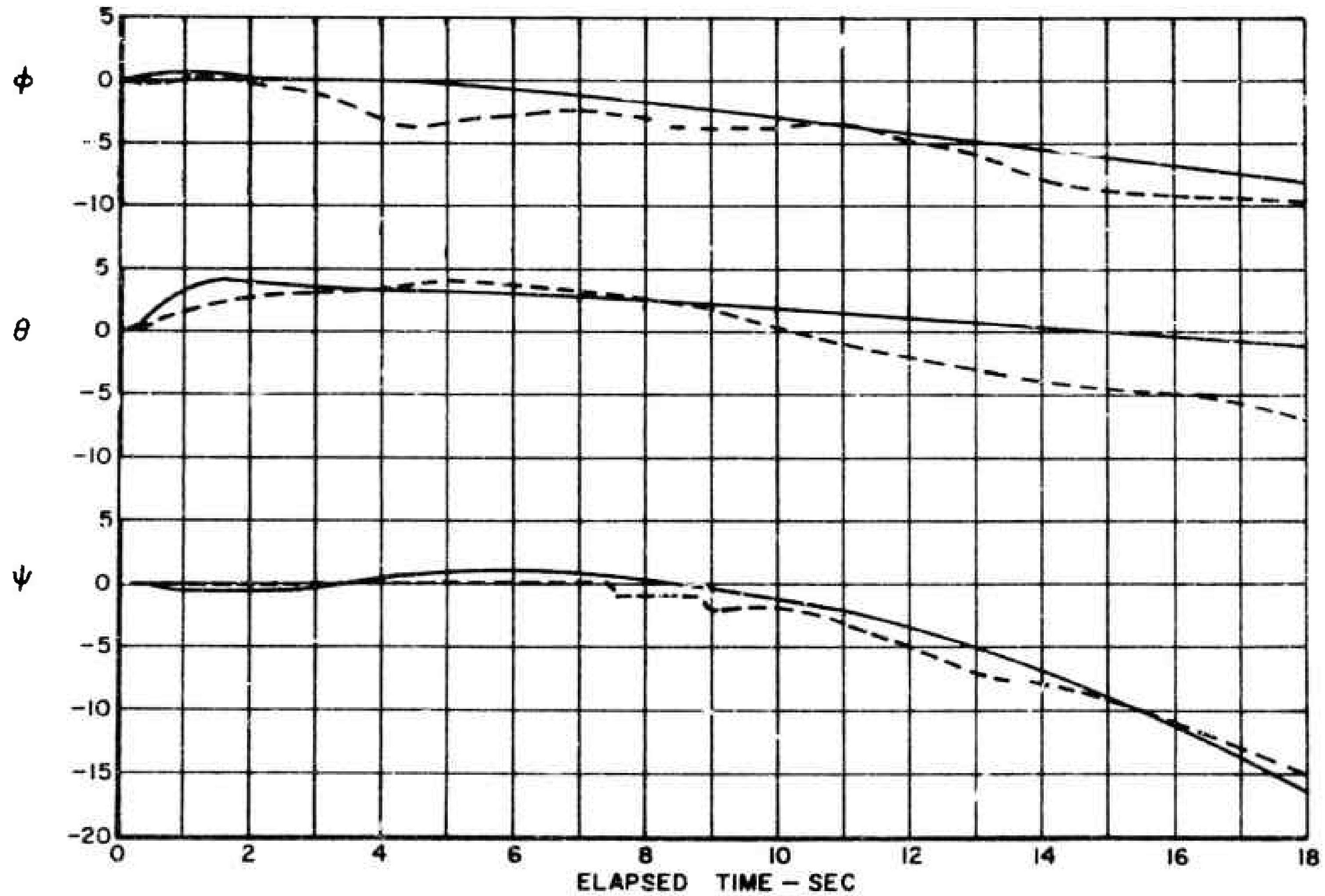

(b) ATTITUDES, DEGREES

Figure 2. Continued.

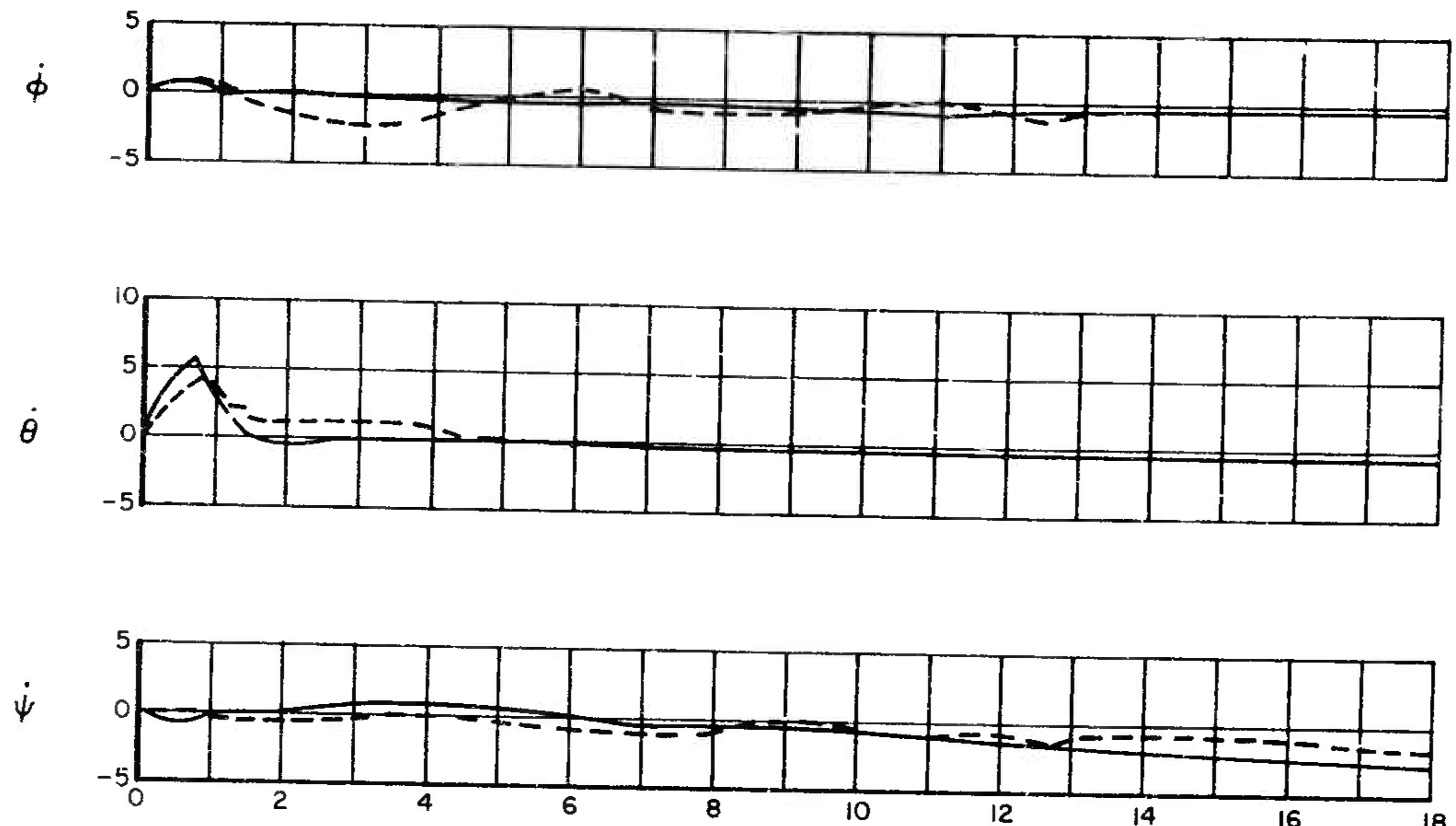

(c) ANGULAR RATES, DEG/SEC

Figure 2. Concluded.

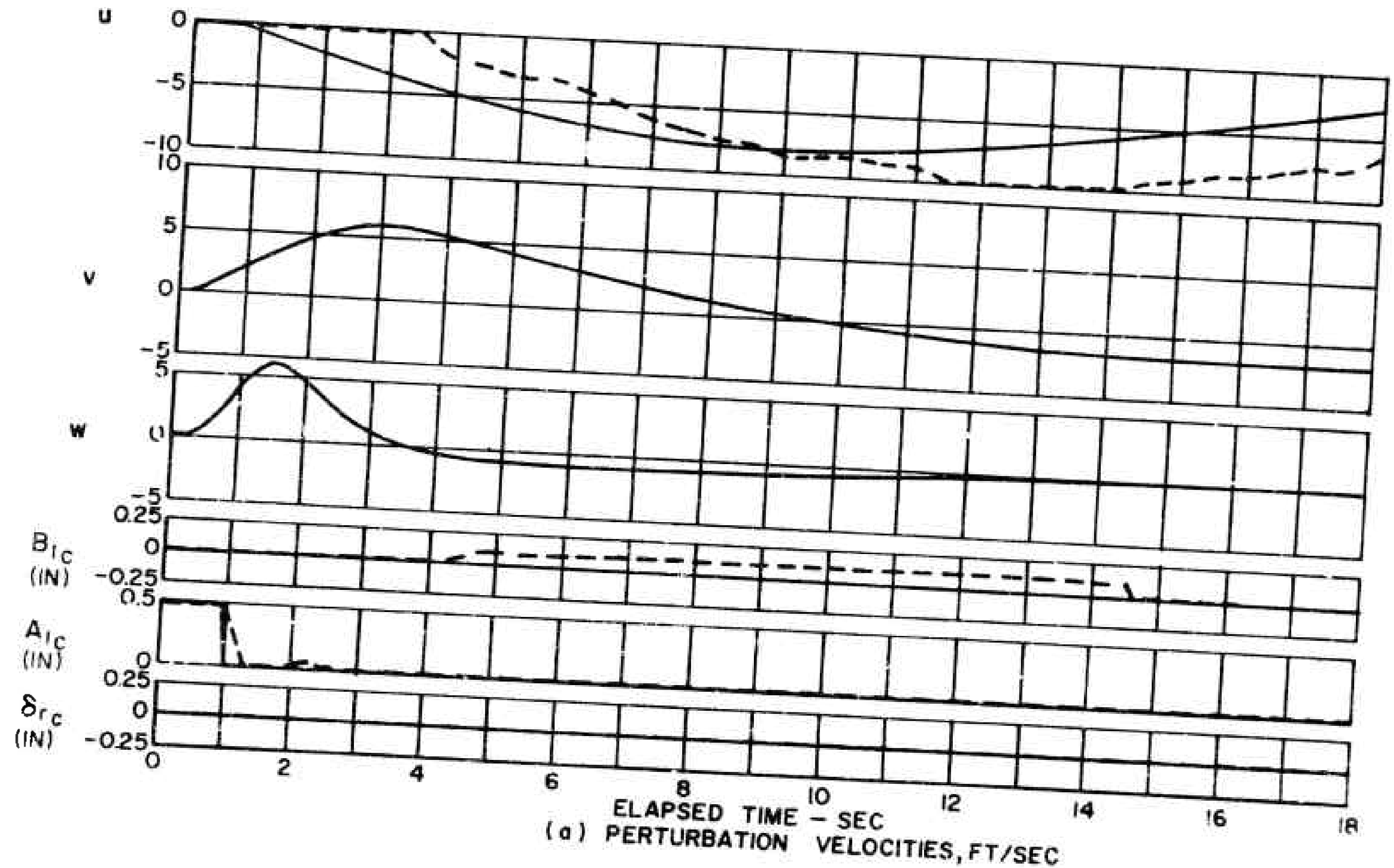

Figure 3. Response of the Articulated Rotor Compound Helicopter Due to Pulse Input of the Lateral Control, A_{1c} = +0.5", V = 125 KTS.

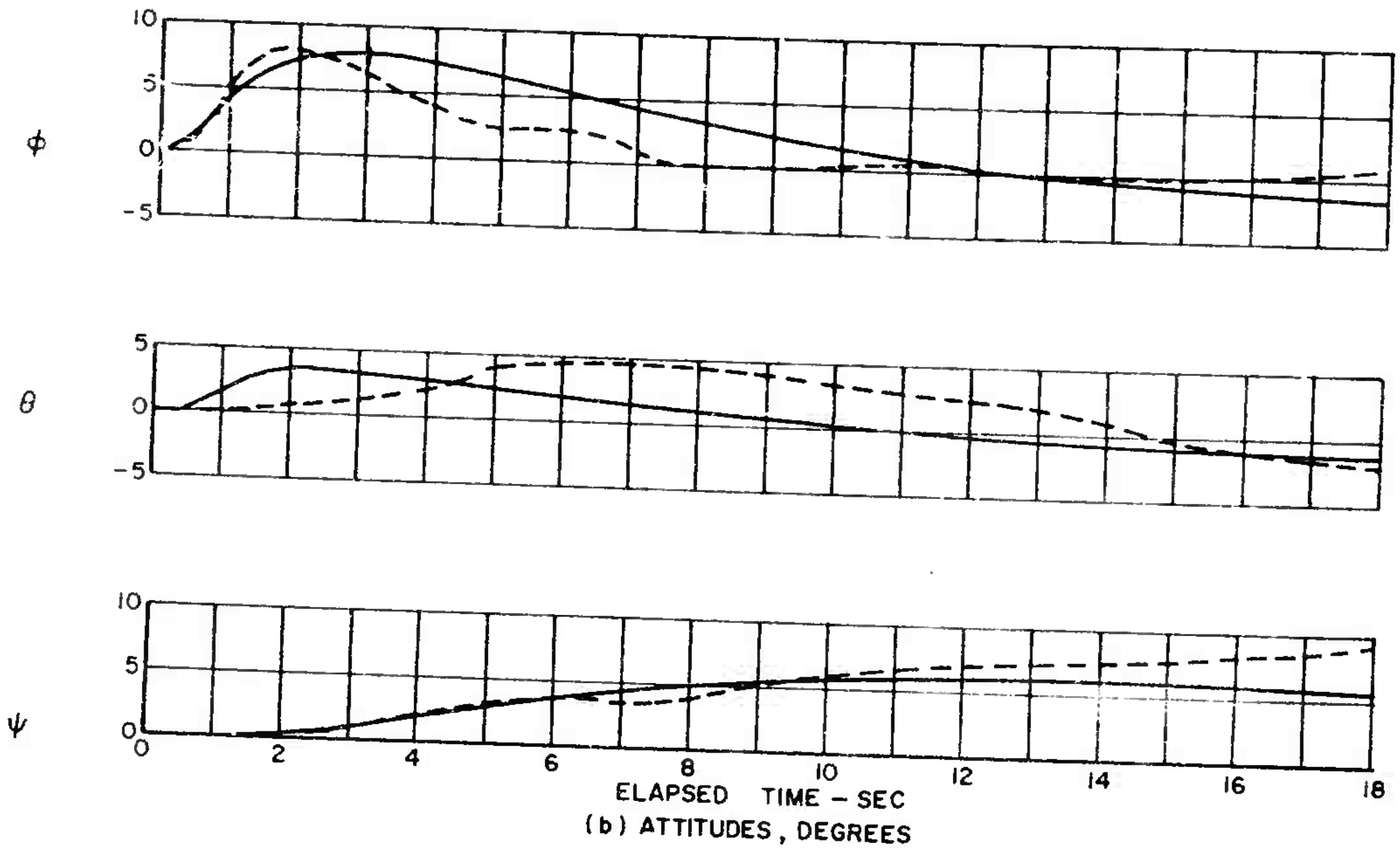

Figure 3. Continued.

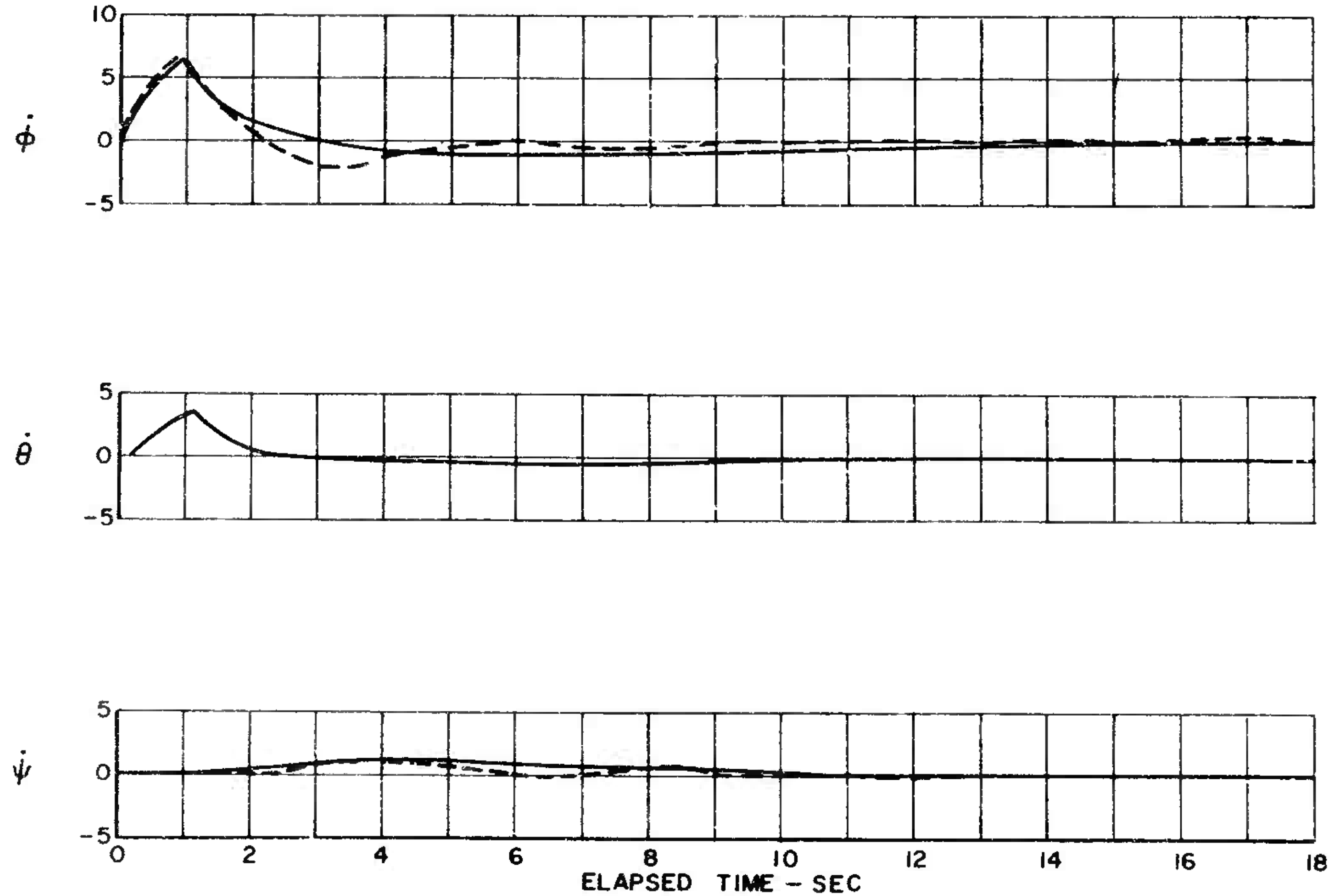

(c) ANGULAR RATES, DEG/SEC

Figure 3. Concluded.

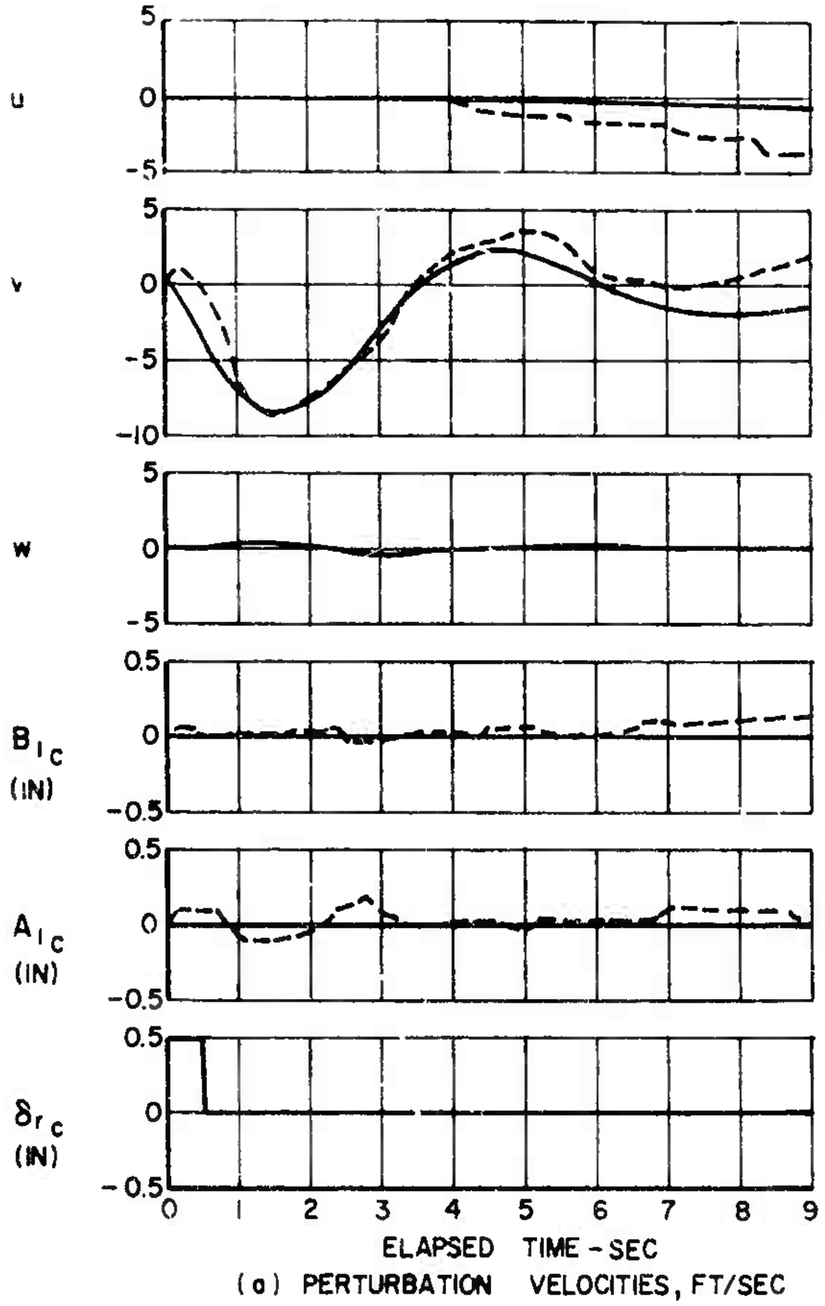

Figure 4. Response of the Articulated Rotor Compound Helicopter Due to Pulse Input of the Directional Control, δ_{r_C} = +0.5", V = 125 KTS.

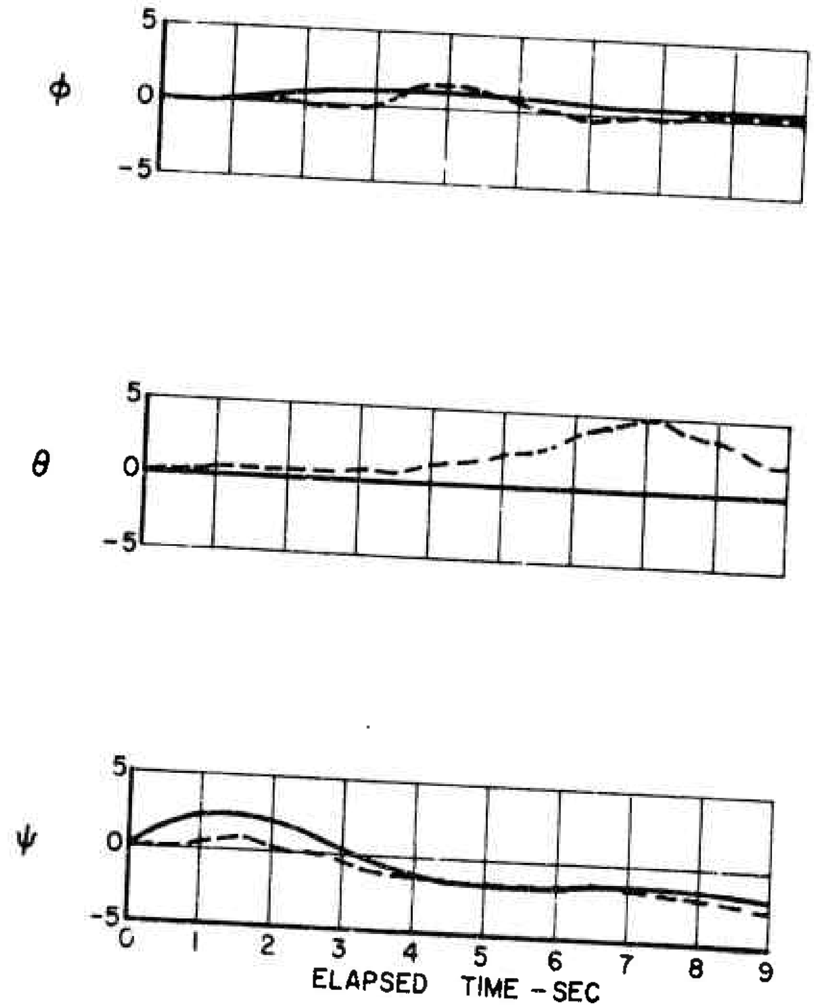

(b) ATTITUDES, DEGREES

Figure 4. Continued.

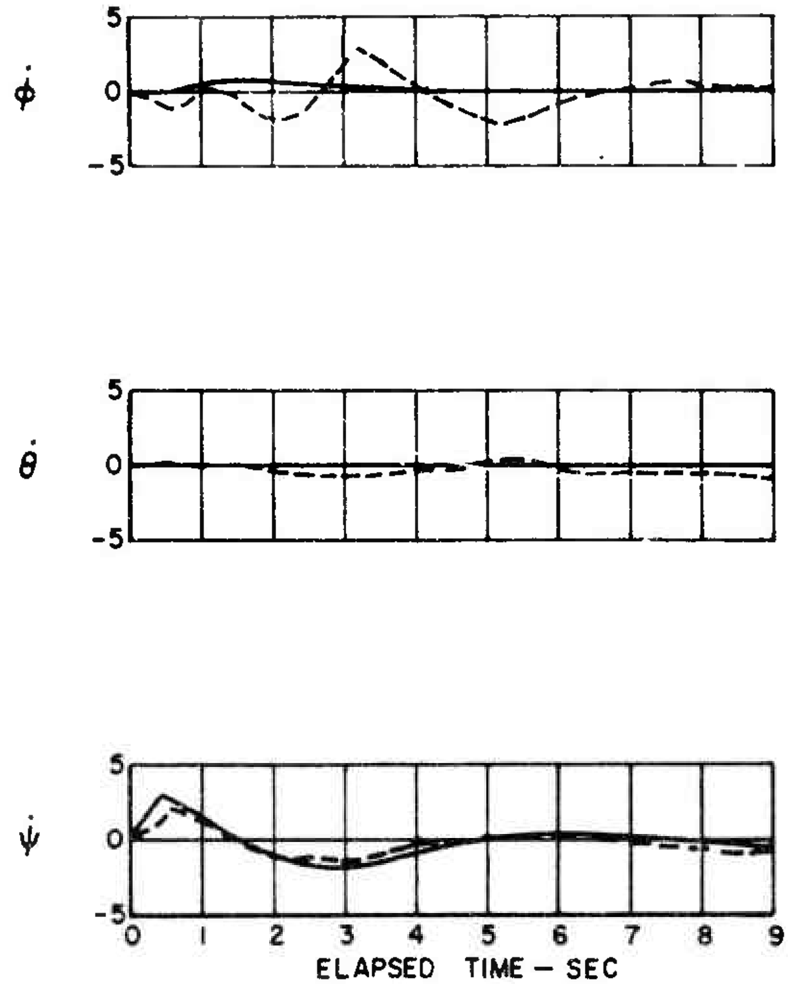

(c) ANGULAR RATES, DEG/SEC

Figure 4. Concluded.

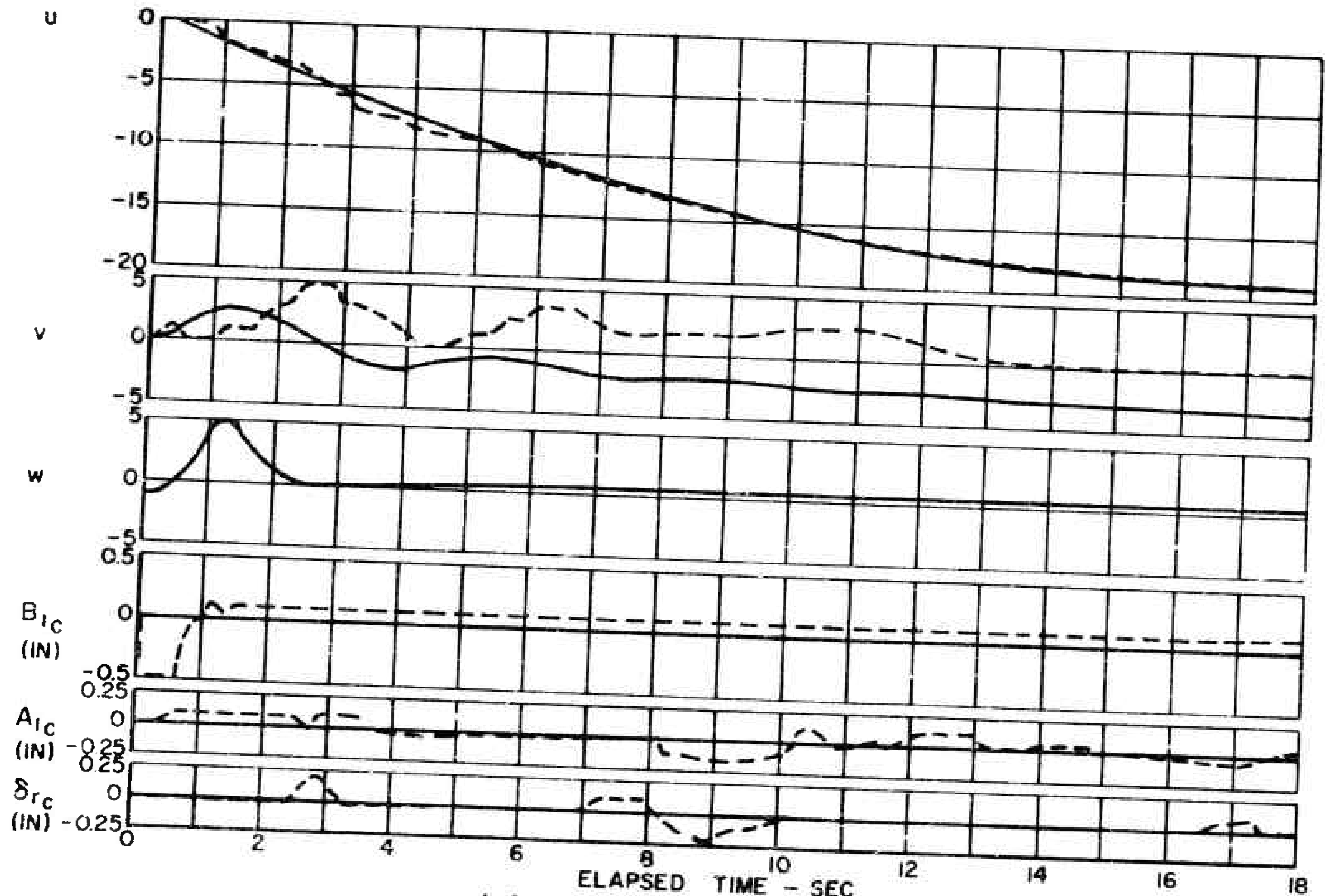

(a) PERTURBATION VELOCITIES, FT/SEC

Figure 5. Response of the Articulated Rotor Compound Helicopter Due to Pulse Input of the Longitudinal Control, B_{1c} = -0.5", V = 150 KTS.

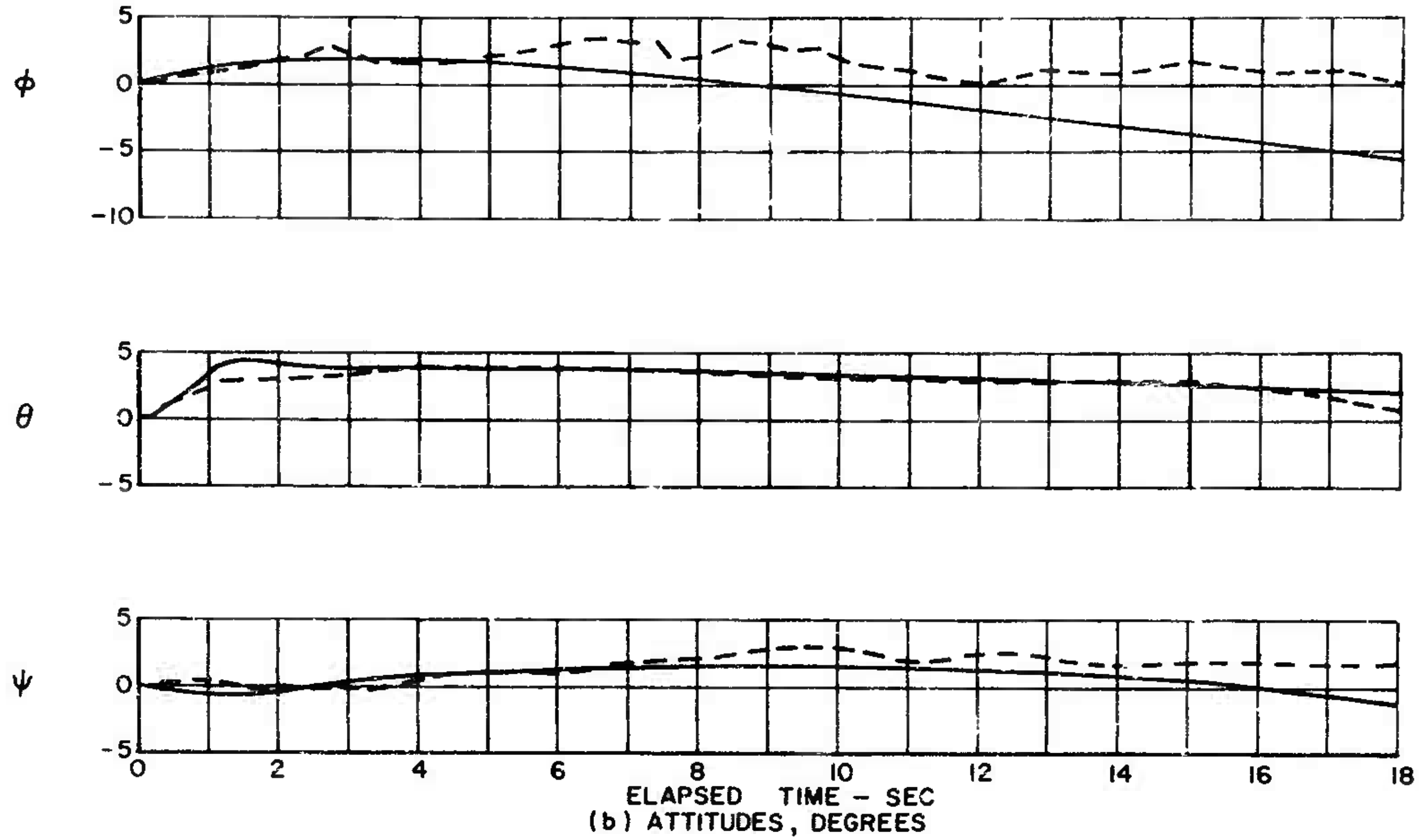

Figure 5. Continued.

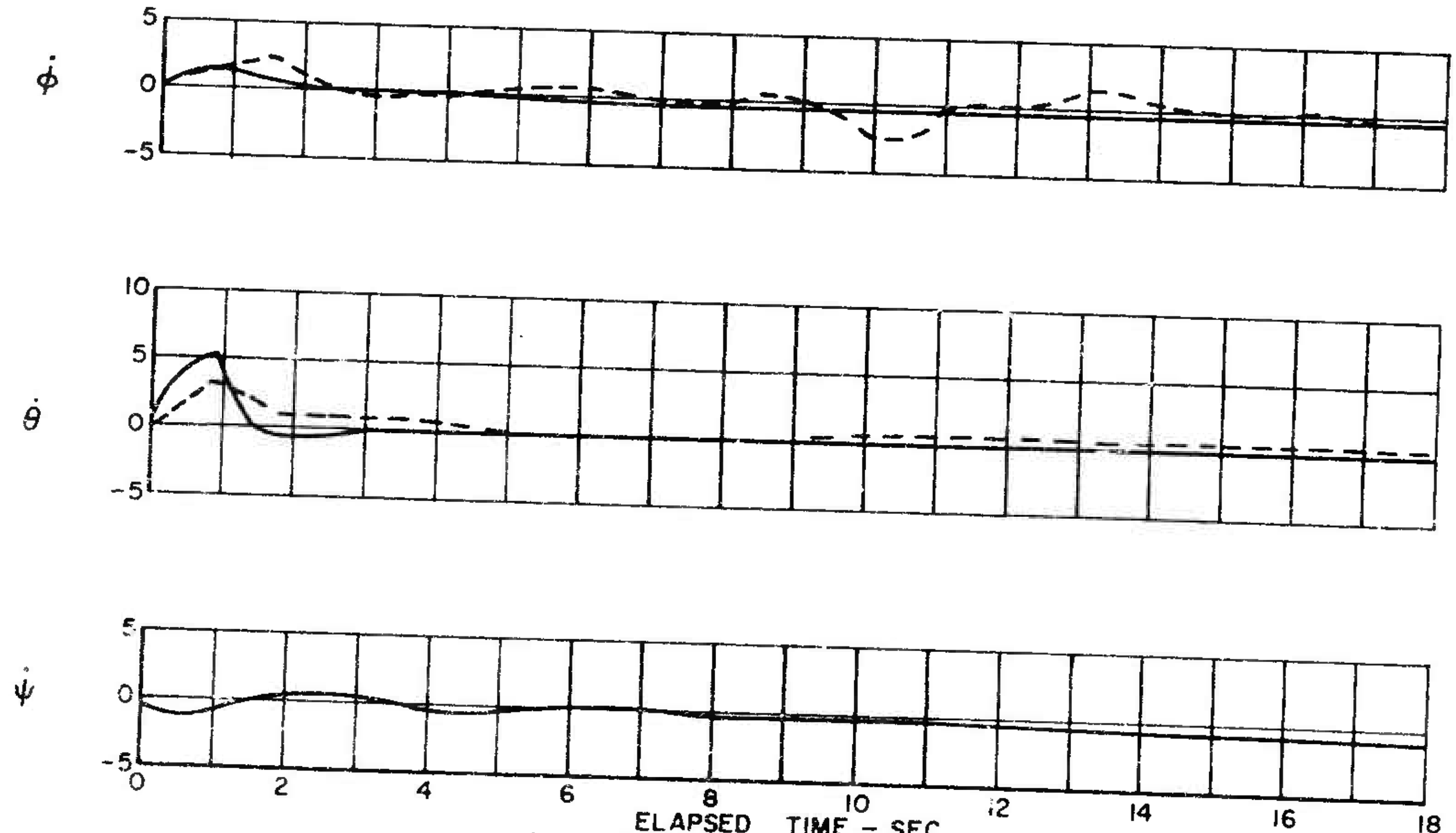

(c) ANGULAR RATES, DEG/SEC

Figure 5. Concluded.

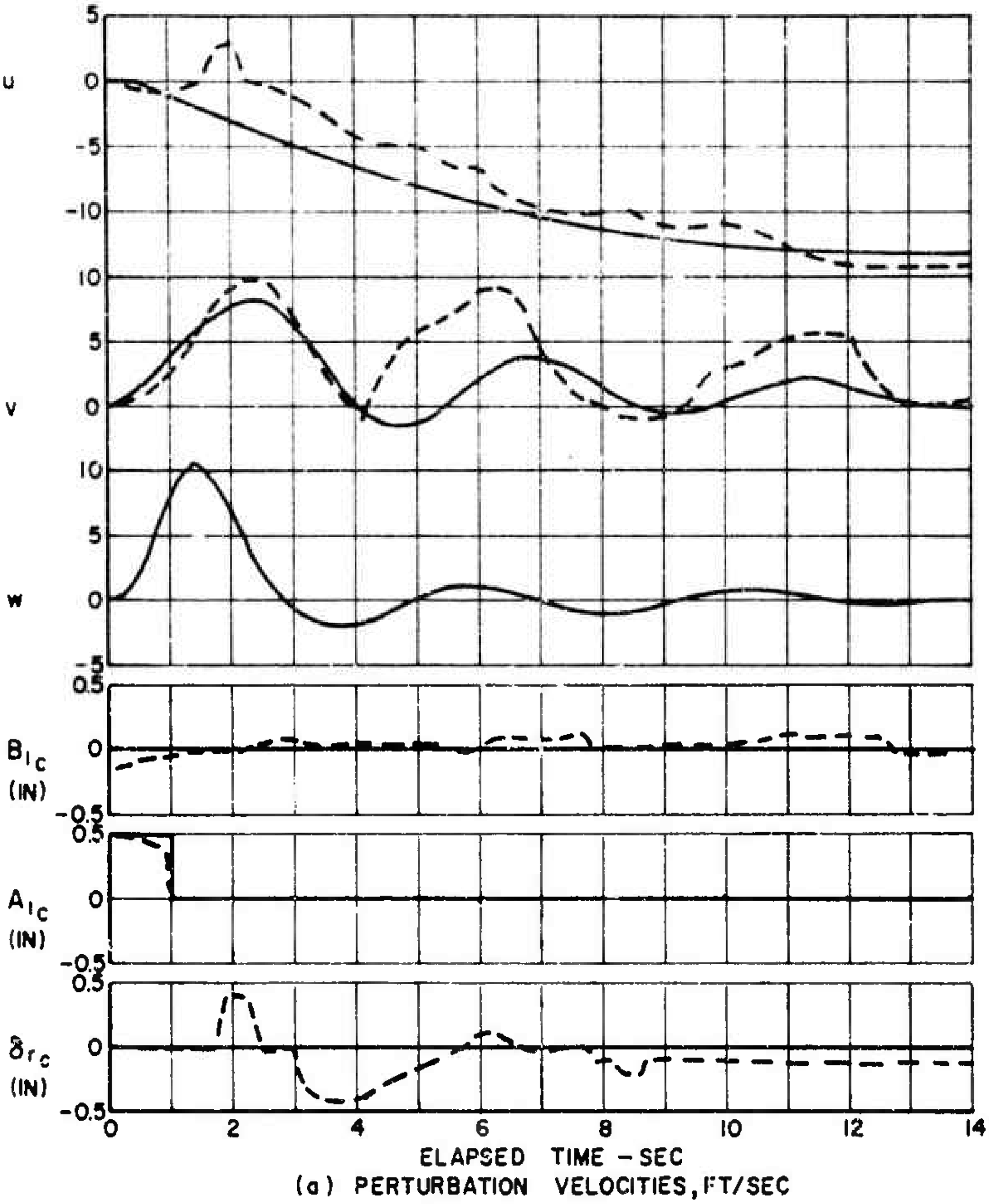

Figure 6. Response of the Articulated Rotor Compound Helicopter Due to Pulse Input of the Lateral Control A_{1c} = +0.5", V = 150 KTS.

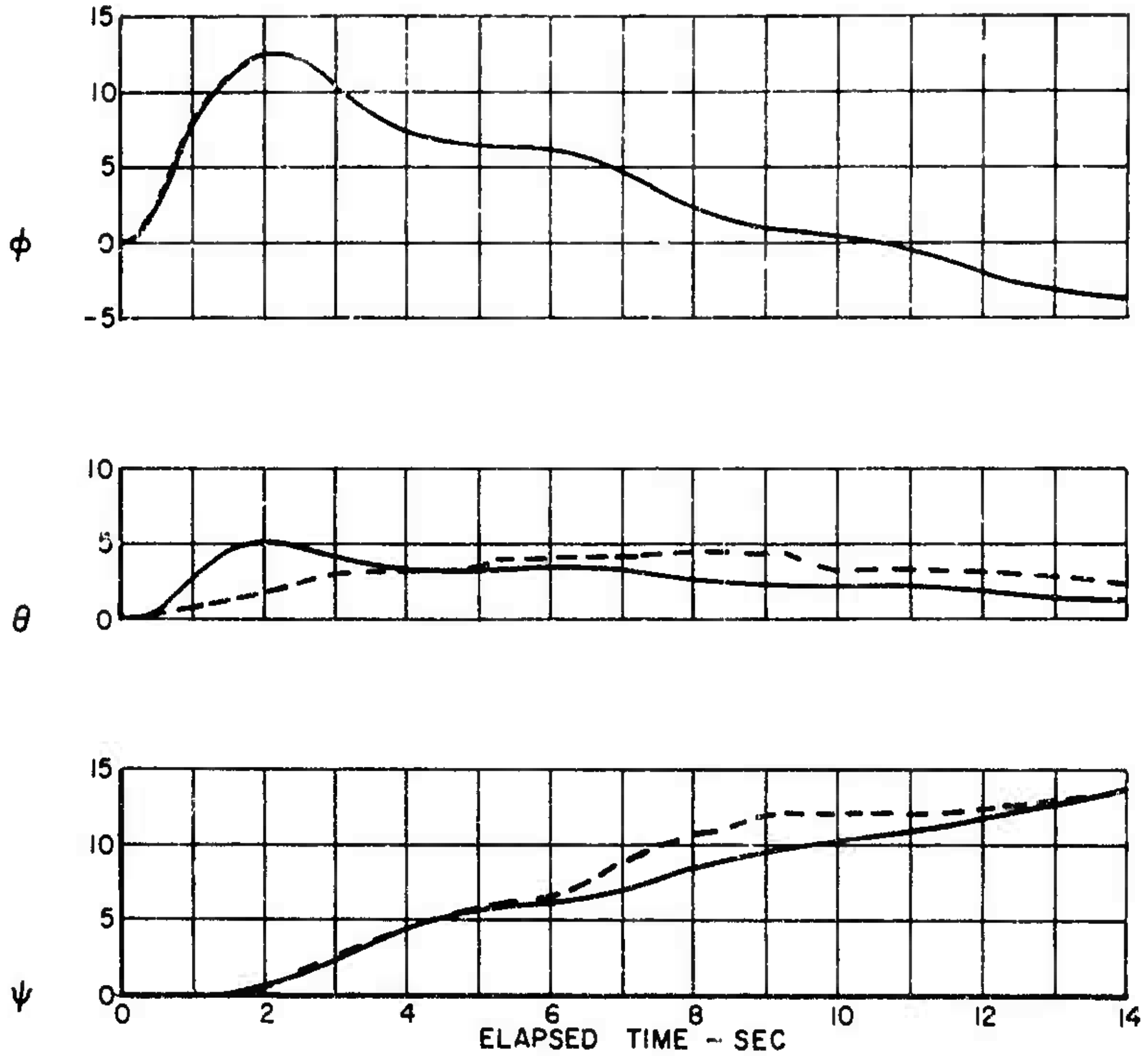

(b) ATTITUDES, DEGREES

Figure 6. Continued.

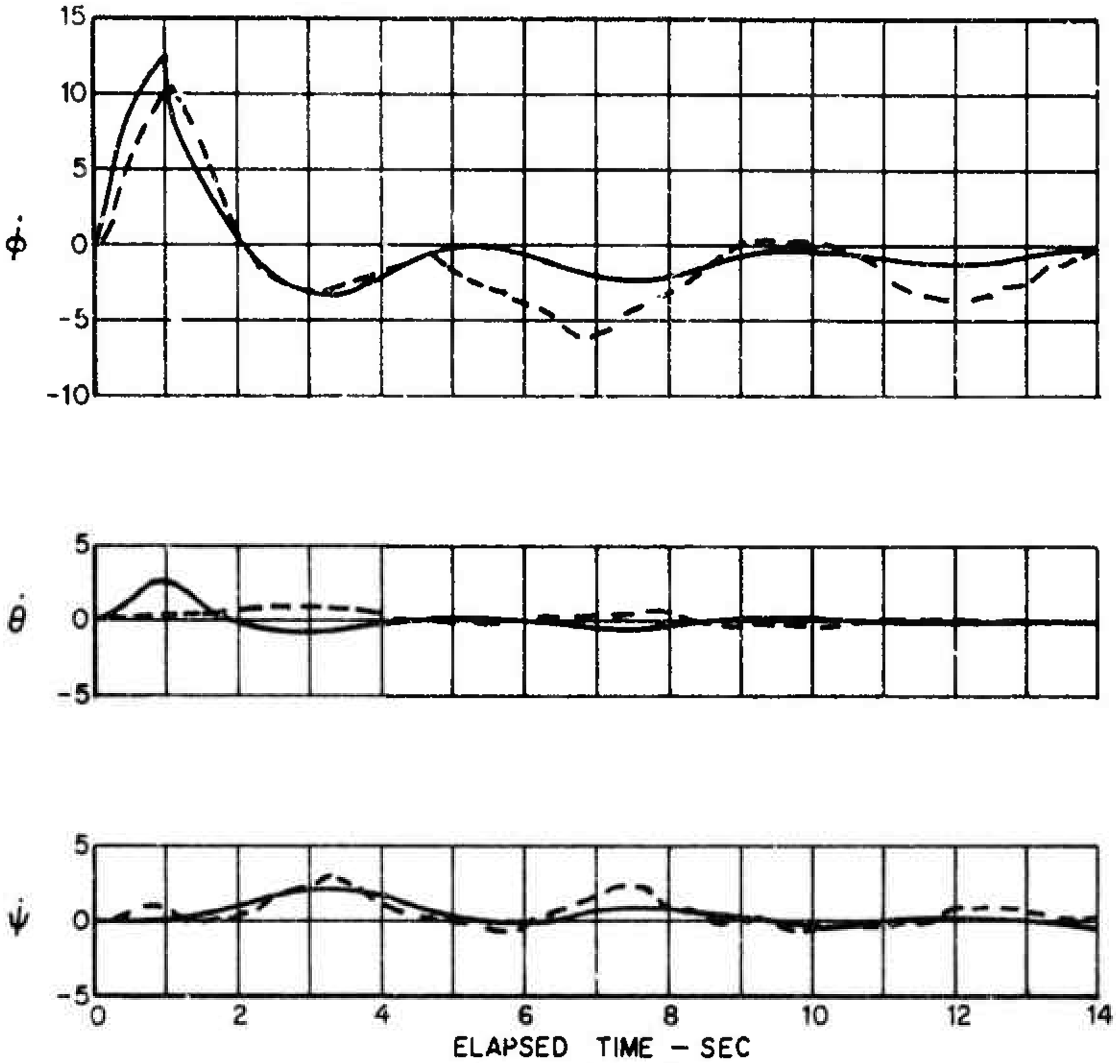

(c) ANGULAR RATES, DEG/SEC

Figure 6. Concluded.

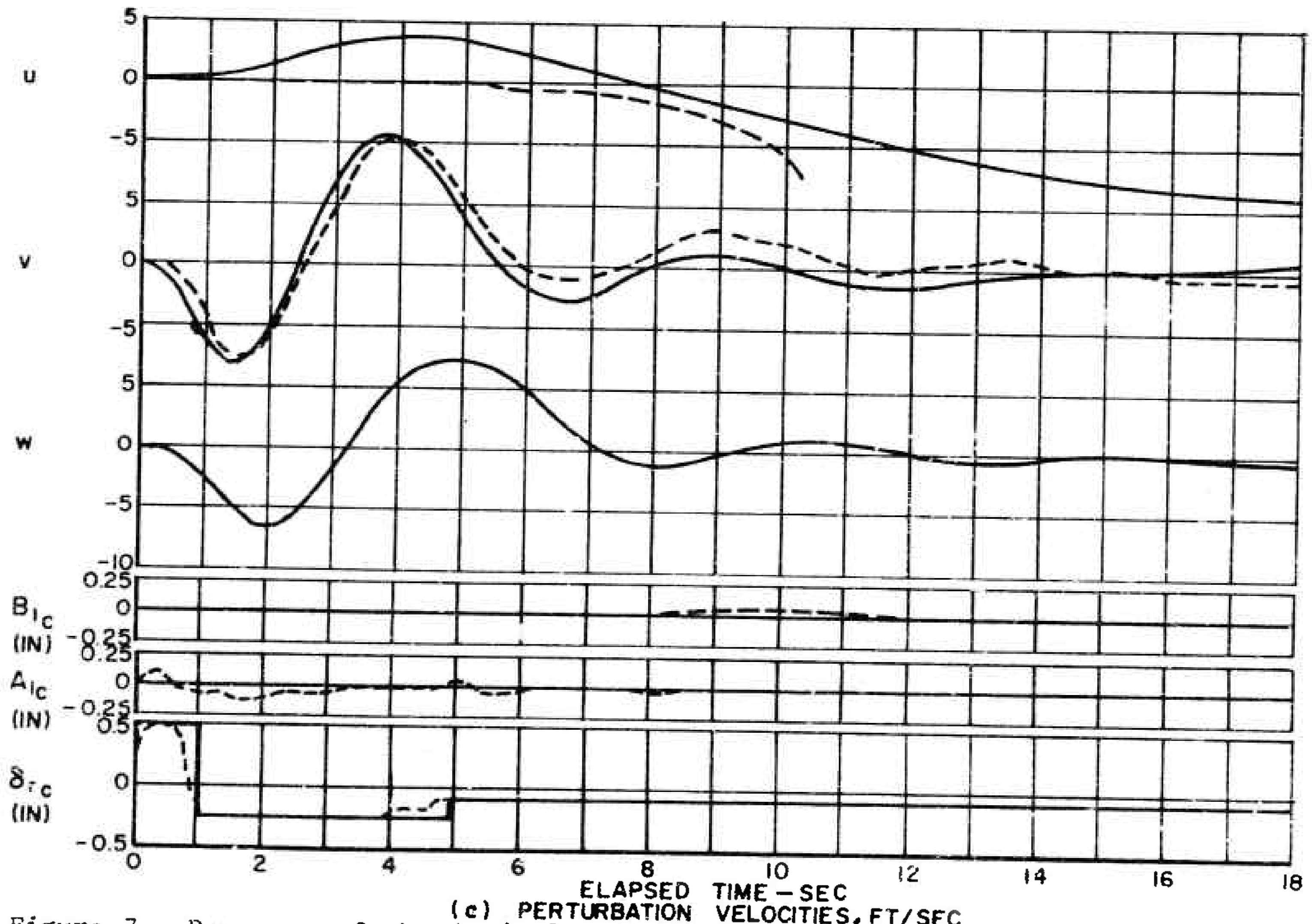

Figure 7. Response of the Articulated Rotor Compound Helicopter Due to Pulse Input of the Direction Control, δ_{rc} = +0.5", V = 150 KTS.

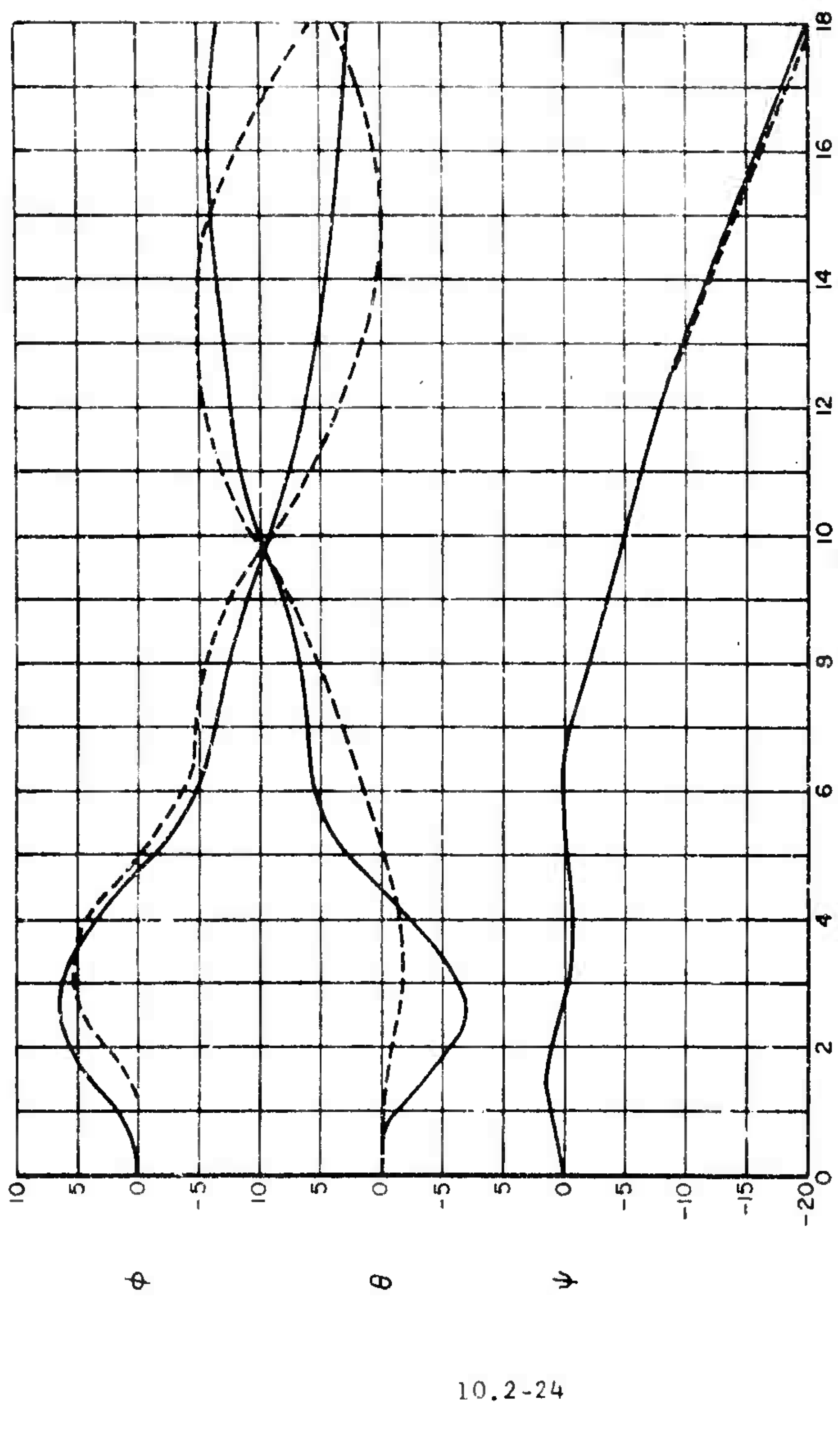

(b) ATTITUDES, DEGREES

Figure 7. Continued.

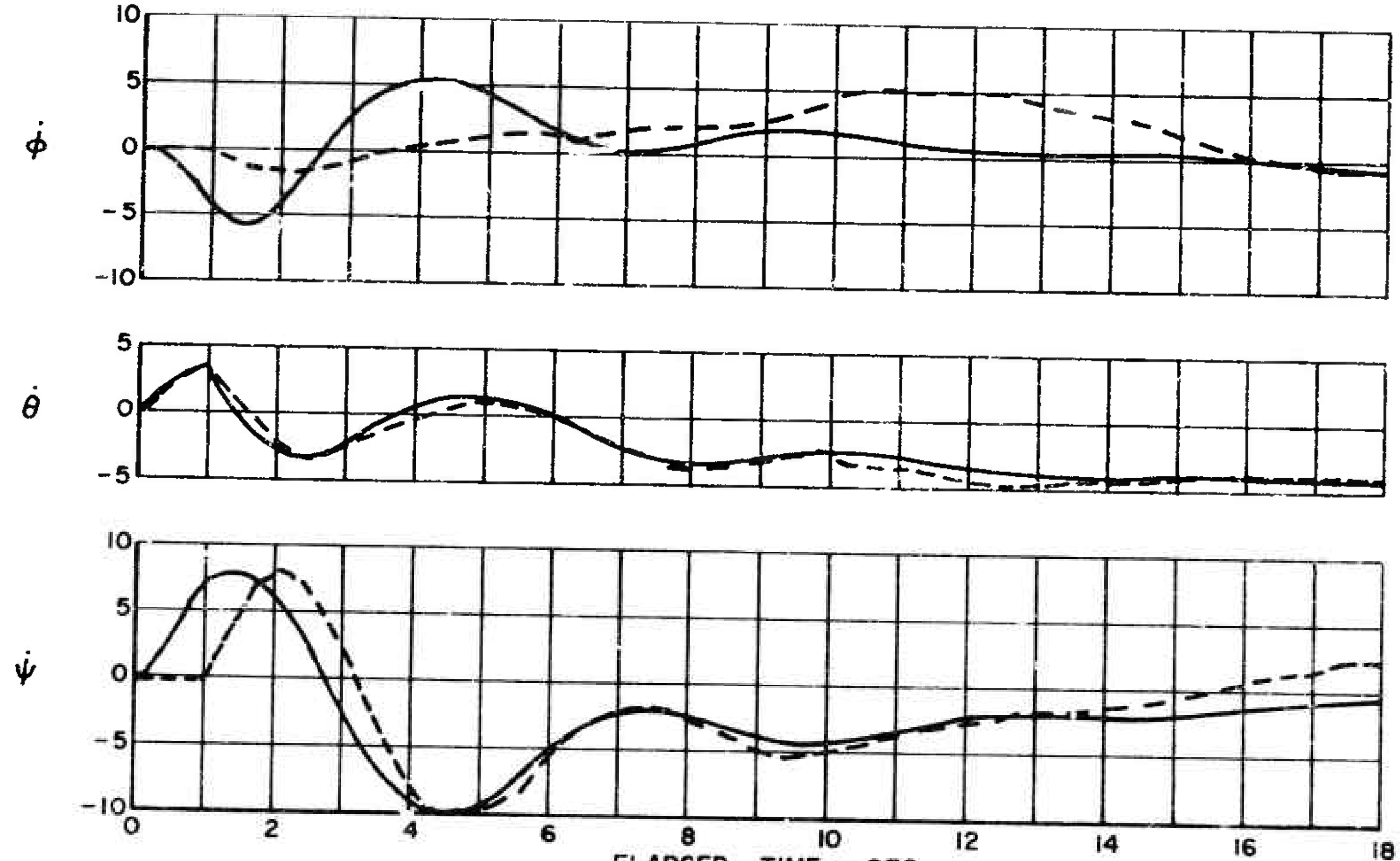

(c) ANGULAR RATES, DEG/SEC

Figure 7. Concluded

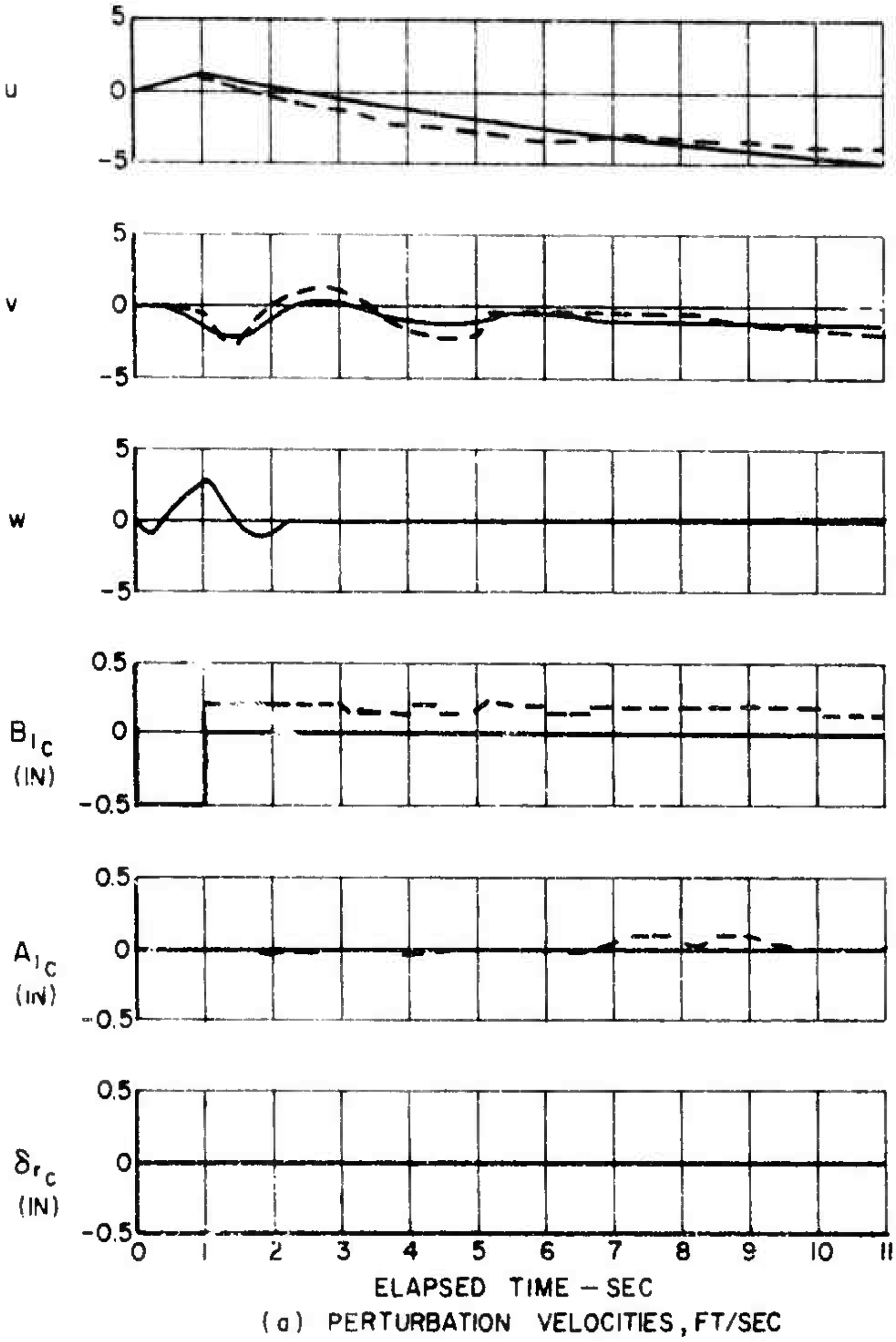

Figure 8. Response of the Articulated Rotor Compound Helicopter Due to Pulse Input of the Longitudinal Control, B_{1c} = -0.5", V = 180 KTS.

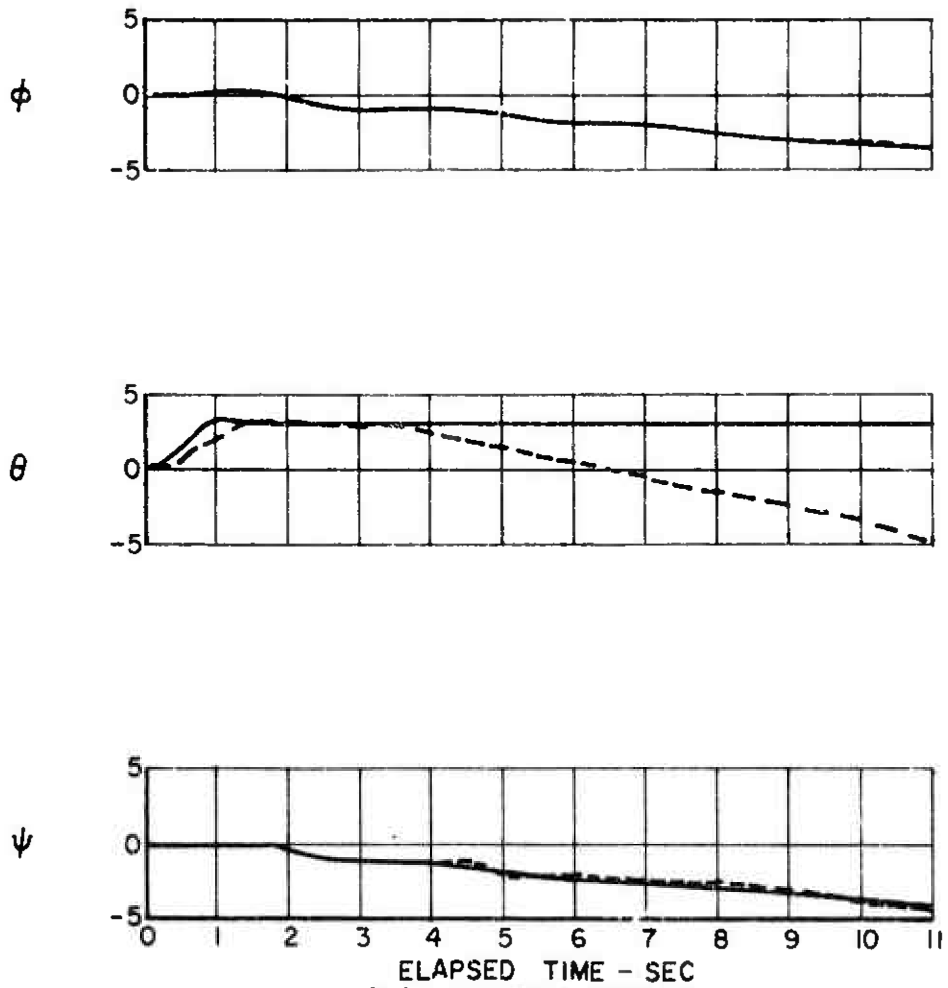

(b) ATTITUDES, DEGREES

Figure 8. Continued.

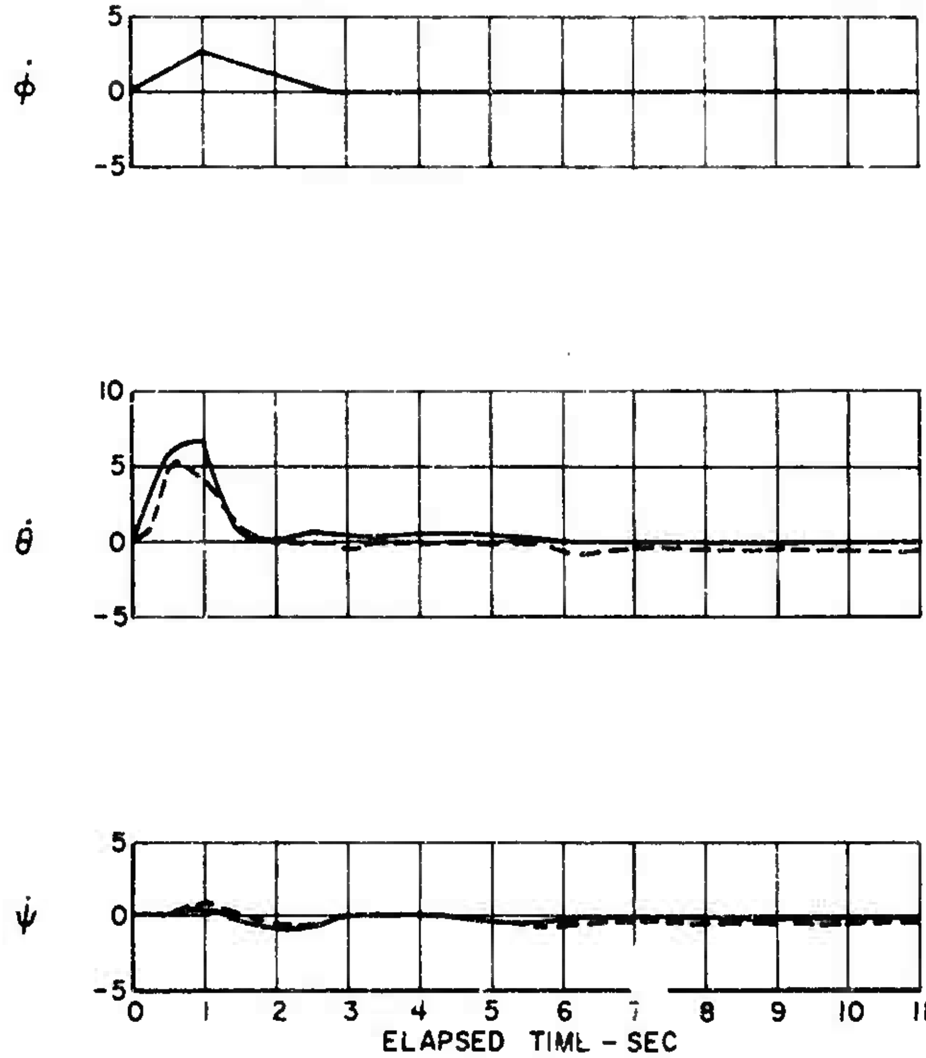

(c) ANGULAR RATES, DEG/SEC

Figure 8. Concluded.

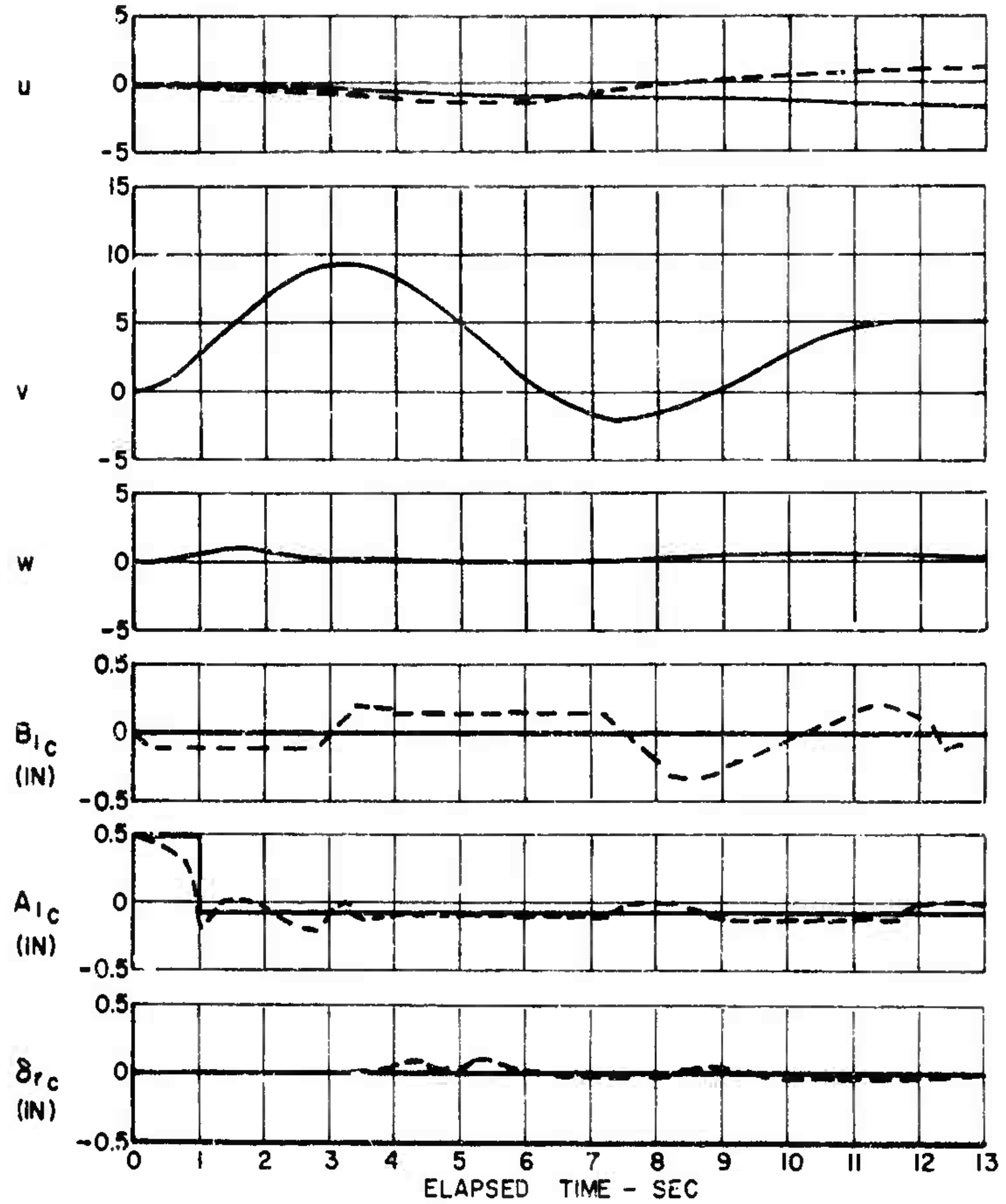

(a) PERTURBATION VELOCITIES, FT/SEC

Figure 9. Response of the Articulated Rotor Compound Helicopter Due to Pulse Input of the Lateral Control, A_{1_C} = +0.5", V = 150 KTS.

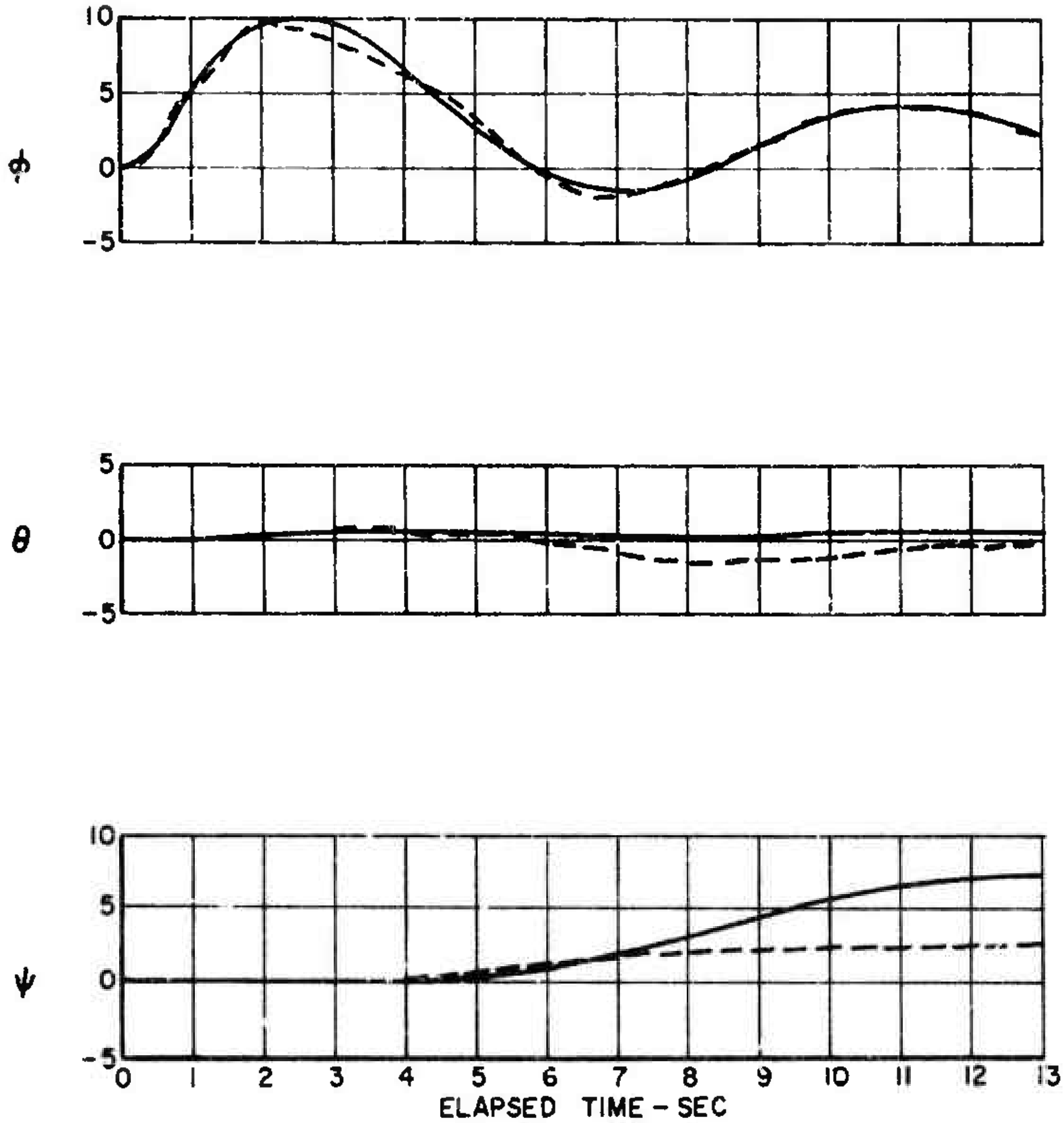

(b) ATTITUDES, DEGREES

Figure 9. Continued.

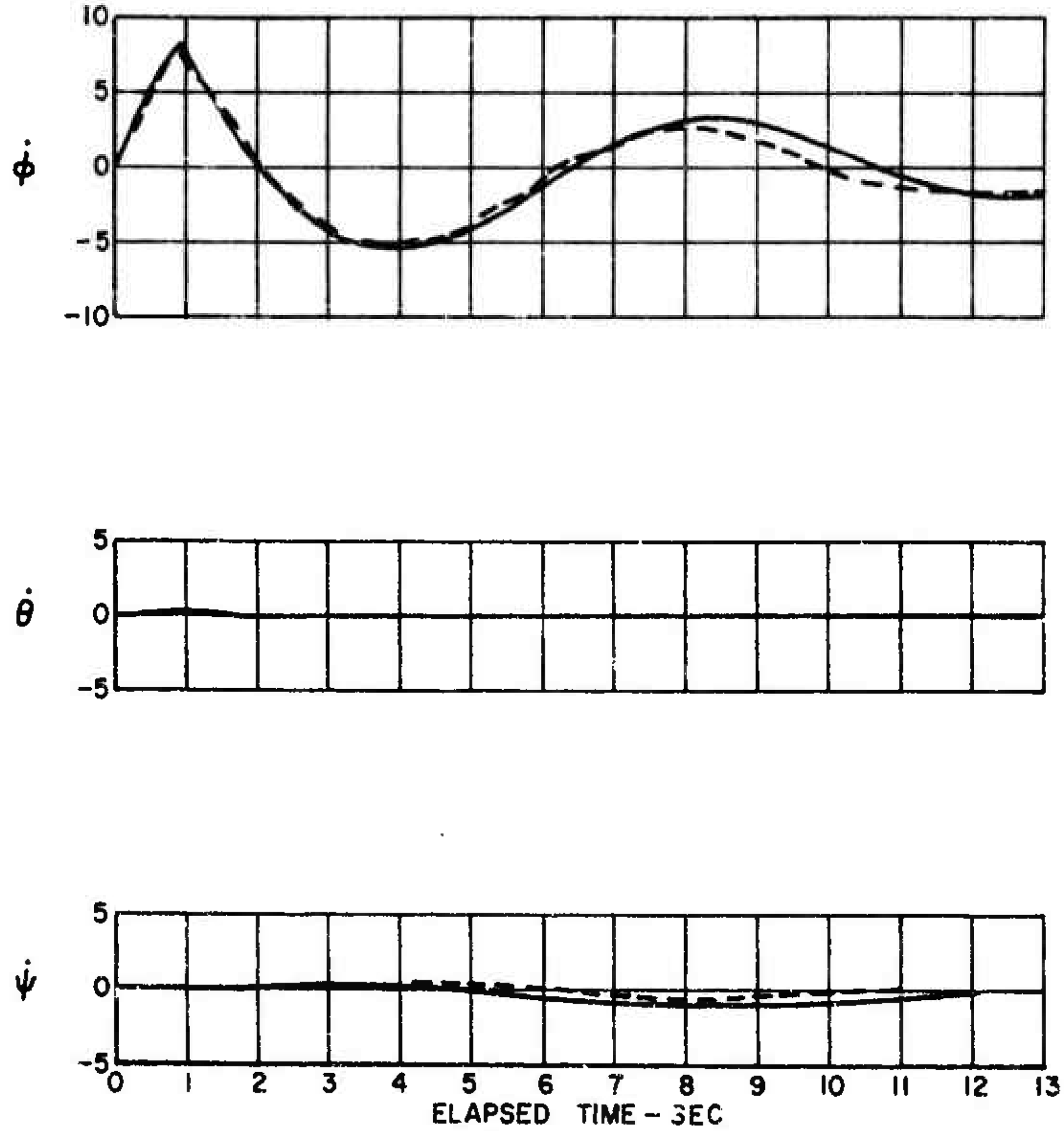

(c) ANGULAR RATES, DEG/SEC

Figure 9. Concluded.

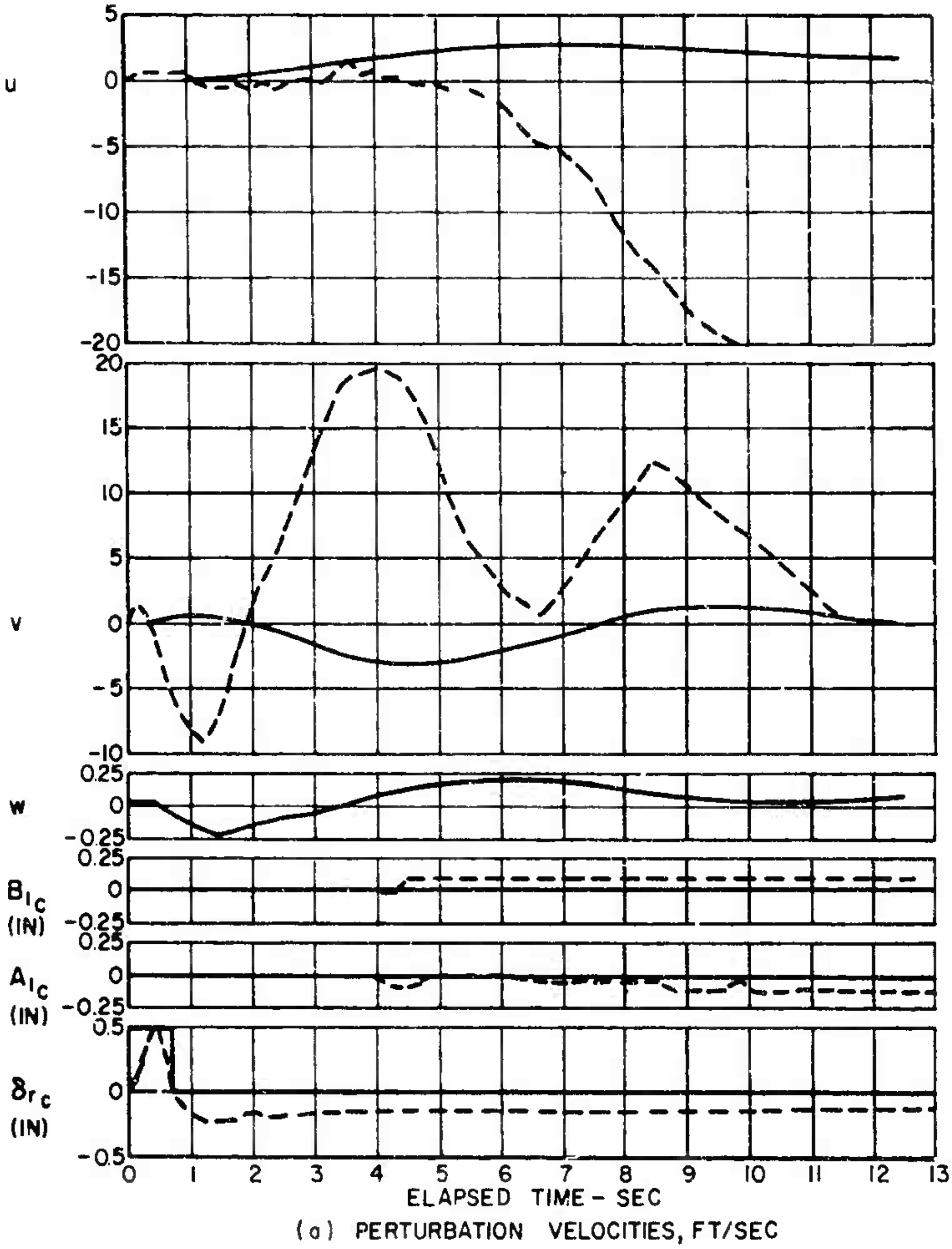

Figure 10. Response of the Articulated Rotor Compound Helicopter Due to Pulse Input of the Directional Control, δ_{r_c} = +0.5" (Ideal Pulse), V = 180 KTS.

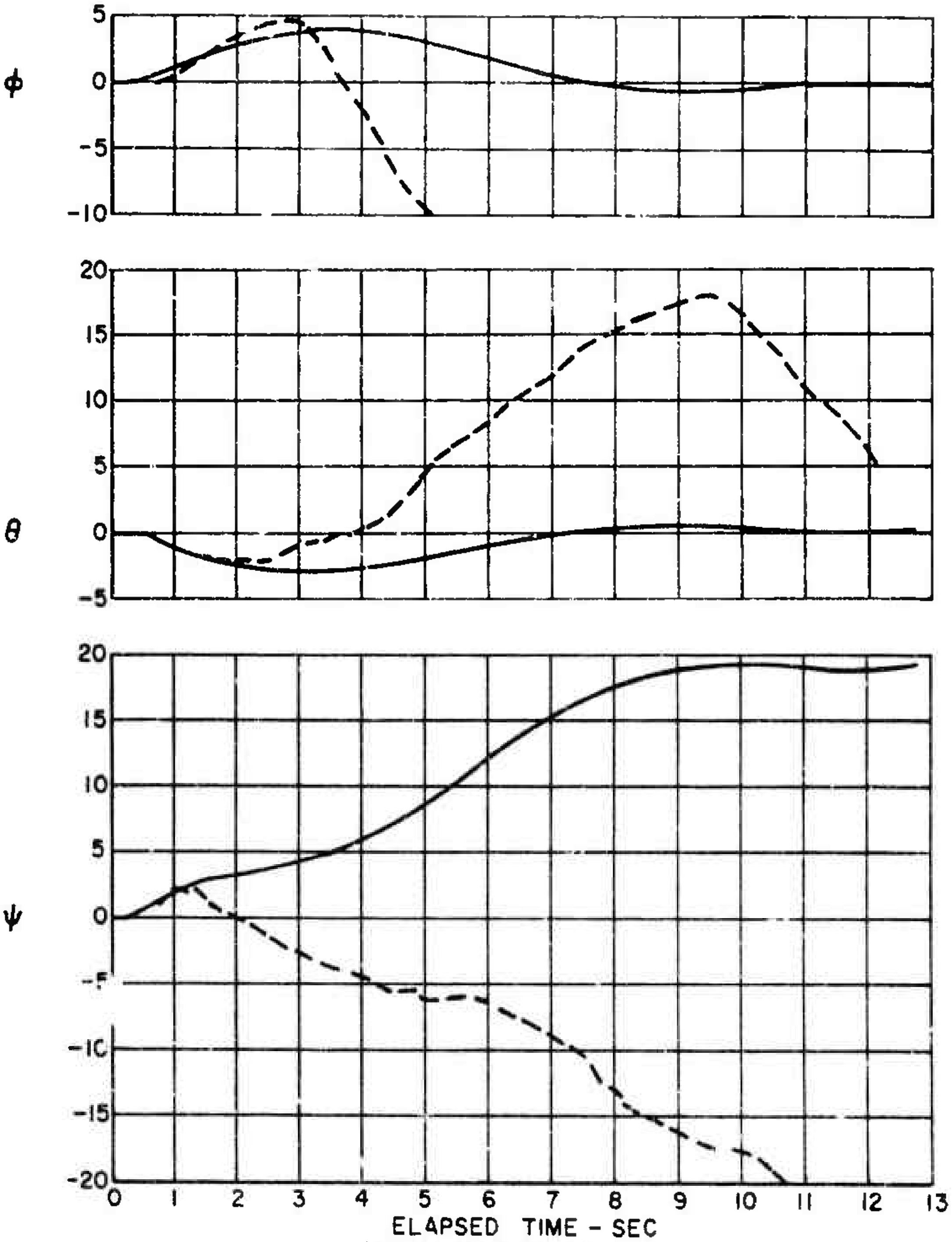

(b) ATTITUDES, DEGREES

Figure 10. Continued.

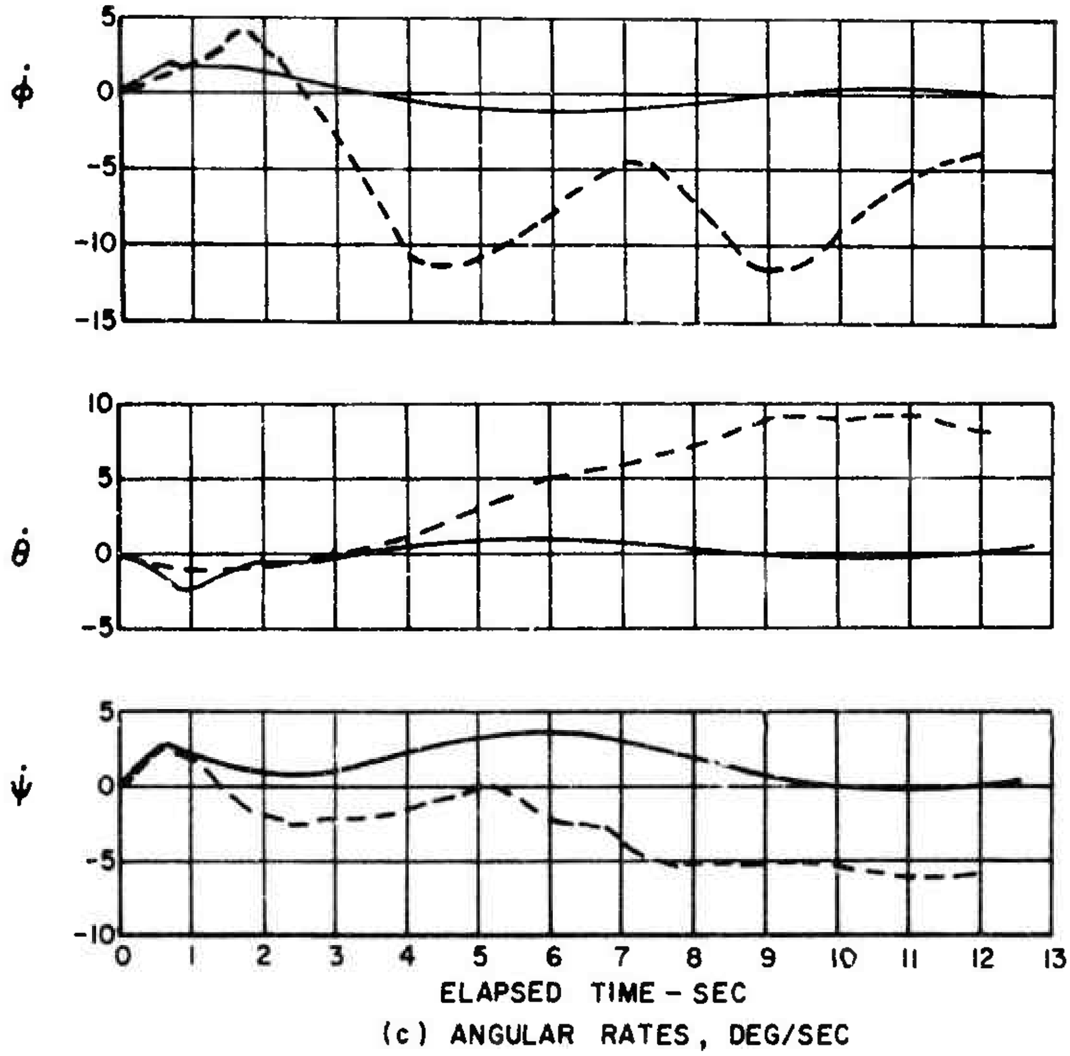

Figure 10. Concluded.

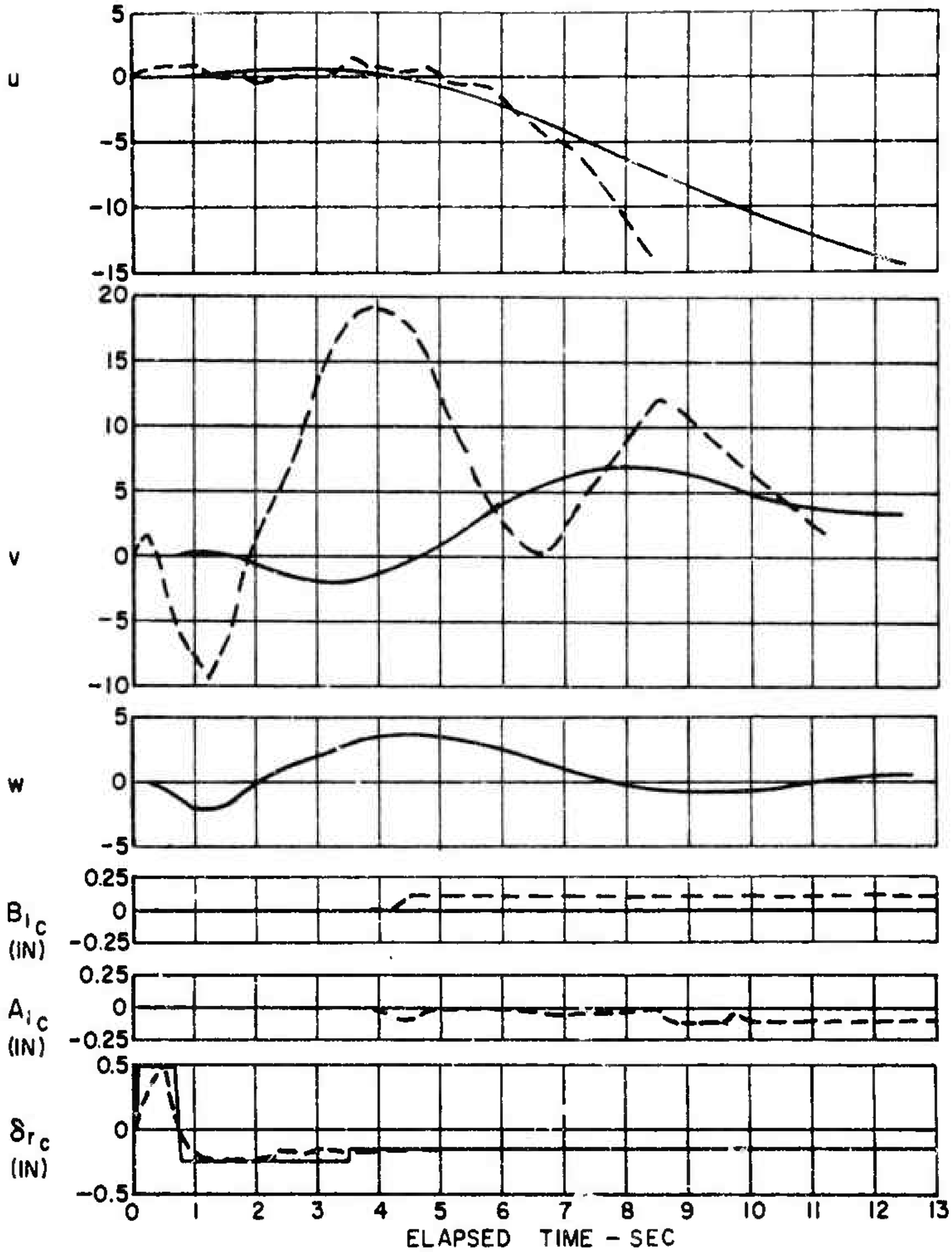

(a) PERTURBATION VELOCITIES, FT/SEC

Figure 11. Response of the Articulated Rotor Compound Helicopter Due to Pulse Input of the Directional Control, δ_{r_C} = +0.5" (Simulated Pulse), V = 180 KTS.

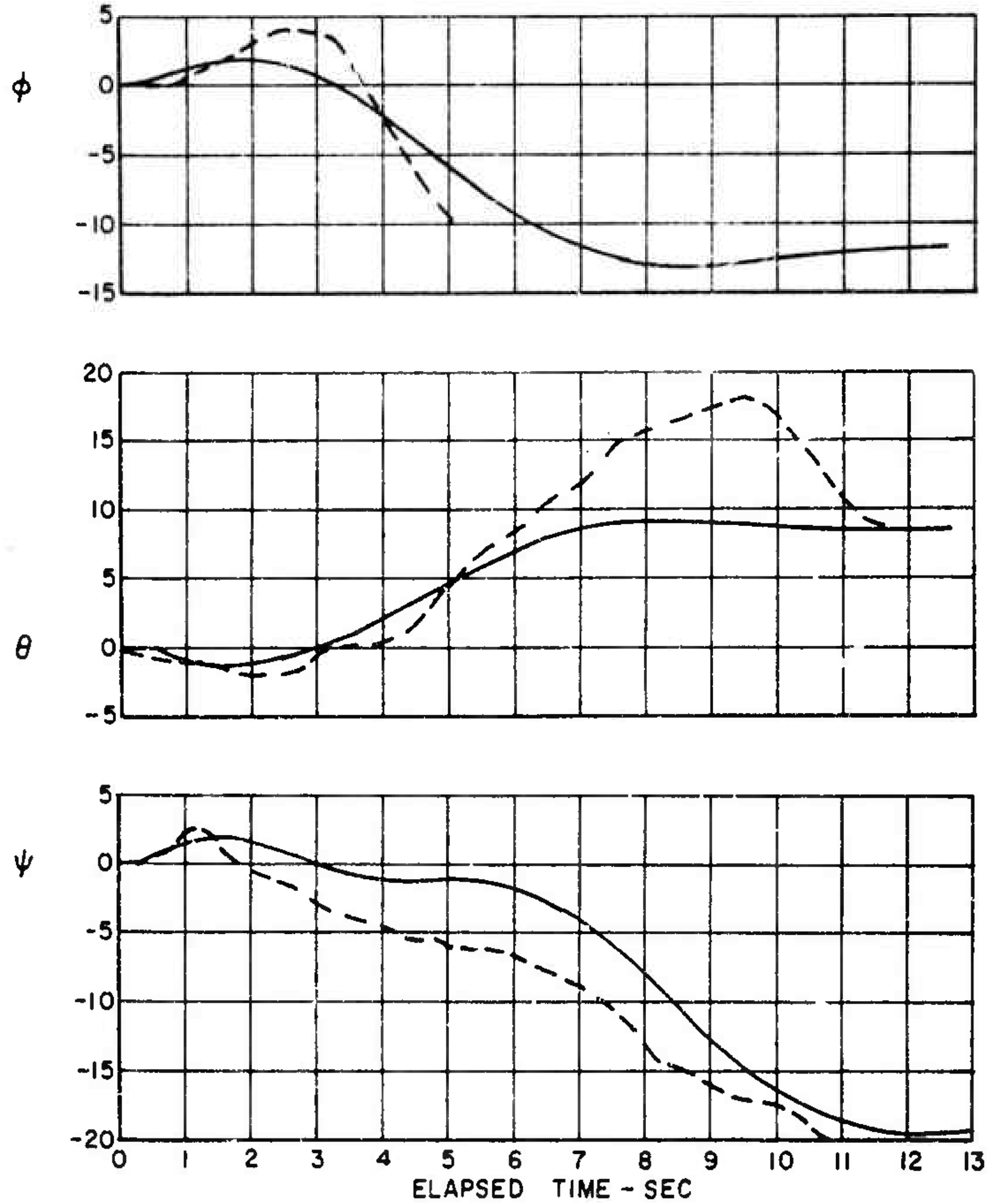

(b) ATTITUDES, DEGREES

Figure 11. Continued.

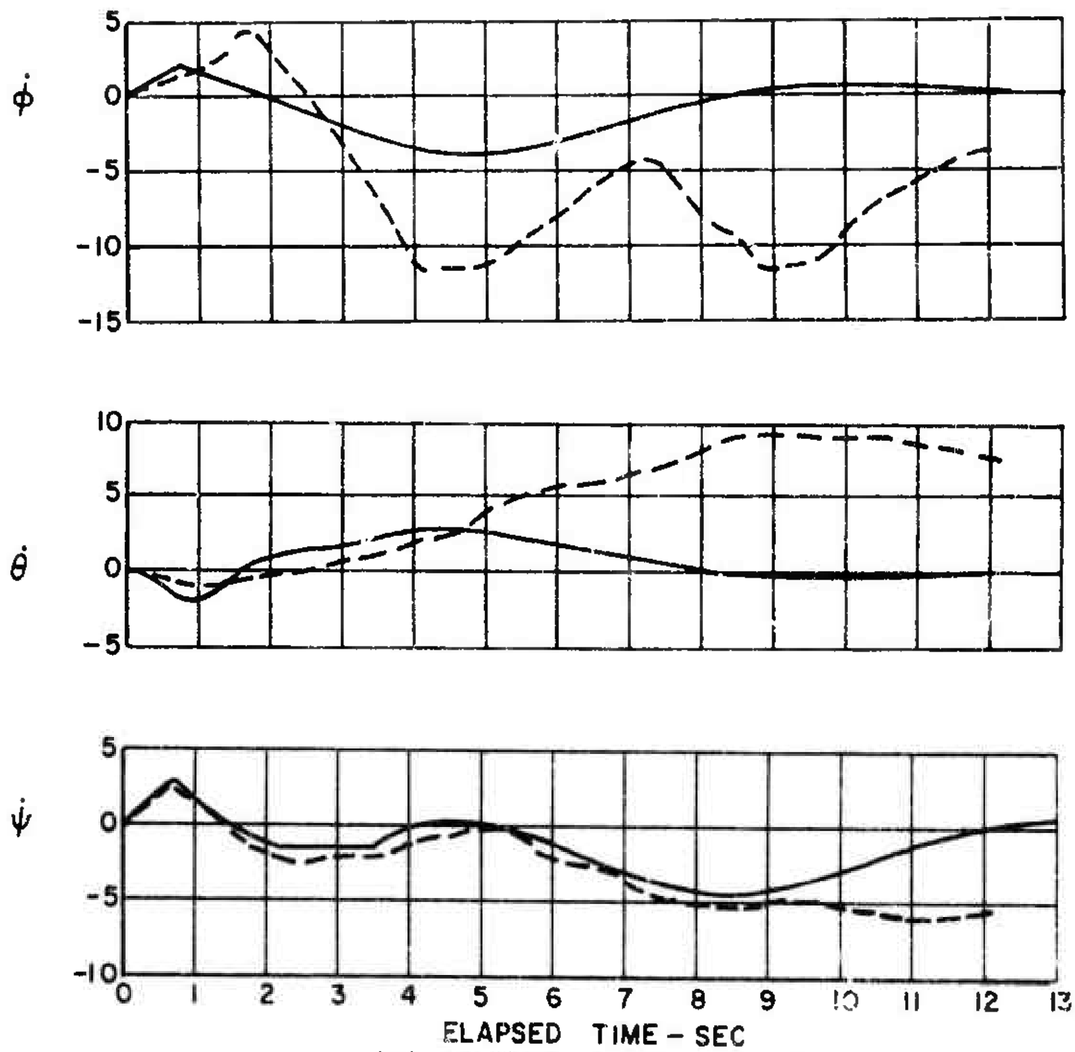

(c) ANGULAR RATES, DEG/SEC

Figure 11. Concluded.

Similar data for forward speeds of 150 and 180 knots are presented in the sets of Figures 5, 6, and 7 and Figures 8, 9, 10, and 11 respectively. Figures 10 and 11 show aircraft responses due to two different pulse inputs of the directional control δ_{r_C} at 180 knots. Figure 10 shows responses due to an "ideal" square pulse input, whereas in Figure 11 an attempt is made to simulate actual rudder control motion introduced by the pilot during the test program. Superimposed on all of these figures are the available flight test data obtained for the sample helicopter from Reference 1.

Furthermore, each figure shows the actual flight test control motions as applied by the pilot in addition to the pulse inputs used in the analog computer program. As can be noted from these figures, the pilot was not always able to apply one control at a time, holding other controls fixed at neutral positions. As a result while applying one specific control motion, excursions from neutral of the other controls were introduced. These excursions of other control motions were not simulated in the analog computer program; consequently, poorer correlation is expected of the analog results based on a single control disturbance with the corresponding data where more than one control motion was unintentionally applied.

A good example of this can be seen in Figure 6 in which the effect of a one-half-inch right lateral stick pulse (A_{1_C}) is examined. Although the analog and flight test (A_{1_C})^{C} control motions are closely duplicated, the rudder control excursions (δ_{r_C}) are even more violent than the A_{1_C} pulse. Also, the longitudinal control (B_{1_C}), which is relatively steady for this flight test, is varying forward and aft up to $\pm 20\%$ of the magnitude of the A_{1_C} pulse. Thus, as can be seen from Figure 6, the correlation between the analog computer results and the flight test data is only fair. For a true assessment of the correlation achieved between the theory and the flight test data in this case, it would be necessary to feed control motions to all three axes into the analog computer. This could be achieved using curve followers to exactly duplicate the flight test control motions.

Figures 10 and 11 illustrate an attempt to partially match the analog control input δ_{r_C} with the flight test control input. Figure 10 shows that a simple square pulse does not yield good correlations for any of the measured responses. However, in Figure 11, where the two steps to the control input after the pulse are added, the correlation between the theory and the flight test is substantially improved.

If the longitudinal and lateral controls of 0.1" forward step at 4.3 second and 0.1" left step after nine seconds respectively, were simultaneously applied, even better correlation would be achieved.

Despite the difficulty of maintaining and simulating the flight test control motions, satisfactory to good correlations are generally obtained between the analog computer results and the corresponding full-scale flight test data.

A summary of the correlations achieved for this sample compound helicopter is presented in Table VI. The same rating system as in Section 10.1 is herein used. It should be noted that an attempt was made to exactly match the control inputs in Figures 7, 8, and 11 and that only the results from Figure 11 are evaluated in Table VI. Also, where control excursions took place for other controls than the one whose effect was being examined, the correlation was judged before the secondary flight test control excursions could have a significant effect on the aircraft responses.

For all these cases, the correlation obtained between the theoretical and the flight test responses is excellent. The previously noted trend for the degree of correlation to improve with the higher speed cases is not evident for this set of data. However, where poor correlation occurred it was usually a result of improper estimates of cross-coupling effects as discussed in the previous section.

Nevertheless, the theoretical methods presented in this handbook appear to be more than adequate for predicting the full-scale flight test responses due to control motions for the sample articulated rotor compound helicopter.

TABLE VI

SUMMARY OF CORRELATION OBTAINED BETWEEN THEORETICAL AND FLIGHT TEST RESPONSES FOR THE ARTICULATED ROTOR COMPOUND HELICOPTER

Control Pulse	Vo (Kn)	Parameter									Figure Number
		u	v	w	ϕ	θ	ψ	$\dot{\phi}$	$\dot{\theta}$	$\dot{\psi}$	
B_{1c}	125	VG	P	---	G	G	E	G	E	VG	2
	150	E	F	---	P	E	VG	G	VG	---	5
	180	E	E	---	---	VG	E	---	VG	E	8*
A_{1c}	125	G	---	---	G	F	E	E	---	E	3
	150	G	P	---	E	G	E	VG	G	VG	6
	180	G	---	---	E	G	E	E	---	E	9*
δ_{r_c}	125	F	E	---	G	P	G	F	E	E	4
	150	P	E	---	VG	F	E	VG	P	E	7*
	180	G	P	---	F	G	VG	F	G	E	11*

* CONTROL PULSES MATCHED

CORRELATION RATINGS: E-excellent
VG-very good
G-good
F-fair
P-poor

LITERATURE CITED

1. Bain, Lawrence J., and Landgrebe, Anton J., INVESTIGATION OF COMPOUND HELICOPTER AERODYNAMIC INTERFERENCE EFFECTS. Sikorsky Aircraft Division, United Aircraft Corporation, USAAVLABS Technical Report 67-44, U. S. Army Aviation Materiel Laboratories, Fort Eustis, Virginia, November 1967, AD665427.

10.3 DYNAMIC STABILITY RESPONSES OF A HINGELESS ROTOR COMPOUND HELICOPTER

10.3.1 Description of the Sample Compound Helicopter

The compound helicopter considered in this section is the hingeless rotor research vehicle illustrated in Figure 1. This aircraft was developed from a medium utility-type helicopter, principally by adding a 70-square-foot wing and an auxiliary jet engine to the port side of the fuselage. The four-bladed main rotor has a hingeless hub, whereas the two-bladed tail rotor has a teetering hub. A mechanical control gyro mounted on the main rotor hub acts as a two-axis stabilization system. This aircraft uses only convention helicopter controls throughout its operational speed range. A summary of the pertinent design parameters is presented in Table I.

To facilitate the dynamic stability and control computations, the hingeless rotor was mathematically represented as an equivalent flapping rotor with a hinge offset of $e_v = 1.91$, as calculated using the methods described in Section 5.2. For these calculations, the first natural bending frequency of the rigidly attached elastic blade was taken from Reference 1 as $\omega_1 = 1.088\,\Omega$. Furthermore, the gyro stabilizer was modeled as a mechanical gyro with two-axis acceleration feedback such as a Bell bar or Hiller control rotor.

For correlation purposes, the operating condition assumed in these sample calculations correspond to forward speeds of 158, 193, and 221 knots and air density ratios of $\rho/\rho_0 = 0.813$, $\rho/\rho_0 = 0.796$, and $\rho/\rho_0 = 0.801$ respectively. The rotor tip speeds assumed were $\Omega R = 669.5$ ft/sec at 158 and 193 knots and $\Omega R = 663$ ft/sec at 221 knots.

10.3.2 Analog Computer Program

The analog computer program for this compound helicopter was developed utilizing the total stability derivatives presented in Tables II, III, and IV. These derivatives were obtained using the design parameters given in Subsection 10.3.1 and the methods described in this report. The analog computer schematic diagram representing the equations of motions for this aircraft is shown in Figure 2. The settings of the potentiometers P and Q shown in Figure 2 are presented in Tables V, VI, and VII for the 158, 193, and 221 knots respectively. These

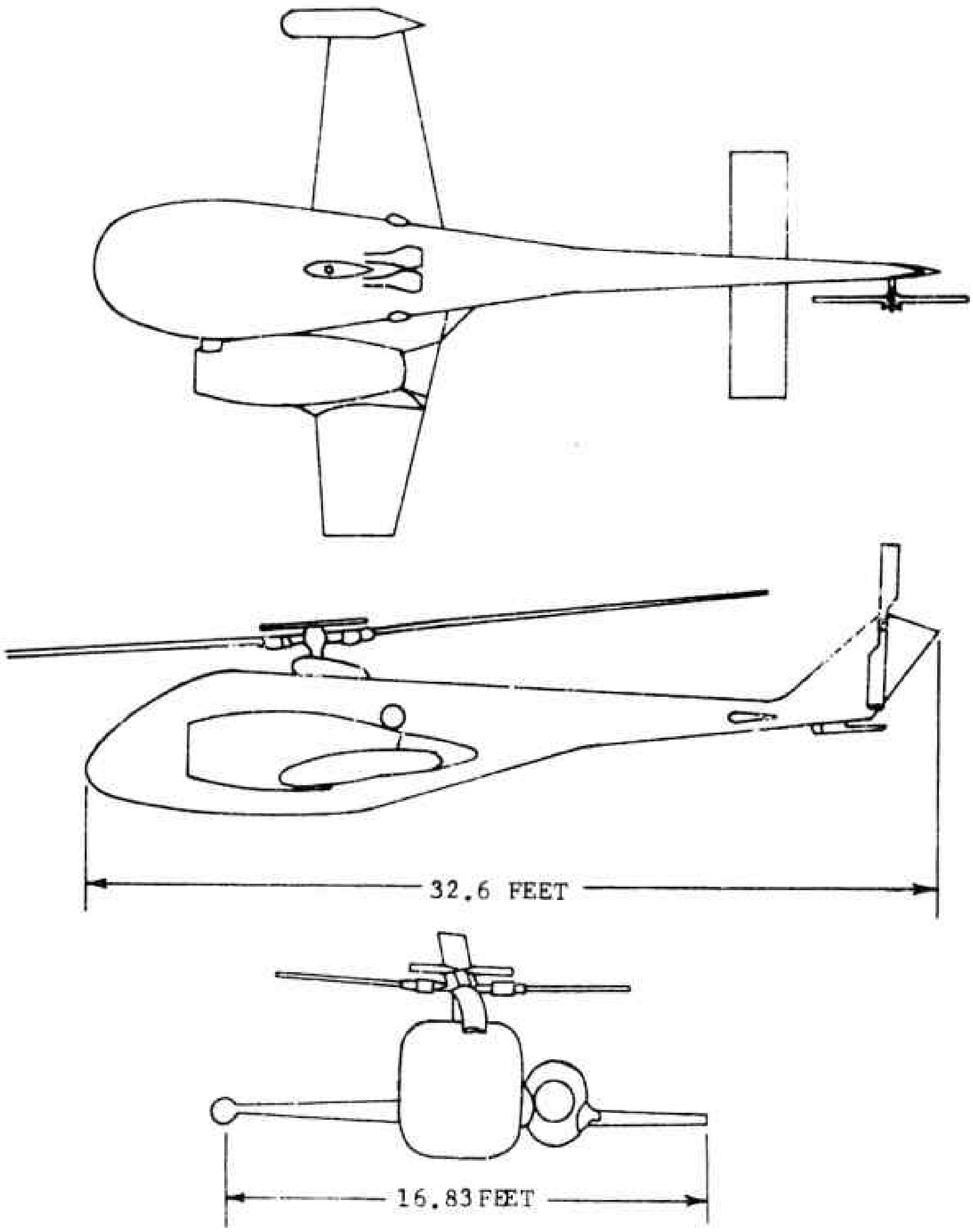

Figure 1. Sample Hingeless Rotor Compound Helicopter General Arrangement.

TABLE I

DESIGN PARAMETERS FOR HINGELESS ROTOR COMPOUND HELICOPTER

Main Rotor	Tail Rotor	Fuselage	Auxiliary Jet
$\theta_{1_F} = -5^\circ$	$\theta_{1TR} = -4.35^\circ$	$W = 4500$ lb	$n = 1$
$a_F = 5.73$	$a_{TR} = 5.73$	$A_{X_{FUS}} = 21.49$ ft^2	$i_P = 7^\circ$
$i_F = -6^\circ$	$i_{TR} = 0^\circ$	$A_{Y_{FUS}} = 84.08$ ft^2	$A_{ii} = 2$ ft^2
$b_F = 4$	$b_{TR} = 2$	$A_{Z_{FUS}} = 76.66$ ft^2	$R_{ii} = 0.80$ ft
$R_F = 17.5$ ft	$R_{TR} = 3$ ft	$\ell_{FUS} = 32.6$ ft	$\ell_{X_P} = 1.32$ ft
$e_{V_F} = 1.91$ ft	$e_{TR} = 0$		$\ell_{Y_P} = -3.26$ ft
$\sigma_F = 0.0818$	$\sigma_{TR} = 0.1503$		$\ell_{Z_P} = 0.75$ ft
$\gamma_F = 5.183$	$\gamma_{TR} = 1.88$		
$\ell_{X_F} = -0.318$ ft	$\ell_{X_{TR}} = -21.48$ ft		
$\ell_{Y_F} = 0.318$ ft	$\ell_{Y_{TR}} = -0.683$ ft		
$\ell_{Z_F} = -3.33$ ft	$\ell_{Z_{TR}} = -3.86$ ft		
$M_{S_F} = 21.38$ slug-ft			

TABLE I - Concluded

Wing	Horizontal Tail	Vertical Tail
$a_W = 3.93$	$a_T = 3.73$	$a_{VT} = 1.33$
$i_W = -0.9^\circ$	$i_T = -0.25^\circ$	$i_{VT} = -5.6^\circ$
$(AR)_W = 4.05$	$(AR)_T = 4.1$	$(AR)_{VT} = 0.95$
$S_W = 70\ ft^2$	$S_T = 19.8\ ft^2$	$S_{VT} = 12.68\ ft^2$
$\ell_{X_W} = 0.57\ ft$	$\ell_{X_T} = -15.89\ ft$	$\ell_{X_{VT}} = -20.4\ ft$
$\ell_{Y_W} = -0.10\ ft$	$\ell_{Y_T} = 0.32\ ft$	$\ell_{Y_{VT}} = 0.32\ ft$
$\ell_{Z_W} = 1.67\ ft$	$\ell_{Z_T} = -0.83\ ft$	$\ell_{Z_{VT}} = -2.37\ ft$
$\alpha_{o_W} = -1.15^\circ$	$\alpha_{o_T} = 0^\circ$	$\alpha_{o_{VT}} = -3.8^\circ$
$b_W = 16.83\ ft$	$b_T = 9\ ft$	$b_{VT} = 3.5\ ft$
$\lambda_W = 0.5$		$\lambda_{VT} = 0.7$
Airfoil: NACA 23012	Airfoil: NACA 0015	Airfoil: NACA 4424 (Modified)

TABLE II

TOTAL STABILITY DERIVATIVES FOR THE HINGELESS ROTOR COMPOUND HELICOPTER AT 158 KNOTS

Eq. / Var.	X	Y	Z	M	N	L
θ	-4547.	0	-643.80	0	0	0
$\dot{\theta}$	-5125.	-38.023	37733.	-16486.	3656.	-3030.
$\ddot{\theta}$	0	0	0	-3180.	0	0
ϕ	0	4592.	0	0	0	0
$\dot{\phi}$	-43.520	5158	-40.164	3504	-93.950	-10670.
$\ddot{\phi}$	0	0	0	0	0	-1500.
ψ	0	643.80	0	0	0	0
$\dot{\psi}$	-8.605	-37776.	-0.270	123.490	-5906.	973.44
$\ddot{\psi}$	0	0	0	0	-3800	0
u	-3.684	-1.767	-29.556	-26.906	7.002	9.691
$\dot{u}$	-142.61	0	0	0	0	0
v	-0.274	-21.190	-0.112	-1.273	302.03	-59.599
$\dot{v}$	0	-142.61	0	0	0	0
w	18.237	-1.080	-205.28	-161.29	-83.617	47.433
$\dot{w}$	0	0	-142.42	0	0	0
A_1	1.638	1613.	-11.511	-9.121	-513.45	-114162.
B_1	81.164	279.89	34441.	-89574.	28521.	-17998
δ_r	-248.25	3795.	-33.563	46.774	-81669.	14672.

TABLE III

TOTAL STABILITY DERIVATIVES FOR THE HINGELESS ROTOR COMPOUND HELICOPTER AT 193 KNOTS

Var. \ Eq.	X	Y	Z	M	N	L
θ	-4611.	0	-538.	0	0	0
$\dot{\theta}$	-5284.	-22.120	46569.	-18214.	1678.	-2944.
$\ddot{\theta}$	0	0	0	-3180	0	0
ϕ	0	4642.	0	0	0	0
$\dot{\phi}$	-26.969	5315.	-40.645	3600.	397.49	-10061.
$\ddot{\phi}$	0	0	0	0	0	-1500.
ψ	0	537.73	0	0	0	0
$\dot{\psi}$	-11.276	-46694.	-1.460	112.37	-6284.	992.30
$\ddot{\psi}$	0	0	0	0	-3800.	0
u	-3.973	-2.128	-26.833	-16.127	14.616	6.429
$\dot{u}$	-144.160	0	0	0	0	0
v	-0.184	-26.316	-0.103	-1.993	327.21	-54.163
$\dot{v}$	0	-144.16	0	0	0	0
w	19.441	-1.202	-228.20	-199.33	-61.132	73.173
$\dot{w}$	0	0	-143.99	0	0	0
A_1	1.262	1027.	-10.820	-7.647	-326.97	-116115.
B_1	-1247.	381.27	43552.	-75383.	27153.	-30303.
δ_r	-356.68	4102.	-39.681	129.13	-88324.	15859.

TABLE IV

TOTAL STABILITY DERIVATIVES FOR THE HINGELESS ROTOR COMPOUND HELICOPTER AT 221 KNOTS

Eq. / Var.	X	Y	Z	M	N	L
θ	-4672.	0	-428.24	0	0	0
$\dot{\theta}$	-4853.	-7.163	53896.	-19034.	562.87	-2765.
$\ddot{\theta}$	0	0	0	-3180.	0	0
ϕ	0	4692.	0	0	0	0
$\dot{\phi}$	-17.578	4865.	-40.290	3702.	833.16	-9534.
$\ddot{\phi}$	0	0	0	0	0	-1500.
ψ	0	428.24	0	0	0	0
$\dot{\psi}$	9.903	-54051.	1.595	80.333	-7091.	1072.
$\ddot{\psi}$	0	0	0	0	-3800.	0
u	-5.438	-2.615	-21.732	-21.803	45.905	-1.238
$\dot{u}$	-145.71	0	0	0	0	0
v	-1.255	-30.441	-0.215	-1.031	396.30	-59.206
$\dot{v}$	0	-145.71	0	0	0	0
w	19.569	0.357	-252.09	-221.29	-57.061	108.49
$\dot{w}$	0	0	-145.56	0	0	0
A_1	-0.071	563.00	0.778	0.485	-179.01	-115349.
B_1	-2383.	-133.11	52273.	-26489.	23287.	-80368.
δ_r	-53.997	4480.	-4.647	-302.36	-96249.	17297.

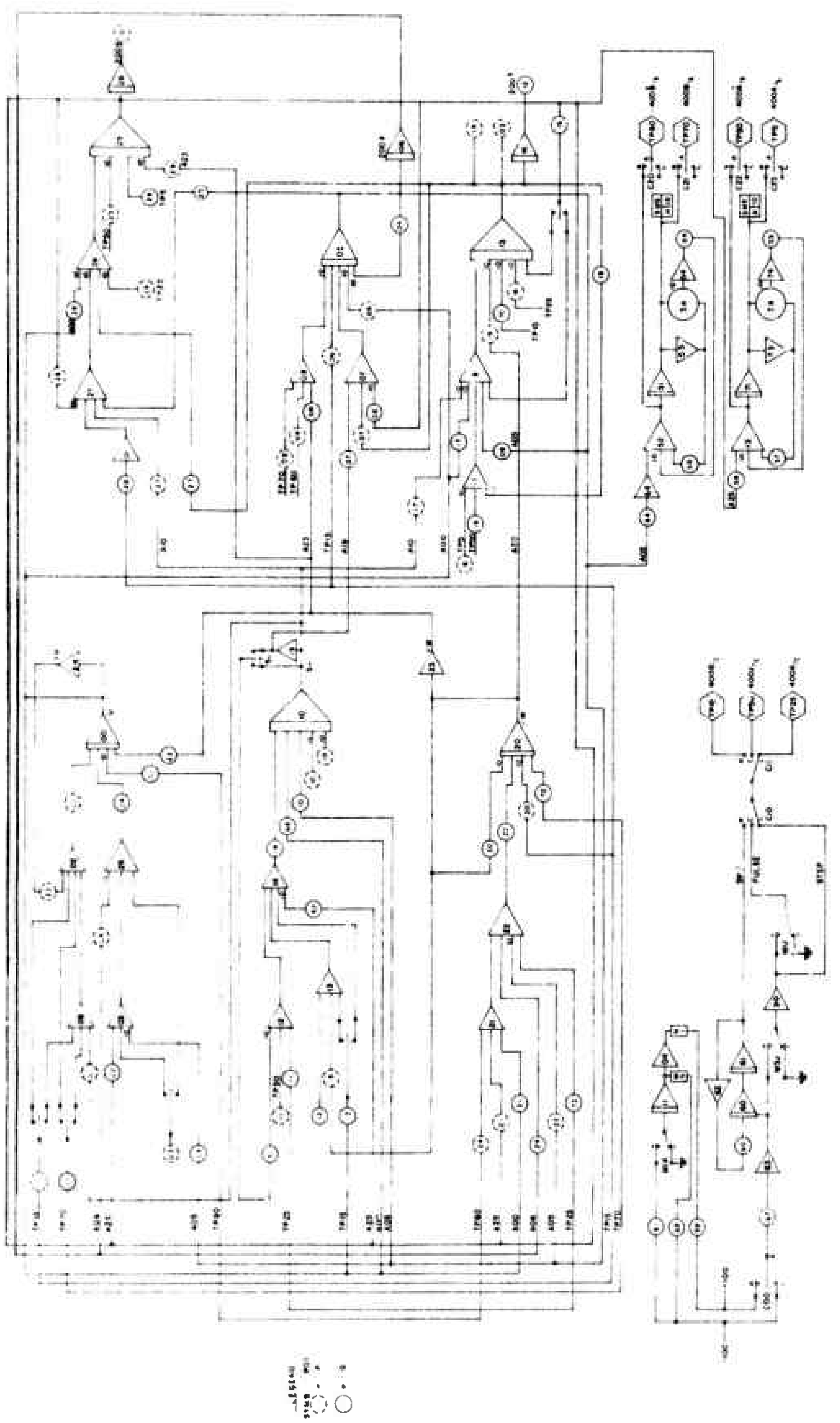

Figure 2. Analog Computer Schematic for the Rigid Rotor Compound Helicopter.

TABLE V

ANALOG COMPUTER POTENTIOMETER SETTINGS FOR THE HINGELESS ROTOR COMPOUND HELICOPTER AT 158 KNOTS

Pot. No.	Setting	Pot. No.	Setting	Pot. No.	Setting	Pot. No.	Setting
P00	0.0085	P10	0.0805	P20	0.0604	Q50	—
Q00	0.0085	Q10	0.0067	Q20	0.1441	Q51	0.0178
P01	0.0023	P11	0.1696	P21	0.0042	Q52	0.6040
Q01	—	Q11	0.1696	Q21	0.6226	Q53	0.0006
P02	0.1667	P12	—	P22	0.3974	Q54	0.1400
Q02	0.0092	Q12	0.1354	Q22	0.3333	Q55	—
P03	0.0018	P13	0.0454	P23	0.1550	Q56	0.1875
Q03	0.1078	Q13	0.0294	Q23	0.1279	Q57	0.5000
P04	0.0956	P14	0.6622	P24	—	Q58	0.5000
Q04	0.1667	Q14	0.8333	Q24	0.0678	Q59	0.2000
P05	0.1692	P15	—	P25	0.3805	Q60	1.0000
Q05	0.5184	Q15	0.0247	Q25	0.2020	Q61	0.1000
P06	0.1014	P16	0.0067	P26	0.7111	Q62	—
Q06	0.1102	Q16	—	Q26	0.5999	Q63	0.1085
P07	0.0388	P17	0.3180	P27	0.1589	Q64	0.1875
Q07	0.0160	Q17	0.0360	Q27	0.6490	Q65	—
P08	0.1408	P18	0.0[illegible]7	P28	0.6324	Q66	—
Q08	0.1408	Q18	0.3753	Q28	0.1300	Q67	—
P09	—	P19	0.4400	P29	0.3805	Q68	0.0620
Q09	0.9622	Q19	0.1554	Q29	—	Q69	0.1000

TABLE VI

ANALOG COMPUTER POTENTIOMETER SETTINGS FOR THE HINGELESS ROTOR COMPOUND HELICOPTER AT 193 KNOTS

Pot. No.	Setting	Pot. No.	Setting	Pot. No.	Setting	Pot. No.	Setting
P00	0.1298	P10	0.0805	P20	0.0756	Q50	—
Q00	0.1298	Q10	0.0038	Q20	0.1585	Q51	0.0219
P01	0.0015	P11	0.1069	P21	0.0042	Q52	0.7560
Q01	—	Q11	0.1069	Q21	0.5591	Q53	0.0006
P02	0.1667	P12	—	P22	0.4851	Q54	0.1400
Q02	0.0056	Q12	0.1119	Q22	0.3333	Q55	—
P03	0.0023	P13	0.0500	P23	0.1654	Q56	0.1875
Q03	0.1100	Q13	0.0397	Q23	0.1349	Q57	0.5000
P04	0.0960	P14	0.8098	P24	—	Q58	0.5000
Q04	0.1667	Q14	0.8333	Q24	0.0560	Q59	0.2000
P05	0.1014	P15	—	P25	0.3871	Q60	1.0000
Q05	0.5728	Q15	0.1046	Q25	0.1963	Q61	0.1000
P06	0.1254	P16	0.0043	P26	0.6707	Q62	—
Q06	0.1132	Q16	—	Q26	1.0101	Q63	0.1106
P07	0.0353	P17	0.3444	P27	0.1444	Q64	0.1875
Q07	0.0252	Q17	0.0770	Q27	0.6615	Q65	—
P08	0.1185	P18	0.0043	P28	0.9760	Q66	—
Q08	0.1185	Q18	0.3573	Q28	0.0860	Q67	—
P09	—	P19	0.3218	P29	0.3871	Q68	0.07[illegible]8
Q09	0.4417	Q19	0.1654	Q29	—	Q69	0.1000

TABLE VII

ANALOG COMPUTER POTENTIOMETER SETTINGS FOR THE HINGELESS ROTOR COMPOUND HELICOPTER AT 221 KNOTS

Pot. No.	Setting	Pot. No.	Setting	Pot. No.	Setting	Pot. No.	Setting
P00	0.2453	P10	0.0805	P20	0.0898	Q50	—
Q00	0.2453	Q10	0.0012	Q20	0.1732	Q51	0.0251
P01	0.0103	P11	0.0579	P21	0.0042	Q52	0.8980
Q01	—	Q11	0.0579	Q21	0.4479	Q53	—
P02	0.1667	P12	—	P22	0.5554	Q54	0.1400
Q02	0.0036	Q12	0.0882	Q22	0.3333	Q55	—
P03	0.0020	P13	0.0147	P23	0.2239	Q56	0.1875
Q03	0.0999	Q13	0.0137	Q23	0.1343	Q57	0.5000
P04	0.0962	P14	0.9274	P24	—	Q58	0.5000
Q04	0.1667	Q14	0.8333	Q24	0.0441	Q59	0.1500
P05	0.1372	P15	—	P25	0.3845	Q50	1.0000
Q05	0.5986	Q15	0.2193	Q25	0.1843	Q61	0.1000
P06	0.1392	P16	0.0023	P26	0.6356	Q62	—
Q06	0.1164	Q16	—	Q26	2.6789	Q63	0.1002
P07	0.0253	P17	0.4172	P27	0.1579	Q64	0.1875
Q07	0.0128	Q17	0.2420	Q27	0.7145	Q65	—
P08	0.0416	P18	0.0023	P28	1.4460	Q66	—
Q08	0.0416	Q18	0.3064	Q23	0.0166	Q67	—
P09	—	P19	0.3004	P29	0.3845	Q68	0.0897
Q09	0.1481	Q19	0.1866	Q29	—	Q69	0.1000

settings were obtained by normalizing the total derivatives in Tables II, III, and IV and then multiplying the normalized derivatives by the appropriate scaling factors required for use on the Pace 221 R computer.

10.3.3 Stability Responses of the Hingeless Rotor Compound Helicopter

The time history responses of the hingeless rotor compound helicopter to pulse inputs of the longitudinal and lateral cyclic controls B_{1_C} and A_{1_C} respectively are shown in Figures 3 through 8 for the three flight speeds considered. The responses due to rudder pedal control δ_{r_C} were not obtained because not enough amplifiers were available on the Pace 221 R analog computer to include the rudder control circuitry along with that of the stability augmentation system. Figures 3 and 4 show that the coupled responses due to the longitudinal and lateral cyclic, respectively, for a forward speed of 158 kts. Similar data for speeds of 193 kts and 221 kts are shown in the sets of Figures 5 and 6 and Figures 7 and 8 respectively. Also presented on the longitudinal control response traces are the corresponding flight test data obtained from NASA and later published as Reference 2. No test data were available for correlation with the lateral control responses at the same flight conditions investigated herein. However, included on Figures 4 and 8 are roll rate responses to lateral stick pulses obtained from Reference 3 for approximately the same test conditions as those evaluated on the analog computer.

Using the correlation rating system described in Section 10.1.3, the responses of the hingeless rotor compound helicopter to longitudinal control pulses were evaluated and are presented in Table VIII. Since very little test data is available for correlation purposes, a complete evaluation of the accuracy of the theoretical methods for predicting the hingeless rotor compound helicopter dynamic stability characteristics is not possible at this time. However, from the limited correlations shown in Table VIII, it appears that the analytical methods presented in this handbook are also suitable for hingeless rotor aircraft. The correlation shown between the roll rate data from Reference 3 and the analog responses to lateral control pulses illustrated in Figures 4 and 8 also substantiate the validity of the theoretical methods.

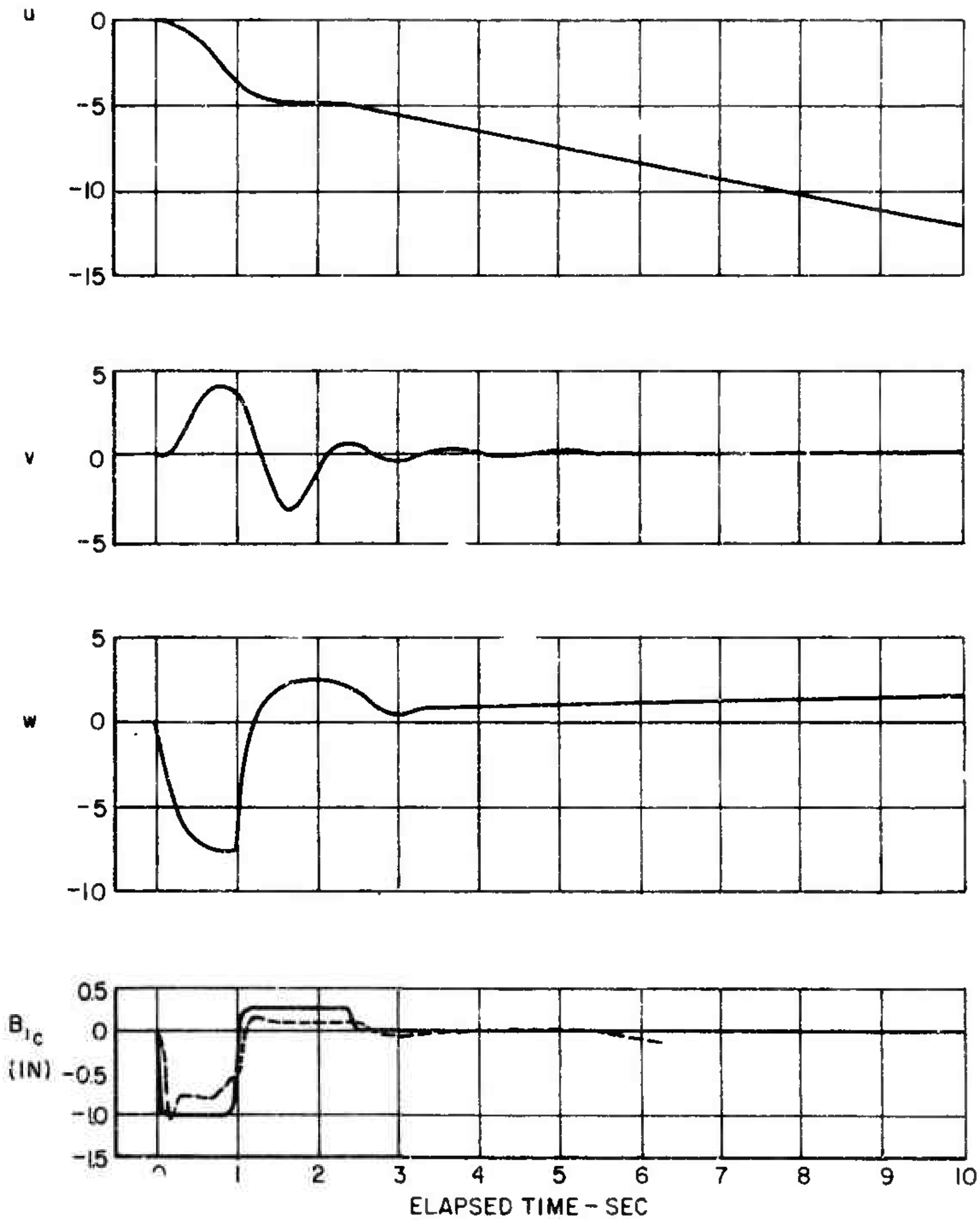

(a) PERTURBATION VELOCITIES-FT/SEC

Figure 3. Response of the Hingeless Rotor Compound Helicopter Due to Pulse Input of the Longitudinal Control, B_{1_C} = -1", V = 158 KTS.

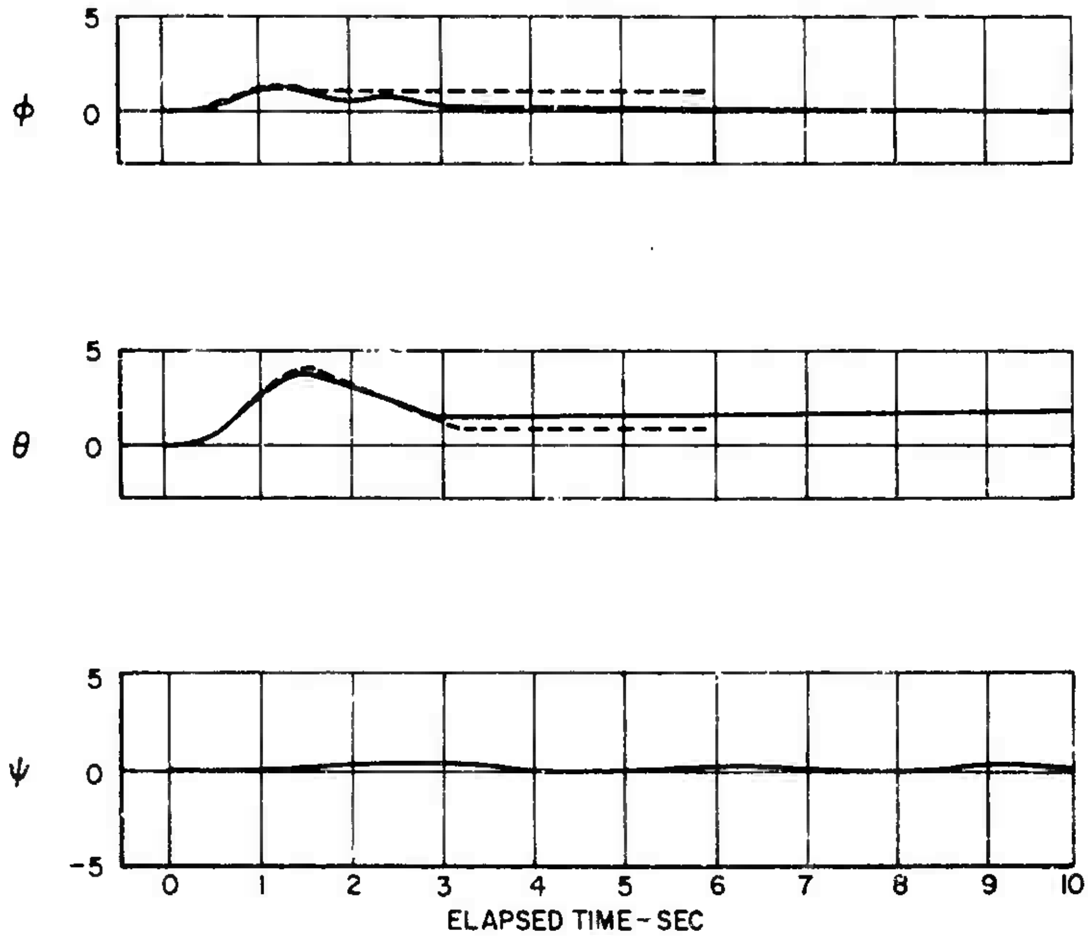

(b) ATTITUDES, DEGREES

Figure 3. Continued.

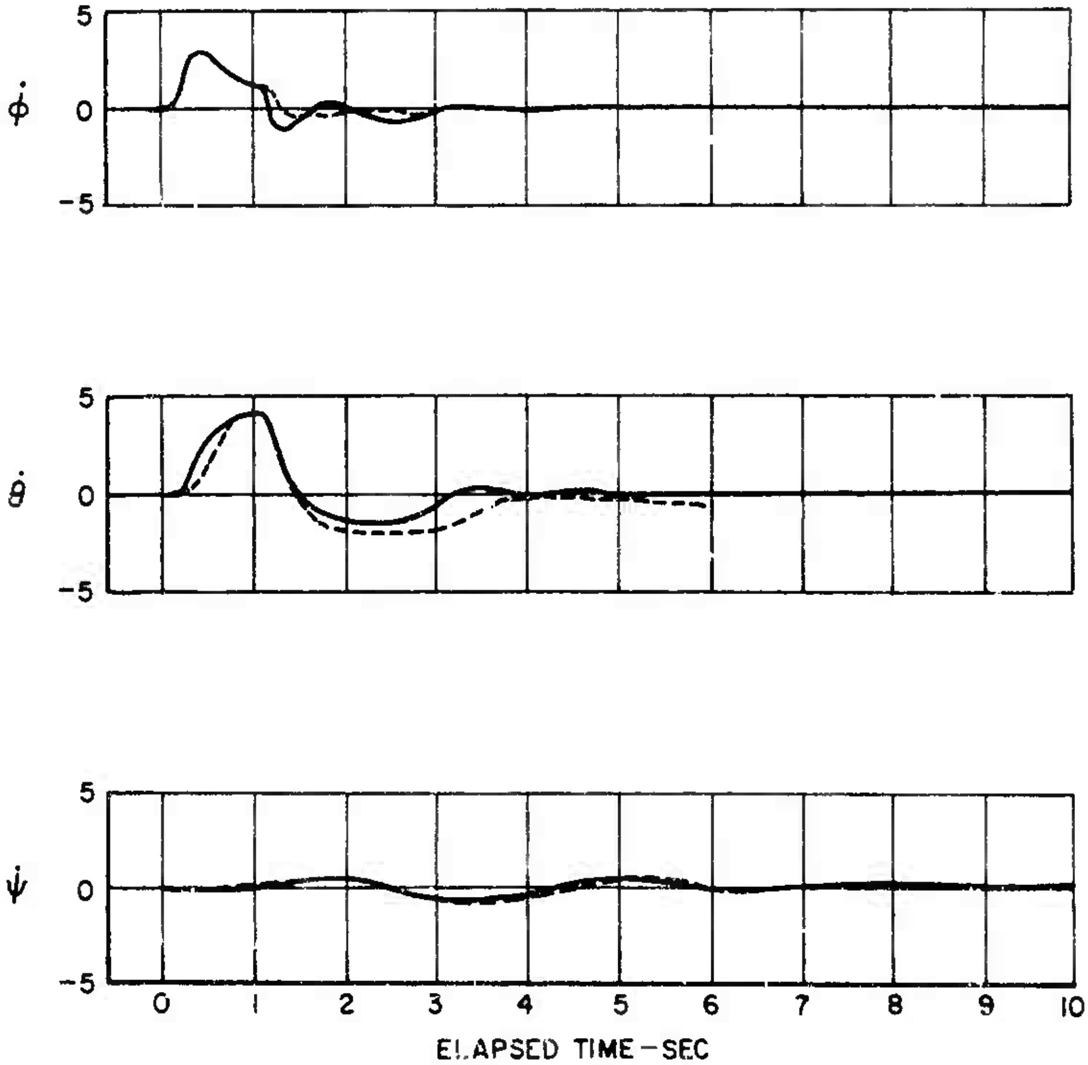

(c) ANGULAR RATES, DEG/SEC

Figure 3. Concluded

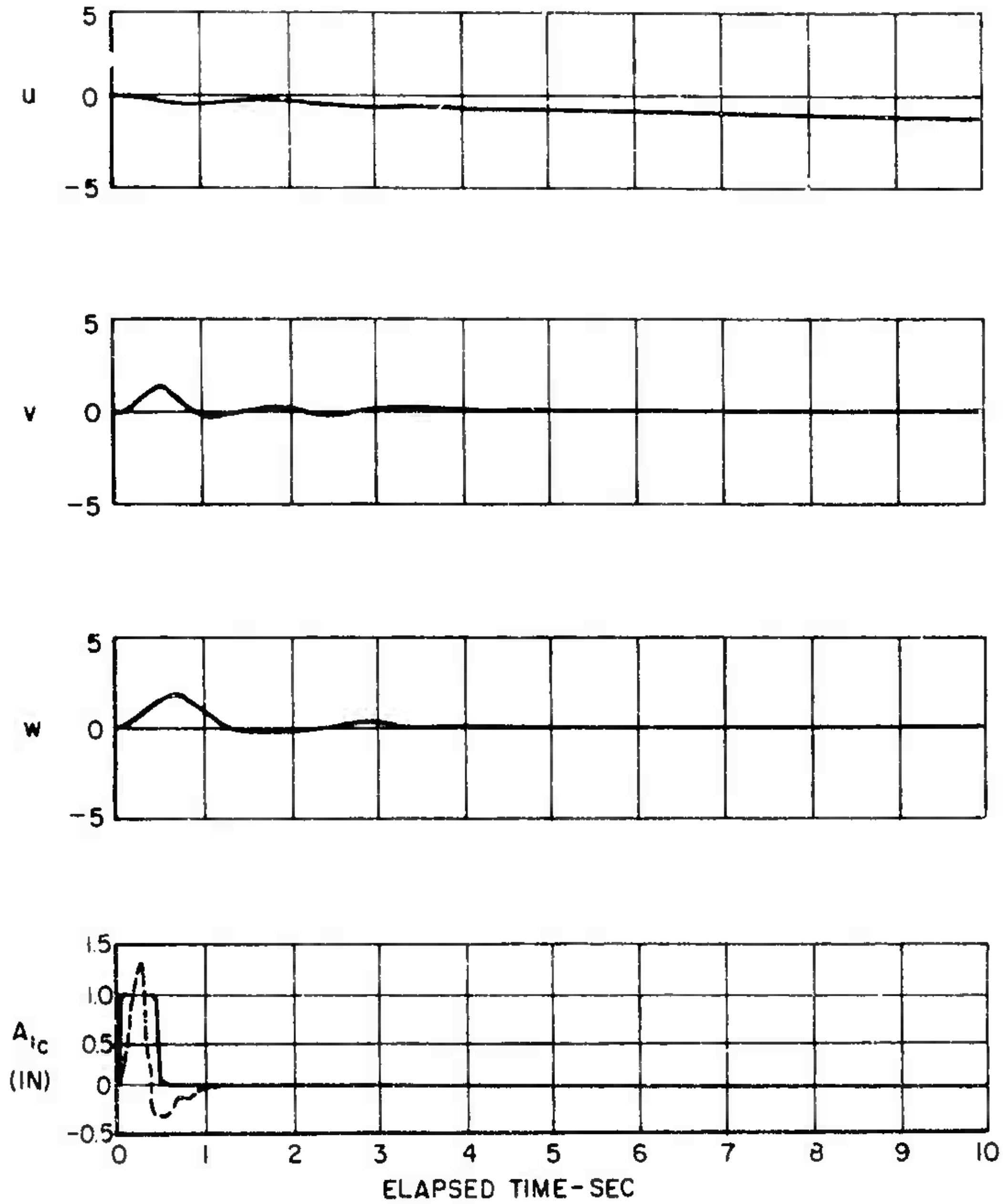

(a) PERTURBATION VELOCITIES—FT/SEC

Figure 4. Response of the Hingeless Rotor Compound Helicopter Due to Pulse Input of the Lateral Control, A_{1_C} = +1", V = 158 KTS.

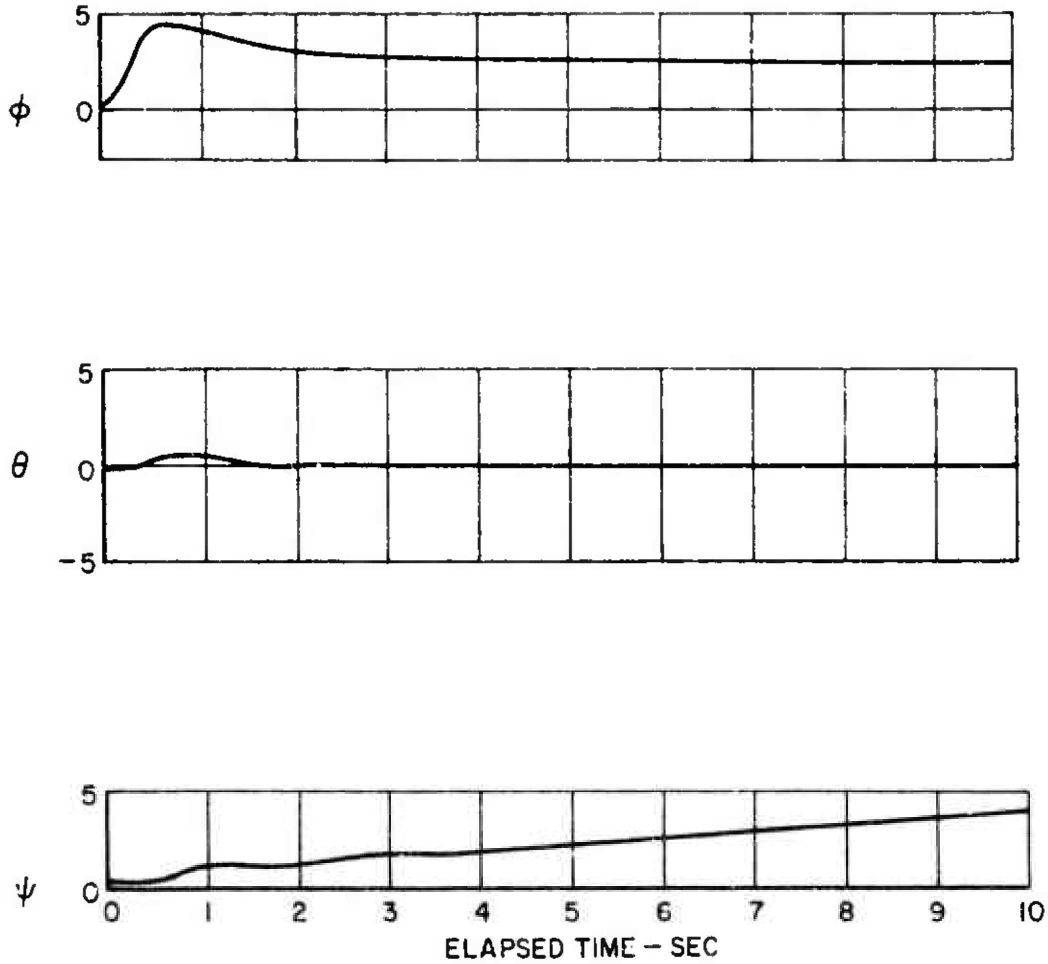

(b) ATTITUDES, DEGREES

Figure 4. Continued.

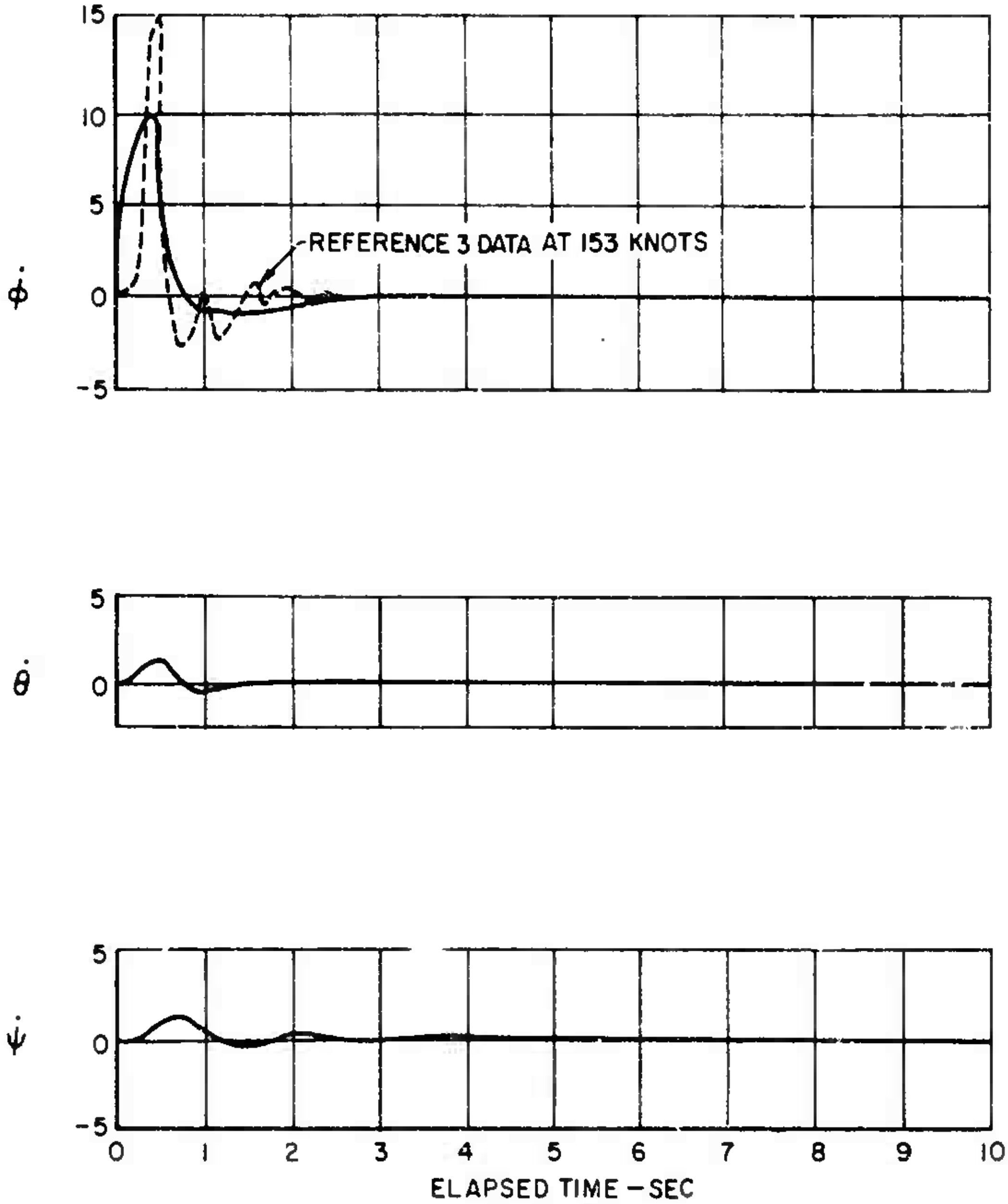

(c) ANGULAR RATES, DEG/SEC

Figure 4. Concluded.

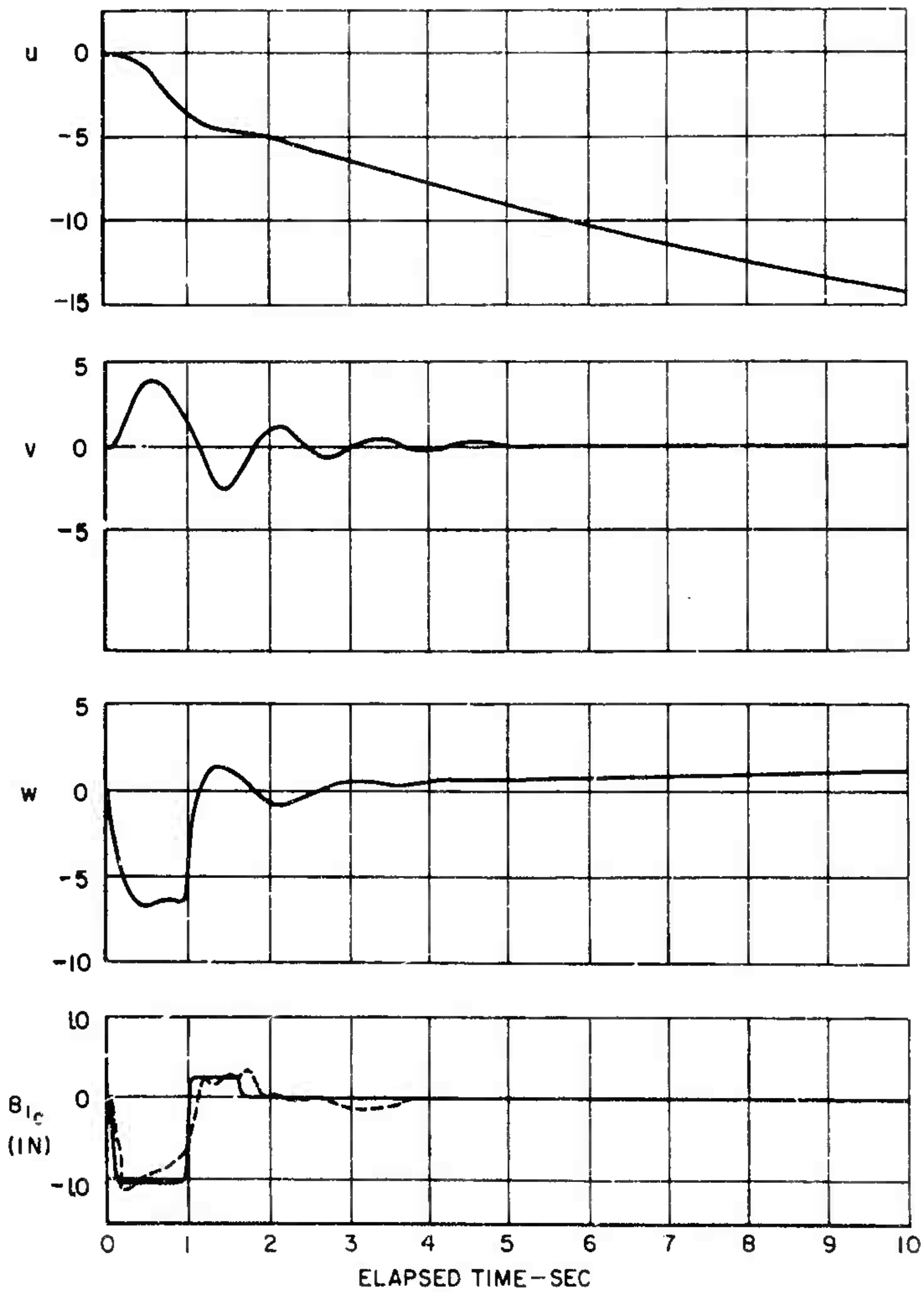

(a) PERTURBATION VELOCITIES-FT/SEC

Figure 5. Response of the Hingeless Rotor Compound Helicopter Due to Pulse Input of the Longitudinal Control, B_{1c} = -1", V = 193 KTS.

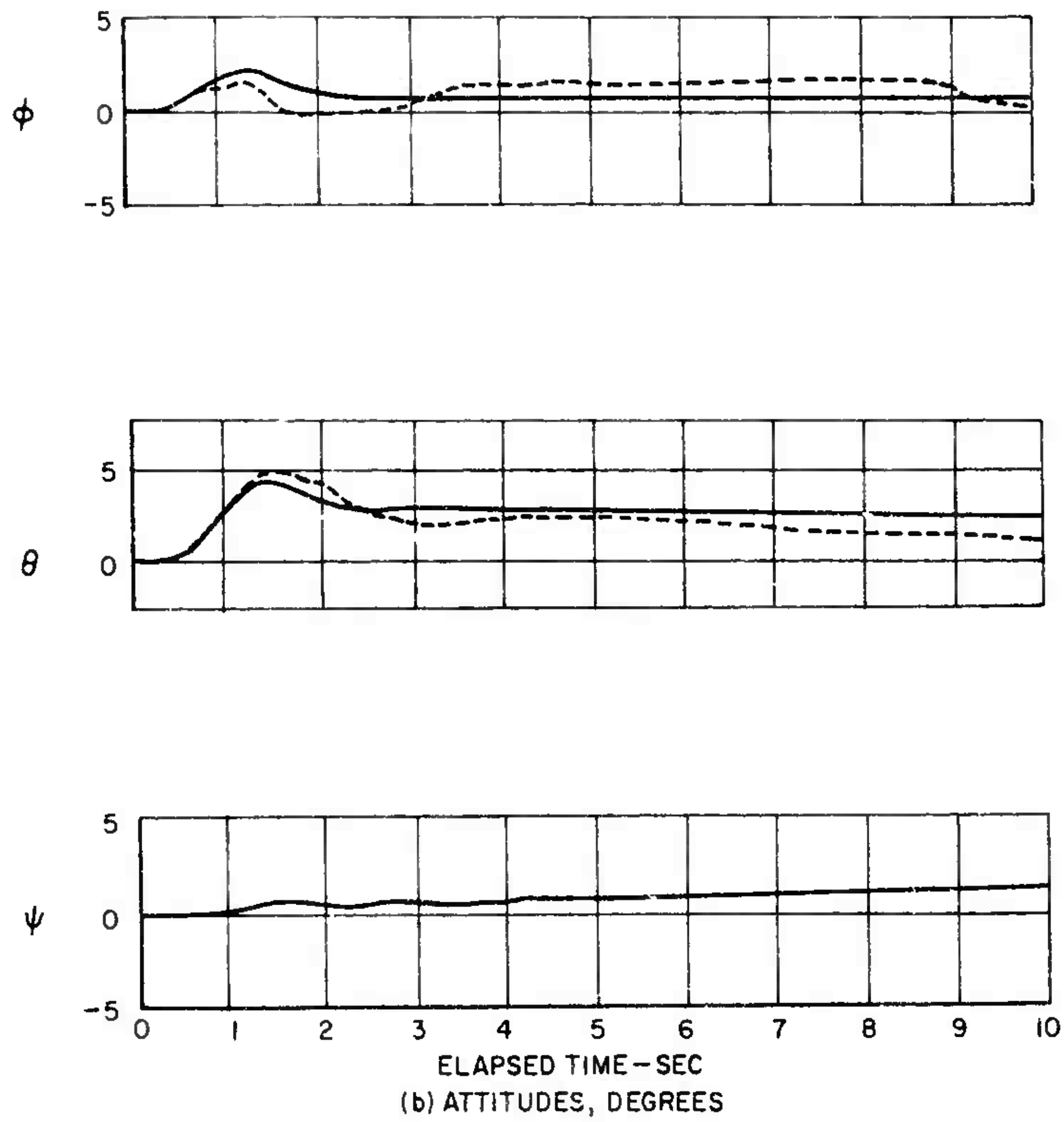

Figure 5. Continued.

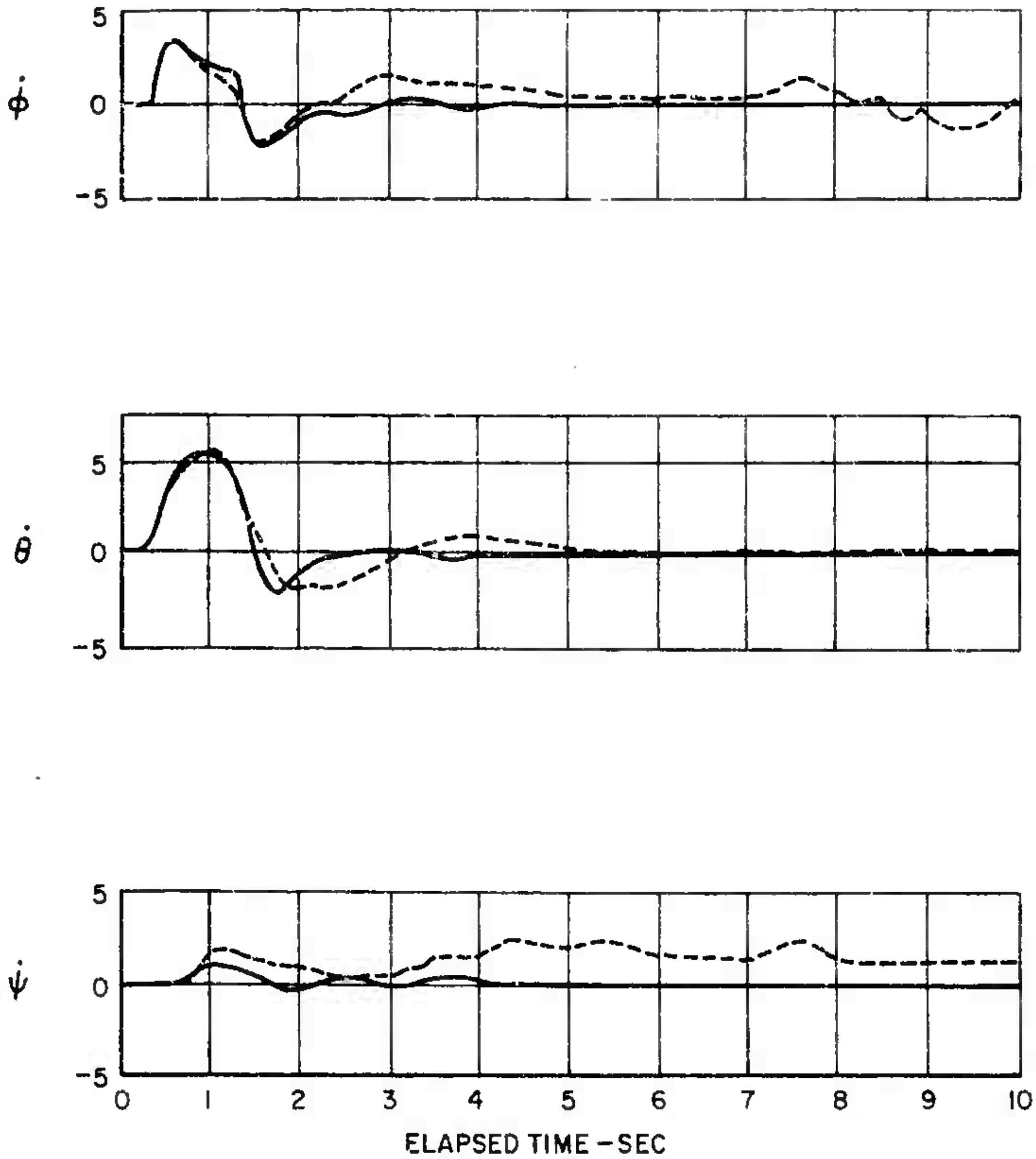

(c) ANGULAR RATES, DEG/SEC

Figure 5. Concluded.

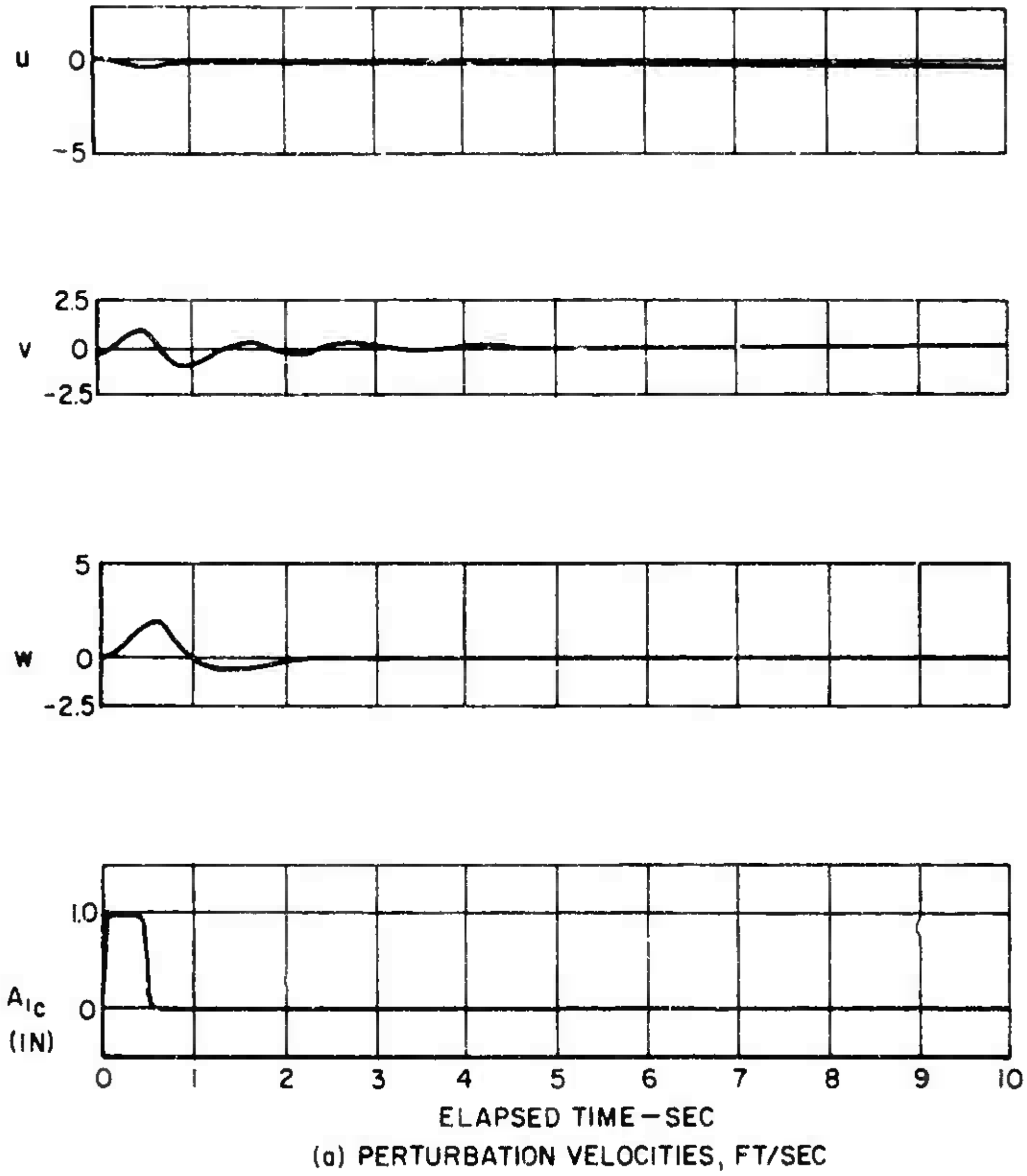

Figure 6. Response of the Hingeless Rotor Compound Helicopter Due to Pulse Input of the Lateral Control, A_{1_C} = +1", V = 193 KTS.

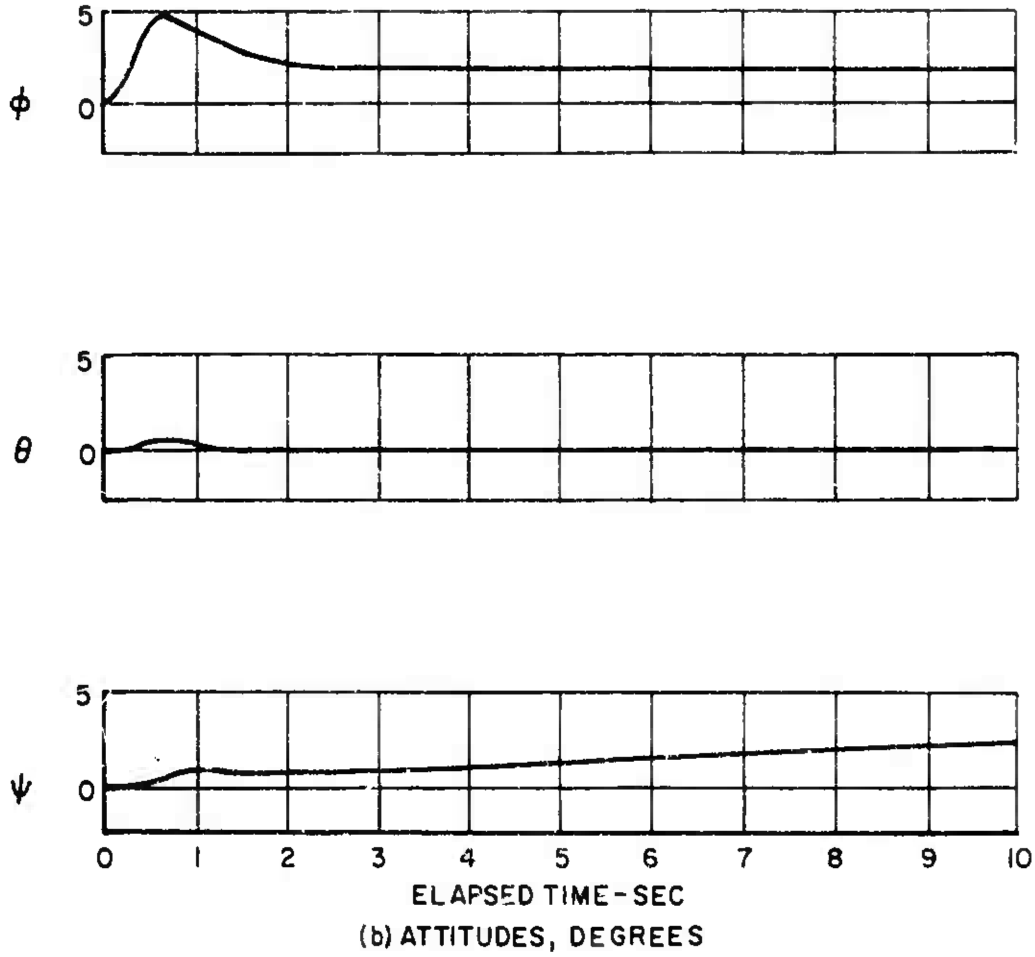

Figure 6. Continued.

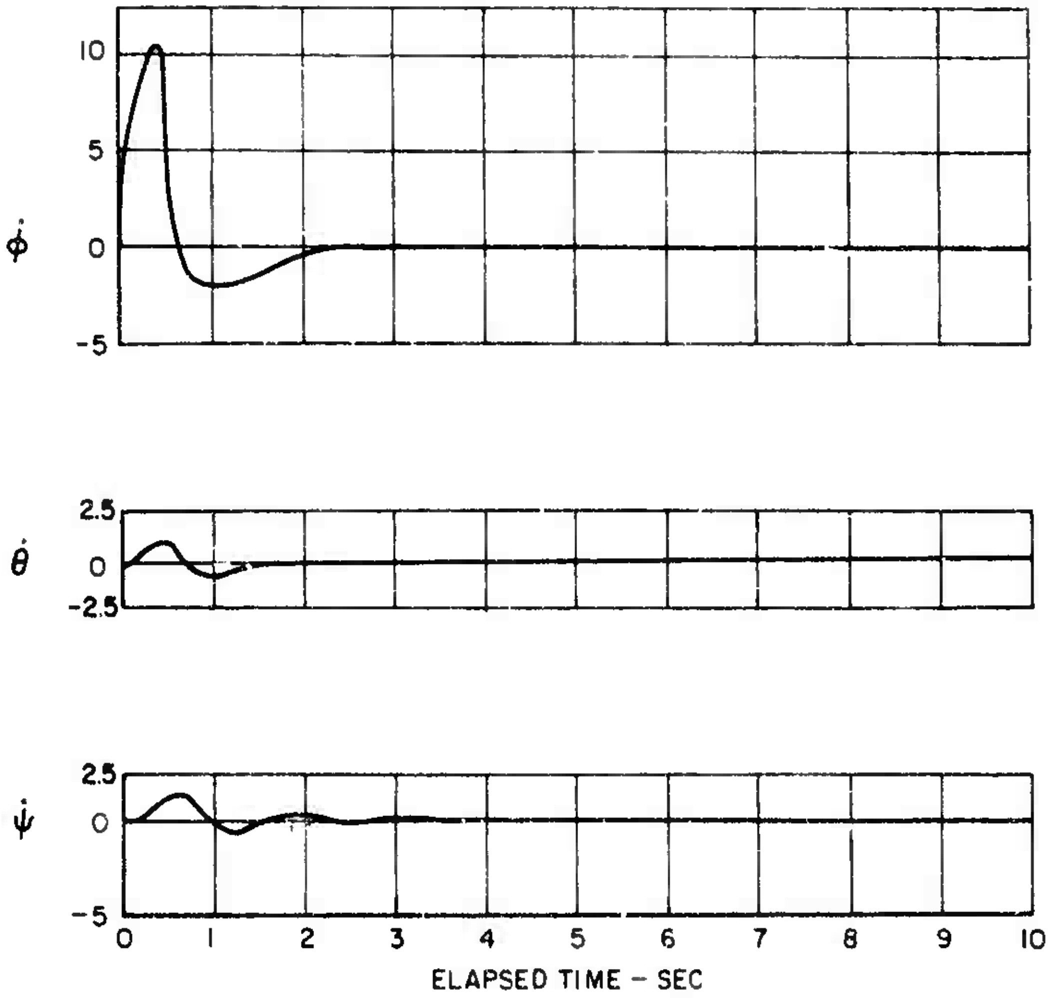

(c) ANGULAR RATES, DEG/SEC

Figure 6. Concluded.

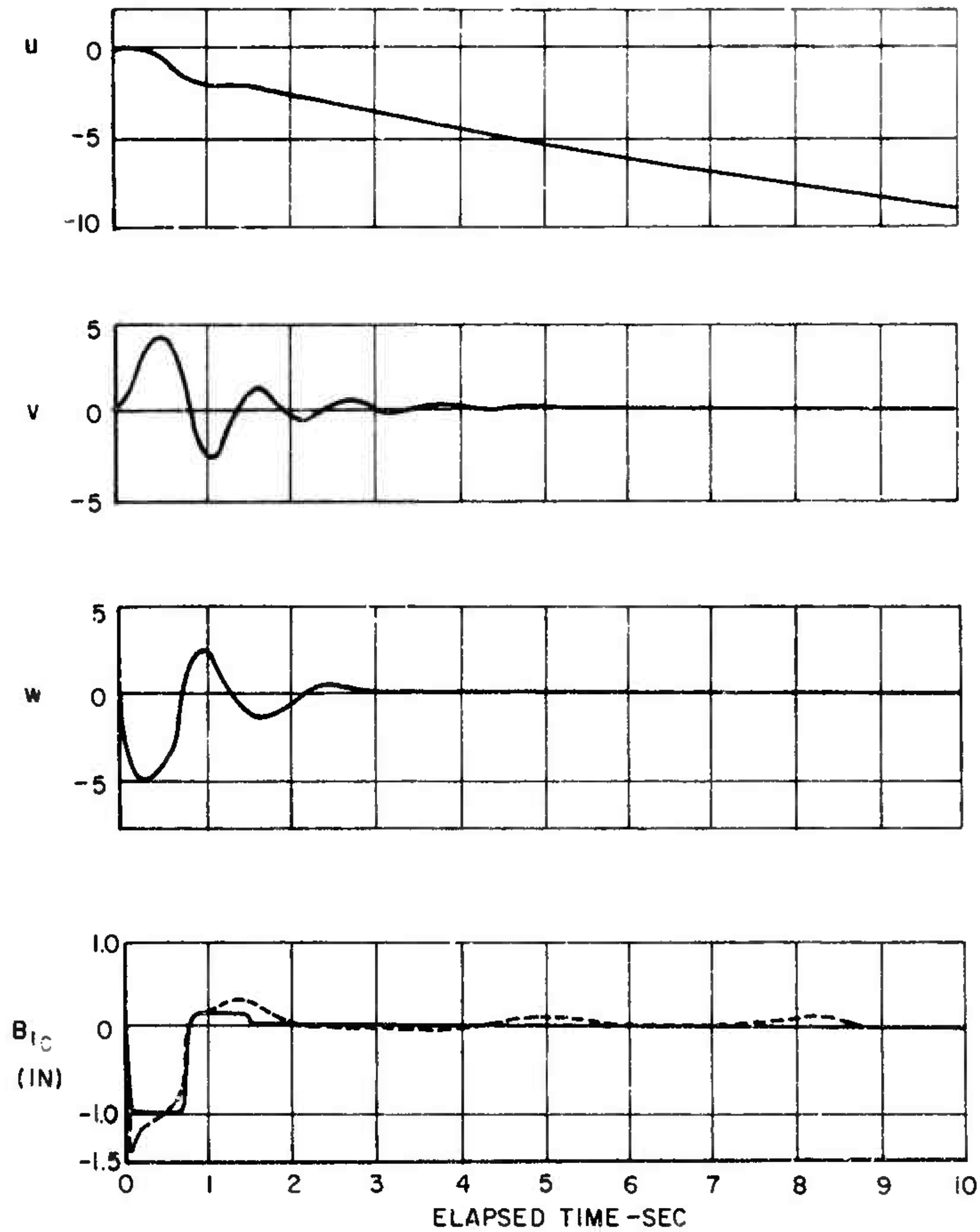

(a) PERTURBATION VELOCITIES, FT/SEC

Figure 7. Response of the Hingeless Rotor Compound Helicopter Due to Pulse Input of the Longitudinal Control, B_{1_C} = -1", V = 221 KTS.

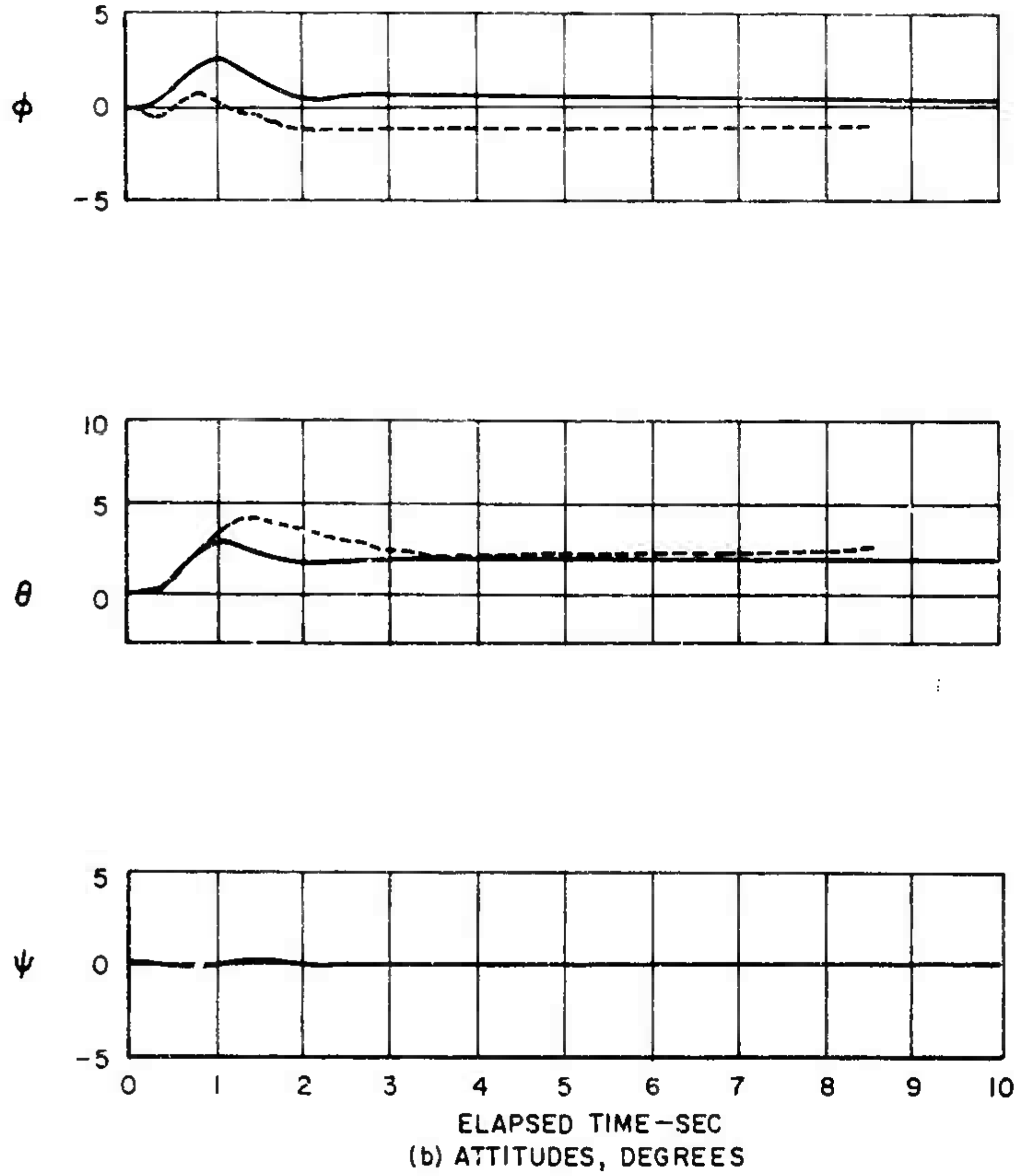

Figure 7. Continued.

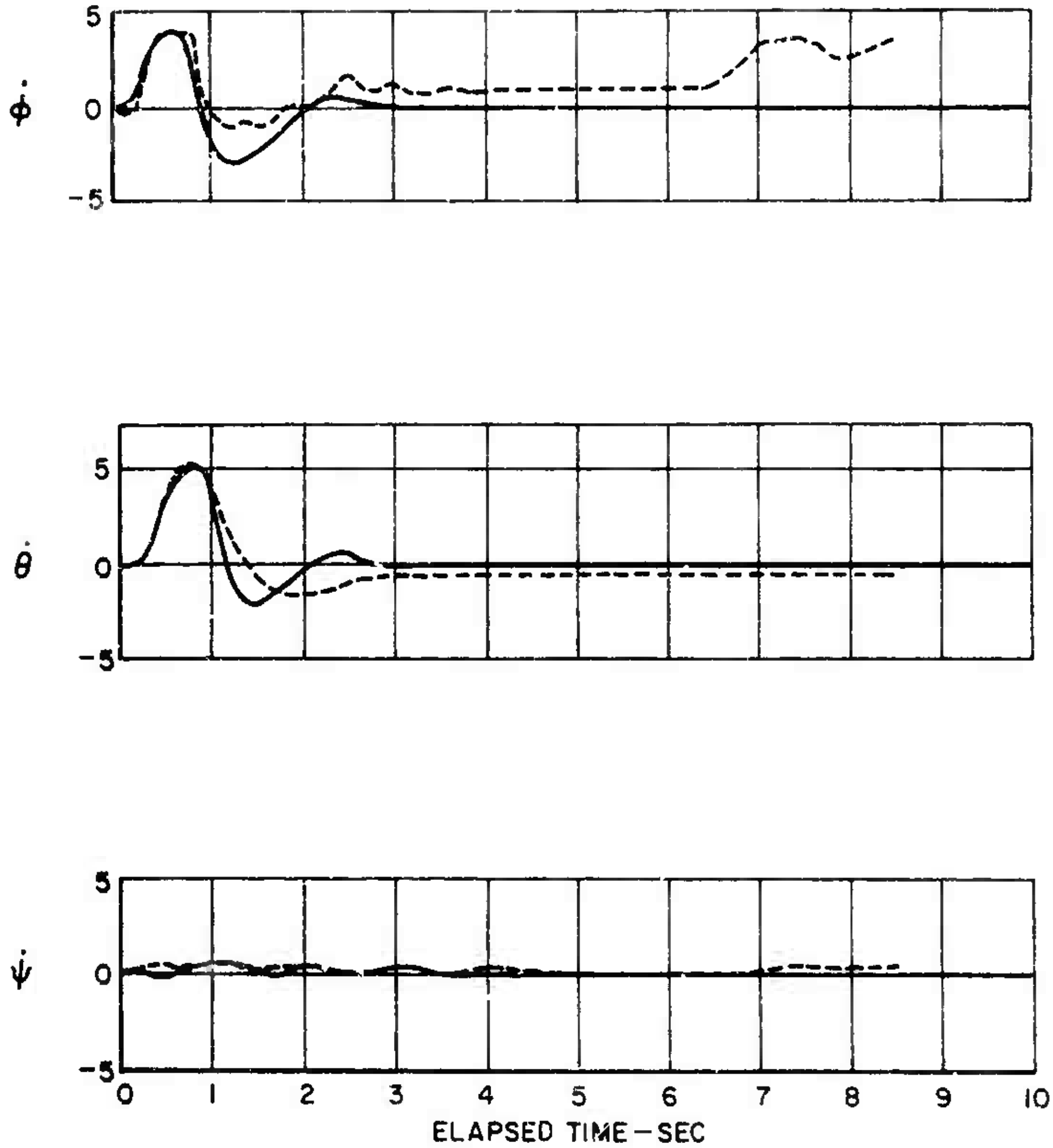

(c) ANGULAR RATES DEG/SEC

Figure 7. Concluded.

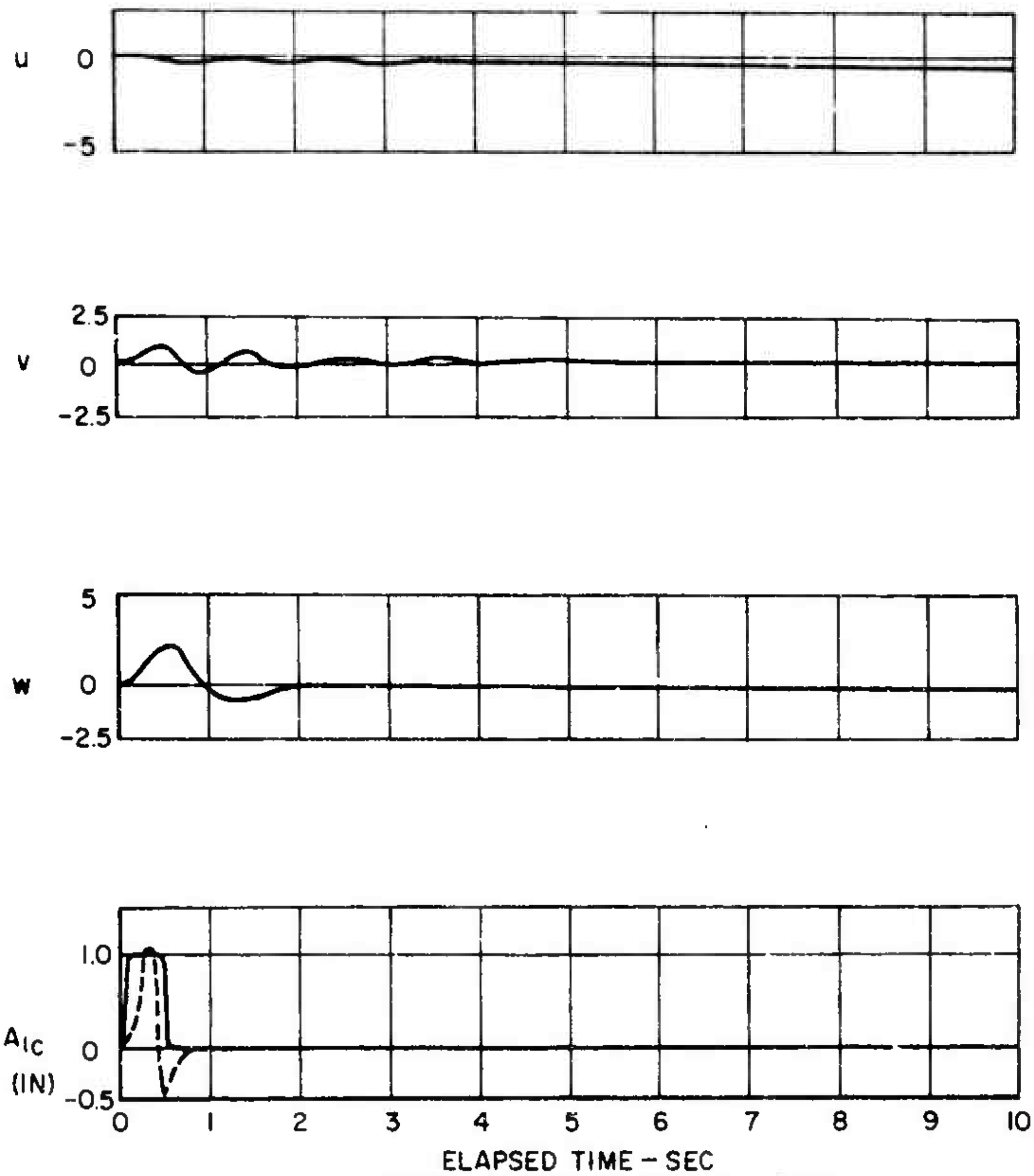

(a) PERTURBATION VELOCITIES, FT/SEC

Figure 8. Response of the Hingeless Rotor Compound Helicopter Due to Pulse Input of the Lateral Cyclic, A_{1C} = +1", V = 221 KTS.

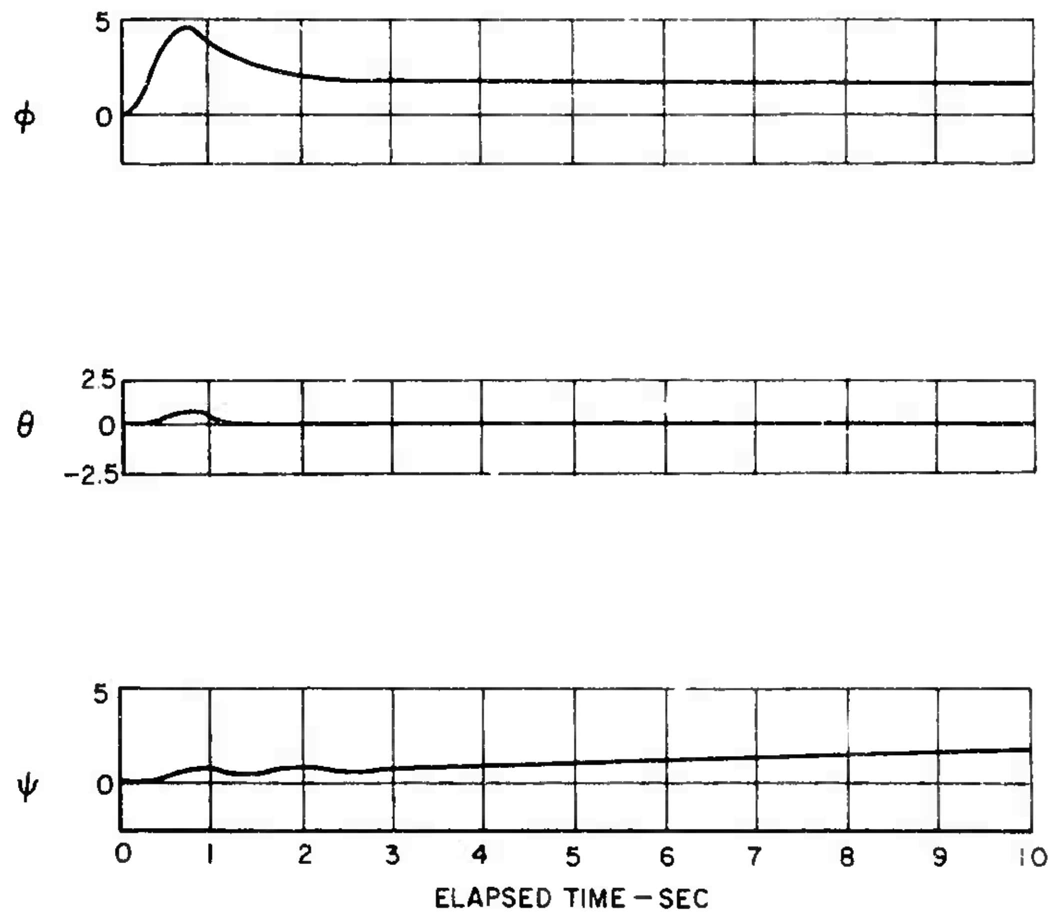

(b) ATTITUDES, DEGREES

Figure 8. Continued.

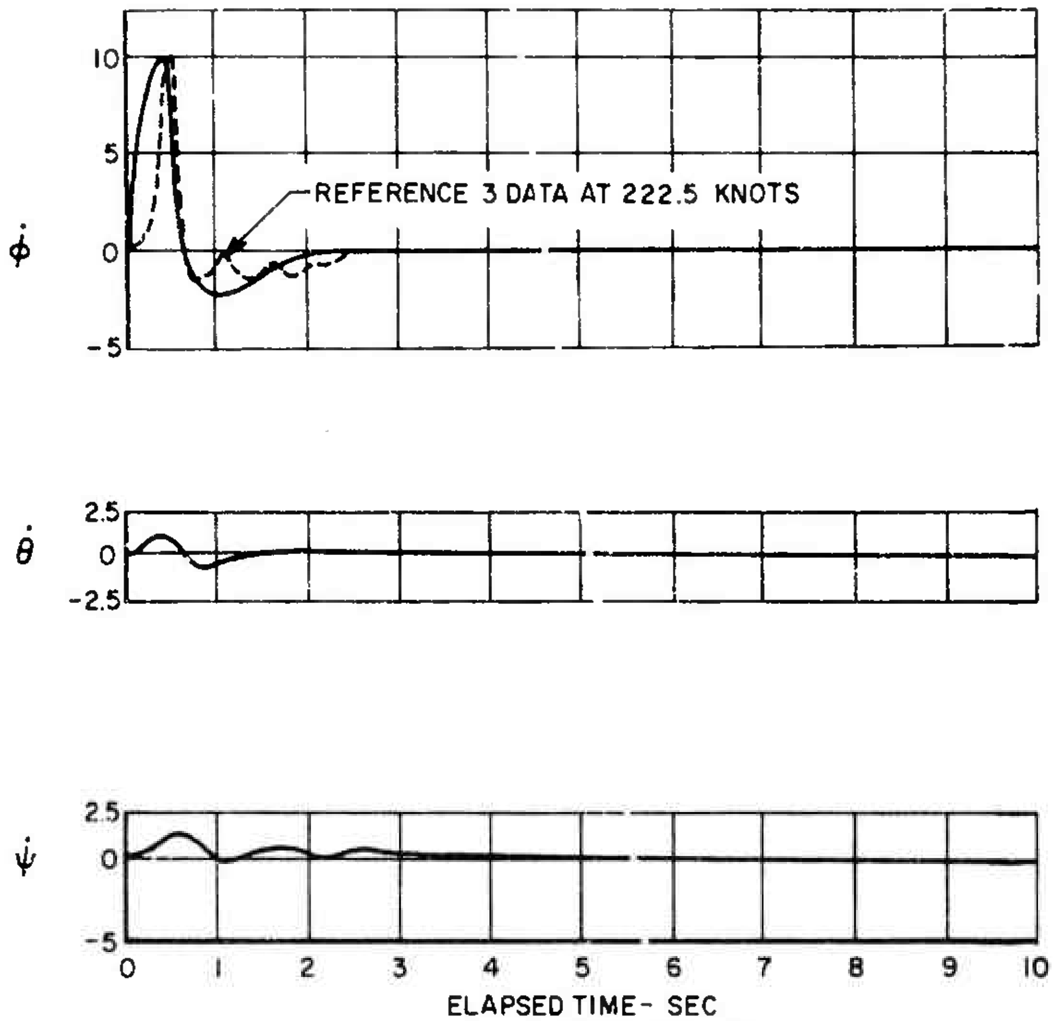

(c) ANGULAR RATES, DEG/SEC

Figure 8. Concluded.

TABLE VIII

SUMMARY OF CORRELATIONS OBTAINED BETWEEN THEORETICAL AND FLIGHT TEST RESPONSES FOR THE HINGELESS ROTOR COMPOUND HELICOPTER

Control Pulse	Vo (Kn)	Parameter									Figure Number
		u	v	w	ϕ	θ	ψ	$\dot{\phi}$	$\dot{\theta}$	$\dot{\psi}$	
B_{1c}	158	---	---	---	G	VG	---	VG	VG	E	3
	193	---	---	---	F	VG	---	G	VG	P	5
	221	---	---	---	P	G	---	F	VG	VG	7

CORRELATION RATINGS:
E - excellent
VG - very good
G - good
F - fair
P - poor

Based on these correlations, it should also be noted that the stability methods presented in this handbook are adequate for predicting the effects of the stability augmentation system such as used on the sample hingeless rotor compound helicopter.

LITERATURE CITED

1. Sweers, J. E., IN-FLIGHT MEASUREMENT AND CORRELATION WITH THEORY OF BLADE AIRLOADS AND RESPONSES ON THE XH-51A COMPOUND HELICOPTER ROTOR - VOLUME III; THEORETICAL PREDICTION OF AIRLOADS AND STRUCTURAL LOADS AND CORRELATION WITH FLIGHT TEST MEASUREMENTS, Lockheed - California Company; USAAVLABS Technical Report 68-22C, U. S. Army Aviation Materiel Laboratories, Fort Eustis, Virginia, May 1968, AD674195.

2. Jenkins, Julian L., Jr., and Deal, Perry L., AN INVESTIGATION OF THE LEVEL FLIGHT AND MANEUVERING CHARACTERISTICS OF A HINGELESS ROTOR COMPOUND HELICOPTER; Langley Working Paper 768, Langley Research Center, Langley Station, Hampton, Virginia, July, 1969.

3. Lentine, F. P., Groth, W. P., and Oglesby, T. H., RESEARCH IN MANEUVERABILITY OF THE XH-51A COMPOUND HELICOPTER, Lockheed - California Company; USAAVLABS Technical Report 68-23, U. S. Army Aviation Materiel Laboratories, Fort Eustis, Virginia, June 1968, AD675445.

10.4 OVERALL APPRAISAL OF THE THEORETICAL METHODS

The correlation results presented in the preceding sections indicate that the theoretical methods and procedures presented in this handbook are more than adequate for accurate assessment of the dynamic stability and control characteristics of generalized compound helicopter configuration. The degree of accuracy obtained in the final results is dependent on the accuracy of the available input data and the ability to theoretically simulate aircraft control motions.

SECTION 11. SAMPLE CALCULATIONS

In order to better illustrate the stability methods presented in the previous sections, a complete sample calculation is herein performed for a typical single rotor compound helicopter. Because of the inherent complexity of the computations pertaining to compound helicopters, the available test data were utilized wherever possible.

The computations presented in this section are performed according to the sequence of operations outlined in the previous sections. Specifically, the sample calculations are initiated with the aircraft trim computations followed by local and total stability derivatives and are ended with the solution of the stability characteristic equation and analog computations of aircraft response.

11.1 DESCRIPTION OF THE SAMPLE COMPOUND HELICOPTER

The sample compound helicopter selected for the computations is a medium utility research helicopter consisting of a main rotor, tail rotor, wings, tail surfaces, and auxiliary jet engines, as illustrated in Figure 1. The main and the tail rotors consist of six and five fully articulated blades respectively. The wing has an NACA 63_2A415 series airfoil section, the horizontal tailplane, a modified NACA 0010 section, and the vertical tail, a modified NACA 0012 section. The fuselage characteristics derived from model tests of Reference 1 for a similar fuselage shape are presented in Figure 2.

The fuselage total drag (curve "a") includes the drag of the two nacelles and supporting pylons, the rotor pylon, main jet intakes, and interference drag. Test data for configuration "A" in Section 5.3 were used to estimate the fuselage lateral characteristics.

Although the aircraft has no stability augmentation system, it does have airplane-type control surfaces integrated with the helicopter controls. The applicable integrated control rigging curves from Reference 2 are presented in Figure 3, 4, and 5.

The aircraft operating conditions assumed in this sample calculation correspond to a forward speed of 125 knots or V_0 = 221.125 ft/sec, a rotor tip speed of ΩR = 660 ft/sec and a density altitude corresponding to 3,000 ft.

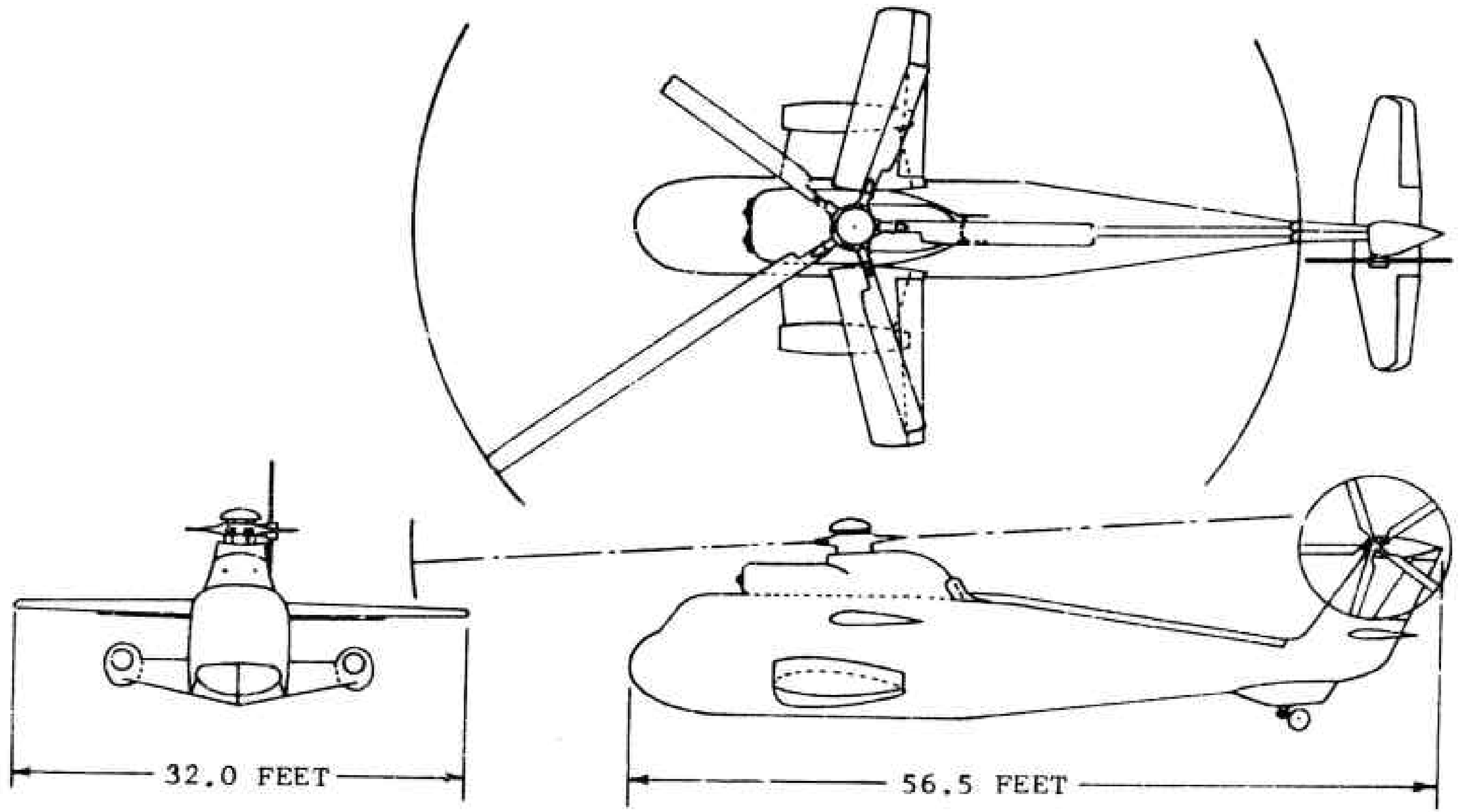

Figure 1. General Arrangement of a Sample Compound Helicopter.

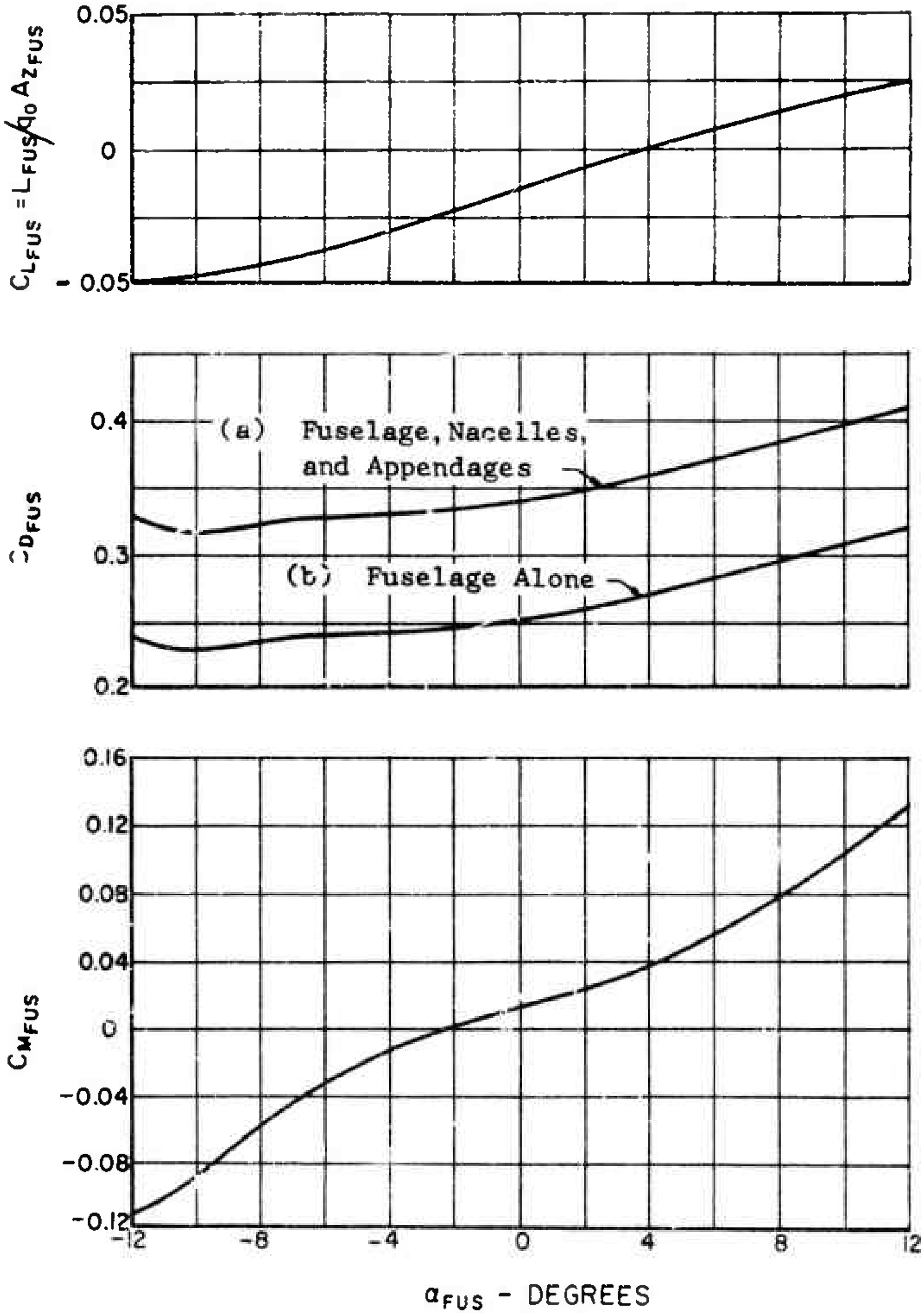

Figure 2. Fuselage Characteristics for the Sample Compound Helicopter ($\beta_S = 0$).

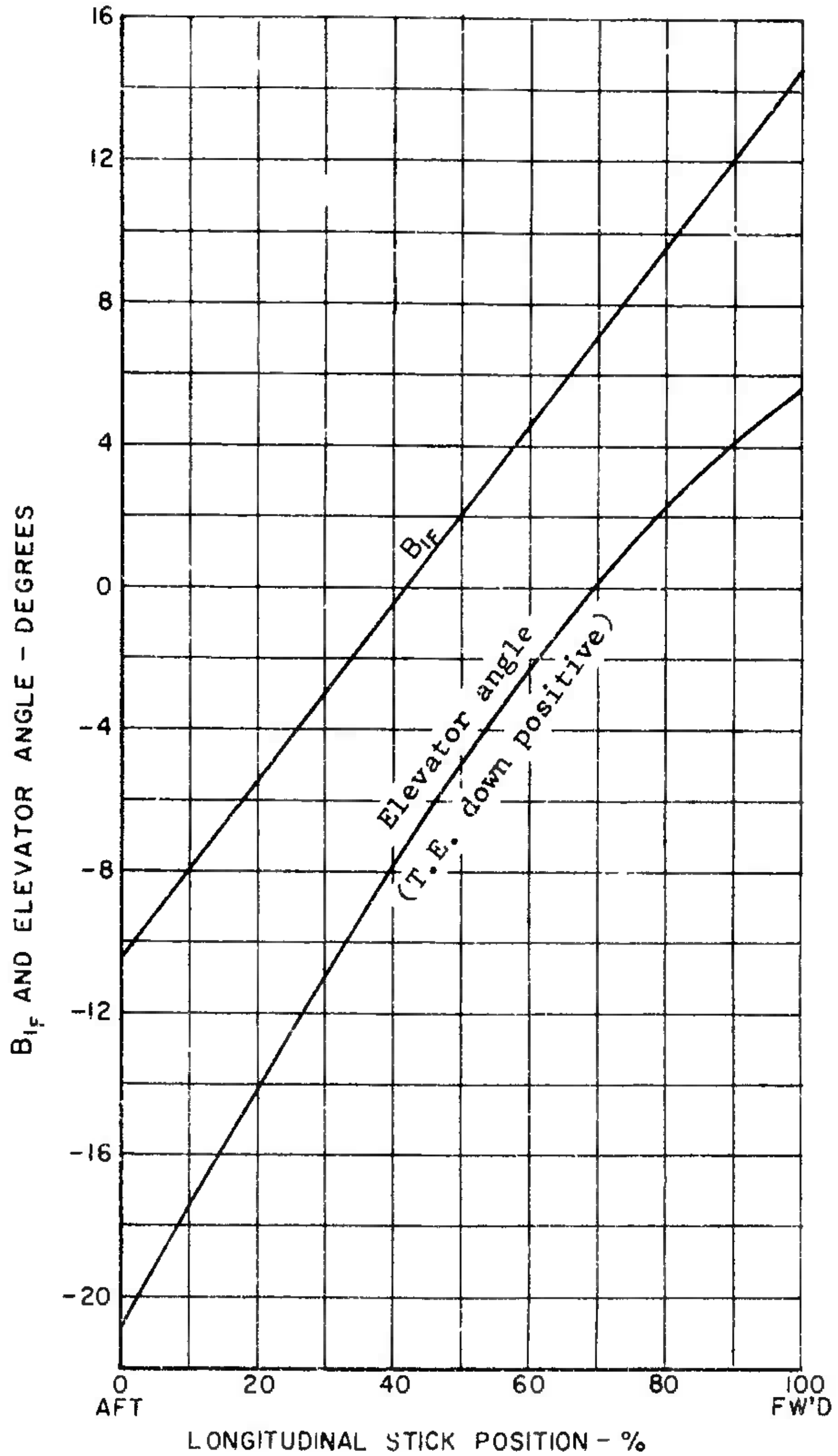

Figure 3. Longitudinal Control Rigging.

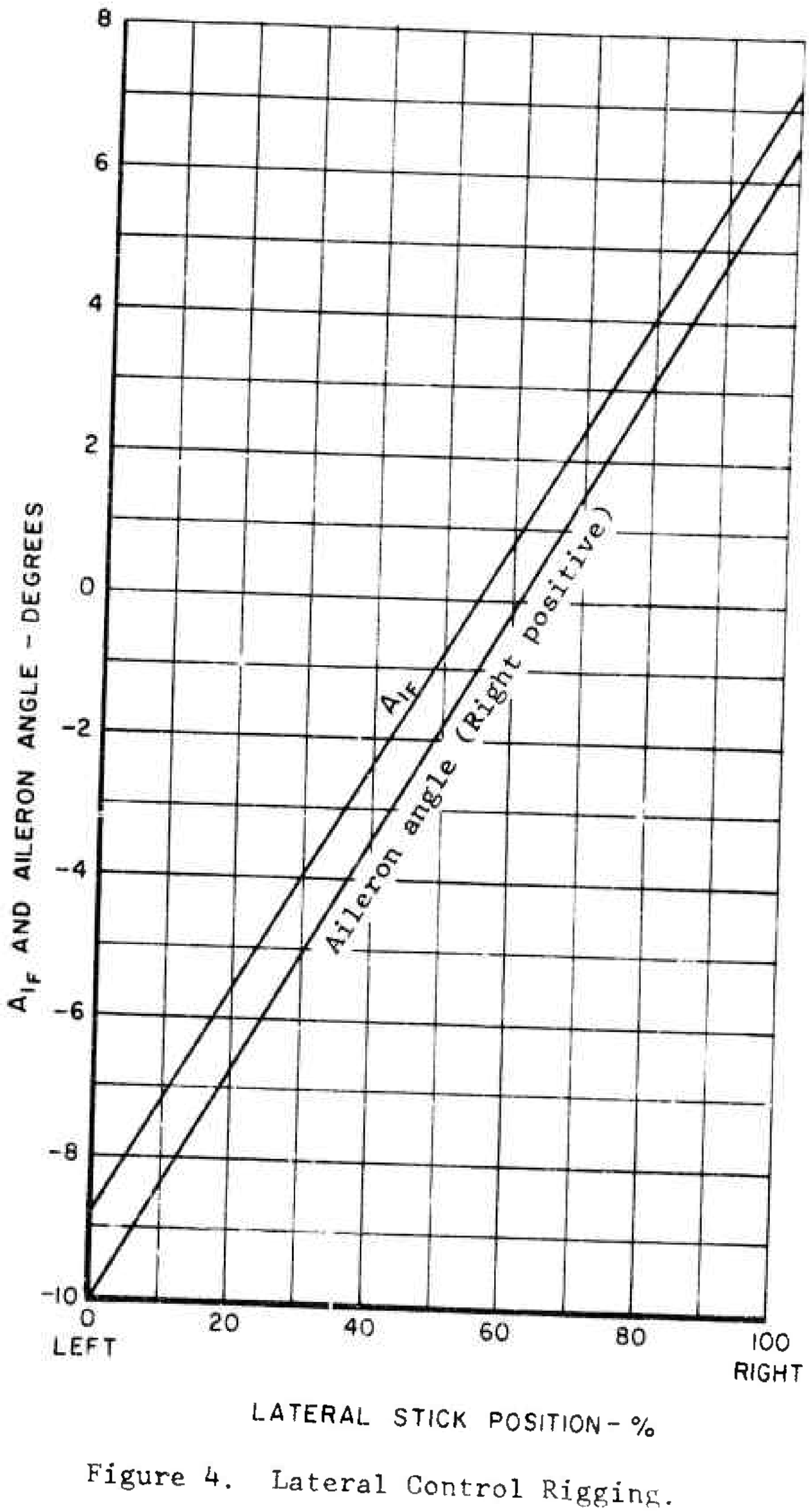

Figure 4. Lateral Control Rigging.

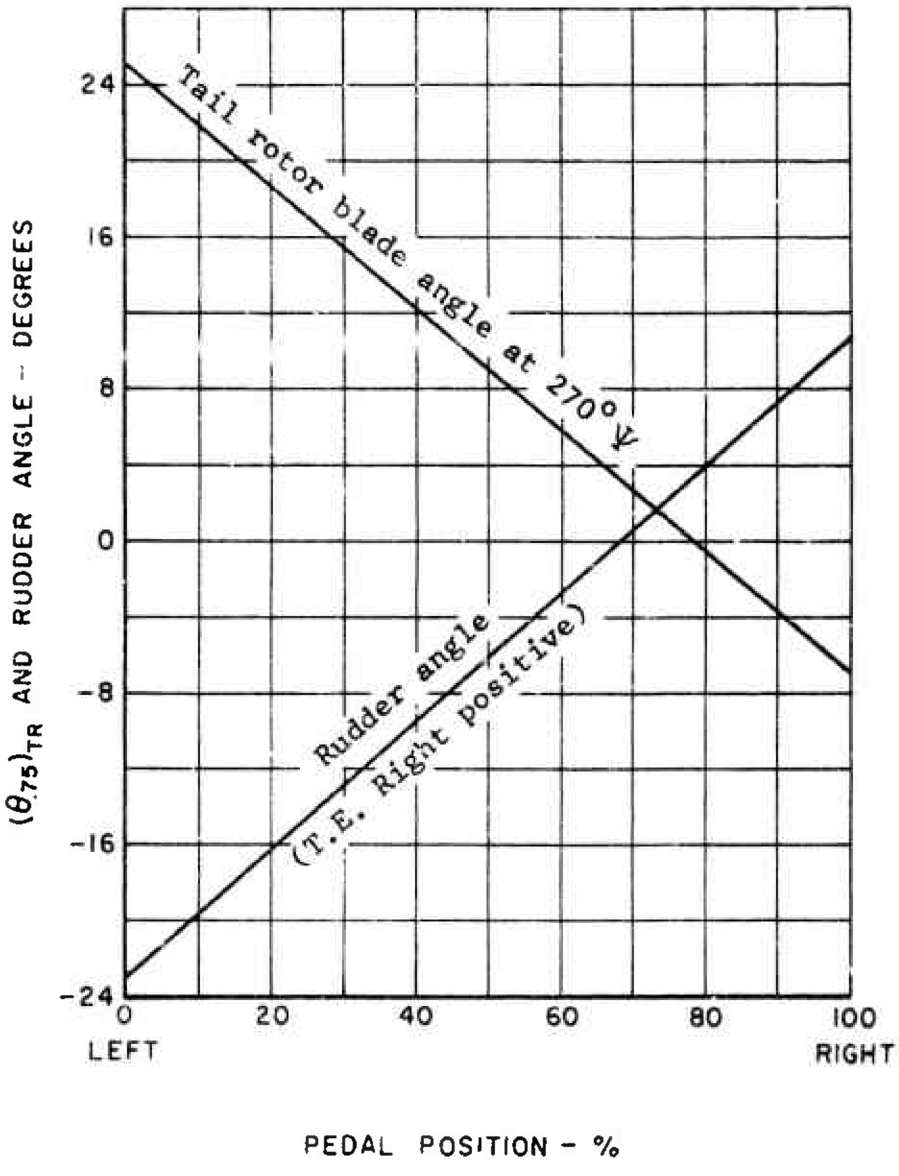

Figure 5. Directional Control Rigging.

LITERATURE CITED

1. Bain, Lawrence J., Landgrebe, Anton J., INVESTIGATION OF COMPOUND HELICOPTER AERODYNAMIC INTERFERENCE EFFECTS, Sikorsky Aircraft Division, United Aircraft Corporation, USAAVLABS Technical Report 67-44, U. S. Army Aviation Materiel Laboratories, Fort Eustis, Virginia, November 1967, AD 665427.

2. Dinkeloo, C., S-61F INTEGRATED CONTROLS FLIGHT TEST DATA, Sikorsky Aircraft SER-611435, February 28, 1969.

11.2 TRIM CALCULATIONS

The sample trim calculations for a single rotor compound helicopter are performed using the analytical procedure outlined in Section 5.1 as follows:

(a) Determine the required compound helicopter design parameters as shown in Table I. The lift curve slopes for the wing, a_W, the horizontal tail, a_T, and the vertical tail, a_{VT}, are obtained using the methods in Section 5.4.

(b) Determine the following operating conditions for the sample aircraft:

V_o = 221 ft/sec

$(\Omega R)_F$ = 660 ft/sec

$(\Omega R)_{TR}$ = 660 ft/sec

V_S = 1104.4 ft/sec

Altitude = 3,000 ft (ρ = 0.002176 slug/ft^3)

Then compute

$$q_o = \frac{1}{2}\rho V_o^2 = \frac{0.002176}{2} \times (221)^2 = 53.2 \text{ lb/ft}^2$$

$$\mu_F = \frac{V_o}{(\Omega R)_F} = \frac{221}{660} = 0.335$$

$$(M_T)_F = \frac{V_o + (\Omega R)_F}{V_S} = \frac{221 + 660}{1104.4} = 0.798$$

$$(T.F.)_F = \left[\rho \pi R^2 (\Omega R)^2\right]_F = 0.002176 \times 3.14 \times 31^2 \times 660^2 = 2.86 \times 10^6 \text{ lb}$$

$$\mu_{TR} = \frac{V_o}{(\Omega R)_{TR}} = \frac{221}{660} = 0.335$$

$$(M_T)_{TR} = \frac{V_o + (\Omega R)_{TR}}{V_S} = \frac{221 + 660}{1104.4} = 0.798$$

$$(T.F.)_{TR} = \left[\rho \pi R^2 (\Omega R)^2\right]_{TR} = 0.002176 \times 3.14 \times 5.17^2 \times 660^2 = 7.95 \times 10^4 \text{ lb}$$

TABLE I

DESIGN PARAMETERS FOR THE SAMPLE COMPOUND HELICOPTER

Main Rotor	Tail Rotor	Fuselage	Auxiliary Jets
$\theta_{1_F} = -4^\circ$	$\theta_{1_{TR}} = 0^\circ$	$W = 18900$ lb	$n = 2$
$a_F = 5.73$	$a_{TR} = 5.73$	$A_{X_{FUS}} = 68\ ft^2$	$i_P = 6^\circ$
$i_F = -4^\circ$	$i_{TR} = 0^\circ$	$A^*_{X_{FUS}} = 95\ ft^2$	$A_{ij} = 1.92\ ft^2$
$b_F = 6$	$b_{TR} = 5$	$A_{Y_{FUS}} = 388\ ft^2$	$R_{ij} = 0.78$ ft
$R_F = 31$ ft	$R_{TR} = 5.17$ ft	$A_{Z_{FUS}} = 276\ ft^2$	$\ell_{X_{P_T}} = 0$
$e_F = 1.05$ ft	$e_{TR} = 0.32$ ft	$\ell_{FUS} = 56.5$ ft	$\ell_{Y_{P_T}} = \pm 8$ ft
$\sigma_F = 0.092$	$\sigma_{TR} = 0.188$		$\ell_{Z_{P_T}} = 2.98$ ft
$\gamma_F = 9.78$	$\gamma_{TR} = 3.89$		$\ell_{X_{P_N}} = 5.75$ ft
$\ell_{X_F} = 0.47$ ft	$\ell_{X_{TR}} = -36$ ft		$\ell_{Y_{P_N}} = \pm 8$ ft
$\ell_{Y_F} = 0$	$\ell_{Y_{TR}} = -2$ ft		$\ell_{Z_{P_N}} = 2.63$ ft
$\ell_{Z_F} = -6.91$ ft	$\ell_{Z_{TR}} = -7.31$ ft		
$M_{S_F} = 92.93$ slug-ft			

* Includes rotor pylon and auxiliary jet engine pylons and nacelles.

TABLE I - Concluded

Wing	Horizontal Tail	Vertical Tail	Nacelle Pylon (Stub Wing)
$a_W = 4.83$	$a_T = 4.42$	$a_{VT} = 1.84$	$a_{SW} = 2.39$
$i_W = 0^\circ$	$i_T = 0^\circ$	$i_{VT} = 0^\circ$	$i_{SW} = 0^\circ$
$(AR)_W = 6.04$	$(AR)_T = 5.26$	$(AR)_{VT} = 1.50$	$(AR)_{SW} = 1.84$
$S_W = 170\ ft^2$	$S_T = 76.20\ ft^2$	$S_{VT} = 52\ ft^2$	$S_{SW(exp)} = 72.75\ ft^2$
$\ell_{XW} = -0.29$ ft	$\ell_{XT} = -35.70$ ft	$\ell_{XVT} = -34.40$ ft	$\ell_{XSW} = 3.5$ ft
$\ell_{YW} = \pm 7.08$ ft	$\ell_{YT} = \pm 3.66$ ft	$\ell_{YVT} = 0$	$\ell_{YSW} = \pm 5.75$ ft
$\ell_{ZW} = -1.25$ ft	$\ell_{ZT} = -0.77$ ft	$\ell_{ZVT} = -3.14$ ft	$\ell_{ZSW} = 3.4$ ft
$\alpha_{oW} = -2.8^\circ$	$\alpha_{oT} = 0^\circ$	$\alpha_{oVT} = 0^\circ$	$\alpha_{oSW} = 0^\circ$
$b_W = 32$ ft	$b_T = 20$ ft		

$$\sum_{i=1}^{n} T_{P_i} = \sum_{i=1}^{2} (960) = 1920 \text{ lb}$$

(c) Obtain fuselage lift and drag coefficients for $\alpha_{FUS} = 2.5^\circ$. This angle is chosen after examining the operating conditions in step (b) in order to reduce the number of iterations required for convergence to trim.

Using Figure 2, of Section 11.1 for $\alpha_{FUS} = 2.5^\circ$, obtain

$C_{L_{FUS}} = -0.006$ (hub and nacelle lift are negligible)

$C_{D_{FUS}} = 0.349$ (includes auxiliary jet nacelle drag)

Using the values for $A_{Z_{FUS}}$ and $A_{X_{FUS}}$ from step (a) and q_0 from step (b), compute

$$L_{FUS} = C_{L_{FUS}} q_0 A_{Z_{FUS}} = -0.006 \times 53.2 \times 276$$

$$= -88.1 \text{ lb}$$

$$D_{FUS} = C_{D_{FUS}} q_0 A_{X_{FUS}} = 0.349 \times 53.2 \times 95$$

$$= 1763 \text{ lb}$$

Also, from rotating hub test data conservatively estimate the hub drag as

$$\frac{D_{HUB}}{q_0} = 7 \text{ ft}^2$$

Include this hub drag in the total fuselage drag estimate, thus:

$$D_{FUS_{TOT}} = D_{FUS} + D_{HUB} = 1763 + 372 = 2135 \text{ lb}$$

(d) Using the values of the wing and horizontal tail parameters from step (a), calculate the first approximation of the wing and tail lift and drag forces by initially neglecting the interference angles, ϵ, thus:

$$\alpha_W = (\alpha_{FUS} + \epsilon_{FUS}) + (i_W - \epsilon_W)$$

$$= (2.5 + 0) + (0 - 0) = 2.5^\circ = 0.0436 \text{ rad}$$

$$\alpha_{o_W} = -2.8^\circ = -0.0489 \text{ rad}$$

$$C_{L_W} = a_W(\alpha_W - \alpha_{o_W}) = 4.83(0.0436 + 0.0489) = 0.447$$

$$L_W = C_{L_W} q_o S_W = 0.447 \times 53.2 \times 170 = 4040.5 \text{ lb}$$

$$C_{D_W} = \left[C_{d_o} + \frac{C_L^2}{\pi A\!\!R}\right]_W = 0.01 + \frac{0.447^2}{3.14 \times 6.04} = 0.0205$$

$$D_W = C_{D_W} q_o S_W = 0.0205 \times 53.2 \times 170 = 185.5 \text{ lb}$$

$$\alpha_T = (\alpha_{FUS} + \epsilon_{FUS}) + (i_T - \epsilon_T)$$

$$= (2.5 + 0) + (0 - 0) = 2.5^\circ = 0.0436 \text{ rad}$$

$$\alpha_{o_T} = 0^\circ = 0 \text{ rad}$$

$$C_{L_T} = a_T(\alpha_T - \alpha_{o_T}) = 4.42(0.0436 - 0) = 0.193$$

$$L_T = C_{L_T} q_o S_T = 0.193 \times 53.2 \times 76.2 = 781.7 \text{ lb}$$

$$C_{D_T} = \left[C_{d_o} + \frac{C_L^2}{\pi A\!\!R}\right]_T = 0.01 + \frac{0.193^2}{3.14 \times 5.26} = 0.0122$$

$$D_T = C_{D_T} q_o S_T = 0.0122 \times 53.2 \times 76.2 = 49.6 \text{ lb}$$

For this sample aircraft, allowance must be made for the lift forces generated by the large pylons and stub wings supporting the nacelles of the auxiliary propulsion units. The pylon drag is included in the total fuselage drag curve shown in Figure 2 of Section 11.1. Using the stub wing parameters presented in Table I, calculate the additional lift, thus:

$$L_{SW} = a_{SW}\alpha_{FUS}\, q_0\, S_{SW}$$

$$= \frac{2.39 \times 2.5 \times 53.2 \times 72.75}{57.3} = 403.2 \text{ lb}$$

(e) Calculate the first approximation for the main rotor lift and drag forces, thus:

$$L_F = W - L_{FUS} - L_W - L_{SW} - L_T - \sum_{i=1}^{n} T_{P_i} \sin(i_{P_i} + \alpha_{FUS})$$

$$= 18900 + 88.1 - 4040.5 - 403.2 - 781.7$$

$$- 1920 \sin(6^\circ + 2.5^\circ) = 13478.9 \text{ lb}$$

$$D_F = -D_{FUS_{TOT}} - D_W - D_T + \sum_{i=1}^{n} T_{P_i} \cos(i_{P_i} + \alpha_{FUS})$$

$$= -2135 - 185.5 - 49.6 + 1920 \cos(6^\circ + 2.5^\circ)$$

$$= -471.4 \text{ lb}$$

Calculate the corresponding lift coefficient for the first approximation, thus:

$$\left(\frac{C_L}{\sigma}\right)_F = \left[\frac{L}{(T.F.)\sigma}\right]_F = \frac{13478.9}{2.86\times10^6\times0.092} = 0.0512$$

(f) Using Section 5.8 or the pertinent test data, obtain the following downwash interference factors

$K_{F_{FUS}} = 1.00$

$K_{F_W} = 1.08$

$(K_{F_T} + K_{W_T}) = (K_{F_{TR}} + K_{W_{TR}}) = 3.112$

Then compute the downwash interference angles ϵ_{FUS}, ϵ_W, ϵ_T, and ϵ_{TR} respectively, using the value of $(C_L'/\sigma)_F$ from step (e) thus:

$$\epsilon_{FUS} = K_{F_{FUS}} \left[\frac{\sigma}{2\mu^2} \left(\frac{C_L'}{\sigma}\right) 57.3 \right] = 1.00 \left[\frac{0.092 \times .0512 \times 57.3}{2 \times 0.335^2} \right]$$

$$= 1.00 \left[1.20 \right] = 1.20^\circ$$

Hence.

$\epsilon_W = 1.08 \times 1.20 = 1.30^\circ$

$\epsilon_T = \epsilon_{TR} = 3.112 \times 1.20 = 3.73^\circ$

(g) Using the downwash angles obtained in step (f), calculate the better approximations for wing and horizontal tail angle of attack and the corresponding forces, thus:

$\alpha_W = (\alpha_{FUS} + \epsilon_{FUS}) + (i_W - \epsilon_W)$

$= (2.5 + 1.2) + (-1.3) = 2.4^\circ = 0.0419$ rad

$\alpha_{o_W} = -2.8^\circ = -0.0489$ rad

$C_{L_W} = a_W(\alpha_W - \alpha_{o_W}) = 4.83(0.0419 + 0.0489) = 0.438$

$L_W = C_{L_W} q_o S_W = 0.438 \times 53.2 \times 170 = 3964.1$ lb

$C_{D_W} = \left[C_{d_o} + \frac{C_L^2}{\pi A\!\!R}\right]_W = 0.01 + \frac{0.438^2}{3.14 \times 6.04} = 0.0201$

$D_W = C_{D_W} q_o S_W = 0.0201 \times 53.2 \times 170 = 181.96$ lb

$\alpha_T = (\alpha_{FUS} + \epsilon_{FUS}) + (i_T - \epsilon_T)$

$= (2.5 + 1.2) + (-3.73) = -0.03^\circ = -0.00052$ rad

$\alpha_{o_T} = 0$

$C_{L_T} = a_T(\alpha_T - \alpha_{o_T}) = 4.42\ (-0.00052) = -0.00229$

$L_T = C_{L_T} q_o S_T = -0.00229 \times 53.2 \times 76.2 = -9.3$ lb

$C_{D_T} = \left[C_{d_o} + \frac{C_L^2}{\pi A\!\!R}\right]_T = 0.01 + \frac{(-0.00229)^2}{3.14 \times 5.26} = 0.010$

$D_T = C_{D_T} q_o S_T = 0.01 \times 53.2 \times 76.2 = 40.54$ lb

The value of the stub wing lift remains unchanged.

$L_{SW} = 403.2$ lb

(h) Calculate the second approximation for the main rotor lift and drag forces, thus:

$L_F = W - L_{FUS} - L_W - L_{SW} - L_T - \sum_{i=1}^{n} T_{P_i} \sin(i_{P_i} + \alpha_{FUS})$

$= 18900 + 88.1 - 3964.1 - 403.2 + 9.3 - 1920 \sin(6^\circ + 2.5^\circ)$

$= 14{,}346.3$ lb

$$D_F = -D_{FUS} - D_W - D_T + \sum_{i=1}^{n} T_{P_i}\cos(i_{P_i} + \alpha_{FUS})$$

$$= -2135.2 - 181.96 - 40.54 + 1920\cos(6^\circ + 2.5^\circ)$$

$$= -458.8 \text{ lb}$$

Also compute the corresponding rotor lift and drag coefficients

$$\left(\frac{C_L'}{\sigma}\right)_F = \left[\frac{L}{(T.F.)\sigma}\right]_F = \frac{14,346.3}{2.86 \times 10^6 \times 0.092} = 0.0545$$

$$\left(\frac{C_D'}{\sigma}\right)_F = \left[\frac{D}{(T.F.)\sigma}\right]_F = \frac{-458.8}{2.86 \times 10^6 \times 0.092} = -0.00174$$

(i) Calculate the chart values of rotor lift and drag coefficients corresponding to a rotor solidity of $\sigma = 0.1$ using the methods in Reference 1 , thus:

$$(\Delta\sigma) = \sigma_F - 0.1 = 0.092 - 0.1 = -0.008$$

$$\left[\left(\frac{C_L'}{\sigma}\right)_F\right]_{0.1} = \left(\frac{C_L'}{\sigma}\right)_F = 0.0545$$

$$\left[\left(\frac{C_D'}{\sigma}\right)_F\right]_{0.1} = \left[\frac{C_D'}{\sigma} - \frac{\Delta\sigma}{2\mu^2}\left(\frac{C_L'}{\sigma}\right)^2\right]_F$$

$$= -0.00174 + \frac{0.008}{2(0.335)^2}(0.0545)^2 = -0.00166$$

(j) Using the values of $[(C_L'/\sigma)_F]_{0.1}$, $[(C_D'/\sigma)_F]_{0.1}$ from step (i) and θ_{1_F} , μ_F , M_{T_F} from steps (a) and (b), enter Figures 25 and 28 of Reference 1, and by interpolating to the desired value of $[(C_L'/\sigma)_F]_{0.1}$ obtain the first approximations for the following main rotor trim parameters:

$$\left[(\alpha_c)_F\right]_{0.1} = -6.57^\circ = -0.1147 \text{ rad}$$

$a_{1_F} = 4.25^{\circ} = 0.0741$ rad

$(\frac{C_Q}{\sigma})_F = 0.00256$

$\lambda_F = -0.0443$

Note that a_{0_F}, b_{1_F}, and $(\theta_{.75})_F$, need only be calculated after final trim has been established.

(k) Calculate main rotor angle of attack (α_{c_F}) and rotor torque (Q_F) as follows:

$$\alpha_{c_F} = \left[(\alpha_c)_{a.1} + \frac{\Delta\sigma}{2\mu^2}(\frac{C_L'}{\sigma})\right]_F$$

$$= -0.1147 - \frac{0.008}{2(0.335)^2} \times 0.0545 = -0.1166 \text{ rad} = -6.68^{\circ}$$

$$Q_F = \left[\frac{C_Q}{\sigma}(T.F.)\sigma R\right]_F$$

$$= 0.00256 \times 2.86 \times 10^6 \times 0.092 \times 31 = 20{,}812 \text{ ft-lb}$$

(1) Using the previously determined downwash interference factors from step (f), compute the new downwash interference angles ϵ_{FUS}, ϵ_W, ϵ_T, and ϵ_{TR} respectively, using the value of $(C_L'/\sigma)_F$ from step (h).

Thus:

$$\epsilon_{FUS} = K_{FUS}\left[\frac{\sigma}{2\sqrt{\mu^2+\lambda^2}}(\frac{C_L'}{\sigma})(57.3)\right]_F$$

$$= 1.00\left[\frac{0.092 \times 0.0545 \times 57.3}{2\sqrt{(0.335)^2 + (-0.0443)^2}}\right]$$

$$= 1.00 \left[1.28\right] = 1.28^{\circ}$$

Hence,

$\epsilon_W = 1.08 \times 1.28 = 1.38^\circ$

$\epsilon_T = \epsilon_{TR} = 3.112 \times 1.28 = 3.98^\circ$

(m) Using the design parameters and the initial trim values obtained in the steps above, determine the relationship between α_{FUS} and $C_{M_{FUS}}$ as follows: First, calculate the hub pitching moment by the following steps

$$B_{1_F} = (\alpha_{FUS} + \epsilon_{FUS}) - \alpha_{C_F} + i_F$$

$$= 2.5 + 1.28 + 6.68 - 4 = 6.46^\circ = 0.1127 \text{ rad}$$

The hub moment due to rotor control forces is then obtained from

$$M_{HUB} = \left[\frac{eb\Omega^2 M_S}{2}(a_1 - B_1)\right]_F$$

$$= \frac{1.05 \times 6 \times 92.93}{2}\left[\frac{660}{31}\right]^2 (0.0741 - 0.1127)$$

$$= -5124.4 \text{ ft-lb}$$

Since the fuselage pitching moment curve does not include the pitching moment due to drag of the rotating hub, this contribution must be precomputed and included in the computations, thus:

$$-\ell_{Z_F} D_{HUB} = 6.91 \times 372 = 2570.5 \text{ ft-lb}$$

The normal force at the intake of the auxiliary jet engines is estimated from Section 5.7 as

$$N_{P_i} = \left(\frac{N_{P_i}}{A_{ii}}\right)A_{ii} = 15.6 \times 1.92 = 30 \text{ lb}$$

Because of the length of the expression relating α_{FUS} and $C_{M_{FUS}}$ calculate the numerator, NUM , and denominator, DEN , separately as follows:

$$\begin{aligned} NUM = {} & \ell_{x_F} L_F - \ell_{z_F} D_F + \ell_{x_W} L_W - \ell_{z_W} D_W + \ell_{x_{SW}} L_{SW} + \ell_{x_T} L_T \\ & - \ell_{z_T} D_T + \sum_{i=1}^{n} T_{P_i} \ell_{z_{PT}} - \sum_{i=1}^{n} N_{P_i} i_{P_i} \ell_{z_{PN}} + \sum_{i=1}^{n} N_{P_i} \ell_{x_{PN}} \\ & - \ell_{z_F} D_{HUB} + M_{HUB} + C_{M_{FUS}} q_0 A_{x_{FUS}} \ell_{FUS} \\ = {} & 0.47 \times 14346.3 - 6.91 \times 458.8 - 0.29 \times 3964.1 + 1.25 \times \\ & 181.96 + 3.5 \times 403.2 + 35.7 \times 9.3 + 0.77 \times 40.5 + 2 \times 960 \times \\ & 2.98 - 2 \times 30 \times 0.104 \times 2.68 + 2 \times 30 \times 5.75 + 2570.5 - 5124.4 \\ & + 53.2 \times 68 \times 56.5 \times C_{M_{FUS}} \\ = {} & 7953.09 + 204390.56\, C_{M_{FUS}} \end{aligned}$$

$$\begin{aligned} DEN = {} & -(\ell_z L + \ell_x D)_F - (\ell_z L + \ell_x D)_W - (\ell_z L + \ell_x D)_T \\ = {} & 6.91 \times 14346.3 + 0.47 \times 458.8 + 1.25 \times 3964.1 \\ & + 0.29 \times 181.96 - 0.77 \times 9.3 + 35.7 \times 40.5 \\ = {} & 105795.15 \end{aligned}$$

Then

$$\alpha_{FUS} = \frac{NUM}{DEN} - \epsilon_{FUS}$$

$$\alpha_{FUS} = \frac{7953.09 + 204390.56\, C_{M_{FUS}}}{105795.15} - \frac{1.28}{57.3}$$

$$= 0.0529 + 1.9319\, C_{M_{FUS}}$$

$$\therefore \alpha_{FUS}^{\circ} = 3.03 + 110.70\, C_{M_{FUS}}$$

Superimpose the linear relationship between $C_{M_{FUS}}$ and α_{FUS}° from the above equation on the experimental fuselage pitching moment curve $C_{M_{FUS}}$ vs. α_{FUS}° as shown in Figure 1. If the two curves intersect, the point of intersection yields the new fuselage trim angle for each successive iteration. The final trim point is obtained when the calculated linear curve of $C_{M_{FUS}}$ vs. α_{FUS}° intersects the experimental curve at the same trim angle of attack, α_{FUS}, for which the last iteration was performed. If, as in this example, no intersection is obtained, use better judgement in selecting a more appropriate initial value of α_{FUS}. Since the calculated value of $C_{M_{FUS}}$ corresponding to the initially assumed α_{FUS}= 2.5 is too low, an increase in α_{FUS} is indicated.

Therefore, for the second iteration choose a trim angle of attack

$$\alpha_{FUS} = 3.0^{\circ} = 0.0524 \text{ rad}$$

(n) Using $\alpha_{FUS} = 3^{\circ}$, enter the fuselage charts. Figure 2 of Section 11.1 and Figures 5,6, and 11 of Section 5.3, and obtain the following longitudinal fuselage characteristics

$C_{L_{FUS}} = -0.004$	$C_{Y_{FUS}} = 0.0049$
$C_{D_{FUS}} = 0.350$	$C_{\ell_{FUS}} = -0.0019$
$C_{M_{FUS}} = 0.030$	$C_{N_{FUS}} = -0.0075$

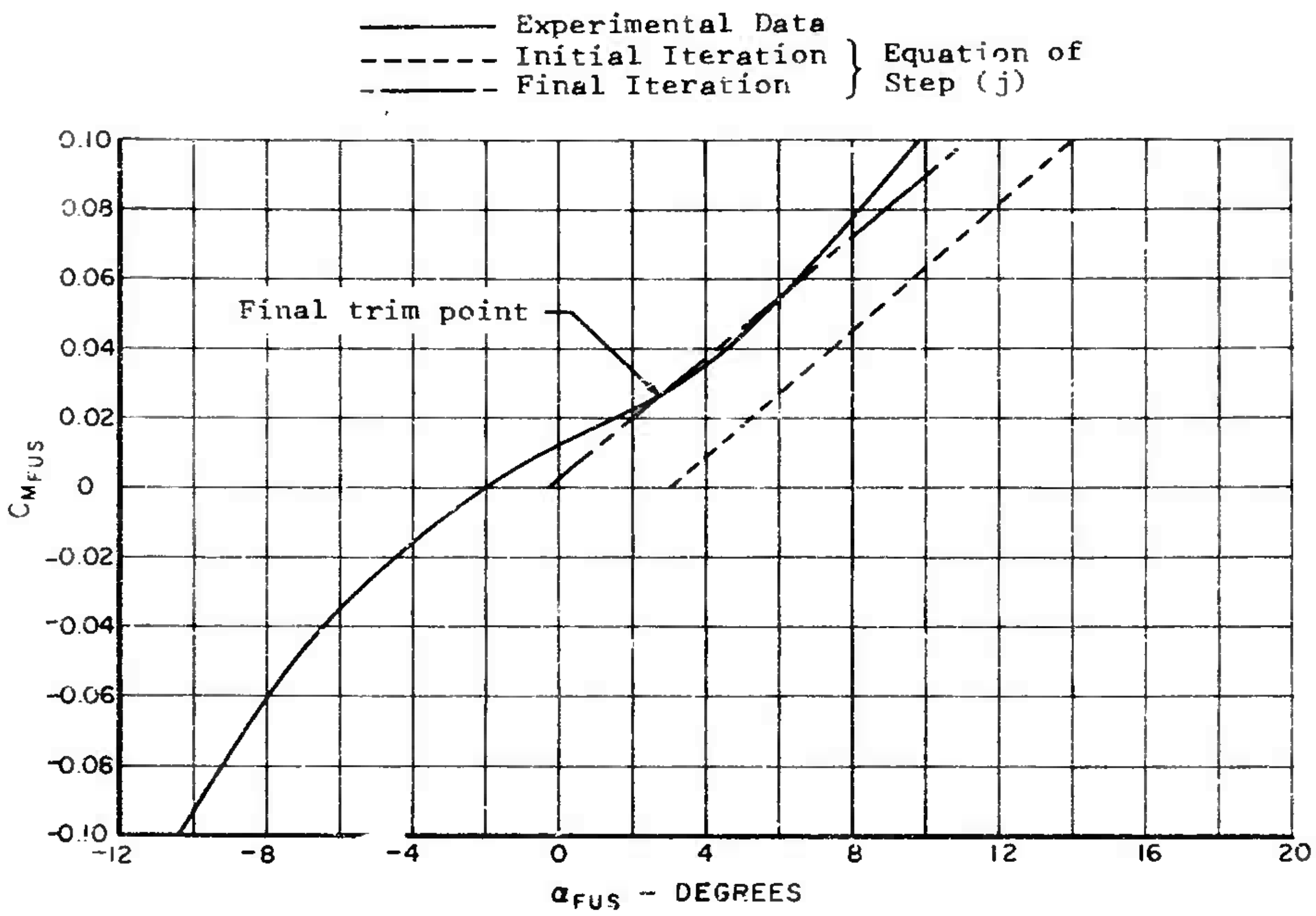

Figure 1. Superposition of the Calculated and the Experimental Fuselage Pitching Moment Data.

Then compute the corresponding fuselage forces and moments, thus:

$L_{FUS} = C_{L_{FUS}} q_0 A_{Z_{FUS}}$ $= -0.004 \times 53.2 \times 276$

$= -58.733$ lb

$D_{FUS} = C_{D_{FUS}} q_0 A^{*}_{X_{FUS}}$ $= 0.35 \times 53.2 \times 95$

$= 1768.9$ lb

$M_{FUS} = C_{M_{FUS}} q_0 A_{X_{FUS}} \ell_{FUS}$ $= 0.03 \times 53.2 \times 68 \times 56.5$

$= 6131.83$ ft-lb

$Y_{FUS} = C_{Y_{FUS}} q_0 A_{Y_{FUS}}$ $= 0.0049 \times 53.2 \times 388$

$= 101$ lb

$\mathcal{L}_{FUS} = C_{\mathcal{L}_{FUS}} q_0 A_{X_{FUS}} \ell_{FUS}$ $= -0.0019 \times 53.2 \times 68 \times 56.5$

$= 388$ ft-lb

$N_{FUS} = C_{N_{FUS}} q_0 A_{X_{FUS}} \ell_{FUS}$ $= -0.0075 \times 53.2 \times 68 \times 56.5$

$= -1532.96$ ft-lb

(o) Using the values of N_{FUS} from step (n), and Q_F from step (k), determine tail rotor thrust and tail rotor lift coefficient, thus:

$$T_{TR} = \frac{N_{FUS} + Q_F}{-\ell_{X_{TR}}} = \frac{-1532.96 + 20811.79}{36} = 535.52 \text{ lb}$$

$$\left(\frac{C_L'}{\sigma}\right)_{TR} = \left[\frac{T}{(T.F.)\sigma}\right]_{TR} = \frac{535.52}{7.95 \times 10^4 \times 0.188} = 0.0358$$

(p) With the values of $\theta_{1_{TR}}$, μ_{TR}, and $M_{T_{TR}}$ from steps (a) and (b), $(C_L'/\sigma)_{TR}$ from step (o), and $(\alpha_C)_{TR} = 0$, enter the appropriate performance charts of Reference 1 (interpolate between the charts if necessary), and obtain the following tail rotor parameters:

$\left[\left(\frac{C_D'}{\sigma}\right)_{TR}\right]_{0.1} = 0.00247$ $\left(\frac{C_Q}{\sigma}\right)_{TR} = 0.00096$

$\lambda_{TR} = 0.00576$ $\qquad (\theta_{75})_{TR} = 2.1^{\circ} = 0.03364$ rad

Then compute

$$\left(\frac{C_D'}{\sigma}\right)_{TR} = \left[\left(\frac{C_D'}{\sigma}\right)_{0.1} + \frac{\Delta\sigma}{2\mu^2}\left(\frac{C_L'}{\sigma}\right)^2\right]_{TR}$$

$$= 0.00247 + \frac{(0.188 - 0.1)(0.0358)^2}{2 \times (.335)^2}$$

$$= 0.00297$$

$$D_{TR} = \left[\frac{C_D'}{\sigma}(T.F.)\sigma\right]_{TR}$$

$$= 0.00297 \times 7.95 \times 10^4 \times 0.188 = 44.39 \text{ lb}$$

$$Q_{TR} = \left[\frac{C_Q}{\sigma}(T.F.)\sigma R\right]_{TR}$$

$$= 0.00096 \times 7.95 \times 10^4 \times 0.188 \times 5.17 = 74.13 \text{ ft-lb}$$

(q) From the trim values obtained in the steps above, determine the new lifting surface characteristics as follows:

$$\alpha_W = \alpha_{FUS} + \epsilon_{FUS} + i_W - \epsilon_W - \alpha_{o_W}$$

$$= 3 + 1.28 + 0 - 1.38 + 2.8 = 5.7^{\circ} = 0.0995 \text{ rad}$$

$$C_{L_W} = a_W \alpha_W = 4.83 \times 0.0995 = 0.480$$

$$C_{D_W} = \left[C_{d_o} + \frac{C_L^2}{\pi AR}\right]_W = 0.01 + \frac{(0.480)^2}{3.14 \times 6.04} = 0.0222$$

$$L_W = C_{L_W} q_o S_W = 0.480 \times 53.2 \times 170 = 4343.7 \text{ lb}$$

$D_W = C_{D_W} q_o S_W = 0.0222 \times 53.2 \times 170 = 200.3$ lb

$\alpha_T = \alpha_{FUS} + \epsilon_{FUS} + i_T - \epsilon_T - \alpha_{o_T}$

$= 3 + 1.28 + 0 - 3.98 - 0 = 0.30^\circ = 0.00521$ rad

Using a trim value of B_{1_F} from step (m). the elevator angle which is coupled with B_{1_F} can be read from the longitudinal control rigging curves presented in Figure 3 of Section 11.1:

$\delta_e = -0.4^\circ = -0.00698$ rad

Using the parameters in step (a) and the methods in Section 5.6, calculate the elevator control derivative, thus:

$C_{L_{\delta_e}} = 1.547$/rad

The horizontal tail lift coefficient is now obtained as

$C_{L_T} = a_T \alpha_T + C_{L_{\delta_e}} \delta_e$

$= 4.42 \times 0.00521 - 1.547 \times 0.00698 = 0.0122$

and

$$C_{D_T} = \left[C_{d_o} + \frac{C_L^2}{\pi A\!\!R}\right]_T = 0.01 + \frac{(0.0122)^2}{3.14 \times 5.26} = 0.01$$

$L_T = C_{L_T} q_o S_T = 0.0122 \times 53.2 \times 76.2 = 49.6$ lb

$D_T = C_{D_T} q_o S_T = 0.01 \times 53.2 \times 76.2 = 40.7$ lb

Also calculate the lift of the stub wing for the new trim conditions, as

$$L_{SW} = a_{SW}\ \alpha_{SW}\ q_o\ S_{SW}$$

$$= 2.39 \times 0.0524 \times 53.2 \times 72.75 = 483.8 \text{ lb}$$

(r) Using the trim parameters obtained above and assuming $A_{1_F} = \phi = Y_{TR} = \gamma_c = \beta_S = 0$, the X and Z equations from Section 4 are solved simultaneously to obtain a better approximation for the main rotor lift and drag, thus:

$$K_1 = W\alpha - L_{FUS}(\alpha - \epsilon_{FUS}) - L_W(\alpha - \epsilon_W) - L_{SW}(\alpha - \epsilon_{FUS}) - L_T(\alpha - \epsilon_T)$$

$$+ D_{FUS} + D_W + D_T + D_{TR} - \sum_{i=1}^{n}\left[T_{P_i} \cos i_{P_i} - N_{P_i} \sin i_{P_i}\right]$$

$$= 18900(0.0747) + 58.7(0.0524) - 4343.7(0.0506)$$

$$- 483.8(0.0524) - 49.6(0.0052) + 2141.3 + 200.3$$

$$+ 40.66 + 44.39 - 1920(0.9945) + 63.7(0.1045)$$

$$= 1694.3 \text{ lb}$$

$$K_2 = D_{FUS}(\alpha - \epsilon_{FUS}) + D_W(\alpha - \epsilon_W) + D_T(\alpha - \epsilon_T) + D_{TR}(\alpha - \epsilon_{TR})$$

$$+ L_{FUS} + L_W + L_{SW} + L_T + \sum_{i=1}^{n}\left[T_{P_i} \sin i_{P_i} + N_{P_i} \cos i_{P_i}\right] - W$$

$$= 2141.3(0.0524) + 200.3(0.0506) + 40.7(0.0052)$$

$$+ 44.39(0.0052) - 58.7 + 4343.7 + 483.8 + 49.6$$

$$+ 1920(0.1045) + 63.7(0.9945) - 18900$$

$$= -13694.8 \text{ lb}$$

$$L_F = \frac{K_1\alpha - K_2}{1+\alpha^2} = \frac{1694.3(0.0747) + 13694.8}{1 + (0.0747)^2} = 13744.7 \text{ lb}$$

$$D_F = L\alpha - K_1 = 13744.7(0.0747) - 1694.3 = -667.53 \text{ lb}$$

Then obtain

$$\left(\frac{C_L'}{\sigma}\right)_F = \left[\left(\frac{C_L'}{\sigma}\right)_F\right]_{0.1} = \left[\frac{L}{(T.F.)\sigma}\right]_F = \frac{13744.7}{2.86\text{x}10^6\text{x}0.092} = 0.0522$$

$$\left(\frac{C_D'}{\sigma}\right)_F = \left[\frac{D}{(T.F.)\sigma}\right]_F = \frac{-700.8}{2.86\text{x}10^6\text{x}0.092} = -0.00254$$

$$\left[\left(\frac{C_D'}{\sigma}\right)_F\right]_{0.1} = \left[\frac{C_D'}{\sigma} - \frac{\Delta\sigma}{2\mu^2}\left(\frac{C_L'}{\sigma}\right)^2\right]_F$$

$$= -0.00254 + \frac{0.008(0.0522)^2}{2\text{x}(0.335)^2} = -0.00245$$

(s) Repeat steps (f) through (r) with new values of $[(C_L'/\sigma)_F]_{0.1}$ and $[(C_L'/\sigma)_F]_{0.1}$ until convergence is achieved, yielding the final trim values as shown in Table II.

(t) Using the final trim values from Table II, calculate main rotor side force, thus:

$$Y_F = \Big[(T.F.)\sigma\frac{a}{2}\Big(-\frac{3}{4}\mu\,\theta_{.75}a_0 + \frac{1}{3}\theta_{.75}b_1 + \frac{3}{8}\mu^2\theta_{.75}b_1$$

$$+ \frac{3}{4}\lambda b_1 + \frac{1}{6}a_0a_1 - \frac{3}{2}\mu\lambda a_0 - \mu^2 a_0a_1 + \frac{1}{4}\mu a_1b_1 + \frac{1}{8}\mu^2\lambda b_1\Big)\Big]_F$$

$$= \frac{2.86\text{x}10^6\text{x}0.092\text{x}5.73}{2}\Big[-\frac{3}{4}\text{x}0.335\text{x}0.112\text{x}0.0497$$
$$+ \frac{1}{3}\text{x}0.112\text{x}0.0242 + \frac{3}{8}(0.335)^2\text{x}0.112\text{x}0.0242$$
$$- \frac{3}{4}\text{x}0.053\text{x}0.0242 + \frac{1}{6}\text{x}0.0497\text{x}0.0752 + \frac{3}{2}\text{x}0.335$$
$$\text{x}0.053\text{x}0.0497 - (0.335)^2\text{x}0.0497\text{x}0.0752$$
$$+ \frac{1}{4}\text{x}0.335\text{x}0.0752\text{x}0.0242 - \frac{1}{8}(0.335)^2\text{x}0.053\text{x}0.0242\Big]$$
$$= 240.9 \text{ lb}$$

TABLE II

FINAL LONGITUDINAL TRIM VALUES FOR THE SAMPLE COMPOUND HELICOPTER

Main Rotor	Tail Rotor	Fuselage	Wing
$\alpha_{c_F} = -7.74^\circ$ (-0.155 rad)	$\alpha_{TR} = 0.21^\circ$ (0.00366 rad)	$\alpha = 4.03^\circ$ (0.0703 rad)	$\alpha_W = 2.70^\circ$ (0.0472 rad)
L_F = 13747 lb	T_{TR} = 644 lb	$\alpha_{FUS} = 2.30^\circ$ (0.0489 rad)	L_W = 4194 lb
D_F = -683 lb	D_{TR} = 51.3 lb	L_{FUS} = -70.5 lb	D_W = 193 lb
Q_F = 22607 ft-lb	Q_{TR} = 66.4 lb	D_{FUS} = 2136 lb	$\epsilon_W = 1.32^\circ$ (0.0231 rad)
λ_F = -0.053	λ_{TR} = -0.00658	M_{FUS} = 5355 ft-lb	**Tailplane**
$\theta_{75_F} = 6.40^\circ$ (0.112 rad)	$\theta_{.75_{TR}} = 2.60^\circ$ (0.0453 rad)	$\epsilon_{FUS} = 1.23^\circ$ (0.0214 rad)	$\alpha_T = 0.21^\circ$ (0.00366 rad)
$a_{0_F} = 2.85^\circ$ (0.0497 rad)	$a_{0_{TR}} = 2.32^\circ$ (0.0405 rad)		L_T = 66.3 lb
$a_{1_F} = 4.31^\circ$ (0.0752 rad)	$a_{1_{TR}} = 2.54^\circ$ (0.0442 rad)		D_T = 40.6 lb
$b_{1_F} = 1.39^\circ$ (0.0242 rad)	$b_{1_{TR}} = 1.065^\circ$ (0.0186 rad)		$\epsilon_T = 3.82^\circ$ (0.0666 rad)
$B_{1_F} = 7.77^\circ$ (0.136 rad)	$\epsilon_{TR} = 3.82^\circ$ (0.0666 rad)		$\delta_e = 0.9^\circ$ (0.0157 rad)

(u) From the rigging curve in Figure 4 of Section 11.1, establish the following linear relationships between helicopter and aerodynamic control surface movement:

$$\delta_{a_R}^{\circ} = -1^{\circ} + A_{1_F}^{\circ}$$

$$\delta_{a_L}^{\circ} = +1^{\circ} - A_{1_F}^{\circ}$$

$$\delta_r^{\circ} = 3.2^{\circ} - (\theta_{.75})_{TR}^{\circ}$$

Using the parameters in step (a) and the methods in Section 5.6, calculate the following control derivatives

$$C_{L_{\delta_r}} = \partial(L_{VT}/q_0 S_{VT})/\partial\delta_r = 0.458/\text{rad}$$

$$C_{\mathcal{L}_{\delta_a}} = \partial(\mathcal{L}_W/q_0 S_W b_W)/\partial\delta_a = 0.183/\text{rad (per aileron)}$$

Then calculate the lift of the vertical tail, thus:

$$L_{VT} = (a_{VT}\beta_S + C_{L_{\delta_r}}\delta_r)\, q_0 S_{VT}$$

$$= (a_{VT}\beta_S + C_{L_{\delta_r}}\left[\frac{3.2}{57.3} - (\theta_{.75})_{TR}\right])\, q_0 S_{VT}$$

$$= (1.84\beta_S + 0.458\ \left[0.05584 - 0.0453\right])\ x53.2x52$$

$$= 13.33 + 5090.14\beta_S \text{ lb}$$

Also compute the wing rolling moment, thus

$$\mathcal{L}_W = -L_W\,\ell_{Y_W}$$

$$\mathcal{L}_W = q_0 S_W b_W C_{\mathcal{L}_{\delta_a}} (\delta_{a_R} - \delta_{a_L})$$

$$= q_0 S_W b_W C_{\mathcal{L}_{\delta_a}} \left[\frac{(-1^\circ + A_{I_F}^\circ) - (1^\circ - A_{I_F}^\circ)}{57.3} \right]$$

$$= 2 q_0 S_W b_W C_{\mathcal{L}_{\delta_a}} \left[-\frac{1}{57.3} + A_{I_F} \right]$$

$$= 2 \times 53.2 \times 170 \times 32 \times 0.183 \left[-0.01745 + A_{I_F} \right]$$

$$= -1848 + 105923 A_{I_F} \text{ ft-lb}$$

Test data from Reference 2 indicate that only about one-third of the total horizontal tail lift is produced by the left tail panel. This gives rise to a rolling moment due to the assymmetric tail lift of:

$$\mathcal{L}_T = -L_T \ell_{Y_T} = -\frac{1}{3} L_T \ell_{Y_{T_L}} - \frac{2}{3} L_T \ell_{Y_{T_R}}$$

$$= -\frac{L_T}{3} \ell_{Y_{T_R}}$$

$$= -\frac{66.3 \times 3.66}{3} = -80.9 \text{ ft-lb}$$

(v) It is convenient in this case to represent the lateral fuselage characteristics for fuselage shape "A" in Section 5.3 in the form of linearized equations as a function of α_{FUS} and β_S, thus:

$$C_{Y_{FUS}} = 0.004 + 0.0201 \alpha_{FUS} - 0.212 \beta_S$$

$$C_{N_{FUS}} = -0.0041 - 0.067 \alpha_{FUS} - 0.333 \beta_S$$

$$C_{\mathcal{L}_{FUS}} = -0.0018 - 0.372 \beta_S$$

(w) Using the above trim conditions solve the sideforce, rolling, and yawing moment equations from Section 4, making the usual small angle assumptions and obtain β_S, A_{1_F}, and ϕ, thus:

$$Y = \left[(L_F - Y_F A_{1_F})\alpha_F - D_F\right]\beta_S + L_F A_{1_F} + Y_F + \left[L_{FUS}\alpha_{FUS} - D_{FUS}\right]\beta_S$$

$$+ C_{Y_{FUS}} q_0 A_{Y_{FUS}} + \left[L_W \alpha_W - D_W\right]\beta_S + \left[L_T \alpha_T - D_T\right]\beta_S - L_{VT}$$

$$- D_{TR}\beta_S + T_{TR} + W\phi = 0$$

$$Y = \left[(13746.6 - 240.9A_{1_F}) \times 0.0703 + 682.6\right]\beta_S$$

$$+ 13746.6A_{1_F} + 240.9 + \left[-70.5 \times 0.0489 - 2136.2\right]\beta_S$$

$$+ \left[0.004 + 0.0201 \times 0.0489 - 0.212\beta_S\right] \times 53.2 \times 388$$

$$+ \left[4194.3 \times 0.0472 - 192.9\right]\beta_S + \left[66.3 \times 0.0037 - 40.6\right]\beta_S$$

$$- 13.33 - 5090.14\beta_S - 51.3\beta_S + 643.8 + 18900\phi$$

$$= -10044.2\beta_S - 16.9A_{1_F}\beta_S + 13746.6A_{1_F} + 973.9$$

$$+ 18900\phi$$

$$\mathcal{L} = \left[(-L_F\alpha + D_F)\beta_S - L_F A_{1_F} - Y_F\right]\ell_{Z_F} - L_W \ell_{Y_W} - (L_W\alpha - D_W)\ell_{Z_W}\beta_S$$

$$- L_T \ell_{Y_T} - (L_T\alpha_T - D_T)\ell_{Z_T}\beta_S + L_{VT}\ell_{Z_{VT}} - D_{TR}\ell_{Y_{TR}}\alpha_{TR}$$

$$- (T_{TR} - D_{TR}\beta_S)\ell_{Z_{TR}} + C_{\mathcal{L}_{FUS}} q_0 A_{X_{FUS}} \ell_{FUS} + \left[\frac{eb\Omega^2 M_S}{2}(b_1 + A_1)\right]_F = 0$$

$$\mathcal{L} = \left[(-13746.6 \times 0.0703 - 682.6)\beta_S - 13746.6A_{1_F} - 240.9\right]$$

$$\times(-6.91) - 1848 + 105923A_{1_F} - (4194.3 \times 0.0472 - 192.9)$$

$$\times(-1.25)\beta_S - 80.9 - (66.3 \times 0.00366 - 40.6)(-0.77)\beta_S$$

$$-(13.33 + 5090.14\beta_S)(3.14) + 51.3 \times 2 \times 0.00366$$

$$+ (643.8 - 51.3\beta_S)(7.31) + (-0.0018 - 0.0372\beta_S) \times 53.2 \times 68 \times 56.5 + \frac{1.05 \times 6 \times 92.93}{2}\left(\frac{660}{31}\right)^2 (0.0242 + A_{1_F})$$

$$= -12603.5\beta_S + 333806.5A_{1_F} + 7239.5$$

$$N = \left[(L_F a_F - D_F)\beta_S + L_F A_{1_F} + Y_F\right] \ell_{X_F} + (L_W a_W - D_W)\ell_{X_W}\beta_S - L_W \ell_{Y_W} a_W + (L_T a_T - D_T)\ell_{X_T}\beta_S - L_T \ell_{Y_T} a_T - L_{VT}\ell_{X_{VT}} + (-D_{TR}\beta_S + T_{TR})\ell_{X_{TR}} - (-D_{TR} - T_{TR}\beta_S)\ell_{Y_{TR}} + C_{N_{FUS}} q_0 A_{X_{FUS}} \ell_{FUS} + Q_F = 0$$

$$N = \left[(13746.6 \times 0.0703 + 682.6)\beta_S + 13746.6A_{1_F} + 240.9\right] \times 0.466 - (4194.3 \times 0.0472 - 192.9) \times 0.292\beta_S + (-1848 + 105923A_{1_F}) \times 0.0472 - (66.3 \times 0.00366 - 40.6) \times 35.7\beta_S - 80.9 \times 0.00366 + (13.33 + 5090.14\beta_S) \times 34.4 - (-51.3\beta_S + 643.8) \times 36 + (-51.3 - 643.8\beta_S) \times 2 + (-0.0041 - 0.067 \times 0.0489 - 0.333\beta_S) \times 53.2 \times 68 \times 56.5 + 22607.3$$

$$= 109705.3\beta_S + 11409.9A_{1_F} - 1693.2$$

Solve for A_{1_F} in terms of β_S from the yawing moment equation, thus

$$A_{1_F} = -9.615\beta_S + 0.148$$

Substitute this equation into the rolling moment equation and obtain the trim value for the sideslip angle

$$\beta_S = 0.0176 \text{ rad} = 1.009 \text{ deg}$$

Using the value of β_S above, solve for the main rotor lateral cyclic tilt, thus

$$A_{1_F} = -\ 0.0209 \text{ rad} = -\ 1.199 \text{ deg}$$

Substitute the final trim values of β_S and A_{1_F} into the Y-force equation and obtain the trim value of aircraft roll attitude, thus

$$\phi = -\ 0.0269 \text{ rad} = -\ 1.544 \text{ deg}$$

(x) Finally, using the lateral trim values from step (w), compute the final values of the lateral forces and moments, thus:

$$L_{VT} = 13.33 + 5090.14 \times 0.0176 = 103 \text{ lb}$$

$$C_{L_{VT}} = \frac{L_{VT}}{q_o S_{VT}} = \frac{103}{53.2 \times 52} = 0.0372$$

$$D_{VT} = \left[C_{d_o} + \frac{C_L^2}{\pi A\!\!\!R}\right]_{VT} q_o S_{VT}$$

$$= \left[0.01 + \frac{(0.0372)^2}{3.14 \times 1.5}\right] \times 53.2 \times 52 = 28.4 \text{ lb}$$

$$Y_{FUS} = C_{Y_{FUS}} q_o A_{Y_{FUS}}$$

$$= (0.004 + 0.0201 \times 0.0489 - 0.212 \times 0.0176) \times 53.2 \times 388$$

$$= 25.6 \text{ lb}$$

$$N_{FUS} = C_{N_{FUS}} q_o A_{X_{FUS}} \ell_{FUS}$$

$$= (-\ 0.0041 - 0.067 \times 0.0489 - 0.333 \times 0.0176) \times 53.2 \times 68 \times 56.5$$

$$= -\ 2706.1 \text{ ft-lb}$$

$$\mathcal{L}_{FUS} = C_{\mathcal{L}_{FUS}} q_0 A_{X_{FUS}} \ell_{FUS}$$

$$= (-0.0018 - 0.0372 \times 0.0176) \times 53.2 \times 68 \times 56.5$$

$$= -500.7 \text{ ft-lb}$$

(y) Summarize the final lateral trim values as shown below

$\mathcal{L}_{FUS} = -500.7$ ft-lb

$N_{FUS} = -2706.1$ ft-lb

$Y_{FUS} = 25.6$ lb

$L_{VT} = 103$ lb

$D_{VT} = 28.4$ lb

$\phi = -1.544^\circ = -0.0269$ rad

$A_{I_F} = -1.199^\circ = -0.0209$ rad

$\beta_S = 1.009^\circ = 0.0176$ rad

$Y_F = 240.9$ lb

LITERATURE CITED

1. Tanner, W. H., CHARTS FOR ESTIMATING ROTARY WING PERFORMANCE IN HOVER AND AT HIGH FORWARD SPEEDS, United Aircraft Corporation; NASA Contractor Report CR-114, National Aeronautics and Space Administration, Washington, D. C., November 1964.

2. Dinkeloo, C., S-61F INTEGRATED CONTROLS FLIGHT TEST DATA, Sikorsky Aircraft SER-611435, February 28, 1969.

11.3 STABILITY DERIVATIVES FOR THE SAMPLE COMPOUND HELICOPTER

The stability derivatives for a compound helicopter are evaluated utilizing the analytical procedure outlined in Section 7. These derivatives are computed at the trim conditions obtained in Section 11.2. Although no Mach number corrections are required for this sample case, the main rotor derivatives are corrected for solidity and twist, and the tail rotor derivatives are corrected for solidity using methods and charts presented in Reference 1. The stability derivatives for the sample compound helicopter are computed for six degrees of freedom of aircraft longitudinal motion, as shown on the following pages.

11.3.1 Front Rotor Isolated Derivatives

(a) Obtain the required front rotor trim parameters from Section 11.2.

$\mu = 0.335$ $\quad M_T = 0.8$ $\quad \theta_1 = -4^\circ$

$\sigma = 0.092$ $\quad T.F. = 2.86 \times 10^6$ $\quad \Omega R = 660$ ft/sec

$\left(\frac{C_L'}{\sigma}\right) = 0.0522$ $\quad \left(\frac{C_D'}{\sigma}\right) = -0.00259$

$L_F = 13746.6$ lb $\quad D_F = -682.6$ lb

$\lambda_F = -0.05303$ $\quad \theta_{.75_F} = 6.4^\circ = 0.1118$ rad

$K_{WF} = 0$ $\quad \epsilon_F = 0$

(b) Using the trim values from step (a), enter the isolated rotor derivative charts given in Section 7.5 and read off the following nondimensional isolated rotor derivatives for the front rotor:

(i) μ -Derivatives

$$\left[\left(\frac{\partial(\frac{C_L'}{\sigma})}{\partial\mu}\right)_F\right]_{0.1} = -0.0746 \qquad \left[\left(\frac{\partial(\frac{C_D'}{\sigma})}{\partial\mu}\right)_F\right]_{0.1} = 0.0200$$

$$\left[\left(\frac{\partial(\frac{C_Q}{\sigma})}{\partial\mu}\right)_F\right]_{0.1} = -0.0060 \qquad \left[\left(\frac{\partial a_1}{\partial\mu}\right)_F\right]_{0.1} = 0.1600$$

$$\left[\left(\frac{\partial b_1}{\partial\mu}\right)_F\right]_{0.1} = 0.0426 \qquad \left[\left(\frac{\partial\lambda}{\partial\mu}\right)_F\right]_{0.1} = -0.1010$$

(ii) α_c -Derivatives

$$\left[\left(\frac{\partial(\frac{C_L'}{\sigma})}{\partial\alpha_c}\right)_F\right]_{0.1} = 0.4210 \qquad \left[\left(\frac{\partial(\frac{C_D'}{\sigma})}{\partial\alpha_c}\right)_F\right]_{0.1} = 0.0480$$

$$\left[\left(\frac{\partial(\frac{C_Q}{\sigma})}{\partial\alpha_c}\right)_F\right]_{0.1} = -0.00781 \qquad \left[\left(\frac{\partial a_1}{\partial\alpha_c}\right)_F\right]_{0.1} = 0.0257$$

$$\left[\left(\frac{\partial b_1}{\partial\alpha_c}\right)_F\right]_{0.1} = 0.1890 \qquad \left[\left(\frac{\partial\lambda}{\partial\alpha_c}\right)_F\right]_{0.1} = 0.2700$$

(iii) $\theta_{.75}$ -Derivatives

The $\theta_{.75}$ -derivatives are not required for this analysis since the collective pitch control of the main rotor remains fixed.

(c) Estimate the effect of -4° of blade twist on the isolated derivatives using data of Reference 1 and add these correction factors to the isolated derivatives computed in step (b), thus:

(i) μ -Derivatives

$$\left[\left(\frac{\partial(\frac{C_L'}{\sigma})}{\partial\mu}\right)_F\right]_{0.1} = -0.0746 + 0.0053 = -0.0693$$

$$\left[\left(\frac{\partial(\frac{C_D'}{\sigma})}{\partial\mu}\right)_F\right]_{0.1} = 0.0200 + 0.0033 = 0.0233$$

$$\left[\left(\frac{\partial(\frac{C_Q}{\sigma})}{\partial\mu}\right)_F\right]_{0.1} = -0.0060 + 0.0005 = -0.0055$$

$$\left[\left(\frac{\partial a_1}{\partial\mu}\right)_F\right]_{0.1} = 0.1600 - 0.0090 = 0.1510$$

$$\left[\left(\frac{\partial b_1}{\partial\mu}\right)_F\right]_{0.1} = 0.0426 - 0.0068 = 0.0358$$

$$\left[\left(\frac{\partial\lambda}{\partial\mu}\right)_F\right]_{0.1} = -0.1010 - 0.0060 = -0.1070$$

(ii) α_c-Derivatives

$$\left[\left(\frac{\partial(\frac{C_L'}{\sigma})}{\partial\alpha_c}\right)_F\right]_{0.1} = 0.4210 + 0.0020 = 0.4230$$

$$\left[\left(\frac{\partial(\frac{C_D'}{\sigma})}{\partial\alpha_c}\right)_F\right]_{0.1} = 0.0480 - 0.0070 = 0.0410$$

$$\left[\left(\frac{\partial(\frac{C_Q}{\sigma})}{\partial\alpha_c}\right)_F\right]_{0.1} = -0.00781 + 0.0022 = -0.00561$$

$$\left[\left(\frac{\partial a_1}{\partial\alpha_c}\right)_F\right]_{0.1} = 0.0257$$

$$\left[\left(\frac{\partial b_1}{\partial\alpha_c}\right)_F\right]_{0.1} = 0.189$$

$$\left[\left(\frac{\partial\lambda}{\partial\alpha_c}\right)_F\right]_{0.1} = 0.270$$

(d) No Mach number corrections are required for this main rotor.

(e) Using the solidity corrections given in Subsection 7.4.1, correct the μ -derivatives obtained in step (c) to the correct rotor solidity of σ =0.092, thus:

$$\Delta\sigma_F = \sigma_F - 0.1 = 0.092 - 0.1 = -0.008$$

$$K_1 = \frac{1}{1+\left[\frac{\Delta\sigma}{2\mu^2}\left(\frac{\partial(\frac{C_L'}{\sigma})}{\partial\alpha_C}\right)_{0.1}\right]_F}$$

$$= \frac{1}{1 - \frac{0.008}{2(0.335)^2} \times 0.423} = 1.015$$

$$\left[\frac{\partial(\frac{C_L'}{\sigma})}{\partial\mu}\right]_F = K\left\{\left[\frac{\partial(\frac{C_L'}{\sigma})}{\partial\mu}\right]_{0.1} + \frac{\Delta\sigma}{\mu^3}\left(\frac{C_L'}{\sigma}\right)\left[\frac{\partial(\frac{C_L'}{\sigma})}{\partial\alpha_C}\right]_{0.1}\right\}_F$$

$$= 1.015\left\{-0.0693 - \frac{0.008\text{x}0.0522\text{x}0.4230}{(0.335)^3}\right\}$$

$$= -0.0751$$

Similarly, for the remaining μ -derivatives obtain:

$$\left[\frac{\partial(\frac{C_D'}{\sigma})}{\partial\mu}\right]_F = 0.0235 \qquad \left[\frac{\partial(\frac{C_Q}{\sigma})}{\partial\mu}\right]_F = -0.00551$$

$$\left(\frac{\partial a_1}{\partial\mu}\right)_F = 0.1510 \qquad \left(\frac{\partial b_1}{\partial\mu}\right)_F = 0.0332$$

$$\left(\frac{\partial\lambda}{\partial\mu}\right)_F = -0.1110$$

Finally, using the fully corrected μ -derivatives from above, and the trim parameters from step (a), calculate $[\partial(C_Y'/\sigma)/\partial\mu]_F$ using the expressions in Subsection 7.5.1.7 as follows

$$\left(\frac{\partial a_0}{\partial\mu}\right) = \frac{\gamma_F}{2}\left[\frac{\theta_{.75}}{2}\mu + \frac{1}{3}\frac{\partial\lambda}{\partial\mu}\right]$$

$$= \frac{9.78}{2}\left[\frac{0.1118 \times 0.335}{2} + \frac{0.111}{3}\right]$$

$$= -0.0890$$

$$\left[\frac{\partial\left(\frac{C_Y'}{\sigma}\right)}{\partial\mu}\right]_F = \frac{a_F}{2}\left\{\frac{\partial a_0}{\partial\mu}\left[a_1\left(\frac{1}{6}-\mu^2\right)-\frac{3}{4}\mu(\theta_{.75}+2\lambda)\right]\right.$$

$$+\frac{\partial a_1}{\partial\mu}\left[a_0\left(\frac{1}{6}-\mu^2\right)+\frac{1}{4}\mu b_1\right]$$

$$+\frac{\partial b_1}{\partial\mu}\left[\theta_{.75}\left(\frac{1}{3}+\frac{3}{8}\mu^2\right)+\lambda\left(\frac{3}{4}+\frac{1}{8}\mu^2\right)+\frac{1}{4}\mu a_1\right]$$

$$+\frac{\partial\lambda}{\partial\mu}\left[b_1\left(\frac{3}{4}+\frac{1}{8}\mu^2\right)-\frac{3}{2}\mu a_0\right]$$

$$\left.+\frac{1}{4}b_1\left[\mu(3\theta_{.75}+\lambda)+a\right]-a_0\left[\frac{3}{4}\theta_{.75}+\frac{2}{3}\lambda-2\mu a_1\right]\right\}_F$$

$$=\frac{5.73}{2}\left\{-0.089\left[0.0752\left(\frac{1}{6}-0.335^2\right)-\frac{3\text{x}0.335}{4}\right.\right.$$

$$\left.\text{x}(0.1118-0.1061)\right]+0.1511\left[0.0497\left(\frac{1}{6}\right.\right.$$

$$\left.\left.-0.335^2\right)+\frac{0.335\text{x}0.0242}{4}\right]+0.0332\left[0.1118\right.$$

$$\text{x}\left(\frac{1}{3}+\frac{3\text{x}0.335^2}{8}\right)-0.053\left(\frac{3}{4}+\frac{0.335^2}{8}\right)$$

$$\left.+\frac{0.335\text{x}0.0752}{4}\right]-0.1108\left[0.0242\left(\frac{3}{4}+\frac{0.335^2}{8}\right)\right.$$

$$\left.-\frac{3\text{x}0.335\text{x}0.0497}{2}\right]+0.00605\left[0.335(0.335\right.$$

$$\left.-0.053)+0.0752\right]-0.0497\left[\frac{0.335}{4}\right.$$

$$\left.-\frac{2\text{x}0.053}{3}-2\text{x}0.335\text{x}0.0752\right]$$

$$=0.0073$$

(f) Using the solidity corrections given in Subsection 7.4.2, correct the α_c-derivatives found in step (c) to the correct solidity of $\sigma = 0.092$, thus:

$$\left[\frac{\partial(\frac{C_L'}{\sigma})}{\partial \alpha_c}\right]_F = K_1\left[\left(\frac{\partial(\frac{C_L'}{\sigma})}{\partial \alpha_c}\right)_F\right]_{0.1} = 1.015 \times 0.423 = 0.430$$

Similarly, for the remaining α_c-derivatives obtain:

$$\left[\frac{\partial(\frac{C_D'}{\sigma})}{\partial \alpha_c}\right]_F = 0.0432 \qquad \left[\frac{\partial(\frac{C_Q}{\sigma})}{\partial \alpha_c}\right]_F = 0.00571$$

$$\left(\frac{\partial a_1}{\partial \alpha_c}\right)_F = 0.0261 \qquad \left(\frac{\partial b_1}{\partial \alpha_c}\right)_F = 0.1920$$

$$\left(\frac{\partial \lambda}{\partial \alpha_c}\right)_F = 0.2740$$

Finally, substitute the fully corrected values of the α_c -derivatives from above and the trim parameters from step (a) into the expressions in Subsection 7.5.2.7 and obtain:

$$\left[\frac{\partial(\frac{C_Y'}{\sigma})}{\partial \alpha_c}\right]_F = 0.00295$$

(g) Using the equations of Subsection 7.3.1 and the values obtained in steps (a), (e), and (f) above, calculate the following main rotor dimensional derivatives:

(i) <u>u_F -Derivatives</u>

$$\frac{\partial L_F}{\partial u_F} = \left[\frac{(T.F.)\sigma}{\Omega R}\right]_F\left[\frac{\partial(\frac{C_L'}{\sigma})}{\partial \mu}\right]_F = 390(-0.0751) = -30.0 \text{ lb-sec/ft}$$

$$\frac{\partial D_F}{\partial u_F} = \left[\frac{(T.F.)\sigma}{\Omega R}\right]_F\left[\frac{\partial(\frac{C_D'}{\sigma})}{\partial \mu}\right]_F = 390 \times 0.0235 = 9.39 \text{ lb-sec/ft}$$

$$\frac{\partial Y_F}{\partial u_F} = \left[\frac{(T.F.)\sigma}{\Omega R}\right]_F\left[\frac{\partial(\frac{C_Y'}{\sigma})}{\partial \mu}\right]_F = 390 \times 0.0073 = 2.91 \text{ lb-sec/ft}$$

$$\frac{\partial Q_F}{\partial u_F} = \left[\frac{(T.F.)\sigma}{\Omega}\right]_F \left[\frac{\partial(\frac{C_Q}{\sigma})}{\partial \mu}\right]_F = 12366\times(-0.00551) = -68.1 \text{ lb-sec}$$

$$\frac{\partial a_{1F}}{\partial u_F} = \left(\frac{1}{\Omega R}\right)_F \left(\frac{\partial a_1}{\partial \mu}\right)_F = \frac{1}{660}\times 0.151 = 0.000229 \text{ rad-sec/ft}$$

$$\frac{\partial b_{1F}}{\partial u_F} = \left(\frac{1}{\Omega R}\right)_F \left(\frac{\partial b_1}{\partial \mu}\right)_F = \frac{1}{660}\times 0.0332 = 0.0000503 \text{ rad-sec/ft}$$

$$\frac{\partial \mathcal{L}_{HUB_F}}{\partial u_F} = \left[\frac{eb\Omega^2 M_S}{2}\right]_F \left(\frac{\partial b_1}{\partial u}\right)_F$$

$$= 1.3268 \times 10^5 \times 0.0000503 = 6.67 \text{ lb-sec}$$

$$\frac{\partial M_{HUB_F}}{\partial u_F} = \left[\frac{eb\Omega^2 M_S}{2}\right]_F \left(\frac{\partial a_1}{\partial u}\right)_F$$

$$= 1.3268 \times 10^5 \times 0.000229 = 30.4 \text{ lb-sec}$$

(ii) α_F -Derivatives

$$\frac{\partial L_F}{\partial \alpha_F} = \left[(T.F.)\sigma\right]_F \left[\frac{\partial(\frac{C_L'}{\sigma})}{\partial \alpha_c}\right]_F$$

$$= 26.33 \times 10^4 \times 0.430 = 11.32 \times 10^4 \text{ lb/rad}$$

$$\frac{\partial D_F}{\partial \alpha_F} = \left[(T.F.)\sigma\right]_F \left[\frac{\partial(\frac{C_Q'}{\sigma})}{\partial \alpha_c}\right]_F$$

$$= 26.33 \times 10^4 \times 0.0432 = 1.14 \times 10^4 \text{ lb/rad}$$

$$\frac{\partial Y_F}{\partial \alpha_F} = \left[(T.F.)\sigma\right]_F \left[\frac{\partial(\frac{C_Y'}{\sigma})}{\partial \alpha_c}\right]_F$$

$$= 26.33 \times 10^4 \times 0.00295 = 777 \text{ lb/rad}$$

$$\frac{\partial Q_F}{\partial \alpha_F} = \left[(T.F.)\sigma R\right]_F \left[\frac{\partial(\frac{C_Q}{\sigma})}{\partial \alpha_c}\right]_F$$

$$= 8.16\times 10^6 \times(-0.00566) = -4.619\times 10^4 \text{ ft-lb/rad}$$

$$\frac{\partial a_{1_F}}{\partial \alpha_F} = \left(\frac{\partial a_1}{\partial \alpha_c}\right)_F = 0.0261$$

$$\frac{\partial b_{1_F}}{\partial \alpha_F} = \left(\frac{\partial b_1}{\partial \alpha_c}\right)_F = 0.192$$

$$\frac{\partial \mathcal{L}_{HUB_F}}{\partial \alpha_F} = \left[\frac{eb\Omega^2 M_S}{2}\right]_F \left(\frac{\partial b_{1_F}}{\partial \alpha_F}\right)$$

$$= 13.2688 \times 10^4 \times 0.192 = 2.55 \times 10^4 \text{ ft-lb/rad}$$

$$\frac{\partial M_{HUB_F}}{\partial \alpha_F} = \left[\frac{eb\Omega^2 M_S}{2}\right]_F \left(\frac{\partial a_{1_F}}{\partial \alpha_F}\right)$$

$$= 13.2688 \times 10^4 \times 0.0261 = 3462 \text{ ft-lb/rad}$$

(iii) β_S -Derivatives

$$\frac{\partial a_{1_F}}{\partial \beta_S} = b_{1_F} = 0.0242 \text{ rad}$$

$$\frac{\partial b_{1_F}}{\partial \beta_S} = -a_{1_F} = -0.07521 \text{ rad}$$

$$\frac{\partial Q_F}{\partial \beta_S} = \left(\frac{\partial Q_F}{\partial a_{1_F}}\right)\left(\frac{\partial a_{1_F}}{\partial \beta_S}\right) + \left(\frac{\partial Q_F}{\partial b_{1_F}}\right)\left(\frac{\partial b_{1_F}}{\partial \beta_S}\right)$$

$$= \left[\left(\frac{\partial Q_F}{\partial u_F}\right)\left(\frac{\partial u_F}{\partial a_{1_F}}\right)\left(\frac{\partial a_{1_F}}{\partial \beta_S}\right)\right] + \left[\left(\frac{\partial Q_F}{\partial u_F}\right)\left(\frac{\partial u_F}{\partial b_{1_F}}\right)\left(\frac{\partial b_{1_F}}{\partial \beta_S}\right)\right]$$

$$= \left[(-68.1)\left(\frac{1}{0.000229}\right)(0.0242)\right]$$

$$+ \left[(-67.8)\left(\frac{1}{0.0000503}\right)(-0.07521)\right] = -5927 \text{ ft-lb}$$

$$\frac{\partial \mathcal{L}_{HUB_F}}{\partial \beta_S} = -M_{HUB_F} = 8013 \text{ ft-lb}$$

$$\frac{\partial M_{HUB_F}}{\partial \beta_S} = \mathcal{L}_{HUB_F} = 434 \text{ ft-lb}$$

(iv) q -Derivatives

$$\frac{\partial a_{1_F}}{\partial q} = \left(\frac{\partial a_1}{\partial q}\right)_F = -\left[\frac{34}{\gamma\Omega(1.883-\mu^2)}\right]_F = -0.0922 \text{ /sec}$$

$$\frac{\partial b_{1_F}}{\partial q} = \left(\frac{\partial b_1}{\partial q}\right)_F = -\left[\frac{1.883}{\Omega(1.883+\mu^2)}\right]_F = -0.04432 \text{ /sec}$$

(v) p -Derivatives

$$\frac{\partial a_{1_F}}{\partial p} = \left(\frac{\partial a_1}{\partial p}\right)_F = \left[\frac{1.883}{\Omega(1.883-\mu^2)}\right]_F = 0.04994 \text{ /sec}$$

$$\frac{\partial b_{1_F}}{\partial p} = \left(\frac{\partial b_1}{\partial p}\right)_F = -\left[\frac{34}{\gamma\Omega(1.883+\mu^2)}\right]_F = -0.08183 \text{ /sec}$$

(vi) r -Derivatives

$$\frac{\partial a_{1_F}}{\partial r} = \left(\frac{\partial a_1}{\partial r}\right)_F = -\frac{\partial a_{1_F}}{\partial \Omega} = \left(\frac{\partial a_1}{\partial \mu}\right)_F\left(\frac{\mu}{\Omega}\right)_F = 0.151\left(\frac{0.335}{21.29}\right) = 0.00238 \text{ /sec}$$

$$\frac{\partial b_{1_F}}{\partial r} = \left(\frac{\partial b_1}{\partial \mu}\right)_F\left(\frac{\mu}{\Omega}\right)_F = 0.0332\left(\frac{0.335}{21.29}\right) = 0.00052 \text{ /sec}$$

(vii) a_{1_F} -Derivatives

$$\frac{\partial L_F}{\partial a_{1_F}} = -D_F = 683 \text{ lb/rad}$$

$$\frac{\partial D_F}{\partial a_{1_F}} = L_F = 13747 \text{ lb/rad}$$

$$\frac{\partial Y_F}{\partial a_{1_F}} = 0$$

$$\left[\frac{\partial(\frac{C_Q}{\sigma})}{\partial a_1}\right]_F = -\frac{a}{2}\left[a_1\left(\frac{1}{4}+\frac{3}{8}\mu^2\right)+\frac{1}{2}\mu\lambda\right]_F = -0.03747 \text{ rad}$$

$$\frac{\partial Q_F}{\partial a_{1_F}} = \left[(TF)\sigma R\right]_F\left[\frac{\partial(\frac{C_Q}{\sigma})}{\partial a_1}\right]_F$$

$$= (8.16\times10^6)\times(-0.03747) = -305811 \text{ ft-lb/rad}$$

(viii) b_{1_F} -Derivatives

$$\frac{\partial L_F}{\partial b_{1_F}} = -Y_F = -241 \text{ lb/rad}$$

$$\frac{\partial D_F}{\partial b_{1_F}} = 0$$

$$\frac{\partial Y_F}{\partial b_{1_F}} = L_F = 13747 \text{ lb/rad}$$

$$\left[\frac{\partial(\frac{C_Q}{\sigma})}{\partial b_1}\right]_F = -\frac{a}{2}\left[b_1(\frac{1}{4} + \frac{1}{8}\mu^2) - \frac{1}{3}\mu a_o\right]_F = -0.00240/\text{rad}$$

$$\frac{\partial Q_F}{\partial b_{1_F}} = \left[(T.F.)\sigma R\right]_F \left[\frac{\partial(\frac{C_Q}{\sigma})}{\partial b_1}\right]_F$$

$$= 8.16\times10^6\times(-0.00240) = -1.96\times10^4 \text{ ft-lb/rad}$$

11.3.2 Tail Rotor Isolated Derivatives

(a) Obtain the following tail rotor trim parameters from Section 11.2.

$\mu = 0.335$	$M_T = 0.8$
$\sigma = 0.188$	$T.F. = 7.95 \times 10^4$
$\theta_1 = 0^\circ$	$\Omega R = 660$ ft/sec
$(\frac{C_L'}{\sigma})_{TR} = 0.0431$	$(\frac{C_D'}{\sigma})_{TR} = 0.00343$
$T_{TR} = 643.8$ lb	$D_{TR} = 51.3$ lb
$\lambda_{TR} = -0.00658$	$\theta_{.75_{TR}} = 2.6^\circ = 0.0453$ rad
$K_{F_{TR}} + K_{W_{TR}} = 3.112$	$\epsilon_{TR} = 3.82^\circ$

(b) Using the trim values from step (a), enter the isolated rotor derivative charts given in Section 7.5 and read off the following nondimensional isolated rotor derivatives for the tail rotor.

(i) μ -Derivatives

$$\left[\left(\frac{\partial\left(\frac{C_L'}{\sigma}\right)}{\partial\mu}\right)_{TR}\right]_{0.1} = 0.0511 \qquad \left[\left(\frac{\partial\left(\frac{C_0'}{\sigma}\right)}{\partial\mu}\right)_{TR}\right]_{0.1} = 0.0177$$

$$\left[\left(\frac{\partial\left(\frac{C_0}{\sigma}\right)}{\partial\mu}\right)_{TR}\right]_{0.1} = -0.00689 \qquad \left[\left(\frac{\partial a_1}{\partial\mu}\right)_{TR}\right]_{0.1} = 0.1480$$

$$\left[\left(\frac{\partial b_1}{\partial\mu}\right)_{TR}\right]_{0.1} = 0.0708 \qquad \left[\left(\frac{\partial\lambda}{\partial\mu}\right)_{TR}\right]_{0.1} = 0.0119$$

(ii) α_c -Derivatives

$$\left[\left(\frac{\partial\left(\frac{C_L'}{\sigma}\right)}{\partial\alpha_c}\right)_{TR}\right]_{0.1} = 0.0408 \qquad \left[\left(\frac{\partial\left(\frac{C_0'}{\sigma}\right)}{\partial\alpha_c}\right)_{TR}\right]_{0.1} = 0.0766$$

$$\left[\left(\frac{\partial\left(\frac{C_0}{\sigma}\right)}{\partial\alpha_c}\right)_{TR}\right]_{0.1} = -0.0280 \qquad \left[\left(\frac{\partial a_1}{\partial\alpha_c}\right)_{TR}\right]_{0.1} = 0.2410$$

$$\left[\left(\frac{\partial b_1}{\partial\alpha_c}\right)_{TR}\right]_{0.1} = 0.1750 \qquad \left[\left(\frac{\partial\lambda}{\partial\alpha_c}\right)_{TR}\right]_{0.1} = 0.2700$$

(iii) $\theta_{.75}$ -Derivatives

$$\left[\left(\frac{\partial\left(\frac{C_L'}{\sigma}\right)}{\partial\theta_{.75}}\right)_{TR}\right]_{0.1} = 0.9490 \qquad \left[\left(\frac{\partial\left(\frac{C_0'}{\sigma}\right)}{\partial\theta_{.75}}\right)_{TR}\right]_{0.1} = 0.0892$$

$$\left[\left(\frac{\partial\left(\frac{C_0}{\sigma}\right)}{\partial\theta_{.75}}\right)_{TR}\right]_{0.1} = -0.0155 \qquad \left[\left(\frac{\partial a_1}{\partial\theta_{.75}}\right)_{TR}\right]_{0.1} = 1.0000$$

$$\left[\left(\frac{\partial b_1}{\partial\theta_{.75}}\right)_{TR}\right]_{0.1} = 0\ 4600 \qquad \left[\left(\frac{\partial\lambda}{\partial\theta_{.75}}\right)_{TR}\right]_{0.1} = -0.1260$$

(c) No twist corrections are required for this tail rotor.

(d) No Mach number corrections are required for this tail rotor.

(e) Using the solidity corrections given in Subsection 7.4.1, correct the tail rotor μ -derivatives found in step (b) to the correct solidity of σ = 0.188, thus

$$\Delta\sigma_{TR} = \sigma_{TR} - 0.1 = 0.188 - 0.1 = 0.088$$

$$K_1 = \frac{1}{1 + \left[\frac{\Delta\sigma}{2\mu^2}\left(\frac{\partial(\frac{C_L'}{\sigma})}{\partial\alpha_c}\right)_{0.1}\right]_{TR}}$$

$$= \frac{1}{1 + \left[\frac{0.088}{2\ (0.335)^2} \times 0.0408\right]} = 0.984$$

$$\left[\frac{\partial(\frac{C_L'}{\sigma})}{\partial\mu}\right]_{TR} = K_1\left\{\left[\frac{\partial(\frac{C_L'}{\sigma})}{\partial\mu}\right]_{0.1} + \frac{\Delta\sigma}{\mu^3}\left(\frac{C_L'}{\sigma}\right)\left[\frac{\partial(\frac{C_L'}{\sigma})}{\partial\alpha_c}\right]_{0.1}\right\}_{TR}$$

$$= 0.984 \quad 0.0511 + \left\{\frac{0.088 \times 0.0431 \times 0.0408}{(0.335)^3}\right\}$$

$$= 0.0543$$

Similarly, for the other μ -derivatives obtain:

$$\left[\frac{\partial(\frac{C_D'}{\sigma})}{\partial\mu}\right]_{TR} = 0.0213 \qquad \left[\frac{\partial(\frac{C_Q}{\sigma})}{\partial\mu}\right]_{TR} = -0.00911$$

$$\left(\frac{\partial a_1}{\partial\mu}\right)_{TR} = 0.1670 \qquad \left(\frac{\partial b_1}{\partial\mu}\right)_{TR} = 0.0847$$

$$\left(\frac{\partial\lambda}{\partial\mu}\right)_{TR} = 0.0333$$

Finally, using the fully corrected μ -derivatives from above, and the trim parameters from step (a), calculate $[\partial (C_Y'/\sigma)/\partial\mu]_{TR}$, using the expressions in Subsection 7.5.1.7 to obtain:

$$\left[\frac{\partial(\frac{C_Y'}{\sigma})}{\partial\mu}\right]_{TR} = 0.00719$$

(f) Using the solidity corrections given in Sub-section 7.4.2, correct the α_c -derivatives found in step (b) to the correct solidity of σ = 0.188, thus:

$$\left[\frac{\partial(\frac{C_L'}{\sigma})}{\partial\alpha_c}\right]_{TR} = K_1\left[\left(\frac{\partial(\frac{C_L'}{\sigma})}{\partial\alpha_c}\right)_{TR}\right]_{0.1} = 0.984 \times 0.0408 = 0.0402$$

Similarly, for the remaining α_c -derivatives obtain:

$$\left[\frac{\partial(\frac{C_D'}{\sigma})}{\partial\alpha_c}\right]_{TR} = 0.0740 \qquad \left[\frac{\partial(\frac{C_Q}{\sigma})}{\partial\alpha_c}\right]_{TR} = -0.0276$$

$$\left(\frac{\partial a_1}{\partial\alpha_c}\right)_{TR} = 0.2380 \qquad \left(\frac{\partial b_1}{\partial\alpha_c}\right)_{TR} = 0.1720$$

$$\left(\frac{\partial\lambda}{\partial\alpha_c}\right)_{TR} = 0.2660$$

Finally, substitute the fully corrected α_c derivatives from above and the trim parameters from step (a) into the expressions in Subsection 7.5.2.7 and obtain:

$$\left[\frac{\partial(\frac{C_Y'}{\sigma})}{\partial\alpha_c}\right]_{TR} = 0.00283$$

(g) Using the solidity corrections given in Subsection 7.4.3, correct the θ_{75} -derivatives found in step (b) to the correct solidity of σ = 0.188, thus:

$$\left[\frac{\partial(\frac{C_L'}{\sigma})}{\partial\theta_{.75}}\right]_{TR} = K_1\left[\left(\frac{\partial(\frac{C_L'}{\sigma})}{\partial\theta_{.75}}\right)_{TR}\right]_{01} = 0.984 \times 0.949 = 0.934$$

Similarly, for the remaining $\theta_{.75}$ -derivatives obtain:

$$\left[\frac{\partial(\frac{C_D'}{\sigma})}{\partial\theta_{.75}}\right]_{TR} = 0.0927 \qquad \left[\frac{\partial(\frac{C_Q}{\sigma})}{\partial\theta_{.75}}\right]_{TR} = -0.00523$$

$$\left(\frac{\partial a_1}{\partial\theta_{75}}\right)_{TR} = 0.9120 \qquad \left(\frac{\partial b_1}{\partial\theta_{75}}\right)_{TR} = 0.3960$$

$$\left(\frac{\partial\lambda}{\partial\theta_{75}}\right)_{TR} = -0.2250$$

Finally, substitute the fully corrected θ_{75} -derivatives from above and the trim parameters from step (a) into the expressions in Subsection 7.5.3.7 and obtain

$$\left[\frac{\partial(\frac{C_Y'}{\sigma})}{\partial\theta_{.75}}\right]_{TR} = 0.0177$$

(h) Using the equations in Subsection 7.3.7 and the values obtained in steps (a), (e), (f), and (g) above, calculate the following tail rotor dimensional derivatives:

(i) u_{TR} -Derivatives

$$\frac{\partial T_{TR}}{\partial u_{TR}} = \left[\frac{(T.F.)\sigma}{\Omega R}\right]_{TR}\left[\frac{\partial(\frac{C_L'}{\sigma})}{\partial\mu}\right]_{TR} = 22.6 \times 0.0543 = 1.229 \text{ lb-sec/ft}$$

$$\frac{\partial D_{TR}}{\partial u_{TR}} = \left[\frac{(T.F.)\sigma}{\Omega R}\right]_{TR}\left[\frac{\partial(\frac{C_D'}{\sigma})}{\partial\mu}\right]_{TR} = 22.6 \times 0.0213 = 0.4820 \text{ lb-sec/ft}$$

$$\frac{\partial Y_{TR}}{\partial u_{TR}} = \left[\frac{(T.F)\sigma}{\Omega R}\right]_{TR}\left[\frac{\partial(\frac{C_Y'}{\sigma})}{\partial \mu}\right]_{TR} = 22.6\text{x}0.00719 = 0.16280 \text{ lb-sec/ft}$$

$$\frac{\partial Q_{TR}}{\partial u_{TR}} = \left[\frac{(T.F)\sigma}{\Omega}\right]_{TR}\left[\frac{\partial(\frac{C_Q}{\sigma})}{\partial \mu}\right]_{TR} = 117\text{x}(-0.00911) = -1.06583 \text{ lb-sec}$$

(ii) α_{TR}-Derivatives

$$\frac{\partial T_{TR}}{\partial \alpha_{TR}} = \frac{\partial D_{TR}}{\partial \alpha_{TR}} = \frac{\partial Y_{TR}}{\partial \alpha_{TR}} = \frac{\partial Q_{TR}}{\partial \alpha_{TR}} = 0$$

(iii) β_S -Derivatives

$$\frac{\partial T_{TR}}{\partial \beta_S} = -\left[(T.F)\sigma\right]_{TR}\left[\frac{\partial(\frac{C_L'}{\sigma})}{\partial \alpha_c}\right]_{TR} = -(14944)\text{x}0.0402 = -600 \text{ lb/rad}$$

$$\frac{\partial D_{TR}}{\partial \beta_S} = -\left[(T.F)\sigma\right]_{TR}\left[\frac{\partial(\frac{C_D'}{\sigma})}{\partial \alpha_c}\right]_{TR} = -(14944)\text{x}0.0740 = -1106 \text{ lb/rad}$$

$$\frac{\partial Y_{TR}}{\partial \beta_S} = -\left[(T.F)\sigma\right]_{TR}\left[\frac{\partial(\frac{C_Y'}{\sigma})}{\partial \alpha_c}\right]_{TR} = -(14944)\text{x}0.00283 = -42.3 \text{ lb/rad}$$

$$\frac{\partial Q_{TR}}{\partial \beta_S} = -\left[(T.F)\sigma R\right]_{TR}\left[\frac{\partial(\frac{C_Q}{\sigma})}{\partial \alpha_c}\right]_{TR} = -(77217)\text{x}(-0.0276) = 2127 \ \frac{\text{ft-lb}}{\text{rad}}$$

(iv) $\theta_{0_{TR}}$ -Derivatives

$$\frac{\partial T_{TR}}{\partial \theta_{0_{TR}}} = \left[(T.F)\sigma\right]_{TR}\left[\frac{\partial(\frac{C_L'}{\sigma})}{\partial \theta_{75}}\right]_{TR} = 14944\text{x}0.934 = 13963 \text{ lb/rad}$$

$$\frac{\partial D_{TR}}{\partial \theta_{0_{TR}}} = \left[(T.F)\sigma\right]_{TR}\left[\frac{\partial(\frac{C_D'}{\sigma})}{\partial \theta_{75}}\right]_{TR} = 14944\text{x}0.0927 = 1385 \text{ lb/rad}$$

$$\frac{\partial Y_{TR}}{\partial \theta_{0_{TR}}} = \left[(T.F)\sigma\right]_{TR}\left[\frac{\partial(\frac{C_Y'}{\sigma})}{\partial \theta_{75}}\right]_{TR} = 14944\text{x}0.0177 = 264 \text{ lb/rad}$$

$$\frac{\partial Q_{TR}}{\partial \theta_{0_{TR}}} = \left[(T.F)\sigma R\right]_{TR}\left[\frac{\partial(\frac{C_Q}{\sigma})}{\partial \theta_{75}}\right]_{TR} = 77217\text{x}(-0.00523) = -404 \text{ ft-lb/sec}$$

11.3.3 Fuselage Isolated Derivatives

(a) Obtain the following fuselage trim parameters from Section 11.2

$V_0 = 221$ ft/sec $\qquad q_0 = 53.2$ lb/ft^2

$\alpha = 4.03^\circ = 0.0703$ rad

$\beta_S = 1.01^\circ = 0.0176$ rad

$\alpha_{FUS} = 2.80^\circ = 0.0489$ rad

$K_{FFUS} = 1.0$

$\epsilon_{FUS} = 1.23^\circ = 0.0214$ rad

$L_{FUS} = -70.5$ lb $\qquad \mathcal{L}_{FUS} = -500.7$ ft-lb

$D_{FUS} = 2136$ lb $\qquad M_{FUS} = 5355$ ft-lb

$Y_{FUS} = 25.6$ lb $\qquad N_{FUS} = -2706$ ft-lb

Also determine the fuselage moments of inertia

$I_{XX} = 14920$ slug-ft^2

$I_{YY} = 59800$ slug-ft^2

$I_{ZZ} = 56800$ slug-ft^2

(b) Using the fuselage trim values from step (a) above, enter the fuselage charts given in Figure 2, Section 11.1, and the charts for fuselage configuration "A", Section 5.3, and determine

$$\frac{\partial C_{L_{FUS}}}{\partial \alpha_{FUS}} = 0.229/\text{rad} \qquad \frac{\partial C_{L_{FUS}}}{\partial \beta_S} = 0$$

$$\frac{\partial C_{D_{FUS}}}{\partial \alpha_{FUS}} = 0.338/\text{rad} \qquad \frac{\partial C_{D_{FUS}}}{\partial \beta_S} = 0.113/\text{rad}$$

$$\frac{\partial C_{Y_{FUS}}}{\partial \alpha_{FUS}} = 0.0201/\text{rad} \qquad \frac{\partial C_{Y_{FUS}}}{\partial \beta_S} = -0.212/\text{rad}$$

$$\frac{\partial C_{\mathcal{L}_{FUS}}}{\partial \alpha_{FUS}} = 0 \qquad \frac{\partial C_{\mathcal{L}_{FUS}}}{\partial \beta_S} = -0.0372/\text{rad}$$

$$\frac{\partial C_{M_{FUS}}}{\partial \alpha_{FUS}} = 0.401/\text{rad} \qquad \frac{\partial C_{M_{FUS}}}{\partial \beta_S} = 0$$

$$\frac{\partial C_{N_{FUS}}}{\partial \alpha_{FUS}} = -0.067/\text{rad} \qquad \frac{\partial C_{N_{FUS}}}{\partial \beta_S} = -0.333/\text{rad}$$

(c) Using the equations of Subsections 7.3.3 and the values obtained in steps (a) and (b) above, compute the following fuselage dimentional derivatives

(i) u_{FUS} -Derivatives

$$\frac{\partial L_{FUS}}{\partial u_{FUS}} = \frac{2}{V_0} L_{FUS} = \frac{2(-70.5)}{221.125} = -0.637 \text{ lb-sec/ft}$$

$$\frac{\partial D_{FUS}}{\partial u_{FUS}} = \frac{2}{V_0} D_{FUS} = \frac{2(2136)}{221.125} = 19.3 \text{ lb-sec/ft}$$

$$\frac{\partial Y_{FUS}}{\partial u_{FUS}} = \frac{2}{V_0} Y_{FUS} = \frac{2(25.6)}{221.125} = 0.231 \text{ lb-sec/ft}$$

$$\frac{\partial \mathcal{L}_{FUS}}{\partial u_{FUS}} = \frac{2}{V_0} \mathcal{L}_{FUS} = \frac{2(-500.7)}{221.125} = -4.53 \text{ lb-sec}$$

$$\frac{\partial M_{FUS}}{\partial u_{FUS}} = \frac{2}{V_o} M_{FUS} = \frac{2(5355)}{221.125} = 48.4 \text{ lb-sec}$$

$$\frac{\partial N_{FUS}}{\partial u_{FUS}} = \frac{2}{V_o} N_{FUS} = \frac{2(-2706)}{221.125} = -24.5 \text{ lb-sec}$$

(ii) $\underline{\alpha_{FUS}\text{ -Derivatives}}$

$$\frac{\partial L_{FUS}}{\partial \alpha_{FUS}} = q_o A_{Z_{FUS}} \left(\frac{\partial C_{L_{FUS}}}{\partial \alpha_{FUS}}\right)$$

$$= 53.2 \times 276 \times 0.229 = 3365 \text{ lb/rad}$$

$$\frac{\partial D_{FUS}}{\partial \alpha_{FUS}} = q_o A_{X_{FUS}} \left(\frac{\partial C_{D_{FUS}}}{\partial \alpha_{FUS}}\right)$$

$$= 53.2 \times 95 \times 0.338 = 1708 \text{ lb/rad}$$

$$\frac{\partial Y_{FUS}}{\partial \alpha_{FUS}} = q_o A_{Y_{FUS}} \left(\frac{\partial C_{Y_{FUS}}}{\partial \alpha_{FUS}}\right)$$

$$= 53.2 \times 388 \times 0.0201 = 414 \text{ lb/rad}$$

$$\frac{\partial \mathcal{L}_{FUS}}{\partial \alpha_{FUS}} = q_o A_{X_{FUS}} \ell_{FUS} \left(\frac{\partial C_{\mathcal{L}_{FUS}}}{\partial \alpha_{FUS}}\right) = 0$$

$$\frac{\partial M_{FUS}}{\partial \alpha_{FUS}} = q_o A_{X_{FUS}} \ell_{FUS} \left(\frac{\partial C_{M_{FUS}}}{\partial \alpha_{FUS}}\right)$$

$$= 53.2 \times 68 \times 56.5 \times 0.401 = 81961 \text{ ft-lb/rad}$$

$$\frac{\partial N_{FUS}}{\partial \alpha_{FUS}} = q_o A_{X_{FUS}} \ell_{FUS} \left(\frac{\partial C_{N_{FUS}}}{\partial \alpha_{FUS}}\right)$$

$$= -53.2 \times 68 \times 56.5 \times 0.067 = -13702 \text{ ft-lb/rad}$$

(iii) Fuselage β_S -Derivatives

$$\frac{\partial L_{FUS}}{\partial \beta_S} = q_o A_{Z_{FUS}} \left(\frac{\partial C_{L_{FUS}}}{\partial \beta_S}\right) = 0$$

$$\frac{\partial D_{FUS}}{\partial \beta_S} = q_o A_{X_{FUS}} \left(\frac{\partial C_{D_{FUS}}}{\partial \beta_S}\right)$$

$$= 53.2 \times 95 \times 0.113 = 571 \text{ lb/rad}$$

$$\frac{\partial Y_{FUS}}{\partial \beta_S} = q_o A_{Y_{FUS}} \left(\frac{\partial C_{Y_{FUS}}}{\partial \beta_S}\right)$$

$$= -53.2 \times 388 \times 0.212 = -4376 \text{ lb/rad}$$

$$\frac{\partial \mathcal{L}_{FUS}}{\partial \beta_S} = q_o A_{X_{FUS}} \ell_{FUS} \left(\frac{\partial C_{\mathcal{L}_{FUS}}}{\partial \beta_S}\right)$$

$$= -53.2 \times 68 \times 56.5 \times 0.0372 = -7603 \text{ ft-lb/rad}$$

$$\frac{\partial M_{FUS}}{\partial \beta_S} = q_o A_{X_{FUS}} \ell_{FUS} \left(\frac{\partial C_{M_{FUS}}}{\partial \beta_S}\right) = 0$$

$$\frac{\partial N_{FUS}}{\partial \beta_S} = q_o A_{X_{FUS}} \ell_{FUS} \left(\frac{\partial C_{N_{FUS}}}{\partial \beta_S}\right)$$

$$= 53.2 \times 68 \times 56.5 \times 0.333 = -68160 \text{ ft-lb/rad}$$

11.3.4 Wing Isolated Derivatives

(a) Obtain the following wing trim parameters from Section 11.2:

V_o = 221 ft/sec $\qquad$ q_o = 53.2 lb/ft^2

α = 4.03^o = 0.0703 rad

$\alpha_W = 2.70^\circ = 0.0472$ rad

$K_{FW} = 1.08$

$\epsilon_W = 1.32^\circ = 0.0231$

$L_W = 4194$ lb $\qquad D_W = 193$ lb

$\mathcal{L}_W = -1848 + 105923 A_{I_F}$ ft-lb

$A_{I_F} = -1.2^\circ = -0.0209$ rad

$\therefore \mathcal{L}_W = -1848 + 105923\ (-0.0209) = -4062$ ft-lb

$a_W = 4.83$/rad

(b) Using the equations in Subsection 7.3.4 and the values obtained in step (a) above, compute the following wing dimensional derivatives:

(i) <u>u_W -Derivatives</u>

$$\frac{\partial L_W}{\partial u_W} = \frac{2}{V_0} L_W = \frac{2 \times 4194}{221} = 37.9 \text{ lb-sec/ft}$$

$$\frac{\partial D_W}{\partial u_W} = \frac{2}{V_0} D_W = \frac{2 \times 193}{221} = 1.74 \text{ lb-sec/ft}$$

$$\frac{\partial \mathcal{L}_W}{\partial u_W} = \frac{2}{V_0} \mathcal{L}_W = \frac{-2 \times 4062}{221} = -36.7 \text{ lb-sec}$$

(ii) <u>α_W -Derivatives</u>

$$\frac{\partial L_W}{\partial \alpha_W} = q_0 a_W S_W = 53.2 \times 4.83 \times 170 = 43682 \text{ lb/rad}$$

$$\frac{\partial D_W}{\partial \alpha_W} = \frac{2L_W}{\pi(AR)_W} a_W = \frac{2 \times 4194}{3.14 \times 6.04} \times 4.83 = 2135 \text{ lb/rad}$$

The remaining wing derivatives can be neglected.

11.3.5 Horizontal Tail Isolated Derivatives

(a) Obtain the following horizontal tailplane trim parameters from Section 11.2:

V_0 = 221 ft/sec q_0 = 53.2 lb/ft^2

α = 4.03° = 0.0703 rad

α_T = 0.210° = 0.00366 rad

$K_{FT} + K_{WT}$ = 3.112

ϵ_T = 3.816° = 0.0666 rad

L_T = 66.3 lb D_T = 40.6 lb

$\mathcal{L}_T$ = -80.9 ft-lb a_T = 4.42/rad

(b) Using the equations in Subsection 7.3.4 and the values obtained in step (a) above, compute the following horizontal tailplane dimensional derivatives:

(i) u_T -Derivatives

$$\frac{\partial L_T}{\partial u_T} = \frac{2}{V_0} L_T = \frac{2 \times 66.3}{221} = 0.599 \text{ lb-sec/ft}$$

$$\frac{\partial D_T}{\partial u_T} = \frac{2}{V_0} D_T = \frac{2 \times 40.6}{221} = 0.367 \text{ lb-sec/ft}$$

$$\frac{\partial \mathcal{L}_T}{\partial u_T} = \frac{2}{V_0}\mathcal{L}_T = \frac{-2 \times 80.9}{221} = 0.732 \text{ lb-sec}$$

(ii) <u>α_T -Derivatives</u>

$$\frac{\partial L_T}{\partial \alpha_T} = q_0\, a_T\, S_T = 53.2 \times 4.42 \times 76.2 = 17918 \text{ lb/rad}$$

$$\frac{\partial D_T}{\partial \alpha_T} = \frac{2 L_T}{\pi (AR)_T}\, a_T = \frac{2 \times 66.3}{3.14 \times 5.26} \times 4.42 = 35.5 \text{ lb/rad}$$

The remaining horizontal tail derivatives can be neglected.

11.3.6 <u>Vertical Tail Isolated Derivatives</u>

(a) Obtain the following vertical tail trim parameters from Section 11.2:

$V_0 = 221$ ft/sec $\qquad q_0 = 53.2$ lb/ft^2

$\alpha = 4.03^\circ = 0.0703$ rad

$\alpha_{VT} = 0.210^\circ = 0.00366$ rad

$\beta_S = 1.01^\circ = 0.0176$ rad

$K_{FVT} + K_{WVT} = 3.112$

$\epsilon_{VT} = 3.816^\circ = 0.0666$ rad

$L_{VT} = 103$ lb $\qquad D_{VT} = 28.6$ lb

$a_{VT} = 1.84$

(b) Using the equations in Subsection 7.3.6 and the values obtained in step (a) above, compute the following vertical tail dimensional derivatives:

(i) u_{VT} -Derivatives

$$\frac{\partial L_{VT}}{\partial u_{VT}} = \frac{2}{V_0} L_{VT} = \frac{2 \times 103}{221} = 0.931 \text{ lb-sec/ft}$$

$$\frac{\partial D_{VT}}{\partial u_{VT}} = \frac{2}{V_0} D_{VT} = \frac{2 \times 28.4}{221} = 0.257 \text{ lb-sec/ft}$$

(ii) α_{VT} -Derivatives

$$\frac{\partial L_{VT}}{\partial \alpha_{VT}} = \frac{\partial D_{VT}}{\partial \alpha_{VT}} = 0$$

(iii) β_S -Derivatives

$$\frac{\partial L_{VT}}{\partial \beta_S} = q_0 a_{VT} S_{VT} = 53.2 \times 1.84 \times 52 = 5090 \text{ lb/rad}$$

$$\frac{\partial D_{VT}}{\partial \beta_S} = \frac{2 L_{VT}}{\pi (AR)_{VT}} a_{VT} = \frac{2 \times 103}{3.14 \times 1.5} \times 1.84 = 80.4 \text{ lb/rad}$$

11.3.7 Auxiliary Propulsion (Jet) Isolated Derivatives

(a) Obtain the auxiliary jet engine trim parameters from Section 11.2

V_0 = 221 ft/sec $\qquad$ q_0 = 53.2 lb/ft^2

$\alpha = 4.03^\circ = 0.0703$ rad

$\alpha_{FUS} = 2.80^\circ = 0.0489$ rad

$\alpha_{P_j} = i_{P_j} + \alpha_{FUS} = 6 + 2.8 = 8.8^\circ$

$T_{P_i} = 960$ lb

$N_{P_i} = 123.3$ lb

(b) Using the values in step (a) above obtain the auxiliary propulsive unit derivatives from Section 5.7 as follows:

(i) u_{P_i} -Derivatives

At the values of T_{P_i} and V_0 given in step (a), graphically obtain the slope $\partial T_{P_i}/\partial u_{P_i}$ from Figure 1 in Section 5.7 as:

$$\frac{\partial T_{P_i}}{\partial u_{P_i}} = -0.49 \text{ lb-sec/ft}$$

Also, from Section 5.7 for an auxiliary engine mounted low on the fuselage, calculate

$$\frac{\partial N_{P_i}}{\partial u_{P_i}} = \frac{2 q_0 A_i}{V_0}\left[2 \sin \alpha_{P_i} - K_{FUS}\left(\frac{\lambda}{\mu} - \frac{\partial \lambda}{\partial \mu}\right)_F \cos \alpha_{P_i}\right]$$

$$= \frac{2 \times 53.2 \times 7.66}{221}\left[2 \times 0.153 - 1.0 \times \left(\frac{-0.053}{0.335} + 0.1108\right) \times 0.998\right] = 1.30 \text{ lb-sec/ft}$$

(ii) α_{P_i} -Derivatives

$$\frac{\partial T_{P_i}}{\partial \alpha_{P_i}} = 0$$

At the value of q_0 given in step (a), graphically obtain the slope $\partial(N_{P_i}/A_i)/\partial \alpha_{P_i}$ from Figure 2 in Section 5.7 as:

$$\frac{\partial\left(\frac{N_{P_i}}{A_i}\right)}{\partial \alpha^{\circ}_{P_i}} = 1.85 \text{ lb/ft}^2\text{-deg}$$

Then

$$\left[\frac{\partial N}{\partial \alpha}\right]_{P_i} = \left[\frac{\partial \frac{N}{A_i}}{\partial \alpha^{\circ}} A_i\right]_{P_i} \times 57.3 = 1.85 \times 7.66 \times 57.3 = 812 \text{ lb/rad}$$

(iii) β_S Derivatives

$$\frac{\partial T_{P_i}}{\partial \beta_S} = 0$$

From symmetry,

$$\frac{\partial N_{P_i}}{\partial \beta_S} = \frac{\partial N_{P_i}}{\partial \alpha_{P_i}} = 812 \text{ lb/rad}$$

LITERATURE CITED

1. Kisielowski, E., Perlmutter, A. A., and Tang, J., STABILITY AND CONTROL HANDBOOK FOR HELICOPTERS, USAAVLABS Technical Report 67-63, U. S. Army Aviation Materiel Laboratories, Fort Eustis, Virginia, August 1967, AD662259.

11.4 TOTAL STABILITY DERIVATIVES

The total stability derivatives for the sample compound helicopter are now easily evaluated utilizing the analytical procedures outlined in Section 7.1 and the isolated derivatives computed in Section 11.3.
The derivatives thus computed for the sample compound helicopter for six degrees of freedom of aircraft motion are presented in Table I. This table also includes the control derivatives required for the aircraft response calculations.

TABLE I

TOTAL STABILITY DERIVATIVES FOR THE SAMPLE COMPOUND HELICOPTER

Var. \ Eq.	X	Y	Z	M	N	L
θ	-18855.	0	-1329.	0	0	0
$\dot{\theta}$	-7788.	-634.88	127219.	-126275.	29567.	-10368.
$\ddot{\theta}$	0	0	0	-59800.	0	0
ϕ	0	18900.	0	0	0	0
$\dot{\phi}$	-664.66	7976.	-57.241	11211.	-10933.	-18468.
$\ddot{\phi}$	0	0	0	0	0	-14920.
ψ	0	1329.	0	0	0	0
$\dot{\psi}$	-116.61	-128911.	-53.776	1059.	-32671.	3362.
$\ddot{\psi}$	0	0	0	0	-56800.	0
u	-32.129	4.153	-40.994	-267.92	-106.64	33.043
$\dot{u}$	-586.96	0	0	0	0	0
v	-1.059	-40.916	-7.221	7.694	623.65	-60.777
$\dot{v}$	0	-586.96	0	0	0	0
w	57.893	-5.656	-765.66	-936.29	-262.98	65.683
$\dot{w}$	0	0	-579.41	269.33	0	0
A_1	3.274	13742.	-46.461	-0.973	6404.	68399.
B_1	3386.	1589.	107369.	-171026.	46935.	-14480.
δ_r	1384.	-15231	269.49	-8.803	546299.	-102610.

11.5 STABILITY CHARACTERISTICS EQUATION

The dynamic stability of an aircraft is assessed by examining the coefficients and the roots of the stability characteristic equations. The uncoupled longitudinal mode and uncoupled lateral mode characteristic equations for the sample compound helicopter are obtained by following the analytical procedure outlined in Section 8.0 and by utilizing the aircraft total derivatives computed in Subsection 11.4.

The computations of aircraft stability characteristics involving more than three degrees of freedom of aircraft motion are most conveniently performed utilizing a digital or analog computer program. A typical analog computer program that can be used for this purpose is described in Section 10.

11.5.1 Uncoupled Longitudinal Mode

11.5.1.1 Coefficients of the Characteristic Equation

(a) Utilizing the total aircraft stability derivatives presented in Table I of Subsection 11.4, compute the following terms:

$$G_1 = Z_{\dot{w}} M_{\ddot{\theta}} - M_{\dot{w}} Z_{\ddot{\theta}} = (-579)(-59800) = 34.6\text{x}10^6$$

$$G_2 = Z_w M_{\ddot{\theta}} + Z_{\dot{w}} M_{\dot{\theta}} - M_w Z_{\ddot{\theta}} - M_{\dot{w}} Z_{\dot{\theta}}$$

$$= (-766)(-59800) + (-579)(-126275) - (269)(127219)$$

$$= 84.7 \times 10^6$$

$$G_3 = Z_{\ddot{\theta}} M_u - Z_u M_{\ddot{\theta}} = -(-41)(-59800) = -2.45 \times 10^6$$

$$G_4 = Z_u M_{\dot{w}} - M_u Z_{\dot{w}}$$

$$= (-41)(269) - (-268)(-579) = -0.166 \times 10^6$$

$G_5 = Z_w M_{\dot\theta} - M_w Z_{\dot\theta} - Z_\theta M_{\dot w}$

$= (-766)(-126275)-(-936)(127219)-(-1329)(269)$

$= 216 \times 10^6$

$G_6 = M_u Z_{\dot\theta} - Z_u M_{\dot\theta}$

$= (-268)(127219)-(-41)(-126275) = -39.2 \times 10^6$

$G_7 = Z_u M_w - M_u Z_w$

$= (-41)(-936) - (-268)(-766) = -0.167 \times 10^6$

$G_8 = M_u X_{\dot w} - M_w X_{\dot u}$

$= (-268)(-0.0413) - (-936)(-587) = -0.550 \times 10^6$

$G_9 = X_w M_u - X_u M_w$

$= (57.9)(-268) - (-32.1)(-936) = -0.0456 \times 10^6$

(b) Calculate the coefficients of the longitudinal mode characteristic equation as follows:

$A = G_1 X_{\dot u} = 34.6(-587) \times 10^6 = -20.3 \times 10^9$

$B = G_1 X_u + G_2 X_{\dot u} + G_3 X_{\dot w} + G_4 X_{\ddot\theta}$

$= \left[34.6(-32.1) + 84.7(-587) - 2.45(-0.0413)\right] \times 10^6$

$= -50.8 \times 10^9$

$$C = G_2 X_u + G_3 X_w + G_4 X_{\dot\theta} + G_5 X_{\dot u} + G_6 X_{\dot w} + G_7 X_{\ddot\theta}$$

$$= \big[84.7(-32.1) - 2.45(57.9) - 0.166(-7788) + 216(-587) - 39.2(-0.0413)\big] \times 10^6 = -128\text{x}10^9$$

$$D = G_4 X_\theta + G_5 X_u + G_6 X_w + G_7 X_{\dot\theta} + G_8 Z_\theta$$

$$= \big[-0.166(-18855) + 216(-32.1) - 39.2(57.9) -0.167(-7788) - 0.55(-1329)\big] \times 10^6 = -4.05\text{x}10^9$$

$$E = G_7 X_\theta + G_9 Z_\theta$$

$$= \big[-0.167(-18855) - 0.0456(-1329)\big] \times 10^6$$

$$= 3.20 \times 10^9$$

(c) Divide all the coefficients by the coefficient A; obtain the following uncoupled longitudinal mode characteristic equation for the sample compound helicopter:

$$\Lambda^4 + 2.50\,\Lambda^3 + 6.32\,\Lambda^2 + 0.199\,\Lambda - 0.157 = 0$$

11.5.1.2 Criteria for Stability

As discussed in Section 8.4, the necessary and sufficient conditions for stability are that all the coefficients of the characteristic equation (B,C,D, and E) be greater than zero when $A > 0$, and also the Routh discriminant $R^* > 0$.

It can be noted that in the sample case, the normalized coefficient E is smaller than zero when A, B, C, and D are greater than zero. Since there is only one sign change in the normalized coefficients A, B .... E, there will exist at least one positive (unstable) real root.

Therefore, the sample aircraft will possess at least one divergent aperiodic longitudinal mode, regardless of whether the Routh discriminant is positive or negative.

11.5.1.3 Solution of the Characteristic Equation

The solution of the stability characteristic equation (quartic) for the example compound helicopter can be obtained utilizing the analytical method of Section 8.5. The calculative procedure is as follows:

(a) The normalized coefficients (A, B, ... E) of the characteristic equation as computed in Subsection 11.5.1.1 are:

$$A\Lambda^4 + B\Lambda^3 + C\Lambda^2 + D\Lambda + E = 0$$

where

$$A = 1,\ B = 2.50,\ C = 6.32,\ D = 0.199,\ E = -0.157$$

(b) Calculate

$$S^* = BD + C^2 - 4E$$

$$= 2.50(0.199) + (6.32)^2 - 4(-0.157) = 41.016$$

$$R^* = BCD - EB^2 - D^2$$

$$= 2.50(6.32)(0.199) + 0.157(2.50)^2 - 0.199$$

$$= 4.074$$

(c) Compute

$$h_1 = \frac{1}{3}(3S^* - 4C^2)$$

$$= \frac{1}{3}\left[3(41.016) - 4(6.32)^2\right] = -12.173$$

$$h_2 = \frac{1}{27}(18CS^* - 16C^3 - 27R^*)$$

$$= \frac{1}{27}\left[18(6.32)(41.016) - 16(6.32)^3 - 27(4.074)\right]$$

$$= 19.323$$

(d) Evaluate the discriminant (Δ)

$$\Delta = \frac{h_2^2}{4} + \frac{h_1^3}{27}$$

$$= \frac{(19.323)^2}{4} + \frac{(-12.173)^3}{27} = 26.536$$

(e) Determine the value of (Π_n).

Since Δ in step (d) is greater than zero, then

$$\Pi_n = \sqrt[3]{-\frac{h_2}{2} + \sqrt{\Delta}} + \sqrt[3]{-\frac{h_2}{2} - \sqrt{\Delta}}$$

$$= \sqrt[3]{\frac{-19.323}{2} + \sqrt{26.536}} + \sqrt[3]{\frac{-19.323}{2} - \sqrt{26.536}}$$

$$= -4.106$$

(f) Compute

$$\zeta\eta = \Pi_n + \frac{2C}{3} \leq \frac{B^2}{4}$$

$$= -4.106 + \frac{2(6.32)}{3} \leq \frac{(2.50)^2}{4}$$

$$= 0.105 \leq 1.556$$

(g) Calculate

$$s = \frac{C - \zeta\eta}{2} + \sqrt{\left(\frac{C - \zeta\eta}{2}\right)^2 - E}$$

$$= \frac{6.32 - 0.105}{2} + \sqrt{\left(\frac{6.32 - 0.105}{2}\right)^2 + 0.157}$$

$$= 6.235$$

$$\nu = \frac{E}{\varsigma} = \frac{-0.157}{6.235} = -0.025$$

$$\eta = \frac{D - B\varsigma}{\nu - \varsigma} = \frac{0.199 \; -2.495(6.235)}{-0.025 \; -6.235} = 2.453$$

$$\zeta = B - \eta = 2.495 \; -2.453 = 0.042$$

(h) Finally, determine the four roots of the stability quartic, thus:

$$\Lambda_{1,2} = -\frac{\zeta}{2} \pm \sqrt{\left(\frac{\zeta}{2}\right)^2 - \nu}$$

$$= -\frac{0.042}{2} \pm \sqrt{\left(\frac{0.042}{2}\right)^2 + 0.025}$$

$$\therefore \Lambda_1 = 0.139 \qquad \Lambda_2 = -0.181$$

and,

$$\Lambda_{3,4} = -\frac{\eta}{2} \pm \sqrt{\left(\frac{\eta}{2}\right)^2 - \varsigma}$$

$$= -\frac{2.453}{2} \pm \sqrt{\left(\frac{2.453}{2}\right)^2 - 6.235}$$

$$= -1.227 \pm 2.175\, i$$

$$\therefore \Lambda_3 = -1.227 + 2.175\, i$$

$$\Lambda_4 = -1.227 - 2.175\, i$$

11.5.1.4 Roots of the Characteristic Equation

The roots of the characteristic equation computed above consist of one positive real root (Λ_1 = 0.139), one

negative real root (Λ_2 = -0.181), and a pair of complex roots ($\Lambda_{3,4}$ = -1.227 ± 2.175 i).
The positive real root (Λ_1) corresponds to aperiodic divergence having time to double the amplitude of about 4.99 sec. The negative root (Λ_2) corresponds to aperiodic convergence having time to half the amplitude of about 3.83 sec, which corresponds to a time constant of 5.52 sec. The complex pair ($\Lambda_{3,4}$) corresponds to a rapidly convergent oscillation having a period of about 2.89 sec and a time to half the amplitude of 0.56 sec. This corresponds to an oscillation frequency of 0.346 c.p.s. and a time constant of 0.815 sec.
It can be concluded, therefore, that the sample compound helicopter is slightly unstable in the longitudinal mode.

11.5.2 Uncoupled Lateral Mode

11.5.2.1 Coefficients of the Characteristic Equation

(a) Utilizing the total aircraft stability derivatives presented in Table I of Subsection 11.4, compute the following terms:

$$H_1 = L_{\ddot{\phi}} N_{\ddot{\psi}} - N_{\ddot{\phi}} L_{\ddot{\psi}} = (-14920)(-56800) = 847 \times 10^6$$

$$H_2 = L_{\dot{\phi}} N_{\ddot{\psi}} + L_{\ddot{\phi}} N_{\dot{\psi}} - N_{\dot{\phi}} L_{\ddot{\psi}} - N_{\ddot{\phi}} L_{\dot{\psi}}$$

$$= (-18467)(-56800) + (-14920)(-56800) = 1896 \times 10^6$$

$$H_3 = L_{\dot{\phi}} N_{\dot{\psi}} - N_{\dot{\phi}} L_{\dot{\psi}}$$

$$= (-18468)(-32671) - (-10933)(3362) = 640 \times 10^6$$

$$H_4 = N_v L_{\ddot{\psi}} - L_v N_{\ddot{\psi}} = -(-60.8)(-56800) = 3.45 \times 10^6$$

$$H_5 = L_v N_{\ddot{\phi}} - N_v L_{\ddot{\phi}} = -(624)(-14920) = 9.30 \times 10^6$$

$H_6 = N_v L_{\dot\psi} - L_v N_{\dot\psi}$

$= (624)(3362)-(-60.8)(-32671) = 0.111 \times 10^6$

$H_7 = L_v N_{\dot\phi} - N_v L_{\dot\phi}$

$= (-60.8)(-10933)-(624)(-18468) = 12.2 \times 10^6$

(b) Calculate the coefficients of the lateral mode characteristic equation as follows:

$A = H_1 Y_{\dot v} = 847(-587)\times10^6 = -497\times10^9$

$B = H_1 Y_v + H_2 Y_{\dot v}$

$= \left[847(-40.9)+1896(-587)\right] \times10^6 = -1147\times10^9$

$C = H_2 Y_v + H_3 Y_{\dot v} + H_4 Y_{\dot\phi} + H_5 Y_{\dot\psi}$

$= \left[1896(-40.9)+640(-587)-3.45(7976) + 9.30(-128911)\right] \times10^6 = -1679\times10^9$

$D = H_3 Y_v + H_4 Y_\phi + H_5 Y_\psi + H_6 Y_{\dot\phi} + H_7 Y_{\dot\psi}$

$= \left[640(-40.9)-3.45(18900)+9.30(1329)+0.111(7976) +12.2(-128911)\right] \times10^6 = -1649\times10^9$

$E = H_6 Y_\phi + H_7 Y_\psi$

$= \left[0.111(18900)+12.2(1329)\right] \times10^6 = 18.3\times10^9$

(c) Divide all the coefficients by the coefficient A; obtain the following uncoupled lateral mode characteristic equation for the sample compound helicopter:

$$\Lambda\left[\Lambda^4 + 2.306\Lambda^3 + 3.375\Lambda^2 + 3.314\Lambda - 0.037\right] = 0$$

11.5.2.2 Criteria for Stability

In the characteristic equation above, we can consider $\Lambda = 0$ to be a root of the equation and then deal only with the remaining quartic equation. In this quartic equation, only the normalized coefficient E is smaller than zero, while A, B, C, and D are greater than zero. Since there is only one sign change in the normalized coefficients A, B......E, there will exist at least one positive (unstable) real root.

Therefore, the sample aircraft will possess at least one divergent aperiodic lateral mode, regardless of whether the Routh discriminant is positive or negative.

11.5.2.3 Solution of the Characteristic Equation

The solution of the stability characteristic equation (quartic) for the sample compound helicopter can be obtained utilizing the analytical method of Section 8.5. The calculative procedure is as follows:

(a) Determine the normalized coefficients (A, B...E) of the characteristic equation

$$\Lambda^4 + B\Lambda^3 + C\Lambda^2 + D\Lambda + E = 0$$

where

A = 1, B = 2.306, C = 3.375, D = 3.314, E = -0.037

(b) Calculate

$$S^* = BD + C^2 - 4E$$

$$= 2.306(3.314) + (3.375)^2 - 4(-0.037) = 19.180$$

$$R^* = BCD - EB^2 - D^2$$

$$= 2.306(3.375)(3.314) - (-0.037)(2.306)^2 - (3.314)^2$$

$$= 15.003$$

(c) Compute

$$h_1 = \frac{1}{3}(3S^* - 4C^2)$$

$$= \frac{1}{3}\left[3(19.18) - 4(3.375)^2\right]$$

$$= 3.993$$

$$h_2 = \frac{1}{27}\left[18CS^* - 16C^3 - 27R^*\right]$$

$$= \frac{1}{27}\left[18(3.375)(19.18) - 16(3.375)^3 - 27\ (15.1003)\right]$$

$$= 5.371$$

(d) Calculate the discriminant (Δ)

$$\Delta = \frac{h_2^2}{4} + \frac{h_1^3}{27}$$

$$= \frac{(5.371)^2}{4} + \frac{(3.993)^3}{27} = 9.568$$

(e) Determine the value of (Π_n).

Since Δ in step (d) is greater than zero, then

$$\Pi_n = \sqrt[3]{-\frac{h_2}{2} + \sqrt{\Delta}} + \sqrt[3]{-\frac{h_2}{2} - \sqrt{\Delta}}$$

$$= \sqrt[3]{\frac{-5.371}{2} + \sqrt{9.568}} + \sqrt[3]{\frac{-5.371}{2} - \sqrt{9.568}}$$

$$= -1.052$$

(f) Compute

$$\zeta\eta = \Pi_n + \frac{2C}{3} \leq \frac{B^2}{4}$$

$$= -1.052 + \frac{2}{3}(3.375) \leq \frac{(2.306)^2}{4}$$

$$= 1.198 \leq 1.329$$

(g) Calculate

$$\varsigma = \frac{C-\zeta\eta}{2} + \sqrt{\left(\frac{C-\zeta\eta}{2}\right)^2 - E}$$

$$= \frac{3.375 - 1.198}{2} + \sqrt{\left(\frac{3.375-1.198}{2}\right)^2 - (-0.037)}$$

$$= 2.192$$

$$\upsilon = \frac{E}{\varsigma} = \frac{-0.037}{2.192} = -0.016$$

$$\eta = \frac{D - B\varsigma}{\upsilon - \varsigma} = \frac{3.314 - 2.306(2.192)}{-0.016 - 2.192} = 0.788$$

$$\zeta = B - \eta = 2.306 - 0.788 = 1.518$$

(h) Finally, determine the four roots of the stability quartic, thus:

$$\Lambda_{1,2} = -\frac{\zeta}{2} \pm \sqrt{\left(\frac{\zeta}{2}\right)^2 - \upsilon}$$

$$= -\frac{1.518}{2} \pm \sqrt{\left(\frac{1.518}{2}\right)^2 - (-0.016)}$$

$$\therefore \Lambda_1 = 0.010 \qquad \Lambda_2 = -1.528$$

and,

$$\Lambda_{3,4} = -\frac{\eta}{2} \pm \sqrt{\left(\frac{\eta}{2}\right)^2 - \varsigma}$$

$$= -\frac{0.788}{2} \pm \sqrt{\left(\frac{0.788}{2}\right)^2 - 2.192}$$

$$= -0.394 \pm 1.427\ i$$

$$\therefore \Lambda_3 = -0.394 + 1.427\ i$$

$$\Lambda_4 = -0.394 - 1.427\ i$$

and $\Lambda_5 = 0$

11.5.2.4 Roots of the Characteristic Equation

The roots of the characteristic equation computed above consist of one zero root ($\Lambda_5=0$), one positive real root ($\Lambda_1=0.01$), one negative real root ($\Lambda_2=-1.528$), and a pair of complex roots ($\Lambda_{3,4} = -0.394 \pm 1.427\ i$).
The zero root (Λ_5) corresponds to a neutrally stable mode. The positive real root (Λ_1) corresponds to a slow aperiodic divergence having time to double the amplitude of about 69.3 sec. The negative root (Λ_2) corresponds to a very rapid aperiodic convergence having time to half the amplitude of about 0.45 sec, which corresponds to a time constant of 0.65 sec. The complex pair ($\Lambda_{3,4}$) corresponds to a rapidly convergent oscillation having a period of about 4.4 sec and a time to half the amplitude of 1.76 sec. This corresponds to an oscillation frequency of 0.227 c.p.s. and a time constant of 2.54 sec. It can be concluded, therefore, that the sample compound helicopter is only slightly unstable in the lateral mode.

11.6 AIRCRAFT RESPONSE

The most convenient way of computing aircraft response due to control inputs or external disturbances is through the use of an analog computer program, such as discussed in Section 10. The response calculations for the sample compound helicopter are performed in Section 10.2 and will not be duplicated in this section. The dynamic stability response results described in Figures 2, 3, and 4 of Section 10.2 show that the sample aircraft is controllable in all stability modes despite the fact that certain modes exhibit divergent trends (e.g., response of ψ , ϕ , θ due to longitudinal cyclic pulse.

The time to double the amplitude of the divergent modes is generally in excess of 10 seconds and is therefore sufficiently long for the pilot to apply a corrective control input before undesirable excursions have time to develop.

Unclassified

Security Classification

DOCUMENT CONTROL DATA - R & D

(Security classification of title, body of abstract and indexing annotation must be entered when the overall report is classified)

1. ORIGINATING ACTIVITY (Corporate author) Dynasciences Corporation Township Line Road Blue Bell, Pennsylvania	2a. REPORT SECURITY CLASSIFICATION Unclassified 2b. GROUP

3. REPORT TITLE

STABILITY AND CONTROL HANDBOOK FOR COMPOUND HELICOPTERS

4. DESCRIPTIVE NOTES (Type of report and inclusive dates)
Handbook

5. AUTHOR(S) (First name, middle initial, last name)

E. K. Garay
E. Kisielowski

6. REPORT DATE	7a. TOTAL NO. OF PAGES	7b. NO. OF REFS
February 1971	668	74

8a. CONTRACT OR GRANT NO. DAAJ02-69-C-0023 b. PROJECT NO. Task 1F162204A14233 c. d.	9a. ORIGINATOR'S REPORT NUMBER(S) USAAVLABS Technical Report 70-67 9b. OTHER REPORT NO(S) (Any other numbers that may be assigned this report) DCR-314

10. DISTRIBUTION STATEMENT This document is subject to special export controls and each transmittal to foreign governments or foreign nationals may be made only with prior approval of Eustis Directorate, U. S. Army Air Mobility Research and Development Laboratory, Fort Eustis, Virginia 23604.

11. SUPPLEMENTARY NOTES	12. SPONSORING MILITARY ACTIVITY Eustis Directorate U. S. Army Air Mobility R&D Laboratory Fort Eustis, Virginia

13. ABSTRACT

This handbook contains analytical methods and stability data for determining the dynamic stability and control characteristics of generalized single-rotor compound helicopter configurations. The methods used calculation procedures which are considerably simplified through the extensive use of information presented in graphs and charts. These charts are applicable to articulated, teetering, and hingeless rotor sytems and cover a range of flight conditions from hover to high forward speeds.

The charts for low forward speeds (advance ratios, $\mu \leq 0.2$) were obtained from the rotor performance data based on classical rotor theory. However, the high-speed charts ($\mu \gtrsim 0.3$) exclude the major assumptions of classical theory and include blade compressibility, stall, reverse flow, large inflow ratios, etc.

The information presented herein is suitable for extensive digital and analog computer studies as well as for rapid manual computations such as required for preliminary design applications.

DD FORM 1 NOV 65 1473 REPLACES DD FORM 1473, 1 JAN 64, WHICH IS OBSOLETE FOR ARMY USE.

Unclassified

Security Classification

Unclassified

Security Classification

14 KEY WORDS	LINK A		LINK B		LINK C	
	ROLE	WT	ROLE	WT	ROLE	WT
Compound Helicopter						
Dynamic Stability						
Control						
Response						
Stability Augmentation						
Stability Derivatives						
Trim						

Unclassified

Security Classification